

**PHYTOCHEMICAL STUDY OF FLAVONOIDS FROM THE LEAVES
OF *Muntingia calabura*, SYNTHESIS OF FLAVONOID MANNICH
BASE DERIVATIVES AND THEIR ANTICANCER ACTIVITY
AGAINST BREAST CARCINOMA CELL LINES**

By

CHANG CHEW CHEEN

A thesis submitted to the Department of Chemical Science,
Faculty of Science,
Universiti Tunku Abdul Rahman,
in partial fulfillment of the requirements for the degree of
Doctor of Philosophy (Science)
February 2022

ABSTRACT

PHYTOCHEMICAL STUDY OF FLAVONOIDS FROM THE LEAVES OF *Muntingia calabura*, SYNTHESIS OF FLAVONOID MANNICH BASE DERIVATIVES AND THEIR ANTICANCER ACTIVITY AGAINST BREAST CARCINOMA CELL LINES

Chang Chew Cheen

Due to the continuous evolution of multi-drug resistant tumors, the development of new drugs with enhanced efficacy is essential. Hence, there is a growing interest in making chemical modifications to the natural flavonoids to improve the bioactivity. The aim of this study is to extract, isolate and characterize the chemical constituents from the leaves of *Muntingia calabura*, synthesize and characterize flavonoid Mannich base derivatives and evaluate their cytotoxic activity. Initially, dried leaves of *Muntingia calabura* were extracted with 95% ethanol, followed by 1:1 water/ethyl acetate (EA) partition. The EA crude extract was then subjected to continuous column chromatography over silica gel to obtain pure compounds. The pure compounds were characterized by spectroscopic techniques. Subsequently, the isolated flavonoids were subjected to Mannich reaction. The synthesized compounds were characterized by spectroscopic techniques. Cytotoxic activity of the parent compounds and synthesized compounds were evaluated against two breast cancer cell lines i.e., MCF-7, MDA-MB-231, and one normal breast cell line, MCF-10A via MTT assay. A total of eighteen flavonoids were isolated from the leaves of *Muntingia*

calabura. Among them, 3,5-dihydroxy-7-methoxyflavanone (**M1**), 7,8-dihydroxyflavanone (**M17**), and 2',3',4'-trihydroxychalcone (**M6**) were isolated from the leaves of *Muntingia calabura* for the first time. For Mannich bases, a total of twenty flavonoid Mannich bases were synthesized. Cytotoxic activity against MDA-MB-231 cancer cell line showed that flavonoid Mannich bases exhibited greater activity than parent compounds. 5,7-dihydroxy-8-(4-methoxybenzylamine)-2-phenyl-4H-chromen-4-one (**M14f**) showed the highest cytotoxic activity against MDA-MB-231 cell with IC_{50} of $5.75 \pm 0.82 \mu\text{M}$. For MCF-7 cell line, the parent compounds and Mannich bases showed moderate activity with the IC_{50} range of 9.17-68.5 μM . For cytotoxic activity against MCF-10A cell line, parent compounds, 5,7-dihydroxyflavone (**M14**) showed highest toxicity against MCF-10A with IC_{50} of $10.55 \pm 1.05 \mu\text{M}$. The results suggest that synthetic modifications have produced the compounds with improved anticancer activity and selectivity against breast cancer cells.

ACKNOWLEDGEMENTS

I would like to take this opportunity to express my gratitude to my Supervisor, Assoc. Prof. Dr. Sim Kooi Mow for his professional guidance, continuous support throughout this research. I would also like to show my appreciation to my co-supervisor Assoc. Prof. Dr. Lim Tuck Meng for his invaluable supervision and support during this study. They have taught me a great deal about the research work.

I would also like to acknowledge Prof. Rusea Go, from Universiti Putra Malaysia for the plant identification. I also wish to extend my sincere thanks to Prof. Mallikarjuna Rao Pichika and Ms Mak Kit Kay, from International Medical University for help in cytotoxic assay study.

I would like to thank all the lab officers Mr Leong Thung Lim, Mr Nicholas Ooh Keng Fei, Mr Seou Chi Kien, and Mr Goh Wee Sheng. It is their kind help and support that have made my study and life in UTAR a wonderful time. I also wish to extend my sincere thanks to my colleagues Dr. Ooi Mei Lee, Dr. Ooi Zhong Xian, Dr. Phoon Lee Quen, Dr. Teo Kah Cheng, Dr. Sangeetha a/p Arullappan, Dr. Lim Chaw Jiang and ex-colleague Dr. Neo Kian Eang for their help, support, and encouragement during this study. I would especially like to thank my friends Dr. Lee Choy Sin and Dr. Lye Huey Shi for giving insights suggestions and assistance when I had challenging time in my study.

Special thanks to Universiti Tunku Abdul Rahman (UTAR) for providing research fund and scholarship for this study. I would also like to extend my thanks to my previous FYP students. Finally, I wish to thank my parents and siblings for their caring and support throughout my study.

APPROVAL SHEET

This thesis entitled “**PHYTOCHEMICAL STUDY OF FLAVONOIDS FROM THE LEAVES OF *Muntingia calabura*, SYNTHESIS OF FLAVONOID MANNICH BASE DERIVATIVES AND THEIR ANTICANCER ACTIVITY AGAINST BREAST CARCINOMA CELL LINES**” was prepared by **CHANG CHEW CHEEN** and submitted as partial fulfillment of the requirements for the degree of Doctor of Philosophy (Science) at Universiti Tunku Abdul Rahman.

Approved by:



(Assoc. Prof. Dr. Sim Kooi Mow)
Supervisor
Department of Chemical Science
Faculty of Science
Universiti Tunku Abdul Rahman

Date: 5/7/2022



(Assoc. Prof. Dr. Lim Tuck Meng)
Co-supervisor
Department of Chemical Science
Faculty of Science
Universiti Tunku Abdul Rahman

Date: 5 July 2022

FACULTY OF SCIENCE
UNIVERSITI TUNKU ABDUL RAHMAN

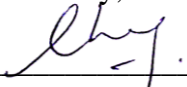
Date: 18/6/2022

SUBMISSION OF THESIS

It is hereby certified that **CHANG CHEW CHEEN** (ID No:**11ADD06526**) has completed this thesis entitled “**PHYTOCHEMICAL STUDY OF FLAVONOIDS FROM THE LEAVES OF *Muntingia calabura*, SYNTHESIS OF FLAVONOID MANNICH BASE DERIVATIVES AND THEIR ANTICANCER ACTIVITY AGAINST BREAST CARCINOMA CELL LINES**” under the supervision of Assoc. Prof Dr. Sim Kooi Mow (Supervisor) from the Department of Chemical Science, Faculty of Science, and Assoc. Prof Dr. Lim Tuck Meng (Co-Supervisor) from the Department of Chemical Science, Faculty of Science.

I understand that University will upload softcopy of my thesis in pdf format into UTAR Institutional Repository, which may be made accessible to UTAR community and public.

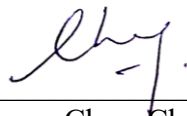
Yours truly,



(Chang Chew Cheen)

DECLARATION

I hereby declare that the dissertation is based on my original work except for quotations and citations which have been duly acknowledged. I also declare that it has not been previously or concurrently submitted for any other degree at UTAR or other institutions.

Name 
(Chang Chew Cheen)

Date 18/6/2022

TABLE OF CONTENTS

| | Page |
|---|---------------|
| ABSTRACT | ii |
| ACKNOWLEDGEMENTS | iv |
| APPROVAL SHEET | vi |
| SUBMISSION SHEET | vii |
| LIST OF TABLES | xiv |
| LIST OF FIGURES | xviii |
| LIST OF ABBREVIATIONS | xxviii |
| | |
| CHAPTER | |
| | |
| 1.0 INTRODUCTION | 1 |
| 1.1 Natural products | 1 |
| 1.2 Botany of Plant Species Studied | 2 |
| 1.2.1 Taxonomy | 2 |
| 1.2.2 <i>Muntingia calabura</i> | 3 |
| 1.2.3 Ethnomedical Uses of <i>Muntingia calabura</i> | 6 |
| 1.3 Anticancer of Flavonoids | 7 |
| 1.4 Mannich reaction | 9 |
| 1.5 Problem statement | 10 |
| 1.6 Objectives | 11 |
| | |
| 2.0 LITERATURE REVIEW | 12 |
| 2.1 Introduction | 12 |
| 2.2 Chemical Constituents from the Roots of <i>Muntingia calabura</i> and Their Biological Activities | 12 |
| 2.3 Chemical Constituents from the Leaves of <i>Muntingia calabura</i> and Their Biological Activities | 15 |
| 2.4 Chemical Constituents from the Stem barks of <i>Muntingia calabura</i> and Their Biological Activities | 23 |
| 2.5 Chemical Constituents from the Fruits of <i>Muntingia calabura</i> | 26 |
| 2.6 Phytochemical Study of <i>Muntingia calabura</i> Leaves Extracts and Their Biological Activities | 26 |
| 2.7 Flavonoid Mannich Bases | 27 |
| 2.7.1 Chalcone Mannich Bases with Cytotoxic Activity | 28 |
| 2.7.2 Flavone Mannich Bases with Cytotoxic Activity | 34 |
| | |
| 3.0 Materials and Methods | |
| 3.1 Plant materials | 40 |
| 3.2 Chemicals and Reagents | 40 |
| 3.2.1 Solvents and Materials Used for Extraction and Isolation | 40 |

| | |
|--|-----------|
| 3.2.2 Chemicals and Reagents Used for Structure Elucidation | 41 |
| 3.2.3 Chemicals and Reagents used for Mannich Reaction | 42 |
| 3.2.4 Chemicals and Reagents Used for Cytotoxic activity | 43 |
| 3.3 Instruments | 44 |
| 3.3.1 Ultra-Violet Visible (UV-Vis) Spectrophotometer | 44 |
| 3.3.2 Fourier Transform Infra Red (FTIR) Spectrophotometer | 44 |
| 3.3.3 Mass Spectrometry | 44 |
| 3.3.4 Nuclear Magnetic Resonance (NMR) | 44 |
| 3.3.5 Melting Point Apparatus | 45 |
| 3.3.6 Polarimeter | 45 |
| 3.3.7 Rotary Evaporator | 45 |
| 3.4 Methodology | 45 |
| 3.4.1 Extraction of the leaves of <i>Muntingia calabura</i> | 45 |
| 3.4.2 Chromatography Methods | 46 |
| 3.4.2.1 Column Chromatography (CC) | 46 |
| 3.4.2.2 Thin Layer Chromatography | 47 |
| 3.5 TLC Visualization Methods | 47 |
| 3.5.1 UV light | 47 |
| 3.5.2 Iodin vapour | 47 |
| 3.6 Mannich Reaction | 48 |
| 3.6.1 Synthesis of Monoamine Chalcone Mannich base Derivatives | 48 |
| 3.6.2 Synthesis of Monoamine Flavone Mannich base Derivatives | 49 |
| 3.6.3 Synthesis of Diamine Flavone Mannich base Derivatives | 50 |
| 3.7 Cytotoxic Activity | 51 |
| 3.7.1 Cell culture | 51 |
| 3.7.2 Preparation of Test Compounds | 52 |
| 3.7.3 Cell Seeding and Treatment | 52 |
| 3.7.4 MTT assay | 52 |
| 3.7.5 Statistical Analysis | 53 |
| 4.0 Results and Discussion | 54 |
| 4.1 Extraction and Isolation | 54 |
| 4.2 Isolated Compounds from the Leaves of <i>Muntingia calabura</i> | 59 |
| 4.2.1 Characterization and Structure Elucidation of Flavanone | 59 |
| 4.2.1.1 Characterization of (2 <i>S</i> , 3 <i>S</i>) 3,5-dihydroxy-7-methoxyflavanone (M1) | 59 |
| 4.2.1.2 Characterization of (2 <i>R</i> , 3 <i>R</i>) 3,5-dihydroxy-6,7-dimethoxyflavanone (M12) | 65 |
| 4.2.1.3 Characterization of (2 <i>R</i> , 3 <i>R</i>) 3,5,7-trihydroxyflavanone (M13) | 69 |
| 4.2.1.4 Characterization of (2 <i>S</i>) 7,8-dihydroxyflavanone (M17) | 73 |
| 4.2.1.5 Characterization of (2 <i>R</i> , 3 <i>R</i>) 3,5,7-trihydroxy-8-methoxyflavanone (M18) | 78 |

| | |
|---|-----|
| 4.2.2 Characterization and Structure Elucidation of Chalcones | 82 |
| 4.2.2.1 Characterization of 2',4'-dihydroxy-3'-methoxychalcone (M2) | 82 |
| 4.2.2.2 Characterization of 2',4'-dihydroxychalcone (M4) | 87 |
| 4.2.2.3 Characterization of 2',3',4'-trihydroxychalcone (M6) | 92 |
| 4.2.3 Characterization and Structure Elucidation of Flavones | 96 |
| 4.2.3.1 Characterization of 3,5-dihydroxy-6,7-dimethoxyflavone (M3) | 96 |
| 4.2.3.2 Characterization of 3, 5, 7-trihydroxy-8-methoxyflavone (M5) | 101 |
| 4.2.3.3 Characterization of 5-hydroxy-3,7-dimethoxyflavone (M7) | 106 |
| 4.2.3.4 Characterization of 3,5-dihydroxy-7-methoxyflavone (M8) | 111 |
| 4.2.3.5 Characterization of 5-dihydroxy-7-methoxyflavone (M9) | 115 |
| 4.2.3.6 Characterization of 5-hydroxy-3,7,8-trimethoxyflavone (M10) | 119 |
| 4.2.3.7 Characterization of 5,7-dihydroxy-3,8-dimethoxyflavone (M11) | 124 |
| 4.2.3.8 Characterization of 5,7-dihydroxyflavone (M14) | 128 |
| 4.2.3.9 Characterization of 5-hydroxy-6,7-dimethoxyflavone (M15) | 132 |
| 4.2.3.10 Characterization of 5,4'-dihydroxy-7-methoxyflavone (M16) | 136 |
| 4.3 Synthesis of Flavonoid Mannich Base Derivatives | 141 |
| 4.3.1 Synthesis of 2',4'-dihydroxy-3'-methoxychalcone (M2) Mannich Bases | 142 |
| 4.3.1.1 Characterization of 1-[3-methoxy-5-(piperidin-4-yl)methyl-2,4-dihydroxyphenyl]-3-phenyl-2-propen-1-one (M2a) | 145 |
| 4.3.1.2 Characterization of 1-[3-methoxy-5-(morpholino-4-yl) methyl-2,4-dihydroxyphenyl]-3-phenyl-2-propen-1-one (M2b) | 153 |
| 4.3.2 Synthesis of 2',4'-dihydroxychalcone (M4) Mannich Bases | 160 |
| 4.3.2.1 Characterization of 1-[3-methoxy-5-(piperidin-4-yl) methyl-2,4-dihydroxyphenyl]-3-phenyl-2-propen-1-one (M4a) | 162 |
| 4.3.2.2 Characterization of 1-[3-(morpholino-4-yl) methyl-2,4-dihydroxyphenyl]-3-phenyl-2-propen-1-one (M4b) | 169 |
| 4.3.3 Synthesis of 3,5,7-trihydroxy-8-methoxyflavone (M5) Mannich Bases | 176 |

| | | |
|---------|--|-----|
| 4.3.3.1 | Characterization of 3,5,7-trihydroxy-8-methoxy-6-(pyrrolidin-1-ylmethyl)-2-phenyl-4H-chromen-4-one (M5a) | 178 |
| 4.3.3.2 | Characterization of 3,5,7-trihydroxy-8-methoxy-6-(piperidin-1-ylmethyl)-2-phenyl-4H-chromen-4-one (M5b) | 185 |
| 4.3.3.3 | Characterization of 3,5,7-trihydroxy-8-methoxy-6-(4-methylpiperazin-1-ylmethyl)-2-phenyl-4H-chromen-4-one (M5c) | 192 |
| 4.3.3.4 | Characterization of 3,5,7-trihydroxy-8-methoxy-6-(morpholinomethyl)-2-phenyl-4H-chromen-4-one (M5d) | 199 |
| 4.3.3.5 | Characterization of 3,5,7-trihydroxy-8-methoxy-6-(thiomorpholinomethyl)-2-phenyl-4H-chromen-4-one (M5e) | 206 |
| 4.3.4 | Synthesis of 5,7-dihydroxyflavone (M14) Monoamine Mannich Bases | 213 |
| 4.3.4.1 | Characterization of 5,7-dihydroxy-8-(pyrrolidine-1-ylmethyl)-2-phenyl-4H-chromen-4-one (M14a) | 215 |
| 4.3.4.2 | Characterization of 5,7-dihydroxy-8-(piperidin-1-ylmethyl)-2-phenyl-4H-chromen-4-one (M14b) | 222 |
| 4.3.4.3 | Characterization of 5,7-dihydroxy-8-(4-methylpiperazin-1-ylmethyl)-2-phenyl-4H-chromen-4-one (M14c) | 229 |
| 4.3.4.4 | Characterization of 5,7-dihydroxy-8-(morpholinomethyl)-2-phenyl-4H-chromen-4-one (M14d) | 236 |
| 4.3.4.5 | Characterization of 5,7-dihydroxy-8-(thiomorpholinomethyl)-2-phenyl-4H-chromen-4-one (M14e) | 243 |
| 4.3.4.6 | Characterization of 5,7-dihydroxy-8-(4-methoxybenzylamine)-2-phenyl-4H-chromen-4-one (M14f) | 250 |
| 4.3.5 | Synthesis of 5,7-dihydroxyflavone (M14) Diamine Mannich Bases | 257 |
| 4.3.5.1 | Characterization of 5,7-dihydroxy-6,8-bis(pyrrolidine-1-ylmethyl)-2-phenyl-4H-chromen-4-one (M14g) | 259 |
| 4.3.5.2 | Characterization of 5,7-dihydroxy-6,8-bis(piperidin-1-ylmethyl)-2-phenyl-4H-chromen-4-one (M14h) | 267 |
| 4.3.5.3 | Characterization of 5,7-dihydroxy-6,8-bis(4-methylpiperazin-1-ylmethyl)-2-phenyl-4H-chromen-4-one (M14i) | 275 |

| | | |
|------------|---|------------|
| 4.3.5.4 | Characterization of 5,7-dihydroxy-6,8-bis(morpholinomethyl)-2-phenyl-4H-chromen-4-one (M14j) | 283 |
| 4.3.5.5 | Characterization of 5,7-dihydroxy-6,8-bis(thiomorpholinomethyl)-2-phenyl-4H-chromen-4-one (M14k) | 291 |
| 4.4 | Cytotoxic Activity | 299 |
| 5.0 | Conclusions | 305 |
| 5.1 | Conclusion | 305 |
| 5.2 | Future Studies | 307 |
| | References | 309 |
| | Appendices | |

LIST OF TABLES

| Table | | Page |
|-------|--|------|
| 1.1 | Taxonomy of <i>Muntingia calabura</i> | 3 |
| 3.1 | Chemicals and materials used for extraction and isolation | 40 |
| 3.2 | Reagents and cuvettes used for UV-vis analysis | 41 |
| 3.3 | Chemicals used for IR analysis | 41 |
| 3.4 | Reagents used for LC-MS analysis | 41 |
| 3.5 | Deuterated solvents for NMR analysis | 42 |
| 3.6 | Chemicals and reagents used for Mannich reaction | 42 |
| 3.7 | Chemical reagents and materials used for cytotoxic activity | 43 |
| 3.8 | Reactants and mol ratio used for the synthesis of chalcone Mannich base derivatives | 49 |
| 3.9 | Reactants and mol ratio used for the synthesis of monoamine flavone Mannich base derivatives | 50 |
| 3.10 | Reactants used for the synthesis of diamine flavone Mannich base derivatives | 51 |
| 4.1 | ^1H , ^{13}C and HMBC spectral data of M1 (CDCl_3) | 62 |
| 4.2 | ^1H , ^{13}C and HMBC spectral data of M12 (acetone- d_6) | 66 |
| 4.3 | ^1H , ^{13}C and HMBC spectral data of M13 (acetone- d_6) | 70 |
| 4.4 | ^1H , ^{13}C and HMBC spectral data of M17 (acetone- d_6) | 75 |
| 4.5 | ^1H , ^{13}C and HMBC spectral data of M18 (acetone- d_6) | 79 |
| 4.6 | ^1H , ^{13}C and HMBC spectral data of M2 (CDCl_3) | 84 |
| 4.7 | ^1H , ^{13}C and HMBC spectral data of M4 (acetone- d_6) | 89 |

| | | |
|------|--|-----|
| 4.8 | ^1H , ^{13}C and HMBC spectral data of M6 (acetone- d_6) | 93 |
| 4.9 | ^1H , ^{13}C and HMBC spectral data of M3 (CDCl_3) | 98 |
| 4.10 | ^1H , ^{13}C and HMBC spectral data of M5 (acetone- d_6) | 103 |
| 4.11 | ^1H , ^{13}C and HMBC spectral data of M7 (CDCl_3) | 108 |
| 4.12 | ^1H , ^{13}C and HMBC spectral data of M8 (acetone- d_6) | 112 |
| 4.13 | ^1H , ^{13}C and HMBC spectral data of M9 (CDCl_3) | 116 |
| 4.14 | ^1H , ^{13}C and HMBC spectral data of M10 (CDCl_3) | 121 |
| 4.15 | ^1H , ^{13}C and HMBC spectral data of M11 (acetone- d_6) | 125 |
| 4.16 | ^1H , ^{13}C and HMBC spectral data of M14 ($\text{DMSO-}\text{d}_6$) | 131 |
| 4.17 | ^1H , ^{13}C and HMBC spectral data of M15 (acetone- d_6) | 133 |
| 4.18 | ^1H , ^{13}C and HMBC spectral data of M16 (acetone- d_6) | 138 |
| 4.19 | Summary Physical Properties of M2a | 146 |
| 4.20 | ^1H , ^{13}C and HMBC spectral data of M2 and M2a (CDCl_3) | 150 |
| 4.21 | Summary Physical Properties of M2b | 154 |
| 4.22 | ^1H , ^{13}C and HMBC spectral data of M2 and M2b (CDCl_3) | 157 |
| 4.23 | Summary Physical Properties of M4a | 163 |
| 4.24 | ^1H , ^{13}C and HMBC spectral data of M4 and M4a (CDCl_3) | 166 |
| 4.25 | Summary Physical Properties of M4b | 170 |
| 4.26 | ^1H , ^{13}C and HMBC spectral data of M4 and M4b (CDCl_3) | 173 |
| 4.27 | Summary Physical Properties of M5a | 179 |
| 4.28 | ^1H , ^{13}C and HMBC spectral data of M5 (acetone- d_6) and M5a (CDCl_3) | 182 |

| | | |
|------|--|-----|
| 4.29 | Summary Physical Properties of M5b | 186 |
| 4.30 | ^1H , ^{13}C and HMBC spectral data of M5 (acetone- d_6) and M5b (CDCl_3) | 189 |
| 4.31 | Summary Physical Properties of M5c | 193 |
| 4.32 | ^1H , ^{13}C and HMBC spectral data of M5 (acetone- d_6) and M5c (CDCl_3) | 196 |
| 4.33 | Summary Physical Properties of M5d | 200 |
| 4.34 | ^1H , ^{13}C and HMBC spectral data of M5 (acetone- d_6) and M5d (CDCl_3) | 203 |
| 4.35 | Summary Physical Properties of M5e | 207 |
| 4.36 | ^1H , ^{13}C and HMBC spectral data of M5 (acetone- d_6) and M5e (CDCl_3) | 210 |
| 4.37 | Summary Physical Properties of M14a | 216 |
| 4.38 | ^1H , ^{13}C and HMBC spectral data of M14 ($\text{DMSO-}\text{d}_6$) and M14a (CDCl_3) | 219 |
| 4.39 | Summary Physical Properties of M14b | 223 |
| 4.40 | ^1H , ^{13}C and HMBC spectral data of M14 ($\text{DMSO-}\text{d}_6$) and M14b (CDCl_3) | 226 |
| 4.41 | Summary Physical Properties of M14c | 230 |
| 4.42 | ^1H , ^{13}C and HMBC spectral data of M14 ($\text{DMSO-}\text{d}_6$) and M14c (CDCl_3) | 233 |
| 4.43 | Summary Physical Properties of M14d | 237 |
| 4.44 | ^1H , ^{13}C and HMBC spectral data of M14 ($\text{DMSO-}\text{d}_6$) and M14d (CDCl_3) | 240 |
| 4.45 | Summary Physical Properties of M14e | 244 |

| | | |
|------|--|-----|
| 4.46 | ¹ H, ¹³ C and HMBC spectral data of M14 (DMSO-d ₆) and M14e (CDCl ₃) | 247 |
| 4.47 | Summary Physical Properties of M14f | 251 |
| 4.48 | ¹ H, ¹³ C and HMBC spectral data of M14 (DMSO-d ₆) and M14f (DMSO-d ₆) | 254 |
| 4.49 | Summary Physical Properties of M14g | 260 |
| 4.50 | ¹ H, ¹³ C and HMBC spectral data of M14 (DMSO-d ₆) and M14g (CDCl ₃) | 264 |
| 4.51 | Summary Physical Properties of M14h | 268 |
| 4.52 | ¹ H, ¹³ C and HMBC spectral data of M14 (DMSO-d ₆) and M14h (CDCl ₃) | 272 |
| 4.53 | Summary Physical Properties of M14i | 276 |
| 4.54 | ¹ H, ¹³ C and HMBC spectral data of M14 (DMSO-d ₆) and M14i (CDCl ₃) | 280 |
| 4.55 | Summary Physical Properties of M14j | 284 |
| 4.56 | ¹ H, ¹³ C and HMBC spectral data of M14 (DMSO-d ₆) and M14j (CDCl ₃) | 288 |
| 4.57 | Summary Physical Properties of M14k | 292 |
| 4.58 | ¹ H, ¹³ C and HMBC spectral data of M14 (DMSO-d ₆) and M14k (CDCl ₃) | 296 |
| 4.59 | Cytotoxic results of parent compounds and synthesized Mannich Bases against cancer and normal cell | 300 |

LIST OF FIGURES

| Figures | | Page |
|---------|---|------|
| 1.1 | Trees of <i>Muntingia calabura</i> (Mahmood, et al.,2014) | 4 |
| 1.2 | Leaves of <i>Muntingia calabura</i> (Mahmood, et al.,2014) | 5 |
| 1.3 | Flowers of <i>Muntingia calabura</i> (Mahmood, et al.,2014) | 5 |
| 1.4 | Fruits of <i>Muntingia calabura</i> (Mahmood, et al., 2014) | 6 |
| 2.1 | Structure of chemical constituents from <i>Muntingia calabura</i> roots | 14 |
| 2.2 | Structure of chemical constituents from <i>Muntingia calabura</i> leaves | 19 |
| 2.3 | Structure of chemical constituents from <i>Muntingia calabura</i> stem barks | 24 |
| 2.4 | Structure of compounds 71 and 72 | 29 |
| 2.5 | Structure of compounds 73 , 74 and 75 | 30 |
| 2.6 | Structure of compounds 76 , 77 , 78 and 79 | 32 |
| 2.7 | Structure of compounds 80 , 81 and 82 | 33 |
| 2.8 | Structure of compounds 83 and 84 | 34 |
| 2.9 | Structure of compounds 85 , 86 , 87 and 88 | 36 |
| 2.10 | Structure of compounds 89-96 | 38 |
| 2.11 | Structure of compounds 97 and 98 | 39 |
| 4.1 | Chromatographic purification of the leaves of <i>Muntingia calabura</i> | 57 |
| 4.2 | ¹ H NMR (400 MHz, CDCl ₃) of (2 <i>S</i> , 3 <i>S</i>) 3,5-dihydroxy-7-methoxyflavone (M1) | 63 |
| 4.3 | ¹³ C NMR (100 MHz, CDCl ₃) of (2 <i>S</i> , 3 <i>S</i>) 3,5-dihydroxy-7- methoxyflavanone (M1) | 64 |

| Figures | Page |
|--|-------------|
| 4.4 ¹ H NMR (400 MHz, acetone-d ₆) of (2 <i>R</i> , 3 <i>R</i>) 3,5-dihydroxy-6,7-dimethoxyflavanone (M12) | 67 |
| 4.5 ¹³ C NMR (100 MHz, acetone-d ₆) of (2 <i>R</i> , 3 <i>R</i>) 3,5-dihydroxy-6,7 dimethoxyflavanone (M12) | 68 |
| 4.6 ¹ H NMR (400 MHz, acetone-d ₆) of (2 <i>R</i> , 3 <i>R</i>) 3,5,7-trihydroxyflavanone (M13) | 71 |
| 4.7 ¹³ C NMR (100 MHz, acetone-d ₆) of (2 <i>R</i> , 3 <i>R</i>) 3,5,7-trihydroxyflavanone (M13) | 72 |
| 4.8 ¹ H NMR (400 MHz, acetone-d ₆) of (2 <i>S</i>) 7,8-dihydroxyflavanone (M17) | 76 |
| 4.9 ¹³ C NMR (100 MHz, acetone-d ₆) of (2 <i>S</i>) 7,8-dihydroxyflavanone (M17) | 77 |
| 4.10 ¹ H NMR (400 MHz, acetone-d ₆) of (2 <i>R</i> , 3 <i>R</i>) 3,5,7-trihydroxy-8-methoxyflavanone (M18) | 80 |
| 4.11 ¹³ C NMR (100 MHz, acetone-d ₆) of (2 <i>R</i> , 3 <i>R</i>) 3,5,8-trihydroxy-8-methoxyflavanone (M18) | 81 |
| 4.12 ¹ H NMR (400 MHz, CDCl ₃) of 2',4'-dihydroxy-3'-methoxychalcone (M2) | 85 |
| 4.13 ¹³ C NMR (100 MHz, CDCl ₃) of 2',4'-dihydroxy-3'-methoxychalcone (M2) | 86 |
| 4.14 ¹ H NMR (400 MHz, acetone-d ₆) of 2',4'-dihydroxychalcone (M4) | 90 |
| 4.15 ¹³ C NMR (100 MHz, acetone-d ₆) of 2', 4'-dihydroxychalcone (M4) | 91 |
| 4.16 ¹ H NMR (400 MHz, acetone-d ₆) of 2', 3', 4'-trihydroxychalcone (M6) | 94 |
| 4.17 ¹³ C NMR (100 MHz, acetone-d ₆) of 2', 3', 4'-trihydroxychalcone (M6) | 95 |
| 4.18 ¹ H NMR (400 MHz, CDCl ₃) of 3,5-dihydroxy-7,8-dimethoxyflavone (M3) | 99 |
| 4.19 ¹³ C NMR (100 MHz, CDCl ₃) of 3,5-dihydroxy-7,8-dimethoxyflavone (M3) | 100 |

| | | |
|------|---|-----|
| 4.20 | ¹ H NMR (400 MHz, acetone-d ₆) of 3, 5, 7-trihydroxy-8-methoxyflavone (M5) | 104 |
| 4.21 | ¹³ C NMR (100 MHz, acetone-d ₆) of 3, 5, 7-trihydroxy-8-methoxyflavone (M5) | 105 |
| 4.22 | ¹ H NMR (400 MHz, CDCl ₃) of 5-hydroxy-3,7-dimethoxyflavone (M7) | 109 |
| 4.23 | ¹³ C NMR (100 MHz, CDCl ₃) of 5-hydroxy-3,7-dimethoxyflavone (M7) | 110 |
| 4.24 | ¹ H NMR (400 MHz, acetone-d ₆) of 3, 5-dihydroxy-7-methoxyflavone (M8) | 113 |
| 4.25 | ¹³ C NMR (100 MHz, acetone-d ₆) of 3, 5-dihydroxy-7-methoxyflavone (M8) | 114 |
| 4.26 | ¹ H NMR (400 MHz, CDCl ₃) of 5-hydroxy-7-methoxyflavone (M9) | 117 |
| 4.27 | ¹³ C NMR (100 MHz, CDCl ₃) of 5-hydroxy-7-methoxyflavone (M9) | 118 |
| 4.28 | ¹ H NMR (400 MHz, CDCl ₃) of 5-hydroxy-3,7,8-trimethoxyflavone (M10) | 122 |
| 4.29 | ¹³ C NMR (100 MHz, CDCl ₃) of 5-hydroxy-3,7,8-trimethoxyflavone (M10) | 123 |
| 4.30 | ¹ H NMR (400 MHz, acetone-d ₆) of 5,7-dihydroxy-3,8-dimethoxyflavone (M11) | 126 |
| 4.31 | ¹³ C NMR (100 MHz, acetone-d ₆) of 5,7-dihydroxy-3,8-dimethoxyflavone (M11) | 127 |
| 4.32 | ¹ H NMR (400 MHz, DMSO-d ₆) of 5,7-dihydroxyflavone (M14) | 129 |
| 4.33 | ¹³ C NMR (100 MHz, DMSO-d ₆) of 5,7-dihydroxyflavone (M14) | 130 |
| 4.34 | ¹ H NMR (400 MHz, acetone-d ₆) of 5-hydroxy-6,7-dimethoxyflavone (M15) | 134 |
| 4.35 | ¹³ C NMR (100 MHz, acetone-d ₆) of 5-hydroxy-6,7-dimethoxyflavone (M15) | 135 |
| 4.36 | ¹ H NMR (400 MHz, acetone-d ₆) of 5,4'-dihydroxy-3,7-dimethoxyflavone (M16) | 139 |

| | | |
|------|--|-----|
| 4.37 | ¹³ C NMR (100 MHz, acetone-d ₆) of 5,4'-dihydroxy-3,7-methoxyflavone (M16) | 140 |
| 4.38 | Synthesis route of chalcone M2 based Mannich bases with mol ratio chalcone: formaldehyde: amine 1:2:2 | 142 |
| 4.39 | Formation of iminium ion | 143 |
| 4.40 | Reaction mechanism of M2 Chalcone Mannich bases | 144 |
| 4.41 | ¹ H NMR (400 MHz, CDCl ₃) of 1-[3-methoxy-5-(piperidin-4-yl) methyl-2,4-dihydroxyphenyl]-3-phenyl-2-propen-1-one (M2a) | 148 |
| 4.42 | ¹³ C NMR (100 MHz, CDCl ₃) of 1-[3-methoxy-5-(piperidin-4-yl) methyl-2,4-dihydroxyphenyl]-3-phenyl-2-propen-1-one (M2a) | 149 |
| 4.43 | HMQC Spectrum of 1-[3-methoxy-5-(piperidin-4-yl) methyl-2,4-dihydroxyphenyl]-3-phenyl-2-propen-1-one (M2a) | 151 |
| 4.44 | HMBC Spectrum of 1-[3-methoxy-5-(piperidin-4-yl) methyl-2,4-dihydroxyphenyl]-3-phenyl-2-propen-1-one (M2a) | 152 |
| 4.45 | ¹ H NMR (400 MHz, CDCl ₃) of 1-[3-methoxy-5-(morpholino-4-yl) methyl-2,4-dihydroxyphenyl]-3-phenyl-2-propen-1-one (M2b) | 155 |
| 4.46 | ¹³ C NMR (100 MHz, CDCl ₃) of 1-[3-methoxy-5-(morpholino-4-yl) methyl-2,4-dihydroxyphenyl]-3-phenyl-2-propen-1-one (M2b) | 156 |
| 4.47 | HMQC Spectrum of 1-[3-methoxy-5-(morpholino-4-yl) methyl-2,4-dihydroxyphenyl]-3-phenyl-2-propen-1-one (M2b) | 158 |
| 4.48 | HMBC Spectrum of 1-[3-methoxy-5-(morpholino-4-yl) methyl-2,4-dihydroxyphenyl]-3-phenyl-2-propen-1-one (M2b) | 159 |
| 4.49 | Synthesis route of chalcone M4 Mannich bases with mol ratio chalcone: formaldehyde: amine 1:2:2 | 160 |
| 4.50 | Reaction mechanism of chalcone M4 Mannich bases | 161 |

| | | |
|------|--|-----|
| 4.51 | ¹ H NMR (400 MHz, CDCl ₃) of 1-[3-(piperidin-1-yl)methyl-2,4-dihydroxyphenyl]-3-phenyl-2-propen-1-one (M4a) | 164 |
| 4.52 | ¹³ C NMR (100 MHz, CDCl ₃) of 1-[3-(piperidin-1-yl)methyl-2,4-dihydroxyphenyl]-3-phenyl-2-propen-1-one (M4a) | 165 |
| 4.53 | HMQC Spectrum of 1-[3-(piperidin-1-yl)methyl-2,4-dihydroxyphenyl]-3-phenyl-2-propen-1-one (M4a) | 167 |
| 4.54 | HMBC Spectrum of 1-[3-(piperidin-1-yl)methyl-2,4-dihydroxyphenyl]-3-phenyl-2-propen-1-one (M4a) | 168 |
| 4.55 | ¹ H NMR (400 MHz, CDCl ₃) of 1-[3-(morpholino-4-yl) methyl-2,4-dihydroxyphenyl]-3-phenyl-2-propen-1-one (M4b) | 171 |
| 4.56 | ¹³ C NMR (100 MHz, CDCl ₃) of 1-[3-(morpholino-4-yl) methyl-2,4-dihydroxyphenyl]-3-phenyl-2-propen-1-one (M4b) | 172 |
| 4.57 | HMQC Spectrum of 1-[3-(morpholino-4-yl)methyl-2,4-dihydroxyphenyl]-3-phenyl-2-propen-1-one (M4b) | 174 |
| 4.58 | HMBC Spectrum of 1-[3-(morpholino-4-yl)methyl-2,4-dihydroxyphenyl]-3-phenyl-2-propen-1-one (M4b) | 175 |
| 4.59 | Synthesis route of flavone M5 Mannich bases with mol ratio flaone: formaldehyde: amine 1:3:3 | 176 |
| 4.60 | Reaction mechanism of flavone M5 Mannich bases | 177 |
| 4.61 | ¹ H NMR (400 MHz, CDCl ₃) of 3,5,7-trihydroxy-8-methoxy-6-(pyrrolidin-1-ylmethyl)-2-phenyl-4H-chromen-4-one (M5a) | 180 |
| 4.62 | ¹³ C NMR (100 MHz, CDCl ₃) of 3,5,7-trihydroxy-8-methoxy-6-(pyrrolidin-1-ylmethyl)-2-phenyl-4H-chromen-4-one (M5a) | 181 |
| 4.63 | HMQC Spectrum of 3,5,7-trihydroxy-8-methoxy-6-(pyrrolidin-1-ylmethyl)-2-phenyl-4H-chromen-4-one (M5a) | 183 |

| | | |
|------|---|-----|
| 4.64 | HMBC Spectrum of 3,5,7-trihydroxy-8-methoxy-6-(pyrrolidin-1-ylmethyl)-2-phenyl-4H-chromen-4-one (M5a) | 184 |
| 4.65 | ¹ H NMR (400 MHz, CDCl ₃) of 3,5,7-trihydroxy-8-methoxy-6-(piperidin-1-ylmethyl)-2-phenyl-4H-chromen-4-one (M5b) | 187 |
| 4.66 | ¹³ C NMR (100 MHz, CDCl ₃) of 3,5,7-trihydroxy-8-methoxy-6-(piperidin-1-ylmethyl)-2-phenyl-4H-chromen-4-one (M5b) | 188 |
| 4.67 | HMQC Spectrum of 3,5,7-trihydroxy-8-methoxy-6-(piperidin-1-ylmethyl)-2-phenyl-4H-chromen-4-one (M5b) | 190 |
| 4.68 | HMBC Spectrum of 3,5,7-trihydroxy-8-methoxy-6-(piperidin-1-ylmethyl)-2-phenyl-4H-chromen-4-one (M5b) | 191 |
| 4.69 | ¹ H NMR (400 MHz, CDCl ₃) of 3,5,7-trihydroxy-8-methoxy-6-(4-methylpiperazin-1-ylmethyl)-2-phenyl-4H-chromen-4-one (M5c) | 194 |
| 4.70 | ¹³ C NMR (100 MHz, CDCl ₃) of 3,5,7-trihydroxy-8-methoxy-6-(4-methylpiperazin-1-ylmethyl)-2-phenyl-4H-chromen-4-one (M5c) | 195 |
| 4.71 | HMQC Spectrum of 3,5,7-trihydroxy-8-methoxy-6-(4-methylpiperazin-1-ylmethyl)-2-phenyl-4H-chromen-4-one (M5c) | 197 |
| 4.72 | HMBC Spectrum of 3,5,7-trihydroxy-8-methoxy-6-(4-methylpiperazin-1-ylmethyl)-2-phenyl-4H-chromen-4-one (M5c) | 198 |
| 4.73 | ¹ H NMR (400 MHz, CDCl ₃) of 3,5,7-trihydroxy-8-methoxy-6-(morpholinomethyl)-2-phenyl-4H-chromen-4-one (M5d) | 201 |
| 4.74 | ¹³ C NMR (100 MHz, CDCl ₃) of 3,5,7-trihydroxy-8-methoxy-6-(morpholinomethyl)-2-phenyl-4H-chromen-4-one (M5d) | 202 |
| 4.75 | HMQC Spectrum of 3,5,7-trihydroxy-8-methoxy-6-(morpholinomethyl)-2-phenyl-4H-chromen-4-one (M5d) | 204 |

| | | |
|------|---|-----|
| 4.76 | HMBC Spectrum of 3,5,7-trihydroxy-8-methoxy-6-(morpholinomethyl)-2-phenyl-4H-chromen-4-one (M5d) | 205 |
| 4.77 | ¹ H NMR (400 MHz, CDCl ₃) of 3,5,7-trihydroxy-8-methoxy-6-(thiomorpholinomethyl)-2-phenyl-4H-chromen-4-one (M5e) | 208 |
| 4.78 | ¹³ C NMR (100 MHz, CDCl ₃) of 3,5,7-trihydroxy-8-methoxy-6-(thiomorpholinomethyl)-2-phenyl-4H-chromen-4-one (M5e) | 209 |
| 4.79 | HMQC Spectrum of 3,5,7-trihydroxy-8-methoxy-6-(thiomorpholinomethyl)-2-phenyl-4H-chromen-4-one (M5e) | 211 |
| 4.80 | HMBC Spectrum of 3,5,7-trihydroxy-8-methoxy-6-(thiomorpholinomethyl)-2-phenyl-4H-chromen-4-one (M5e) | 212 |
| 4.81 | Synthesis route of flavone M14 monoamine Mannich bases with mol ratio flavone: formaldehyde: amine 1:2:2 | 213 |
| 4.82 | Reaction mechanism of flavone M14 monoamine Mannich bases | 214 |
| 4.83 | ¹ H NMR (400 MHz, CDCl ₃) of 5,7-dihydroxy-8-(pyrrolidine-1-ylmethyl)-2-phenyl-4H-chromen-4-one (M14a) | 217 |
| 4.84 | ¹³ C NMR (100 MHz, CDCl ₃) of 5,7-dihydroxy-8-(pyrrolidine-1-ylmethyl)-2-phenyl-4H-chromen-4-one (M14a) | 218 |
| 4.85 | HMQC Spectrum of 5,7-dihydroxy-8-(pyrrolidine-1-ylmethyl)-2-phenyl-4H-chromen-4-one (M14a) | 220 |
| 4.86 | HMBC Spectrum of 5,7-dihydroxy-8-(pyrrolidine-1-ylmethyl)-2-phenyl-4H-chromen-4-one (M14a) | 221 |
| 4.87 | ¹ H NMR (400 MHz, CDCl ₃) of 5,7-dihydroxy-8-(piperidin-1-ylmethyl)-2-phenyl-4H-chromen-4-one (M14b) | 224 |
| 4.88 | ¹³ C NMR (100 MHz, CDCl ₃) of 5,7-dihydroxy-8-(piperidin-1-ylmethyl)-2-phenyl-4H-chromen-4-one (M14b) | 225 |

| | | |
|-------|---|-----|
| 4.89 | HMQC Spectrum of 5,7-dihydroxy-8-(piperidin-1-ylmethyl)-2-phenyl-4H-chromen-4-one (M14b) | 227 |
| 4.90 | HMBC Spectrum of 5,7-dihydroxy-8-(piperidin-1-ylmethyl)-2-phenyl-4H-chromen-4-one (M14b) | 228 |
| 4.91 | ¹ H NMR (400 MHz, CDCl ₃) of 5,7-dihydroxy-8-(4-methylpiperazin-1-ylmethyl)-2-phenyl-4H-chromen-4-one (M14c) | 231 |
| 4.92 | ¹³ C NMR (100 MHz, CDCl ₃) of 5,7-dihydroxy-8-(4-methylpiperazin-1-ylmethyl)-2-phenyl-4H-chromen-4-one (M14c) | 232 |
| 4.93 | HMQC Spectrum of 5,7-dihydroxy-8-(4-methylpiperazin-1-ylmethyl)-2-phenyl-4H-chromen-4-one (M14c) | 234 |
| 4.94 | HMBC Spectrum of 5,7-dihydroxy-8-(4-methylpiperazin-1-ylmethyl)-2-phenyl-4H-chromen-4-one (M14c) | 235 |
| 4.95 | ¹ H NMR (400 MHz, CDCl ₃) of 5,7-dihydroxy-8-(morpholinomethyl)-2-phenyl-4H-chromen-4-one (M14d) | 238 |
| 4.96 | ¹³ C NMR (100 MHz, CDCl ₃) of 5,7-dihydroxy-8-(morpholinomethyl)-2-phenyl-4H-chromen-4-one (M14d) | 239 |
| 4.97 | HMQC Spectrum of 5,7-dihydroxy-8-(morpholinomethyl)-2-phenyl-4H-chromen-4-one (M14d) | 241 |
| 4.98 | HMBC Spectrum of 5,7-dihydroxy-8-(morpholinomethyl)-2-phenyl-4H-chromen-4-one (M14d) | 242 |
| 4.99 | ¹ H NMR (400 MHz, CDCl ₃) of 5,7-dihydroxy-8-(thiomorpholinomethyl)-2-phenyl-4H-chromen-4-one (M14e) | 245 |
| 4.100 | ¹³ C NMR (100 MHz, CDCl ₃) of 5,7-dihydroxy-8-(thiomorpholinomethyl)-2-phenyl-4H-chromen-4-one (M14e) | 246 |
| 4.101 | HMQC Spectrum of 5,7-dihydroxy-8-(thiomorpholinomethyl)-2-phenyl-4H-chromen-4-one (M14e) | 248 |

| | | |
|-------|--|-----|
| 4.102 | HMBC Spectrum of 5,7-dihydroxy-8-(thiomorpholinomethyl)-2-phenyl-4H-chromen-4-one (M14e) | 249 |
| 4.103 | ¹ H NMR (400 MHz, CDCl ₃) of 5,7-dihydroxy-8-(4-methoxybenzylamine)-2-phenyl-4H-chromen-4-one (M14f) | 252 |
| 4.104 | ¹³ C NMR (100 MHz, CDCl ₃) of 5,7-dihydroxy-8-(4-methoxybenzylamine)-2-phenyl-4H-chromen-4-one (M14f) | 253 |
| 4.105 | HMQC Spectrum of 5,7-dihydroxy-8-(4-methoxybenzylamine)-2-phenyl-4H-chromen-4-one (M14f) | 255 |
| 4.106 | HMBC Spectrum of 5,7-dihydroxy-8-(4-methoxybenzylamine)-2-phenyl-4H-chromen-4-one (M14f) | 256 |
| 4.107 | Synthesis route of flavone M14 diamine Mannich bases with mol ratio flavone: formaldehyde: amine 1:3:3 | 257 |
| 4.108 | Reaction mechanism of flavone M14 diamine Mannich bases | 258 |
| 4.109 | ¹ H NMR (400 MHz, CDCl ₃) of 5,7-dihydroxy-6,8-bis(pyrrolidine-1-ylmethyl)-2-phenyl-4H-chromen-4-one (M14g) | 262 |
| 4.110 | ¹³ C NMR (100 MHz, CDCl ₃) of 5,7-dihydroxy-6,8-bis(pyrrolidine-1-ylmethyl)-2-phenyl-4H-chromen-4-one (M14g) | 263 |
| 4.111 | HMQC Spectrum of 5,7-dihydroxy-6,8-bis(pyrrolidine-1-ylmethyl)-2-phenyl-4H-chromen-4-one (M14g) | 265 |
| 4.112 | HMBC Spectrum of 5,7-dihydroxy-6,8-bis(pyrrolidine-1-ylmethyl)-2-phenyl-4H-chromen-4-one (M14g) | 266 |
| 4.113 | ¹ H NMR (400 MHz, CDCl ₃) of 5,7-dihydroxy-6,8-bis(piperidin-1-ylmethyl)-2-phenyl-4H-chromen-4-one (M14h) | 270 |
| 4.114 | ¹³ C NMR (100 MHz, CDCl ₃) of 5,7-dihydroxy-6,8-bis(piperidin-1-ylmethyl)-2-phenyl-4H-chromen-4-one (M14h) | 271 |

| | | |
|-------|--|-----|
| 4.115 | HMQC Spectrum of 5,7-dihydroxy-6,8-bis(piperidin-1-ylmethyl)-2-phenyl-4H-chromen-4-one (M14h) | 273 |
| 4.116 | HMBC Spectrum of 5,7-dihydroxy-6,8-bis(piperidin-1-ylmethyl)-2-phenyl-4H-chromen-4-one (M14h) | 274 |
| 4.117 | ¹ H NMR (400 MHz, CDCl ₃) of 5,7-dihydroxy-6,8-bis(4-methylpiperazin-1-ylmethyl)-2-phenyl-4H-chromen-4-one (M14i) | 278 |
| 4.118 | ¹³ C NMR (100 MHz, CDCl ₃) of 5,7-dihydroxy-6,8-bis(4-methylpiperazin-1-ylmethyl)-2-phenyl-4H-chromen-4-one (M14i) | 279 |
| 4.119 | HMQC Spectrum of 5,7-dihydroxy-6,8-bis(4-methylpiperazin-1-ylmethyl)-2-phenyl-4H-chromen-4-one (M14i) | 281 |
| 4.120 | HMBC Spectrum of 5,7-dihydroxy-6,8-bis(4-methylpiperazin-1-ylmethyl)-2-phenyl-4H-chromen-4-one (M14i) | 282 |
| 4.121 | ¹ H NMR (400 MHz, CDCl ₃) of 5,7-dihydroxy-6,8-bis(morpholinomethyl)-2-phenyl-4H-chromen-4-one (M14j) | 286 |
| 4.122 | ¹³ C NMR (100 MHz, CDCl ₃) of 5,7-dihydroxy-6,8-bis(morpholinomethyl)-2-phenyl-4H-chromen-4-one (M14j) | 287 |
| 4.123 | HMQC Spectrum of 5,7-dihydroxy-6,8-bis(morpholinomethyl)-2-phenyl-4H-chromen-4-one (M14j) | 289 |
| 4.124 | HMBC Spectrum of 5,7-dihydroxy-6,8-bis(morpholinomethyl)-2-phenyl-4H-chromen-4-one (M14j) | 290 |
| 4.125 | ¹ H NMR (400 MHz, CDCl ₃) of 5,7-dihydroxy-6,8-bis(thiomorpholinomethyl)-2-phenyl-4H-chromen-4-one (M14k) | 294 |
| 4.126 | ¹³ C NMR (100 MHz, CDCl ₃) of 5,7-dihydroxy-6,8-bis(thiomorpholinomethyl)-2-phenyl-4H-chromen-4-one (M14k) | 295 |

| | | |
|-------|--|-----|
| 4.127 | HMQC Spectrum of 5,7-dihydroxy-6,8-bis(thiomorpholinomethyl)-2-phenyl-4H-chromen-4-one (M14k) | 297 |
| 4.128 | HMBC Spectrum of 5,7-dihydroxy-6,8-bis(thiomorpholinomethyl)-2-phenyl-4H-chromen-4-one (M14k) | 298 |

LIST OF ABBREVIATIONS

| | |
|------------------------|--|
| ^1H | Proton |
| ^{13}C | Carbon |
| Å | Angstrom |
| β | Beta |
| δ | Chemical shift |
| δ_{C} | Chemical shift of carbon |
| δ_{H} | Chemical shift of proton |
| λ_{max} | Maximum wavelength |
| μg | Microgram |
| μL | Microliter |
| Acetone- d_6 | Deuterated acetone |
| A549 | Human lung cancer cell line |
| brs | Broad singlet |
| CDCl_3 | Deuterated chloroform |
| d | Doublet |
| DCM | Dichloromethane |
| dd | Doublet of doublet |
| DEPT | Distortionless Enhancement by Polarization Transfer |
| DMEM/F-12 | Dulbecco's Modified Eagle Medium/Nutrient Mixture F-12 |
| DMSO | Dimethylsulfoxide |
| FTIR | Fourier-Transform Infrared Spectroscopy |
| HCC1954 | Epithelial breast cancer cell |

| | |
|------------------|---|
| HeLa | Human cervical cancer cell |
| HepG2 | Human hepatocellular liver cell |
| HMBC | Heteronuclear Multiple Bond Coherence |
| HMQC | Heteronuclear Multiple Quantum Coherence |
| HREIMS | High Resolution Electrospray Ionization Mass Spectrometry |
| HT-1080 | Human fibrosarcoma |
| HT-29 | Human colon cancer cell |
| Hz | Hertz |
| IC ₅₀ | Half maximal inhibitory concentration |
| IMU | International Medical University |
| IR | Infrared |
| <i>J</i> | Coupling constant in Hertz |
| KB | Human nasopharyngeal carcinoma |
| KBr | Potassium bromide |
| KB-V1 | drug-resistant KB |
| LC-MS | Liquid Chromatography-Mass Spectrometry |
| m | Multiplet |
| m/z | Mass-to-charge ratio |
| MCF-7 | Human breast cancer cell |
| MCF-10A | Normal breast cancer cell |
| MDA-MB-231 | Breast adenocarcinoma |
| Mel2 | Human melanoma |
| mM | Milimoles |
| mol | Mole |
| mp | Melting point |

| | |
|----------------|--|
| MTT | 3-(4,5-dimethylthiazol-2-yl)-2,5-diphenyltetrazolium bromide |
| nm | Nanometer |
| NMR | Nuclear Magnetic Resonance |
| O-H | Oxygen-Hydrogen (or Hydroxyl) |
| P-388 | Leukemia cancer cell |
| ppm | Part per million |
| R _f | Retention factor |
| s | Singlet |
| SK-LU-1 | Human lung cancer cell |
| SK-OV-3 | Ovarian cancer cell |
| TLC | Thin Layer Chromatography |
| UV-Vis | Ultraviolet-Visible |

CHAPTER 1

INTRODUCTION

1.1 Natural products

Natural products are substances that generated by living organisms naturally. Natural products are included primary metabolites and secondary metabolites. Primary metabolites are those chemical substances that play an important role in the metabolism and reproduction of the cells. Examples of primary metabolites are amino acid, sugars (carbohydrates) and nucleic acids. On the other hand, secondary metabolites refer to the organic compounds that are not directly involved in the growth of organism. Secondary metabolites can be classified into few main classes which included alkaloid, flavonoid, retinoid, steroid, terpenoid and xanthone (Dias et al., 2012; Ouyang et al., 2014; Buhian et al., 2016).

Historically, natural products are the most significant sources of new leads for pharmaceutical developments and mostly are from plants (McChesney et al., 2007; Yun et al., 2012). Around 80% people in developing countries still rely on traditional medicines as their primary healthcare. Medicinal plants are sources of vital therapeutic aids to alleviate illness and approximately 85% of traditional medicine is plant extracts (Mahmood et al., 2014). The interest in herbal medicine and products has increased, and this has stimulated scientist to

explore and understand pharmacologically active constituents in medicinal plants (Che and Zhang, 2019).

Secondary metabolites such as polyphenols, flavonoids, quinones and tannins are the sources of plant natural products used in medicine. They are known for their potent cytotoxic, antimicrobial and antioxidant activities (Buhian et al., 2016). Plants have produced many important drugs, from morphine that was discovered in the early nineteenth century to the paclitaxel and artemisinin recently (Che and Zhang, 2019).

McChesney et al. (2007) reported that around 10,000 of the world's plants were documented medicinal use, however it is roughly 150-200 of such agents are incorporated in western medicine. Hence, it shows that many more important discoveries in plants for drug development. In addition, Mahmood et al. (2014) reported that there is large amount of medicinal plants still remain for possible valuable pharmaceutical application to be investigated.

1.2 Botany of Plant Species Studied

1.2.1 Taxonomy

Elaeocarpaceae is a family belongs to Angiosperm (flowering plants). This family consists of 15 genera and more than 500 species which are origin

from South America (Crayn, Rossetto and Maynard, 2006). Trees are evergreen and small size growing of shrubs. Trees and shrubs were known by opposite or alternate simple leaves with stipules and petioles with enlargements at both ends. Besides, flowers are large in clusters, bisexual, with 4-5 sepals, stamens were inserted to disk, pistil with superior ovary and fruit a capsule or berry (Little, Woodbury and Wadsworth, 1974). Table 1.1 shows the taxonomy of *Muntingia calabura*.

Table 1.1: Taxonomy of *Muntingia calabura*

| | |
|-----------------|------------------|
| Kingdom | Plantae |
| Division | Magnoliophyta |
| Class | Monocotyledonae |
| Order | Malvales |
| Family | Elaeocarpaceae |
| Genus | <i>Muntingia</i> |
| Species | <i>calabura</i> |

1.2.2 *Muntingia calabura*

Muntingia calabura is the sole species of genus *Muntingia*. It is native to southern Mexico, Central America, South America, Trinidad, the Greater Antilles and St. Vincent. It also greatly cultivated in warm areas in India and Southeast Asia such as Malaysia. In Malaysia, it is commonly cultivated as roadside trees (Mortan, 1987; Mahmood et al., 2004).

Muntingia calabura is known as ‘Kerukup siam’ in Malaysia, whereas known as ‘Jamaica Cherry’ throughout the world. It is a fast growing tree can reach to a height of around 7.5–12 m with the branches spreading nearly horizontally. The leaves are around 5-12.5 cm long and 1-6.5 cm wide, oblong, oblique base with dark green colour. It is irregularly toothed, upper surface was minutely hairy, whereas brown-, or gray- hairy on underside. The flowers are around 1.25-2 cm wide, with five green sepals, five white petals, many prominent yellow stamens, and born singly or 2’s, 3’s in the leaf axils. It has abundant fruits which are in sphere shape and around 1-1.25 cm wide. Its fruits are yellow or red with tender, thin and smooth skin. The fruits are soft, with juicy pulp, and filled with tiny, yellowish seeds. It is very sweet, with fig-like flavour and musky. Figures 1.1, 1.2, 1.3 and 1.4 show the trees, leaves, flowers and fruits of *Muntingia calabura*, respectively.



Figure 1.1: Trees of *Muntingia calabura*



Figure 1.2: Leaves of *Muntingia calabura*



Figure 1.3: Flowers of *Muntingia calabura*



Figure 1.4: Fruits of *Muntingia calabura*

1.2.3 Ethnomedical Uses of *Muntingia calabura*

Muntingia calabura was claimed by Peruvian folklore medicine that it has medicinal values (Zakaria et al., 2007). Various parts of this tree were documented in Southeast Asia and tropical America have medicinal uses (Kaneda et al., 1991; Nshimo et al., 1993). The flowers were used to treat headaches, and as an antispasmodic, antidyspeptic, and diaphoretic in Philippines. In Colombia, flowers infusions are drunk as a tranquillizer and tonic.

The roots of this species were used as an abortifacient in Malaysia and as an emmenagogue in Vietnam (Kaneda et al., 1991). The barks were boiled in water and used to reduce swelling in the lower hands and feet. Its leaves are drunk as a tea like beverage to reduce swelling of the prostate gland or to relieve gastric ulcers. In addition, the leaves are also used to alleviate colds and headaches (Zakaria et al., 2007).

1.3 Anticancer of Flavonoids

Cancer, the uncontrolled growth of cells, is one of the most deadly types of disease that claims millions of lives worldwide each year. According to World Health Organization (WHO), it is responsible for 8.2 million deaths (13% of all death worldwide) and expected to increase to 30 million the next 20 years. As 25% of female cancer patients suffer from it, breast cancer has become an important issue (Peña-Morán et al., 2016).

Plant-derived compounds or semisynthetic drugs, natural compounds chemically modified to show a better activity and/ or less toxicity were used for cancer treatment (Peña-Morán et al., 2016). Flavonoids are polyphenol compounds which widely present as constituents in flowering plants and is one of the most widespread secondary metabolites of all plant phenolics (Kandaswami et al., 2005; Tapas, Sakakar and Kakde, 2008).

Flavonoids are phenyl substituted chromones consisting of 15 carbons basic skeleton (C6-C3-C6). It is composed of benzo ring A, the heterocyclic ring C and a phenyl, the aromatic ring B (Kandaswami et al., 2005). The major flavonoid classes are flavones, flavanones, flavonols, flavanols, isoflavones, chalcones and aurones.

Compounds such as quercetin, chrysin, epicatechin, and taxifolin show wide range of biological activities ranging from antioxidant properties, antimicrobial to cancer chemoprevention (Mohammed et al., 2010). The studies of specific anticancer activities of certain flavones have intensified the research to more active and selective flavonoid derivatives. Flavone scaffold such as quercetin and chrysin which undergo numerous chemical modifications has allowed synthesis of large number of substituted flavonoids (Mohammed et al., 2010).

This resulted in the development of research in the modification of the chemical structure. As reported by Newman and Cragg (2012), almost 80% of new drugs discovered in the field of cancer research were derived from natural sources or semi-synthetic modifications. The biological activities of flavonoids greatly depend on their structure characteristics such as degree of hydroxylation and substitution. With a small modification in the chemical structure may lead to a significant change in biological activities (Hoang et al., 2018).

1.4 Mannich reaction

Mannich reaction has become a suitable method for the modification of existing chemical structure. It is a three-component single pot reaction that involves a secondary amine reacts with an aldehyde and an active hydrogen compound to form compounds known as Mannich bases (Nor-Eljaleel et al., 2015).

It is also one of the very important reactions to synthesize drugs and natural products. Besides, the Mannich reaction was regarded as an effective way to introduce aminomethyl substituents in the molecules so that the biological activity of the compounds can be enhanced (Liu et al., 2012). In organic synthesis, it is one of the most important and fundamental reactions for C-C bond forming (Subramaniapillai, 2013).

With the substantial published papers on medicinal chemistry every year, this had shown the most important application of the Mannich reaction is in the medicinal chemistry. This is due to the Mannich bases exhibiting interesting biological activities, and the delivery to the human body can be improved with the aminomethylation of drugs (Roman, 2015).

1.5 Problem statement

Muntingia calabura, known as 'kerukup siam' in Malay, is a common plant in Malaysia and it has recently gained medicinal plant status. Investigations on the leaves, stem bark, and roots of *Muntingia calabura* from Thailand, Philippines, Peru, and Taiwan have shown that the majority of the compounds were flavonoids i.e., flavanones, flavones, flavans, and chalcones. Flavonoids were reported to possess various pharmacological activities such as anticancer, antibacterial, antioxidant, antiviral activity etc.

There were more than 8000 flavonoids isolated from natural sources and scientists are still making attempts to find new flavonoids. There is a growing interest in making the chemical modifications to the natural flavonoids to improve the bioactivity. Due to the continuous evolution of multi-drug resistant tumours, the development of new drugs with enhanced efficacy is essential (Subramaniapillai, 2013). Mannich reaction has become a versatile and convenient synthetic method to produce diverse flavonoid derivatives with better activity than the parent compounds.

1.6 Objectives

- a) To extract, isolate and purify the flavonoids from the leaves of *Muntingia calabura* via chromatographic methods.
- b) To characterize and identify the classes of flavonoid isolates via spectroscopic methods.
- c) To synthesize the flavonoid derivatives from isolates via Mannich reaction.
- d) To characterize the structure of Mannich-base flavonoid derivatives via spectroscopic methods.
- e) To evaluate the cytotoxic activity of parent compounds and synthesized flavonoid derivatives against breast carcinoma cell lines via MTT assay.

CHAPTER TWO

LITERATURE REVIEW

2.1 Introduction

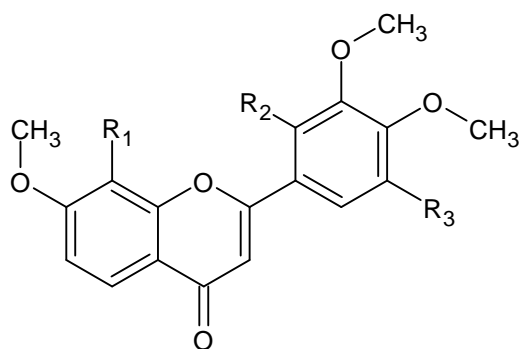
Muntingia calabura was being investigated from 1991 until the present. Different parts of this plant such as leaves, stem bark, and roots were studied, and various phytochemical constituents have been isolated. The biological activity of the isolated chemical constituents was also determined.

2.2 Chemical Constituents from the Roots of *Muntingia calabura* and Their Biological Activities

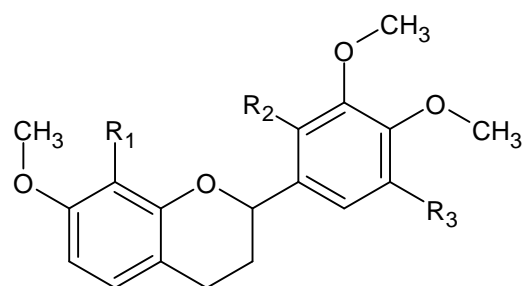
In 1991, Kaneda et al. were the first to attempt isolate chemical constituents from the roots of *Muntingia calabura*. Twelve flavonoids were isolated from the methanol extract of *Muntingia calabura* roots i.e. 7,8,3',4',5'-pentamethoxyflavone (1), 5'-hydroxy-7,8,3',4'-tetramethoxyflavone (2), 8,5'-dihydroxy-7,3',4'-trimethoxyflavone (3), (2*S*)-7,8,3',4',5'-pentamethoxyflavan (4), (2*S*)-5'-hydroxy-7,3',4'-trimethoxyflavan (5), (2*S*)-2'-hydroxy-7,8,3',4',5'-pentamethoxyflavan (6), (2*S*)-8-hydroxy-7,3',4',5'-tetramethoxyflavan (7), (2*S*)-5'-hydroxy-7,8,3',4'-tetramethoxyflavan (8), (2*S*)-8,5'-dihydroxy-7,3',4'-trimethoxyflavan (9), (2*S*)-8,2'-dihydroxy-7,3',4',5'-tetramethoxyflavan (10),

(M),(2*S*),(2''*S*)-(P),(2*S*),(2''*S*)-8,8''-5'-trihydroxy-7,7''-3', 3'''-4' ,4'''-5'''-
heptamethoxy-5, 5''- biflavan (**11**), and (M),(2*S*),(2''*S*),(P),(2*S*),(2''*S*)-8,8''-5',5''-
tetrahydroxy-7,7''-3',3''-4',4''-hexamethoxy-5,5''-biflavan (**12**).

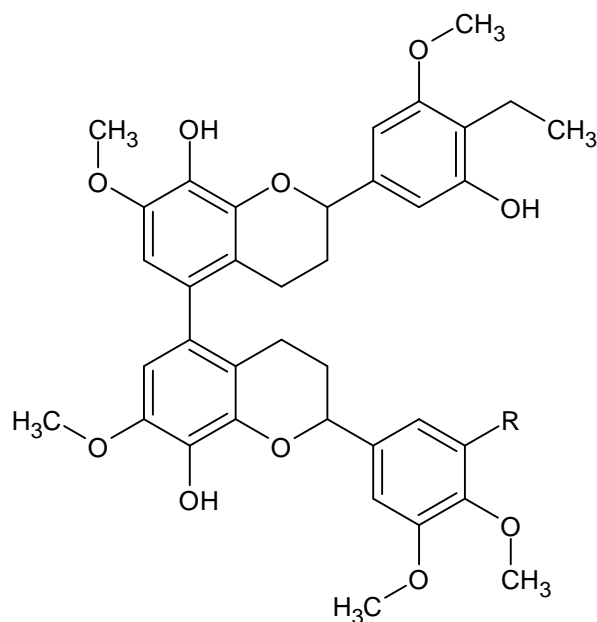
All the compounds showed cytotoxic activity towards P388 cells except compound (**1**). Flavans (**4**) to (**10**) exhibited selectively active toward melanoma (Me12) and KB cells. Compounds (**6**), (**11**) and (**12**), were generally cytotoxic and not preferentially active against KB-V cells. Figure 2.1 shows the structure of chemical constituents of *Muntingia calabura* roots.



- (1) $R_1=R_3=OMe, R_2=H$
 (2) $R_1=OMe, R_2=H, R_3=OH$
 (3) $R_1=R_3=OH, R_2=H$



- (4) $R_1=R_3=OMe, R_2=H$
 (5) $R_1=R_2=H, R_3=OH$
 (6) $R_1=R_3=OMe, R_2=OH$
 (7) $R_1=OH, R_2=H, R_3=OMe$
 (8) $R_1=OMe, R_2=H, R_3=OH$
 (9) $R_1=R_3=OH, R_2=H$
 (10) $R_1=R_2=OH, R_2=OMe$



- (11) $R=OMe$
 (12) $R=OH$

Figure 2.1: Structure of chemical constituents from *Muntingia calabura* roots

2.3 Chemical Constituents from the Leaves of *Muntingia calabura* and Their Biological Activities

Su et al. (2003) attempted to isolate compounds from the leaves of *Muntingia calabura* which collected in Purus, Peru. Fractionation of the ethyl acetate extract of the leaves of *Muntingia calabura* led to the identification of one new flavanone, (2*R*,3*R*)-7-methoxy-3,5,8-trihydroxyflavanone (**13**), and 24 known compounds, (2*S*)-7-hydroxyflavanone (**14**), (2*S*)-5,7-dihydroxyflavanone (**15**), (2*R*,3*R*)-3,5,7-trihydroxyflavanone (**16**), (2*S*)-5-hydroxy-7-methoxyflavanone (**17**), 8-methoxy-3,5,7-trihydroxyflavone (**18**), 3,8-dimethoxy-5,7,4'-trihydroxyflavone (**19**), 3,5-dihydroxy-7,4'-dimethoxyflavone (**20**), 3,5-dihydroxy-7,8-dimethoxyflavone (**21**), 5-hydroxy-3,7,8-trimethoxyflavone (**22**), 5,4'-dihydroxy-3,7,8-trimethoxyflavone (**23**), 5-hydroxy-3,7,8,4'-tetramethoxyflavone (**24**), 7-hydroxyflavone (**25**), 5,7-dihydroxyflavone (**26**), 3-methoxy-5,7,4'-trihydroxyflavone (**27**), 3,3'-dimethoxy-5,7,4'-trihydroxyflavone (**28**), 2',4'-dihydroxychalcone (**29**), 4,2',4'-trihydroxychalcone (**30**), 7-hydroxyisoflavone (**31**), 7,3',4'-trimethoxyisoflavone (**32**), 2',4'-dihydroxydihydrochalcone (**33**), 3,4,5-trihydroxybenzoic acid (**34**), lupenone (**35**), 2 α ,3 β -dihydroxyolean-12-en-28-oic acid (**36**) and (2*S*)-5'-hydroxy-7,8,3',4'-tetramethoxyflavan (**7**).

Chen et al. (2005) carried out phytochemical study on the leaves of *Muntingia calabura* collected from Kaohsiung, Taiwan. CH₃Cl-soluble fraction, *n*-BuOH-soluble and H₂O-soluble fractions that obtained from partition of methanol extract of the leaves of *Muntingia calabura* were subjected to

isolations. A new flavanone, (2S)-(-)-5'-hydroxy-7,3',4'-trimethoxyflavanone (**37**), a new flavonol derivative, muntingone (**38**), two new dihydrochalcones, 2',4'-dihydroxy-3'-methoxydihydrochalcone (**39**), (-)-3'-methoxy-2',4', β -trihydroxydihydrochalcone (**40**), along with sixteen known compounds, 5-hydroxy-7-methoxyflavone (**41**), 3,7-dimethoxy-5-hydroxyflavone (**42**), 5-hydroxy-3,6,7-trimethoxyflavone (**43**), 3,5-dihydroxy-7-methoxyflavone (**44**), 8-methoxy-3,5,7-trihydroxyflavone (**45**), 5,7-dihydroxy-3,8-dimethoxyflavone (**46**), 6,7-dimethoxy-5-hydroxyflavone (**47**), 3,5-dihydroxy-6,7-dimethoxyflavone (**48**), 5-hydroxy-3,7-dimethoxyflavone (**49**), 5,7-dihydroxyflavone (**26**), 7-hydroxy-8-methoxyflavanone (**50**), 4'-hydroxy-7-methoxyflavanone (**51**), and 2',4'-dihydroxy-3'-methoxychalcone (**52**), 7-hydroxyflavanone (**14**), 2',4'-dihydroxychalcone (**29**), and 2',4'-dihydroxydihydrochalcone (**33**) were obtained. Cytotoxic activity of the isolates were evaluated against P-388 and HT-29 cell lines. From the results, compounds **37**, **51**, **29** and **52** exhibit cytotoxicities against P-388 and HT-29 cell lines with IC₅₀ values < 4 μ g/ml. Among the flavanones, compounds **37** and **51** which have substituents at ring B show stronger cytotoxicities than compounds **14** and **50** without substituents at ring B against P-388 cell line. Chalcones **29** and **52** show the most cytotoxic among the isolates with IC₅₀ ranged from 0.21 to 1.31 μ g/ml against both cell lines.

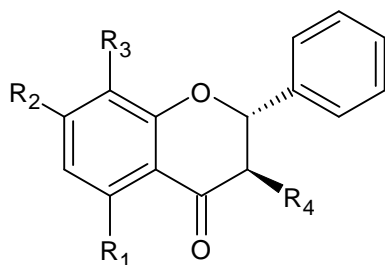
Two years later, Chen et al. again isolated compounds from the CH₃Cl-soluble and n-BuOH-soluble fractions which prepared from the methanol extract *Muntingia calabura* in previous study (Chen et al., 2005). Twenty-two compounds were isolated from this study. Of the isolated compounds, a new

flavanone, (2*R*,3*R*)-(-)-3,5-dihydroxy-6,7-dimethoxyflavanone (**53**), two new dihydrochalcones, 2,3-dihydroxy-4,3',4,5'-tetramethoxydihydrochalcone (**54**), 4,2',4'-trihydroxy-3'-methoxydihydrochalcone (**55**), 7-methoxyflavone (**56**), 5,7-dihydroxy-3-methoxyflavone (**57**), 5,7-dihydroxy-6-methoxyflavone (**58**), 5,4'-dihydroxy-3,7-dimethoxyflavone (**59**), (2*S*)-7,8,3',4',5'-pentamethoxyflavan (**60**), (2*S*)-5'-hydroxy-7,8,3',4'-tetramethoxyflavan (**7**), methyl 4-hydrobenzoate, isovanillic acid, *p*-nitrophenol, methyl gallate, trans-methyl *p*-coumarate, β -sitostenone, mixture of β -sitosterol and stigmasterol, β -amyrenone, α -tocopherylquione, δ -tocopherol, α -tocospiro A, and α -tocospiro B were obtained. Antiplatelet effects of the isolates were evaluated. From the results, compounds **54**, **58**, **60**, **59**, and methyl gallate exhibited significant antiplatelet aggregation activity *in vitro*.

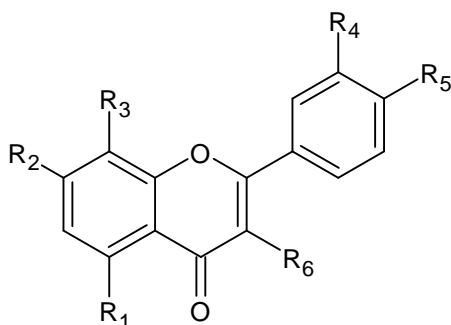
In 2013, Sufian et al. isolated compounds from the leaves of *Muntingia calabura* that collected from Shah Alam, Selangor, Malaysia and studied its antibacterial activity and cytotoxic activity. The methanol extract of *Muntingia calabura* was suspended in water to afford an aqueous methanol solution. The methanol solution was partitioned with petroleum ether and ethyl acetate. The obtained dried petroleum ether extract, dried ethyl acetate extract and H₂O-soluble extract were tested for its antibacterial and cytotoxic activity. Ethyl acetate extract was found to be the most active fraction and was further fractionated by column chromatography. This led to the isolation of four known compounds, 2',4'-dihydroxychalcone (**29**), 5,7-dihydroxy-3,8-dimethoxyflavone (**46**), 5-hydroxy-3,8-dimethoxyflavone (**49**), and 3,5,7-trihydroxy-8-methoxyflavone (**61**). Compound **29** displayed the most significant

antibacterial activity with MIC value of 50 µg/mL and 100 µg/mL against methicillin-sensitive *Staphylococcus aureus* (MSSA) and methicillin-resistant *Staphylococcus aureus* (MRSA), respectively. Compounds **29** and **49** exhibited very strong cytotoxic activity against HL60 with IC₅₀ values of 3.43 µg/mL and 3.34 µg/mL, respectively.

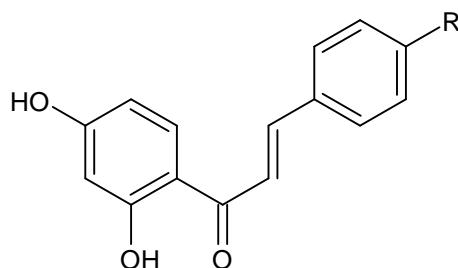
Yusof et al. (2013) also studied the leaves of *Muntingia calabura* which collected in Shah Alam, Selangor, Malaysia. The crude methanol extract of *Muntingia calabura* was partitioned to obtain petroleum ether, ethyl acetate and aqueous partition. The obtained partitions and crude methanol extract were subjected to antinociceptive assay. Petroleum ether was found to exhibit the highest percentage of antinociceptive assay and was further subjected to an isolation process. This led to the identification of one new compound, 8-hydroxy-6-methoxyflavone (calaburone) (**62**), and three known compounds, namely, 5-hydroxy-3,7,8-trimethoxyflavone (**22**), 5-hydroxy-3,7-dimethoxyflavone (**49**), and 2',4'-dihydroxy-3'-methoxychalcone (**52**). From the investigation, compound **52** showed the highest antinociceptive in both phases of the formalin test at the dose of 50 mg/kg. Figure 2.2 shows the structure of chemical constituents from *Muntingia calabura* leaves.



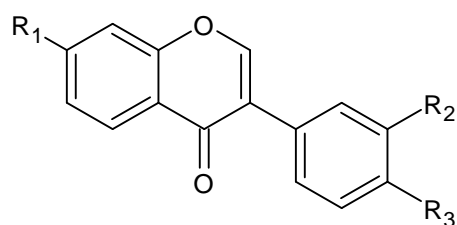
- (13) $R_1=OH$, $R_2=OMe$, $R_3=OH$, $R_4=OH$
 (14) $R_1=H$, $R_2=OH$, $R_3=H$, $R_4=H$
 (15) $R_1=OH$, $R_2=OH$, $R_3=H$, $R_4=OH$
 (16) $R_1=OH$, $R_2=OH$, $R_3=H$, $R_4=OH$
 (17) $R_1=OH$, $R_2=OMe$, $R_3=H$, $R_4=H$



- (18) $R_1=OH$, $R_2=OH$, $R_3=OMe$, $R_4=H$, $R_5=H$, $R_6=OH$
 (19) $R_1=OH$, $R_2=OH$, $R_3=OMe$, $R_4=H$, $R_5=OH$, $R_6=OMe$
 (20) $R_1=OH$, $R_2=OMe$, $R_3=H$, $R_4=H$, $R_5=OMe$, $R_6=OH$
 (21) $R_1=OH$, $R_2=OMe$, $R_3=OMe$, $R_4=H$, $R_5=H$, $R_6=OH$
 (22) $R_1=OH$, $R_2=OMe$, $R_3=OMe$, $R_4=H$, $R_5=H$, $R_6=OMe$
 (23) $R_1=OH$, $R_2=OMe$, $R_3=OMe$, $R_4=H$, $R_5=OH$, $R_6=OMe$
 (24) $R_1=OH$, $R_2=OMe$, $R_3=OMe$, $R_4=H$, $R_5=OMe$, $R_6=OMe$
 (25) $R_1=H$, $R_2=OH$, $R_3=H$, $R_4=H$, $R_5=H$, $R_6=H$
 (26) $R_1=OH$, $R_2=OH$, $R_3=H$, $R_4=H$, $R_5=H$, $R_6=H$
 (27) $R_1=OH$, $R_2=OH$, $R_3=H$, $R_4=H$, $R_5=OH$, $R_6=OMe$
 (28) $R_1=OH$, $R_2=OH$, $R_3=OMe$, $R_4=OMe$, $R_5=OH$, $R_6=OMe$

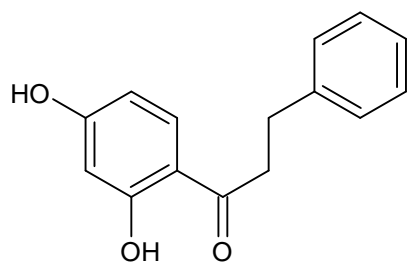


- (29) $R=H$
 (30) $R=OH$

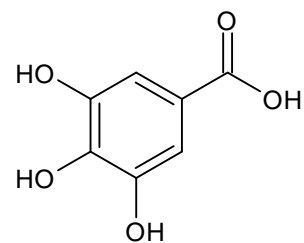


- (31) $R_1=OH$, $R_2=R_3=H$
 (32) $R_1=R_2=R_3=OMe$

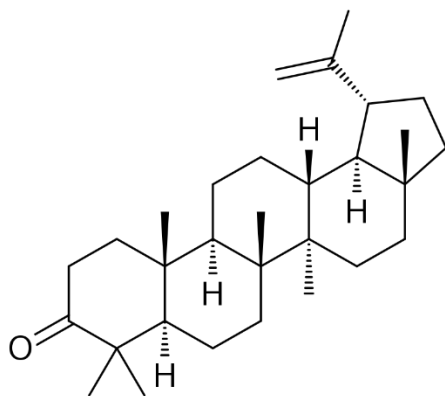
Figure 2.2: Structure of chemical constituents from *Muntingia calabura* leaves



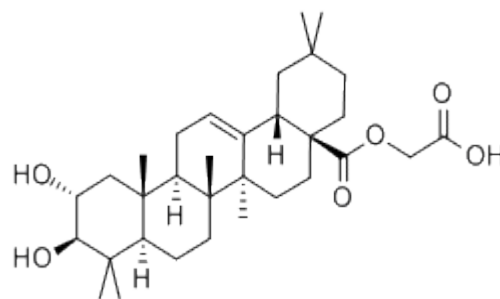
(33)



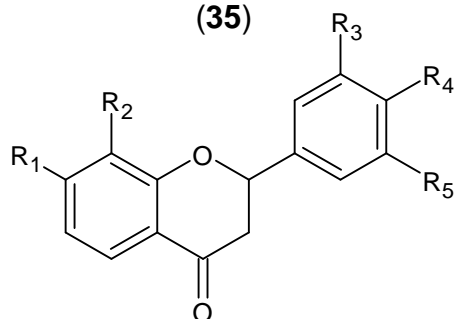
(34)



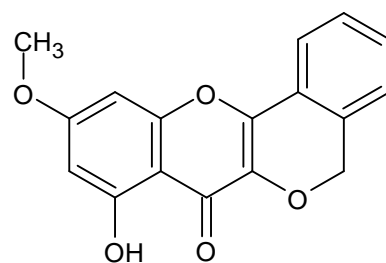
(35)



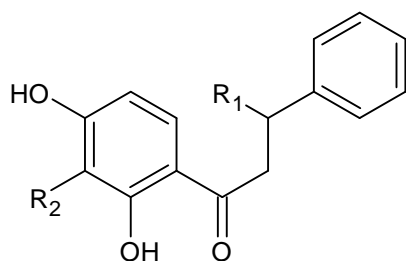
(36)



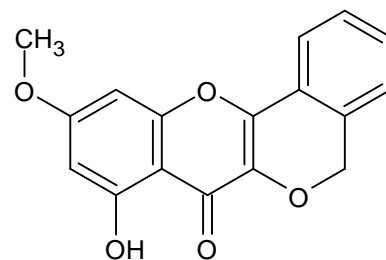
- (37) $R_1=R_3=R_4=OMe$, $R_2=H$, $R_5=OH$
 (50) $R_1=OH$, $R_2=OMe$, $R_3=R_4=R_5=H$
 (51) $R_1=OMe$, $R_2=R_3=R_5=H$, $R_4=OH$



(38)

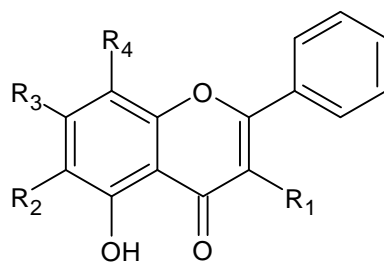


- (39) $R_1=H$, $R_2=OMe$
 (40) $R_1=OH$, $R_2=OMe$

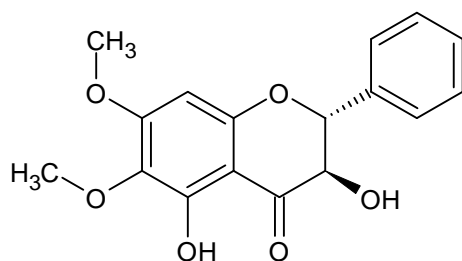


(36)

Figure 2.2: Structure of chemical constituents from *Muntingia calabura* leaves (Cont')

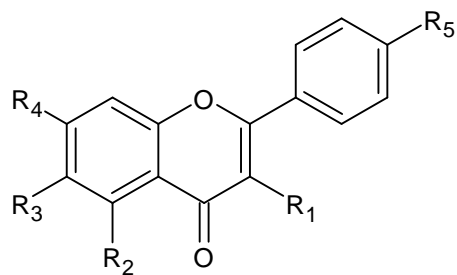


- (41) R₁=H, R₂=H, R₃=OMe, R₄=H
- (42) R₁=OMe, R₂=H, R₃=OMe, R₄=H
- (43) R₁=OMe, R₂=OMe, R₃=OMe, R₄=H
- (44) R₁=OH, R₂=H, R₃=OMe, R₄=H
- (45) R₁=OH, R₂=H, R₃=OH, R₄=OMe
- (46) R₁=OMe, R₂=OMe, R₃=OH, R₄=OMe
- (47) R₁=H, R₂=OMe, R₃=OMe, R₄=H
- (48) R₁=OH, R₂=OMe, R₃=OMe, R₄=H
- (49) R₁=OMe, R₂=H, R₃=OMe, R₄=H



(53)

Figure 2.2: Structure of chemical constituents from *Muntingia calabura* leaves (Con't)

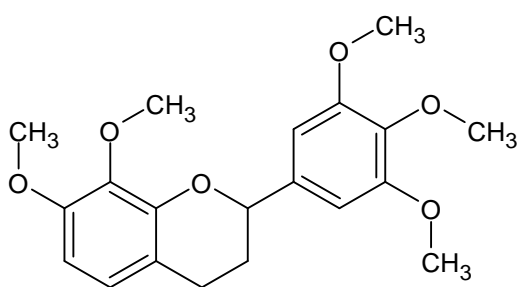


(56) R₁=R₂=R₃=R₅=H, R₄=OMe

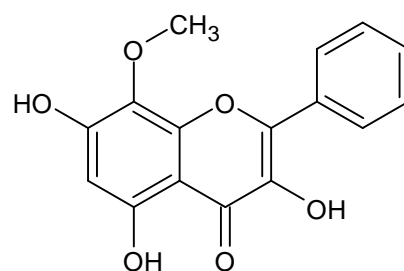
(57) R₁=OMe, R₂=OH, R₃=H, R₄=OH, R₅=H

(58) R₁=H, R₂=OH, R₃=OMe, R₄=OH, R₅=H

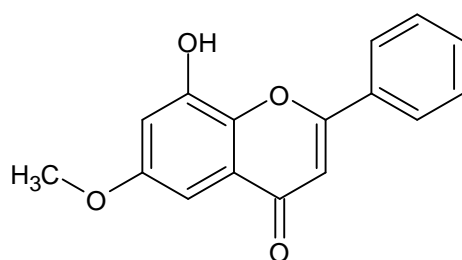
(59) R₁=OMe, R₂=OH, R₃=H, R₄=OMe, R₅=OH



(60)



(61)



(62)

Figure 2.2: Structure of chemical constituents from *Muntingia calabura* leaves (Con't)

2.4 Chemical Constituents from the Stem barks of *Muntingia calabura* and Their Biological Activities

Chen et al. (2004) has studied stem bark of *Muntingia calabura* that collected from Kaohsiung City, Taiwan. The methanol extract of stem bark was partitioned between H₂O-CH₃Cl prior to the isolation processes. Isolation of CHCl₃-soluble fraction led to the identification of two new compounds, 8-hydroxy-7,3',4',5'-tetramethoxyflavone (**63**) and 8,4'-dihydroxy-7,3',5'-trimethoxyflavone (**64**) and 13 known compounds, namely, 6,7-dimethoxy-5-hydroxyflavone (**47**), 5,7-dimethoxyflavone (**65**), 3,5-dihydroxy-6,7-dimethoxyflavone (**48**), (2*S*)-5'-hydroxy-7,8,3',4'-tetramethoxyflavan (**7**), β -sitostenone, 6 β -hydroxystigmast-4-en-3-one, β -sitosterol, syringic acid, vanillic acid, 3-hydroxy-1-(3,5-dimethoxy-4-hydroxyphenyl)propan-1-one, tetracosyl ferulate and, a mixture of 1-tetracosanol, and 1-hexacosanol. Among the isolates, compounds **63**, **64** and 3-hydroxy-1-(3,5-dimethoxy-4-hydroxyphenyl)propan-1-one displayed effective cytotoxicities against the P-388 cell lines with ED₅₀ values 3.56, 3.71 and 3.27 μ g/mL, respectively. Figure 2.3 shows the structure of chemical constituents from *Muntingia calabura* stem bark.

Kuo et al. (2014) investigated stem wood of *Muntingia calabura* which collected from Changjhih Township, Pingtung County, Taiwan. The methanol extract of stem wood was partitioned between CH₂Cl₂ and H₂O (1:1). From the isolation of CH₂Cl₂ fraction, three new compounds namely, 4'-hydroxy-7,8,3',5'-tetramethoxyflavone (**66**), (*R*)-2', β -dihydroxy-3',4'-dimethoxydihydrochalcone (**67**), (*M*),(2*S*),(2"*S*)-,(*P*),(2*S*),(2"*S*)-

7,8,3',4',5',7'',8'',3''',4''',5'''- decamethoxy-5,5'' biflavan (**68**), and twelve known compounds, namely, (2*S*)-8,5'-dihydroxy-7,3',4'-trimethoxyflavan (**9**), (2*S*)-5'-hydroxy-7,8,3',4'-tetramethoxyflavan (**8**), quercetin (**69**), 5-hydroxy-7-methoxyflavone (**41**), 7,8,3',4',5'-pentamethoxyflavone (**1**), (2*S*)-7-hydroxyflavanone (**14**), (2*S*)-7-hydroxy-8-methoxyflavanone (**50**), (*M*),(2*S*),(2''*S*)-,(*P*),(2*S*),(2''*S*)-8,5',8''-trihydroxy-7,3',4',7'',3''',4''',5'''-heptamethoxy-5,5''-biflavan (**70**), gallic acid, (*E*)-ferulic acid, β -sitosterol and β -sitostenone were obtained.

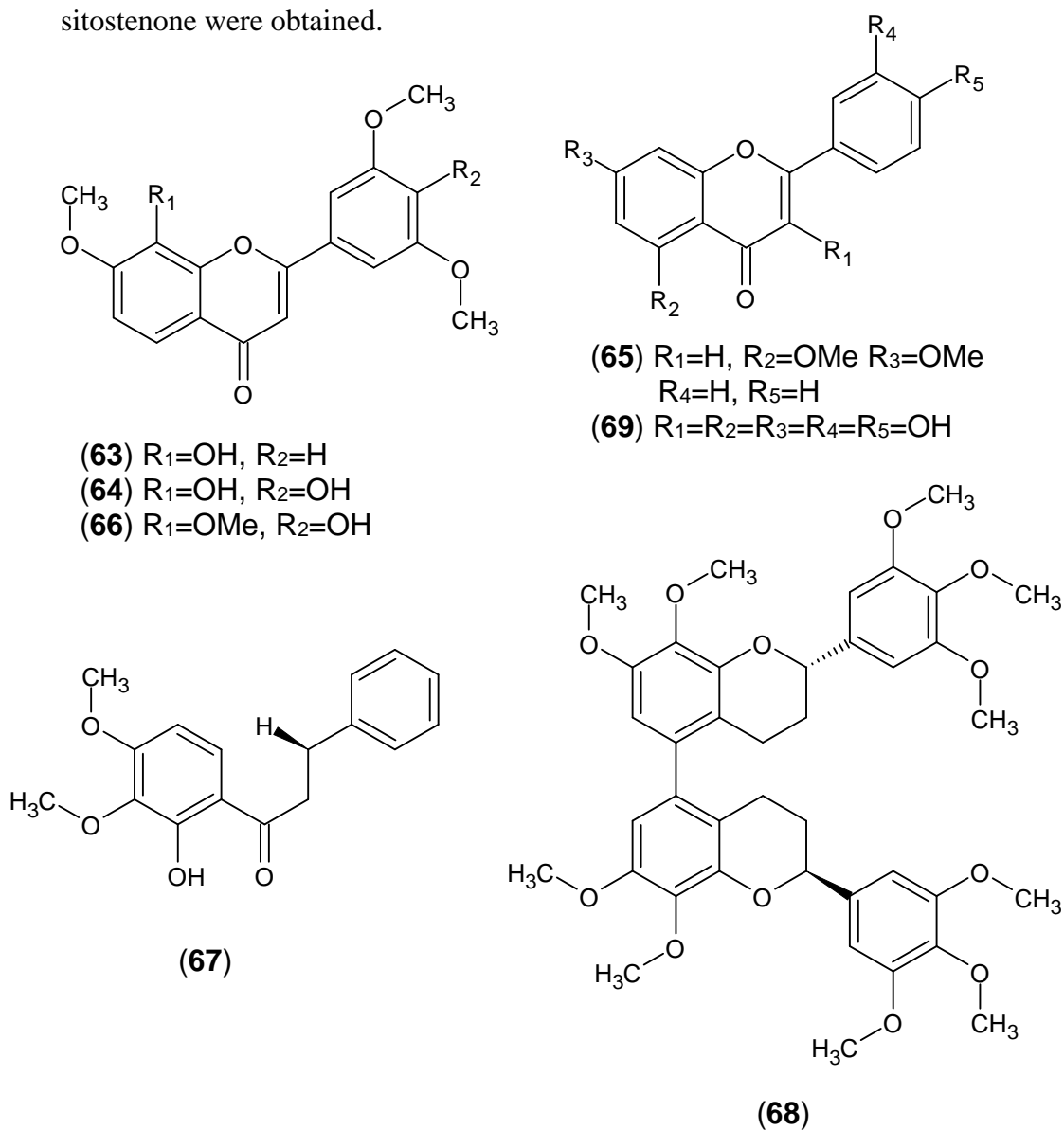
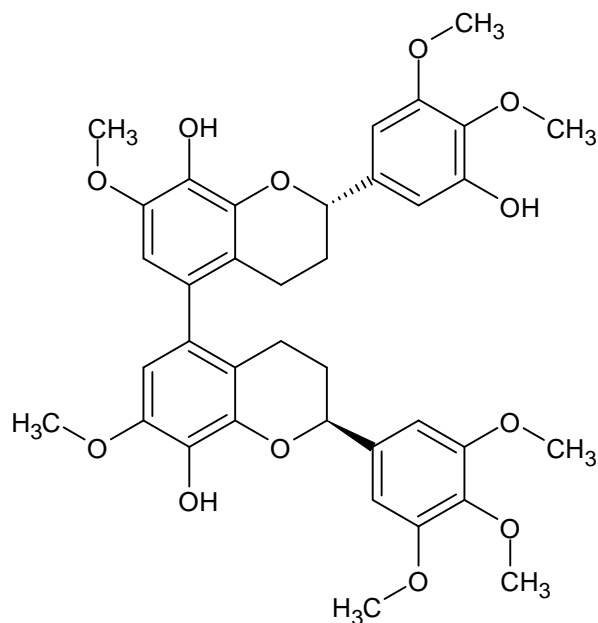


Figure 2.3: Structure of chemical constituents from *Muntingia calabura* stem barks



(70)

Figure 2.3: Structure of chemical constituents from *Muntingia calabura* stem barks (con't)

From the results of anti-inflammatory, compounds (9), (14), (41), (66), (69), and (70) showed inhibition of formyl-L-methionyl-L-leucyl-L-phenylalanine (fMLP)-induced $O_2^{\cdot-}$ generation with $IC_{50} \leq 58.4 \mu M$. Among the isolated compounds, compounds (14), (41), and (69) exhibited the highest inhibition against fMLP-induced superoxide anion generation with IC_{50} values of 4.92 ± 1.71 , 1.77 ± 0.70 , and $3.82 \pm 0.46 \mu M$. These three compounds were suggested to further develop for the treatment of several kinds of inflammatory diseases.

2.5 Chemical Constituents from the Fruits of *Muntingia calabura*

In 2015, Ragasa et al. isolated compounds from the fruits of *Muntingia calabura* that were harvested from San Pedro, Laguna, Philippines. Four compounds were isolated from the dichloromethane extract of the fruits of *Muntingia calabura* i.e. squalene, fatty acids, triglycerides, and a mixture of β -sitosterol and stigmasterol. Squalene and triglycerides were reported first isolated from *Muntingia calabura*.

2.6 Phytochemical Study of *Muntingia calabura* Leaves Extracts and Their Biological Activities

Surjowardojo et al. (2014) carried out qualitative and quantitative phytochemical analysis of the leaves of *Muntingia calabura* that collected from Sawiran Village, Tukur Sub District, Pasuruan Regency, East Jawa Province, Indonesia. The leaves were extracted with polar solvent (water, methanol, and ethanol) and non-polar solvent (chloroform, ether, and citric acid). Methanol had yielded highest extract and % rendement. Saponins, tannins and flavonoids were present in all solvent. However, their concentrations in polar solvent are higher compared to non-polar solvent. From this study, it also suggested that the efficacy of the leaves of *Muntingia calabura* may be due to the presence of these compounds as bioactive constituents. Epigallocatechin gallate and genistein were the bioactive constituents that had been found out from this study and concluded that the extract of leaves of *Muntingia calabura* had the potential as antimicrobial agent.

Buhian et al (2016) had conducted phytochemical screening of the leaves and stems of *Muntingia calabura* and determined the antimicrobial activity of ethanol extract of *Muntingia calabura* leaves and stems. The leaves and stems of *Muntingia calabura* were collected from Paniqui, Tarlac, Philippines. It was reported that the leaves ethanol extract contained higher number of secondary metabolites compared to the stem ethanol extract. There was presence of flavonoids, alkaloids, sterols, saponins, tannins and glycosides in leaves extract while absence of triterpenes. However, triterpenes were found in the stems extract. The leaves and stems extract exhibited antimicrobial activity with minimum inhibition concentration (MIC) value of 2.5 mg/mL against *Pseudomonas aeruginosa*, whereas with MIC value of 1.25 mg/mL against *Staphylococcus aureus*. For *Candida albicans*, stem extract exhibited MIC value of 2.5 mg/mL whereas leaves extract exhibited MIC value of 0.625 mg/mL or lower. This study showed that ethanol extract of *Muntingia calabura* leaves and stems were potential to act as sources of antibacterial agents against *Pseudomonas aeruginosa* and *Staphylococcus aureus*.

2.7 Flavonoid Mannich Bases

Natural products containing nitrogen compound has become the most important class of drugs recently. Mannich bases are one of this kind of compound as this compound was incorporated amine in the compound via Mannich reaction. Drugs that contain amine moiety could enhance

physicochemical properties such as water solubility, enhance bioactivity and bioavailability of bioactive molecules (Nguyen et al., 2015). Mannich reaction was used by many researchers to synthesize various flavonoid Mannich bases to improve their biological activities.

2.7.1 Chalcone Mannich Bases with Cytotoxic Activity

In 2007, Gul et al. synthesized a new series of 4'-hydroxychalcones based Mannich bases and evaluated *in vitro* their cytotoxic activity against PC3-cell lines. Compound **71** (Figure 2.4) exhibited the most potent ($IC_{50} = 3.7 \mu M$) among all the synthesized compounds. From the results, it showed that as the lipophilicity of the compound increases, the potency increases. Compounds **71** and **72** (Figure 2.4) exhibited potency 1.68 and 2.19 times compared to the chalcone precursors showing the incorporation of the 3'-piperidomethyl group has raised the potency. This significant improvement of cytotoxicity suggested that introducing 3'-piperidinomethyl group in 4'-hydrochalcones is a useful molecular modification. Besides, these observations served as guidelines for future modifications as candidate cytotoxic agents.

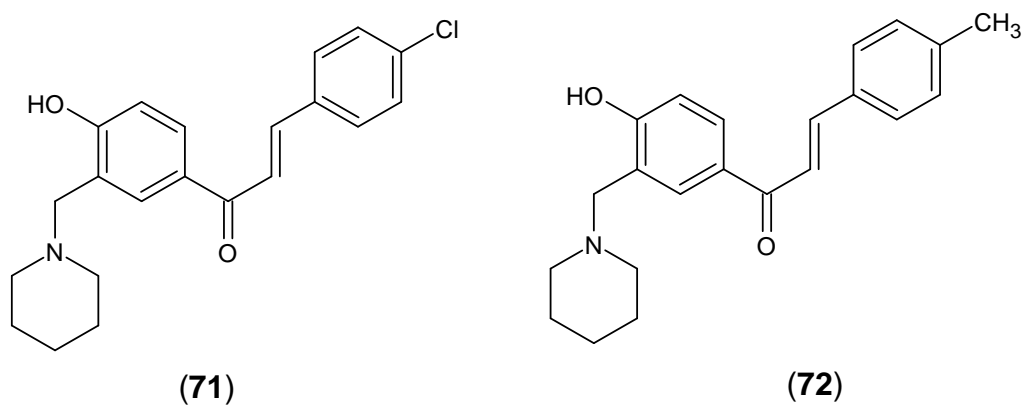


Figure 2.4: Structure of compounds 71 and 72

Hieu et al. (2012) prepared a series of 4'-hydroxychalcone based Mannich bases. The synthesized Mannich bases were evaluated *in vitro* cytotoxic activity against the human lung carcinoma (SK-Lu-1), human hepatocellular carcinoma (HepG2), and human breast cancer (MCF-7).

Three chalcones (4'-hydroxy-4-chlorochalcone, 4'-hydroxy-4-methoxychalcone and 4'-hydroxy-2-methoxychalcone) were used to react with different amines (phenylpiperazine, diethylamine, piperidine, 4-methylpiperidine, morpholine, ethylpiperazine, methylpiperazine, pyrrolidine and 2-methylpiperidine) to form Mannich bases. From the cytotoxic test, compound **73**, (*E*)-1-(4-chloro-phenyl)-3-[3-(4-ethyl-piperazin-1-ylmethyl)-4-hydroxy-phenyl]-propenone exhibited the most potent against three cancer cell lines (HepG2, SK-LU-1, and MCF-7) with IC_{50} values of 1.57, 1.16 and 1.21 $\mu\text{g/mL}$, respectively. Besides, compounds **74**, (*E*)-1-(4-chloro-phenyl)-3-[3-(4-methyl-piperazin-1-ylmethyl)-4-hydroxy-phenyl]-propenone and **75**, (*E*)-3-[3-

(4-ethyl-piperazin-1-ylmethyl)-4-hydroxy-phenyl]-1-(methoxy-phenyl)-propenone showed very significant activity against MCF-7 with IC_{50} values of $2.0 \mu\text{g/ml}$. Results showed that compounds **73** and **75** which incorporating with ethylpiperazine group displayed enhance cytotoxic activity. In addition, 4-chloro group in the B-ring exhibited more enhance cytotoxic activity compared with methoxy group. Figure 2.5 shows the structure of compounds **73**, **74** and **75**.

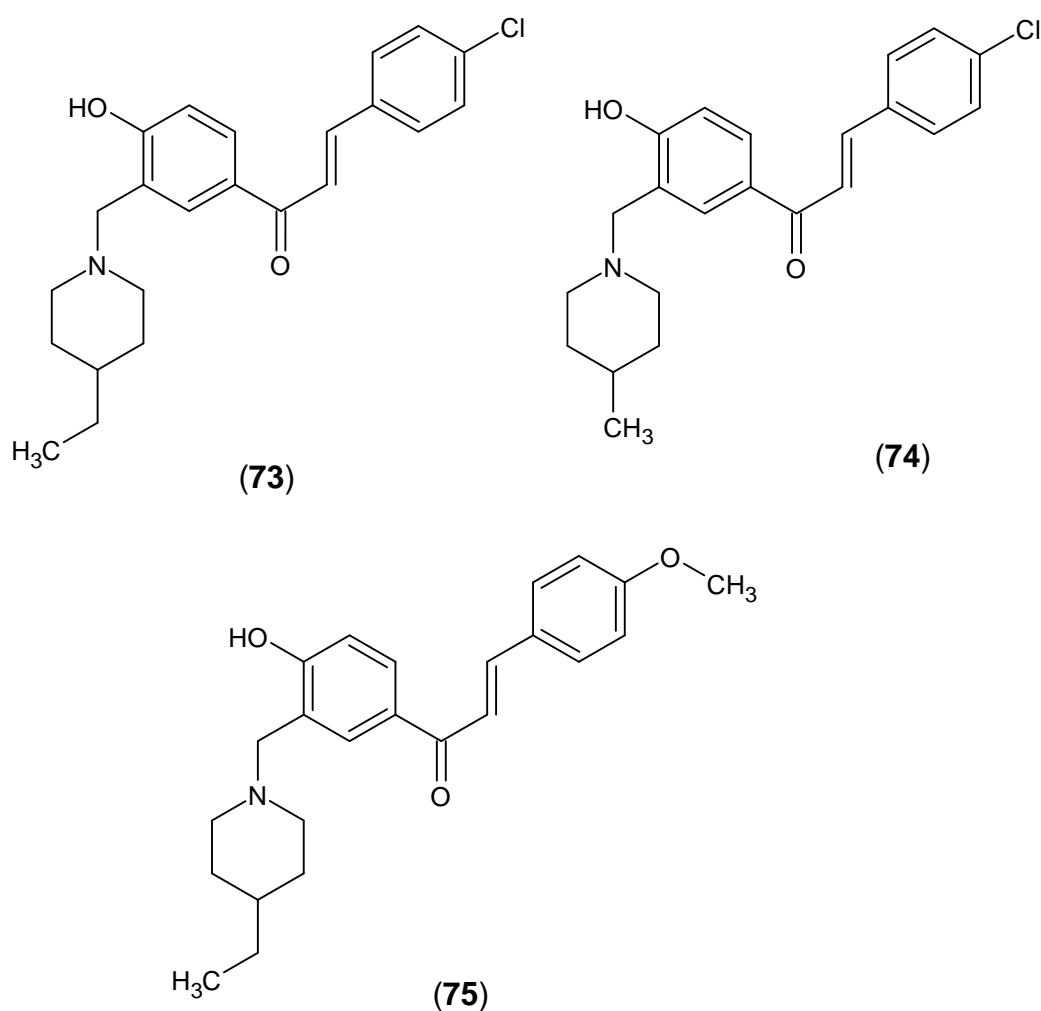


Figure 2.5: Structure of compounds 73, 74 and 75

Yamali et al. (2016) synthesized a series of halogen bearing phenolic chalcones and their corresponding bis Mannich bases. Cytotoxic activity of synthesized compounds were evaluated against human oral squamous cell carcinoma cell lines (HSC-2, HSC-3, HSC-4). The compounds exhibited higher cytotoxicities than reference compounds 5-fluorouracil and Melphalan. Based on potency selectivity expression (PSE) values, compounds **76** (1-[3,5-Bis(piperidin-1-yl) methyl-4-hydroxyphenyl]-3-(4-chlorophenyl)-2-propen-1-one) and **77** (1-[3,5-Bis(piperidin-1-yl)methyl-4-hydroxyphenyl]-3-(4-bromophenyl)-2-propen-1-one) which were bis Mannich bases with piperidine substituents displayed high PSE values with 470 and 413, respectively. Furthermore, compounds **78** (1-[3,5-Bis(morpholino-4-yl) methyl-4-hydroxyphenyl]-3-(4-chlorophenyl)-2-propen-1-one) and **79** (1-[3,5-Bis(morpholino-4-yl) methyl-4-hydroxyphenyl]-3-(4-bromophenyl)-2-propen-1-one) with morpholine as aminoalkyl substituents exhibited higher PSE values with 694.1 and 675.5, respectively. These two compounds with the highest PSE values may act as lead molecules for further anticancer investigations.

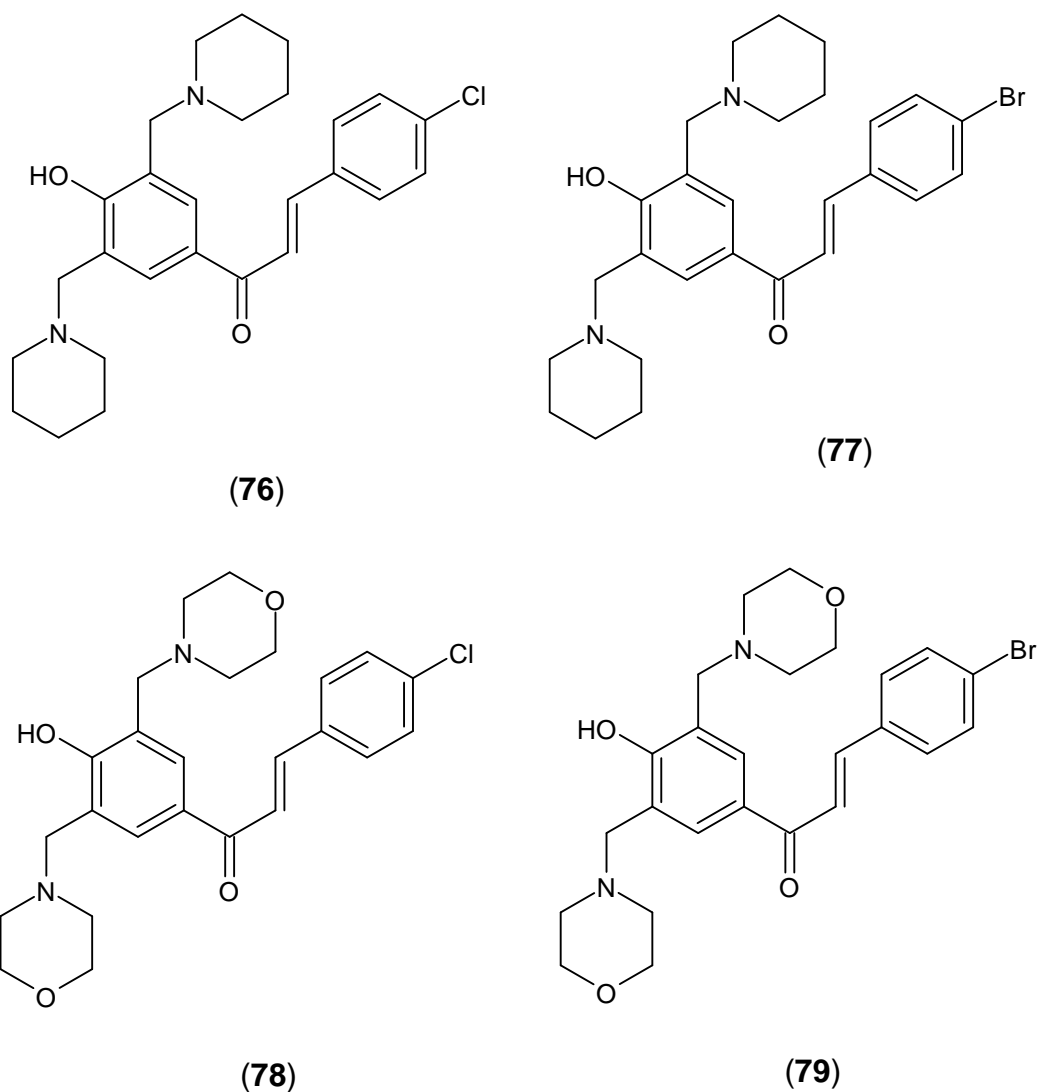


Figure 2.6: Structure of compounds 76, 77, 78 and 79

Fu et al. (2014) synthesized a series of aminomethylated derivatives of isoliquiritigenin via Mannich reaction. The synthesized Mannich bases were evaluated against human mammary cancer cell line MCF-7, human oophoroma cell line HO-8910 and human prostatic cell line PC-3. The amines used for the synthesis were dimethylamine, morpholine, cyclohexylamine, diisopropylamine, diethylamine, sec-butylamine, tert-butylamine, monoethanolamine,

diethanolamine, and pyrrolidine. Cytotoxic activity results showed that compounds **80** and **81** displayed stronger inhibition against PC-3 with IC_{50} of 28.32 μ M and 35.14 μ M for 72 h, respectively compared to parent compound isoliquiritigenin. Compound **81** exhibited strong inhibition against HO-8910 with IC_{50} value of 37.85 μ M and was the only compound showed strong growth inhibition against MCF-7. Compound **82** with the monoethanolamine as substitute displayed much improved activity compared to other derivatives. Whereas, for compound **81** which contains two hydroxyl groups that attached with the nitrogen atom showed the most potent activity. It was concluded that amines containing hydroxyl group which located at 3'-position of A-ring was beneficial to the activity of the compounds. Compound **81** containing the amine with two hydroxyl groups showed more potent cytotoxicities than compound **80** which containing the amine with one hydroxyl group. Figure 2.7 shows the structure of compounds **80**, **81** and **82**.

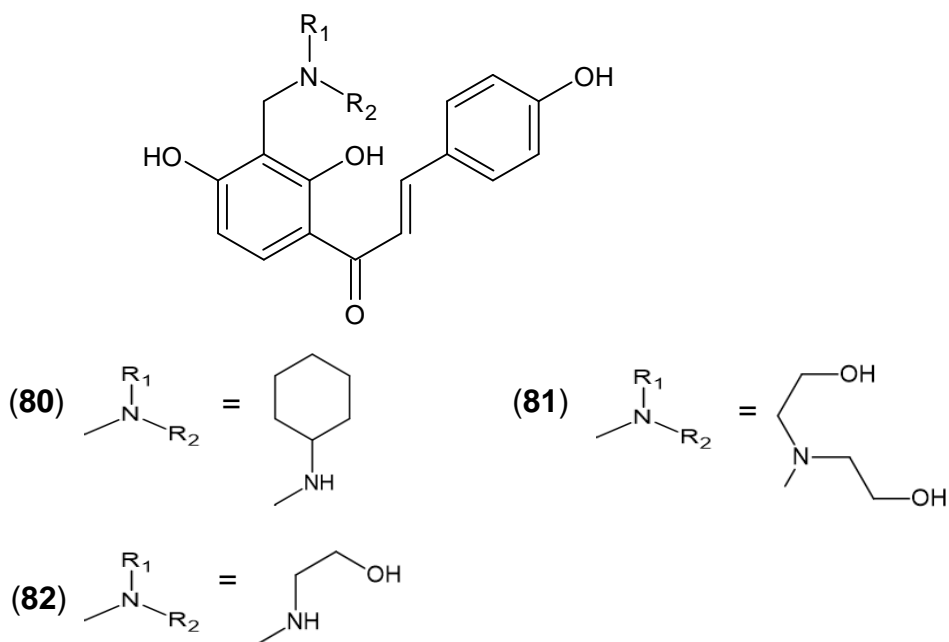
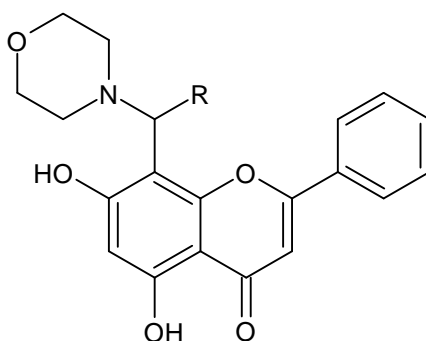


Figure 2.7: Structure of compounds 80, 81 and 82

2.7.2 Flavone Mannich Bases with Cytotoxic Activity

In 2010, Mohammed synthesized a range of mono- and disubstituted chrysin derivatives and evaluated their aromatase inhibition activity. Aromatase is a key target for hormone-dependent tumours treatment, including breast cancer. From the results, some of the synthesized compounds showed more effective aromatase inhibitors than aminoglutethimide which is the benchmark compound. Compound **83** consisting of morpholine as substituent exhibited aromatase inhibition with IC_{50} of 5.90 μ M, which is significantly lower than aminoglutethimide ($IC_{50} = 36.74 \mu$ M), the benchmark inhibitor. Whereas compound **84** also with morpholine as substituent but the aldehyde is *p*-methoxybenzaldehyde instead of formaldehyde as in **83**, exhibited IC_{50} value of 15.63 μ M which is lower than of parent compound, chrysin. These results showed that by adding a substituent, the binding affinity to aromatase active site could be increased. Figure 2.7 shows the structure of compounds **83** and **84**.

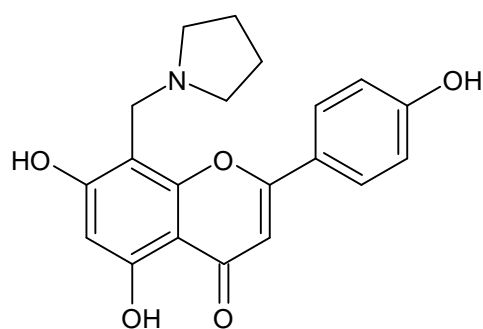


(**83**) R=H

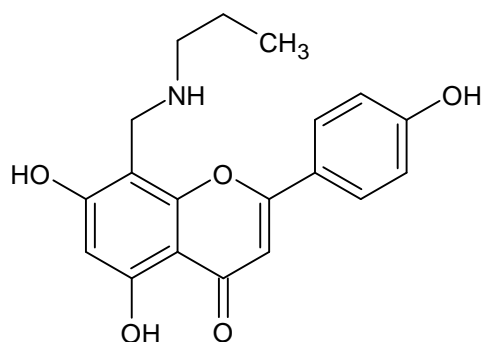
(**84**) R=C₆H₄-*p*OCH₃

Figure 2.8: Structure of compounds 83 and 84

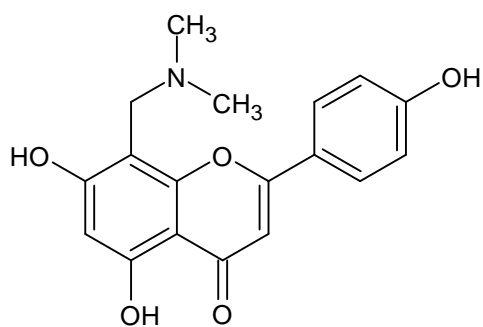
Liu et al. (2012) synthesized a series of nitrogen-containing apigenin analogue via Mannich reaction and evaluated their anticancer activity. Primary and secondary amines (ethylamine, propylamine, isopropylamine, tert-butylamine, dimethylamine, diethylamine, diisopropylamine, cyclohexylamine, pyrrolidine and morpholine) were used to prepare the Mannich bases. Antiproliferative activities of the prepared compounds against HeLa, HepG2, A549, and MCF-7 cancer cell lines were evaluated. From the results, high doses of compounds exhibited more antiproliferative activities. Compound **85** (4',5,7-trihydroxy-8-(pyrrolidin-1-ylmethyl)-2-phenyl-4*H*-chromen-4-one) displayed the strongest antiproliferative activity against A549, MCF-7, HeLa and HepG2 with IC₅₀ values of 223, 166, 40, and 40 µg/mL, respectively. Compounds **85**, **86** (4',5,7-trihydroxy-8-(propylamino)-2-phenyl-4*H*-chromen-4-one) and **87** (4',5,7-trihydroxy-8-(dimethylamino)-2-phenyl-4*H*-chromen-4-one) showed stronger activities against A549 than parent compound apigenin. Compounds **85**, **87** and **88** (4',5,7-trihydroxy-8-(diethylamino)-2-phenyl-4*H*-chromen-4-one) displayed better antiproliferative activities against MCF-7 cells compared with apigenin. In addition, apigenin analogues with a short and more branched alkyl chain at the C-8 position of apigenin improved the antiproliferative activities against HeLa and HepG2. Based on the results obtained, it was concluded that the presence of nitrogen at the C-8 position of apigenin was critical to the antiproliferative activities of the synthesized compounds. Figure 2.8 shows the structures of compounds **85**, **86**, **87** and **88**.



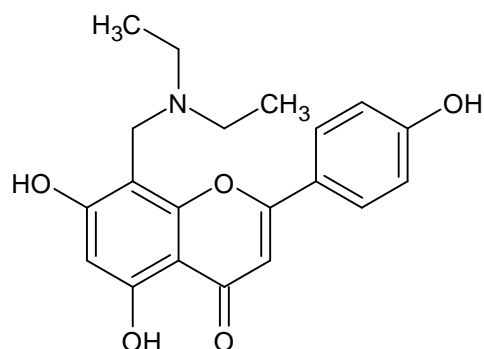
(85)



(86)



(87)



(88)

Figure 2.9: Structure of compounds 85, 86, 87 and 88

Nguyen et al. (2015) synthesized nine novel kaempferide Mannich bases and evaluated their antiproliferative activity against three human cancer cell lines (HCC1954, SK-OV-3, Hela) via standard MTT method. Compounds **89** (3,5,7-trihydroxy-2-(4-methoxyphenyl)-6,8-bis[(dimethylamino)methyl]-4*H*-chromen-4-one, **91** (3,5,7-trihydroxy-2-(4-methoxyphenyl)-6,8-bis[(dipropylamino)methyl]-4*H*-chromen-4-one, **92** (3,5,7-trihydroxy-2-(4-

methoxyphenyl)-6,8-bis(morpholinomethyl)-4*H*-chromen-4-one), **93** (3,5,7-trihydroxy-2-(4-methoxyphenyl)-6,8-bis(piperazin-1-ylmethyl)-4*H*-chromen-4-one), **94** (3,5,7-trihydroxy-2-(4-methoxyphenyl)-6,8-bis(pyrrolidin-1-ylmethyl)-4*H*-chromen-4-one), **95** (3,5,7-trihydroxy-2-(4-methoxyphenyl)-6,8-bis(piperidin-1-ylmethyl)-4*H*-chromen-4-one), **96** (3,5,7-trihydroxy-2-(4-methoxyphenyl)-6,8-bis[(4-methylpiperazin-1-yl)methyl]-4*H*-chromen-4-one) with IC₅₀ values of 12.47-28.24 μM against Hela cells were more potent than the positive control, *cis*-platin with IC₅₀ value of 41.25 μM. Compounds **91**, **92**, **94**, **96** with IC₅₀ values of 8.82-14.97 μM against HCC1954 cells were more potent to positive control, *cis*-platin (IC₅₀ 29.68 μM). Compounds **89**, **90** (3,5,7-trihydroxy-2-(4-methoxyphenyl)-6,8-bis[(diethylamino)methyl]-4*H*-chromen-4-one), **91**, **92**, and **96** with IC₅₀ values of 7.67-18.5 μM against SK-OV-3 were more potent than the positive control, *cis*-platin with IC₅₀ value of 21.27 μM. Figure 2.9 shows the structure of compounds **89-96**. Biological potency was increased with the presence of amine moiety in flavonoid molecule because of (1) extra molecular site for electrophilic attack by cellular constituents; (2) the effect of chemosensitization.

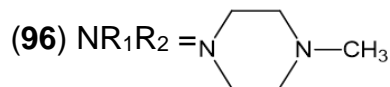
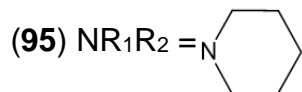
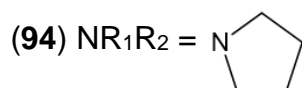
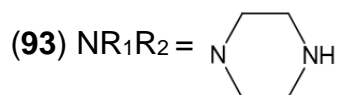
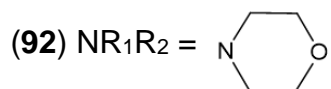
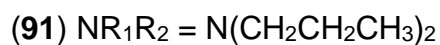
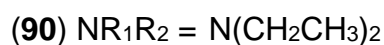
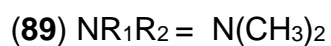
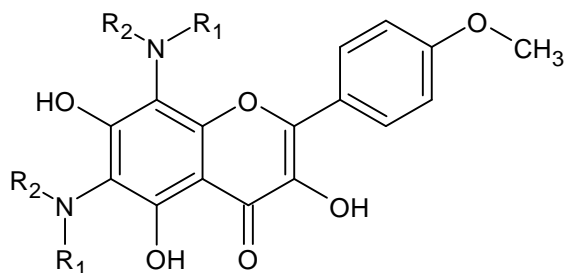
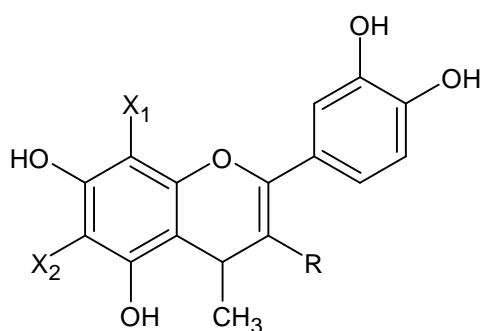


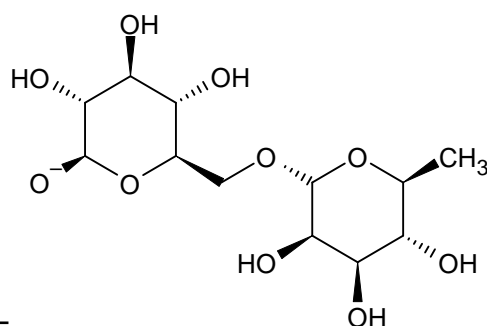
Figure 2.10: Structure of compounds 89-96

Hoang et al. (2018) have synthesized luteolin, quercetin, rutin, and hesperetin based Mannich bases. They reacted the flavonoids with secondary amine (morpholine, pyrrolidine, and 1-methylpiperazine) via Mannich reaction. The synthesized flavonoid derivatives were evaluated against breast cancer cell line MDA-MB-231. It was reported that disubstituted derivatives of hesperetin

and rutin showed greater activity than the parent compounds, whereas all quercetin derivatives displayed lower activity than the parent compounds. Among all the compounds, quercetin (**97**) and 2-(3,4-dihydroxyphenyl)-5,7-dihydroxy-6,8-bis(pyrrolidin-1-ylmethyl)-3-(((2*S*,3*R*,4*S*,5*S*,6*R*)-3,4,5-trihydroxy-6-(((2*R*,3*R*,4*R*,5*R*,6*S*)-3,4,5-trihydroxy-6-methyltetrahydro-2*H*-pyran-2-yl)oxy)methyl)tetrahydro-2*H*-pyran-2-yl)oxy)-4*H*-chromen-4-one (**98**). Figure 2.11 shows the structure of compounds **97** and **98**.



(97) R=OH, X₁=X₂=H



(98) R=



Figure 2.11: Structure of compounds 97 and 98

CHAPTER 3

MATERIALS AND METHODS

3.1 Plant materials

Leaves of *Muntingia calabura* were collected in Kampar, Perak in July 2011. It was identified by plant botanist, Prof. Dr. Rusea Go from Universiti Putra Malaysia. Voucher specimen (RG 6084) was deposited at the Herbarium Biology Department, Faculty of Science, Universiti Putra Malaysia (UPM).

3.2 Chemicals and Reagents

3.2.1 Solvents and Materials Used for Extraction and Isolation

The solvents and materials used for extraction and isolation of the leaves of *Muntingia calabura* were listed in Table 3.1.

Table 3.1 Chemicals and materials used for extraction and isolation

| Solvents/ Materials | Source, Country |
|---------------------------------|-----------------------------|
| 95% ethanol, Industrial grade | Rank Synergy, Malaysia |
| Silica gel (60 Å), 230-240 mesh | Carl Roth, Germany |
| Hexane, Industrial grade | Euro Chemo-Pharma, Malaysia |
| Chloroform, Industrial grade | Merck, Germany |
| Acetone, Industrial grade | Euro Chemo-Pharma, Malaysia |

| | |
|--|-----------------------------------|
| Dichloromethane, Industrial grade | QRec, Malaysia |
| Ethyl acetate, Industrial grade | Synerlab, France |
| Iodin crystal | Fisher Scientific, United Kingdom |
| Sodium sulphate Anhydrous, AR grade | Fisher Scientific, United States |
| TLC silica gel 60 F ₂₅₄ | Merck, Germany |

3.2.2 Chemicals and Reagents Used for Structure Elucidation

Chemicals and reagents used for structure elucidation analysis were shown in Tables 3.2 to 3.5.

Table 3.2: Reagents used for UV-vis analysis

| Reagents/ Materials | Source, Country |
|---------------------|-----------------------------------|
| Methanol, AR grade | Fisher Scientific, United Kingdom |

Table 3.3: Chemicals used for IR analysis

| Chemicals | Source, Country |
|-------------------------|-----------------------------------|
| Potassium bromide (KBr) | Fisher Scientific, United Kingdom |

Table 3.4: Reagents used for LC-MS analysis

| Reagents | Source, Country |
|----------------------|-----------------------------------|
| Methanol, HPLC grade | Fisher Scientific, United Kingdom |

Table 3.5: Deuterated solvents for NMR analysis

| Reagents | Source, Country |
|---|-----------------|
| Deuterated chloroform | Merck, Germany |
| Deuterated acetone, acetone-d ₆ | Merck, Germany |
| Deuterated dimethyl sulfoxide-DMSO-d ₆ | Merck, Germany |

3.2.3 Chemicals and Reagents used for Mannich Reaction

Chemicals and reagents used for Mannich reaction were listed in Table 3.6.

Table 3.6: Chemicals and reagents used for Mannich reaction

| Chemicals/ Reagents | Source, Country |
|--------------------------------|-----------------------------------|
| Pyrrolidine, AR grade | Merck, Germany |
| Piperidine, AR grade | Acros Organics, Belgium |
| 1-methylpiperazine, AR grade | Acros Organics, Belgium |
| Morpholine, AR grade | Merck, Germany |
| Thiomorpholine, AR grade | Sigma Aldrich, Germany |
| 4-methoxybenzylamine, AR grade | Alfa Aesar, India |
| Acetonitrile, AR grade | Fisher Scientific, United Kingdom |
| Formaldehyde, AR grade | Merck, Germany |
| Ethyl acetate, AR grade | Fisher Scientific, United Kingdom |
| Parafilm oil | Sigma Aldrich, United States |

3.2.4 Chemicals and Reagents Used for Cytotoxic activity

Chemical reagents and materials used for cytotoxic activity were shown in Table 3.7.

Table 3.7: Chemical reagents and materials used for cytotoxic activity

| Chemical reagents/ Materials | Source, Country |
|---|------------------------|
| RPMI 1640 medium | Nacalai Tesque, Japan |
| Foetal bovine serum | Sigma-Aldrich, USA |
| Penicillin-streptomycin | Sigma-Aldrich, USA |
| DMEM:F12 | Sigma-Aldrich, USA |
| Horse serum | Sigma-Aldrich, USA |
| Epidermal growth factor (EGF) | Sigma-Aldrich, USA |
| Hydrocortisone | Sigma-Aldrich, USA |
| Insulin | Sigma-Aldrich, USA |
| Dimethyl sulfoxide (DMSO), biological grade | Merck, Germany |
| Trypsin-EDTA | Nacalai Tesque, Japan |
| 96-well plate | Thermo Scientific, USA |
| 3-(4,5-dimethyl thiazol-2-yl)-2,5-dipheyl tetrazolium bromide), MTT dye | Sigma Aldrich, USA |
| Doxorubicin | Merck, Germany |
| MCF-7 | HTB-22, IMU |
| MDA-MB-231 | Crm-HTB-26, IMU |
| MCF-10A | CRL-10317, IMU |

3.3 Instruments

3.3.1 Ultra-Violet Visible (UV-Vis) Spectrophotometer

Ultra-violet spectra were recorded in Shimadzu UV-1700 UUVIS Spectrophotometer, Japan.

3.3.2 Fourier Transform Infra Red (FTIR) Spectrophotometer

Infrared spectra were determined by using Perkin-Elmer Spectrum RX1 IR spectrometer (United States) with KBr technique.

3.3.3 Mass Spectrometry

HR-EIMS were recorded on an Agilent Technologies G6520B Accurate-Mass-Q-TOF LC-MS, United States.

3.3.4 Nuclear Magnetic Resonance (NMR)

^1H and ^{13}C NMR spectra were analysed on a JEOL JNM-ECX 400 MHz spectrometer (Japan), in CDCl_3 , CD_3OD or acetone- d_6 , and $\text{DMSO-}d_6$. Chemical shifts were expressed in δ (ppm) values relative to tetramethylsilane (TMS) as the internal standard.

3.3.5 Melting Point Apparatus

Melting points of compounds were obtained using a Stuart SMP 10 (United Kingdom) melting point apparatus.

3.3.6 Polarimeter

The specific rotation of chiral compounds was obtained on a Jasco 43 Europe P-2000 digital polarimeter, Japan.

3.3.7 Rotary Evaporator

The solvent was evaporated using a rotary evaporator, R-200 (Buchi, Germany).

3.4 Methodology

3.4.1 Extraction of the leaves of *Muntingia calabura*

Dried leaves (3 kg) were extracted with 95 % ethanol (4x4L) at room temperature for one week. The solvent extract was filtered, and the filtrates were evaporated under reduced pressure at 40 °C by rotary evaporator. The obtained ethanol crude extract was then partitioned with water (4x1L): ethyl acetate (4x1L) in 1:1 ratio to obtain ethyl acetate crude extract.

3.4.2 Chromatography Methods

3.4.2.1 Column Chromatography (CC)

Column chromatography over silica gel 60 Å, 230-400 Mesh (40-60 microns) was used for the isolation of crude extract. Different sizes of column (2.5, 3.0, 4.0, 8 cm x 50 cm) were used. The column's size depends on the weight of crude extract. Silica gel was employed as a stationary phase in column chromatography. Solvent of different polarity (hexane, dichloromethane, chloroform, ethyl acetate and acetone) was used as mobile phase to elute out the compounds.

Crude extract was prepared using dry packing method. At first, the crude extract was dissolved in an appropriate amount of solvent (chloroform or acetone), then the mixture was added dropwise to silica gel and mixed evenly with minimum amount of silica gel. The wet mixture was then left dry overnight at room temperature. Sintered glass column was used to pack the column. To pack column, silica gel slurry was prepared by mixing hexane with silica gel. Then the slurry was poured to the column at desired height. The column was tapped with rubber tubing to aid for compact packing. After the column was densely packed, the dry crude extract was introduced onto the packed column. A thin layer of sodium sulphate anhydrous was added on top of the crude extract layer in order to prevent the surface of crude extract was disturbed when solvent was added to the column. A series of mobile phase in increasing polarity was added as eluent to isolate compounds. Isocratic and gradient solvent systems were used in column chromatography. The eluents were collected based on separate colour bands and volume.

3.4.2.2 Thin Layer Chromatography

Thin layer chromatography (TLC) was used to detect the number of compounds that present in the obtained fractions. The developing chamber was prepared by using solvent mixture with different polarity. The base line and solvent front line were drawn 0.5 cm from the bottom and top of the TLC plate. Then, the sample in solution was spotted on the baseline of TLC plate using a microcapillary tube. The plate was then put in the developing chamber until the solvent mobile phase reached to the front line of the TLC plate.

3.5 TLC Visualization Methods

3.5.1 UV light

UV light at 254 nm and 365 nm was used to detect the developed spots on the TLC plate. Any spots were circled lightly with a pencil. The R_f value was determined based on distance travelled by sample divided by distance travelled by solvent as shown below.

$$R_f = \frac{\text{distance travelled by the sample (cm)}}{\text{distance travelled by the solvent (cm)}}$$

3.5.2 Iodin vapour

A few iodine crystals were placed in the iodine chamber to form iodine vapour. The developed TLC plate was put into iodine chamber. After 10 minutes,

the TLC plate was carefully removed from the chamber. The brown spots formed were circled immediately with pencil as the iodine spots will fade over time .

3.6 Mannich Reaction

3.6.1 Synthesis of Monoamine Chalcone Mannich base Derivatives

0.1 mmol of 2',4'-dihydroxy-3'-methoxychalcone (**M2**) was dissolved in 5 ml acetonitrile, then 0.2 mmol of formaldehyde was added to the solution and stirred for 15 mins at room temperature. After 15 mins, 0.2 mmol of secondary amine was added and continued stirred for 30 mins at room temperature. After 30 mins, the mixture was refluxed with stirring at 70 °C, progression of the reaction was monitored by TLC.

After the reaction was completed, the mixture was evaporated under reduced pressure. After evaporation, 15 mL distilled water was added and sonicated for 5 mins. Then, 15 mL ethyl acetate was added to extract organic compound. The washing was repeated twice. The organic layer was separated and dry with sodium sulphate anhydrous. The organic layer was evaporated. TLC was used to determine the purity of the compound. The crude product was recrystallized from absolute ethanol. Same procedures were repeated for synthesis of monoamine 2',4'-dihydroxychalcone (**M4**). Table 3.8 shows the reactants, and mol ratio used for the synthesis of chalcone Mannich base derivatives.

Table 3.8: Reactants and mol ratio used for the synthesis of chalcone Mannich base derivatives

| Chalcone | Amines | Mol ratio (chalcone:formaldehyde: amine) |
|---|---------------|---|
| 2',4'-dihydroxy- 3'-methoxychalcone (M2) | Piperidine | 1:2:2 |
| | Morpholine | 1:2:2 |
| 2',4'- dihydroxychalcone (M4) | Piperidine | 1:2:2 |
| | Morpholine | 1:2:2 |

3.6.2 Synthesis of Monoamine Flavone Mannich base Derivatives

0.1 mmol of 3,5,7-trihydroxy-8-methoxyflavone (**M5**) was dissolved in 5 mL acetonitrile, then 0.2 mmol of formaldehyde was added to the solution and stirred for 15 mins at room temperature. After 15 mins, 0.2 mmol of secondary amine was added and continued stirred for 30 mins at room temperature. After 30 mins, the mixture was refluxed at stirring 70 °C, progression of the reaction was monitored by TLC.

After the reaction was completed, the mixture was evaporated by using rotary evaporator. The obtained solid was washed with cooled distilled water and dried in oven at 60 °C. Thin layer chromatography was carried out in order to determine the purity of the compound. Same procedures were repeated for 5,7-dihydroxyflavone (**M14**). Table 3.9 shows the reactants and mol ratio used for the synthesis of monoamine flavone Mannich base derivatives.

Table 3.9: Reactants and mol ratio used for the synthesis of monoamine flavone Mannich base derivatives

| Flavone | Amines | Mol ratio (flavone:formaldehyde: amine) |
|---|----------------------|--|
| 3,5,7-trihydroxy-8-methoxyflavone (M5) | Pyrrolidine | 1:2:2 |
| | Piperidine | 1:2:2 |
| | 1-methylpiperazine | 1:2:2 |
| | Morpholine | 1:2:2 |
| | Thiomorpholine | 1:2:2 |
| 5,7-dihydroxyflavone (M14) | Pyrrolidine | 1:2:2 |
| | Piperidine | 1:2:2 |
| | 1-methylpiperazine | 1:2:2 |
| | Morpholine | 1:2:2 |
| | Thiomorpholine | 1:2:2 |
| | 4-methoxybenzylamine | 1:2:2 |

3.6.3 Synthesis of Diamine Flavone Mannich base Derivatives

Same procedure in Section 3.6.2 was repeated except the molar ratio (flavone: amine: formaldehyde) 1:3:3 was used instead of 1:2:2. Table 3.10 shows the reactants, and molar ratio used for the synthesis of diamine flavone Mannich base derivatives.

Table 3.10: Reactants used for the synthesis of diamine flavone Mannich base derivatives

| Flavone | Amines | Mol ratio (flavone:formaldehyde:amine) |
|---------------------------------------|--------------------|---|
| 5,7-dihydroxyflavone (M14) | Pyrrolidine | 1:3:3 |
| | Piperidine | 1:3:3 |
| | 1-methylpiperazine | 1:3:3 |
| | Morpholine | 1:3:3 |
| | Thiomorpholine | 1:3:3 |

3.7 Cytotoxic Activity

3.7.1 Cell culture

Three breast cancer cell lines (MCF-7, Estrogen receptor positive; MDA-MB-231, Estrogen receptor negative and Triple negative breast cancer cell line; and MCF-10A, normal breast cancer cell line) were obtained from International Medical University (IMU) Research Laboratory, Malaysia. The MCF-7 and MDA-MB-231 cell lines were cultured in RPMI-1640 supplemented with 10% foetal bovine serum (FBS) and 1% penicillin-streptomycin (100 IU/mL penicillin, and 100 µg/mL streptomycin). MCF-10A were cultured in DMEM:F12 media (Sigma, USA) supplemented with 5% horse serum, 20 ng/ml EGF, 0.5 µg/ml hydrocortisone, 10 µg/ml insulin, and 1% penicillin-streptomycin. The cells were allowed to grow in an incubated condition set at 37°C, 5% CO₂. The breast cancer cells were maintained in T-flasks (T-75) and the media were replaced every two to three days, whenever required.

3.7.2 Preparation of Test Compounds

Stock solutions of all test compounds at 100 mM were prepared using biological grade DMSO as solvent. Serial dilution was performed using the stock solution to prepare the respective working solutions. Doxorubicin was used as the positive control and 0.1% DMSO in respective culture medium was used as the negative control.

3.7.3 Cell Seeding and Treatment

When cells in the T-75 flasks reach the confluency at about 70-80%, the cells were trypsinised using Trypsin-EDTA to detach the cells from the surface of the cell culture flask. Fresh supplemented medium was added to resuspend the cells and was centrifuged at 1500 rpm for 5 minutes. The cell supernatant was discarded, and the cell pellets were resuspended with fresh medium. The cells were seeded in 96- well microplates at 3×10^4 cells/well. The plates were incubated for 24 hours at 37°C, 5% CO₂. The cells were treated with test compounds in the concentration range of 0.781 – 100 µM. The concentration of positive control was tested in the range of 0.0781 – 10 µM. Each concentration was tested in triplicate. The effective concentration of DMSO is not more than 0.1% in each well.

3.7.4 MTT assay

The percentage of viable cells was determined using the (3-(4,5-Dimethylthiazol-2-yl)-2,5-Diphenyltetrazolium Bromide) (MTT) assay. The

MTT assay was performed on the experimental 96-well microplates upon 72 hours of incubation, according to the manufacturer's instructions. Ten microlitres of MTT reagent was added into each well and the plates were allowed to incubate at 37°C, 5% CO₂ for 4 hours. After 4 hours, the medium was carefully decanted without disturbing the purple formazan crystals on the surface of the wells. The crystals were dissolved using DMSO. The contents were gently mixed and the absorbance of the formazan solutions at wavelengths 570 nm and 630 nm were determined using the TECAN Infinite F200 microplate reader. Each experiment was performed in triplicate and was repeated 3 times. The half maximal inhibitory concentration (IC₅₀) values of each treatment were calculated using Microsoft Excel.

3.7.5 Statistical Analysis

GraphPad Prism 9 (GraphPad Software, San Diego, CA) was used to analyse data. Any significances between the means were analysed by using unpaired t-test. It was considered significant as the differences at 5% confidence level.

CHAPTER 4

RESULTS AND DISCUSSION

4.1 Extraction and Isolation

3 kg dried leaves of *Muntingia calabura* were extracted with 95 % ethanol (4x4 L) at room temperature for one week. After filtration and the solvent was evaporated under reduced pressure, the combined ethanol crude extract was partitioned with water (4x1 L) and ethyl acetate (4x1 L) in 1:1 ratio. 298.0 g of ethyl acetate crude extract was obtained after the partition. 198.13 g ethyl acetate crude extract was subjected to column chromatography (8x50 cm) over silica gel, 326 fractions were obtained eluting with hexane, gradually increasing the polarity with ethyl acetate (98:2, 94:6, 90:10, 75:25, 70:30, 50:50, 0:100) , and then followed by increasing polarity of ethyl acetate in ethanol (99:1, 90:10, 75:25, 50:50, 20:80, 0:100). The obtained fractions were chromatographed on TLC. Fractions that showed similar TLC profile were combined to give seventeen major fractions (MF1-MF17).

From the 326 fractions, solids were obtained after some fractions were evaporated. Fraction 47 (1.67 g) obtained as solid and further fractionated over silica gel column (2 cm x 50 cm) eluted with hexane: acetone (95:5) to give compound **M1** (50 mg) and with hexane: acetone (94:6) to give compound **M2** (103 mg). Fraction 52 obtained as solid form (1.78 g) was chromatographed on

silica gel column (5x50 cm) eluting with hexane, gradually increasing polarity with acetone to give 34 subfraction. Subfraction F52-5 (0.49 g) was further fractionated with hexane: chloroform (3:7) to obtain compound **M3** (15.6 mg) and with hexane:chloroform (1:9) to obtain compound **M4** (45 mg). Fraction 53-56 was obtained as yellow solid and afforded compound **M5** (1.1 g). Fraction 57 was obtained as orange crystal and yielded compound **M6** (108 mg). A light yellow crystal compound **M7** (1.19 g) was obtained from fraction 63.

MF4 (0.38 g) was purified by silica gel column (3x50 cm) eluting with hexane: dichloromethane (12:13) to obtain compound **M8** (95.4 mg) and with hexane: dichloromethane (21:29) to give pale yellow compound **M9** (78.1 mg). MF5 (4.97 g) was chromatographed on silica gel column (4x50 cm), eluted with hexane, gradually increasing polarity with acetone (98:2, 96:4, 92:8, 90:10, 80:20, 70:30, 60:40, 50:50, 0:100) to give 32 subfractions. Subfraction MF5-22 yielded additional amount of compound **M3** (32.5 mg). Subfraction MF5-20 to MF5-25 were combined (2.99 g) was further purified by using silica gel column (4x50 cm) eluted with hexane: dichloromethane (55:45) to give additional amount of compound **M2** (23.1 mg) and with hexane: dichloromethane (15:85) to give additional amount of compound **M4** (112.6 mg).

MF6 (4.21 g) eluted with hexane, gradually increasing polarity with acetone was fractioned over silica gel column (5x50 cm) afforded 100 subfractions. Subfraction MF6-8 eluted with hexane: acetone (96:4) yielded additional amount of compound **M7** (20.2 mg) and developed with hexane:

acetone 50:50 to give addition amount of compound **M2** (258.7 mg). Subfraction MF6-17 (0.83 g) was further purified by using silica gel column (4x50 cm) eluting with hexane: dichloromethane (50:50) to obtain addition amount of compound **M9** (126.1 mg) and eluted with hexane: dichloromethane (12:13) to obtain dark yellow compound **M10** (303.5 mg).

MF7 (3.69 g) was chromatographed on silica gel column (4x50 cm) eluting with hexane: acetone (95:5) afforded yellow compound **M11** (26.1 mg). MF8 (10.84 g) was subjected to silica gel column (5x50 cm) eluted with dichloromethane: hexane (90:10) to obtain yellow compound **M12** (315.2 mg), white compound **M13** (153.5 mg) and yellow compound **M14** (646.3 mg). MF9 (3.32 g) was purified by silica gel column (4x50 cm), eluting with hexane, gradually increasing the polarity with acetone (90:10, 80:20, 70:30, 60:40, 50:50, 0:100) to afford white powder compound **M15** (15.2 mg) and additional amount of compound **M14** (22.3 mg)

MF11 (2.20 g) was chromatographed on silica gel column (3x50 cm) developed with hexane, gradually increasing the polarity with acetone. Additional amount of compound **M14** (36.5 mg) was obtained at solvent mixture hexane: acetone (88:12), yellow compound **M16** (15 mg) was yielded with hexane: acetone (86:14). MF11 eluted with hexane: acetone (82:18) to yield pale yellow compound **M17** (7.6 mg) and afforded compound **M18** (18.3 mg) with hexane: acetone (76:24). Chromatographic purification of the leaves of *Muntingia calabura* is shown in Figure 4.1.

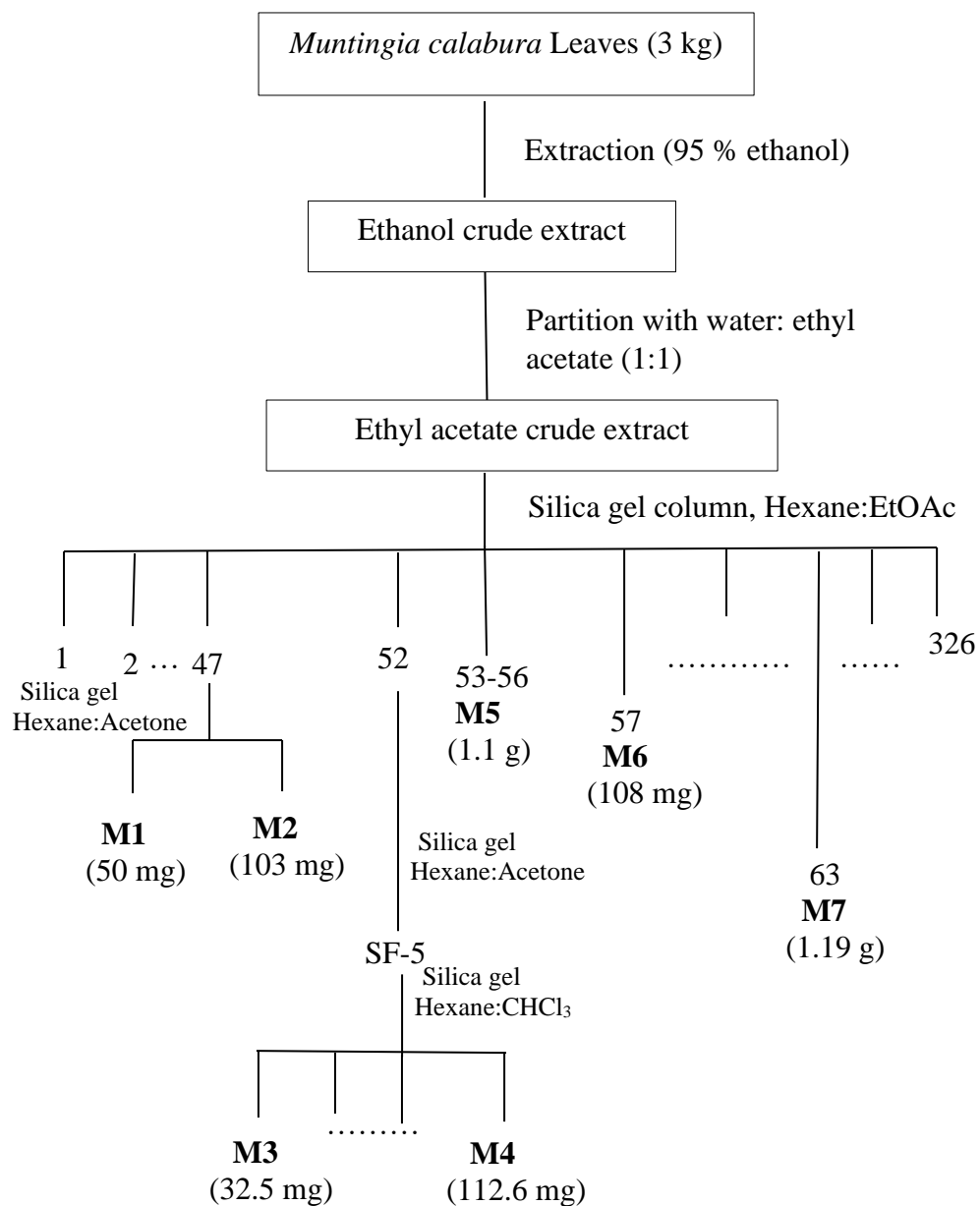


Figure 4.1: Chromatographic purification of the leaves of *Muntingia calabura*

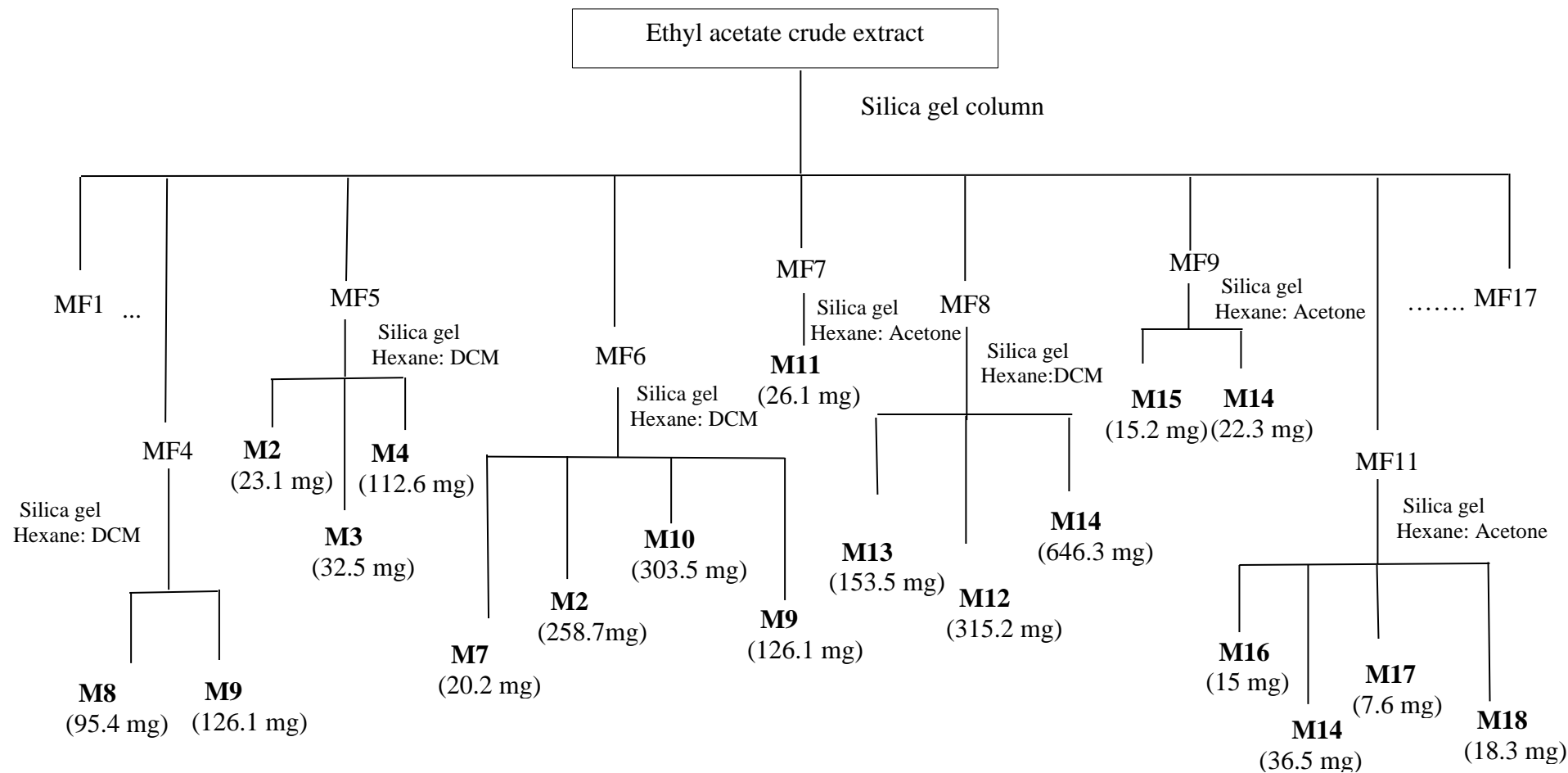


Figure 4.1: Chromatographic purification of the leaves of *Muntingia calabura* (cont')

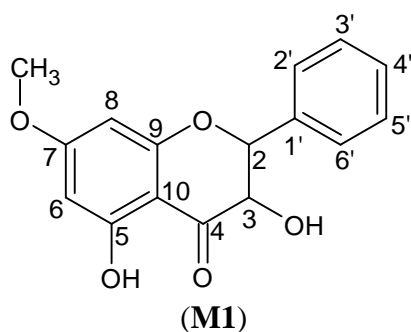
4.2 Isolated Compounds from the Leaves of *Muntingia calabura*

A total of eighteen compounds were isolated from the leaves of *Muntingia calabura* i.e. four flavanone, one flavanone, three chalcones and ten flavones. Among the isolates, three compounds i.e. 3,5-dihydroxy-7-methoxyflavone (**M1**), 2',3',4'-trihydroxychalcone (**M3**) and 7,8-dihydroxyflavanone (**M17**) were isolated from the leaves of *M. calabura* for the first time. The structures of the compounds were determined via spectroscopic methods (IR, UV-vis, 1D NMR, 2D NMR and LC-MS analyses) and compared with literature data.

4.2.1 Characterization and Structure Elucidation of Flavanones

Five flavanones, 3,5-dihydroxy-7-methoxyflavanone (**M1**), 3,5-dihydroxy-6,7-dimethoxyflavanone (**M12**), 3,5,7-trihydroxyflavanone (**M13**), 7,8-dihydroxyflavanone (**M17**) and 3,5,8-trihydroxy-7-methoxyflavanone (**M18**) were isolated from the leaves of *Muntingia calabura*.

4.2.1.1 Characterization of (2*S*, 3*S*) 3,5-dihydroxy-7-methoxyflavanone (**M1**)



Compound **M1** was obtained as a light yellow solid, mp 175-177 °C (Lit. 176-179 °C, Kurkin et al., 1994). Its specific rotation is negative as $[\alpha]_D$: -23.5° ($[\alpha]_D$: -28.1, Urzua et al., 2000). It gave R_f value of 0.28 in mobile phase hexane: chloroform 3:7. The structure was confirmed as 2*S*, 3*S* as the coupling constant was same with the reported data (Urzua et al., 2000). According to Ekalu and Habila (2020), chemical shift of flavonoids is unique. With these chemical shift characteristics, make characterization easier. The HRESIMS (Appendix A1) gave a pseudomolecular ion peak at $m/z = 287.0922 [M+H]^+$ which analysed for $C_{16}H_{14}O_5$ (found 286.0849; calculated 286.0841). The UV absorptions were 342.3 nm and 289.6 nm (Appendix B1), represent bands I and II which are the characteristic of flavanone absorption. Band I is the absorption due to a B-ring cinnamoyl system and band II involves absorption due to A-ring benzoyl system (Kumar and Pandey, 2015). The IR spectrum (Appendix C1) show absorption band at 3467 (OH stretch), 2924 (CH_3 stretch), 1635 (C=O stretch), 1574 (C=C stretch), and 1134 (C-O stretch) cm^{-1} .

The 1H NMR (Figure 4.2) shows characteristic peaks of 3-hydroxyflavanone or flavanonol moiety as doublet at δ_H 5.10 ($J=11.6$ Hz) corresponding to H-2, and doublet at δ_H 4.55 ($J= 11.6$ Hz) indicating H-3 (Weisheng et al., 2017). Two doublets aromatic protons at δ_H 6.06 ($J=2.4$ Hz) and δ_H 6.11(d, $J=2.4$ Hz) corresponding to H-8 and H-6 which is meta coupling proton and one methoxy group at δ_H 3.84 (3H). Two aromatic multiplets at δ_H 7.46 (3H, m), δ_H 7.53 (2H, m) indicate unsubstituted benzene ring B. There was one chelated hydroxide group at δ_H 11.19 (5-OH). 3-OH group was not shown in the spectrum was due to the hydrogen-deuterated proton exchange. In ^{13}C

NMR spectrum (Figure 4.3), there were 13 signals which correspond to 15 carbons of flavonoid skeleton. There was carbonyl carbon at δ_c 195.9 and methoxy carbon at δ_c 55.9. Three signals at δ_c 168.9, δ_c 163.7 and δ_c 162.9 were oxygen link aromatic carbons corresponding to C-5, C-7 and C-9 respectively. Peaks at δ_c 94.8 and δ_c 95.6 were characteristic of the C-8 and C-6 resonances of a 3-hydroxyflavanone. Observations on the ^{13}C NMR spectrum showed that peaks at δ 127.5, δ 128.8, δ 129.4 represented C-2',6', C-3',5' and C-4', respectively, of an unsubstituted B-ring. In the DEPT spectrum (Appendix D1), there were 6 quaternary carbons, 9 methine carbons and one methoxy carbon. In the HMBC spectrum (Appendix D3), the methoxy group at δ 3.84 (7-OCH₃) correlated to C-7 (δ 168.9) was confirmed as well as the correlation of H-6 (δ 6.06) to C-7 (δ 168.9) and correlation of H-8 (δ 6.11) to C-7 (δ 168.9). The 5-OH proton signal at δ_H 11.19 showed correlations with the carbons at δ_c 95.6 (C-6), δ_c 100.9 (C-10), and δ_c 162.9 (C-5). Table 4.1 shows the ^1H , ^{13}C and HMBC spectra data of compound M1.

This compound was reported isolated from *Heliotropium huascoense* and induces the expression of cytokines which are vital to control viral infection in invertebrates (Urzua et al., 2000; Valenzuela et al., 2017). Besides, it showed *in vitro* antiviral activity against infectious salmon anaemia virus.

Table 4.1: ¹H, ¹³C and HMBC spectral data of M1 (CDCl₃)

| Position | δ _H (multiplicity) | *δ _H (multiplicity) | δ _C (C-type) | HMBC |
|--------------------|---------------------------------|---------------------------------|-------------------------|----------------|
| 2 | 5.10 (1H, d, <i>J</i> =11.6 Hz) | 5.07 (1H, d, <i>J</i> =11.9 Hz) | 83.5 (CH) | - |
| 3 | 4.54 (1H, d, <i>J</i> =11.6 Hz) | 4.54 (1H, d, <i>J</i> =11.9 Hz) | 72.5(CH) | - |
| 4 | - | - | 195.9 (C) | - |
| 5 | - | - | 168.9 (C) | - |
| 6 | 6.06 (1H, d, <i>J</i> =2.4 Hz) | 6.05 (1H, d, <i>J</i> =2.3 Hz) | 95.6 (CH) | C-5, 7, 8, 10 |
| 7 | - | - | 163.7 (C) | - |
| 8 | 6.11 (1H, d, <i>J</i> =2.4 Hz) | 6.11 (1H, d, <i>J</i> =2.3 Hz) | 94.8 (CH) | - |
| 9 | - | - | 162.9 (C) | - |
| 10 | - | - | 100.9 (C) | - |
| 1' | - | - | 136.1 (C) | - |
| 2', 6' | 7.53 (2H, m) | 7.54 (2H, m) | 127.5 (CH) | C-2, 3',5', 4' |
| 3', 5' | 7.44 (2H, m) | 7.44 (2H, m) | 128.8 (CH) | C-1', C4' |
| 4' | 7.44 (1H, m) | 7.44 (1H, m) | 129.4 (CH) | C-2',6' |
| 5-OH | 11.19 (1H, s) | 11.18 (1H, s) | - | C-6, 5, 10 |
| 7-OCH ₃ | 3.83 (3H, s) | 3.80 (3H, s) | 55.9 (CH ₃) | C-7 |

*Urzua et al. (2000)

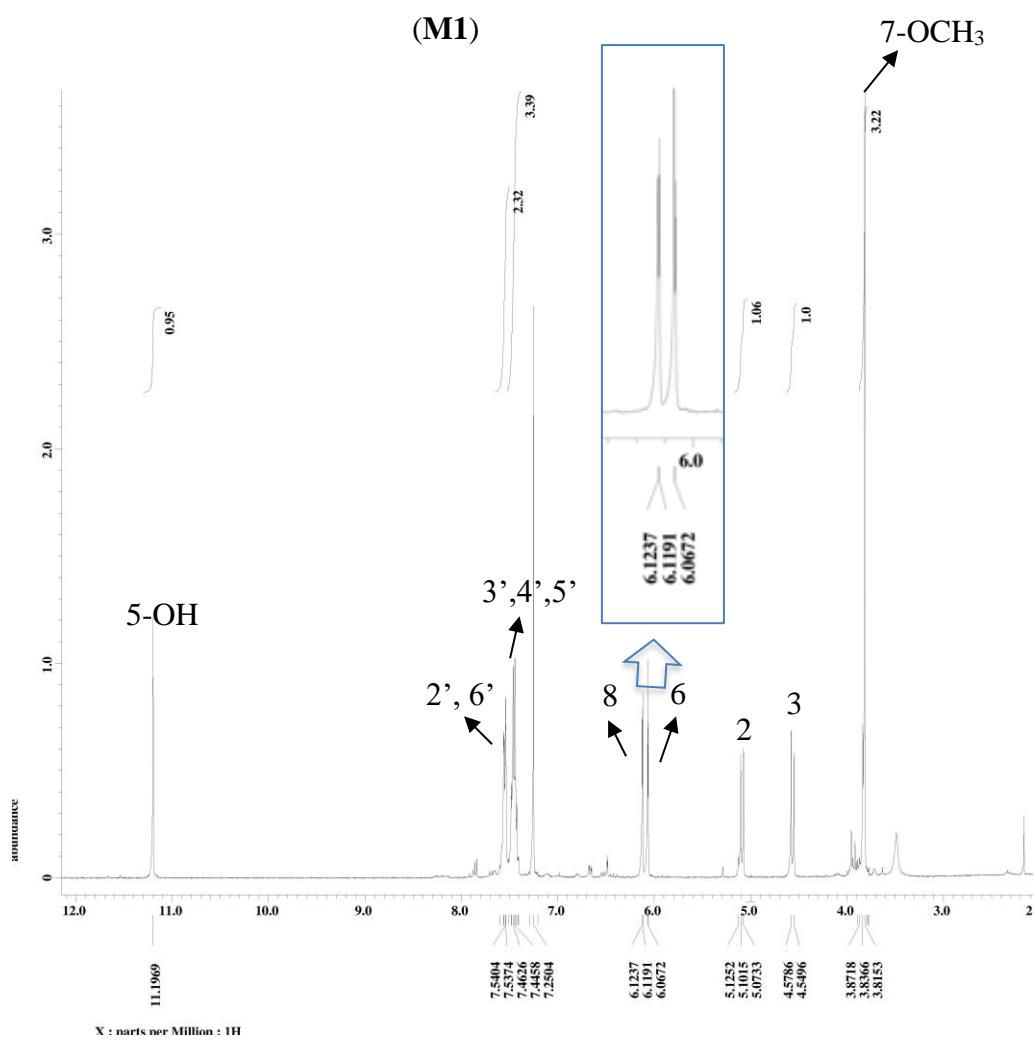
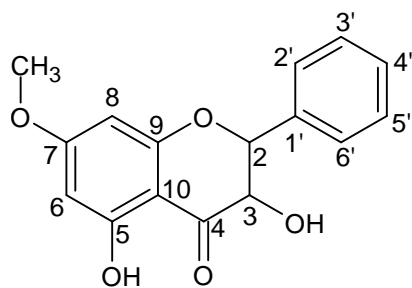


Figure 4.2: ¹H NMR (400 MHz, CDCl₃) of (2*S*, 3*S*) 3,5-dihydroxy-7-methoxyflavone (M1)

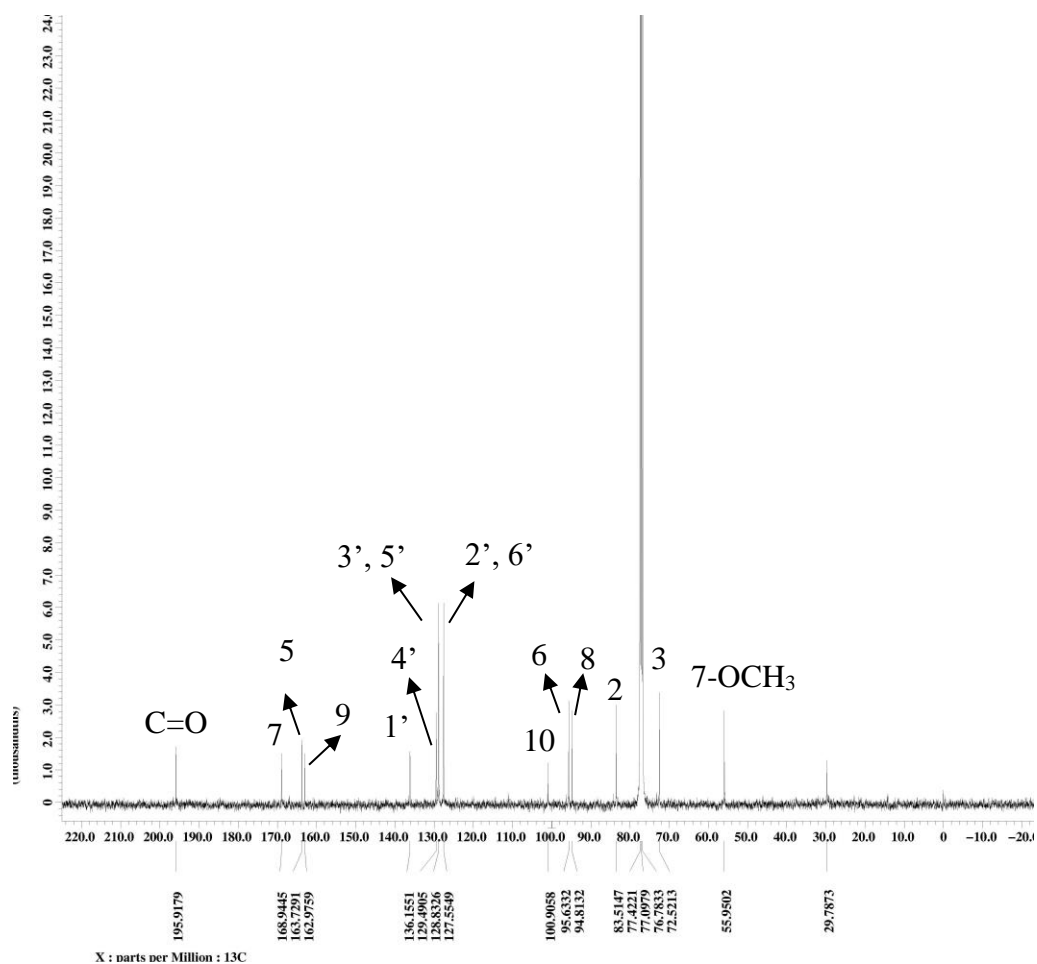
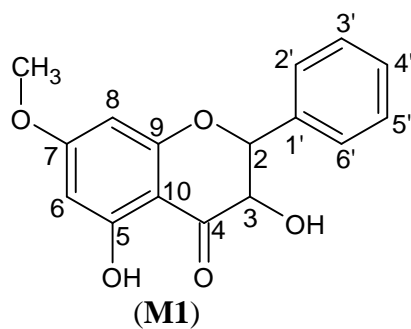
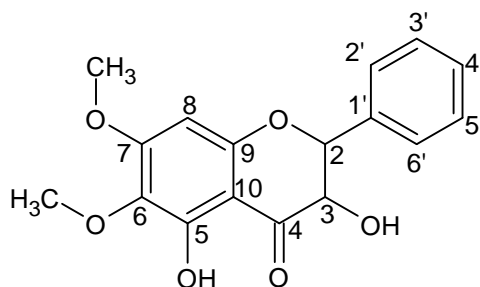


Figure 4.3: ^{13}C NMR (100 MHz, CDCl_3) of (2*S*, 3*S*) 3,5-dihydroxy-7-methoxyflavanone

4.2.1.2 Characterization of (2*R*, 3*R*) 3,5-dihydroxy-6,7-dimethoxyflavanone (**M12**)



(**M12**)

Compound **M12** was isolated as a light yellow solid, mp 186-188 °C (Lit. 189-190 °C, Chen et al., 2007). Its specific rotation is negative as $[\alpha]_D: -23.5^\circ$ (c 0.1, MeOH). The stereochemistry was similar to the reported as 2*R*, 3*R*. It gave R_f value of 0.28 in mobile phase hexane: chloroform 3:7. The HRESIMS (Appendix A2) gave a pseudomolecular ion peak at $m/z = 317.1028$ $[M+H]^+$ which analysed for $C_{17}H_{16}O_6$ (found 316.0955; calculated 316.0947). The UV absorptions were 338 nm and 292 nm (Appendix B2). According to Kumar and Pendey (2013), flavanones show a very strong absorption at Band II between 270 and 295 nm and only a shoulder for Band I at 326 and 327 nm. The IR spectrum (Appendix C2) shows absorption bands at 3435 (OH stretch), 2924 (CH_3 stretch), 1636 (C=O stretch), 1619, 1458 (C=C stretch), and 1136 (C-O stretch) cm^{-1} .

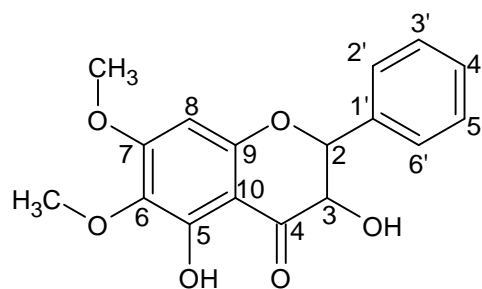
The 1H NMR and ^{13}C NMR of compound **M12** (Figure 4.4; Figure 4.5) were like compound **M1** except for the appearance of one more methoxy group (δ_H 3.71) at C-6 instead of aromatic proton in **M1**. In HMBC (Appendix D6),

it showed correlation between methoxy proton at δ_{H} 3.71 with δ_{C} 130.7 (C-6), and at δ_{H} 3.94 with δ_{C} 159.8 (C-7). H-8 (δ_{H} 6.19) showed correlations with C-10 (δ_{C} 101.3), C-6 (δ_{C} 130.7), C-9 (δ_{C} 158.7), and C-7 (δ_{C} 159.8). Through interpretation of spectra data $\{^1\text{H}, ^{13}\text{C}$ NMR, DEPT (Appendix D4), HMQC (Appendix D5), HMBC (Appendix D6) $\}$ and comparison with literature data (Chen et al., 2007), the compound was confirmed as (2*R*,3*R*) 3,5-dihydroxy-6,7-dimethoxyflavanone. Table 4.2 shows the ^1H , ^{13}C and HMBC spectra data of compound **M12**.

Table 4.2: ^1H , ^{13}C and HMBC spectral data of **M12** (acetone- d_6)

| Position | δ_{H} (multiplicity) | δ_{C} (C-type) | * δ_{C} (C-type) | HMBC |
|--------------------|------------------------------------|------------------------------|--------------------------------|------------------|
| 2 | 5.17 (1H, d, $J=12.2$ Hz) | 83.9 (CH) | 83.8 (CH) | C-2, 1' |
| 3 | 4.67 (1H, d, $J=12.2$ Hz) | 72.5(CH) | 72.5(CH) | C-3, 2', 6' |
| 4 | - | 198.2 (C) | 196.4 (C) | - |
| 5 | - | 154.6 (C) | 154.3 (C) | - |
| 6 | - | 130.7(C) | 130.9 (C) | C-2, 4' |
| 7 | - | 159.8 (C) | 161.7 (C) | - |
| 8 | 6.19 (1H, s) | 92.0 (CH) | 92.2 (CH) | C-10, 6, 9, 7 |
| 9 | - | 158.7 (C) | 158.8 (C) | - |
| 10 | - | 101.3 (C) | 100.9 (C) | - |
| 1' | - | 137.4 (C) | 136.0 (C) | - |
| 2', 6' | 7.57 (2H, m) | 127.6 (CH) | 127.4 (CH) | C-3', 5' |
| 3', 5' | 7.41 (2H, m) | 128.3 (CH) | 128.8 (CH) | C-2', 6', 3 |
| 4' | 7.41 (1H, m) | 128.8 (CH) | 129.5 (CH) | C-2',6' |
| 5-OH | 11.48 (1H, s) | - | - | C-6, 10 |
| 6-OCH ₃ | 3.71 (3H, s) | 59.7 (CH ₃) | 61.0 (CH ₃) | C-7 |
| 7-OCH ₃ | 3.94 (3H, s) | 55.9 (CH ₃) | 56.4 (CH ₃) | C-8 |

*Chen et al. (2007)



(M12)

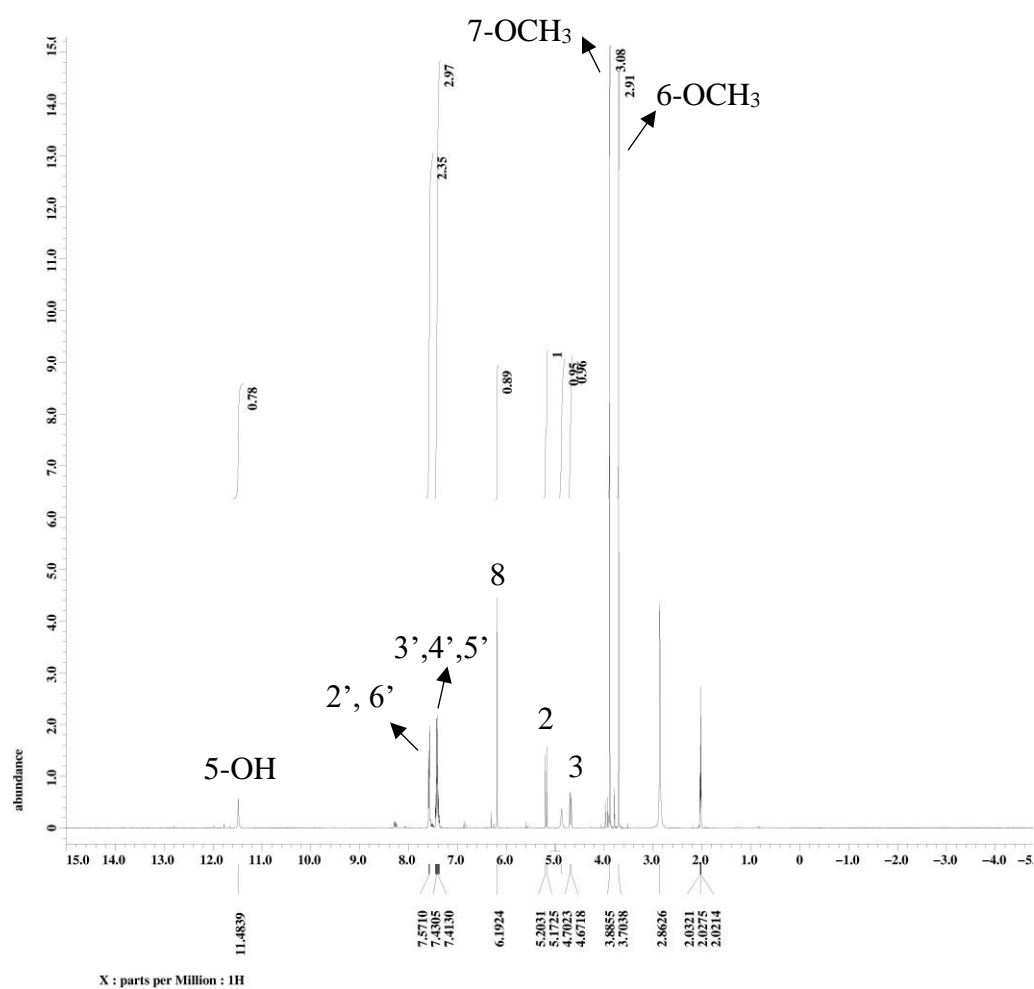
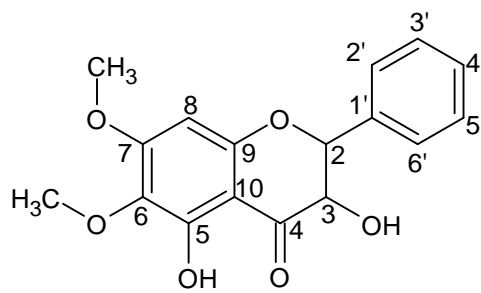


Figure 4.4: ¹H NMR (400 MHz, acetone-d₆) of (2*R*, 3*R*) 3,5-dihydroxy-6,7-dimethoxyflavanone (M12)



(M12)

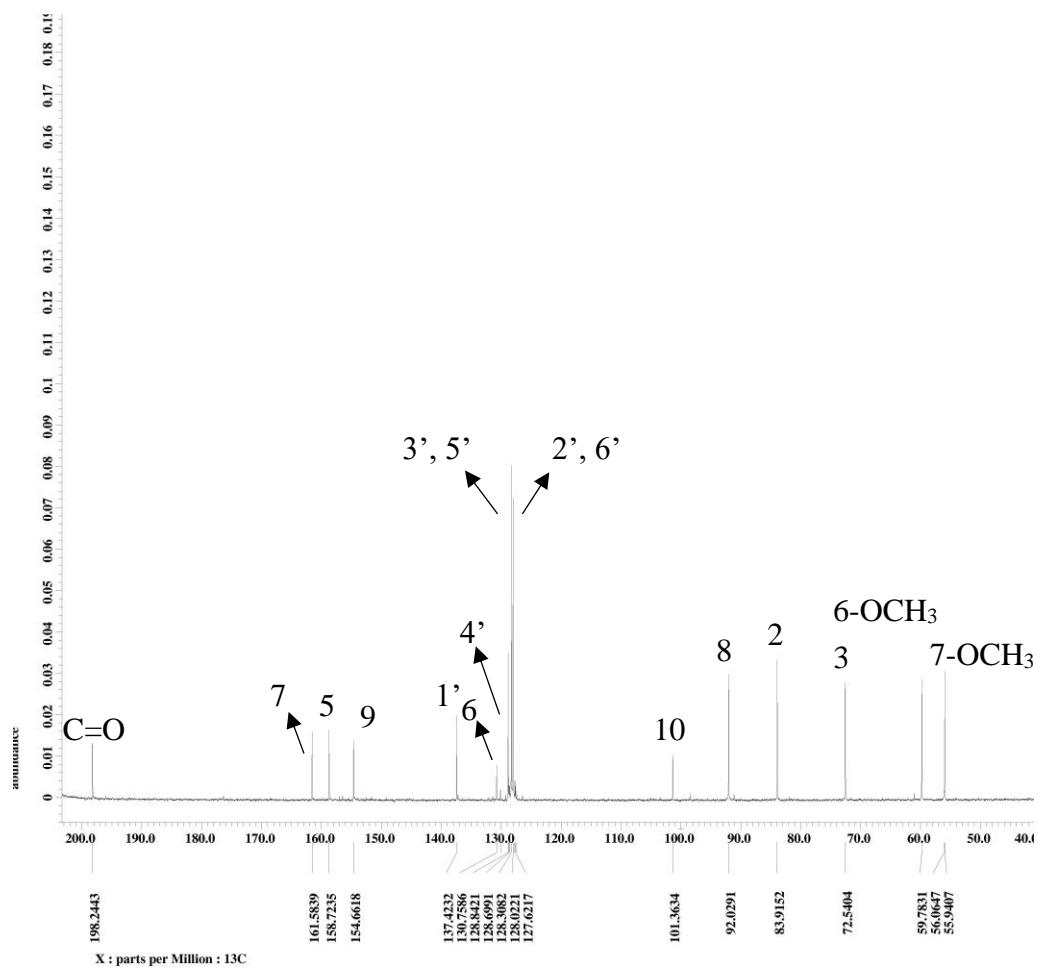
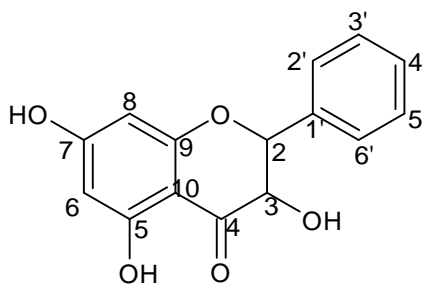


Figure 4.5: ^{13}C NMR (100 MHz, acetone- d_6) of (2*R*, 3*R*) 3,5-dihydroxy-6,7-dimethoxyflavanone (M12)

4.2.1.3 Characterization of (2*R*, 3*R*) 3,5,7-trihydroxyflavanone (M13)



(M13)

Compound **M13** was isolated as a white solid, mp 172-174 °C (Lit. 171-174 °C, Kuroyanagi et al., 1982). Its specific rotation is negative as $[\alpha]_D: +7.6^\circ$ (c 0.1, MeOH). It gave R_f value of 0.21 in mobile phase hexane: acetone 10:4. The HRESIMS (Appendix A3) gave a pseudomolecular ion peak at $m/z = 273.0760$ $[M+H]^+$ which analysed for $C_{15}H_{12}O_5$ (found 272.0690; calculated 272.0684). The UV absorptions were 332 nm and 292 nm (Appendix B3). The IR spectrum (Appendix C3) shows absorption bands at 3420 (OH stretch), 1636 (C=O stretch), 1618 (C=C stretch), and 1136 (C-O stretch) cm^{-1} .

The 1H NMR and ^{13}C NMR of compound **M13** (Figure 4.6; Figure 4.7) show the similar spectra to **M1** except the methoxy group at δ_H 3.84 in **M1** was replaced by OH group in **M13**. According to Kumar and Pandey (2013), flavonoids are hydroxylated phenolic substances. Therefore, based on the spectrum {DEPT (Appendix D7), HMQC (Appendix 8), and HMBC (Appendix 9)}, the substituent at C-7 is confirmed as hydroxy group. The structure of **M13** was confirmed as (2*R*, 3*R*) 3,5,7-trihydroxyflavanone as compared to published data (Kuroyanagi et al., 1982). This compound or

known as pinobanksin was reported isolated from aerial parts of *polygonum nodosum*. Table 4.3 shows the ^1H , ^{13}C and HMBC spectra data of compound **M13**.

Table 4.3: ^1H , ^{13}C and HMBC spectral data of M13 (acetone- d_6)

| Position | δ_{H} (multiplicity) | δ_{C} (C-type) | δ_{C}^* (C-type) | HMBC |
|----------|------------------------------------|------------------------------|--------------------------------|-----------------------|
| 2 | 5.15 (1H, d, $J=11.6$ Hz) | 83.5 (CH) | 83.5 (CH) | C-3, 2', 6', 1', 4 |
| 3 | 4.63 (1H, d, $J=11.6$ Hz) | 72.3 (CH) | 72.5 (CH) | C-2, 1', 4 |
| 4 | - | 197.1 (C) | 196.0 (C) | - |
| 5 | - | 164.2 (C) | 163.6 (C) | - |
| 6 | 5.95 (1H, d, $J=2.4$ Hz) | 96.3 (CH) | 96.9 (CH) | C-5, 7, 8, 10 |
| 7 | - | 167.1 (C) | 167.5 (C) | - |
| 8 | 5.98 (1H, d, $J=2.4$ Hz) | 95.2 (C) | 96.0 (C) | C-6, 9 |
| 9 | - | 163.1 (C) | 163.0 (C) | - |
| 10 | - | 100.6 (C) | 100.5 (C) | - |
| 1' | - | 137.4 (C) | 130.5 (C) | - |
| 2', 6' | 7.56 (2H, m) | 128.0 (CH) | 127.6 (CH) | C-2, 3', 5', 4' |
| 3', 5' | 7.40 (2H, m) | 128.3 (CH) | 128.6 (CH) | C-1', C4' |
| 4' | 7.40(1H, m) | 128.7 (CH) | 129.2 (CH) | C-2', 6' |
| 5-OH | 11.68 (1H, s) | - | - | C-6, 10, 5 |

*Kuroyanagi et al. (1982)

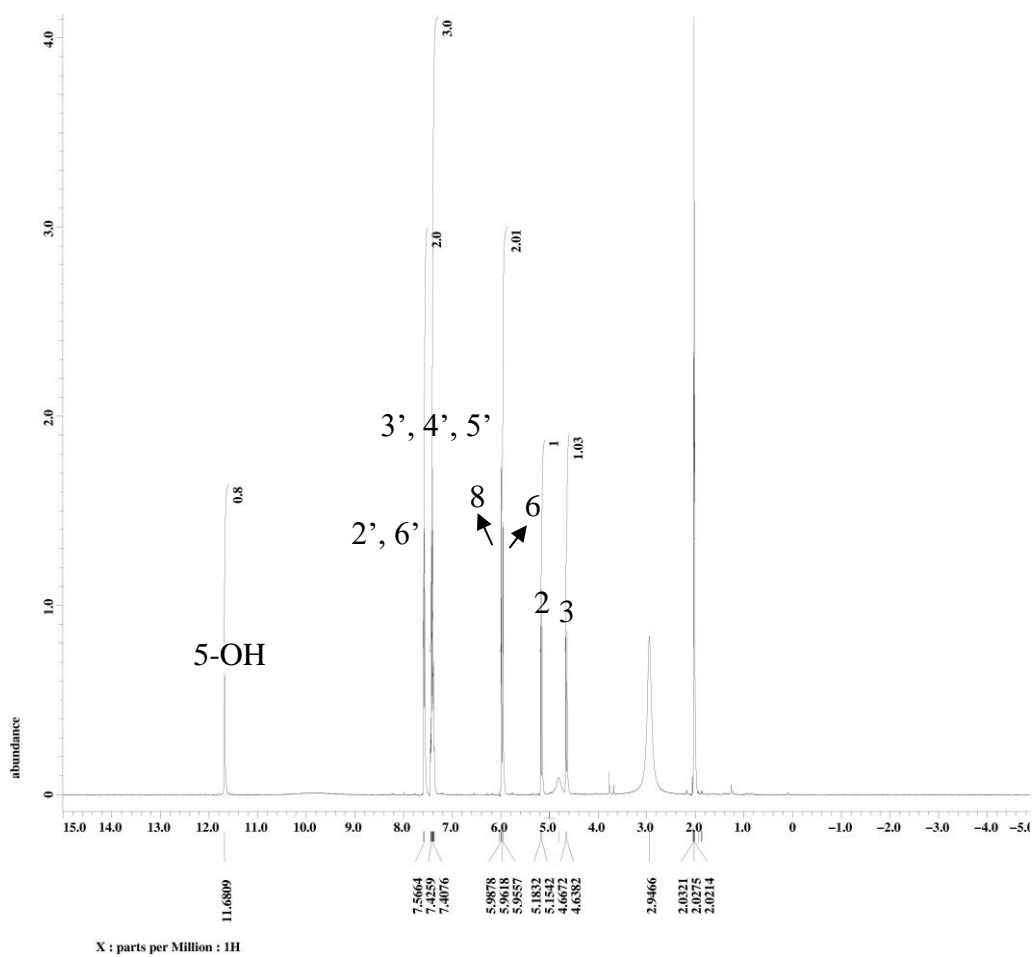
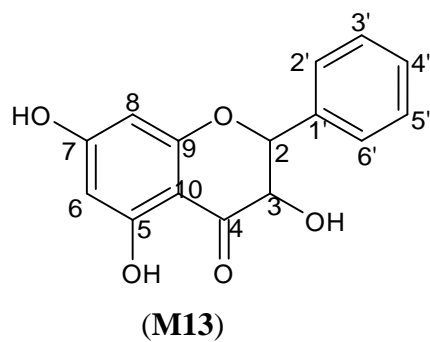
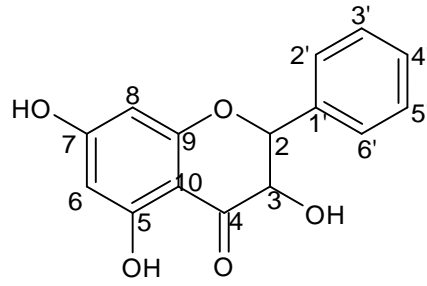


Figure 4.6: ^1H NMR (400 MHz, acetone- d_6) of (2*R*, 3*R*) 3,5,7-trihydroxyflavanone (M13)



(M13)

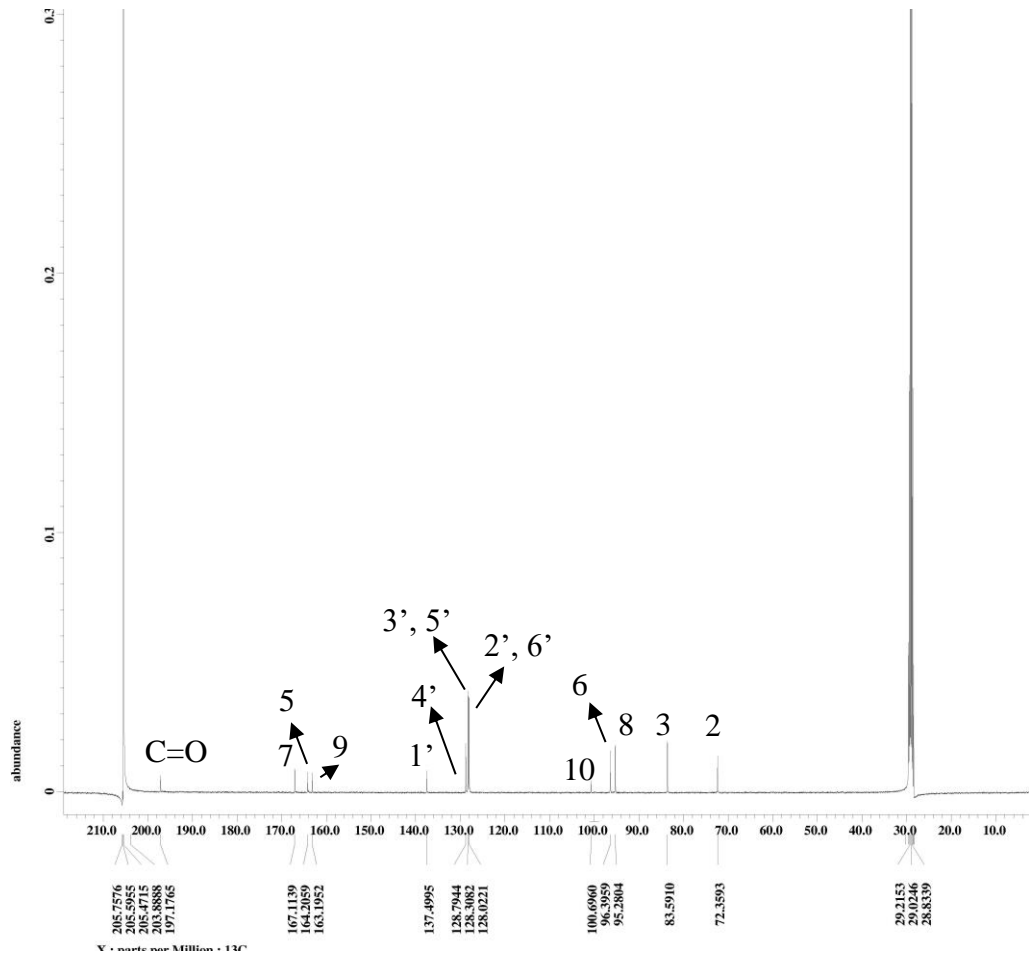
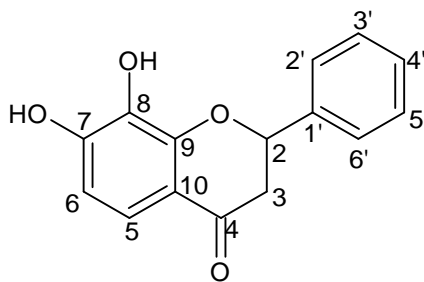


Figure 4.7: ^{13}C NMR (100 MHz, acetone- d_6) of (2*R*, 3*R*) 3,5,7-trihydroxyflavanone (M13)

4.2.1.4 Characterization of (2*S*) 7,8-dihydroxyflavanone (M17)



(M17)

Compound **M17** was isolated as a white solid, mp 162-164 °C (Lit. 164-166 °C, Hahm et al., 2003). Its specific rotation is positive as $[\alpha]_D: +14.3^\circ$. It gave R_f value of 0.14 in mobile phase hexane: acetone 7:2.5. Su et al. (2003) reported that most of the flavanones that obtained from natural sources have the 2*S* absolute configuration. Hence, the absolute configuration for this compound was determined as 2*S*. The HRESIMS (Appendix A4) gave a pseudomolecular ion peak at $m/z = 257.0815$ $[M+H]^+$ which analysed for $C_{15}H_{12}O_4$ (found 256.0742; calculated 256.07356). The UV absorptions were 349.5 nm and 293.3 nm (Appendix B4). The IR spectrum (Appendix C4) shows absorption bands at 3431 (OH stretch), 2359, 2341 (CH_3 stretch), 1637 (C=O stretch), 1617 (C=C stretch), and 1182 (C-O stretch) cm^{-1} .

The 1H NMR of compound **M17** (Figure 4.8) showed characteristic signals of flavanone moiety seen as a doublet of doublets at δ_H 5.53 ($J = 3.0, 12.8$ Hz) and two doublet of doublets further upfield at δ_H 3.07 ($J = 12.8, 16.5$ Hz), 2.74 ($J = 3.0, 16.8$ Hz), corresponding to H-2, H-3 α , and H-3 β respectively. Two aromatic multiplets at δ_H 7.44 (3H, m), δ_H 7.57 (2H, m) indicate

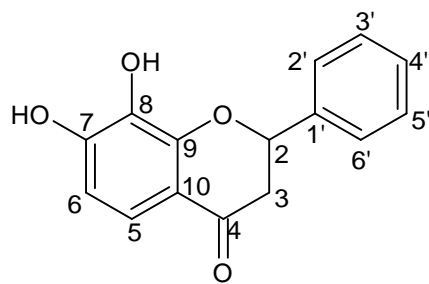
unsubstituted benzene ring B. The presence of hydroxy groups was revealed by the band at 3431(br) cm^{-1} , in the IR spectrum. The hydroxy groups were not appeared in ^1H NMR as deuterated proton exchangeable. The doublet at δ_{H} 6.58 and δ_{H} at 7.28 with coupling constant $J = 8.5$ Hz indicates both are ortho coupling which assigned as H-6 and H-5. In ^{13}C NMR of **M17** (Figure 4.9), δ_{C} 150.7 (C-7), δ_{C} 132.8 (C-8) and δ_{C} 151.9 (C-9) are oxygenated aromatic carbons. δ_{H} 80.3 and δ_{H} 44.3 are C-2, C-3 α and C3 β , respectively. In DEPT spectrum (Appendix D10), shows these carbons are methylene carbons. The structure of **M17** was confirmed by HMQC (Appendix D11) and HMBC (Appendix D12) spectra and compared with literature data (Hahm et al., 2003). This compound was reported isolated from the seeds of *Alpinia Katsumadai* Hayata and reported exhibited cytotoxic activity against cancer cell line A549 and K 562 with IC_{50} 0.20 mmol/mL and 0.056 mmol/mL, respectively (Hahm et al., 2003). Table 4.4 shows the summary NMR spectra data of compound **M17**.

Table 4.4: ¹H, ¹³C and HMBC spectral data of M17 (acetone-d₆)

| Position | δ _H (multiplicity) | δ _C (C-type) | * ^a δ _C (C-type) | HMBC |
|------------|--|-------------------------|--|--------------|
| 2 | 5.53 (1H, dd, <i>J</i> = 12.8, 3.0 Hz) | 80.3 (CH) | 80.4 (CH) | C-2', 6' |
| 3α | 3.07 (1H, dd, <i>J</i> =16.5, 12.8 Hz) | 44.3 (CH ₂) | 44.1 (CH ₂) | C-2, 4 |
| 3β | 2.74 (1H, dd, <i>J</i> = 16.5, 3.0 Hz) | 44.3 (CH ₂) | 44.1 (CH ₂) | C-4 |
| 4 | - | 189.7 (C) | 197.3 (C) | - |
| 5 | 7.28 (1H, d, <i>J</i> = 8.5 Hz) | 109.8 (CH) | 96.2 (CH) | C-4, 7 |
| 6 | 6.58 (1H, d, <i>J</i> = 8.5 Hz) | 118.0 (CH) | 97.1 (CH) | C-8, 9, 10 |
| 7 | - | 150.7 (C) | 168.4 (C) | - |
| 8 | - | 132.8 (C) | 165.4 (C) | - |
| 9 | - | 151.9 (C) | 164.6 (C) | - |
| 10 | - | 114.9 (C) | 103.3 (C) | - |
| 1' | - | 139.6 (C) | 140.4 (C) | - |
| 2', 6' | 7.57 (2H, m) | 126.6 (CH) | 127.3 (CH) | C-2, 3', 5' |
| 3', 4', 5' | 7.44 (3H, m) | 128.6 (CH) | 129.6 (CH) | C-1', 2', 6' |

* Hahm et al. (2003)

^aCD₃OD



(M17)

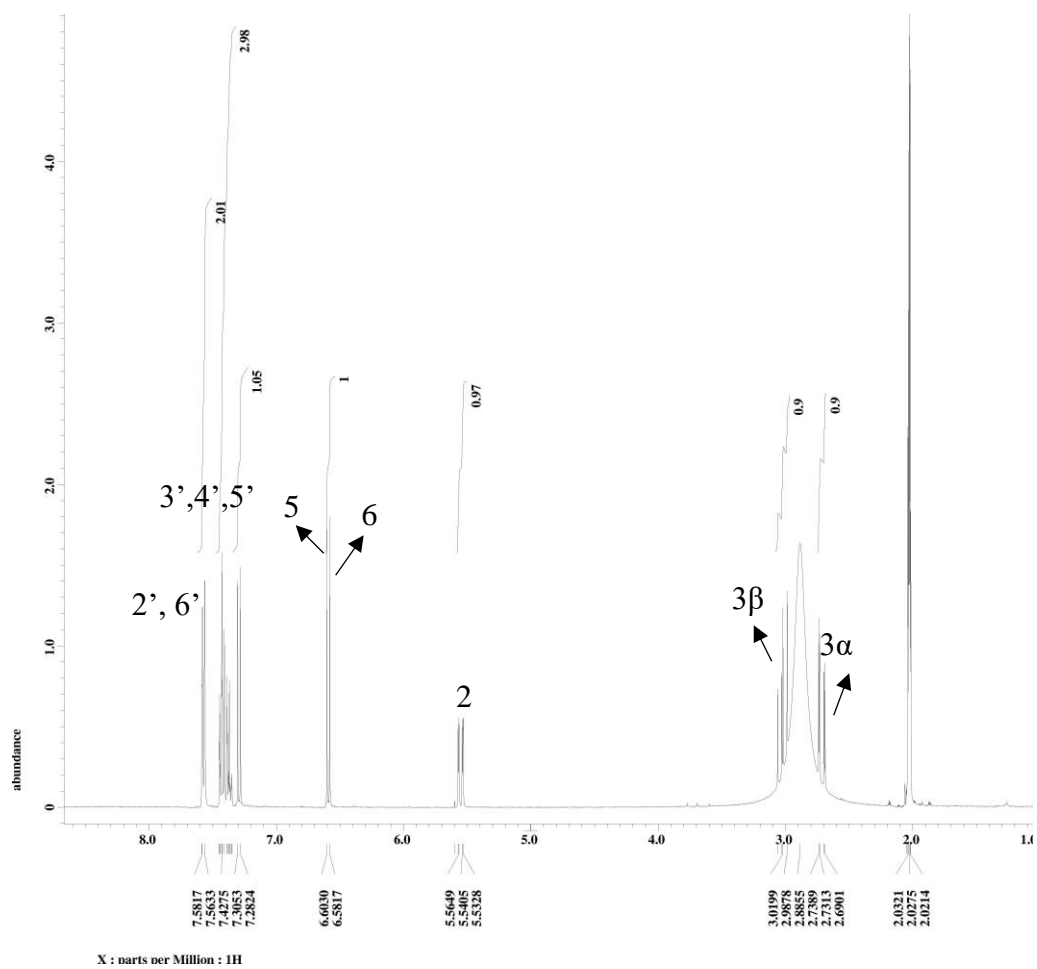
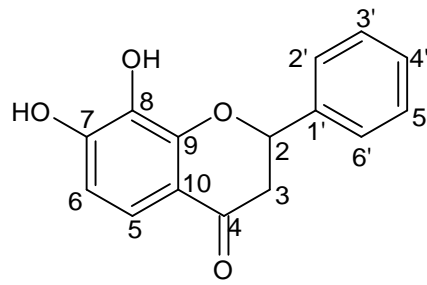


Figure 4.8: ^1H NMR (400 MHz, acetone- d_6) of (2S)-7,8-dihydroxyflavanone (M17)



(M17)

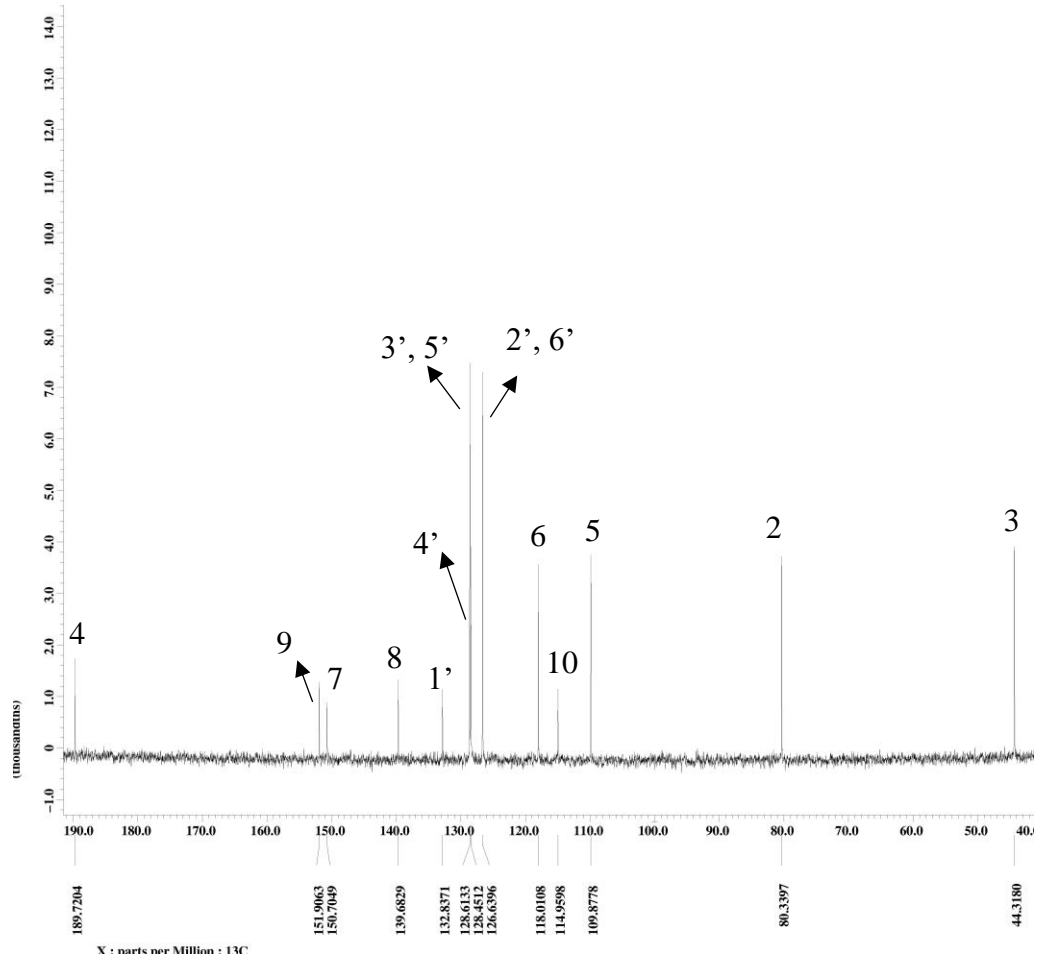
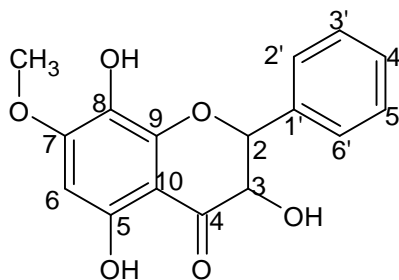


Figure 4.9: ^{13}C NMR (100 MHz, acetone- d_6) of (2S) 7,8-dihydroxyflavanone (M17)

4.2.1.5 Characterization of (2*R*, 3*R*) 3,5,7-trihydroxy-8-methoxyflavanone (M18)



(M18)

Compound **M18** was isolated as a yellow solid, mp 225-226 °C (Lit. 226-228 °C, Su et al., 2003). Its specific rotation is positive as $[\alpha]_D: +7.4^\circ$. The structure was confirmed as 2*R*, 3*R* as the coupling constant was same with the reported data (Su et al., 2003). It gave R_f value of 0.09 in mobile phase hexane: acetone 7:2.5. The HRESIMS (Appendix A5) gave a pseudomolecular ion peak at $m/z = 303.0862$ $[M+H]^+$ which analysed for C₁₆H₁₄O₆ (found 302.0789; calculated 302.0790). The UV absorptions were 358.7 nm and 293.6 nm (Appendix B5). The IR spectrum (Appendix C5) shows absorption bands at 3413 (OH stretch), 1637 (C=O stretch), 1618 (C=C stretch), and 1131 (C-O stretch) cm⁻¹.

The ¹H NMR (Figure 4.10) and ¹³C NMR (Figure 4.11) of compound **M18** are similar to compound **M1** except absence of aromatic H-8, hydroxyl group was present at C-8. In HMBC spectrum (Appendix D15), H-6 at δ_H 6.21 show correlations with C-8 (δ_C 127.3), C-10 (δ_C 100.8) and C-5 (δ_C 156.3).

Hence, hydroxyl group was assigned to C-8. Based on DEPT (Appendix D13), HMQC (Appendix D14), HMBC (Appendix D15) and compared with literature data (Su et al., 2003), the structure of **M18** was confirmed as (2*R*,3*R*) 3,5,7-trihydroxy-8-methoxyflavanone. Table 4.5 shows the ¹H, ¹³C and HMBC spectra data of compound **M18**.

Table 4.5: ¹H, ¹³C and HMBC spectral data of M18 (acetone-d₆)

| Position | δ _H (multiplicity) | δ _C (C-type) | * ^b δ _C (C-type) | HMBC |
|--------------------|---------------------------------|-------------------------|--|----------------|
| 2 | 5.15 (1H, d, <i>J</i> =11.6 Hz) | 83.7 (CH) | 82.9 (CH) | C-2',6' |
| 3 | 4.64 (1H, d, <i>J</i> =11.6 Hz) | 72.8 (CH) | 71.8(CH) | - |
| 4 | - | 197.9 (C) | 198.3(C) | - |
| 5 | - | 156.3 (C) | 155.2 (C) | - |
| 6 | 6.21 (1H, s) | 92.9 (CH) | 92.8 (CH) | C-5, 8, 10 |
| 7 | - | 157.3 (C) | 157.2(C) | - |
| 8 | - | 127.3 (C) | 147.7 (C) | - |
| 9 | - | 147.3 (C) | 155.5 (C) | - |
| 10 | - | 100.8 (C) | 101.0 (C) | - |
| 1' | - | 137.5 (C) | 137.3 (C) | - |
| 2', 6' | 7.58 (2H, m) | 128.1 (CH) | 128.0(CH) | C-2, 3',4', 5' |
| 3', 5' | 7.41 (2H, m) | 128.2 (CH) | 128.5 (CH) | C- 4' |
| 4' | 7.58 (1H, m) | 128.7 (CH) | 128.0 (CH) | C-2',6' |
| 3-OH | - | - | - | - |
| 5-OH | 11.35 (1H, s) | - | - | C-6, 5, 10 |
| 7-OCH ₃ | 3.89 (3H, s) | 55.9 (CH ₃) | 55.9 (CH ₃) | C-7 |

*Su et al. (2003)

^bDMSO-d₆

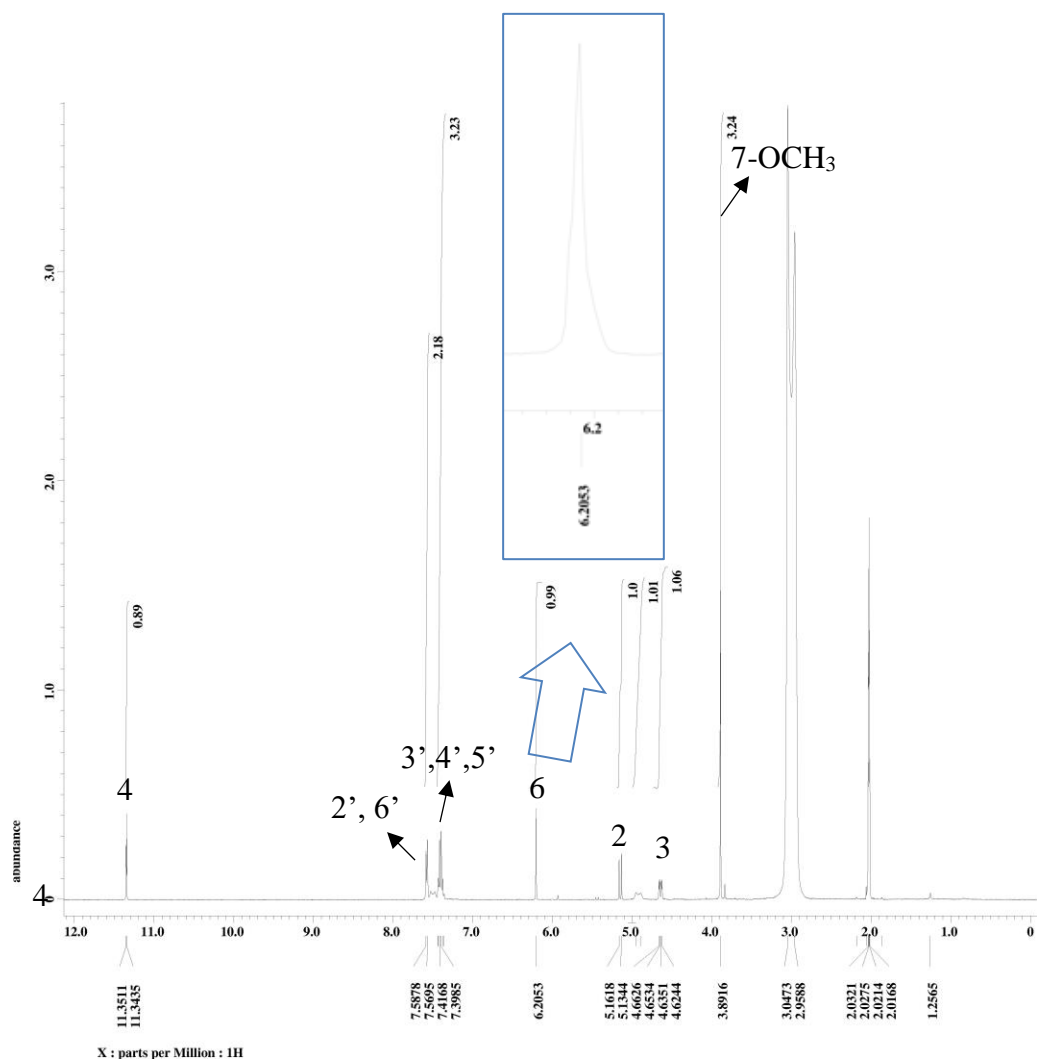
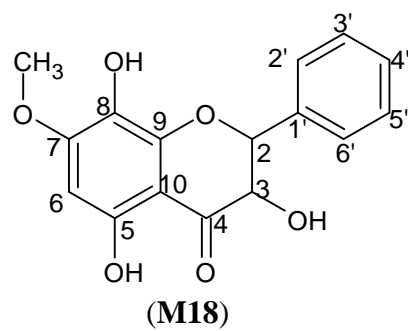
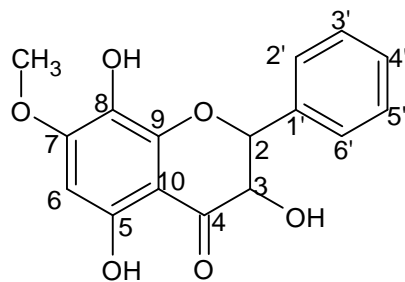


Figure 4.10: ¹H NMR (400 MHz, acetone-d₆) of (2*R*, 3*R*) 3,5,7-trihydroxy-8-methoxyflavanone (M18)



(M18)

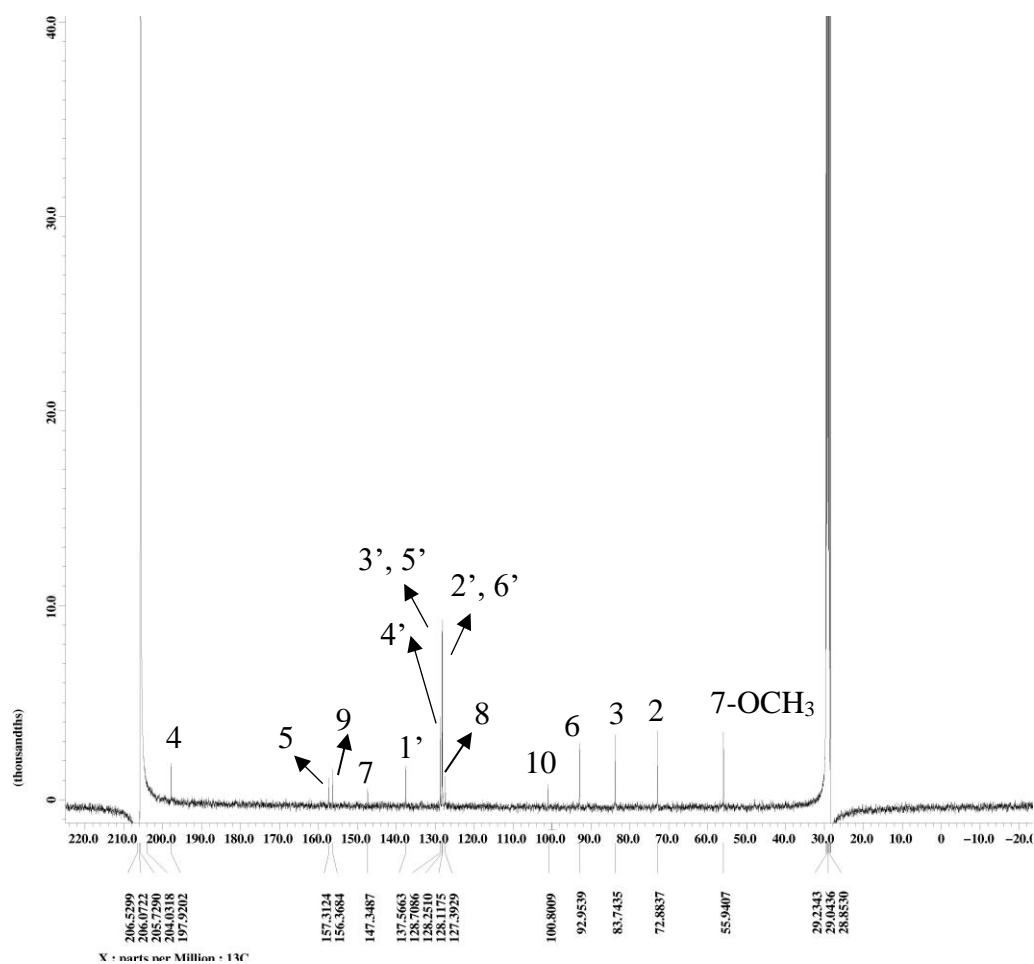
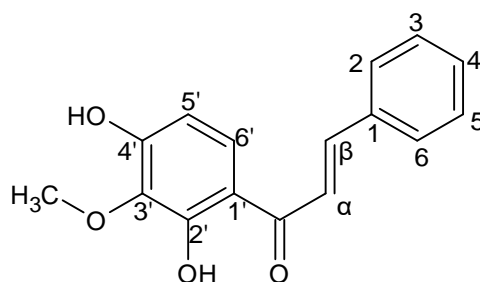


Figure 4.11: ¹³C NMR (100 MHz, acetone-d₆) of (2*R*, 3*R*) 3,5,8-trihydroxy-8-methoxyflavanone (M18)

4.2.2 Characterization and Structure Elucidation of Chalcones

Three chalcones were isolated from the leaves of *Muntingia calabura* i.e. 2',4'-dihydroxy-3'-methoxychalcone (**M2**), 2',4'-dihydroxychalcone (**M4**) and 2',3',4'-trihydroxychalcone (**M6**).

4.2.2.1 Characterization of 2',4'-dihydroxy-3'-methoxychalcone (**M2**)



(**M2**)

Compound **M2** was isolated as an orange solid, mp 127-128 °C (Lit. 126-128 °C, Buckingham & Munasinghe, 2015). It gave R_f value of 0.12 in mobile phase hexane: acetone 10:2. The HRESIMS (Appendix A6) gave a pseudomolecular ion peak at $m/z = 271.0793$ $[M+H]^+$ which analysed for $C_{16}H_{14}O_4$ (found 270.090; calculated 270.089). The UV absorption was 339.30 nm (Appendix B6). Aziz (2014) reported that chalcone only showed one absorption maxima (band I) whereas band II appeared as diminished in UV spectrum. The IR spectrum (Appendix C6) shows absorption bands at 3436 (OH stretch), 2941 (CH_3 stretch), 1634 (C=O stretch), 1593 (C=C stretch), and 1157 (C-O stretch) cm^{-1} .

In the ^1H NMR of **M2** (Figure 4.12), presence of two doublets at δ_{H} 7.58 (d, $J= 15.3$ Hz) and δ_{H} 7.90 (d, $J=15.3$ Hz) indicates the existence of the trans olefin H- α and H- β protons, respectively. A pair of doublets at δ_{H} 6.58 (d, $J= 9.2$ Hz) and at δ_{H} 7.62 (d, $J= 9.2$ Hz) are assigned to ortho-coupled protons at H-5' and H-6', respectively. Two multiplets at δ_{H} 7.42 (3H, H-3, 4, 5) and δ_{H} 7.65 (2H, H-2, 6) are characteristic of monosubstituted ring B. These signals indicate the compound is a chalcone. A signal at δ_{H} 13.57 is assign to phenolic OH chelated to the oxygen of the carbonyl group. A signal of methoxy group could be seen at δ_{H} 4.01.

In the ^{13}C NMR (Figure 4.13), three oxygenated carbons were observed at δ_{c} 157.9, δ_{c} 134.4, and δ_{c} 155.5 corresponding to C-2', C-3' and C-4', respectively. Due to position of C-3' that was ortho to C-2' and C-4' with electron donating hydroxyl group attached, therefore C-3' was at more upfield than C-2' and C-4'. Two quaternary aromatic carbons were observed at δ_{c} 115.1 and δ_{c} 134.8 was assigned to C-1' and C-1 respectively. Signals at δ_{c} 120.3 and δ 144.8 belong to two olefin carbons present in chalcone backbone was assigned as C- α and C- β respectively. Seven aromatic C-H were observed at δ_{c} 106.7 (C-5'), δ_{c} 126.4 (C-6'), δ_{c} 128.7 (C-2,6), δ_{c} 129.1 (C-3,5) and δ_{c} 130.9 (C-4). A methoxy group was detected at δ_{c} 60.9. Based on DEPT spectrum (Appendix D16), HMQC spectrum (Appendix D17), HMBC spectrum (Appendix D18) and comparison with literature data, compound **M2** was confirmed as 2',4'-dihydroxy-3'-methoxychalcone. The NMR data of **M2** was summarized in Table 4.6.

Table 4.6: ¹H, ¹³C and HMBC spectral data of M2 (CDCl₃)

| Position | δ _H (multiplicity) | *δ _H (multiplicity) | δ _C (Carbon type) | *δ _C (Carbon type) | HMBC |
|---------------------|----------------------------------|----------------------------------|------------------------------|-------------------------------|-------------------|
| 1 | - | - | 134.8 (C) | 134.7 (C) | - |
| 2,6 | 7.65 (2H, m) | 7.68 (2H, m) | 128.7 (CH) | 128.6 (CH) | C-1 |
| 3,5 | 7.42 (2H, m) | 7.46 (2H, m) | 129.1 (CH) | 129.0 (CH) | C-1 |
| 4 | 7.42 (1H, m) | 7.46 (1H, m) | 130.9 (CH) | 130.8 (CH) | - |
| α | 7.58 (1H, d, <i>J</i> = 15.3 Hz) | 7.56 (1H, d, <i>J</i> = 15.6 Hz) | 120.3 (CH) | 120.2 (CH) | C-1, β, C=O |
| β | 7.90 (1H, d, <i>J</i> = 15.3 Hz) | 7.92 (1H, d, <i>J</i> = 15.6 Hz) | 144.8 (CH) | 144.7 (CH) | C-1, 2, 6, α, C=O |
| C=O | - | - | 192.7 (C) | 192.6 (C) | - |
| 1' | - | - | 115.1 (C) | 115.0 (C) | - |
| 2' | - | - | 157.9 (C) | 157.8 (C) | - |
| 3' | - | - | 134.4 (C) | 134.3 (C) | - |
| 4' | - | - | 155.5 (C) | 155.3 (C) | - |
| 5' | 6.58 (1H, d, <i>J</i> = 9.2 Hz) | 6.59 (1H, d, <i>J</i> = 9.2 Hz) | 106.7 (CH) | 106.5 (CH) | C-1', 3', 4' |
| 6' | 7.62 (1H, d, <i>J</i> = 9.2 Hz) | 7.64 (1H, d, <i>J</i> = 9.2 Hz) | 126.4 (CH) | 129.3 (CH) | C-1', 2', 4', C=O |
| 2'-OH | 13.57 (1H, s) | 13.57 (1H, s) | - | - | - |
| 3'-OCH ₃ | 4.01 (3H, s) | 4.05 (3H, s) | 60.9 | 60.8 | C3' |
| 4'-OH | 9.27 (1H, s) | - | - | - | - |

*Ghani et. al. (2012)

This compound was reported isolated from the stem bark of *Polythia cauliflora* and showed strong cytotoxic activity against human leukemia HL60 cells with IC₅₀ value of 5.1 µg/ml (Ghani et al., 2012).

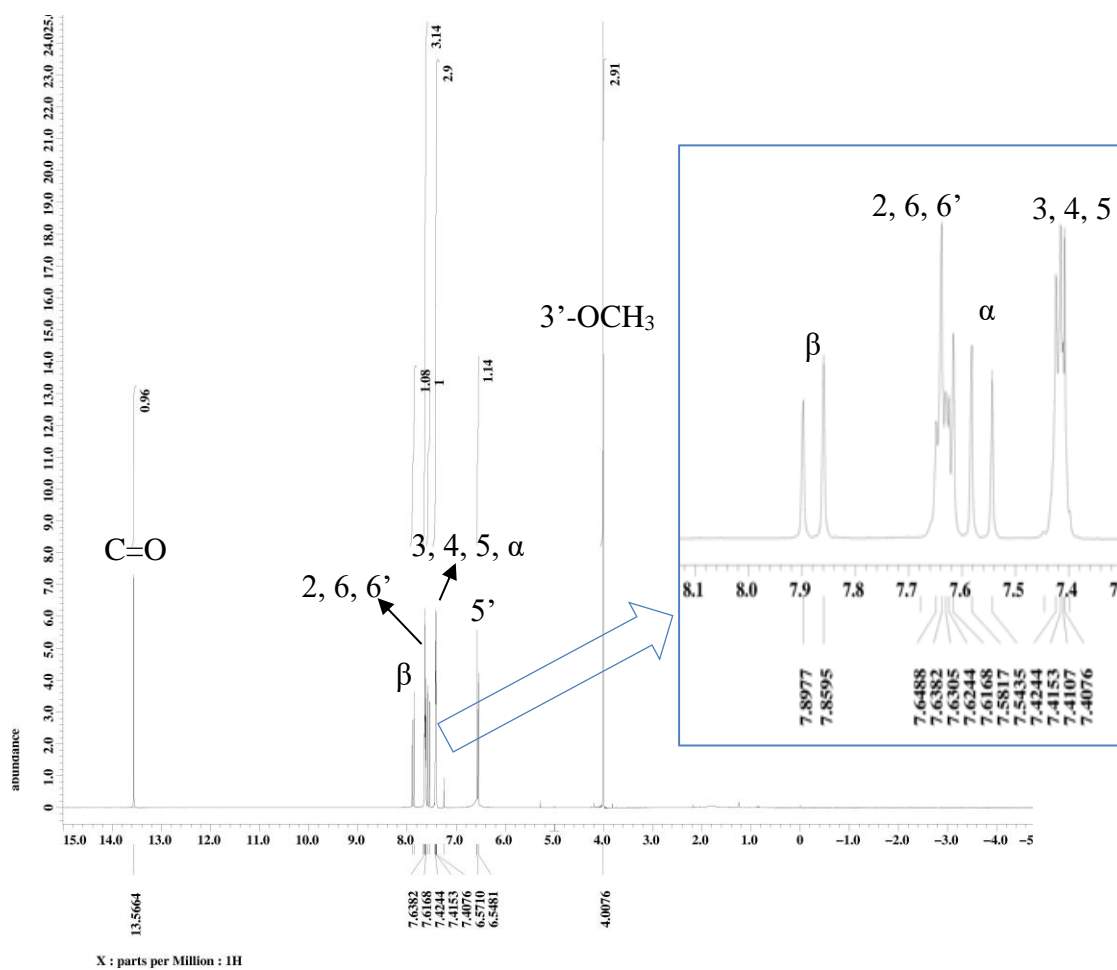
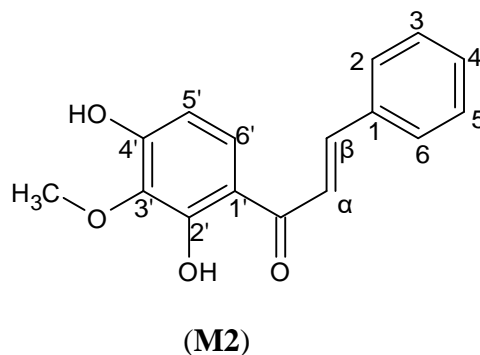


Figure 4.12: ¹H NMR (400 MHz, CDCl₃) of 2',4'-dihydroxy-3'-methoxychalcone (M2)

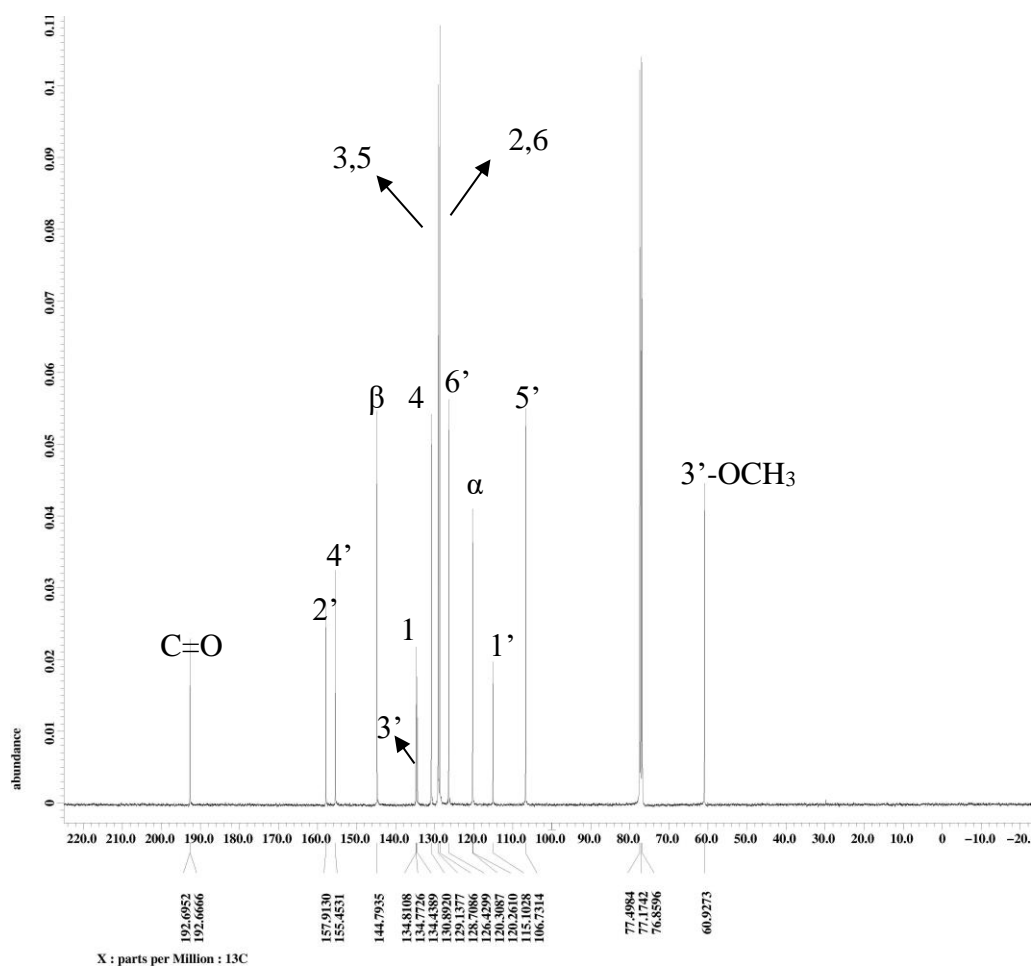
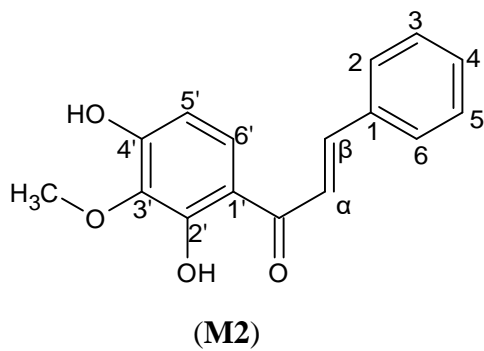
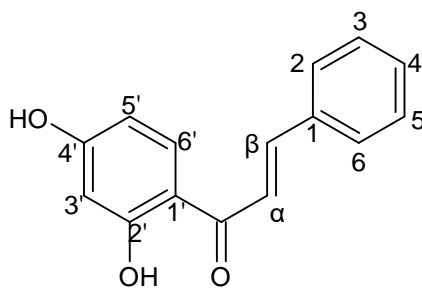


Figure 4.13: ^{13}C NMR (100 MHz, CDCl_3) of 2',4'-dihydroxy-3'-methoxychalcone (M2)

4.2.2.2 Characterization of 2',4'-dihydroxychalcone (M4)



(M4)

Compound **M4** was isolated as a yellow needle crystals, mp 145-146 °C (Lit. 148-149 °C, Nshimo et al., 1991). It gave R_f value of 0.12 in mobile phase hexane: acetone 10:2. The HRESIMS (Appendix A7) gave a pseudomolecular ion peak at $m/z = 241.0869 [M+H]^+$ which analysed for $C_{15}H_{12}O_3$ (found 240.0796; calculated 240.0786). The UV absorptions were 345 nm, 321 nm, and 263 nm (Appendix B7). The IR spectrum (Appendix C7) shows absorption bands at 3413 (OH stretch), 1635 (C=O stretch), 1495 (C=C stretch), and 1145 (C-O stretch) cm^{-1} .

The 1H NMR (Figure 4.14) of compound **M4** shows a pair of doublets at δ_H 7.83 and δ_H 7.92 were signals of H- α and H- β respectively. Two multiplets at δ_H 7.85 and δ_H 7.44 were characteristics of mono-substituted ring B. Signals at δ_H 6.36 (1H, d, $J= 2.4$ Hz) and δ_H 6.46 (1H, dd, $J= 9.3$ Hz, 2.1 Hz) were indicative of two meta-coupled protons which belong to H-3' and H-5', respectively. H-5' coupled to an adjacent proton at δ_H 8.15 (1H, d, $J=9.2$ Hz) which was H-6'.

The ^{13}C NMR (Figure 4.15) of compound **M4** showed similar pattern signals to compound **M2** except aromatic proton present at δ_c 102.9 (C-3') instead of methoxy group. Based on the spectral data {DEPT (Appendix D19), HMQC (Appendix D20), and HMBC (Appendix D21)}, and comparison with literature data, compound **M4** was characterized as 2',4'-dihydroxychalcone. This compound was reported isolated from the stem bark of *Polyalthia cauliflora* (Ghani et al., 2012). Table 4.7 shows the ^1H , ^{13}C NMR, and HMBC data of compound **M4**.

Table 4.7: ¹H, ¹³C and HMBC spectral data of M4 (acetone-d₆)

| Position | δ_{H} (multiplicity) | * δ_{H} (multiplicity) | δ_{C} (Carbon type) | * δ_{C} (Carbon type) | HMBC |
|----------|------------------------------------|--------------------------------------|-----------------------------------|-------------------------------------|------------------------|
| 1 | - | - | 135.1 (C) | 134.7 (C) | - |
| 2,6 | 7.85 (2H, m) | 7.67 (2H, m) | 129.0 (CH) | 128.6 (CH) | C-1, β , 4 |
| 3,5 | 7.44 (2H, m) | 7.45 (2H, m) | 128.9 (CH) | 129.0 (CH) | C-4, 1 |
| 4 | 7.44 (1H, m) | 7.45 (1H, m) | 130.7 (CH) | 130.7 (CH) | C-1 |
| β | 7.92 (1H, d, $J=15.9$ Hz) | 7.91 (1H, d, $J=15.6$ Hz) | 144.7 (CH) | 144.7 (CH) | C-1, C=O |
| α | 7.83 (1H, d, $J=15.9$ Hz) | 7.59 (1H, d, $J=15.6$ Hz) | 120.3 (CH) | 120.3 (CH) | C-1, 6', β , C=O |
| C=O | - | - | 192.0 (C) | 192.0 (C) | - |
| 1' | - | - | 113.6 (C) | 114.4 (C) | - |
| 2' | - | - | 166.9 (C) | 156.4 (C) | - |
| 3' | 6.36 (1H, d, $J=2.4$ Hz) | 6.46 (1H, d, $J=2.4$ Hz) | 102.9 (CH) | 103.8 (CH) | C-5', C1', 4' |
| 4' | - | - | 165.1 (C) | 162.9 (C) | - |
| 5' | 6.46 (1H, dd, $J=9.2, 2.1$ Hz) | 6.49 (1H, dd, $J=9.2, 2.1$ Hz) | 108.1 (CH) | 107.9 (CH) | C-3', C1' |
| 6' | 8.14 (1H, d, $J=9.2$ Hz) | 7.85 (1H, d, $J=9.2$ Hz) | 132.8 (CH) | 132.0 (CH) | C- α , 4', C=O |
| 2'-OH | 13.45 (1H, s) | 13.41 (1H, s) | - | - | C1', C4', C2' |

* Ghani et al. (2012)

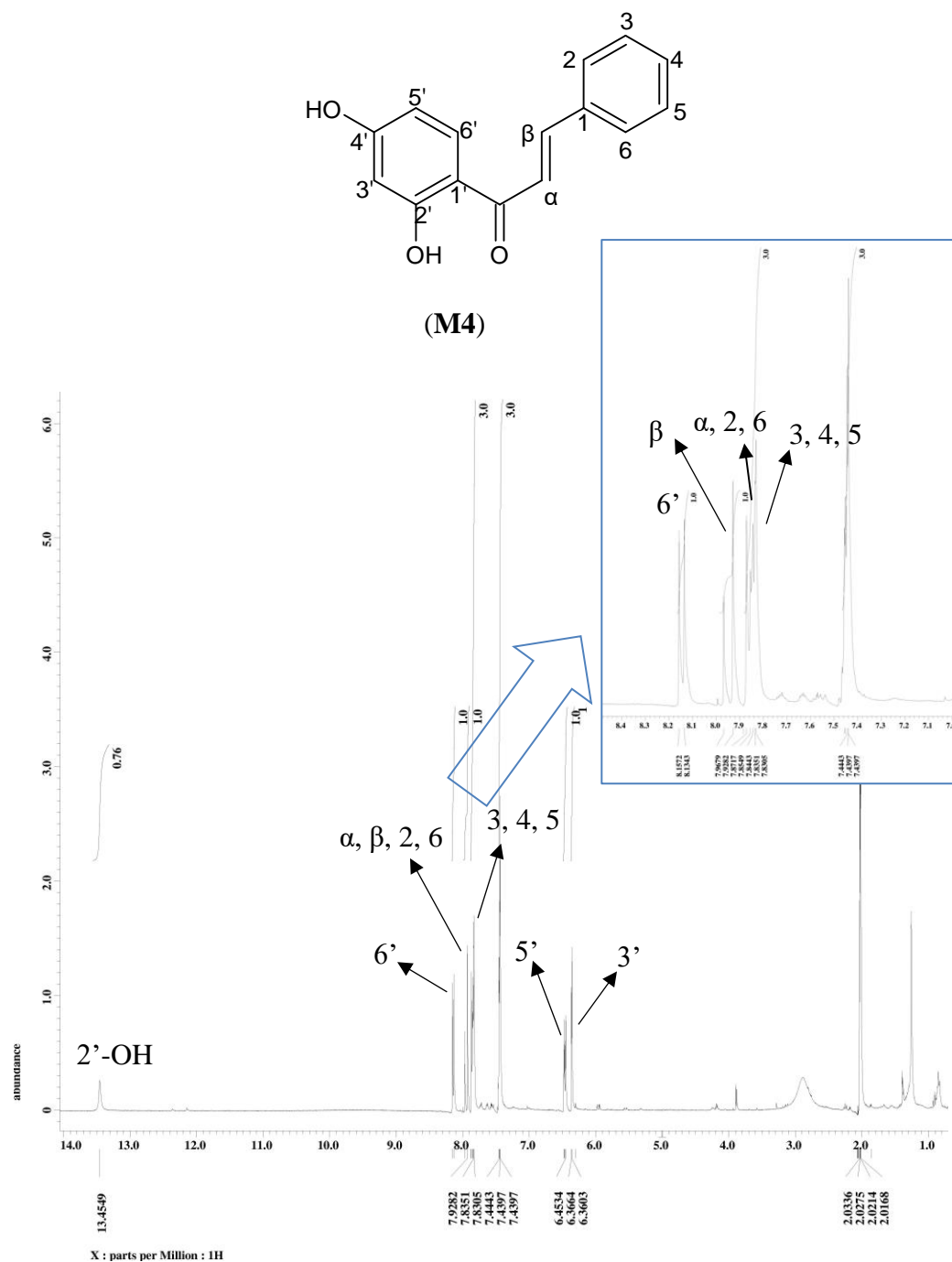
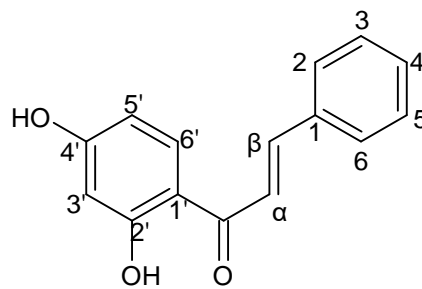


Figure 4.14: ^1H NMR (400 MHz, acetone- d_6) of 2',4'-dihydroxychalcone (M4)



(M4)

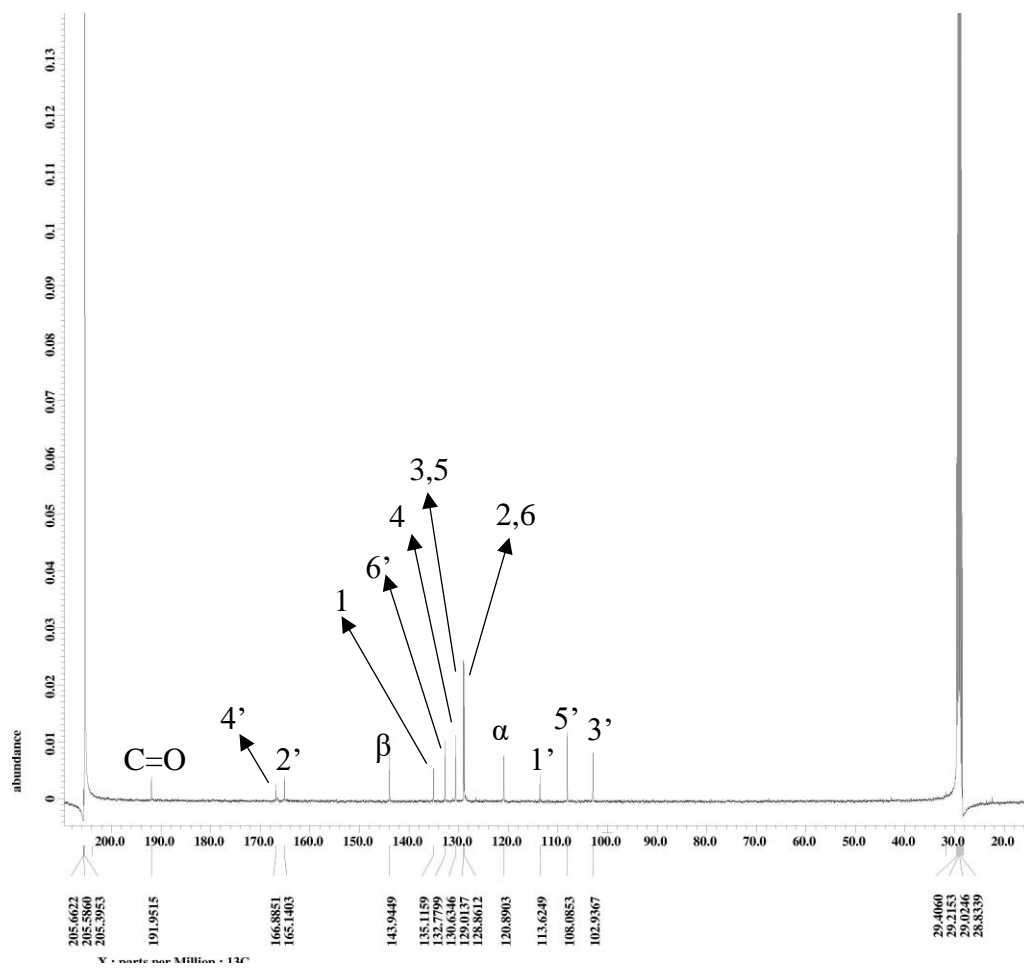
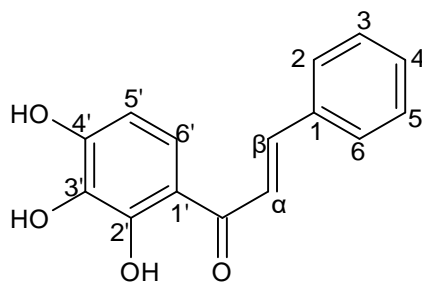


Figure 4.15: ^{13}C NMR (100 MHz, acetone- d_6) of 2',4'-dihydroxychalcone (M4)

4.2.2.3 Characterization of 2',3',4'-trihydroxychalcone (M6)



(M6)

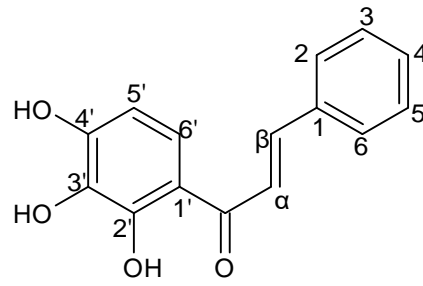
Compound **M6** was isolated as an orange needle crystals, mp 173-175 °C. It gave R_f value of 0.40 in mobile phase chloroform: methanol 10:1. The HRESIMS (Appendix A8) gave a pseudomolecular ion peak at $m/z = 257.0809$ $[M+H]^+$ which analysed for $C_{15}H_{13}O_4$ (found 256.0736; calculated 256.0736). The UV absorptions were 345 nm, 300 nm, and 231 nm (Appendix B8). The IR spectrum (Appendix C8) shows absorption bands at 3436 (OH stretch), 1636 (C=O stretch), 1572 (C=C stretch), and 1171 (C-O stretch) cm^{-1} .

The 1H NMR (Figure 4.17) and ^{13}C NMR (Figure 4.18) of compound **M6** show similar pattern signals as compound **M2** except the hydroxyl group at C-3' replaced 3'-OCH₃ of compound **M2**. In 1H NMR, a downfield signal at δ_H 13.47 was a chelated hydroxyl group at C-2', whereas signal at δ_H 8.86 was hydroxyl group at C-4'. C-3' hydroxyl group was not appeared in 1H NMR due to hydrogen-deuterium exchange. In the HMBC spectrum (Appendix D24), 4'-OH showed correlation with C-5' (δ_c 107.6), C-3' (δ_c 132.5) and C-4' (δ_c 152.2) which confirmed the hydroxy group at C-4'. Based on the spectrals including

DEPT (Appendix D22) and HMQC (Appendix D23), compound M6 was confirmed as 2',3',4'-trihydroxychalcone. Table 4.8 shows the summary data of compound M6.

Table 4.8: ^1H , ^{13}C and HMBC spectral data of M6 (acetone- d_6)

| Position | δ_{H} (multiplicity) | δ_{C} (Carbon type) | HMBC |
|----------|------------------------------------|-----------------------------------|------------------------------|
| 1 | - | 135.0 (C) | - |
| 2,6 | 7.84 (2H, m) | 128.8 (CH) | C-1, 3, 4, 5, β |
| 3,5 | 7.45 (2H, m) | 129.0 (CH) | C-1, 2, 6 |
| 4 | 7.45 (1H, m) | 130.6 (CH) | C-1 |
| β | 7.93 (1H, d, $J = 15.6$ Hz) | 143.9 (CH) | C-6', 1, |
| α | 7.85 (1H, $J = 15.6$ Hz) | 120.8 (CH) | C- β , 1 |
| C=O | - | 192.5 (C) | - |
| 1' | - | 113.8 (C) | - |
| 2' | - | 153.5 (C) | - |
| 3' | - | 132.5 (C) | - |
| 4' | - | 152.2 (C) | - |
| 5' | 6.50 (1H, d, $J = 9.2$ Hz) | 107.6 (CH) | C-1', 3', 4' |
| 6' | 7.72 (1H, d, $J = 9.2$ Hz) | 122.6 (CH) | C-1', α , 3', 2', C=O |
| 2'-OH | 13.47 (1H, s) | - | C-5', 3', 2' |
| 3'-OH | - | - | - |
| 4'-OH | 8.86 (1H, s) | - | C-5', 4', 3' |



(M6)

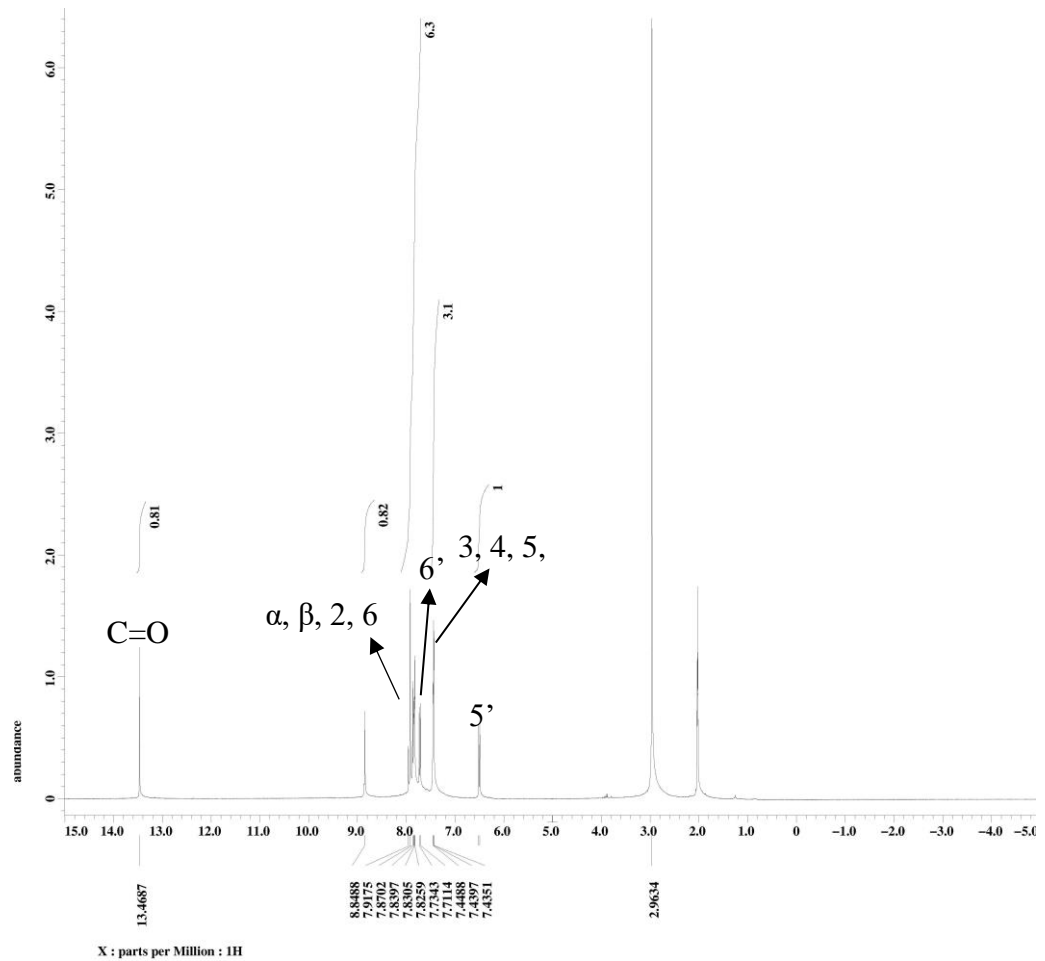


Figure 4.16: ^1H NMR (400 MHz, acetone- d_6) of 2', 3', 4'-trihydroxychalcone (M6)

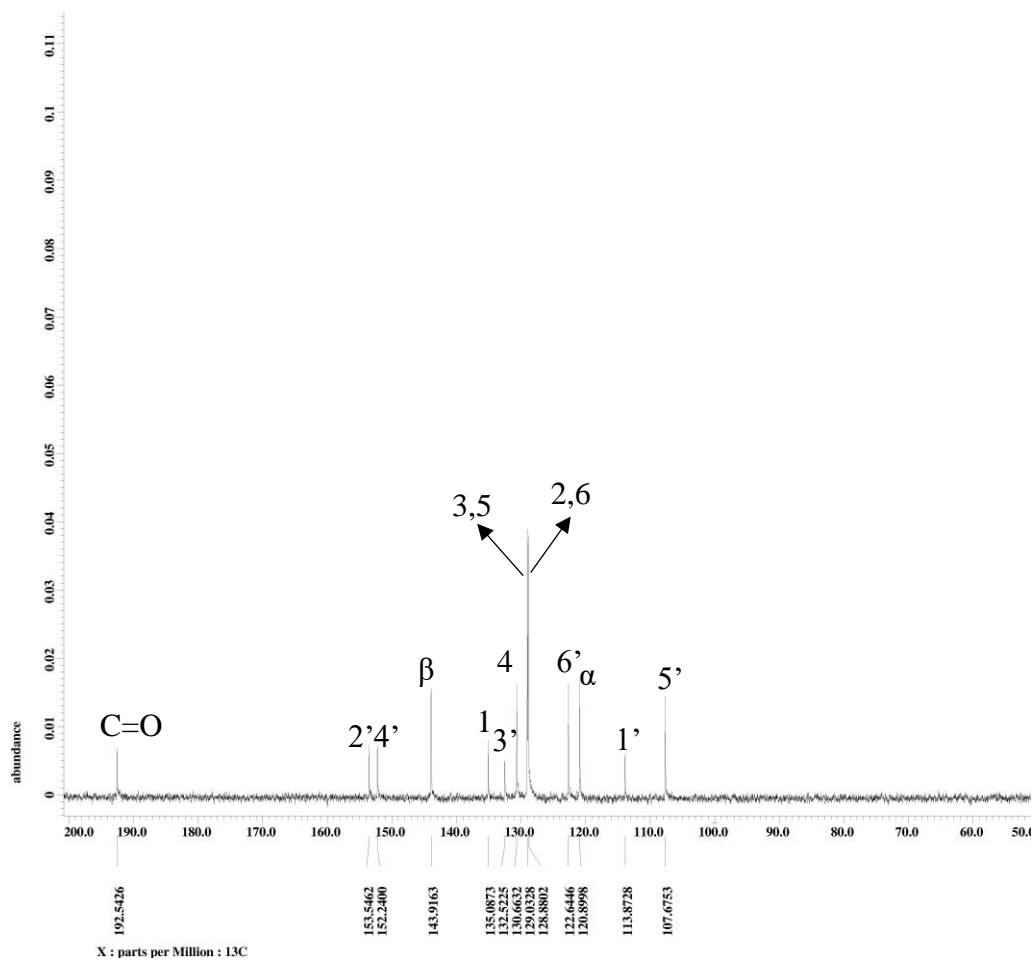
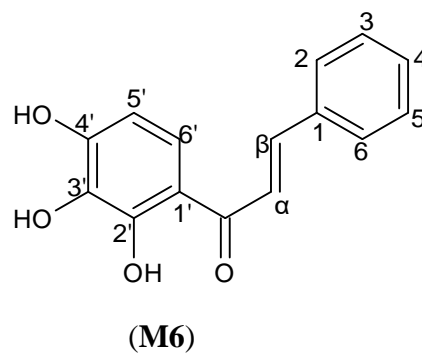
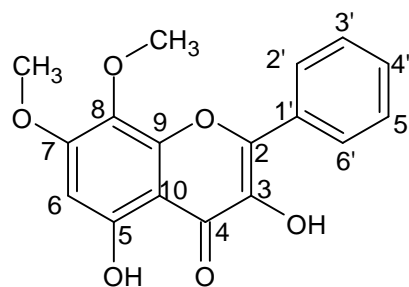


Figure 4.17: ^{13}C NMR (100 MHz, acetone- d_6) of 2',3',4'-trihydroxychalcone (M6)

4.2.3 Characterization and Structure Elucidation of Flavones

Ten flavones were isolated from the leaves of *Muntingia calabura* i.e. 3,5-dihydroxy-6,7-dimethoxyflavone (**M3**), 3,5,7-trihydroxy-8-methoxyflavone (**M5**), 5-hydroxy-3,7-dimethoxyflavone (**M7**), 3,5-dihydroxy-7-methoxyflavone (**M8**), 5-hydroxy-7-methoxyflavone (**M9**), 5-hydroxy-3,7,8-trimethoxyflavone (**M10**), 5,7-dihydroxy-3,8-dimethoxyflavone (**M11**), 5,7-dihydroxyflavone (**M14**), 5-hydroxy-6,7-dimethoxyflavone (**M15**), and 5,4'-dihydroxy-3,7-dimethoxyflavone (**M16**).

4.2.3.1 Characterization of 3,5-dihydroxy-7,8-dimethoxyflavone (**M3**)



(**M3**)

Compound **M3** was isolated as a yellow solid, mp 199-202 °C. It gave R_f value of 0.24 in mobile phase hexane: acetone 8:2. The HRESIMS (Appendix A9) gave a pseudomolecular ion peak at $m/z = 315.0871$ $[M+H]^+$ which analysed for $C_{17}H_{14}O_6$ (found 314.0798; calculated 314.07904). The UV absorptions were 328 nm, and 271 nm (Appendix B9). The IR spectrum (Appendix C9) shows

absorption bands at 3435 (OH stretch), 2973, 2935 (CH₃ stretch), 1652 (C=O stretch), 1619 (C=C stretch), and 1180 (C-O stretch) cm⁻¹.

The ¹H NMR (Figure 4.18) and ¹³C NMR (Figure 4.19) of compound **M3** showed a flavone structure for compound **M3**. In the ¹H NMR of compound **M3**, signals at δ_H 3.92 and δ_H 3.97 indicate the presence of two methoxy groups. Two multiplets at δ_H 7.51 and δ_H 8.17 were characteristic of unsubstituted benzene ring B which assigned to H-3',4',5' and H-2',6' respectively. Signals at δ_H 11.61 was belonging to chelated hydroxyl group at C-5 and δ_H 6.74 was assigned to hydroxyl proton at C-3. An aromatic singlet proton at δ 6.56 was proton at C-6.

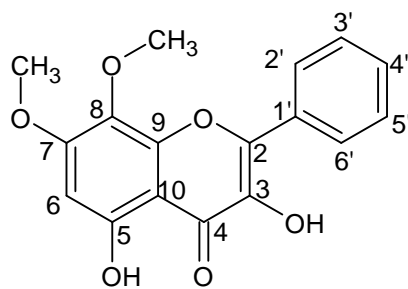
In the ¹³C NMR of compound **M3**, there were 15 carbon signals and two methoxy groups carbon signals. Signal at δc 175.6 was the carbonyl group at C-4 which bonded to hydroxyl group at C-5. Four aromatic oxygenated carbons were observed at δc 152.6 (C-5), δc 136.6 (C-3), δc 159.5 (C-7) and δc 132.3 (C-8). Signal at δc 175.6 was a typical of a hydrogen-bonded 3-hydroxyflavone carbonyl at C-4 for the hydroxyl groups at C-3 and C-5 (Nshimo, 1991). Signals at δc 130.8, δc 127.7, δc 128.7 and δc 130.8 represented C1', C-2',6', C-3',5' and C-4', respectively, of mono substituted flavone B-ring. Two methoxy groups signals were indicated at δc 56.4 (7-OCH₃) and δc 61.0 (8-OCH₃). C-8 methoxy group was more deshielded due to the 8-OCH₃ located near to electronegative oxygen atom at position 1. Signals at δc 104.6 and δc 151.5 were assigned to C-9 and C-10, respectively. C-9 showed a lower chemical shift as C-9 bonded to electronegative oxygen atom. C-6 at δc 90.8 displayed up-field chemical shift as

there were electron donating group at C-5 and C-7. The structure was further confirmed by DEPT (Appendix D25), HMQC (Appendix D26), HMBC (Appendix D27) and comparison with literature data (Su et al., 2003). Table 4.9 shows the summary data of compound **M3**.

Table 4.9: ^1H , ^{13}C and HMBC spectral data of M3 (CDCl_3)

| Position | δ_{H} (multiplicity) | δ_{C} (C-type) | * δ_{C} | HMBC |
|--------------------|---------------------------------------|------------------------------|-----------------------|---------------------|
| 2 | - | 145.5 (C) | 145.3 | - |
| 3 | - | 136.6 (C) | 136.6 | - |
| 4 | - | 175.6 (C) | 175.8 | - |
| 5 | - | 152.6 (C) | 156.4 | - |
| 6 | 6.56 (1H, s) | 90.8 (CH) | 95.2 | C-5, 7, 8, 10 |
| 7 | - | 159.5 (C) | 158.7 | - |
| 8 | - | 132.3 (C) | 129.1 | - |
| 9 | - | 151.5 (C) | 156.4 | - |
| 10 | - | 104.6 (C) | 103.3 | - |
| 1' | - | 130.8 (C) | 130.9 | - |
| 2', 6' | 7.51 (2H, m) | 127.7 (CH) | 127.7 | C-2, 1', 3', 5', 4' |
| 3', 5' | 8.17 (2H, m) | 128.7 (CH) | 128.7 | C-1', 2', 6', 4' |
| 4' | 7.51 (1H, m) | 130.8 (CH) | 130.4 | C-1', 2', 6' |
| 3-OH | 6.74 (1H, s) | - | - | - |
| 5-OH | 11.61 (1H, s) | - | - | C-8, 5, 10 |
| 7-OCH ₃ | 3.96 (3H, s) | 56.4 (CH ₃) | 56.4 | C-7 |
| 8-OCH ₃ | 3.92 (3H, s) | 61.0 (CH ₃) | 61.6 | C-8 |

*Su et al., 2003



(M3)

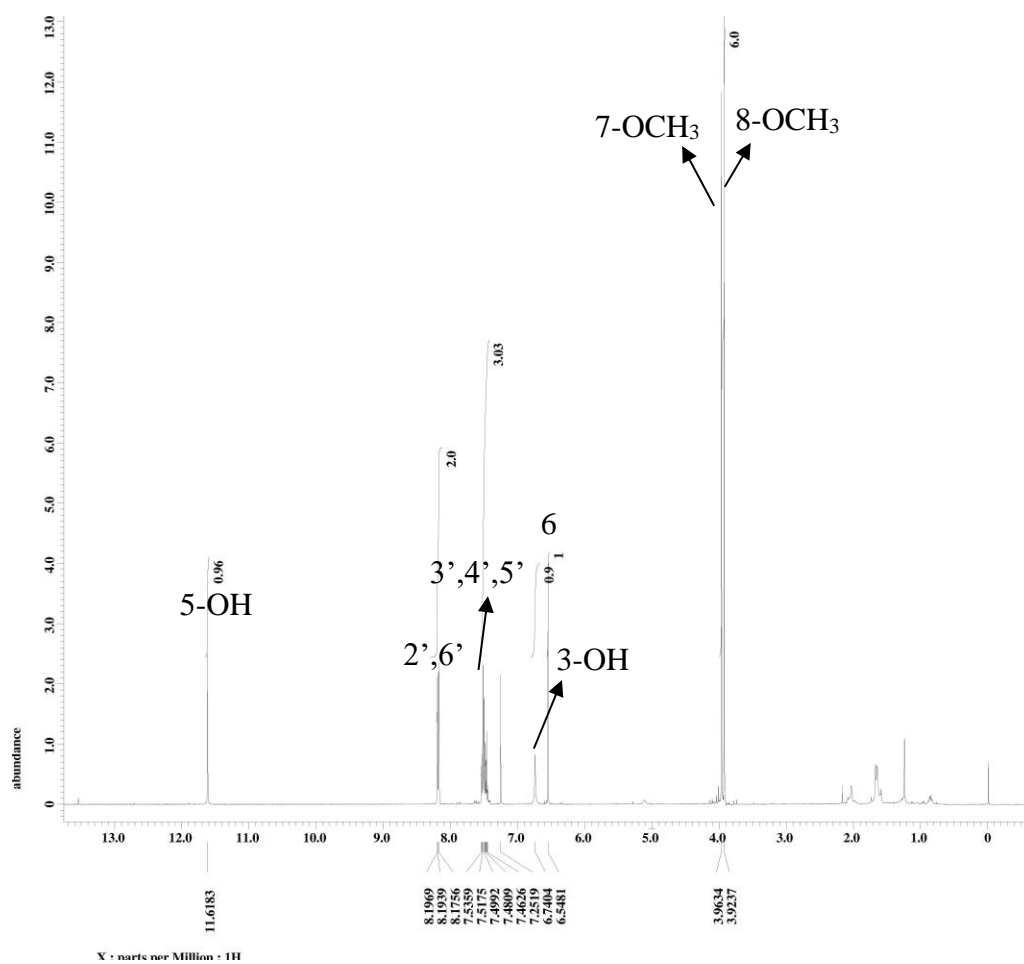


Figure 4.18: ^1H NMR (400 MHz, CDCl_3) of 3,5-dihydroxy-7,8-dimethoxyflavone (M3)

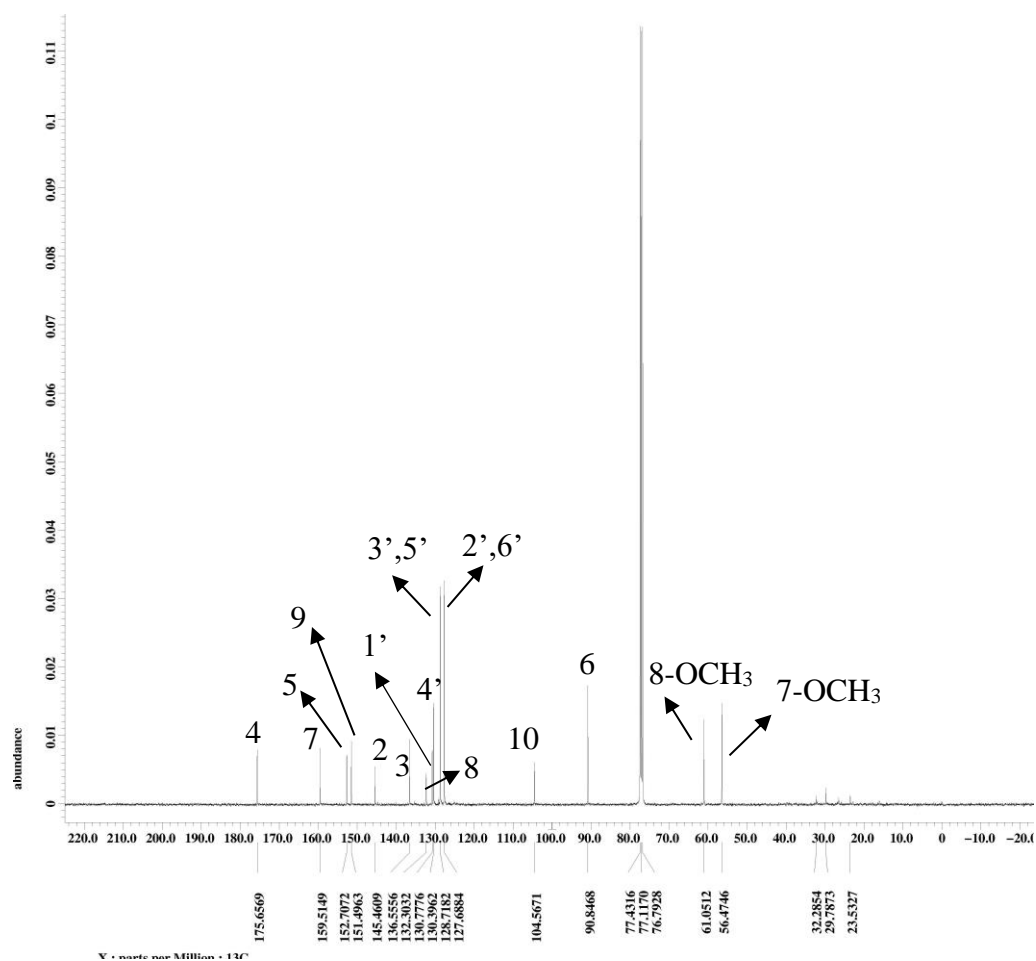
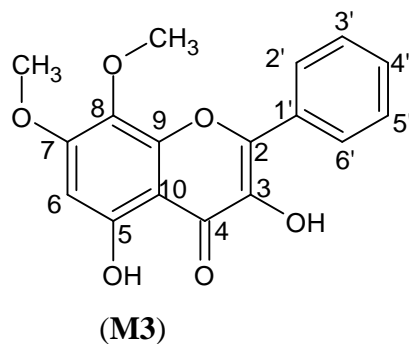
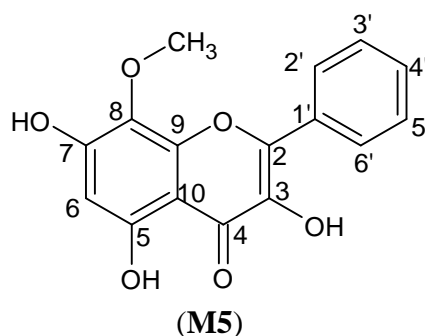


Figure 4.19: ^{13}C NMR (100 MHz, CDCl_3) of 3,5-dihydroxy-7,8-dimethoxyflavone (M3)

4.2.3.2 Characterization of 3, 5, 7-trihydroxy-8-methoxyflavone (**M5**)



Compound **M5** was isolated as a yellow solid, mp 205-207 °C (Lit. 203-205 °C, Nshimo, 1991). It gave R_f value of 0.23 in mobile phase hexane: acetone 7:3. The HRESIMS (Appendix A10) gave a pseudomolecular ion peak at $m/z = 301.0704$ $[M+H]^+$ which analysed for $C_{16}H_{12}O_6$ (found 300.0643; calculated 300.0639). The UV absorptions were 367 nm, 309 and 273 nm (Appendix B10). The IR spectrum (Appendix C10) shows absorption bands at 3393 (OH stretch), 3066 (aromatic CH stretch), 2946 (CH_3 stretch), 1654 (C=O stretch), 1625 (C=C stretch), and 1172 (C-O stretch) cm^{-1} .

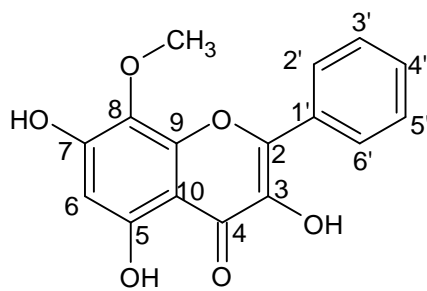
The 1H NMR (Figure 4.20) and ^{13}C NMR (Figure 4.21) of compound **M5** is similar to compound **M3**, except the substitution at C-7 is hydroxy group in **M5** instead of methoxy group in **M3**. One methoxy group at δ_H 3.93 was displayed in 1H NMR spectrum. The structure of compound **M5** was further confirmed by DEPT (Appendix D28), HMQC (Appendix D29), HMBC (Appendix D30) and compared with literature data (Nshimo, 1991). 1H NMR, ^{13}C NMR, and HMBC of compound **M5** was shown in Table 4.10.

This compound was reported isolated from the leaves of *Adenostoma sparsifolium*, bud excretion of *Platanus acerifolia* and leaves of *Muntingia calabura* (Sufian et al., 2013). Nshimo et al. (1993) reported that the cytotoxic activity of this compound was not active against eight cancer cell lines i.e. HT 1080, KB, KB-V1, Lu1, Mel2, P388, BC1 and Col2 with ED₅₀ values of > 10 µg/ml.

Table 4.10: ¹H, ¹³C and HMBC spectral data of M5 (acetone-d₆)

| Proton | δ _H (Multiplicity) | *δ _H (Multiplicity) | δ _C (Type of C) | *δ _C (Type of C) | HMBC |
|--------------------|-------------------------------|--------------------------------|----------------------------|-----------------------------|--------------|
| 2 | - | - | 145.2 (C) | 145.6 (C) | - |
| 3 | - | - | 137.2 (C) | 137.1 (C) | - |
| 4 | - | - | 176.3 (C) | 176.4 (C) | - |
| 5 | - | - | 156.5 (C) | 155.5 (C) | - |
| 6 | 6.30 (1H, s) | 6.33 (1H, s) | 98.4 (CH) | 98.5 (CH) | C-10, 8, 7 |
| 7 | - | - | 157.0 (C) | 156.8 (C) | - |
| 8 | - | - | 127.8 (C) | 127.5 (C) | - |
| 9 | - | - | 149.1 (C) | 148.6 (C) | - |
| 10 | - | - | 103.5 (C) | 103.1 (C) | - |
| 1' | - | - | 131.4 (C) | 131.1 (C) | - |
| 2',6' | 8.28 (2H, m) | 8.20 (2H, m) | 127.6 (CH) | 127.3 (CH) | C-1', 3', 5' |
| 3',5' | 7.57 (2H, m) | 7.58 (2H, m) | 128.7 (CH) | 128.6 (CH) | C-1', 2', 6' |
| 4' | 7.51 (1H, m) | 7.59 (1H, m) | 130.1(CH) | 129.9 (CH) | C-1', 2', 6' |
| 5-OH | 11.77 (1H, s) | 12.10 (1H, s) | - | - | C-6, 10, 7 |
| 8-OCH ₃ | 3.93 (3H, s) | 3.86 (3H, s) | 61.1(CH ₃) | 60.9 (CH ₃) | C-8 |
| 3-OH | 8.35 (1H, s) | - | - | - | - |
| 7-OH | 9.47 (1H, s) | - | - | - | - |

* Nshimo (1991)



(M5)

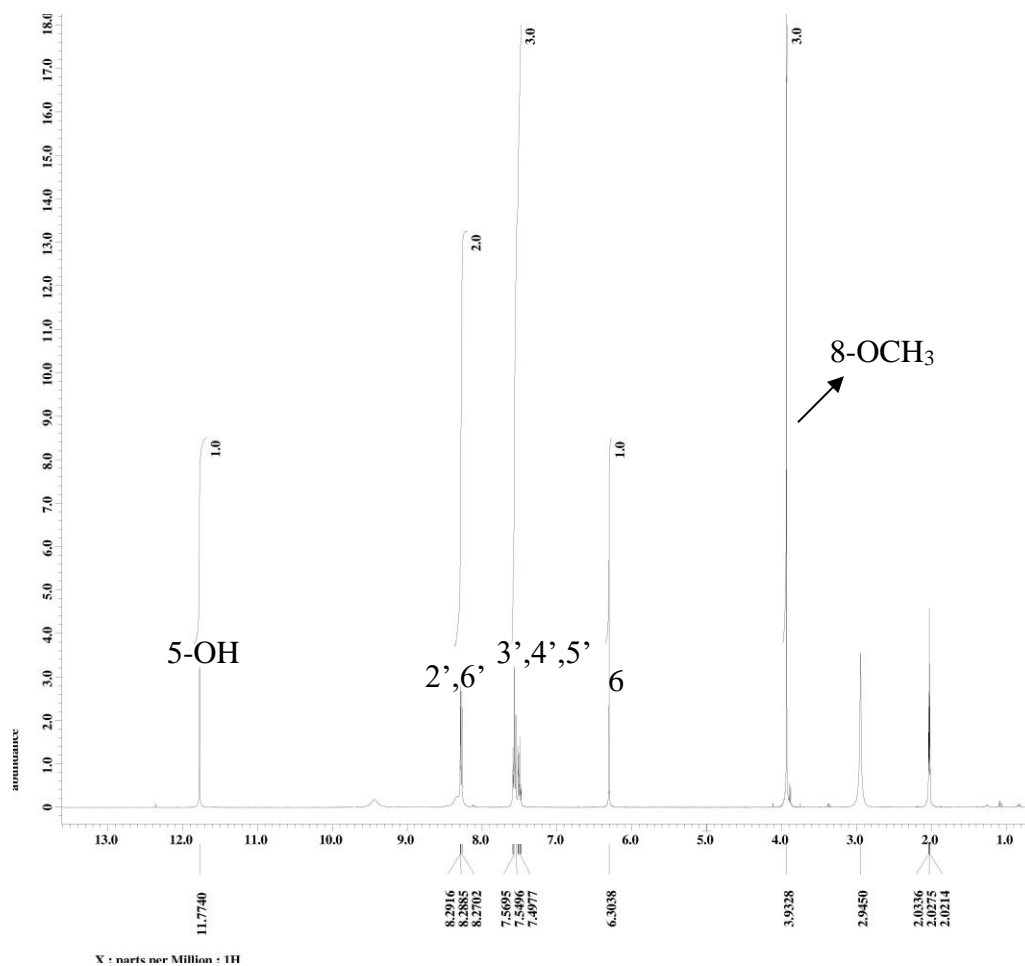
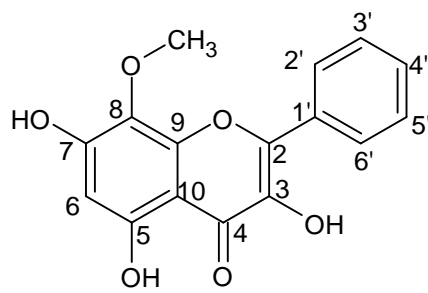


Figure 4.20: ¹H NMR (400 MHz, acetone-d₆) of 3,5,7-trihydroxy-8-methoxyflavone (M5)



(M5)

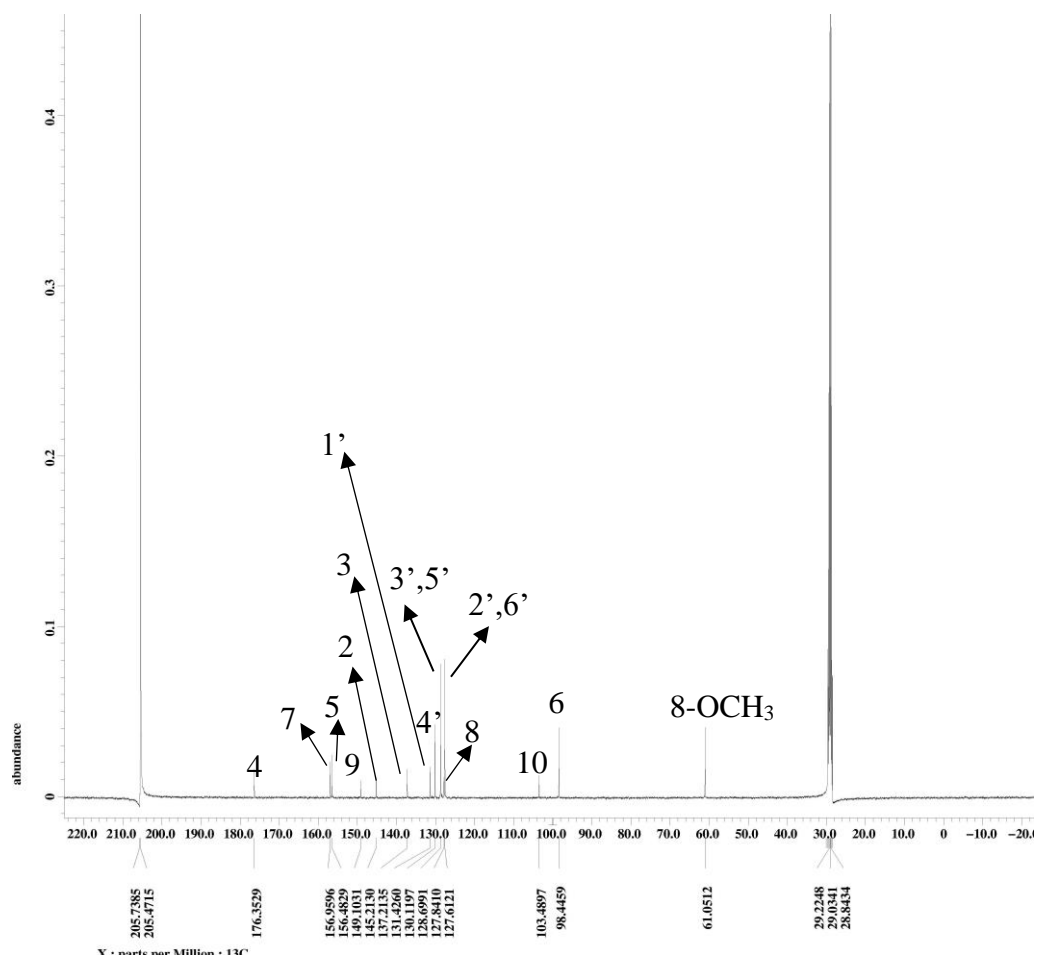
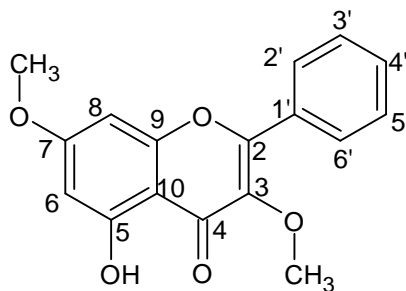


Figure 4.21: ^{13}C NMR (100 MHz, acetone- d_6) of 3,5,7-trihydroxy-8-methoxyflavone (M5)

4.2.3.3 Characterization of 5-hydroxy-3,7-dimethoxyflavone (M7)



(M7)

Compound **M7** was isolated as a yellow solid, mp 142-144 °C (Lit. 143-144 °C, Nshimo et al., 1993). It gave R_f value of 0.23 in mobile phase hexane: acetone 7:3. The HRESIMS (Appendix A11) gave a pseudomolecular ion peak at $m/z = 299.0920$ $[M+H]^+$ which analysed for $C_{17}H_{14}O_5$ (found 298.0841; calculated 298.0841). The UV absorptions were 342.9 nm, 305.9 (sh) and 266.6 nm (Appendix B11). The IR spectrum (Appendix C11) shows absorption bands at 3436 (OH stretch), 2939 (CH_3 stretch), 3066 (aromatic CH stretch), 1651 (C=O stretch), 1606 (C=C stretch), and 1167 (C-O stretch) cm^{-1} .

The 1H NMR of compound **M7** (Figure 4.22) displayed signal at δ_H 3.90 (s, 6H) indicated the presence of two methoxy groups. Resonances at δ_H 7.51 (m, 3H) and δ_H 8.06 (m, 2H) confirmed that the flavonoid has an unsubstituted ring B. Signals at δ_H 6.35 (d, 1H, $J=2.4$ Hz) and δ_H 6.44 (d, 1H, $J=2.4$ Hz) indicated the presence of meta-coupled proton which belong to H-6 and H-8. A downfield signal at δ_H 12.57 indicated chelated hydroxyl group at C-5.

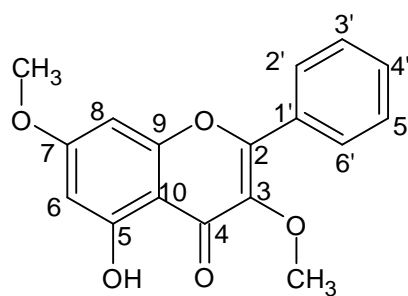
In the ^{13}C NMR of compound **M7** (Figure 4.23), the chemical shifts at δ_{C} 98.0 and δ_{C} 92.2 were characteristic peaks for C-6 and C-8, respectively. Signal at δ_{C} 179.0 was the carbonyl carbon that was hydrogen-bonded to the C-5 hydroxyl group. Peaks at δ_{H} 128.4, δ_{H} 128.7 and δ_{H} 131.0 represented C-2',6', C-3',5', and C-4', respectively, of an unsubstituted flavone B-ring. Peaks at δ_{C} 60.4 and δ_{C} 55.9 were 3-OCH₃, and 7-OCH₃ methoxy group signals, respectively. The position of the methoxy groups at C-3 and C-7 was further confirmed with HMBC (Appendix D33). The structure of **M7** was further confirmed with DEPT (Appendix D31), HMQC (Appendix D32) and compared with literature value (Sufian et al., 2013). Table 4.11 shows the ^1H NMR, ^{13}C NMR, and HMBC data of compound **M7**.

This compound was reported isolated from *Kaempferia parviflora*, rhizomes of *Boesenbrgia pandurate*, leaves of *Muntingia calabura* (Sufian et al., 2013; Nshimo et al., 1993). It showed moderate anti-inflammatory against nitric oxide production with IC₅₀ 41.6 μM and moderate anti-allergic activity. (Sufian et al., 2013).

Table 4.11: ¹H, ¹³C and HMBC spectral data of M7 (CDCl₃)

| Position | δ_{H} (multiplicity) | * δ_{H} (multiplicity) | δ_{C} (C-type) | * δ_{C} | HMBC |
|--------------------|------------------------------------|---|------------------------------|-----------------------|----------------------|
| 2 | - | - | 156.0 (C) | 155.9 | - |
| 3 | - | - | 139.7 (C) | 139.7 | - |
| 4 | - | - | 179.0 (C) | 178.9 | - |
| 5 | - | - | 162.1 (C) | 162.1 | - |
| 6 | 6.35 (1H, d, $J=2.4$ Hz) | 6.39 (1H, d, $J=2.1$ Hz) | 98.0 (CH) | 97.9 | C-5, 7, 8, 10 |
| 7 | - | - | 165.6 (C) | 165.6 | - |
| 8 | 6.44 (1H, d, $J=2.4$ Hz) | 6.49 (1H, d, $J=2.1$ Hz) | 92.2 (C) | 92.2 | - |
| 9 | - | - | 156.9 (C) | 156.9 | - |
| 10 | - | - | 106.2 (C) | 106.2 | - |
| 1' | - | - | 130.5 (C) | 130.5 | - |
| 2', 6' | 8.06 (2H, m) | 8.09 (2H, m) | 128.4 (CH) | 128.4 | C-2, 1', 3', 5', 4' |
| 3', 5' | 7.51 (2H, m) | 7.54 (2H, m) | 128.7 (CH) | 128.6 | C-1', 2', 6', 4' |
| 4' | 7.51 (1H, m) | 7.51 (1H, m) | 131.0 (CH) | 130.9 | C-1', 2', 6', 3', 5' |
| 5-OH | 12.57 (1H, s) | 12.60 (1H, s) | - | - | - |
| 3-OCH ₃ | 3.90 (3H, s) | 3.89 (3H, s) | 60.4 (CH ₃) | 60.3 | C-7 |
| 7-OCH ₃ | 3.90 (3H, s) | 3.90 (3H, s) | 55.9 (CH ₃) | 55.8 | C-3 |

*Sufian et al. (2013)



(M7)

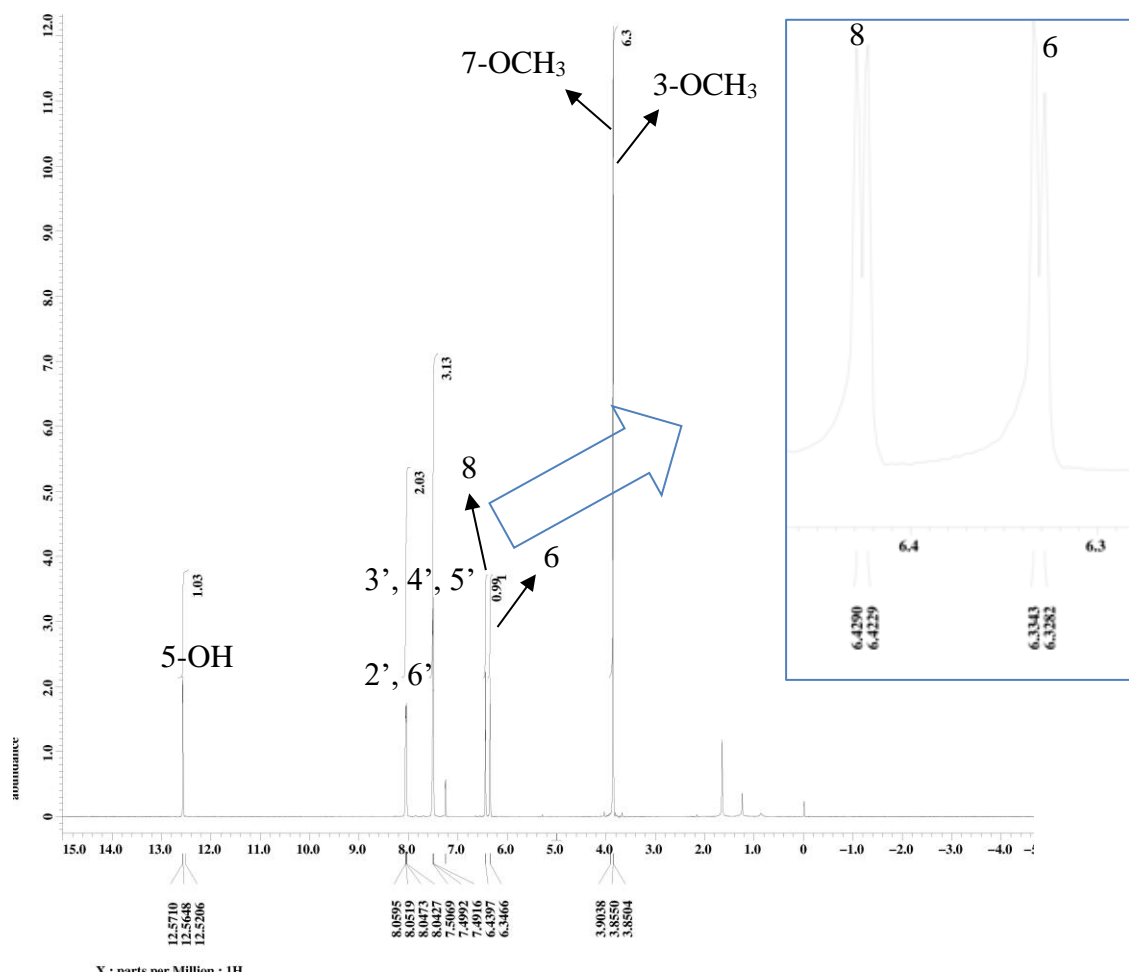
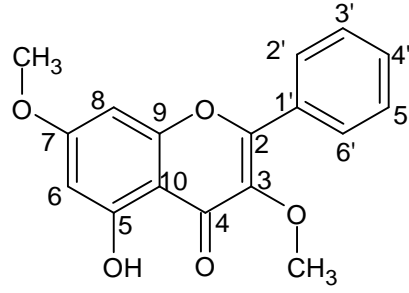


Figure 4.22: ^1H NMR (400 MHz, CDCl_3) of 5-hydroxy-3,7-dimethoxyflavone (M7)



(M7)

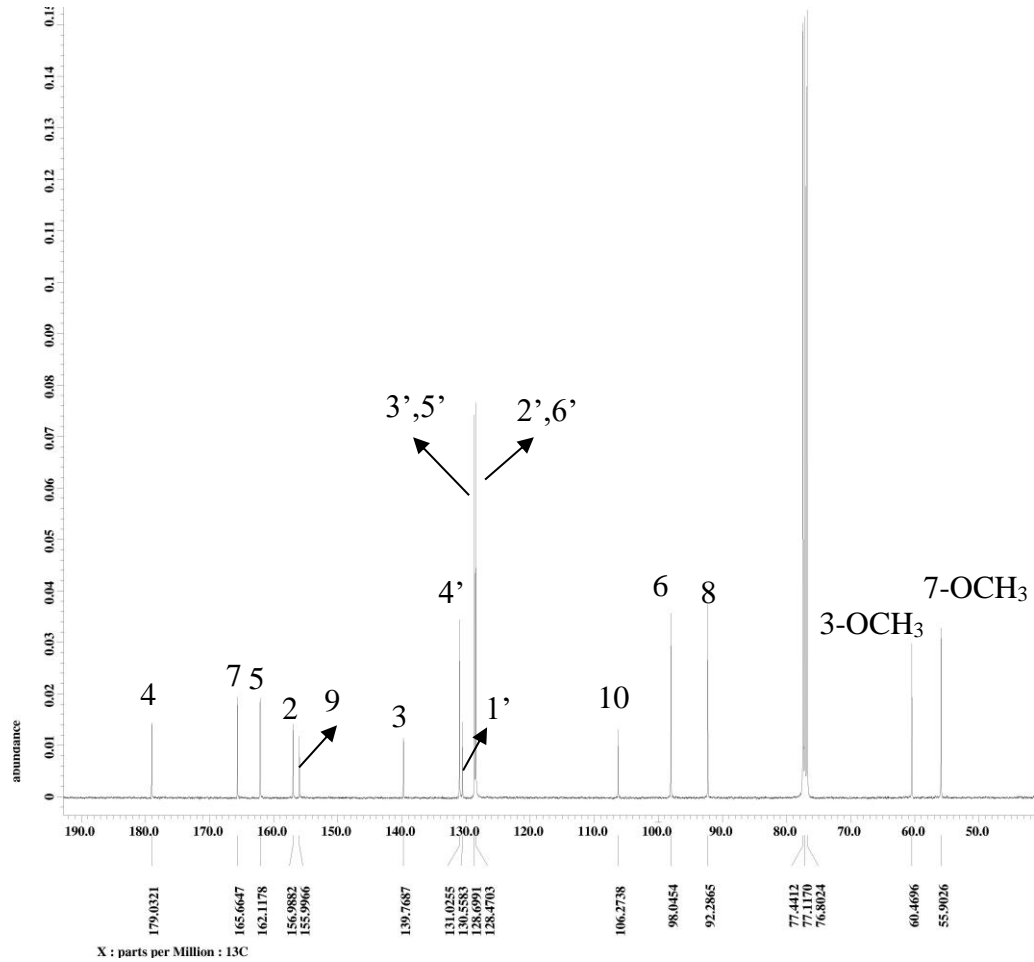
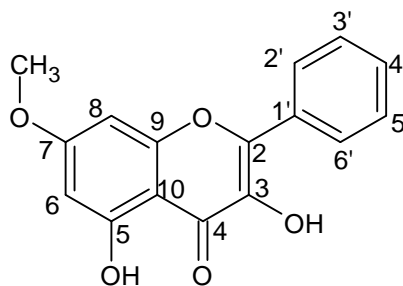


Figure 4.23: ¹³C NMR (100 MHz, CDCl₃) of 5-hydroxy-3,7-dimethoxyflavone (M7)

4.2.3.4 Characterization of 3,5-dihydroxy-7-methoxyflavone (M8)



(M8)

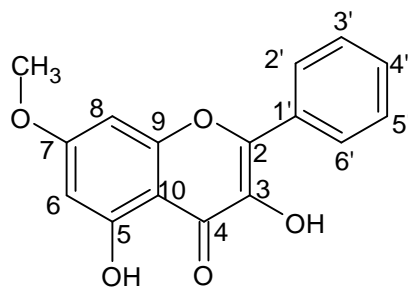
Compound **M8** was isolated as a yellow solid, mp 197-198 °C (Lit. 198-199 °C, Kurkin et al., 1994). It gave R_f value of 0.32 in mobile phase hexane: ethyl acetate 10:1. The HRESIMS (Appendix A12) gave a pseudomolecular ion peak at $m/z = 285.0763$ $[M+H]^+$ which analysed for $C_{16}H_{12}O_5$ (found 284.0690; calculated 284.0684). The UV absorptions were 359 nm, 311 and 266 nm (Appendix B12). The IR spectrum (Appendix C12) shows absorption bands at 3420 (OH stretch), 1637 (C=O stretch), 1618 (C=C stretch), and 1167 (C-O stretch) cm^{-1} .

The 1H NMR (Figure 4.24) and ^{13}C NMR (Figure 4.25) of compound **M8** are similar to compound **M7** except hydroxyl group was present at C-3 instead of methoxy group in **M7**. Hydroxyl group at C-3 was not appeared in 1H NMR due to hydrogen deuterium exchange. The methoxy group (7-OCH₃) was displayed at δ_H 3.91 in 1H NMR and at δ_C 55.6 in ^{13}C NMR. The structure of **M8** was further confirmed by DEPT spectrum (Appendix D34), HMQC spectrum (Appendix D35), and HMBC spectrum (Appendix D36). Table 4.12 shows the summary data of **M8**.

This compound was reported isolated from the buds of *Populus lauriflora* and from the leaves of *Muntingia calabura* (Kurkin et al., 1994; Chen et al., 2005). It exhibited moderate cytotoxic activity towards P-388 and HT-29 with IC_{50} 8.77 ± 0.85 and 15.0 ± 1.6 $\mu\text{g/mL}$, respectively.

Table 4.12: ^1H , ^{13}C and HMBC spectral data of M8 (acetone- d_6)

| Position | δ_{H} (multiplicity) | δ_{C} (C-type) | HMBC |
|--------------------|------------------------------------|------------------------------|------------------|
| 2 | - | 145.6 (C) | - |
| 3 | - | 137.4 (C) | - |
| 4 | - | 176.2 (C) | - |
| 5 | - | 161.1 (C) | - |
| 6 | 6.31 (1H, d, $J = 2.4$ Hz) | 97.6 (CH) | C-5, 7, 8, 10 |
| 7 | - | 166.1 (C) | - |
| 8 | 6.71 (1H, d, $J = 2.4$ Hz) | 92.0 (C) | C-6, 10, 9, 7 |
| 9 | - | 157.1 (C) | - |
| 10 | - | 104.2 (C) | - |
| 1' | - | 131.2 (C) | - |
| 2', 6' | 8.26 (m) | 127.7 (CH) | C-2, 3', 5', 4' |
| 3', 5' | 7.53 (m) | 128.5 (CH) | C-1', 2', 6', 4' |
| 4' | 7.53 (m) | 130.1 (CH) | C-2', 6', 3', 5' |
| 5-OH | 12.02 (s) | - | - |
| 7-OCH ₃ | 3.91 (s) | 55.6 (CH ₃) | C-7 |



(M8)

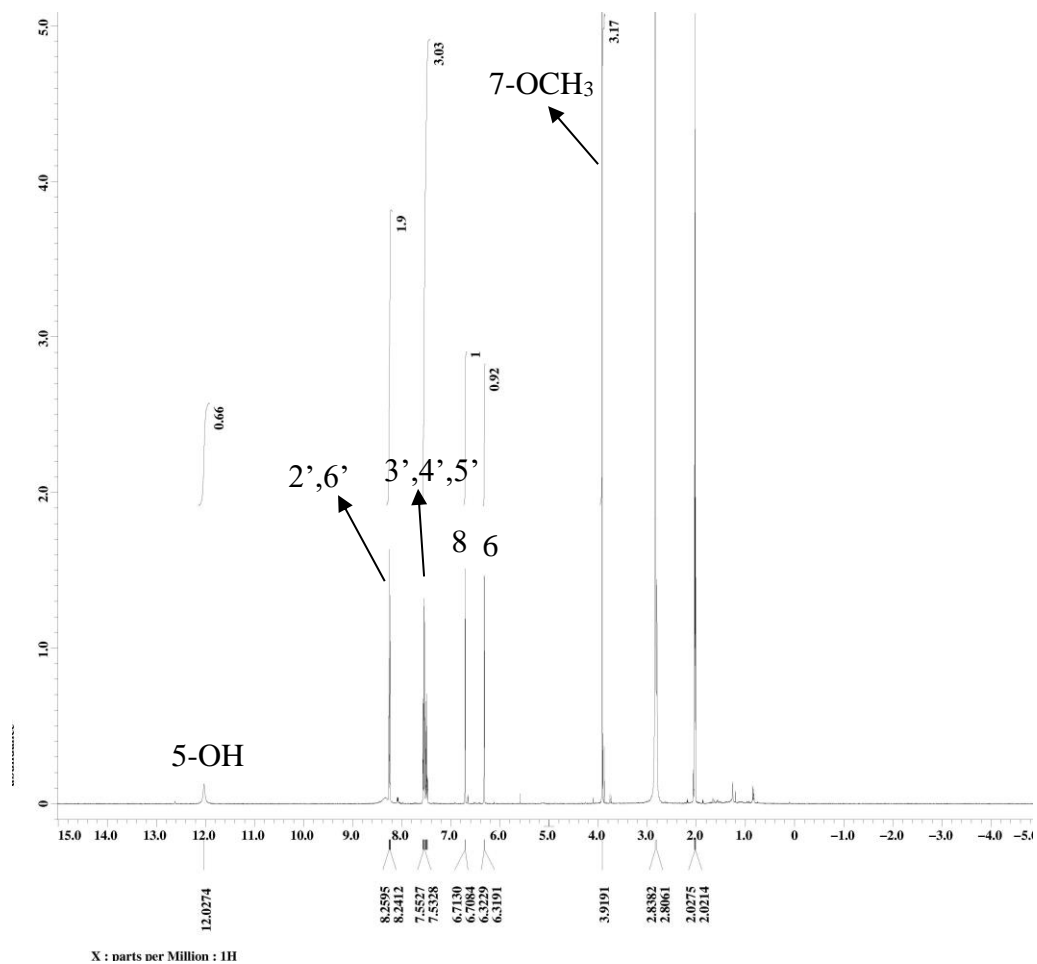
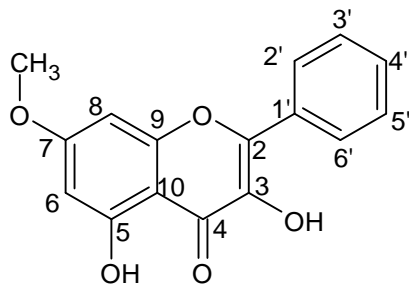


Figure 4.24: ^1H NMR (400 MHz, acetone- d_6) of 3,5-dihydroxy-7-methoxyflavone (M8)



(M8)

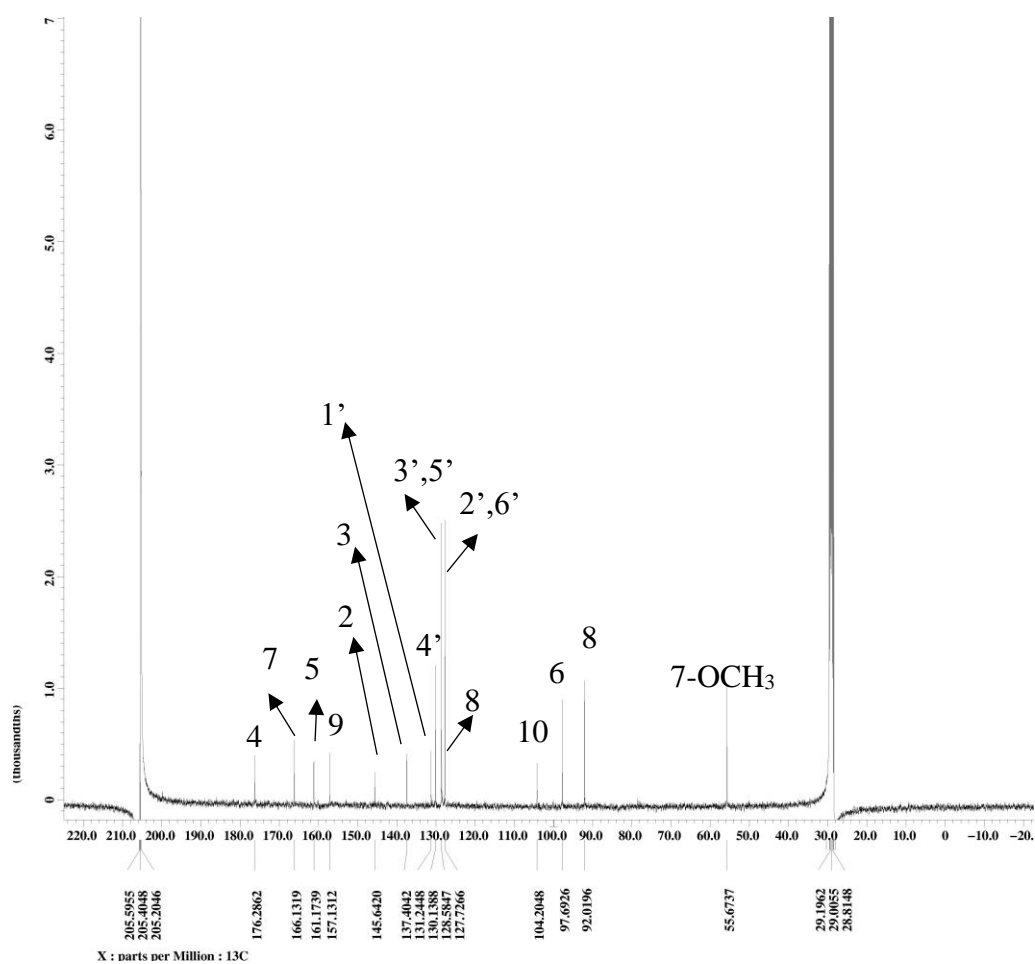
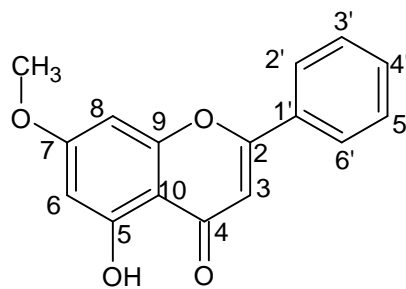


Figure 4.25: ^{13}C NMR (100 MHz, acetone- d_6) of 3, 5-dihydroxy-7-methoxyflavone (M8)

4.2.3.5 Characterization of 5-dihydroxy-7-methoxyflavone (M9)



(M9)

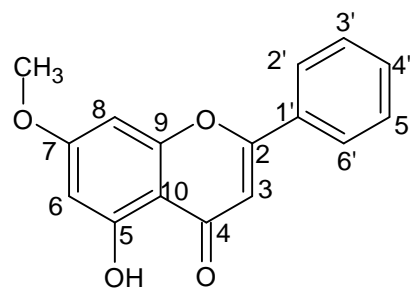
Compound **M9** was isolated as a yellow solid, mp 165-166 °C (Lit. 164-165°C, Rosandy et al., 2013). It gave R_f value of 0.44 in mobile phase hexane: chloroform 3:7. The HRESIMS (Appendix A13) gave a pseudomolecular ion peak at $m/z = 269.0814 [M+H]^+$ which analysed for $C_{16}H_{12}O_4$ (found 268.0742; calculated 268.07356). The UV absorptions were 310 and 268.6 nm (Appendix B13). The IR spectrum (Appendix C13) shows absorption bands at 3411 (OH stretch), 3010 (aromatic CH stretch), 2919 (CH_3 stretch), 1668 (C=O stretch), 1608 (C=C stretch), and 1159 (C-O stretch) cm^{-1} .

The 1H NMR (Figure 4.26) and ^{13}C NMR (Figure 4.27) of compound **M9** is similar to compound **M8** except aromatic proton present at C-3 instead of hydroxy group in **M8**. The structure of **M9** was further confirmed with DEPT spectrum (Appendix D37), HMQC spectrum (Appendix D38), HMBC spectrum (Appendix D39) and compared with published data (Rosandy et al., 2013). Table 4.13 shows the 1H , ^{13}C , and HMBC spectra data of **M9**. This compound was previously isolated from stem bark of *Uvaria rufa* (Rosandy et al., 2013).

Table 4.13: ¹H, ¹³C and HMBC spectral data of M9 (CDCl₃)

| Position | δ _H (multiplicity) | *δ _H (multiplicity) | δ _C (C-type) | *δ _C (C-type) | HMBC |
|--------------------|---------------------------------|---------------------------------|-------------------------|--------------------------|---------------------|
| 2 | - | - | 164.0 (C) | 164.0 (C) | - |
| 3 | 6.79 | 6.67 | 105.9 (CH) | 105.9 (C) | C-2, 4, 10, 1' |
| 4 | - | - | 182.6 (C) | 182.5 (C) | - |
| 5 | - | - | 162.2 (C) | 162.2 (C) | - |
| 6 | 6.23 (1H, d, <i>J</i> = 2.4 Hz) | 6.39 (1H, d, <i>J</i> = 2.4 Hz) | 98.3 (CH) | 98.2 (CH) | C-5, 7, 10 |
| 7 | - | - | 165.7 (C) | 165.6 (C) | - |
| 8 | 6.70 (1H, d, <i>J</i> = 2.4 Hz) | 6.51 (1H, d, <i>J</i> = 2.4 Hz) | 92.7 (CH) | 92.7 (C) | C-10, 9, 7 |
| 9 | - | - | 157.9 (C) | 157.8 (C) | - |
| 10 | - | - | 105.8 (C) | 105.7 (C) | - |
| 1' | - | - | 131.4 (C) | 131.9 (C) | - |
| 2', 6' | 8.05 (2H, m) | 8.26 (2H, m) | 126.4 (CH) | 126.3 (CH) | C-2, 1', 3', 5', 4' |
| 3', 5' | 7.59 (2H, m) | 7.53 (2H, m) | 129.2 (CH) | 129.1 (CH) | C-1', 2', 6', 4' |
| 4' | 7.57 (1H, m) | 7.53 (1H, m) | 131.9 (CH) | 132.1 (CH) | C-2', 6', 3', 5' |
| 5-OH | 12.02 (1H, s) | 12.02 (1H, s) | - | - | - |
| 7-OCH ₃ | 3.95 (3H, s) | 3.91 (3H, s) | 55.8 (CH ₃) | 55.9 (CH ₃) | C-7 |

* Rosandy et al. (2013)



(M9)

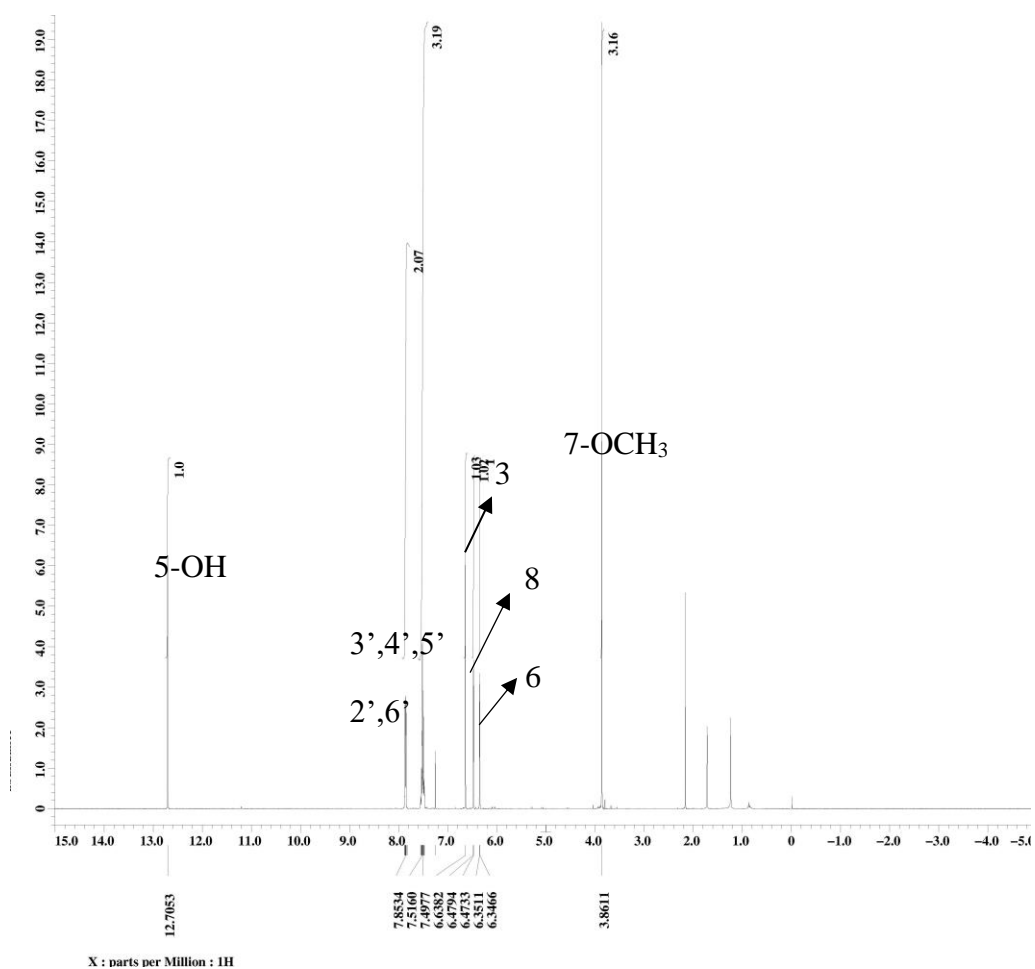
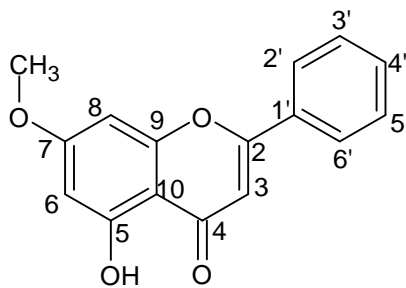


Figure 4.26: ^1H NMR (400 MHz, CDCl_3) of 5-hydroxy-7-methoxyflavone (M9)



(M9)

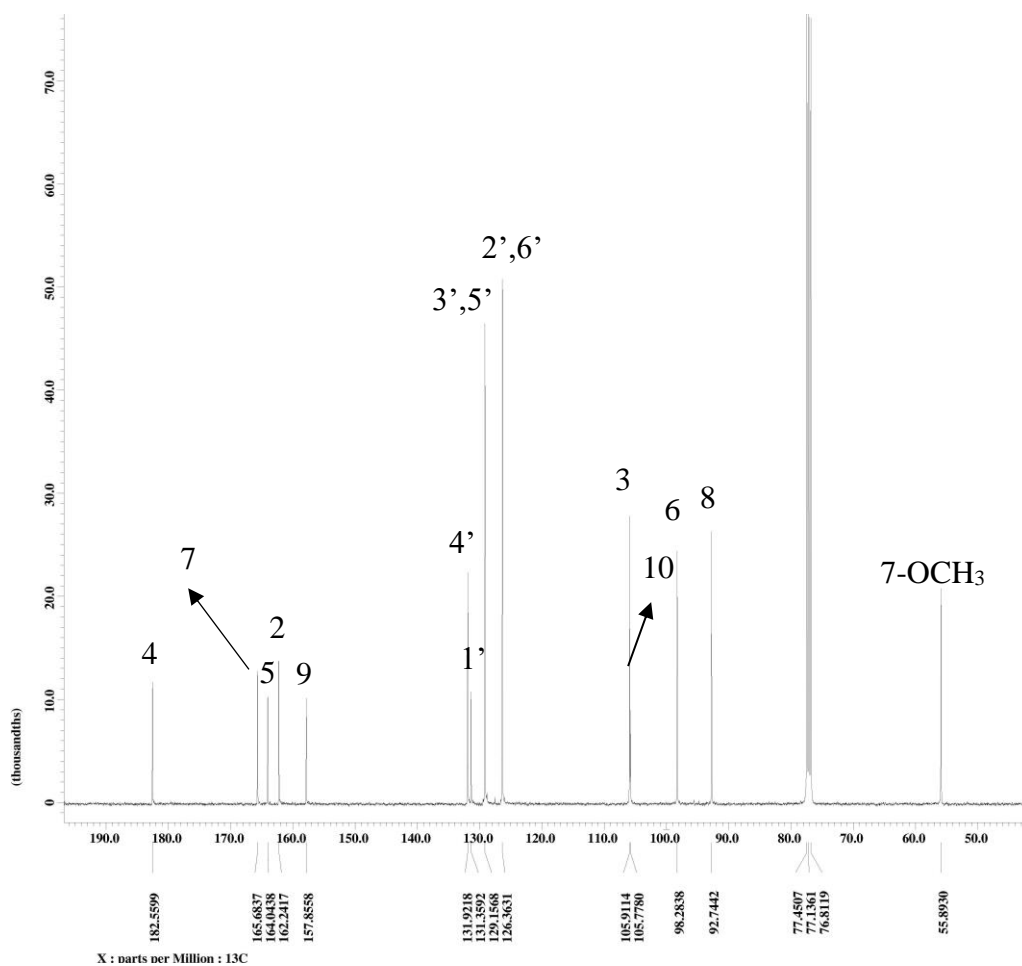
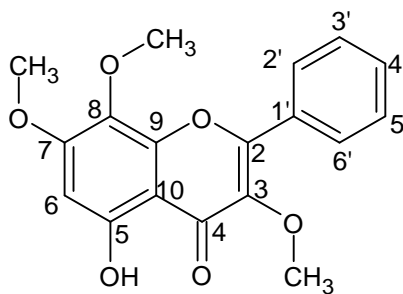


Figure 4.27: ^{13}C NMR (100 MHz, CDCl_3) of 5-hydroxy-7-methoxyflavone (M9)

4.2.3.6 Characterization of 5-hydroxy-3,7,8-trimethoxyflavone (M10)



(M10)

Compound **M10** was isolated as a yellow solid, mp 176-177 °C. It gave R_f value of 0.44 in mobile phase hexane: acetone 8:2. The HRESIMS (Appendix A14) showed a pseudomolecular ion peak at $m/z = 329.1026 [M+H]^+$ which analysed for $C_{18}H_{16}O_6$ (found 328.0947; calculated 328.0946). The UV absorptions were 356.1 and 273.5 nm (Appendix B14). The IR spectrum (Appendix C14) shows absorption bands at 3458 (OH stretch), 2920 (CH₃ stretch), 1635 (C=O stretch), 1619 (C=C stretch), and 1212 (C-O stretch) cm^{-1} .

The 1H NMR (Figure 4.28) and ^{13}C NMR (Figure 4.29) of compound **M10** are similar to compound **M3** except methoxy group is present at C-3 instead of hydroxyl group in **M3**. Signals at δ_H 3.86, 3.89, and 3.90 were methoxy group at C-3 (δ_C 60.5), C-8 (δ_C 61.7), and C-7 (δ_C 56.5), respectively. Due to secondary anisotropic fields generated by pi electrons in aromatic ring A, methoxy protons of 7-OCH₃ and 8-OCH₃ shifted downfield than 3-OCH₃. Whereas, due to 8-OCH₃ located at the increased electron density position that para to hydroxyl group at C-5, 8-OCH₃ shifted upfield than 7-OCH₃. Structure of **M10** was further confirmed

by DEPT (Appendix D40), HMQC (Appendix D41), HMBC (Appendix D42) and compared with literature data (Yusof et al.,2013). Table 4.14 shows the summary data of compound **M10**.

This compound was reported isolated from the leaves of *Muntingia calabura* (Yusof et al., 2013). Yusof et al. (2013) revealed that this compound was not active against antinociceptive activity.

Table 4.14: ^1H , ^{13}C and HMBC spectral data of M10 (CDCl_3)

| Position | δ_{H} (multiplicity) | $^*\delta_{\text{H}}$ (multiplicity) | δ_{C} (C-type) | $^*\delta_{\text{C}}$ (C-type) | HMBC |
|--------------------|------------------------------------|--------------------------------------|------------------------------|--------------------------------|---------------------|
| 2 | - | - | 158.6 (C) | 158.5 (C) | - |
| 3 | - | - | 139.5 (C) | 139.4 (C) | - |
| 4 | - | - | 179.3 (C) | 179.2 (C) | - |
| 5 | - | - | 157.4(C) | 157.4 (C) | - |
| 6 | 6.35 (1H, s) | 6.45 (1H, s) | 95.6 (CH) | 95.5 (CH) | C-7, 8, 10 |
| 7 | - | - | 155.9 (C) | 155.8 (C) | - |
| 8 | - | - | 129.0 (C) | 128.9 (C) | C-6, 10, 9, 7 |
| 9 | - | - | 148.7 (C) | 148.6(C) | - |
| 10 | - | - | 105.5 (C) | 105.4 (C) | - |
| 1' | - | - | 130.7 (C) | 130.6 (C) | - |
| 2', 6' | 8.13 (2H, m) | 8.17 (2H, m) | 128.5 (CH) | 128.4 (CH) | C-1', 3',5', 4' |
| 3', 5' | 7.52 (2H, m) | 7.56 (2H, m) | 128.8 (CH) | 128.7 (CH) | C-1', 2', 4', 6' |
| 4' | 8.13 (1H, m) | 8.17 (1H, m) | 131.1 (CH) | 131.1 (CH) | C-1', 2', 3', 5' 6' |
| 5-OH | 12.41 (1H, s) | 12.41 (1H, s) | - | - | - |
| 3-OCH ₃ | 3.86 (3H, s) | 3.86 (3H, s) | 60.5 (CH ₃) | 60.3 (CH ₃) | C-3 |
| 7-OCH ₃ | 3.90 (3H, s) | 3.90 (3H, s) | 56.5 (CH ₃) | 56.9 (CH ₃) | C-7 |
| 8-OCH ₃ | 3.89 (3H, s) | 3.89 (3H, s) | 61.7 (CH ₃) | 61.6 (CH ₃) | C-8 |

*Yusof et al. (2013)

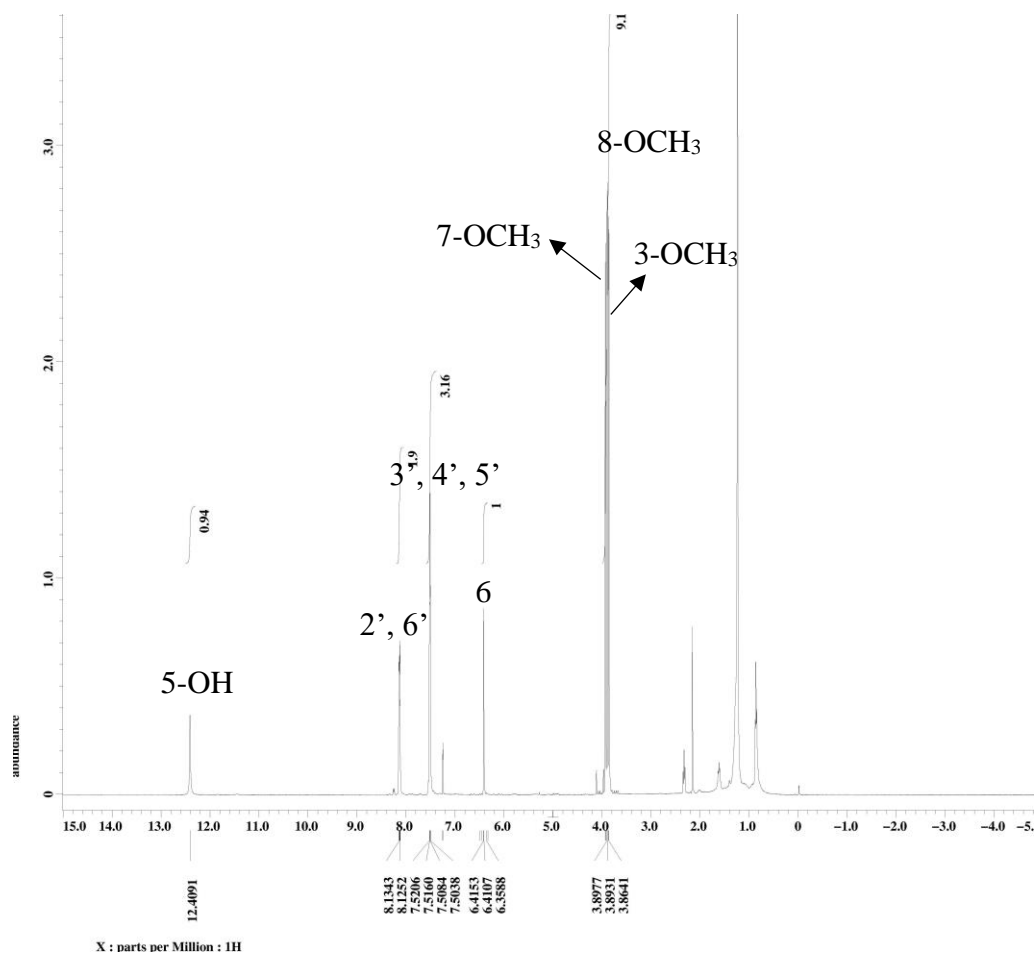
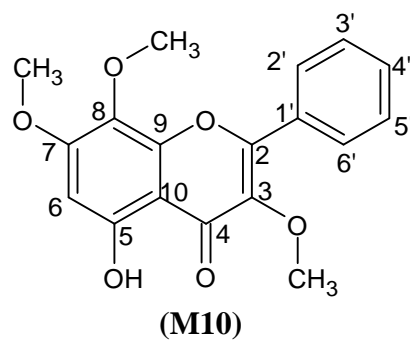
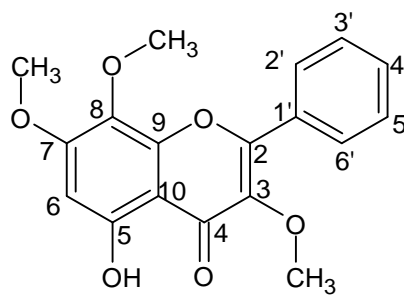


Figure 4.28: ^1H NMR (400 MHz, CDCl_3) of 5-hydroxy-3,7,8-trimethoxyflavone (M10)



(M10)

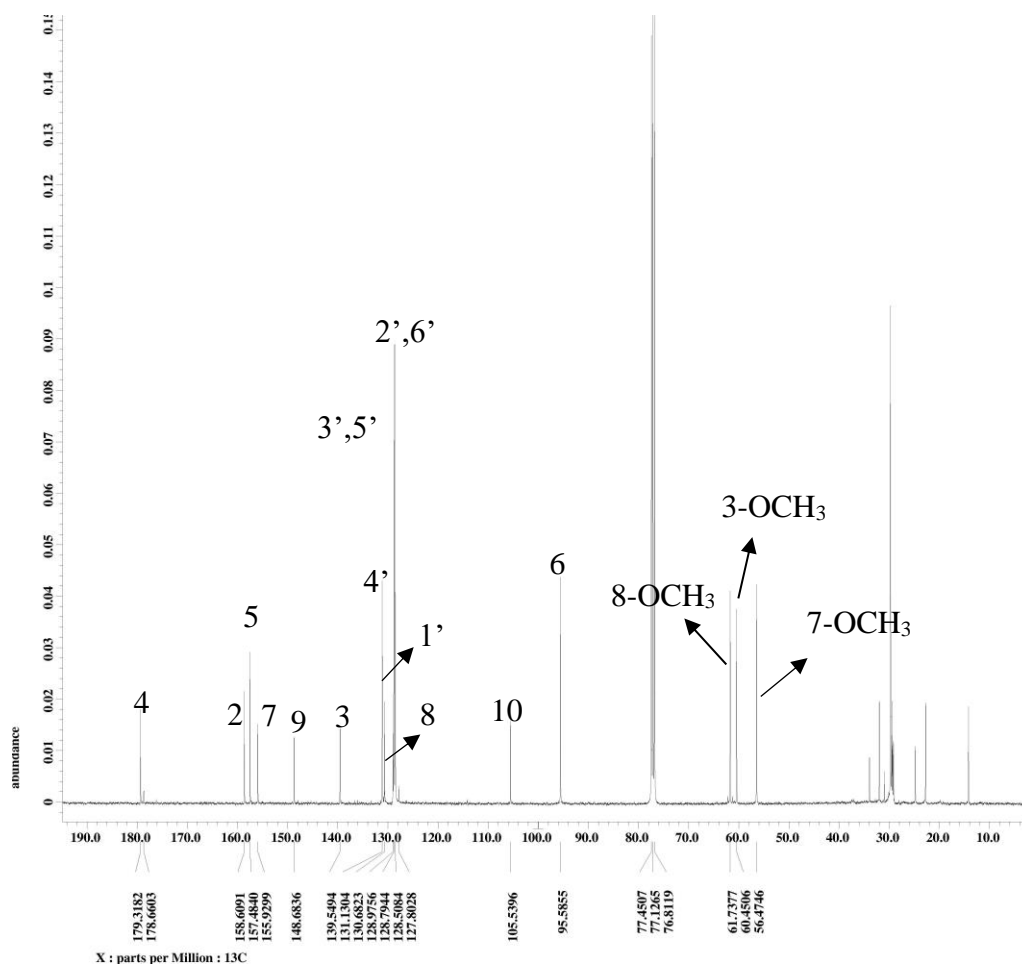
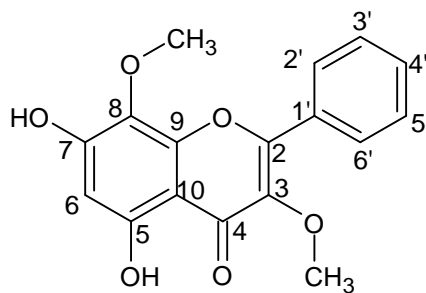


Figure 4.29: ^{13}C NMR (100 MHz, CDCl_3) of 5-hydroxy-3,7,8-trimethoxyflavone (M10)

4.2.3.7 Characterization of 5,7-dihydroxy-3,8-dimethoxyflavone (**M11**)



(**M11**)

Compound **M11** was isolated as a yellow solid, mp 144-146 °C (Lit. 145-148 °C, Urzua et al., 1999). It gave R_f value of 0.36 in mobile phase hexane:dichloromethane 10:6. The HRESIMS (Appendix A15) gave a pseudomolecular ion peak at $m/z = 315.0873$ $[M+H]^+$ which analysed for $C_{17}H_{14}O_6$ (found 314.0796; calculated 314.0790). The UV absorptions were 354 and 274 nm (Appendix B15). The IR spectrum (Appendix C15) shows absorption bands at 3460 (OH stretch), 2957, 2918 (CH_3 stretch), 1637 (C=O stretch), 1617 (C=C stretch), and 1174 (C-O stretch) cm^{-1} .

The 1H NMR (Figure 4.30) and ^{13}C NMR (Figure 4.31) of compound **M11** are similar to compound **M10** except hydroxyl group replace methoxy group at C-7 in **M10**. Downfield exchangeable singlet at δ_H 12.30 was observed, which is generally characteristic for the chelated 5-OH of flavones. Signal of 7-OH was not observed as hydrogen-deuterium exchange. Structure of **M11** was further confirmed by DEPT (Appendix D43), HMQC (Appendix D44), HMBC

(Appendix D45) and compared to published data (Urzúa et al., 1999). This compound was previously isolated from resinous exudates of *Pseudognaphalium robustum* (Urzúa et al., 1999). Table 4.15 shows the summary spectra data of compound **M11**.

Table 4.15: ^1H , ^{13}C and HMBC spectral data of M11 (acetone- d_6)

| Position | δ_{H} (multiplicity) | δ_{C} (C-type) | * δ_{C} (C-type) | HMBC |
|--------------------|---------------------------------------|------------------------------|--------------------------------|-------------------------|
| 2 | - | 155.5 (C) | 155.4 (C) | - |
| 3 | - | 139.3 (C) | 137.5 (C) | - |
| 4 | - | 179.0 (C) | 178.0 (C) | - |
| 5 | - | 157.0 (C) | 155.9 (C) | - |
| 6 | 6.30 (1H, s) | 98.9 (CH) | 99.0 (CH) | C-7, 8, 10 |
| 7 | - | 157.4 (C) | 156.9 (C) | - |
| 8 | - | 127.9 (C) | 127.5 (C) | - |
| 9 | - | 149.2 (C) | 148.5 (C) | - |
| 10 | - | 104.9 (C) | 104.0 (C) | - |
| 1' | - | 130.7 (C) | 130.5 (C) | - |
| 2', 6' | 8.08 (2H, m) | 128.3 (CH) | 128.2 (CH) | C-3', 5', 4', 2 |
| 3', 5' | 7.55 (2H, m) | 128.8 (CH) | 128.6 (CH) | C-2', 6', 4', 1' |
| 4' | 7.55 (2H, m) | 131.0 (CH) | 130.8 (CH) | C-2', 6', 3', 5', 1' |
| 5-OH | 12.30 (1H, s) | - | - | - |
| 3-OCH ₃ | 3.86 (3H, s) | 59.7 (CH ₃) | - | C-3 |
| 8-OCH ₃ | 3.88 (3H, s) | 60.9 (CH ₃) | - | C-8 |

* Urzua et al. (1999)

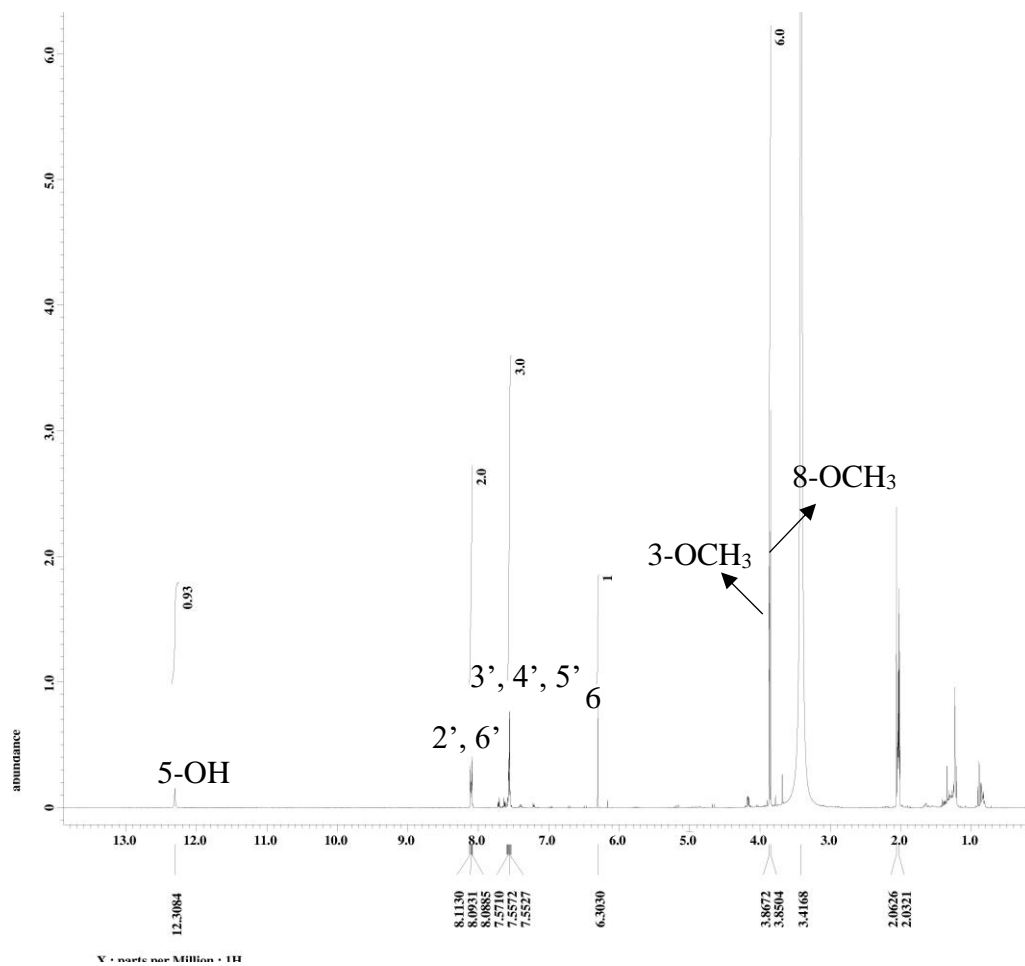
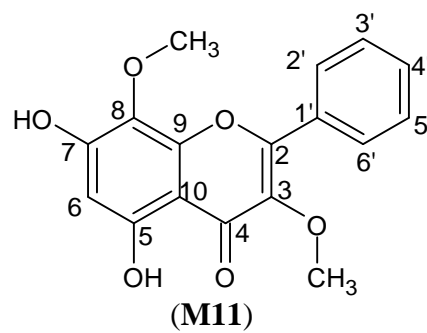


Figure 4.30: ^1H NMR (400 MHz, acetone- d_6) of 5,7-dihydroxy-3,8-dimethoxyflavone (M11)

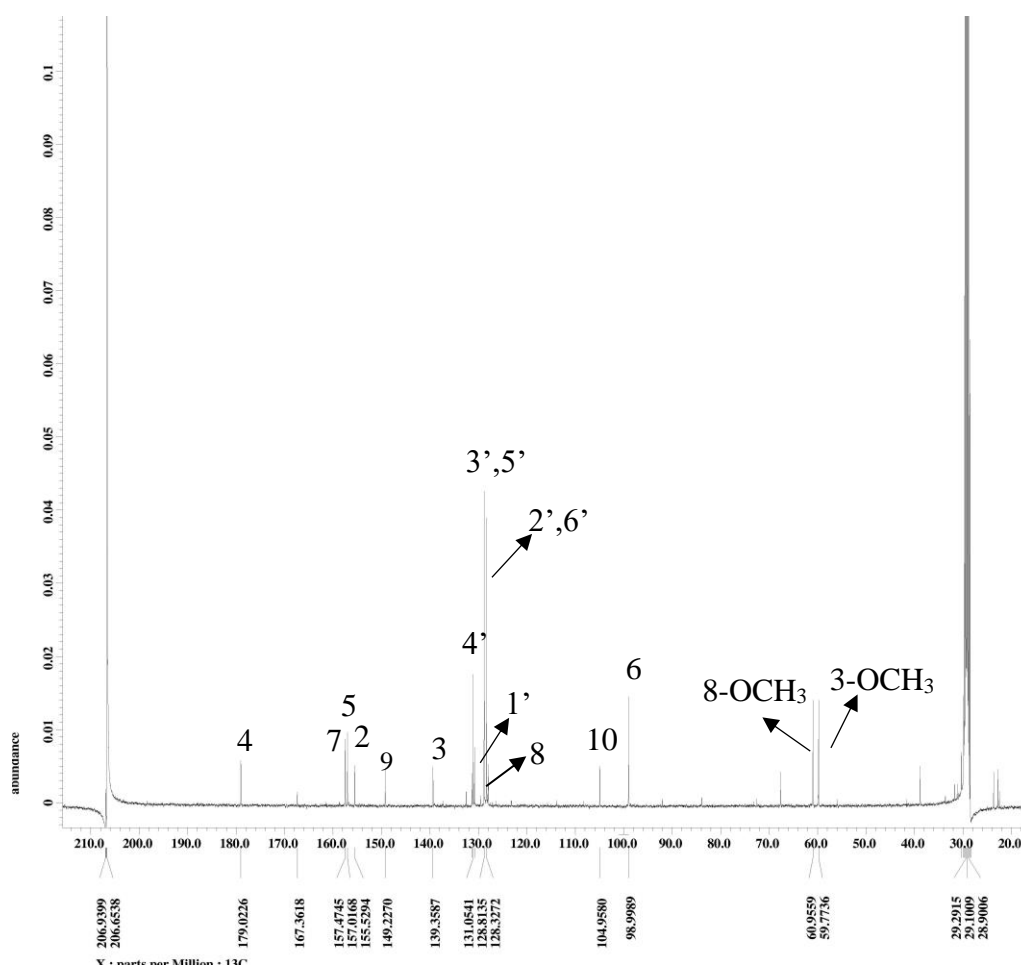
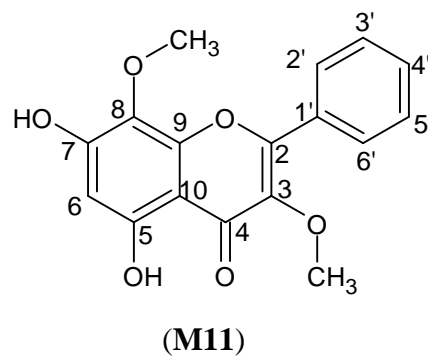
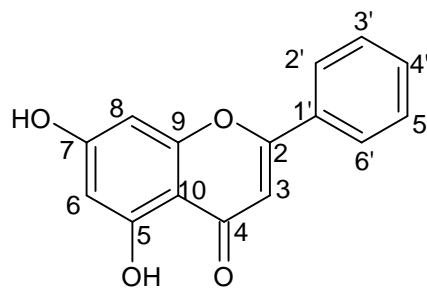


Figure 4.31: ^{13}C NMR (100 MHz, acetone- d_6) of 5,7-dihydroxy-3,8-dimethoxyflavone (M11)

4.2.3.8 Characterization of 5,7-dihydroxyflavone (M14)



(M14)

Compound **M14** was isolated as a yellow solid, mp 286-287 °C (Lit. 283-285 °C, Nshimo, 1991). It gave R_f value of 0.51 in mobile phase hexane: acetone 10:6. The HRESIMS (Appendix A16) gave a pseudomolecular ion peak at $m/z = 255.0549 [M+H]^+$ which analysed for $C_{15}H_{10}O_4$ (found 254.0576; calculated 254.0579). The UV absorptions were 316.4 and 269.3 nm (Appendix B16). The IR spectrum (Appendix C16) shows absorption bands at 3436 (OH stretch), 1651 (C=O stretch), 1613 (C=C stretch), and 1169 (C-O stretch) cm^{-1} .

The 1H NMR (Figure 4.32) and ^{13}C NMR (Figure 4.33) of compound **M14** are similar to compound **M9** except for that 7-OH of **M14** was replaced 7-OCH₃ in **M9**. Signal at δ_H 10.98 indicated the presence of 7-OH. According to above data, the structure of **M14** was elucidated as 5,7-dihydroxyflavone; this was further confirmed by DEPT (Appendix D46), HMQC (Appendix D47), HMBC (Appendix D48) and compared with literature data (Nshimo, 1991). Table 4.16 shows the 1H , ^{13}C , and HMBC spectral data of **M14**. This compound was previously isolated from the leaves of *Muntingia calabura*

(Nshimo, 1991). It was reported to exhibit significant cytotoxic activity towards eight cancer cell lines i.e. HT 1080, KB, KB-V1, Mel2, and P388, with ED₅₀ values range from 3.0 – 4.4 μg/ml.

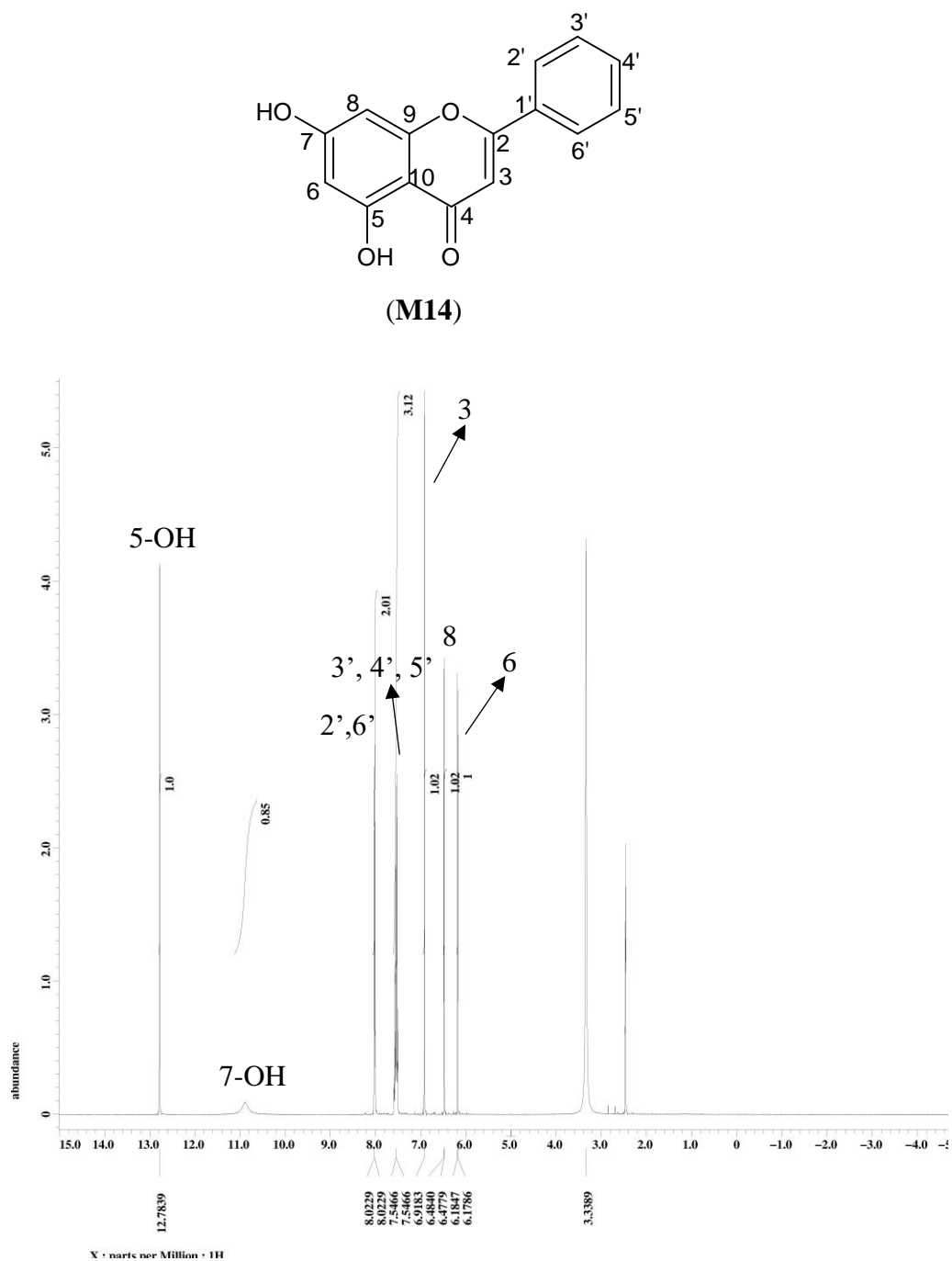
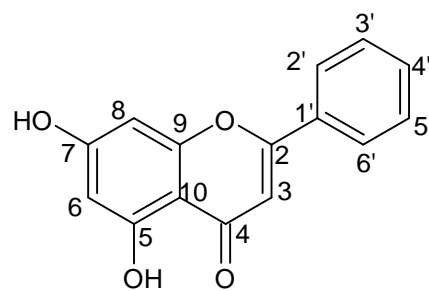


Figure 4.32: ¹H NMR (400 MHz, DMSO-d₆) of 5,7-dihydroxyflavone (M14)



(M14)

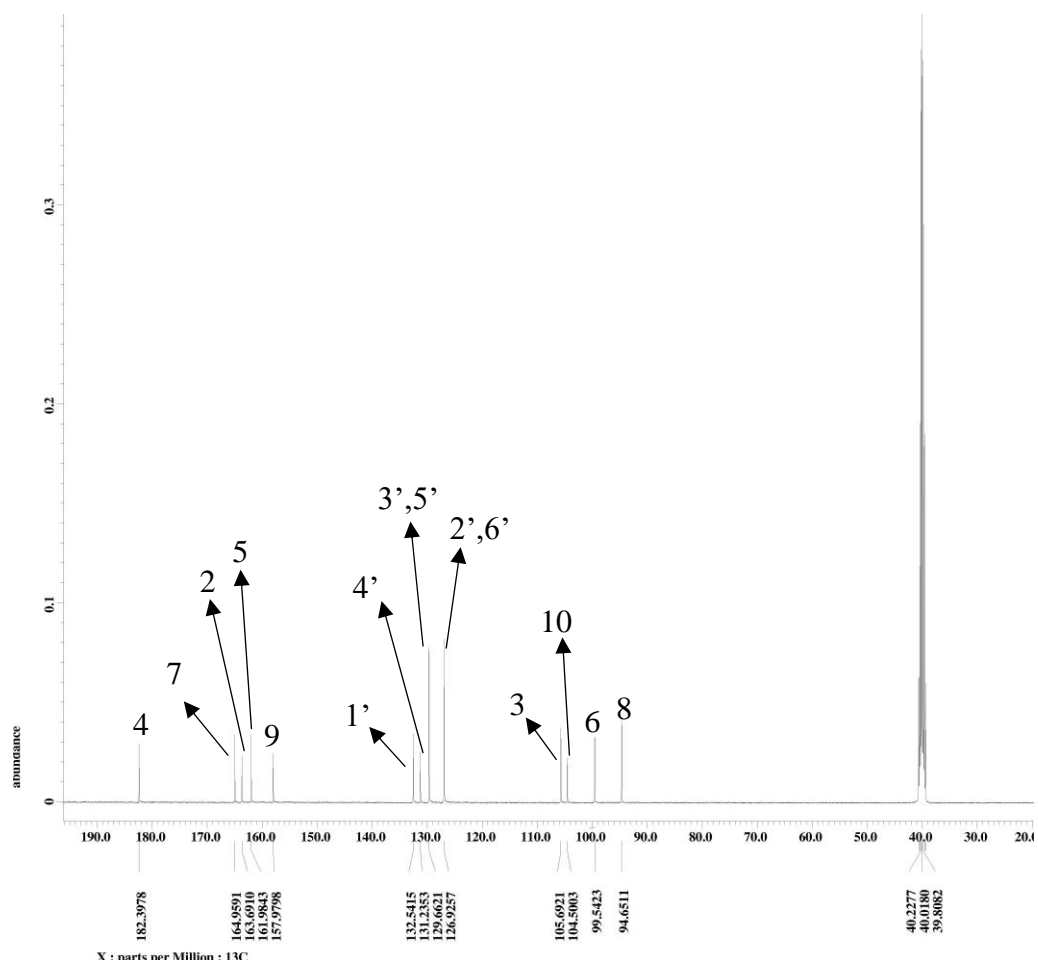


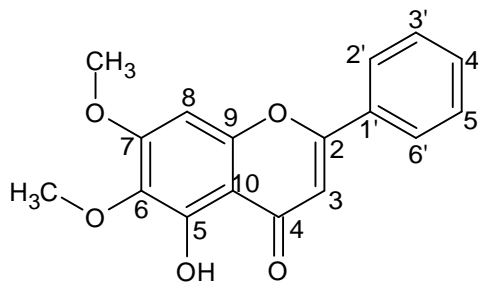
Figure 4.33: ^{13}C NMR (100 MHz, DMSO- d_6) of 5,7-dihydroxyflavone (M14)

Table 4.16: ¹H, ¹³C and HMBC spectral data of M14 (DMSO-d₆)

| Position | δ _H (multiplicity) | *δ _H (multiplicity) | δ _C (C-type) | *δ _C (C-type) | HMBC |
|----------|--------------------------------|--------------------------------|-------------------------|--------------------------|------------------|
| 2 | - | - | 163.6 (C) | 163.0 (C) | - |
| 3 | 6.91 (1H, s) | 6.97 (1H, s) | 105.6 (CH) | 105.0 (CH) | C-2, 1', 10, 4 |
| 4 | - | - | 182.3 (C) | 181.6 (C) | - |
| 5 | - | - | 161.9 (C) | 161.0 (C) | - |
| 6 | 6.17 (1H, d, <i>J</i> =1.8 Hz) | 6.23 (1H, d, <i>J</i> =1.8 Hz) | 99.5 (CH) | 99.0 (CH) | C-5, 7, 8, 10 |
| 7 | - | - | 164.9 (C) | 164.5 (C) | - |
| 8 | 6.47 (1H, d, <i>J</i> =1.8 Hz) | 6.53 (1H, d, <i>J</i> =1.8 Hz) | 94.6 (CH) | 94.0 (CH) | C-6, 7, 9, 10, 4 |
| 9 | - | - | 157.9 (C) | 157.0 (C) | - |
| 10 | - | - | 104.5 (C) | 103.9 (C) | - |
| 1' | - | - | 131.2 (C) | 131.9 (C) | - |
| 2', 6' | 8.03 (2H, m) | 8.09 (2H, m) | 126.9 (CH) | 126.3 (CH) | C-2, 1', 3', 5', |
| 3', 5' | 7.53 (2H, m) | 7.60 (2H, m) | 129.6 (CH) | 129.1 (CH) | C-2',6' |
| 4' | 7.53 (1H, m) | 7.60 (1H, m) | 133.5 (CH) | 130.9 (CH) | C-3', 5' |
| 5-OH | 12.78 (1H, s) | - | - | - | C8, C9, C10 |

* Nshimo (1991)

4.2.3.9 Characterization of 5-hydroxy-6,7-dimethoxyflavone (M15)



(M15)

Compound **M15** was isolated as a yellow solid, mp 164-165 °C (Lit. 163-164 °C, Linlin et al., 2016). It gave R_f value of 0.10 in mobile phase hexane: ethyl acetate 10:1. The HRESIMS (Appendix A17) gave a pseudomolecular ion peak at $m/z = 299.0922$ $[M+H]^+$ which analysed for $C_{17}H_{14}O_5$ (found 298.0849; calculated 298.0841). The UV absorptions were 316 and 273.1 nm (Appendix B17). The IR spectrum (Appendix C17) shows absorption bands at 3436 (OH stretch), 2924 (CH_3 stretch) 1635 (C=O stretch), 1496 (C=C stretch), and 1179 (C-O stretch) cm^{-1} .

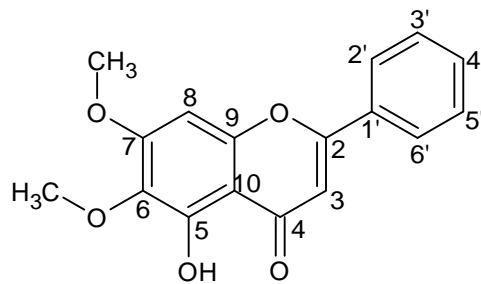
The 1H NMR (Figure 4.34) of compound **M15** was similar to compound **M9** except presence of methoxy group at C-6 in **M15** instead of aromatic proton in **M9**. Two methoxy groups signals at δ_H 3.78 and δ_H 3.98 belong to 7-OCH₃ and 6-OCH₃, respectively. Two aromatic proton singlets appeared at δ_H 6.81 and δ_H 6.88 were assigned to H-3 and H-8, respectively. In ^{13}C NMR (Figure 4.35) of compound **M15**, three carbons signals appeared at δ_c 153.0, δ_c 132.8, and δ_c 159.8 were assigned to C-5, C-6 and C-7, respectively. C-6 appeared at higher field than C-5 and C-7, due to the increased electron density in position C-6 that

was ortho to both C-5 and C-7 with electron donating groups attached. The structure was further confirmed by DEPT (Appendix D49), HMQC (Appendix D50), HMBC (Appendix D51) and compared with literature data (Rosandy et al., 2013). Table 4.17 shows summary data of compound **M15**. This compound was reported isolated from the stem bark of *Uvaria rufa* (Rosandy et al., 2013).

Table 4.17: ¹H, ¹³C and HMBC spectral data of M15 (acetone-d₆)

| Position | δ _H (multiplicity) | δ _C (C-type) | *δ _C (C-type) | HMBC |
|--------------------|----------------------------------|-------------------------|-----------------------------|---------------|
| 2 | - | 164.0 (C) | 164.0 (C) | - |
| 3 | 6.81 (1H, s) | 105.1 (CH) | 104.9 (CH) | C-2, 10 |
| 4 | - | 182.7 (C) | 182.8 (C) | - |
| 5 | - | 153.0 (C) | 157.6 (C) | - |
| 6 | - | 132.8 (C) | 132.0 (C) | - |
| 7 | - | 159.8 (C) | 158.8 (C) | - |
| 8 | 6.88 (1H, s) | 91.2 (CH) | 95.9 (CH) | C-10, 7, 5, 6 |
| 9 | - | 151.7 (C) | 149.5 (C) | - |
| 10 | - | 105.8 (C) | 105.4 (C) | - |
| 1' | - | 131.4 (C) | 131.4 (C) | - |
| 2', 6' | 8.06 (2H, m) | 126.4 (CH) | 126.4 (CH) | C- 3',5', 4' |
| 3', 5' | 7.59 (2H, m) | 129.2 (CH) | 129.2 (CH) | C-1' |
| 4' | 7.59 (1H, m) | 131.9 (CH) | 129.2 (CH) | C-3',5' |
| 5-OH | 12.80 (1H, s) | - | - | C-8, C9, C10 |
| 6-OCH ₃ | 3.98 (3H, s) | 59.7 (CH ₃) | 61.7 (CH ₃) | C-7 |
| 7-OCH ₃ | 3.78 (s) | 56.0 (CH ₃) | 56.4 (CH ₃) | C-6 |

*Rosandy et al. (2013)



(M15)

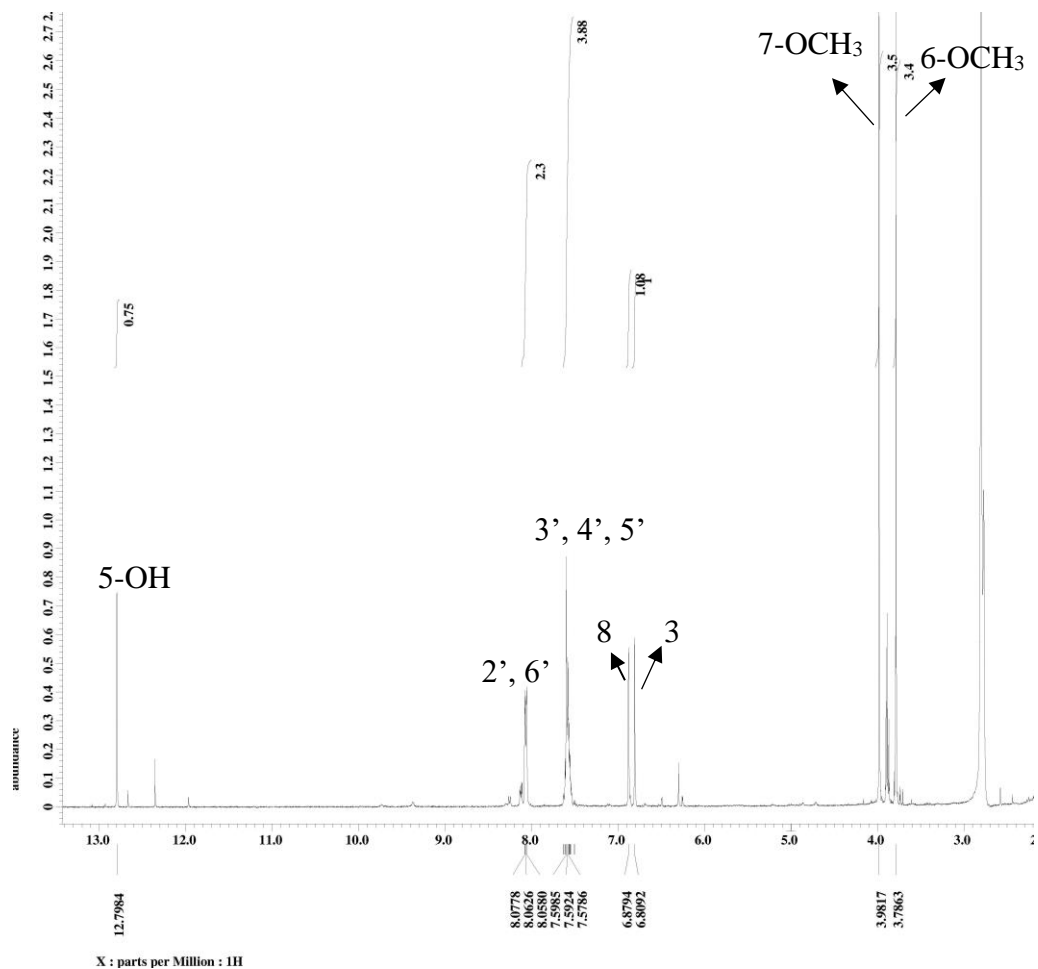


Figure 4.34: ^1H NMR (400 MHz, acetone- d_6) of 5-hydroxy-6,7-dimethoxyflavone (M15)

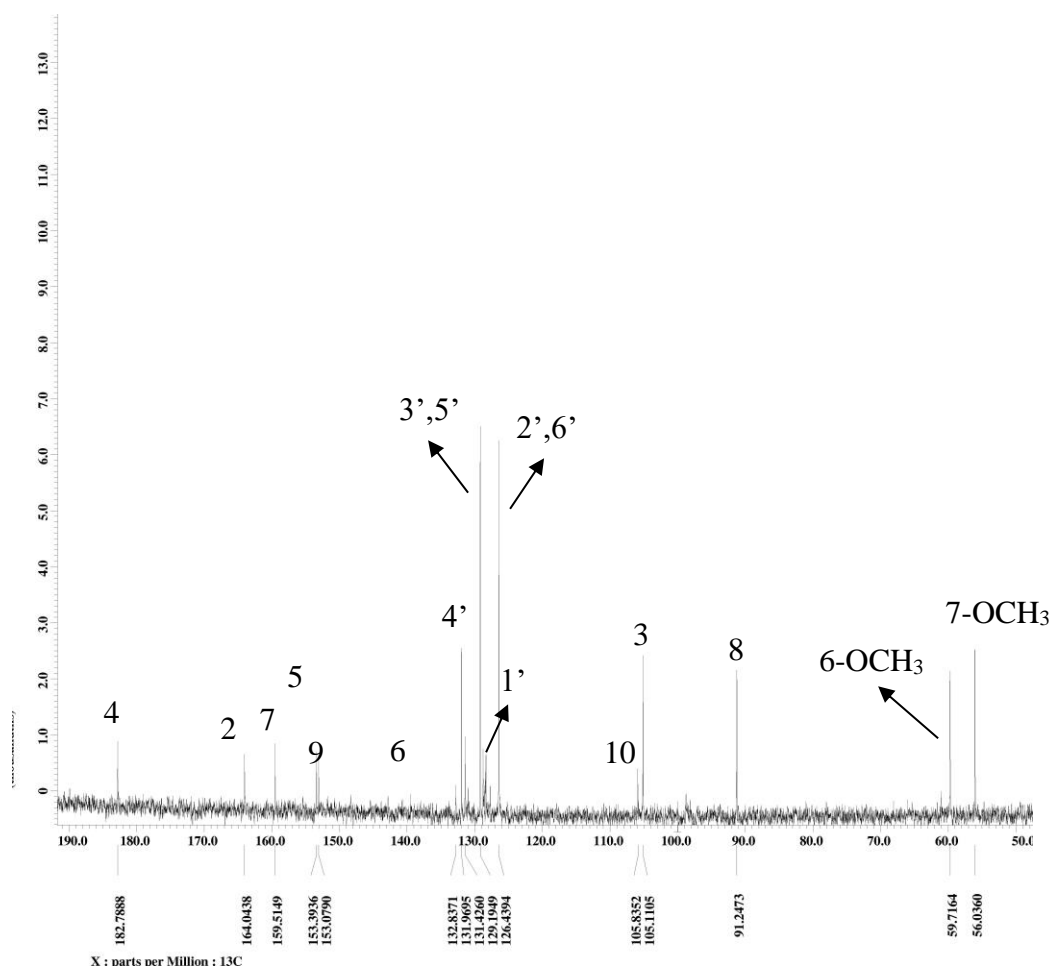
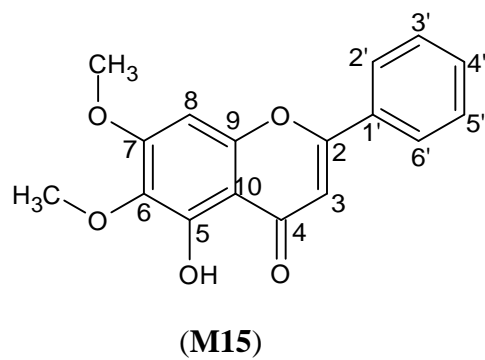
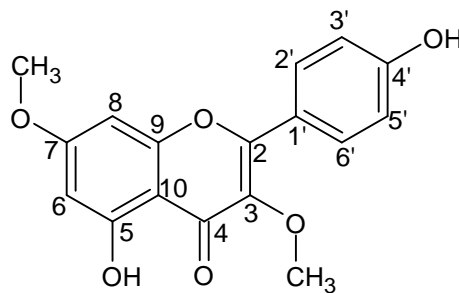


Figure 4.35: ^{13}C NMR (100 MHz, acetone- d_6) of 5-hydroxy-6,7-dimethoxyflavone (M15)

4.2.3.10 Characterization of 5,4'-dihydroxy-3,7-dimethoxyflavone (M16)



(M16)

Compound **M16** was isolated as a yellow solid, mp 219-221 °C (Lit. 220-222 °C, Boghrati et al., 2016). It gave R_f value of 0.49 in mobile phase hexane: ethyl acetate 1:1. The HRESIMS (Appendix A18) gave a pseudomolecular ion peak at $m/z = 315.0872$ $[M+H]^+$ which analysed for $C_{17}H_{14}O_6$ (found 314.0799; calculated 314.0790). The UV absorptions were 350 and 267 nm (Appendix B18). The IR spectrum (Appendix C18) shows absorption bands at 3436 (OH stretch), 1636 (C=O stretch), 1615 (C=C stretch), and 1170 (C-O stretch) cm^{-1} .

The 1H NMR (Figure 4.36) and ^{13}C NMR (Figure 4.37) of compound **M16** is similar to compound **M7** except presence of 4'-OH in compound **M16** instead of aromatic proton in **M7**. In 1H NMR, 4'-OH was appeared at δ_H 9.2. Two aromatic protons were appeared as doublets at δ_H 6.99 ($J= 8.0$ Hz) and at δ_H 8.03 ($J= 8.0$ Hz) due to ortho-coupled proton, were assigned to H-3',5' and H2',6', respectively. The meta position protons of ring A were displayed at δ_H 6.29 (H-6, d, $J= 2.4$ Hz) and δ_H 6.24 (H-8, d, $J=2.4$ Hz). Two methoxy groups at δ_H 3.85 and δ_H 3.90 correlated in the HMBC spectrum (Appendix D54) to the ^{13}C

NMR signals at δ_c 138.5 (C-3), and δ_c 165.7 (C-7), respectively, confirmed that methoxy groups present at C-3 and C-7. The structure of compound **M16** was further confirmed by DEPT (Appendix D52), HMQC (Appendix D53) and compared with literature data (Boghrati et al., 2016). Table 4.18 shows the ^1H , ^{13}C NMR and HMBC data of compound **M16**.

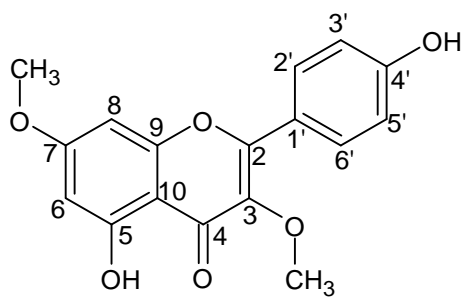
This compound was reported isolated from the aerial parts of *Teucrium polium* var. *gnaphalodes* and showed lowest antioxidant activity among test compounds. However, it showed the most tyrosinase inhibitory activity with IC_{50} value of 0.04 mM which comparable with the IC_{50} of kojic acid as positive control (Boghrati et al., 2016).

Table 4.18: ¹H, ¹³C and HMBC spectral data of M16 (acetone-d₆)

| Position | δ _H (multiplicity) | δ _C (C-type) | * ^b δ _C (C-type) | HMBC |
|--------------------|---------------------------------|-------------------------|--|-------------|
| 2 | - | 156.2 (C) | 164.5 (C) | - |
| 3 | - | 138.5 (C) | 132.3 (C) | - |
| 4 | - | 178.8 (C) | 182.4 (C) | - |
| 5 | - | 162.0 (C) | 153.0 (C) | - |
| 6 | 6.29 (1H, d, <i>J</i> = 2.4 Hz) | 97.7 (CH) | 92.0 (CH) | C-5, 10, 8 |
| 7 | - | 165.7 (C) | 159.0 (C) | - |
| 8 | 6.64 (1H, d, <i>J</i> =2.4 Hz) | 92.0 (CH) | 103.1 (CH) | C-10, 7, 6 |
| 9 | - | 156.9 (C) | 152.5 (C) | - |
| 10 | - | 105.7 (C) | 105.5 (C) | - |
| 1' | - | 121.8 (C) | 131.4 (C) | - |
| 2', 6' | 8.03 (2H, d, <i>J</i> = 8.0 Hz) | 130.4 (CH) | 121.5 (CH) | C- 2, 4' |
| 3', 5' | 6.99 (2H, d, <i>J</i> = 8.0 Hz) | 115.6 (CH) | 116.4 (CH) | C-1', 4' |
| 4'-OH | 9.16 (1H, s) | 160.2 (C) | 161.7(C) | C-3',5', 4' |
| 5-OH | 12.74 (1H, s) | - | - | C-5, 6, 10 |
| 3-OCH ₃ | 3.85 (3H, s) | 59.4 (CH ₃) | 60.4 (CH ₃) | C-3 |
| 7-OCH ₃ | 3.90 (s) | 55.6 (CH ₃) | 56.8 (CH ₃) | C-7 |

* Boghrati, et al. (2016)

^bDMSO-d₆



(M16)

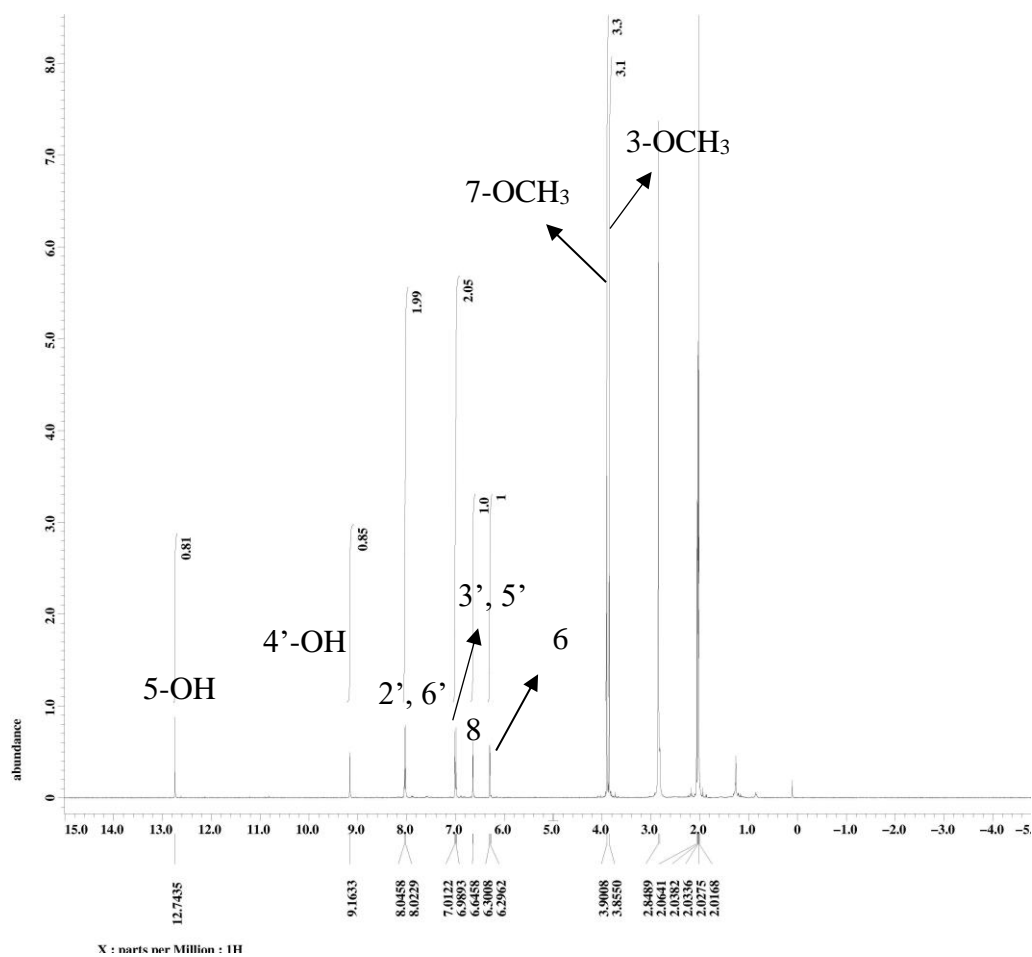
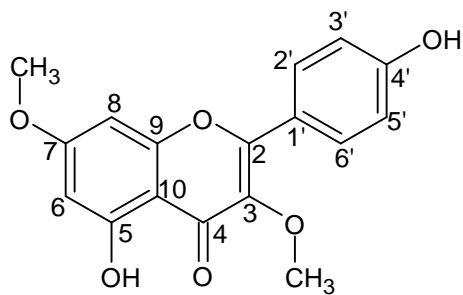


Figure 4.36: ^1H NMR (400 MHz, acetone- d_6) of 5,4'-dihydroxy-3,7-dimethoxyflavone (M16)



(M16)

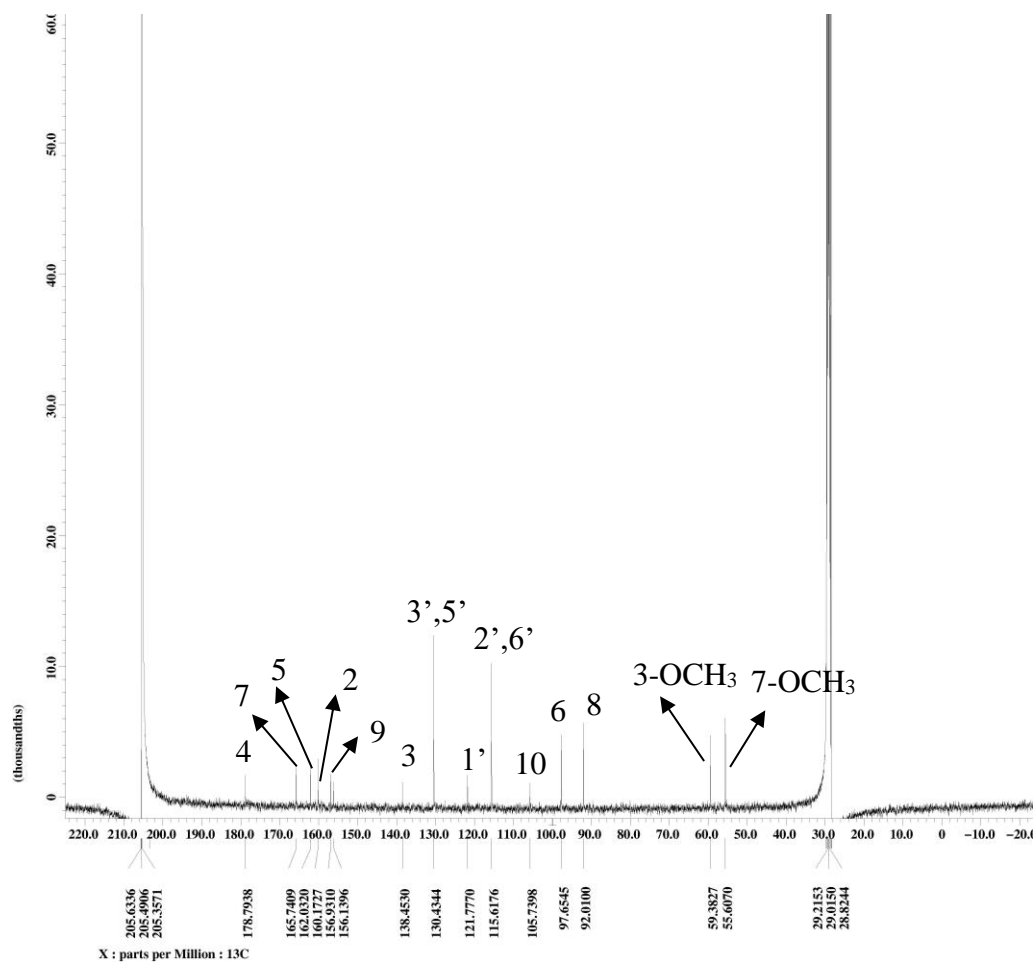


Figure 4.37: ^{13}C NMR (100 MHz, acetone- d_6) of 5,4'-dihydroxy-3,7-methoxyflavone (M16)

4.3 Synthesis of Flavonoid Mannich Base Derivatives

Mannich reaction was used to synthesize flavonoid Mannich base derivatives. It is a three-component condensation reaction that involves formaldehyde, secondary amine and active hydrogen containing substrate (Sujith et al., 2009). The substrates used in this work were isolated from the leaves of *Muntingia calabura*. The amines used in this work were pyrrolidine, piperidine, 1-methylpiperazine, morpholine, thiomorpholine and 4-methoxybenzylamine.

Isolates chalcones 2',4'-dihydroxy-3'-methoxychalcone (**M2**) and 2',4'-dihydroxychalcone (**M4**) were used to synthesize chalcone Mannich base. For flavone Mannich base, flavones 3,5,7-trihydroxy-8-methoxyflavone (**M5**) and 5,7-dihydroxyflavone (**M14**) were used. A total of four chalcone Mannich bases, eleven monosubstituted flavone Mannich bases and six disubstituted flavone Mannich bases were synthesized. Isolated flavanones were not chosen for synthesis due to low yield.

4.3.1 Synthesis of 2',4'-dihydroxy-3'-methoxychalcone (M2) Mannich Bases

Isolate 2',4'-dihydroxy-3'-methoxychalcone (**M2**) was used to synthesis chalcone Mannich bases via Mannich reaction. The reaction route was shown in Figure 4.38.

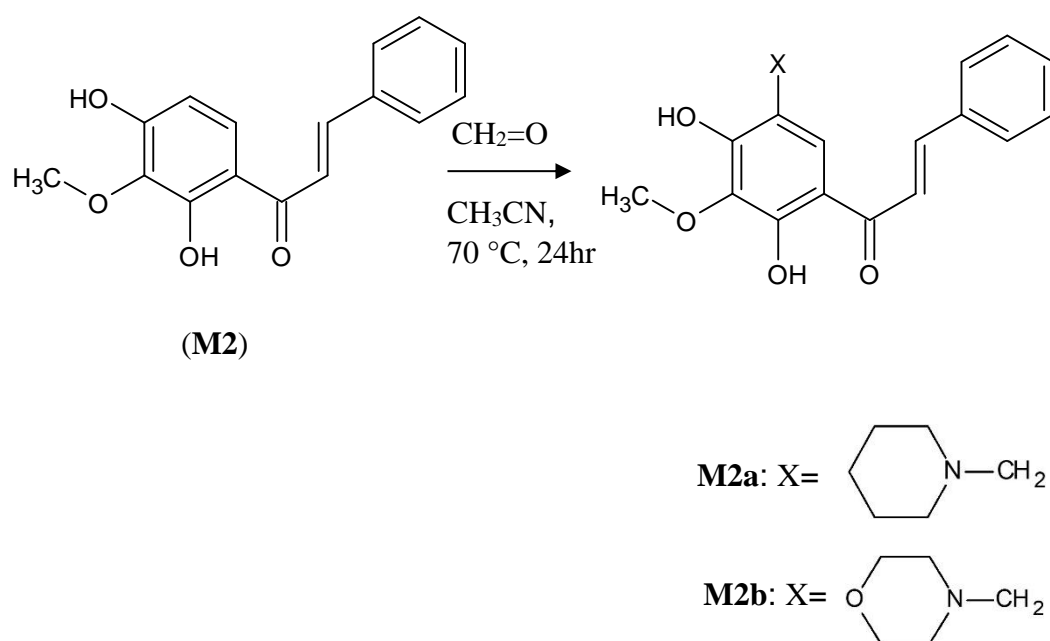


Figure 4.38: Synthesis route of chalcone M2 based Mannich bases with mol ratio chalcone: formaldehyde: amine 1:2:2

Mannich chalcones (**M2a** & **M2b**) were prepared by reaction of **M2** chalcone with formaldehyde, secondary amine (piperidine in **M2a**; morpholine in **M2b**) in mol ratio 1:2:2, respectively, and stirred under reflux in acetonitrile for 24 hr at 70 °C.

The reaction mechanism involves the formation of iminium ion (Figure 4.39) which is the condensation between formaldehyde and secondary amine. Then, followed by the electrophilic attack of the iminium ion on the aromatic B-ring of the chalcone substrate at C5' which is ortho to hydroxyl group. The reaction mechanism is shown in Figure 4.40. Zhang et al. (2019) reported that formation of *o*-substituted Mannich chalcone bases is attributed to the hydrogen bonding between *o*-hydroxy group and nitrogen which form a stable six-membered ring.

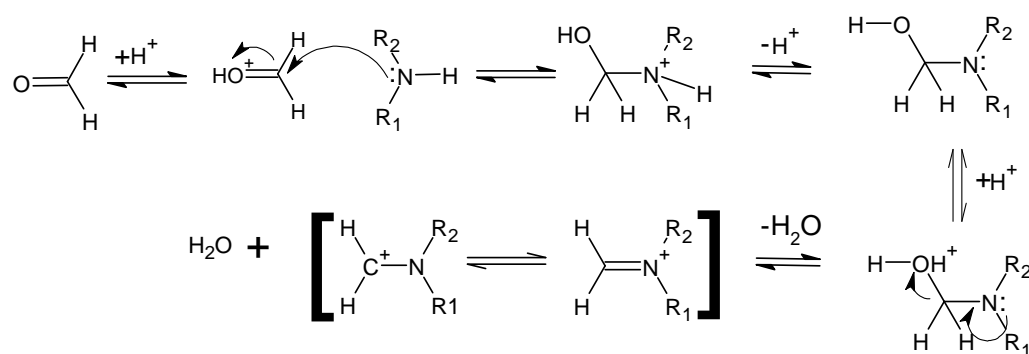


Figure 4.39: Formation of iminium ion

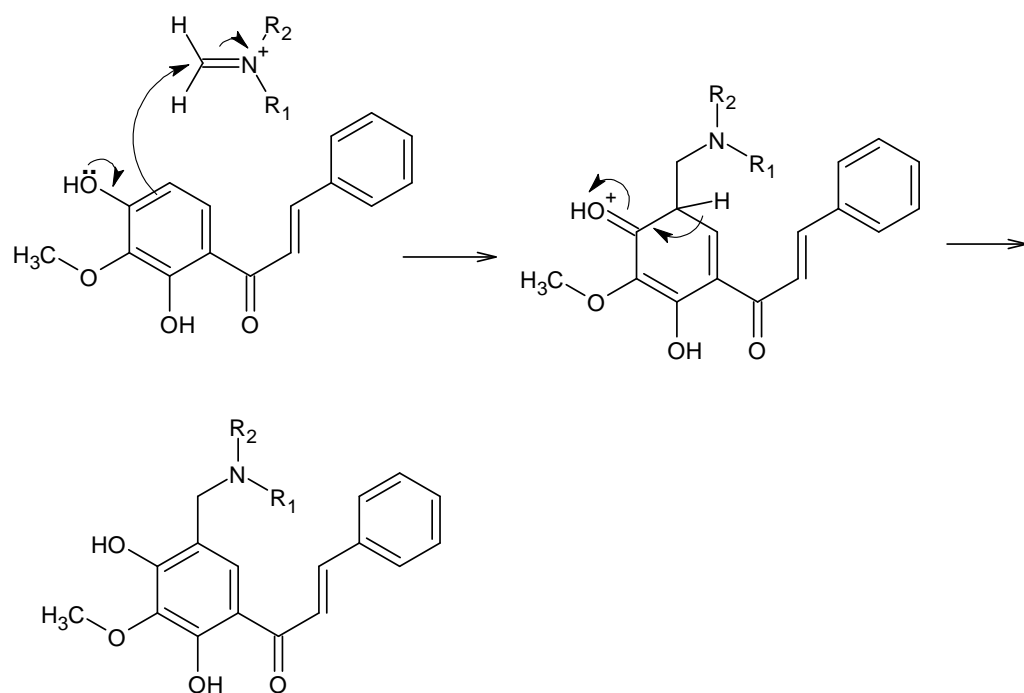
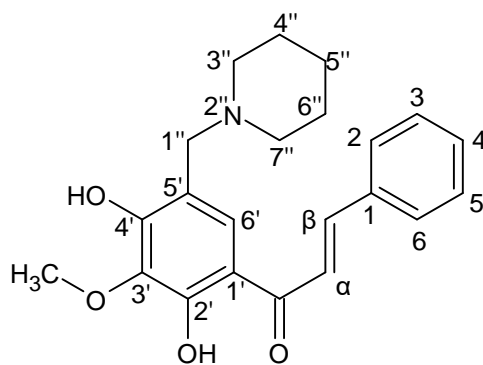


Figure 4.40: Reaction mechanism of M2 Chalcone Mannich bases

4.3.1.1 Characterization of 1-[3-methoxy-5-(piperidin-4-yl) methyl-2,4-dihydroxyphenyl]-3-phenyl-2-propen-1-one (M2a)



(M2a)

Compound **M2a** was obtained as dark orange solid, mp 100-101 °C. It showed R_f value of 0.31 on a TLC plate eluted with mobile phase hexane:acetone 6:4. The percentage yield of **M2a** was obtained at 65.9%. The HRESIMS (Appendix A19) gave a pseudomolecular ion peak at $m/z = 368.1862$ $[M+H]^+$ which analysed for $C_{22}H_{25}NO_4$ (found 367.1789; calculated 367.1784). Table 4.19 shows the summary physical properties of **M2a**.

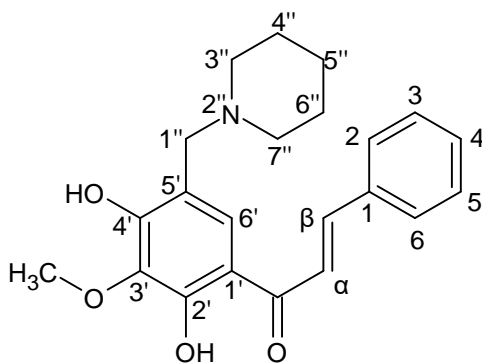
The IR spectrum of **M2a** (Appendix C19) shows absorption bands at 3414 (OH stretch), 2931 (CH_3 stretch), 1637 (C=O stretch), 1617 (C=C stretch), 1170 (C-N stretch), 1033 (C-O-C stretch) cm^{-1} .

Table 4.19: Summary Physical Properties of M2a

| Compound | M2a |
|-------------------------|---|
| IUPAC Name | 1-[3-methoxy-5-(piperidin-4-yl) methyl-2,4-dihydroxyphenyl]-3-phenyl-2-propen-1-one |
| Molecular formula | C ₂₂ H ₂₅ NO ₄ |
| Molecular weight, g/mol | 367.1789 |
| Physical appearance | Dark orange solid |
| Percentage yield, % | 65.9 |
| Obtained Mass, mg | 24.2 |
| R _f value | 0.31 |
| Melting point, °C | 100-101 |

The ¹H NMR of **M2a** (Figure 4.41) was similar to the **M2** (Figure 4.12) except for the appearance of signal for methylene protons and piperidine protons. The singlet at δ_H 3.76 indicated the presence of methylene protons instead of the doublet at δ_H 6.58 (H-5') observed for chalcone **M2**. The piperidine protons were observed as multiplets of four protons at δ_H 1.68, broad singlet of four protons at δ_H 2.61 for characteristic of CH₂NCH₂ of the piperidine moiety. Singlet at δ_H 1.51 was assigned to CH₂ protons of piperidine. In ¹³C NMR of **M2a** (Figure 4.42), methylene protons were observed at δ_c 60.8. Characteristic peaks of piperidine were observed at δ_c 23.6 (C-5''), δ 25.3 (C-4'', 6'') and δ 44.3 (C-3'', 7''). Aminomethylation at C-5' was confirmed through HMBC spectrum (Figure 4.44). The methylene protons at δ_H 3.76 (5'-CH₂) showed three-bond correlations with carbon signals at δ_c 44.3 (C-3'',7''), δ_c 159.1 (C-4'), and δ_c

125.1 (C-6'). Also, two bonds correlations also observed between these methylene protons and a carbon resonance at δ_c 112.6 (C-5'), show that piperidinomethyl group was attached to C-5'. The structure was further confirmed by DEPT spectrum (Appendix D55) and HMQC spectrum (Figure 4.43). Table 4.20 shows the summary NMR data of **M2** and **M2a**.



(M2a)

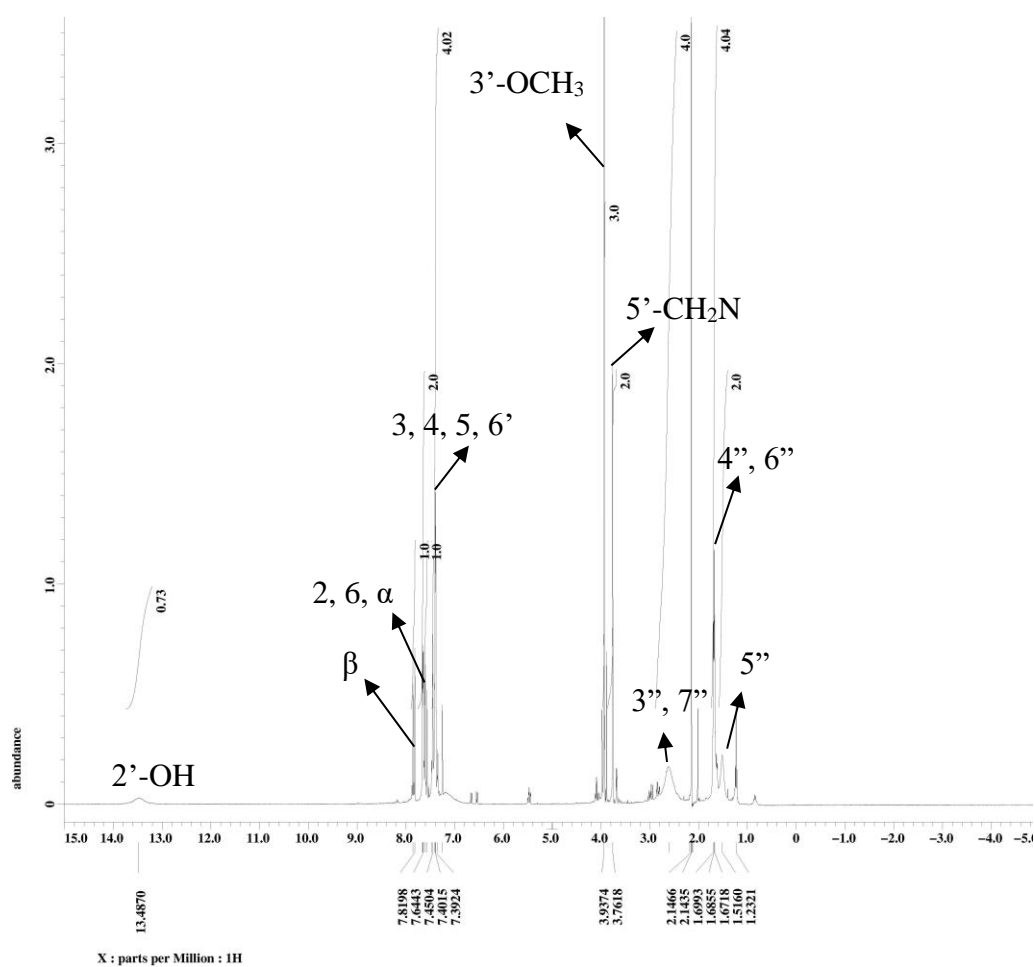
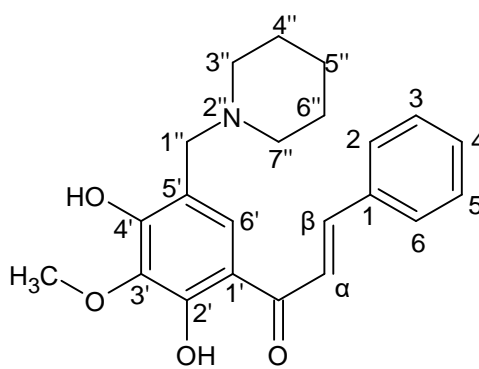


Figure 4.41: ^1H NMR (400 MHz, CDCl_3) of 1-[3-methoxy-5-(piperidin-4-yl)methyl-2,4-dihydroxyphenyl]-3-phenyl-2-propen-1-one (M2a)



(M2a)

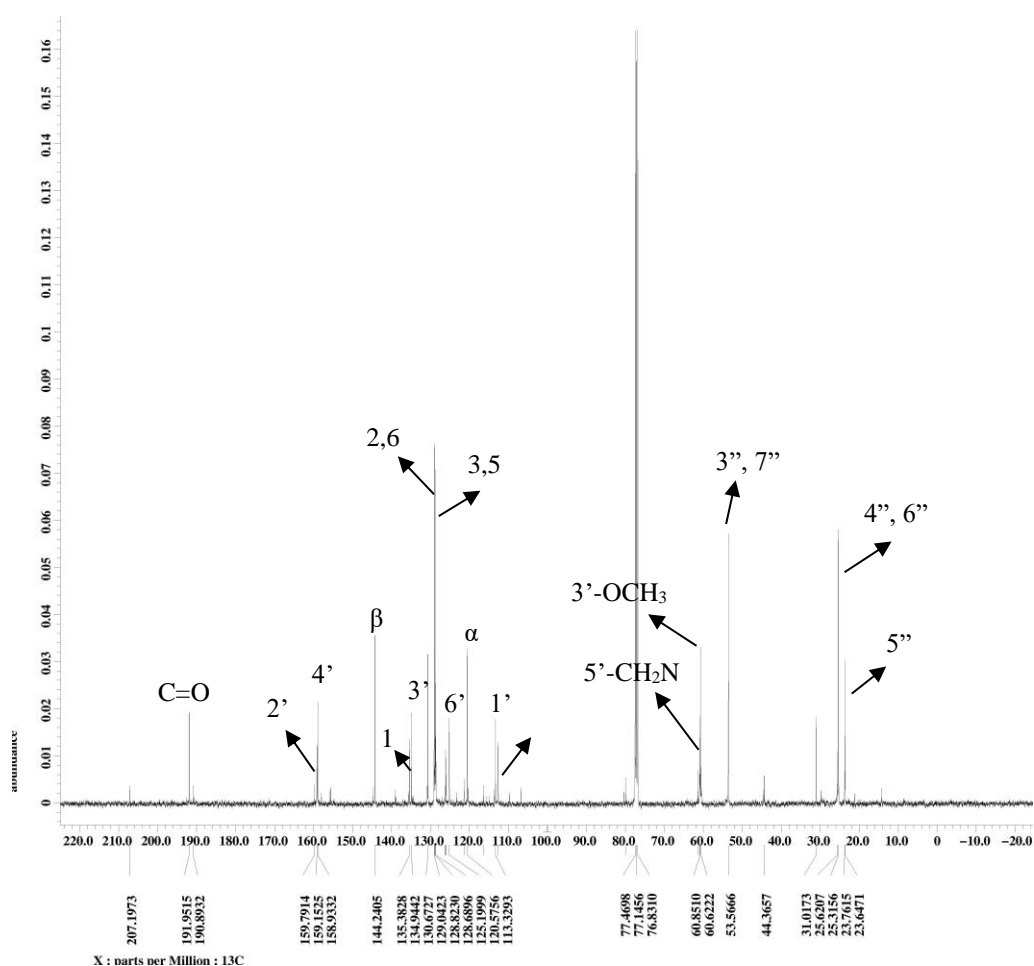
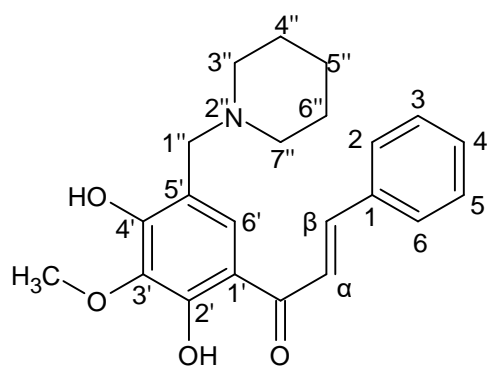


Figure 4.42: ^{13}C NMR (100 MHz, CDCl_3) of 1-[3-methoxy-5-(piperidin-4-yl)methyl-2,4-dihydroxyphenyl]-3-phenyl-2-propen-1-one (M2a)

Table 4.20: ^1H , ^{13}C and HMBC spectral data of M2 and M2a (CDCl_3)

| | M2 | M2a | M2 | M2a | M2a |
|----------------------|------------------------------------|--------------------------------------|-----------------------------------|-------------------------------------|------------------------|
| Position | δ_{H} (multiplicity) | $^*\delta_{\text{H}}$ (multiplicity) | δ_{C} (Carbon type) | $^*\delta_{\text{C}}$ (Carbon type) | HMBC |
| 1 | - | - | 134.8 (C) | 135.3 (C) | - |
| 2,6 | 7.65 (2H, m) | 7.64 (2H, m) | 128.7 (CH) | 128.8 (CH) | C- 3, 4, 5 |
| 3,5 | 7.42 (2H, m) | 7.42 (2H, m) | 129.1 (CH) | 129.0 (CH) | C-2,6 |
| 4 | 7.42 (1H, m) | 7.42 (1H, m) | 130.9 (CH) | 130.6 (CH) | C-2,6 |
| α | 7.58 (1H, d, $J = 15.3$ Hz) | 7.56 (1H, $J=15.3$ Hz) | 120.3 (CH) | 120.5 (CH) | C-1, C=O |
| β | 7.90 (1H, d, $J = 15.3$ Hz) | 7.81 (d, $J=15.3$ Hz) | 144.8 (CH) | 144.2 (CH) | C-2, 6, C=O |
| C=O | - | - | 192.7 (C) | 191.9 (C) | - |
| 1' | - | - | 115.1 (C) | 113.3 (C) | - |
| 2' | - | - | 157.9 (C) | 159.7 (C) | - |
| 3' | - | - | 134.4 (C) | 134.9 (C) | - |
| 4' | - | - | 155.5 (C) | 159.1 (C) | - |
| 5' | 6.58 (1H, d, $J = 9.2$ Hz) | - | 106.7 (CH) | 112.6 (CH) | - |
| 6' | 7.62 (1H, d, $J = 9.2$ Hz) | 7.39 (1H, m) | 126.4 (CH) | 125.1 (CH) | C- 3', 4', C=O |
| 2'-OH | 13.57 (1H, s) | 13.48 (1H, s) | - | - | - |
| 3'-OCH ₃ | 4.01(3H, s) | 3.94 (3H, s) | 60.9 (CH ₃) | 60.6 (CH ₃) | C3' |
| 4'-OH | 9.27 (1H, s) | - | - | - | - |
| 5'-CH ₂ N | - | 3.76 (2H, s) | - | 60.8 (CH ₂) | C-3'', 7'', 5', 6', 4' |
| 5''-CH ₂ | - | 1.51 (2H, s) | - | 23.6 (CH ₂) | C-4'', 6'', 3'', 7'' |
| 4'', 6'' | - | 1.68 (2H, m) | - | 25.3 (CH ₂) | - |
| 3'', 7'' | - | 2.61 (2H, br s) | - | 44.3 (CH ₂) | - |



(M2a)

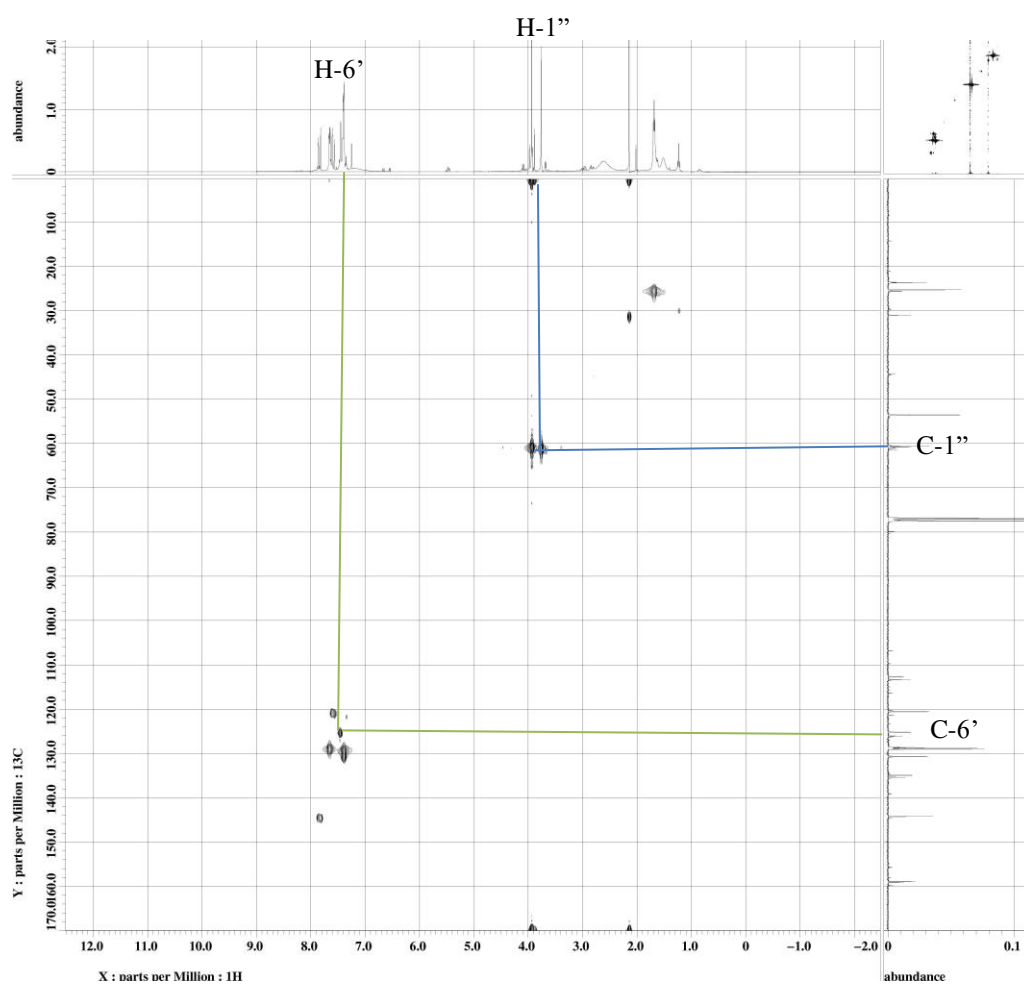
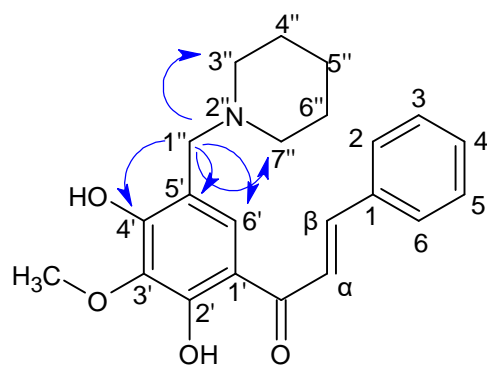


Figure 4.43: HMQC Spectrum of 1-[3-methoxy-5-(piperidin-4-yl) methyl-2,4-dihydroxyphenyl]-3-phenyl-2-propen-1-one (M2a)



(M2a)

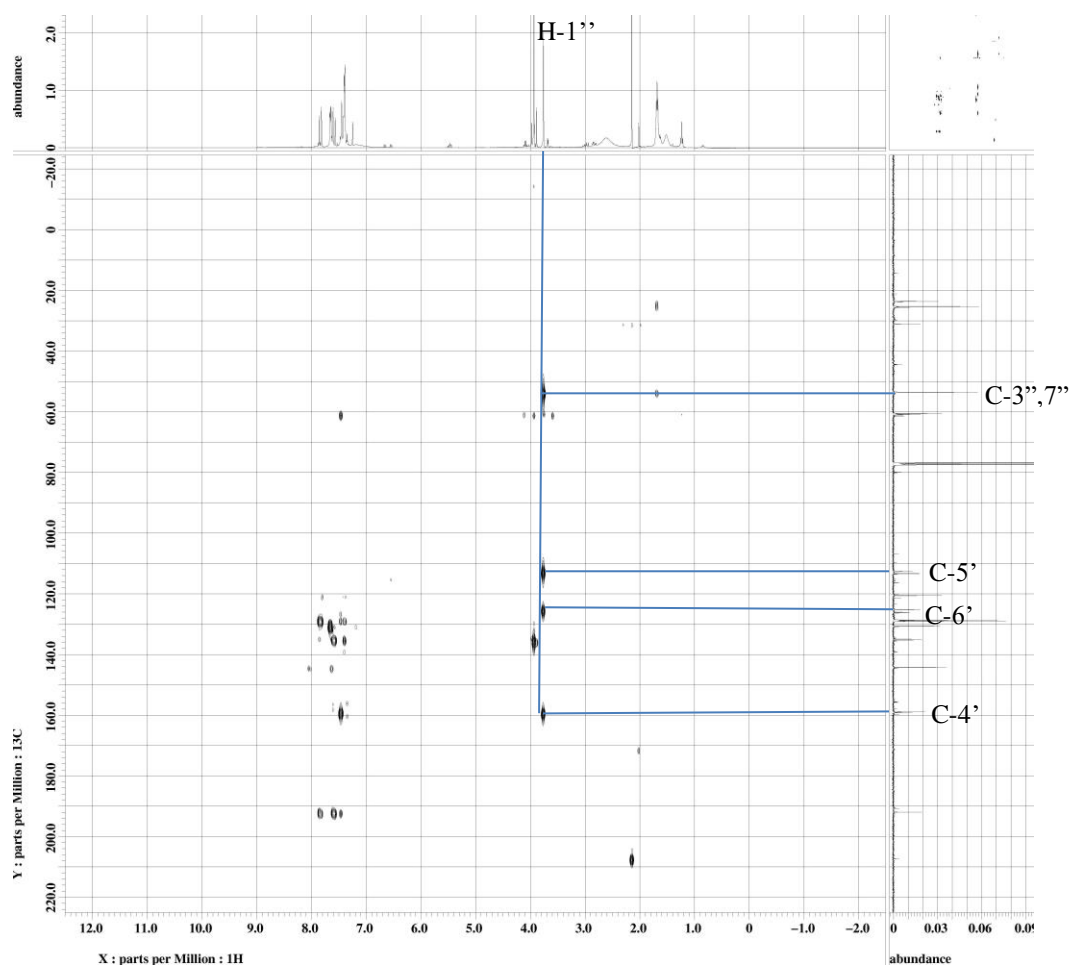
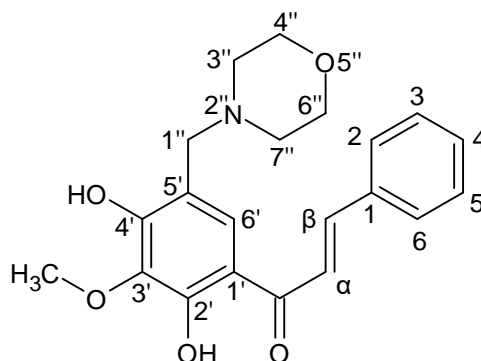


Figure 4.44: HMBC Spectrum of 1-[3-methoxy-5-(piperidin-4-yl) methyl-2,4-dihydroxyphenyl]-3-phenyl-2-propen-1-one (M2a)

4.3.1.2 Characterization of 1-[3-methoxy-5-(morpholino-4-yl) methyl-2,4-dihydroxyphenyl]-3-phenyl-2-propen-1-one (M2b)



(M2b)

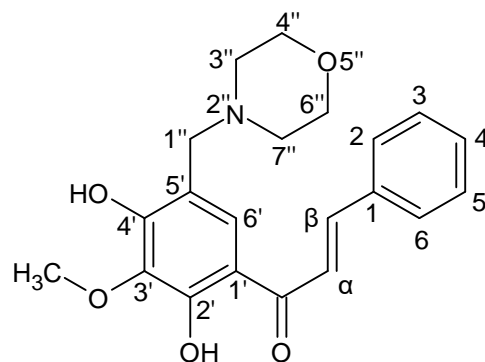
Compound **M2b** was obtained as dark orange solid, mp 220-221 °C. In TLC plate, R_f value of 0.46 was obtained in mobile phase hexane: acetone 6:4. The percentage yield of **M2b** was found to be 61 %. The HRESIMS (Appendix A20) gave a pseudomolecular ion peak at $m/z = 370.1652$ $[M+H]^+$ which analysed for $C_{21}H_{23}NO_5$ (found 369.1580; calculated 369.1576). Table 4.21 shows the summary physical properties of **M2b**.

The IR spectrum of **M2b** (Appendix C20) shows absorption bands at 3413 (OH stretch), 1637 (C=O stretch), 1617 (C=C stretch), 1171 (C-N stretch), 1118 (C-O-C stretch) cm^{-1} .

Table 4.21: Summary Physical Properties of M2b

| Compound | M2b |
|-------------------------|--|
| IUPAC Name | 1-[3-methoxy-5-(morpholino-4-yl) methyl-2,4-dihydroxyphenyl]-3-phenyl-2-propen-1-one |
| Molecular formula | C ₂₁ H ₂₃ NO ₅ |
| Molecular weight, g/mol | 369.1580 |
| Physical appearance | Dark orange solid |
| Percentage yield, % | 61 |
| Obtained Mass, mg | 22.5 |
| R _f value | 0.46 |
| Melting point, °C | 220-221 |

In the ¹H NMR of **M2b** (Figure 4.45), methylene protons were observed at δ_H 3.76. Signals at δ_H 3.76 (s, H-3'', 7'') and δ_H 2.63 (s, H-4'', 6'') were characteristic peaks of morpholine. In ¹³C NMR of **M2b** (Figure 4.46), the methylene carbon signal was appeared at δ_c 61.1. Signals at δ_c 66.6 and δ_c 52.7 were belonging to C-3'', 7'' (CH₂OCH₂), and C-4'', 6'' (CH₂NCH₂), respectively. Aminomethylation also occurred at C-5' as in **M2a**. The position of morpholine aminomethyl side chain in **M2b** was supported by the correlations observed in the HMBC spectrum (Figure 4.48). Structure **M2b** was further confirmed by DEPT spectrum (Appendix D56) and HMQC spectrum (Figure 4.47). Table 4.22 shows the summary NMR data of **M2** and **M2b**.



(M2b)

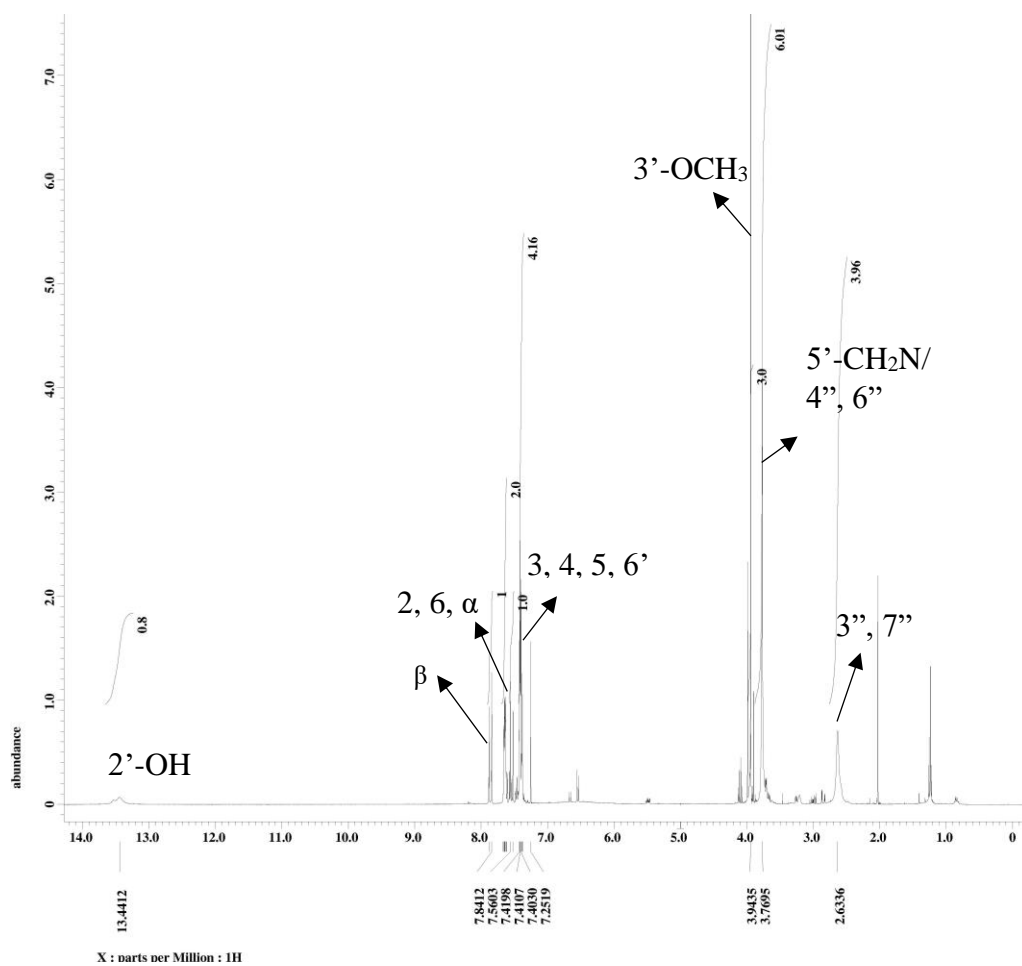


Figure 4.45: ¹H NMR (400 MHz, CDCl₃) of 1-[3-methoxy-5-(morpholino-4-yl) methyl-2,4-dihydroxyphenyl]-3-phenyl-2-propen-1-one (M2b)

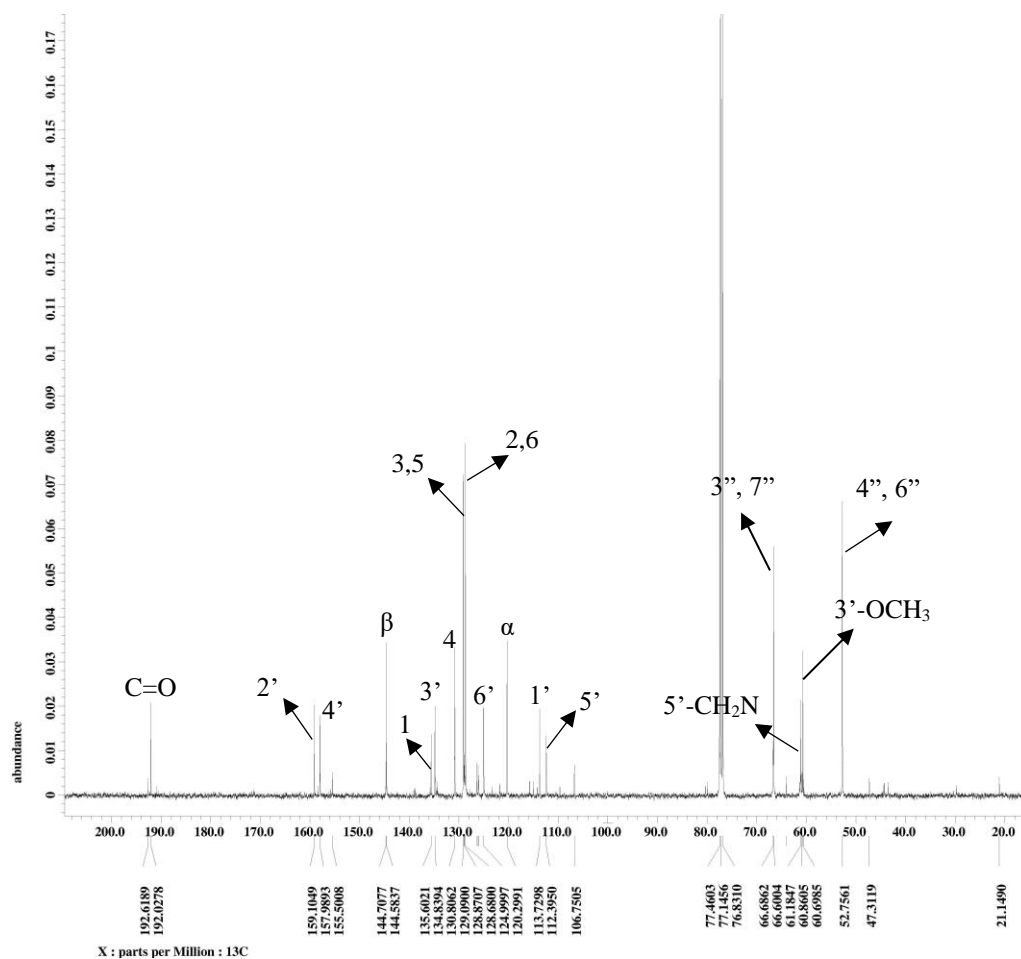
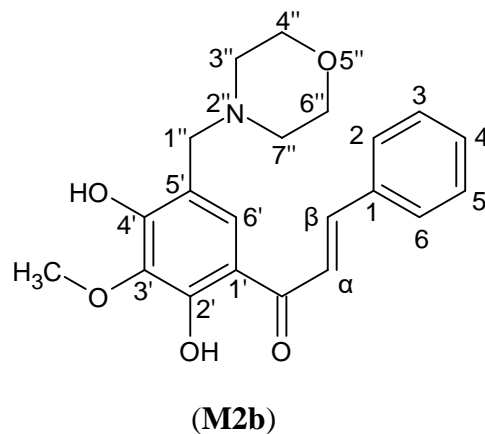


Figure 4.46: ^{13}C NMR (100 MHz, CDCl_3) of 1-[3-methoxy-5-(morpholino-4-yl) methyl-2,4-dihydroxyphenyl]-3-phenyl-2-propen-1-one (M2b)

Table 4.22: ^1H , ^{13}C and HMBC spectral data of M2 and M2b (CDCl_3)

| | M2 | M2b | M2 | M2b | M2b |
|----------------------------------|------------------------------------|--------------------------------------|-----------------------------------|-------------------------------------|------------------------|
| Position | δ_{H} (multiplicity) | $^*\delta_{\text{H}}$ (multiplicity) | δ_{C} (Carbon type) | $^*\delta_{\text{C}}$ (Carbon type) | HMBC |
| 1 | - | - | 134.8 (C) | 135.6 (C) | - |
| 2,6 | 7.65 (2H, m) | 7.63 (2H, m) | 128.7 (CH) | 128.6 (CH) | C- 3, 4, 5 |
| 3,5 | 7.42 (2H, m) | 7.41 (2H, m) | 129.1 (CH) | 129.0 (CH) | C-1, 2, 6 |
| 4 | 7.42 (1H, m) | 7.41 (1H, m) | 130.9 (CH) | 130.8 (CH) | C-1, 2, 6 |
| α | 7.58 (1H, d, $J=15.3$ Hz) | 7.52 (1H, d, $J=15.3$ Hz) | 120.3 (CH) | 120.2 (CH) | C-1, C=O |
| β | 7.90 (1H, d, $J=15.3$ Hz) | 7.84 (1H, d, $J=15.3$ Hz) | 144.8 (CH) | 144.7 (CH) | C-2, 6, C=O |
| C=O | - | - | 192.7 (C) | 192.0 (C) | - |
| 1' | - | - | 115.1 (C) | 113.7 (C) | - |
| 2' | - | - | 157.9 (C) | 159.7 (C) | - |
| 3' | - | - | 134.4 (C) | 134.8 (C) | - |
| 4' | - | - | 155.5 (C) | 159.1 (C) | - |
| 5' | 6.58 (1H, d, $J=9.2$ Hz) | - | 106.7 (CH) | 112.3 (CH) | - |
| 6' | 7.62 (1H, d, $J=9.2$ Hz) | 7.39 (1H, m) | 126.4 (CH) | 124.9 (CH) | C- 3', 4', C=O |
| 2'-OH | 13.57 (1H, s) | 13.48 (1H, s) | - | - | - |
| 3'-OCH ₃ | 4.01 (1H, s) | 3.94 (1H, s) | 60.9 (CH ₃) | 60.6 (CH ₃) | C3' |
| 4'-OH | 9.27 (1H, s) | - | - | - | - |
| 5'-CH ₂ N | - | 3.76 (2H, s) | - | 61.1 (CH ₂) | C-3'', 7'', 5', 6', 4' |
| CH ₂ OCH ₂ | - | 3.76 (4H, s) | - | 66.6 (CH ₂) | - |
| CH ₂ NCH ₂ | - | 2.63 (4H, s) | - | 52.7 (CH ₂) | - |

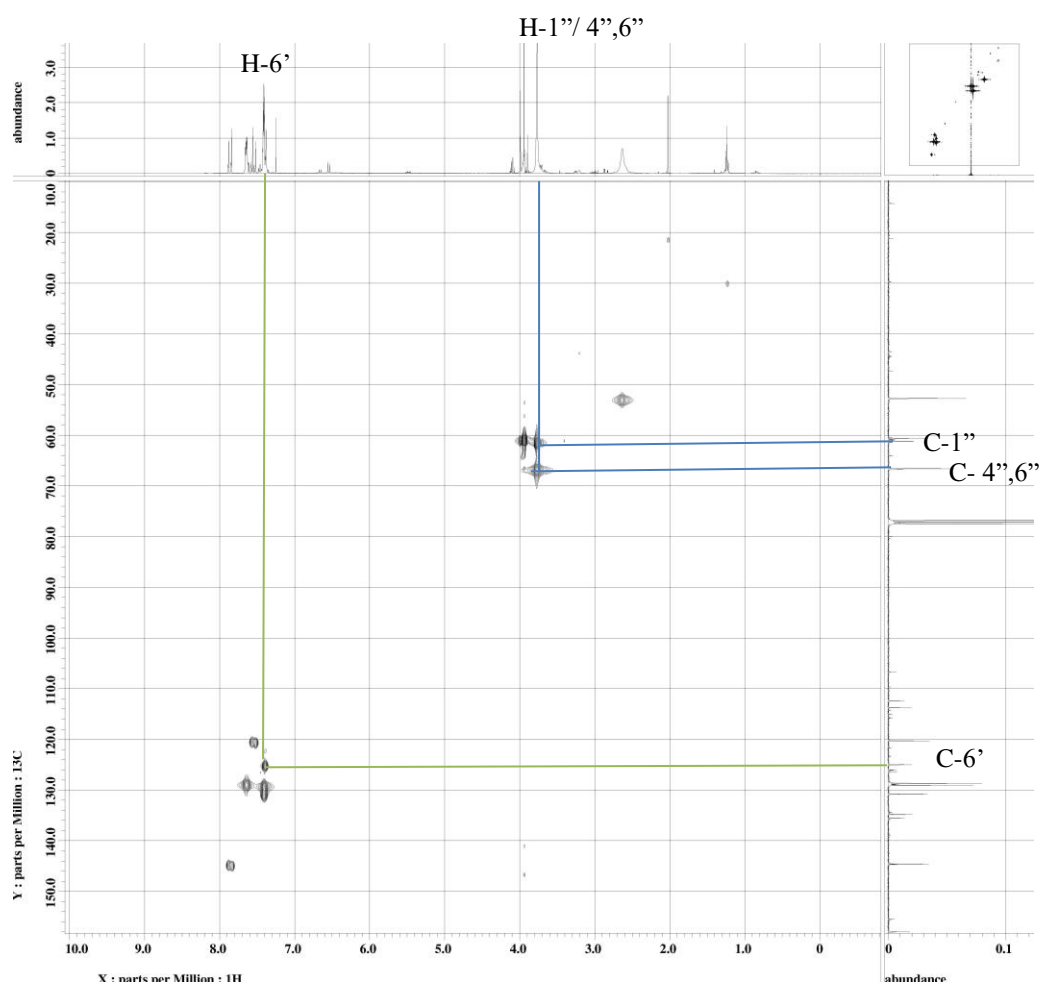
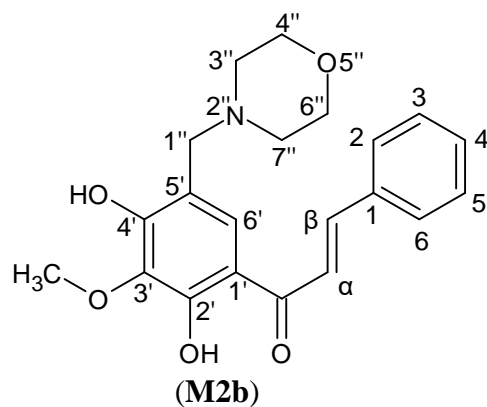
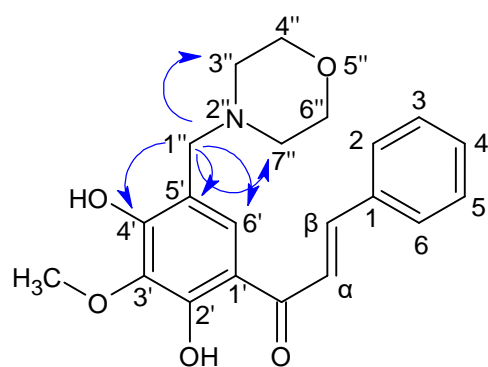


Figure 4.47: HMQC Spectrum of 1-[3-methoxy-5-(morpholino-4-yl)methyl-2,4-dihydroxyphenyl]-3-phenyl-2-propen-1-one (M2b)



(M2b)

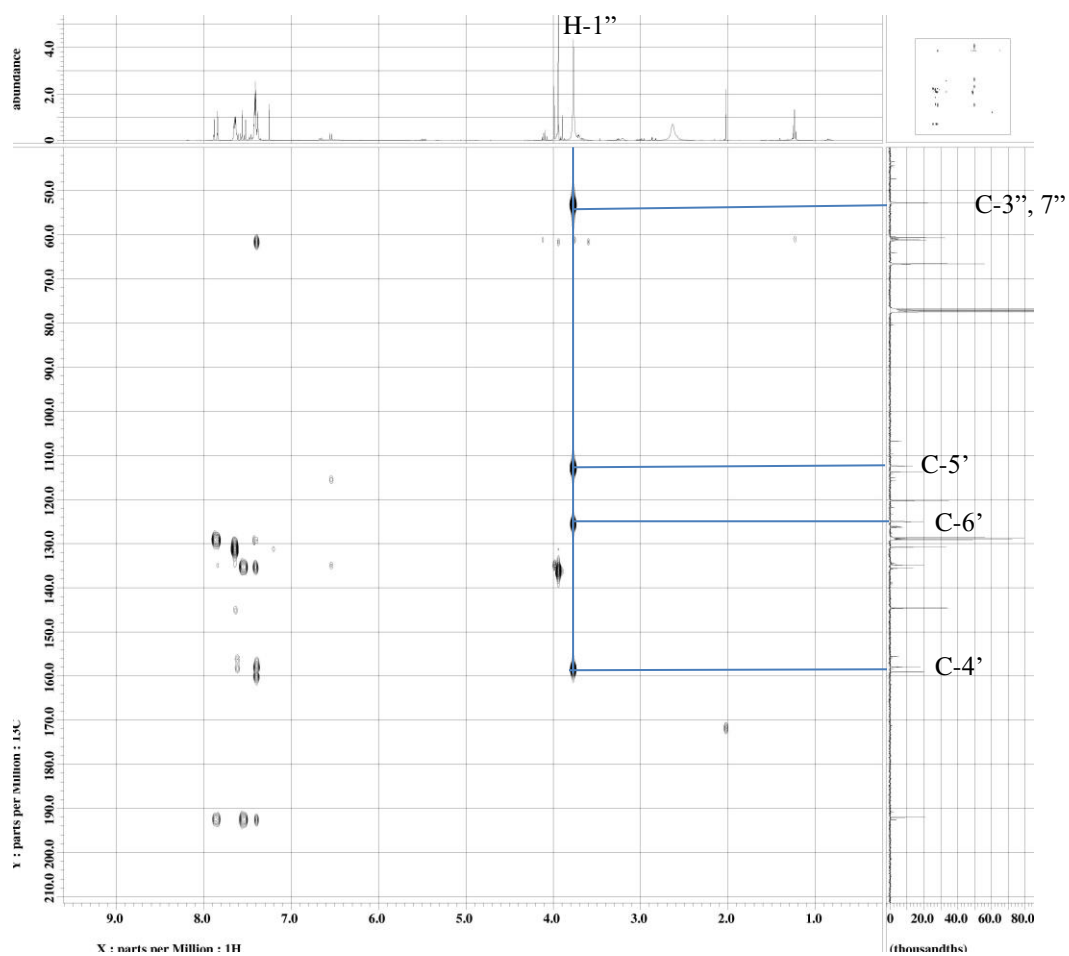


Figure 4.48: HMBC Spectrum of 1-[3-methoxy-5-(morpholino-4-yl) methyl-2,4-dihydroxyphenyl]-3-phenyl-2-propen-1-one (M2b)

4.3.2 Synthesis of 2',4'-dihydroxychalcone (M4) Mannich Bases

Isolate 2',4'-dihydroxychalcone (**M4**) was used to synthesis chalcone Mannich bases via Mannich reaction. The reaction route was shown in Figure 4.49.

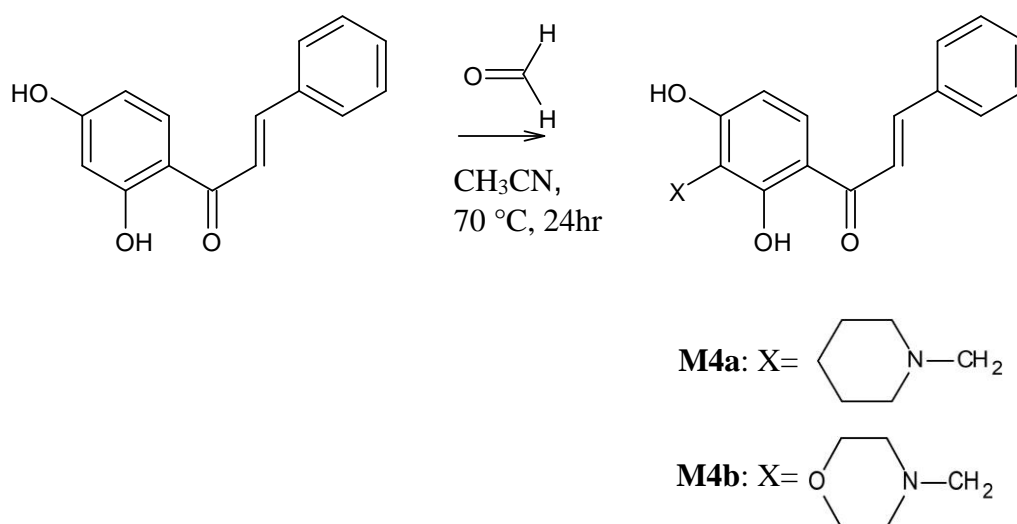


Figure 4.49: Synthesis route of chalcone M4 Mannich bases with mol ratio chalcone: formaldehyde: amine 1:2:2

Mannich chalcones (**M4a** & **M4b**) were prepared by reaction of **M4** chalcone with formaldehyde, secondary amine (piperidine in **M4a**; morpholine in **M4b**) in mol ratio 1:2:2, respectively, and stirred under reflux in acetonitrile for 24 hr at $70\text{ }^\circ\text{C}$.

The reaction mechanism involves the formation of iminium ion (Figure 4.39) which is the condensation between formaldehyde and secondary amine.

Then, followed by the electrophilic attack of the iminium ion on the aromatic B-ring of the chalcone substrate at C3' which is ortho to hydroxyl group. The reaction mechanism was shown in Figure 4.50.

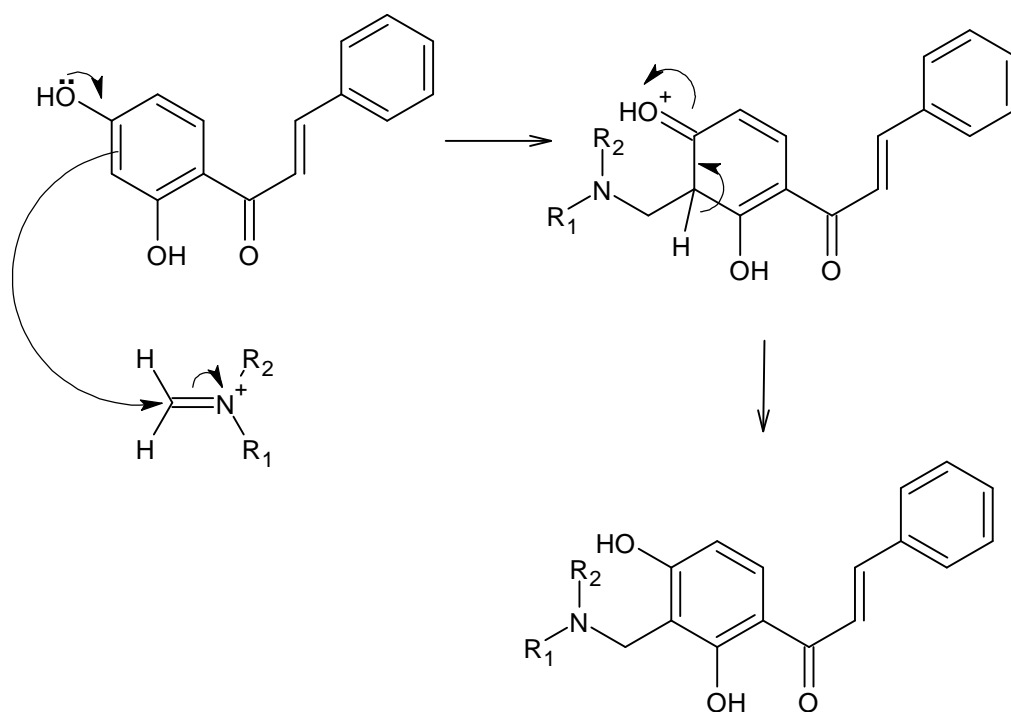
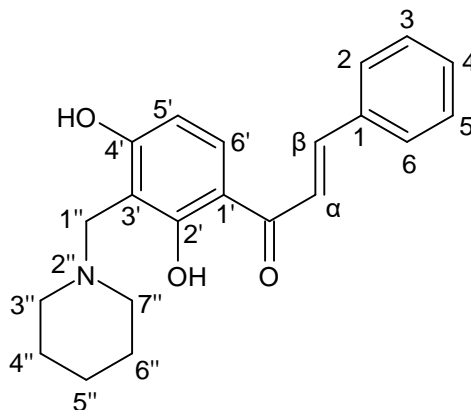


Figure 4.50: Reaction mechanism of chalcone M4 Mannich bases

4.3.2.1 Characterization of 1-[3-methoxy-5-(piperidin-4-yl) methyl-2,4-dihydroxyphenyl]-3-phenyl-2-propen-1-one (M4a)



(M4a)

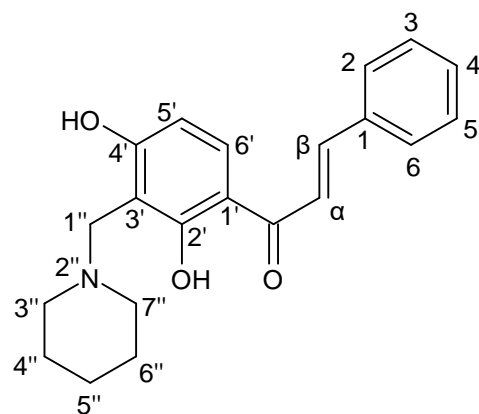
Compound **M4a** was obtained as yellow solid, mp 248-250 °C. It showed R_f value of 0.33 on a TLC plate eluted with mobile phase hexane:acetone 6:3. The percentage yield of **M4a** was obtained at 58.1%. The HRESIMS (Appendix A21) gave a pseudomolecular ion peak at $m/z = 338.1758$ $[M+H]^+$ which analysed for $C_{21}H_{23}NO_3$ (found 337.1685; calculated 337.1677). Table 4.23 shows the summary physical properties of **M4a**.

The IR spectrum of **M4a** (Appendix C21) shows absorption bands at 3413 (OH stretch), 2929 (CH_3 stretch), 1637 (C=O stretch), 1617 (C=C stretch), 1233 (C-N stretch) cm^{-1} .

Table 4.23: Summary Physical Properties of M4a

| Compound | M4a |
|-------------------------|--|
| IUPAC Name | 1-[3-(piperidin-1-yl)methyl-2,4-dihydroxyphenyl]-3-phenyl-2-propen-1-one |
| Molecular formula | C ₂₁ H ₂₃ NO ₃ |
| Molecular weight, g/mol | 367.1789 |
| Physical appearance | Yellow solid |
| Percentage yield, % | 58.1 |
| Obtained Mass, mg | 19.6 |
| R _f value | 0.33 |
| Melting point, °C | 248-250 |

In the ¹H NMR of compound **4a** (Figure 4.51), signal at δ_H 3.93 indicates the presence of methylene protons. Multiplets signals at δ_H 1.24, δ_H 1.71, and δ_H 2.96 were the characteristic peaks of piperidine. The disappearance doublet at δ_H 6.36 (H-3', *J*=2.4 Hz) in compound **4a** showed that the aminomethylation was occurred at C-3'. In ¹³C NMR (Figure 4.52) of compound **4a**, signal at δ_c 53.8 was the methylene carbon and the signal at δ_c 23.4, δ_c 25.2 and δ_c 53.6 were the characteristic peaks of piperidine moiety. In the HMBC spectrum (Figure 4.54), methylene protons showed three bond correlation with C-2' (δ_c 167.9), and C-4' (δ_c 164.3) which was belonging to chalcone ring B. In addition, methylene protons also showed three bonds correlation with C-3'', 7'' (δ_c 53.6) which belong to piperidine moiety. The structure was further confirmed by using DEPT (Appendix D57) and HMQC (Appendix Figure 4.53) spectrums. Table 4.24 shows the summary NMR data of compounds **M4** and **M4a**.



(M4a)

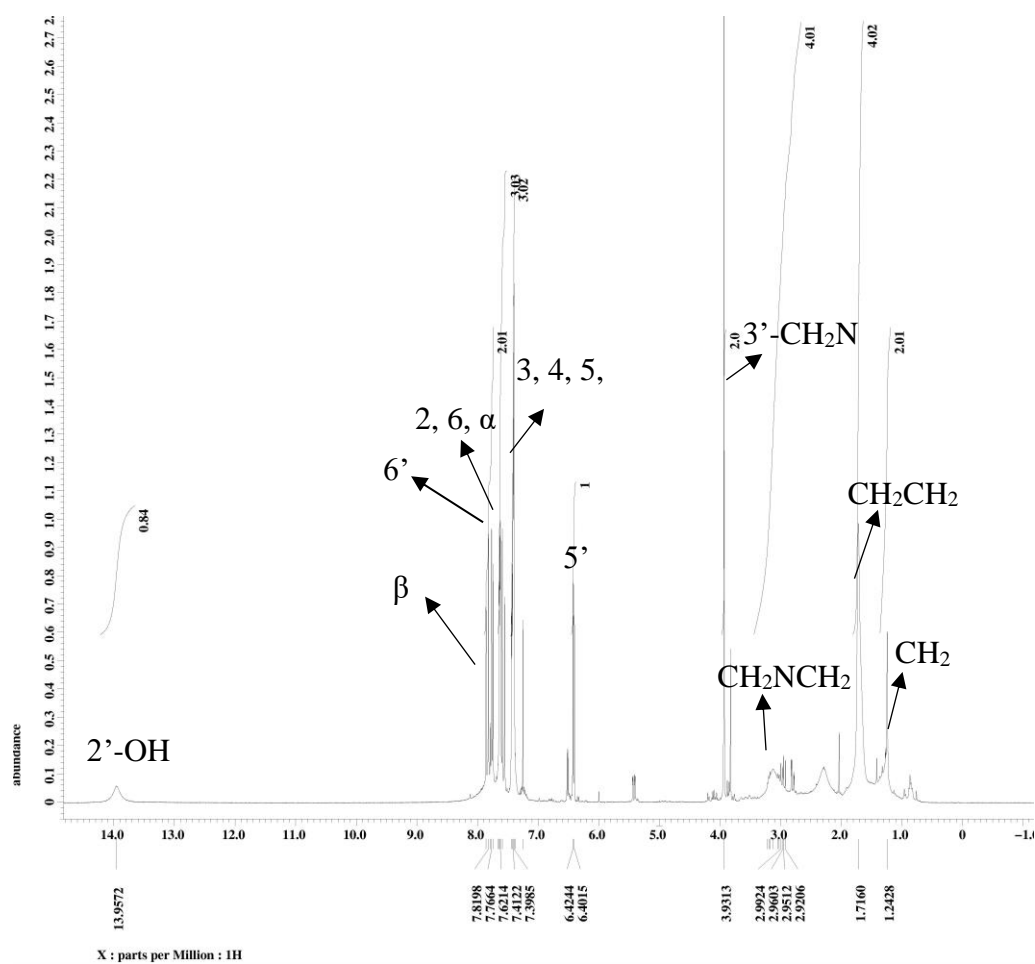
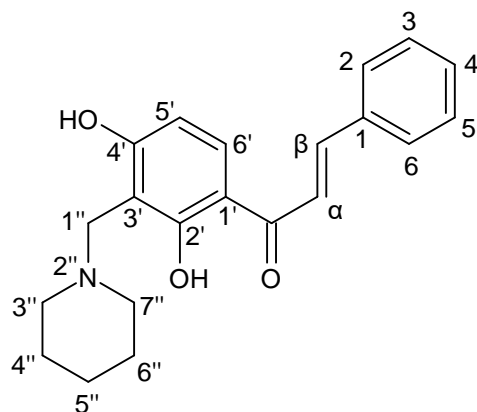


Figure 4.51: ^1H NMR (400 MHz, CDCl_3) of 1-[3-(piperidin-1-yl)methyl-2,4-dihydroxyphenyl]-3-phenyl-2-propen-1-one (M4a)



(M4a)

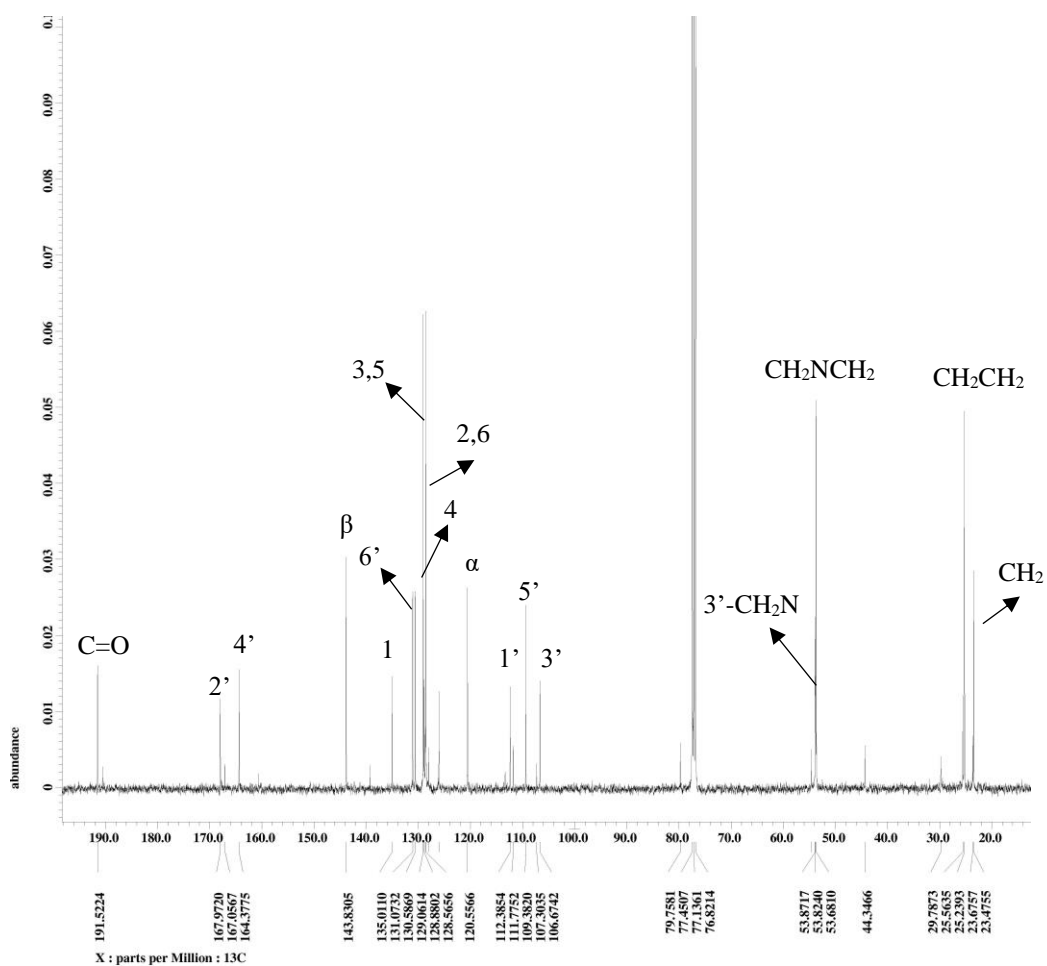
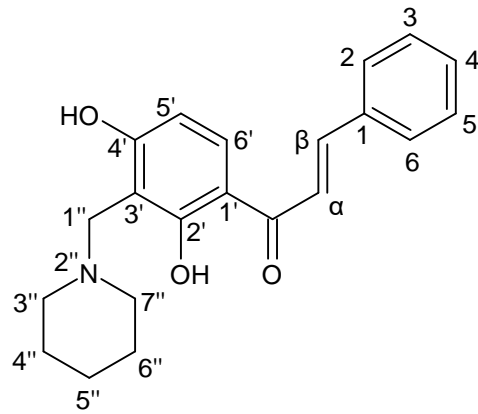


Figure 4.52: ^{13}C NMR (100 MHz, CDCl_3) of 1-[3-(piperidin-1-yl)methyl-2,4-dihydroxyphenyl]-3-phenyl-2-propen-1-one (M4a)

Table 4.24: ^1H , ^{13}C and HMBC spectral data of M4 and M4a (CDCl_3)

| | M4 | M4a | M4 | M4a | M4a |
|----------------------------------|------------------------------------|------------------------------------|-----------------------------------|-----------------------------------|------------------------|
| Position | δ_{H} (multiplicity) | δ_{H} (multiplicity) | δ_{C} (Carbon type) | δ_{C} (Carbon type) | HMBC |
| 1 | - | - | 135.1 (C) | 135.0 (C) | - |
| 2,6 | 7.85 (2H, m) | 7.62 (2H, m) | 129.0 (CH) | 128.5 (CH) | C-3, 4, 5 |
| 3,5 | 7.44 (2H, m) | 7.39 (2H, m) | 128.9 (CH) | 129.0 (CH) | C-1 |
| 4 | 7.44 (1H, m) | 7.39 (2H, m) | 130.7 (CH) | 130.5 (CH) | C-1 |
| β | 7.92 (1H, d, $J=15.9$ Hz) | 7.81 (1H, d, $J=15.3$ Hz) | 144.7 (CH) | 143.8 (CH) | C-2, 6, C=O |
| α | 7.83 (1H, d, $J=15.9$ Hz) | 7.55 (1H, d, $J=15.3$ Hz) | 120.3 (CH) | 120.5 (CH) | C-1, C=O |
| C=O | - | - | 192.0 (C) | 191.5 (C) | - |
| 1' | - | - | 113.6 (C) | 112.3 (C) | - |
| 2' | - | - | 166.9 (C) | 167.9 (C) | - |
| 3' | 6.36 (1H, d, 2.4 Hz) | - | 102.9 (CH) | 106.6 (CH) | C-5', C1', 4' |
| 4' | - | - | 165.1 (C) | 164.3 (C) | - |
| 5' | 6.46 (1H, dd, $J=9.2, 2.1$ Hz) | 6.41 (1H, d, $J=9.2$ Hz) | 108.1 (CH) | 107.9 (CH) | C-3', C1' |
| 6' | 8.15 (1H, d, $J=9.2$ Hz) | 7.76 (1H, d, $J=9.2$ Hz) | 132.8 (CH) | 131.0 (CH) | C-2', 4', C=O |
| 2'-OH | 13.45 (1H, s) | 13.95 (1H, s) | - | - | - |
| 3'-CH ₂ N | - | 3.93 (3H, s) | - | 53.8 (CH ₂) | C-3'', 7'', 5', 4', 2' |
| CH ₂ | - | 1.24 (2H, m) | - | 23.4 (CH ₂) | - |
| CH ₂ CH ₂ | - | 1.71 (4H, m) | - | 25.2 (CH ₂) | - |
| CH ₂ NCH ₂ | - | 2.96 (4H, m) | - | 53.6 (CH ₂) | - |



(M4a)

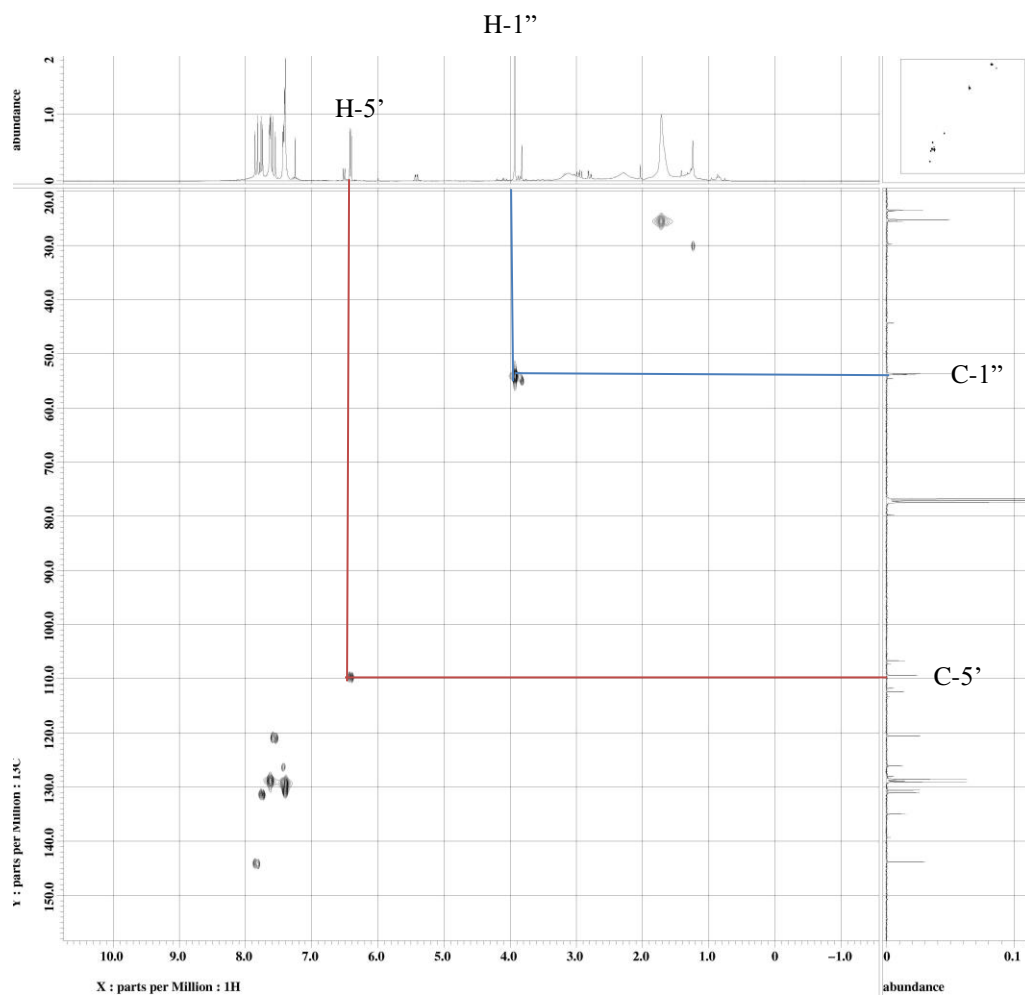
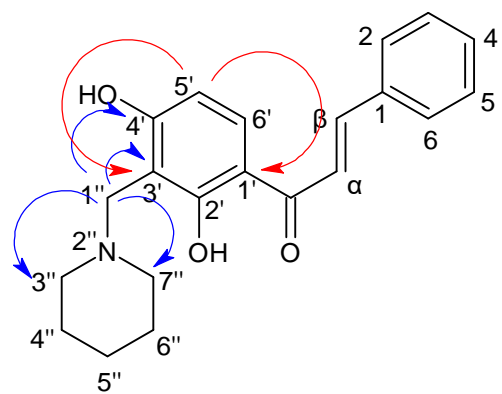


Figure 4.53: HMBC Spectrum of 1-[3-(piperidin-1-yl)methyl-2,4-dihydroxyphenyl]-3-phenyl-2-propen-1-one (M4a)



(M4a)

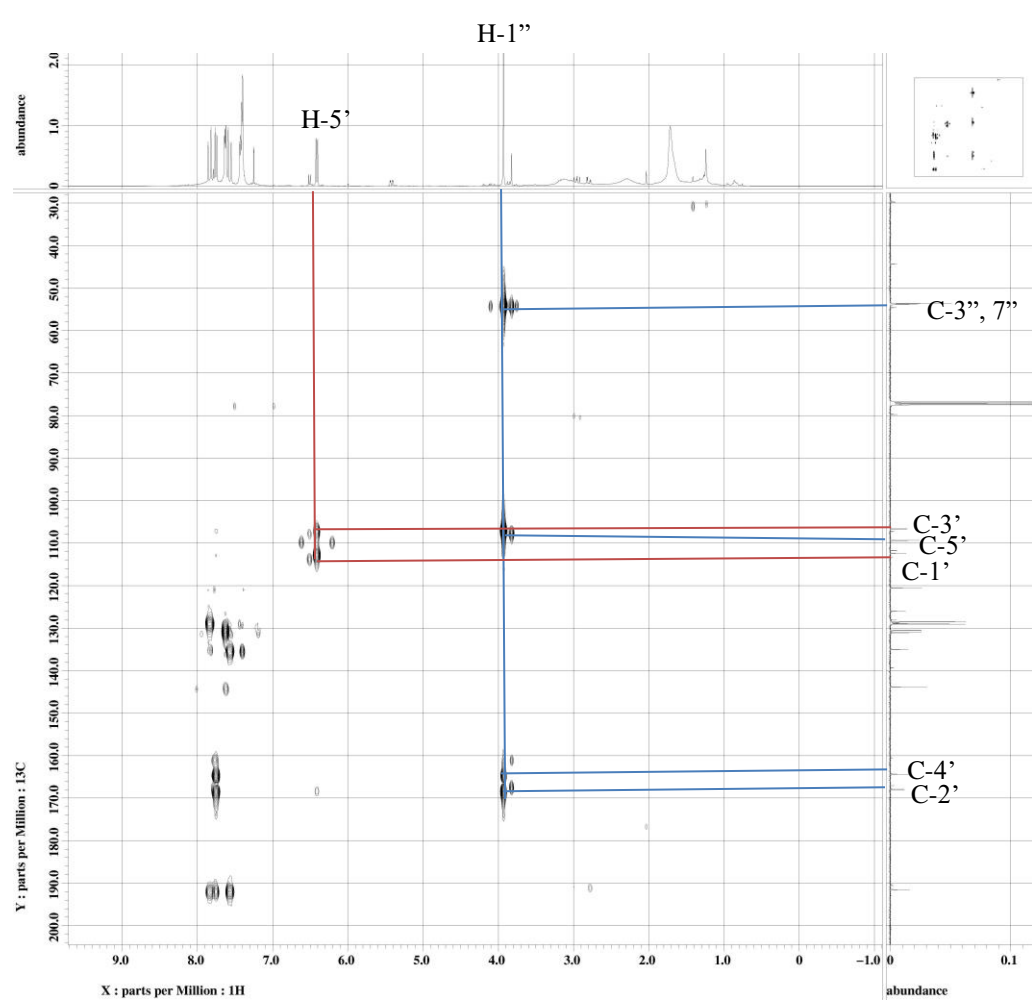
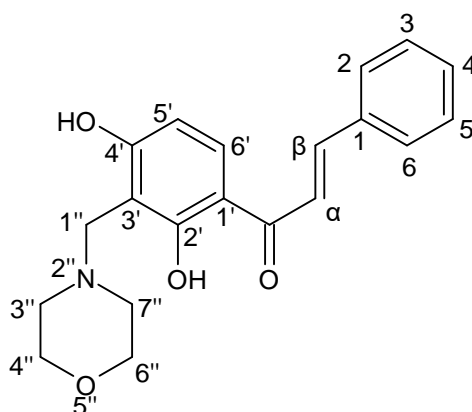


Figure 4.54: HMBC Spectrum of 1-[3-(piperidin-1-yl)methyl-2,4-dihydroxyphenyl]-3-phenyl-2-propen-1-one (M4a)

4.3.2.2 Characterization of 1-[3-(morpholino-4-yl) methyl-2,4-dihydroxyphenyl]-3-phenyl-2-propen-1-one (M4b)



(M4b)

Compound **M4b** was obtained as yellow solid, mp 122-123 °C. In TLC plate, R_f value of 0.35 was obtained in mobile phase hexane:acetone 6:3. The percentage yield of **M4b** was obtained at 65.7%. The HRESIMS (Appendix A22) gave a pseudomolecular ion peak at $m/z = 340.1549 [M+H]^+$ which analysed for $C_{20}H_{21}NO_4$ (found 339.1476; calculated 339.1470). Table 4.25 shows the summary physical properties of **M4b**.

The IR spectrum of **M4b** (Appendix C22) shows absorption bands at 3435 (OH stretch), 1635 (C=O stretch), 1490 (C=C stretch), 1226 (C-N stretch), 1114 (C-O-C stretch) cm^{-1} .

Table 4.25: Summary Physical Properties of M4b

| Compound | M4b |
|-------------------------|--|
| IUPAC Name | 1-[3-(morpholino-4-yl) methyl-2,4-dihydroxyphenyl]-3-phenyl-2-propen-1-one |
| Molecular formula | C ₂₀ H ₂₁ NO ₄ |
| Molecular weight, g/mol | 339.1476 |
| Physical appearance | Yellow solid |
| Percentage yield, % | 65.7 |
| Obtained Mass, mg | 22.3 |
| R _f value | 0.35 |
| Melting point, °C | 122-123 |

The ¹H NMR of compound **M4b** (Figure 4.55) was similar to compound **M4** except the appearance of aliphatic peaks in up field region. Instead of the doublet at δ_H 6.36 (H-3', *J*=2.4 Hz) observed for compound **M4**, characteristic signals of methylene protons at (δ_H 3.89, δ_C 53.9) were shown in the ¹H NMR and ¹³C NMR of compound **M4b** (Figure 4.56). Multiplets signals at (δ_H 2.65, δ_C 52.9) and (δ_H 3.77, δ_C 66.6) were belonging to CH₂NCH₂ and CH₂OCH₂ of morpholine, respectively. The methylene protons was assigned to C-3' as in HMBC (Figure 4.58), H-3' (δ_H 3.89) showed three bonds correlation with C-2' (δ_C 166.1), C-4' (δ_C 164.1). Three bonds correlation also observed for H-3' between C-3'', 7'' (δ_C 52.9) of morpholine moiety. The structure was further confirmed with DEPT (Appendix D58) and HMQC (Figure 4.57) spectra. Gul et. al., (2007) synthesized a series of mono Mannich bases of 4'-hydroxy-3'-piperidinomethylchalcone derivatives with the aminomethylation occurred at

C-3'. It was reported that aminomethylation occurred at the *ortho* position to hydroxyl group. Table 4.26 shows the summary NMR data of compound **M4** and **M4b**.

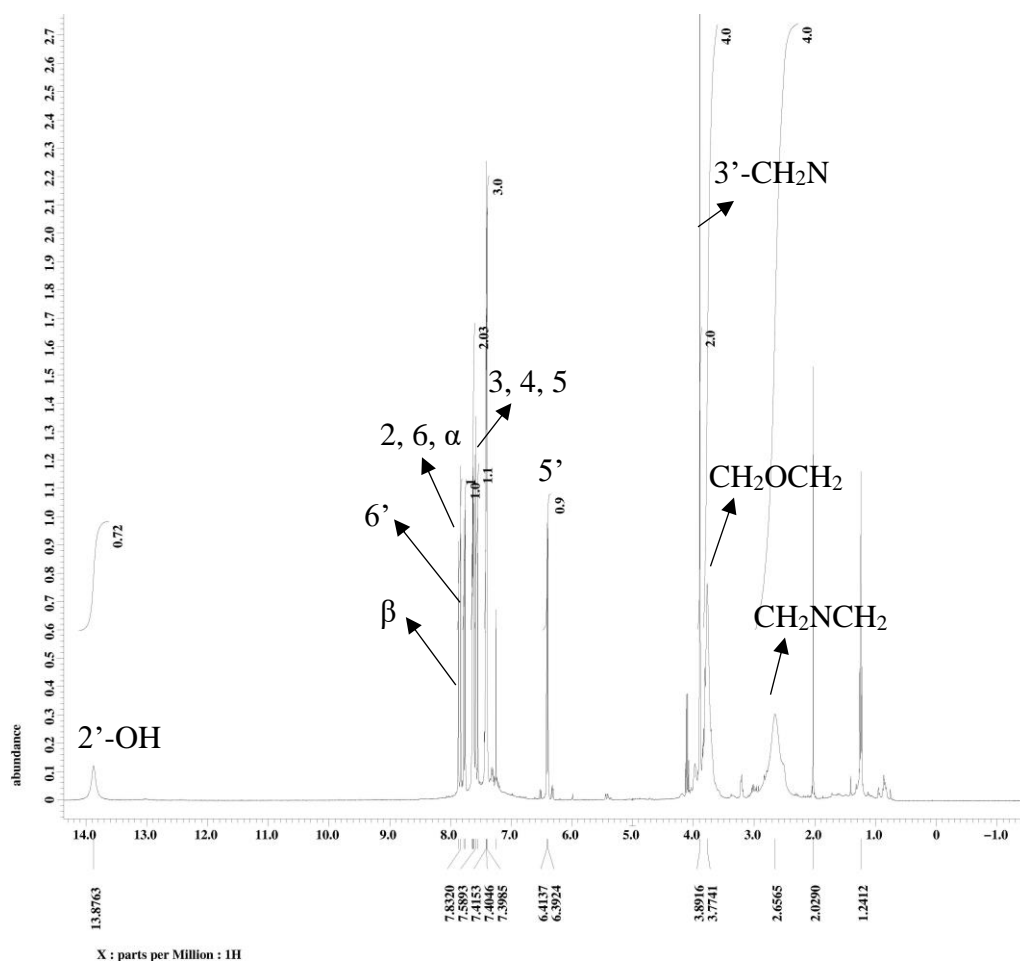
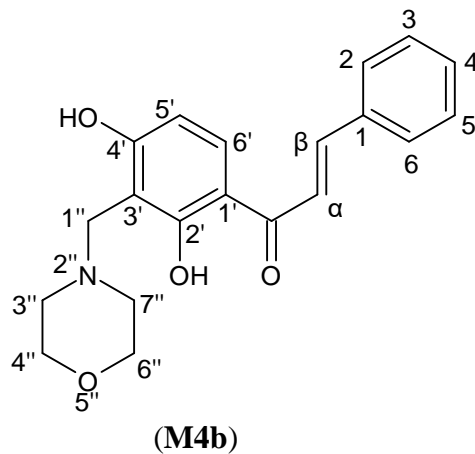


Figure 4.55: ^1H NMR (400 MHz, CDCl_3) of 1-[3-(morpholino-4-yl) methyl-2,4-dihydroxyphenyl]-3-phenyl-2-propen-1-one (**M4b**)

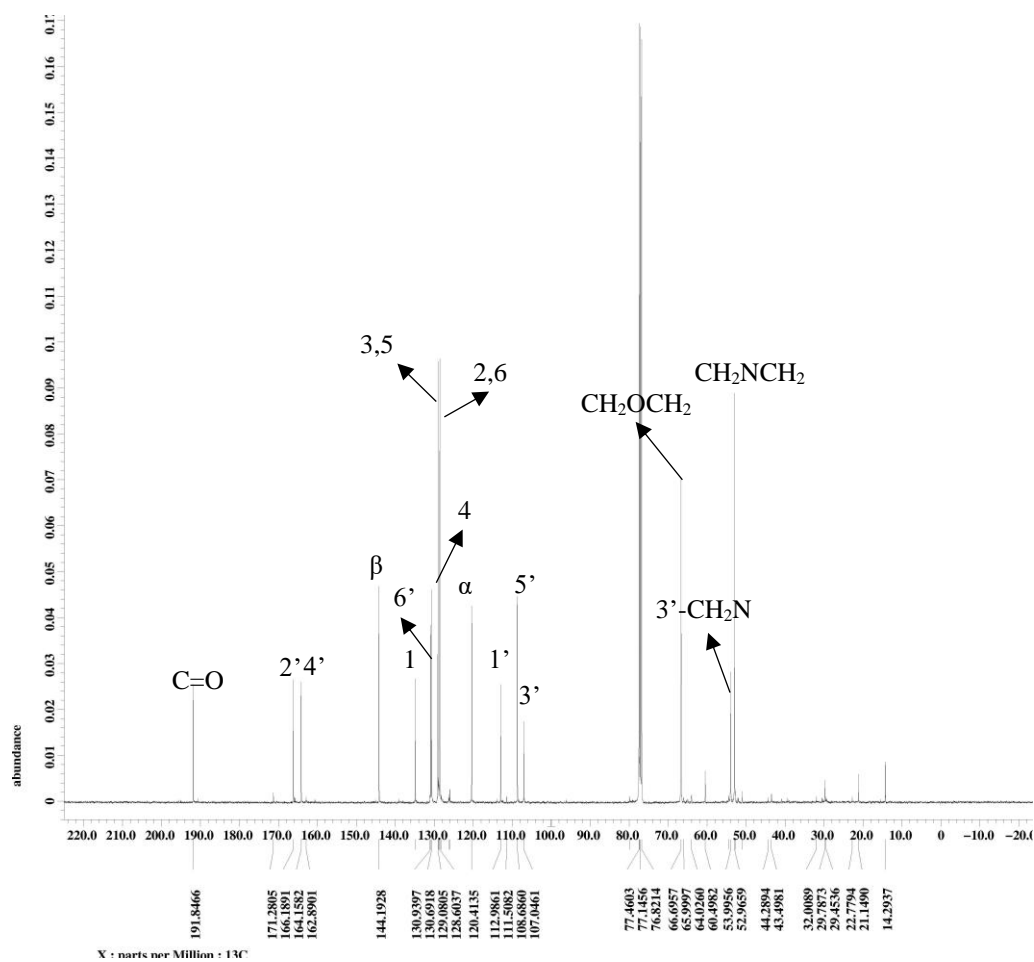
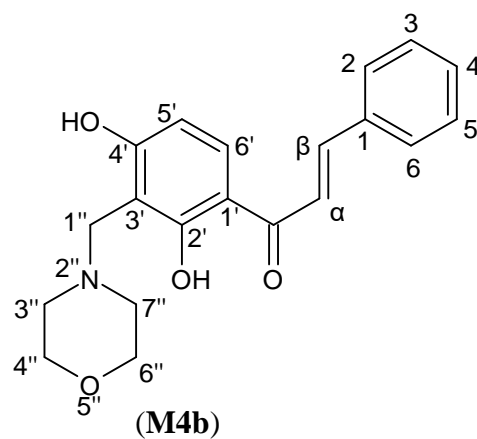
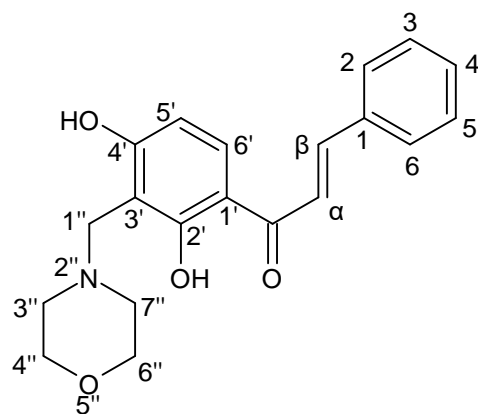


Figure 4.56: ^{13}C NMR (100 MHz, CDCl_3) of 1-[3-(morpholino-4-yl) methyl-2,4-dihydroxyphenyl]-3-phenyl-2-propen-1-one (M4b)

Table 4.26: ¹H, ¹³C and HMBC spectral data of M4 and M4b (CDCl₃)

| | M4 | M4b | M4 | M4b | M4b |
|----------------------------------|---------------------------------------|----------------------------------|------------------------------|------------------------------|------------------------|
| Position | δ _H (multiplicity) | δ _H (multiplicity) | δ _C (Carbon type) | δ _C (Carbon type) | HMBC |
| 1 | - | - | 135.1 (C) | 134.9 (C) | - |
| 2,6 | 7.85 (2H, m) | 7.60 (2H, m) | 129.0 (CH) | 128.6 (CH) | C-3, 4, 5 |
| 3,5 | 7.44 (2H, m) | 7.40 (2H, m) | 128.9 (CH) | 129.0 (CH) | C-1, 2, 6 |
| 4 | 7.44 (1H, m) | 7.40 (1H, m) | 130.7 (CH) | 130.6 (CH) | C-1 |
| β | 7.92 (1H, d, <i>J</i> = 15.9 Hz) | 7.85 (1H, d, <i>J</i> = 15.3 Hz) | 144.7 (CH) | 144.1 (CH) | C-2, 6, C=O |
| α | 7.83 (1H, d, <i>J</i> = 15.9 Hz) | 7.58 (1H, d, <i>J</i> = 15.3 Hz) | 120.3 (CH) | 120.4 (CH) | C-1, C=O |
| C=O | - | - | 192.0 (C) | 191.8 (C) | - |
| 1' | - | - | 113.6 (C) | 112.9 (C) | - |
| 2' | - | - | 166.9 (C) | 166.1 (C) | - |
| 3' | 6.36 (1H, d, <i>J</i> = 2.4 Hz) | - | 102.9 (CH) | 107.6 (CH) | C-5', 1', 4' |
| 4' | - | - | 165.1 (C) | 164.1 (C) | - |
| 5' | 6.46 (1H, dd, <i>J</i> = 9.2, 2.1 Hz) | 6.41 (1H, d, <i>J</i> = 9.2 Hz) | 108.1 (CH) | 108.6 (CH) | C-3', C1', 2' |
| 6' | 8.15 (1H, d, <i>J</i> = 9.2 Hz) | 7.76 (1H, d, <i>J</i> = 9.2 Hz) | 132.8 (CH) | 130.9 (CH) | C-2', 4', C=O |
| 2'-OH | 13.45 (1H, s) | 13.95 (1H, s) | - | - | - |
| 3'-CH ₂ N | - | 3.89 (2H, s) | - | 53.9 (CH ₂) | C-3'', 7'', 3', 4', 2' |
| CH ₂ NCH ₂ | - | 2.65 (4H, m) | - | 52.9 (CH ₂) | - |
| CH ₂ OCH ₂ | - | 3.77 (4H, m) | - | 66.6 (CH ₂) | - |



(M4b)

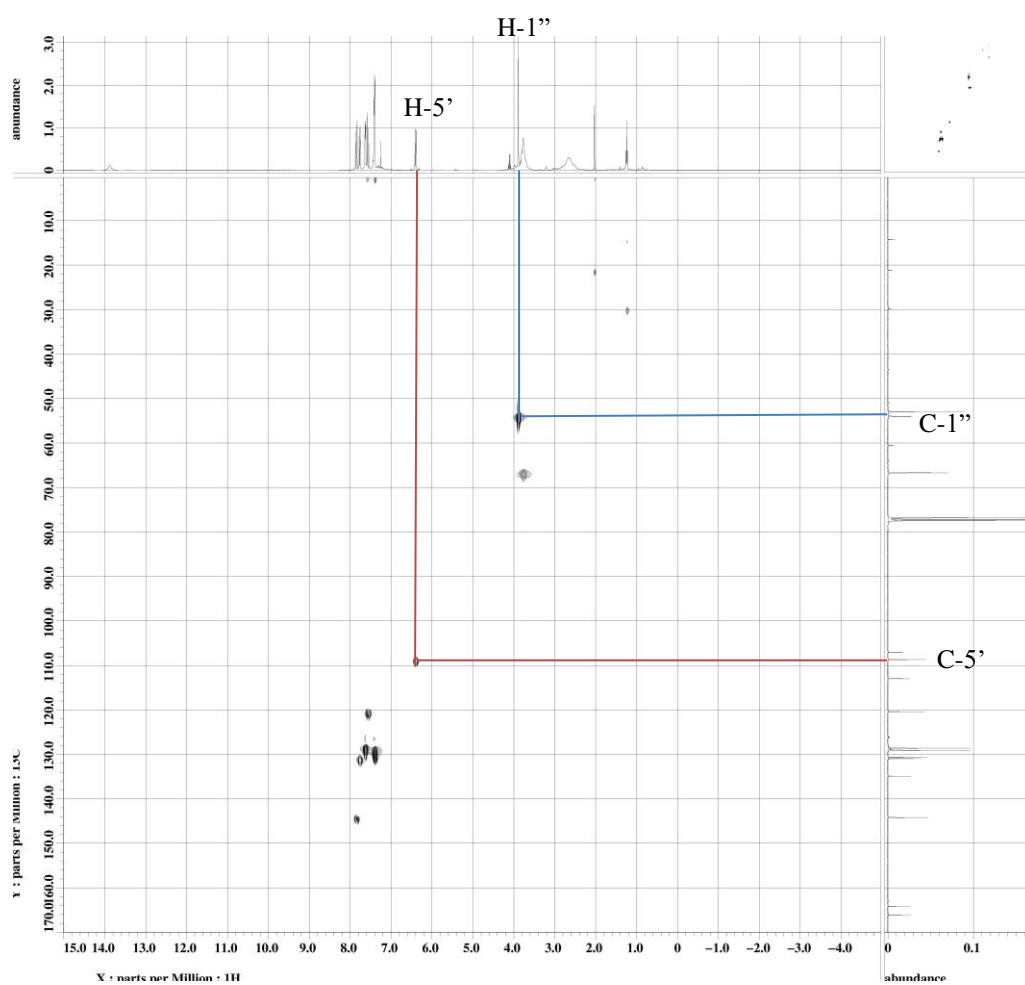
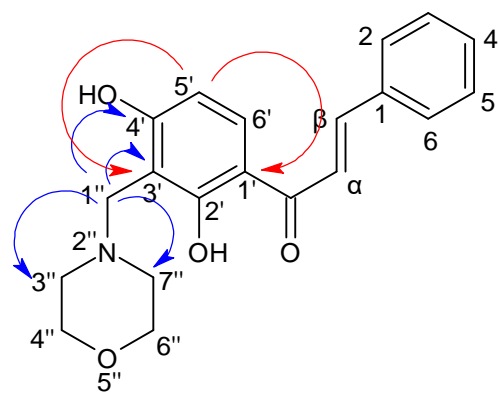


Figure 4.57: HMQC Spectrum of 1-[3-(morpholino-4-yl)methyl-2,4-dihydroxyphenyl]-3-phenyl-2-propen-1-one (M4b)



(M4b)

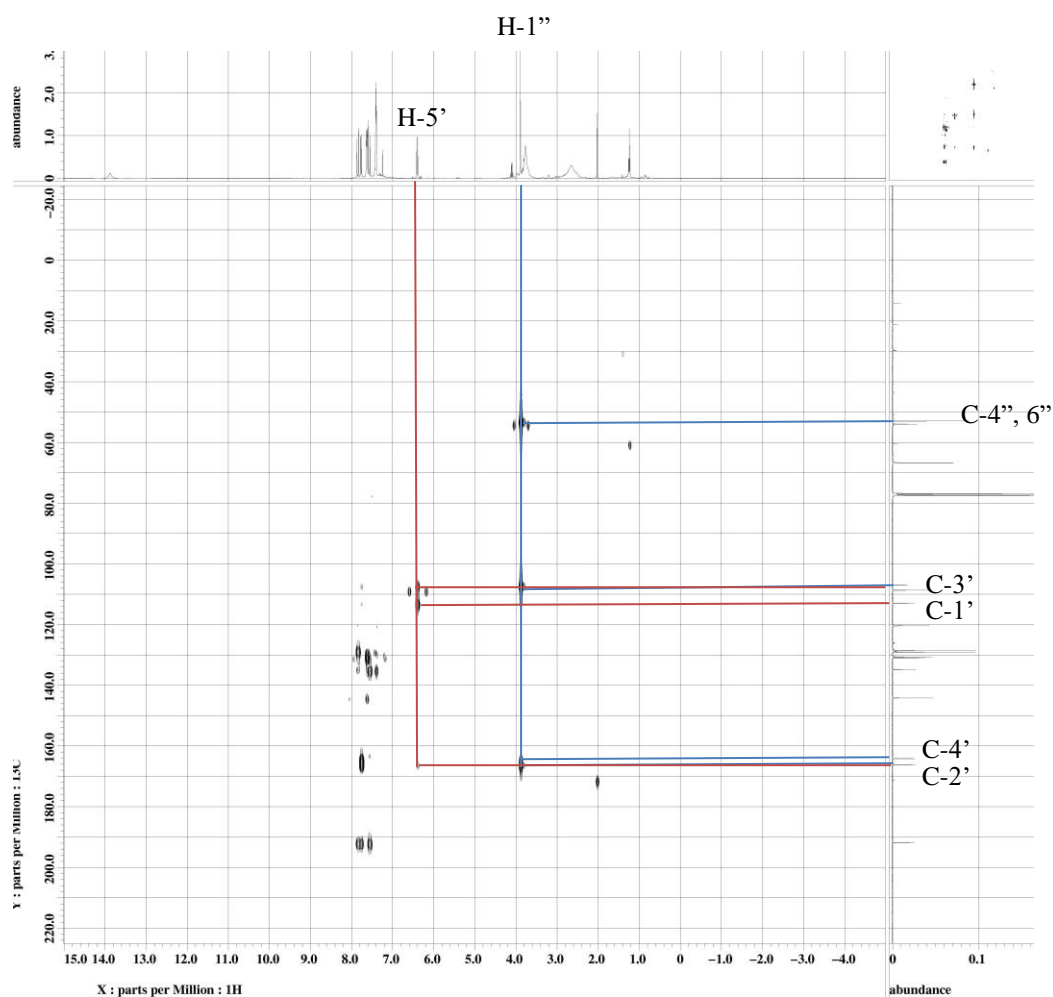


Figure 4.58: HMBC Spectrum of 1-[3-(morpholino-4-yl)methyl-2,4-dihydroxyphenyl]-3-phenyl-2-propen-1-one (M4b)

4.3.3 Synthesis of 3,5,7-trihydroxy-8-methoxyflavone (M5) Mannich Bases

Isolate 3,5,7-trihydroxy-8-methoxyflavone (**M5**) was used to synthesize flavone Mannich bases via Mannich reaction. The reaction route was shown in Figure 4.59.

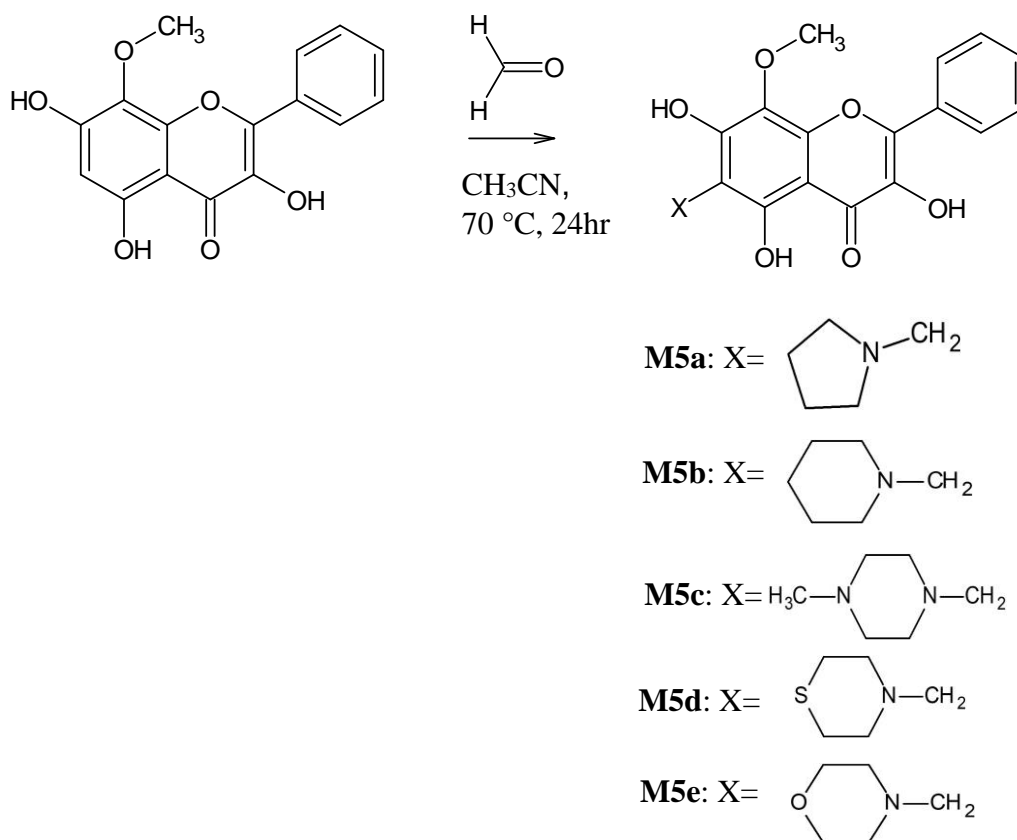


Figure 4.59: Synthesis route of flavone M5 Mannich bases with mol ratio flacone: formaldehyde: amine 1:3:3

Mannich flavones (**M5a-M5e**) were prepared by reaction of **M5** flacone with formaldehyde, secondary amine (pyrrolidine in **M5a**; piperidine in **M5b**; 1-methylpiperazine in **M5c**; thiomorpholine in **M5d**; morpholine in **M5e**) in mol

ratio 1:3:3, respectively, and stirred under reflux in acetonitrile for 24 hr at 70 °C.

The reaction mechanism involves the formation of iminium ion (Figure 4.39) which is the condensation between formaldehyde and secondary amine. Then, followed by the electrophilic attack of the iminium ion on the aromatic A-ring of the flavone substrate at C6 which is ortho to hydroxyl group. The reaction mechanism was shown in Figure 4.60.

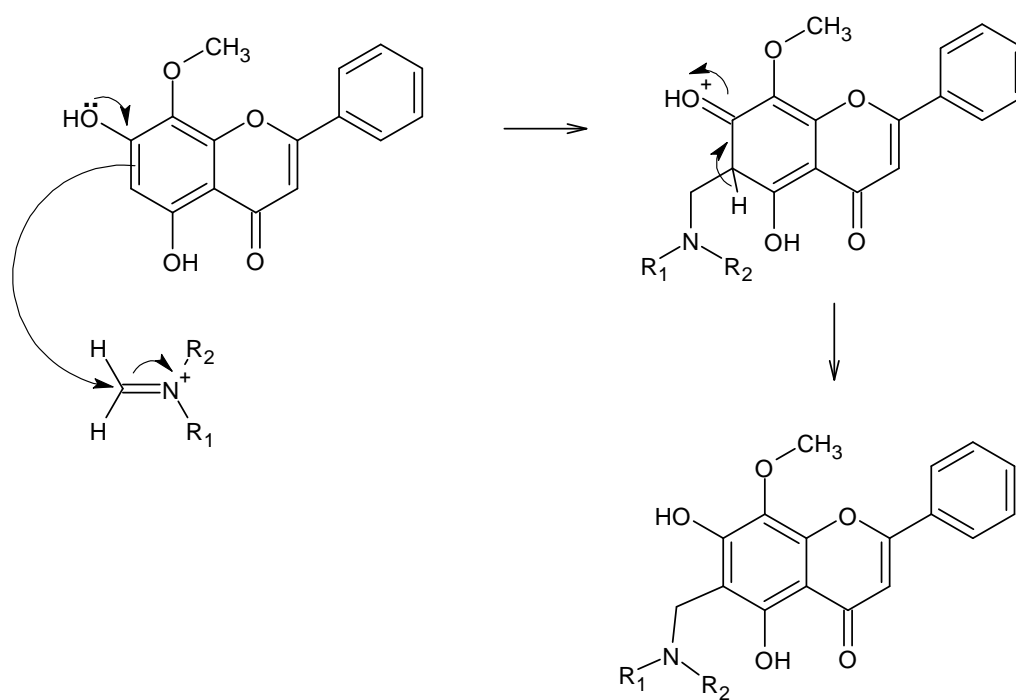
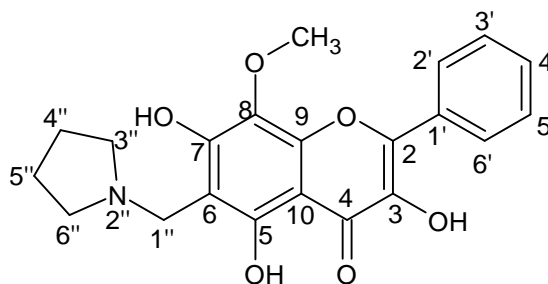


Figure 4.60: Reaction mechanism of flavone M5 Mannich bases

4.3.3.1 Characterization of 3,5,7-trihydroxy-8-methoxy-6-(pyrrolidin-1-ylmethyl)-2-phenyl-4H-chromen-4-one (M5a)



(M5a)

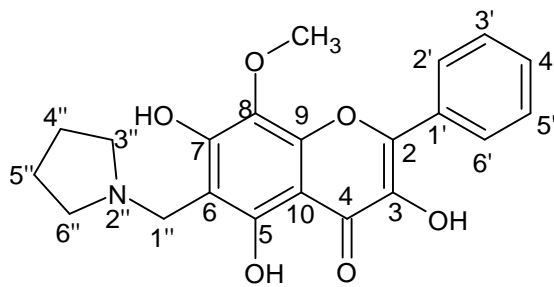
Compound **M5a** was obtained as dark yellow solid, mp 231-232 °C. In TLC plate, R_f value of 0.08 was obtained in mobile phase hexane:acetone 6:4. The percentage yield of **M5a** was obtained at 47.5%. The HRESIMS (Appendix A23) gave a pseudomolecular ion peak at $m/z = 384.1442 [M+H]^+$ which analysed for $C_{21}H_{21}NO_6$ (found 383.1370; calculated 383.1369). Table 4.23 shows the summary physical properties of **M5a**.

The IR spectrum of **M5a** (Appendix C23) shows absorption bands at 3414 (OH stretch), 2982, 2951 (CH_3 stretch), 1637 (C=O stretch), 1618 (C=C stretch), 1298 (C-N stretch), 1186 (C-O stretch), 1047 (C-O-C stretch) cm^{-1} .

Table 4.27: Summary Physical Properties of M5a

| Compound | M5a |
|-------------------------|--|
| IUPAC Name | 3,5,7-trihydroxy-8-methoxy-6-(pyrrolidin-1-ylmethyl)-2-phenyl-4H-chromen-4-one |
| Molecular formula | C ₂₁ H ₂₁ NO ₆ |
| Molecular weight, g/mol | 383.1370 |
| Physical appearance | Dark yellow solid |
| Percentage yield, % | 47.5 |
| Obtained Mass, mg | 18.2 |
| R _f value | 0.08 |
| Melting point, °C | 231-232 |

In the ¹H NMR of compound **M5a** (Figure 4.61), signal at δ_H 4.37 indicated the presence of methylene protons. Multiplets signals at δ_H 1.95, δ_H 3.57 were the characteristic peaks of pyrrolidine. The disappearance singlet at δ_H 6.30 (H-6) in compound **M5a** showed that the aminomethylation was occurred at C-6. In ¹³C NMR (Figure 4.62) of compound **M5a**, signal at δ_c 45.9 was the methylene carbon and the signals at δ_c 23.2 and δ_c 53.2 were the characteristic peaks of pyrrolidine moiety. In the HMBC spectrum (Figure 4.64), methylene protons displayed two bond correlations with C-6 (δ_c 100.9), and three bonds correlations with C-5 (δ_c 155.5). In addition, methylene protons also showed three-bond correlations with C-3'', 6'' (δ_c 53.2) which belong to pyrrolidine moiety. The structure was further confirmed by using DEPT (Appendix D59) and HMQC (Figure 4.63) spectrums. Table 4.28 shows the summary NMR data of compounds **M5** and **M5a**.



(M5a)

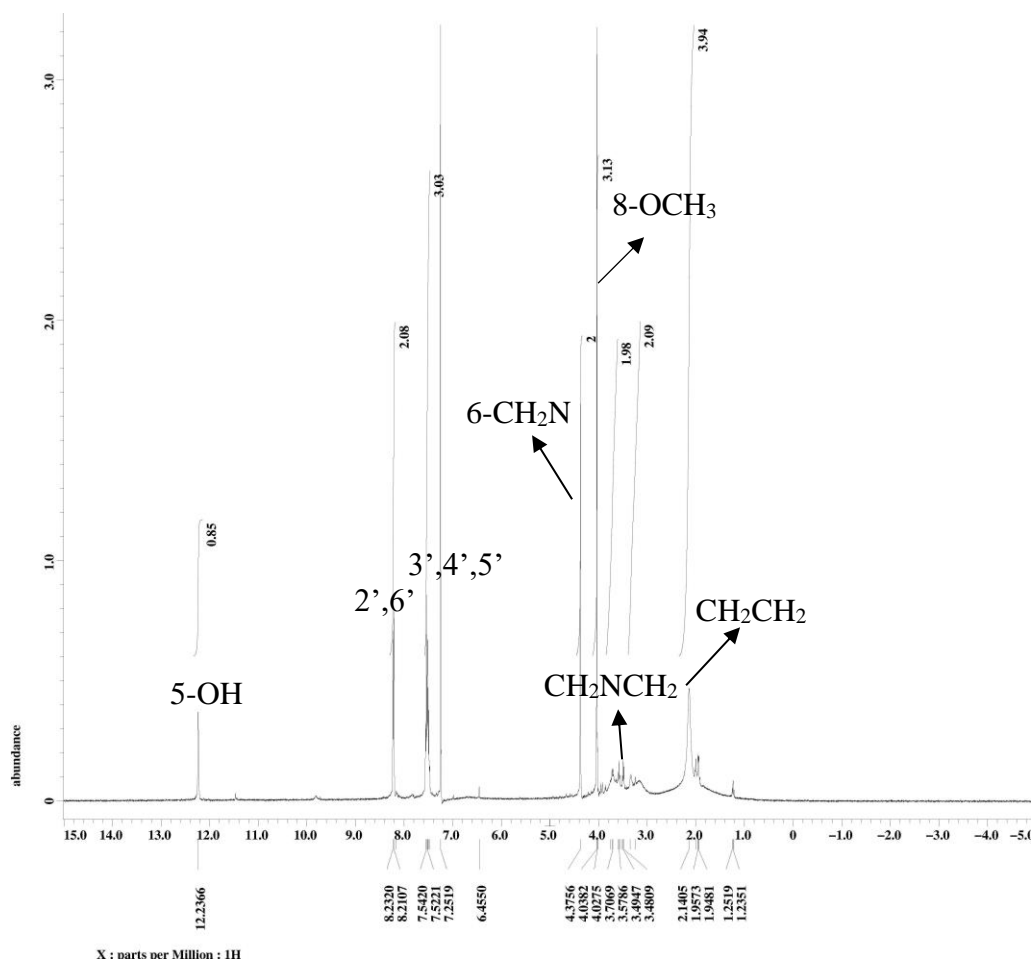


Figure 4.61: ¹H NMR (400 MHz, CDCl₃) of 3,5,7-trihydroxy-8-methoxy-6-(pyrrolidin-1-ylmethyl)-2-phenyl-4H-chromen-4-one (M5a)

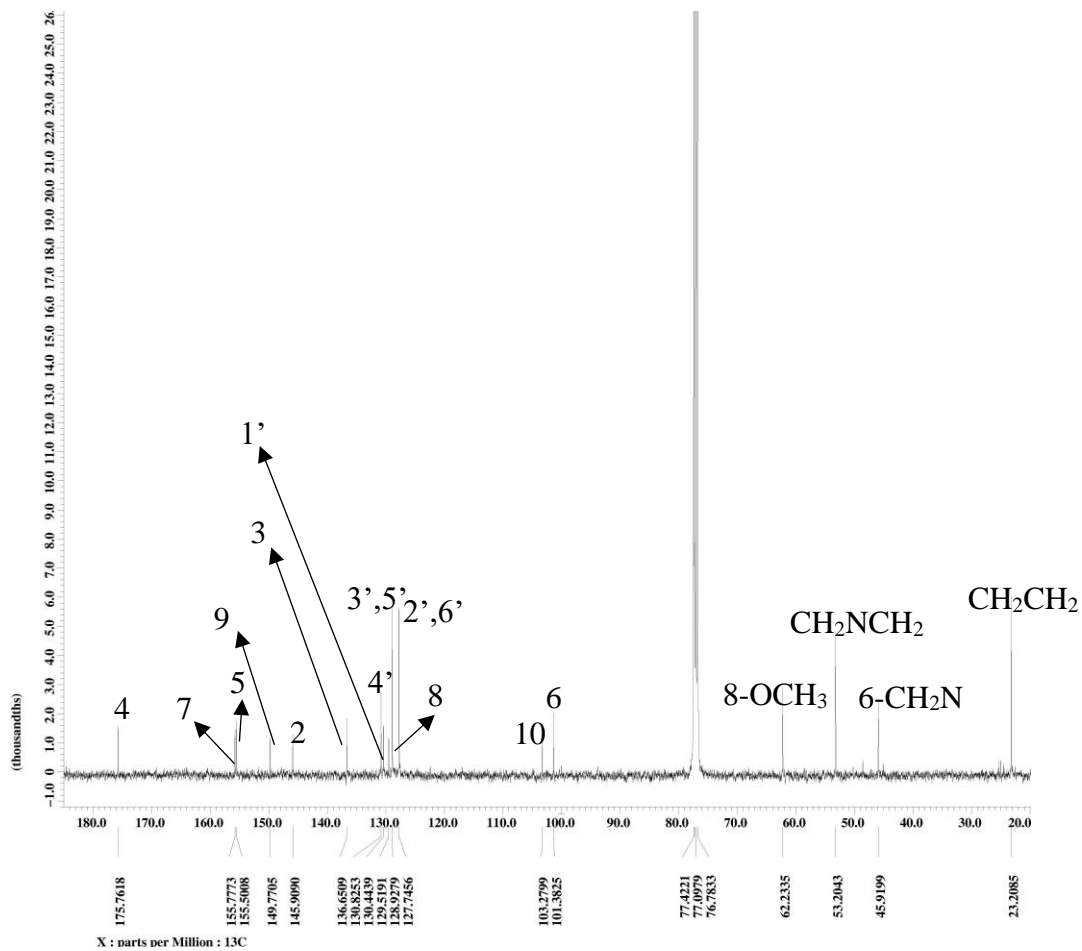
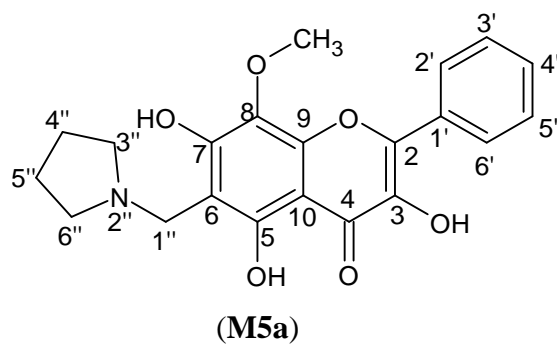


Figure 4.62: ^{13}C NMR (100 MHz, CDCl_3) of 3,5,7-trihydroxy-8-methoxy-6-(pyrrolidin-1-ylmethyl)-2-phenyl-4H-chromen-4-one (M5a)

Table 4.28: ¹H, ¹³C and HMBC spectral data of M5 (acetone-d₆) and M5a (CDCl₃)

| | M5 | M5a | M5 | M5a | M5a |
|---------------------|-------------------------------|-------------------------------|----------------------------|----------------------------|------------------|
| Proton | δ _H (Multiplicity) | δ _H (Multiplicity) | δ _c (Type of C) | δ _c (Type of C) | HMBC |
| 2 | - | - | 145.2 (C) | 145.9 (C) | - |
| 3 | - | - | 137.2 (C) | 136.6 (C) | - |
| 4 | - | - | 176.3 (C) | 175.7 (C) | - |
| 5 | - | - | 156.5 (C) | 155.5 (C) | - |
| 6 | 6.30 (1H, s) | - | 98.4 (C) | 100.9 (C) | - |
| 7 | - | - | 157.0 (C) | 155.7 (C) | - |
| 8 | - | - | 127.8 (C) | 129.5 (C) | - |
| 9 | - | - | 149.1 (C) | 149.7 (C) | - |
| 10 | - | - | 103.5 (C) | 103.2 (C) | - |
| 1' | - | - | 131.4 (C) | 130.8 (C) | - |
| 2',6' | 8.28 (2H, m) | 8.20 (2H, m) | 127.6 (CH) | 127.7 (CH) | C-2, 3', 4', 5' |
| 3',5' | 7.57 (2H, m) | 7.54 (2H, m) | 128.7 (CH) | 128.9 (CH) | C-1', 2',6' |
| 4' | 7.51 (1H, m) | 7.52 (1H, m) | 130.1(CH) | 130.4 (CH) | C-1', 2',6' |
| 5-OH | 11.77 (1H, s) | 12.10 (1H, s) | - | - | C-6, 10, 5 |
| 8-OCH ₃ | 3.93 (3H, s) | 3.86 (3H, s) | 61.1(CH ₃) | 62.2 (CH ₃) | C-8 |
| 3-OH | 8.35 (1H, s) | - | - | - | - |
| 7-OH | 9.47 (1H, s) | - | - | - | - |
| 6-CH ₂ N | - | 4.37 (2H, s) | - | 45.9 (CH ₂) | C-3'', 6'', 6, 5 |
| 4'', 5'' | - | 1.95 (4H, m) | - | 23.2 (CH ₂) | - |
| 3'', 6'' | - | 3.57 (4H, m) | - | 53.2 (CH ₂) | - |

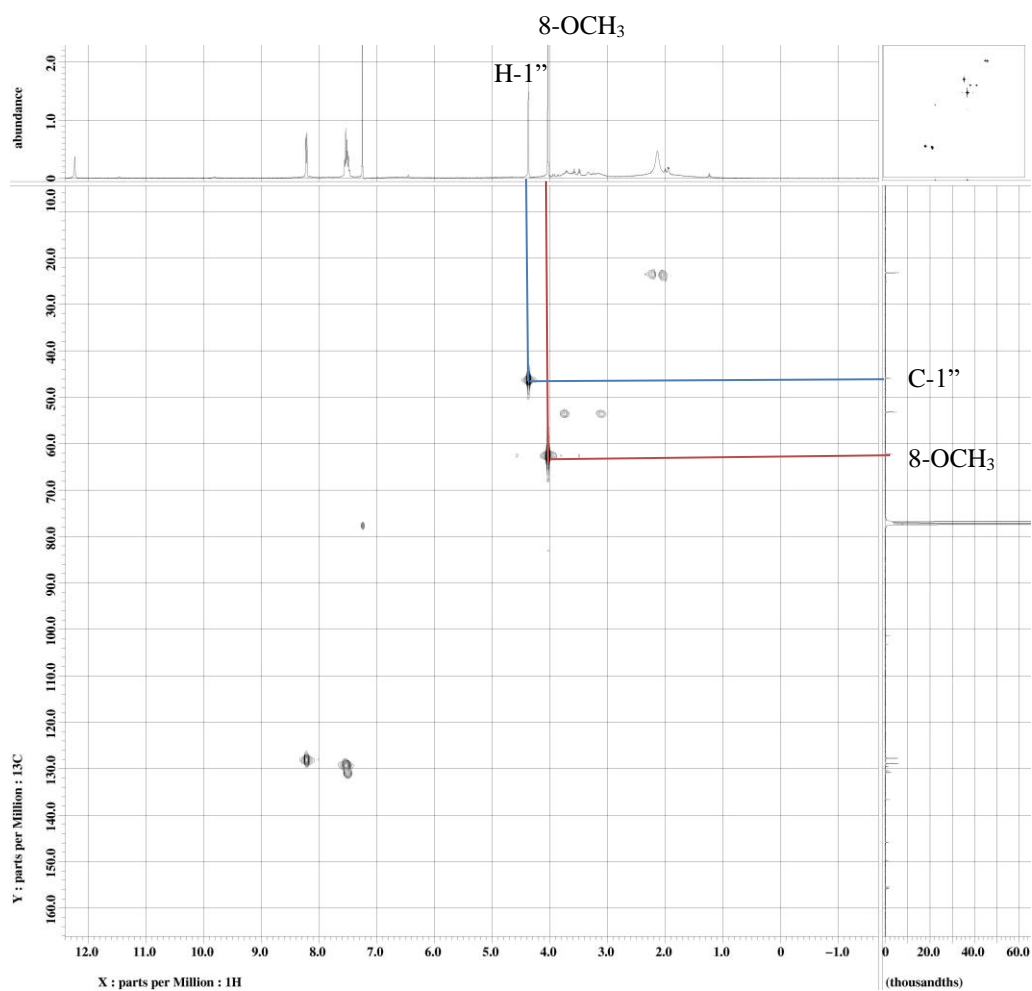
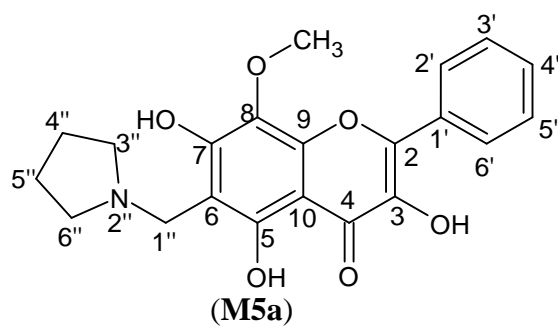
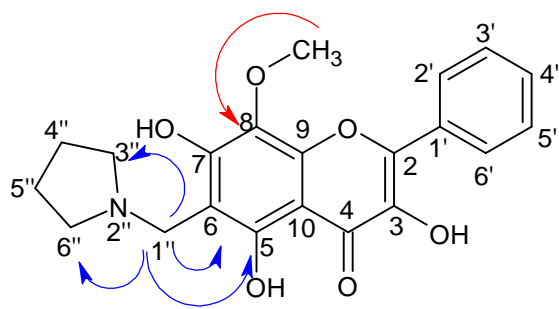


Figure 4.63: HMBC Spectrum of 3,5,7-trihydroxy-8-methoxy-6-(pyrrolidin-1-ylmethyl)-2-phenyl-4H-chromen-4-one (M5a)



(M5a)

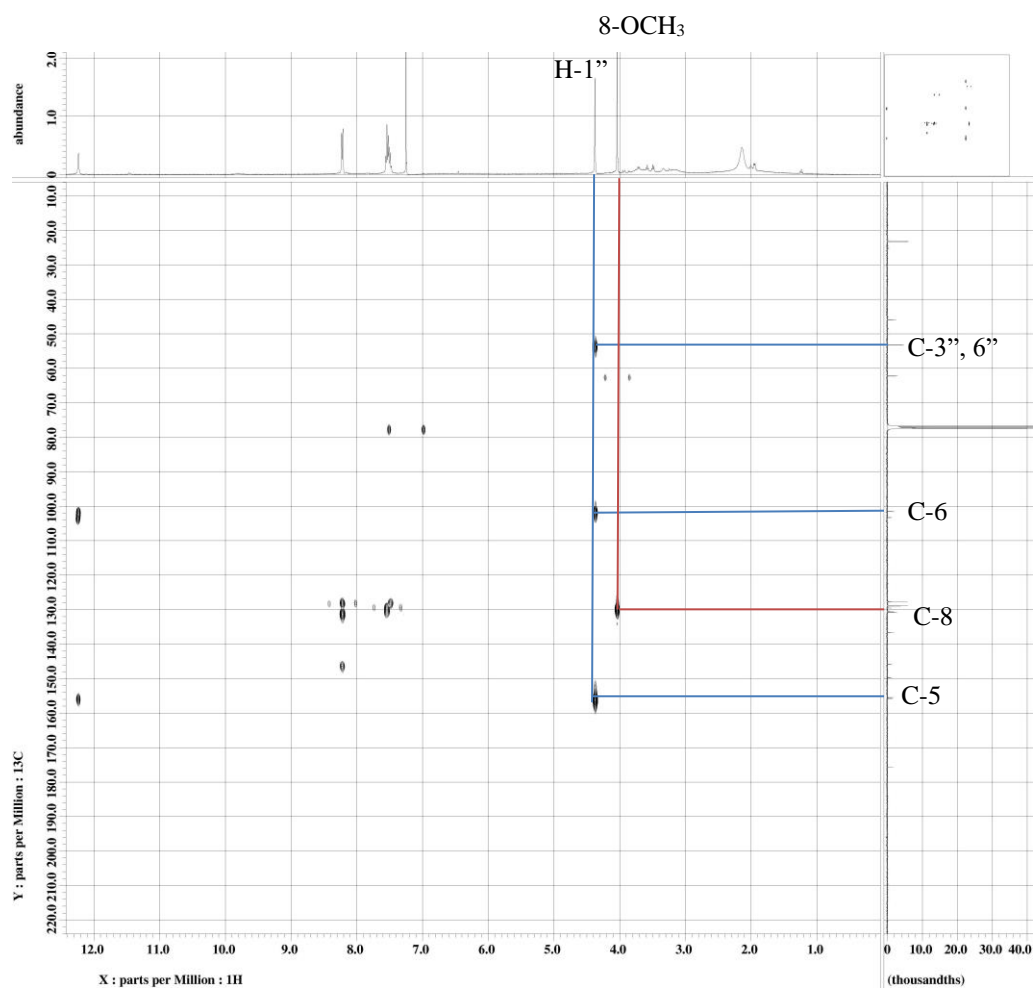
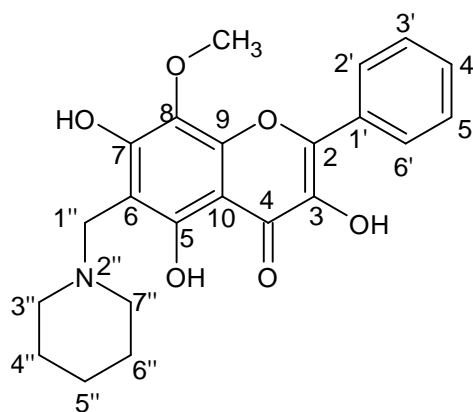


Figure 4.64: HMBC Spectrum of 3,5,7-trihydroxy-8-methoxy-6-(pyrrolidin-1-ylmethyl)-2-phenyl-4H-chromen-4-one (M5a)

4.3.3.2 Characterization of 3,5,7-trihydroxy-8-methoxy-6-(piperidin-1-ylmethyl)-2-phenyl-4H-chromen-4-one (M5b)



(M5b)

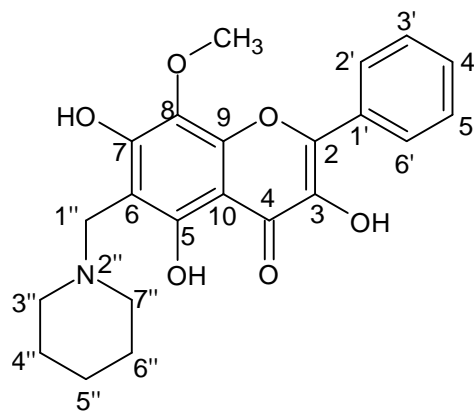
Compound **M5b** was obtained as yellow solid, mp 223-224 °C. It showed R_f value of 0.25 on a TLC plate eluted with mobile phase hexane:acetone 6:4. The percentage yield of **M5b** was obtained at 67.5%. The HRESIMS (Appendix A24) gave a pseudomolecular ion peak at $m/z = 398.1600$ $[M+H]^+$ which analysed for $C_{22}H_{23}NO_6$ (found 397.1527; calculated 397.1525). Table 4.29 shows the summary physical properties of **M5b**.

The IR spectrum of **M5b** (Appendix C24) shows absorption bands at 3433 (OH stretch), 1636 (C=O stretch), 1490 (C=C stretch), 1199 (C-N stretch), 1187 (C-O stretch), 1047 (C-O-C stretch) cm^{-1} .

Table 4.29: Summary Physical Properties of M5b

| Compound | M5b |
|-------------------------|---|
| IUPAC Name | 3,5,7-trihydroxy-8-methoxy-6-(piperidin-1-ylmethyl)-2-phenyl-4H-chromen-4-one |
| Molecular formula | C ₂₂ H ₂₃ NO ₆ |
| Molecular weight, g/mol | 397.1527 |
| Physical appearance | Yellow solid |
| Percentage yield, % | 67.5 |
| Obtained Mass, mg | 26.8 |
| R _f value | 0.25 |
| Melting point, °C | 223-224 |

In the ¹H NMR of compound **M5b** (Figure 4.65), signal at δ_H 4.28 belongs to methylene protons. Characteristic peaks of piperidine were appeared at δ_H 2.21, δ_H 2.81 and δ_H 3.63. In ¹³C NMR (Figure 4.66) of compound **M5b**, signal at δ_C 49.0 was the methylene carbon and the signals at δ_C 22.0, δ_C 22.9 δ_C 52.9 were the characteristic peaks of piperidine moiety. The position of aminomethylation was confirmed by using HMBC spectrum (Figure 4.68). In the HMBC spectrum, methylene protons displayed two bonds correlations with C-6 (δ_C 100.9), and three bonds correlations with C-5 (δ_C 155.9). Besides, methylene protons also displayed three bonds correlations with C-3'', 7'' (δ_C 52.9) which belong to piperidine moiety. The structure was further confirmed by using DEPT (Appendix D60) and HMQC (Figure 4.67) spectra. Table 4.30 shows the summary NMR data of compounds **M5** and **M5b**.



(M5b)

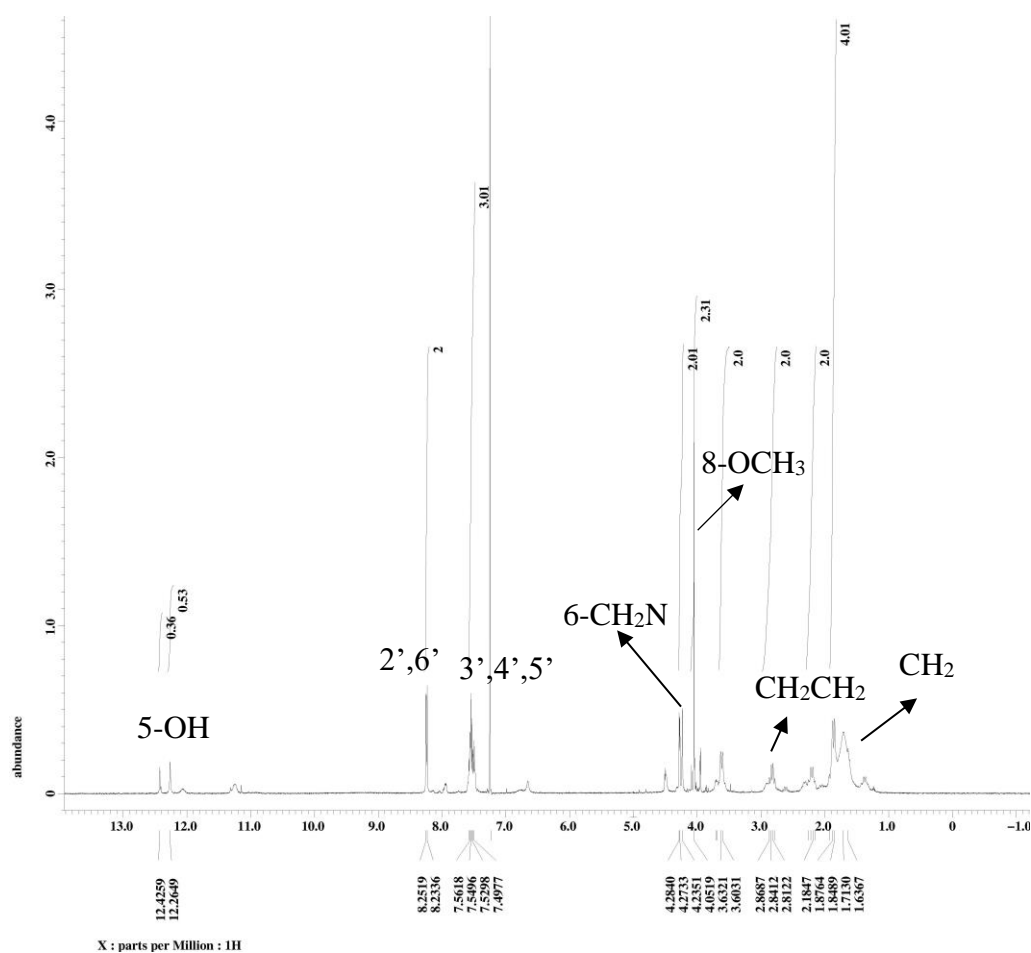
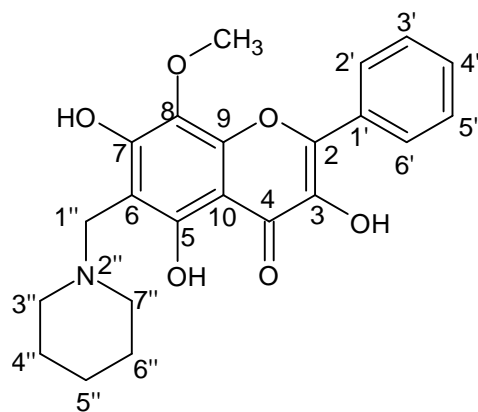


Figure 4.65: ^1H NMR (400 MHz, CDCl_3) of 3,5,7-trihydroxy-8-methoxy-6-(piperidin-1-ylmethyl)-2-phenyl-4H-chromen-4-one (M5b)



(M5b)

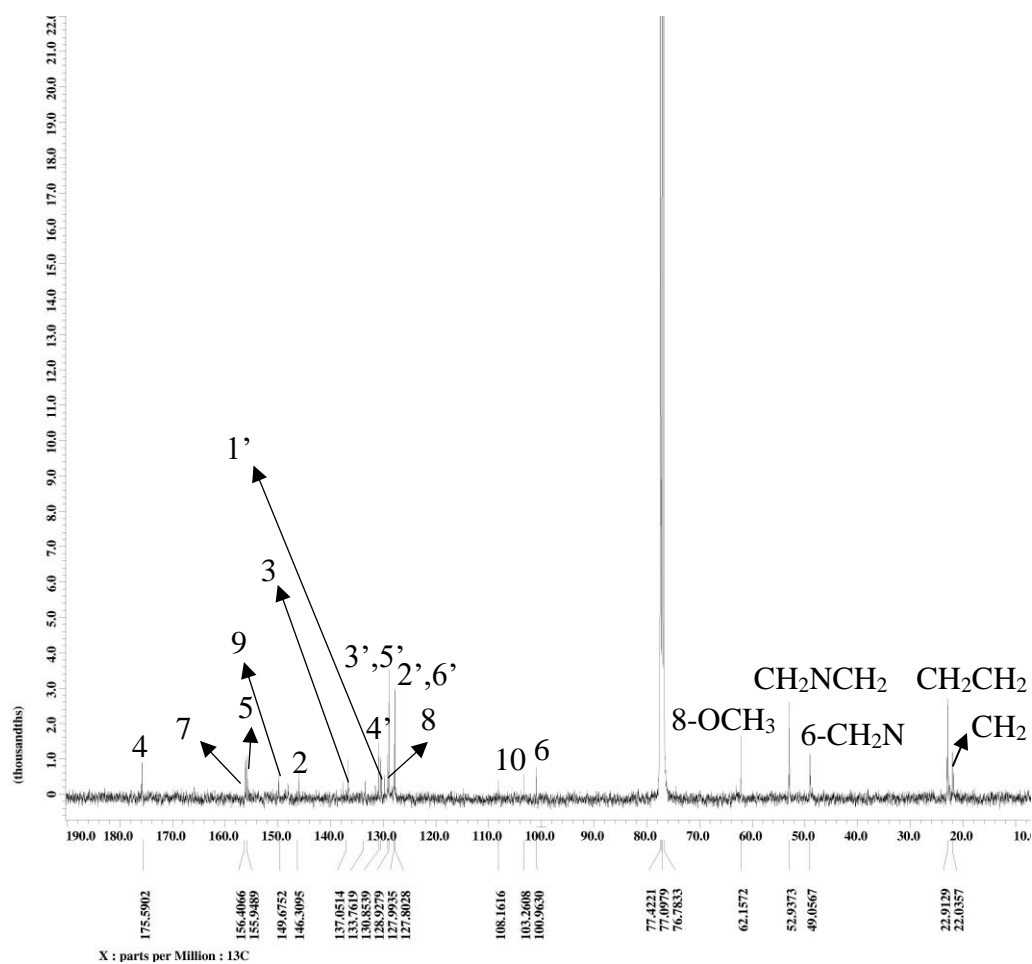


Figure 4.66: ¹³C NMR (100 MHz, CDCl₃) of 3,5,7-trihydroxy-8-methoxy-6-(piperidin-1-ylmethyl)-2-phenyl-4H-chromen-4-one (M5b)

Table 4.30: ^1H , ^{13}C and HMBC spectral data of M5 (acetone- d_6) and M5b (CDCl_3)

| | M5 | M5b | M5 | M5b | M5b |
|----------------------------------|------------------------------------|------------------------------------|---------------------------------|---------------------------------|------------------|
| Proton | δ_{H} (Multiplicity) | δ_{H} (Multiplicity) | δ_{C} (Type of C) | δ_{C} (Type of C) | HMBC |
| 2 | - | - | 145.2 (C) | 146.3 (C) | - |
| 3 | - | - | 137.2 (C) | 137.0 (C) | - |
| 4 | - | - | 176.3 (C) | 175.5 (C) | - |
| 5 | - | - | 156.5 (C) | 155.9 (C) | - |
| 6 | 6.30 (1H, s) | - | 98.4 (C) | 100.9 (C) | - |
| 7 | - | - | 157.0 (C) | 156.4 (C) | - |
| 8 | - | - | 127.8 (C) | 129.8 (C) | - |
| 9 | - | - | 149.1 (C) | 149.6 (C) | - |
| 10 | - | - | 103.5 (C) | 103.2 (C) | - |
| 1' | - | - | 131.4 (C) | 130.4 (C) | - |
| 2',6' | 8.28 (2H, m) | 8.23 (2H, m) | 127.6 (CH) | 127.7 (CH) | C-2, 3', 4', 5' |
| 3',5' | 7.57 (2H, m) | 7.54 (2H, m) | 128.7 (CH) | 128.9 (CH) | C-2', 6' |
| 4' | 7.51 (1H, m) | 7.49 (1H, m) | 130.1(CH) | 130.8 (CH) | C- 2', 6' |
| 5-OH | 11.77 (1H, s) | 12.40 (1H, s) | - | - | C-6, 10, 5 |
| 8-OCH ₃ | 3.93 (3H, s) | 3.86 (3H, s) | 61.1(CH ₃) | 62.1 (CH ₃) | C-8 |
| 3-OH | 8.35 (1H, s) | - | - | - | - |
| 7-OH | 9.47 (s) | - | - | - | - |
| 6-CH ₂ N | - | 4.28 (2H, s) | - | 49.0 (CH ₂) | C-3'', 7'', 6, 5 |
| CH ₂ | - | 2.21(2H, s) | - | 22.0 (CH ₂) | - |
| CH ₂ CH ₂ | - | 2.81 (4H, m) | - | 22.9 (CH ₂) | - |
| CH ₂ NCH ₂ | - | 3.63 (4H, m) | - | 52.9 (CH ₂) | - |

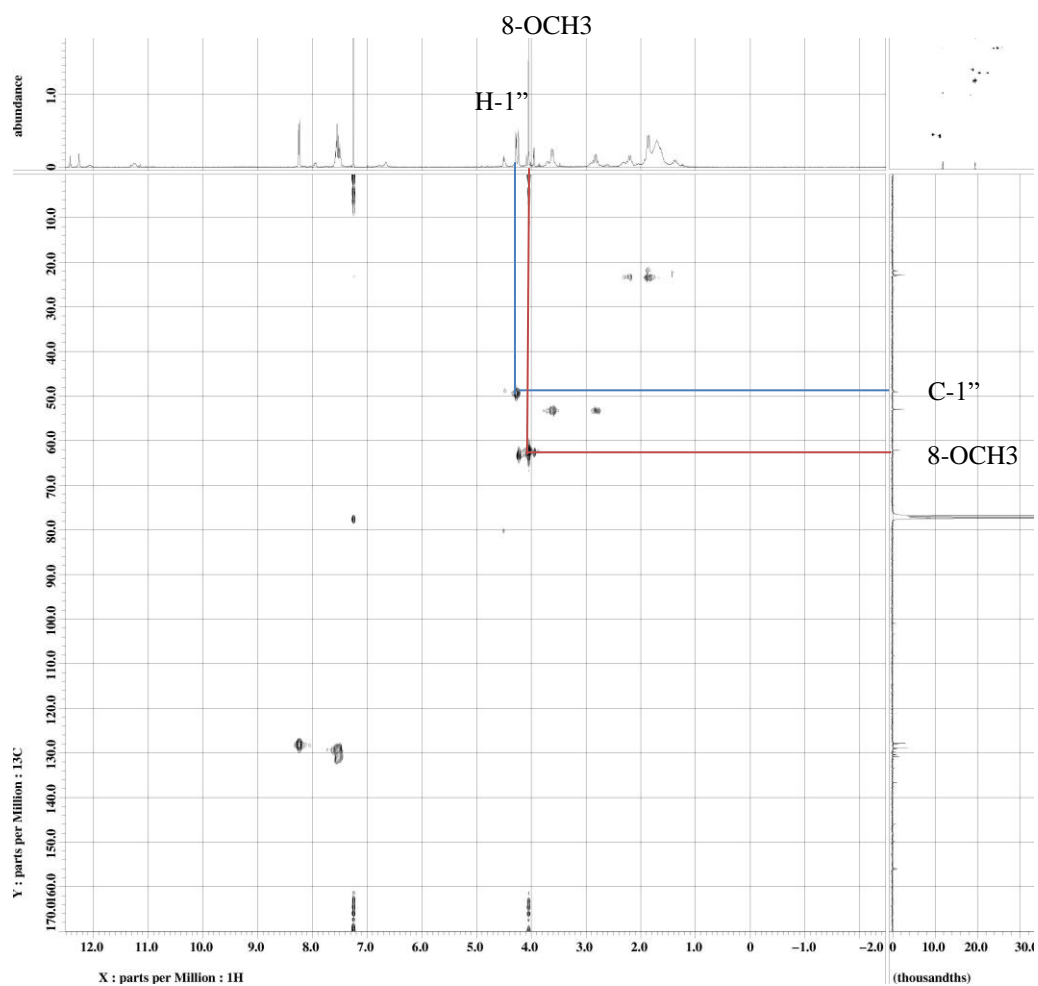
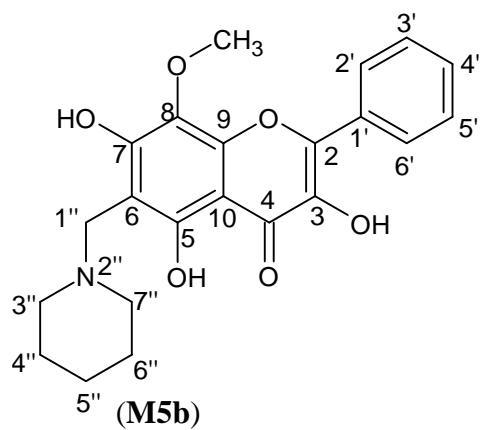
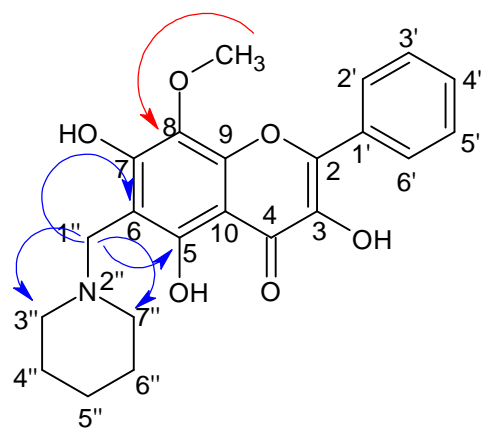


Figure 4.67: HMBC Spectrum of 3,5,7-trihydroxy-8-methoxy-6-(piperidin-1-ylmethyl)-2-phenyl-4H-chromen-4-one (M5b)



(M5b)

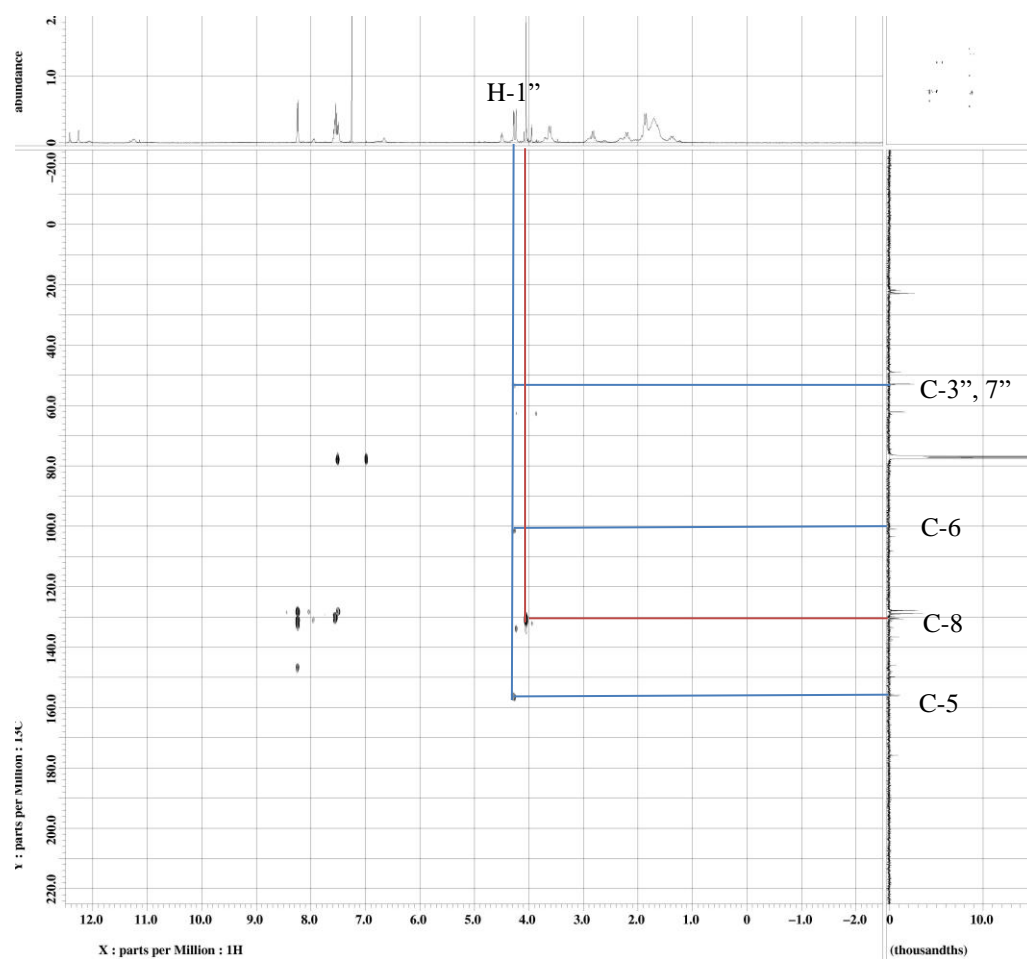
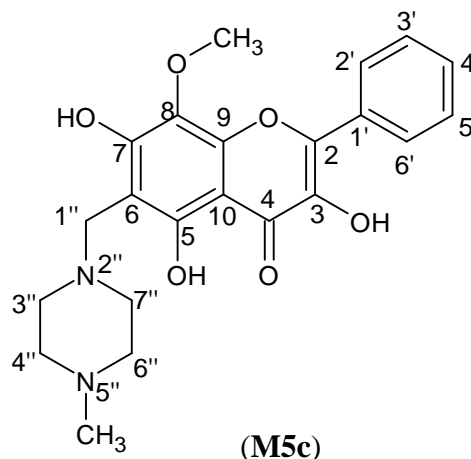


Figure 4.68: HMBC Spectrum of 3,5,7-trihydroxy-8-methoxy-6-(piperidin-1-ylmethyl)-2-phenyl-4H-chromen-4-one (M5b)

4.3.3.3 Characterization of 3,5,7-trihydroxy-8-methoxy-6-(4-methylpiperazin-1-ylmethyl)-2-phenyl-4H-chromen-4-one (M5c)



Compound **M5c** was obtained as yellow solid, mp 172-174 °C. In TLC plate, R_f value of 0.12 was obtained in mobile phase hexane: acetone 6:4. The percentage yield of **M5c** was obtained at 38.3%. The HRESIMS (Appendix A25) gave a pseudomolecular ion peak at $m/z = 413.1725$ $[M+H]^+$ which analysed for $C_{22}H_{24}N_2O_6$ (found 412.1652; calculated 412.1634). Table 4.31 shows the summary physical properties of **M5c**.

The IR spectrum of **M5c** (Appendix C25) shows absorption bands at 3412 (OH stretch), 2933, 2830 (CH_3 stretch), 1637 (C=O stretch), 1618 (C=C stretch), 1305 (C-N stretch), 1149 (C-O stretch), 1048 (C-O-C stretch) cm^{-1} .

Table 4.31: Summary Physical Properties of M5c

| Compound | M5c |
|-------------------------|---|
| IUPAC Name | 3,5,7-trihydroxy-8-methoxy-6-(4-methylpiperazin-1-ylmethyl)-2-phenyl-4H-chromen-4-one |
| Molecular formula | C ₂₂ H ₂₄ N ₂ O ₆ |
| Molecular weight, g/mol | 412.1652 |
| Physical appearance | Yellow solid |
| Percentage yield, % | 38.3 |
| Obtained Mass, mg | 15.8 |
| R _f value | 0.12 |
| Melting point, °C | 172-174 |

In the ¹H NMR of compound **M5c** (Figure 4.69), the multiplets signals at δ_H 2.38 (CH₃-N), δ_H 2.54 (CH₂NCH₂), δ_H 2.68 (CH₂NCH₂) were the characteristic peaks of 1-methylpiperazine. The methylene protons signal was shown at signal δ_H 3.93. The disappearance singlet at δ_H 6.30 (H-6) in compound **M5c** showed that the aminomethylation was occurred at C-6. In ¹³C NMR (Figure 4.70) of compound **M5c**, signal at δ_c 53.1 was the methylene carbon and the signals at δ_c 45.5, δ_c 51.8 and δ_c 54.4 were the characteristic peaks of 1-methylpiperazine moiety. In the HMBC spectrum (Figure 4.72), methylene protons displayed two bonds correlations with C-6 (δ_c 102.1), and three bonds correlations with C-5 (δ_c 153.3), C-7 (δ_c 159.3). Furthermore, methylene protons also show three-bond correlations with C-3'', 7'' (δ_c 51.8) which belong to 1-methylpiperazine moiety. Signal at δ_H 2.38 (CH₃-N) show three-bond correlations with C-4'', 6'' (δ_c 54.4) which confirmed the position of CH₂N-

5''CH₂. The structure was further confirmed by using DEPT (Appendix D61) and HMQC (Figure 4.71) spectrums. Table 4.32 shows the summary NMR data of compounds **M5** and **M5c**.

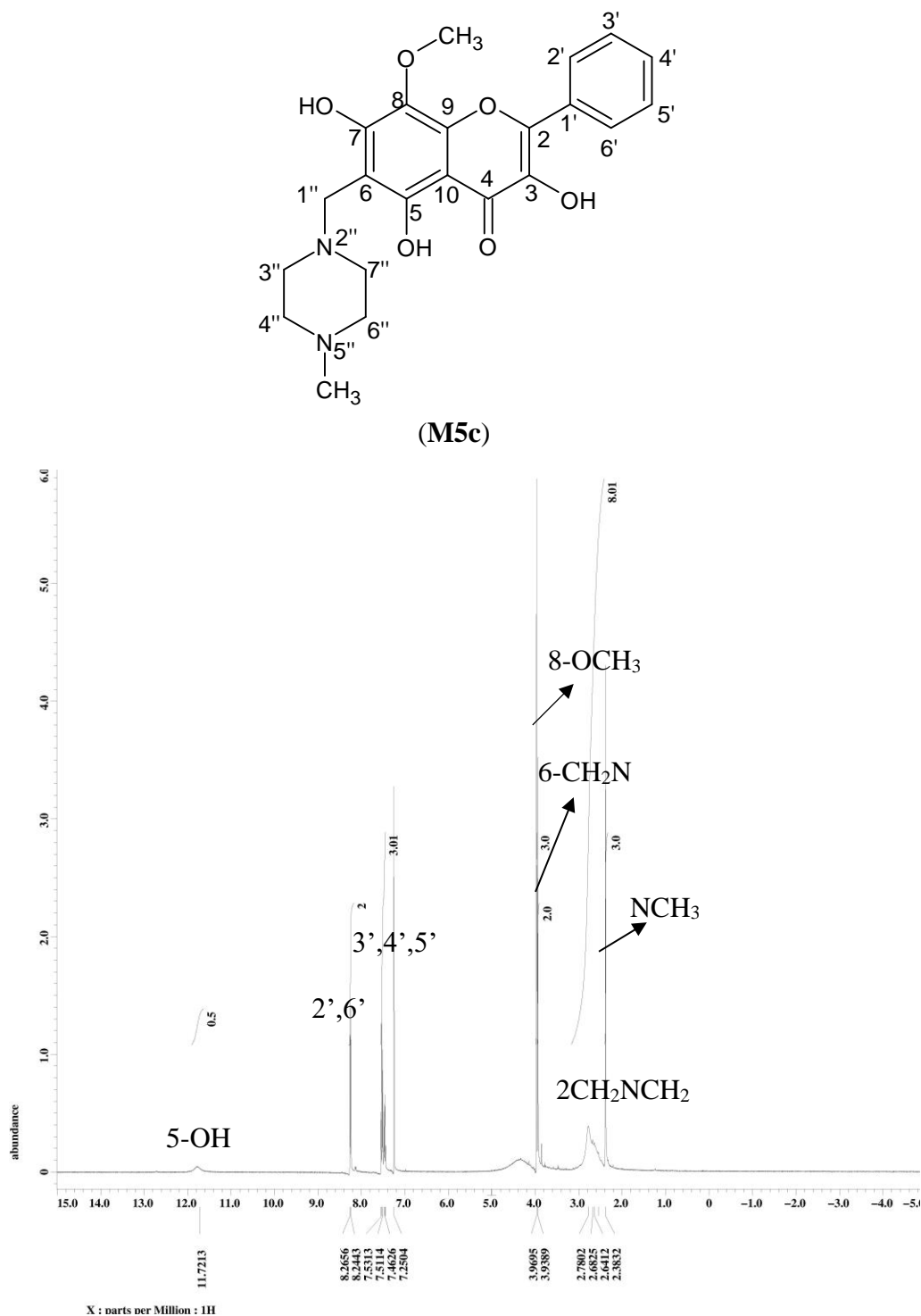
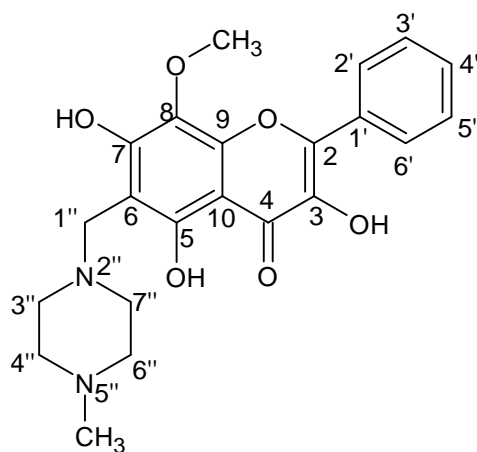


Figure 4.69: ¹H NMR (400 MHz, CDCl₃) of 3,5,7-trihydroxy-8-methoxy-6-(4-methylpiperazin-1-ylmethyl)-2-phenyl-4H-chromen-4-one (**M5c**)



(M5c)

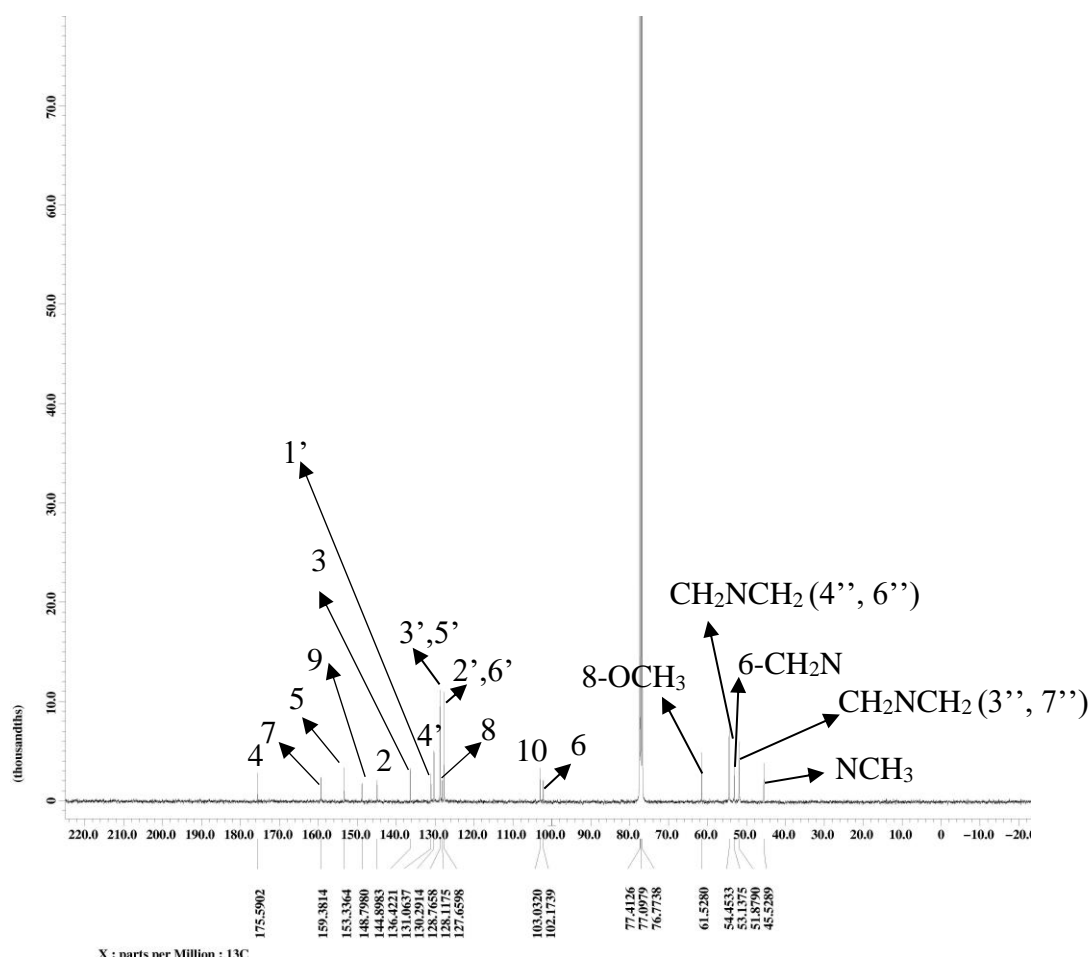


Figure 4.70: ^{13}C NMR (100 MHz, CDCl_3) of 3,5,7-trihydroxy-8-methoxy-6-(4-methylpiperazin-1-ylmethyl)-2-phenyl-4H-chromen-4-one (M5c)

Table 4.32: ¹H, ¹³C and HMBC spectral data of M5 (acetone-d₆) and M5c (CDCl₃)

| | M5 | M5c | M5 | M5c | M5c |
|----------------------------------|-------------------------------|-------------------------------|----------------------------|----------------------------|---------------------|
| Proton | δ _H (Multiplicity) | δ _H (Multiplicity) | δ _c (Type of C) | δ _c (Type of C) | HMBC |
| 2 | - | - | 145.2 (C) | 144.8 (C) | - |
| 3 | - | - | 137.2 (C) | 136.4 (C) | - |
| 4 | - | - | 176.3 (C) | 175.5 (C) | - |
| 5 | - | - | 156.5 (C) | 153.3 (C) | - |
| 6 | 6.30 (1H, s) | - | 98.4 (C) | 102.1 (C) | - |
| 7 | - | - | 157.0 (C) | 159.3 (C) | - |
| 8 | - | - | 127.8 (C) | 128.1 (C) | - |
| 9 | - | - | 149.1 (C) | 148.7 (C) | - |
| 10 | - | - | 103.5 (C) | 103.0 (C) | - |
| 1' | - | - | 131.4 (C) | 131.0 (C) | - |
| 2',6' | 8.28 (2H, m) | 8.23 (2H, m) | 127.6 (CH) | 127.6 (CH) | C-2, 3', 4', 5' |
| 3',5' | 7.57 (2H, m) | 7.58 (2H, m) | 128.7 (CH) | 128.7 (CH) | C-2', 6', 4' |
| 4' | 7.51 (1H, m) | 7.59 (1H, m) | 130.1(CH) | 130.2 (CH) | C- 2', 6' |
| 5-OH | 11.77 (1H, s) | 12.40 (1H, s) | - | - | C-6, 10, 5 |
| 8-OCH ₃ | 3.93 (3H, s) | 3.86 (3H, s) | 61.1(CH ₃) | 61.5 (CH ₃) | C-8 |
| 3-OH | 8.35 (1H, s) | - | - | - | - |
| 7-OH | 9.47 (1H, s) | - | - | - | - |
| 6-CH ₂ N | - | 3.93 (2H, s) | - | 53.1 (CH ₂) | C-3'', 7'', 6, 5, 7 |
| CH ₃ N | - | 2.38 (3H, s) | - | 45.5 (CH ₂) | C-4'', 6'' |
| CH ₂ NCH ₂ | - | 2.54 (4H, m) | - | 51.8 (CH ₂) | - |
| CH ₂ NCH ₂ | - | 2.68 (4H, m) | - | 54.4 (CH ₂) | - |

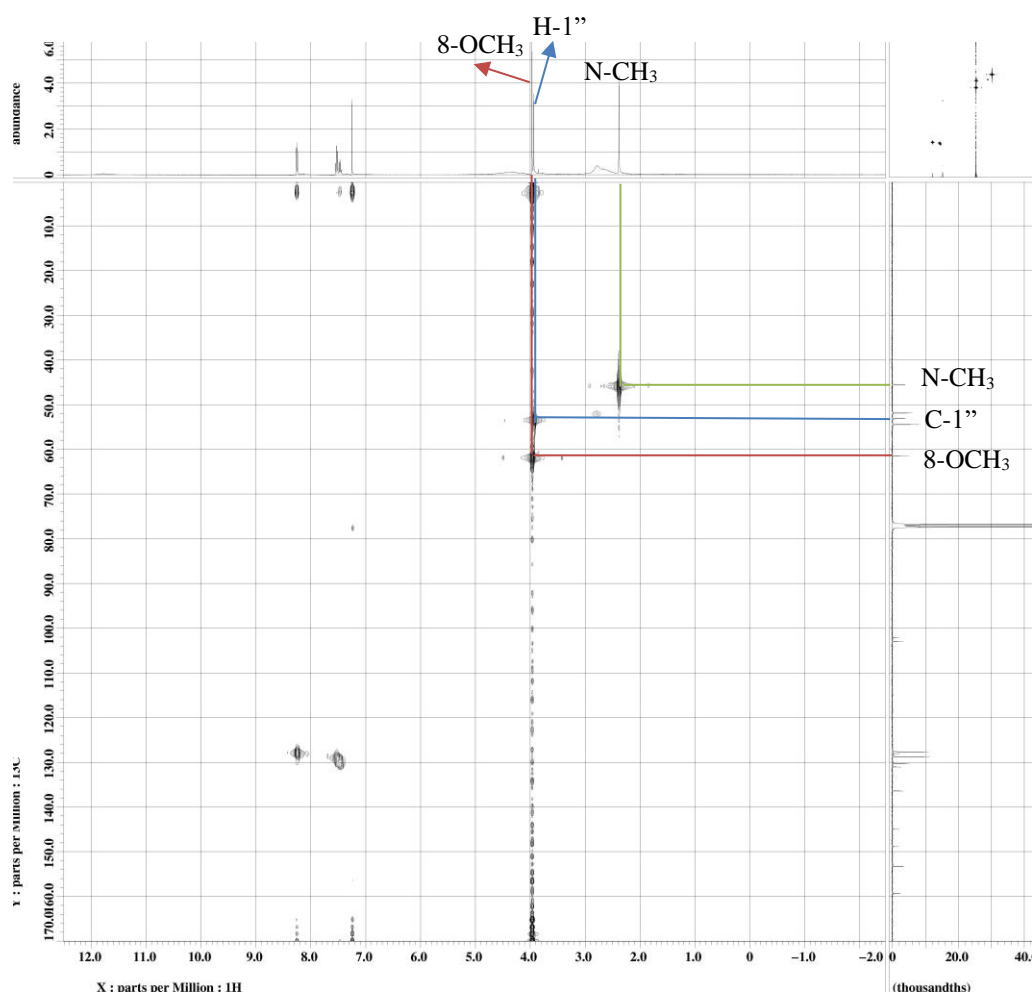
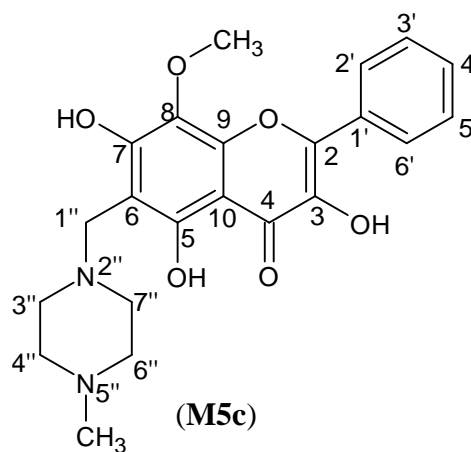
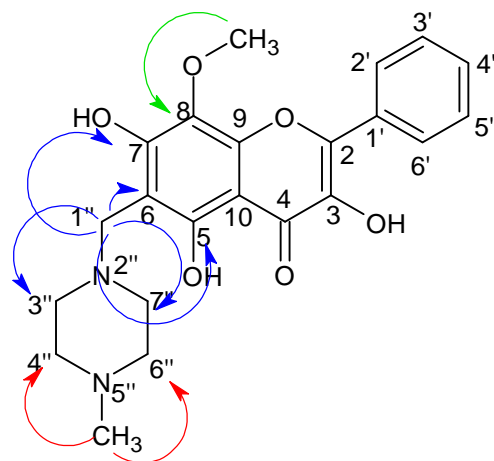


Figure 4.71: HMQC Spectrum of 3,5,7-trihydroxy-8-methoxy-6-(4-methylpiperazin-1-ylmethyl)-2-phenyl-4H-chromen-4-one (M5c)



(M5c)

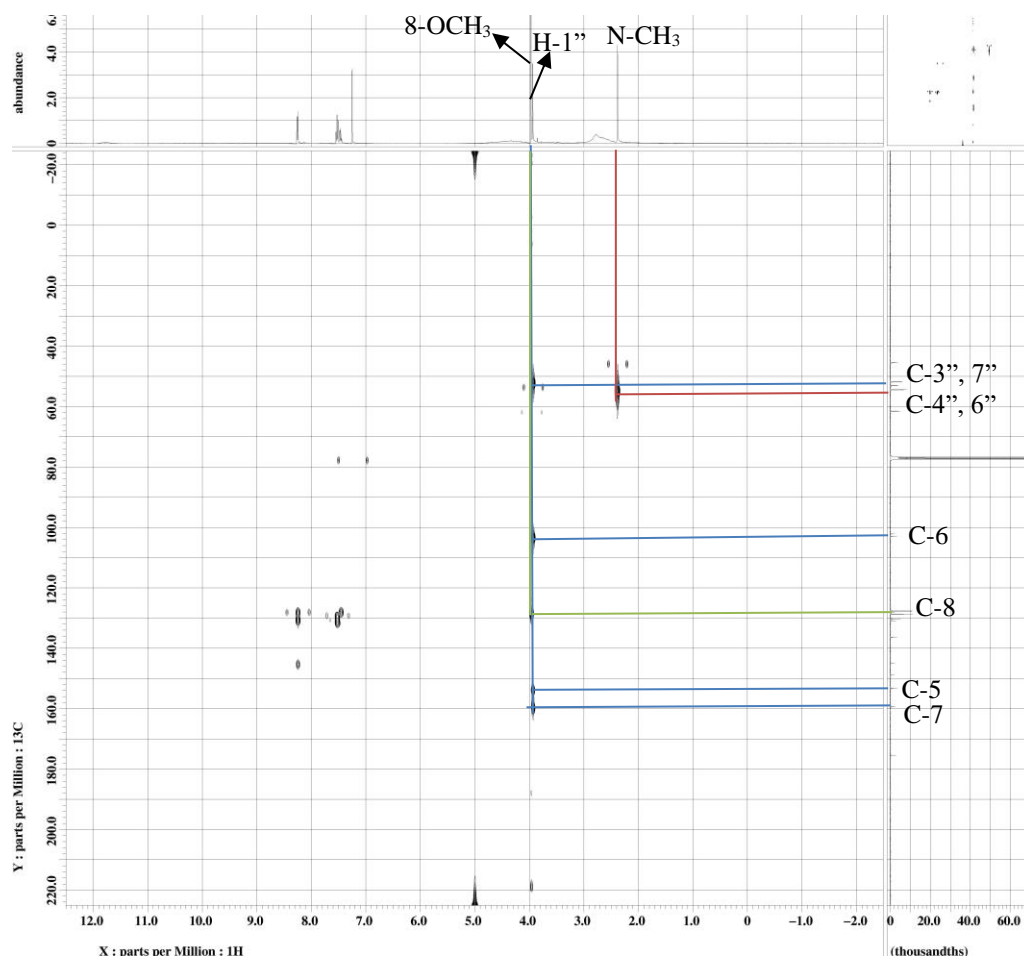
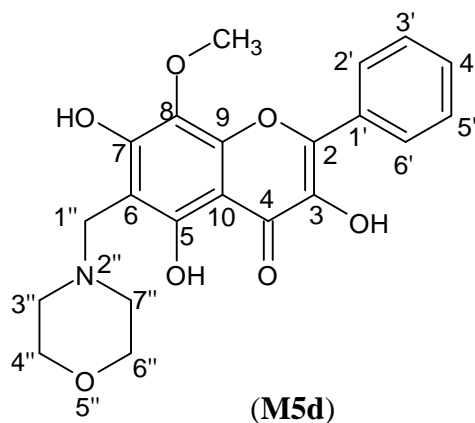


Figure 4.72: HMBC Spectrum of 3,5,7-trihydroxy-8-methoxy-6-(4-methylpiperazin-1-ylmethyl)-2-phenyl-4H-chromen-4-one (M5c)

4.3.3.4 Characterization of 3,5,7-trihydroxy-8-methoxy-6-(morpholinomethyl)-2-phenyl-4H-chromen-4-one (M5d)



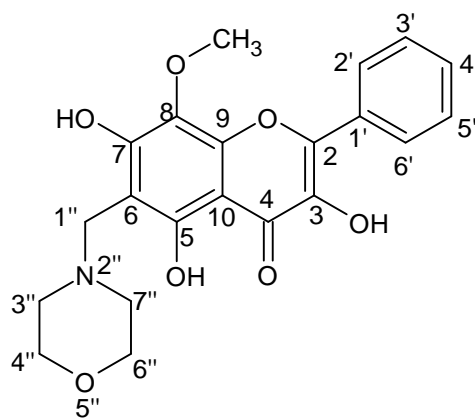
Compound **M5d** was obtained as yellow solid, mp 233-234 °C. In TLC plate, R_f value of 0.16 was obtained in mobile phase hexane:acetone 6:4. The percentage yield of **M5d** was obtained at 58.9%. The HRESIMS (Appendix A26) gave a pseudomolecular ion peak at $m/z = 400.1397$ $[M+H]^+$ which analysed for $C_{21}H_{21}NO_7$ (found 399.1324 ; calculated 399.1318). Table 4.33 shows the summary physical properties of **M5d**.

The IR spectrum of **M5d** (Appendix C26) shows absorption bands at 3413 (OH stretch), 2965, 2943 (CH_3 stretch), 1638 (C=O stretch), 1618 (C=C stretch), 1288 (C-N stretch), 1179 (C-O stretch), 1046 (C-O-C stretch) cm^{-1} .

Table 4.33: Summary Physical Properties of M5d

| Compound | M5d |
|-------------------------|---|
| IUPAC Name | 3,5,7-trihydroxy-8-methoxy-6-(morpholinomethyl)-2-phenyl-4H-chromen-4-one |
| Molecular formula | C ₂₁ H ₂₁ NO ₇ |
| Molecular weight, g/mol | 399.1324 |
| Physical appearance | Yellow solid |
| Percentage yield, % | 58.8 |
| Obtained Mass, mg | 23.5 |
| R _f value | 0.16 |
| Melting point, °C | 233-234 |

In the ¹H NMR of compound **M5d** (Figure 4.73), signal at δ_H 3.91 belongs to methylene protons. Characteristic peaks of morpholine were appeared at δ_H 2.72 (CH₂NCH₂) and δ_H 3.81 (CH₂OCH₂). In ¹³C NMR (Figure 4.74) of compound **M5d**, signal at δ_C 53.8 was the methylene carbon and the signals at δ_C 52.8 and δ_C 61.5 were the characteristic peaks of morpholine moiety. The position of aminomethylation was confirmed by using HMBC spectrum (Figure 4.76). The structure was further confirmed by using DEPT (Appendix D62) and HMQC (Figure 4.75) spectra. Table 4.34 shows the summary NMR data of compounds **M5** and **M5d**.



(M5d)

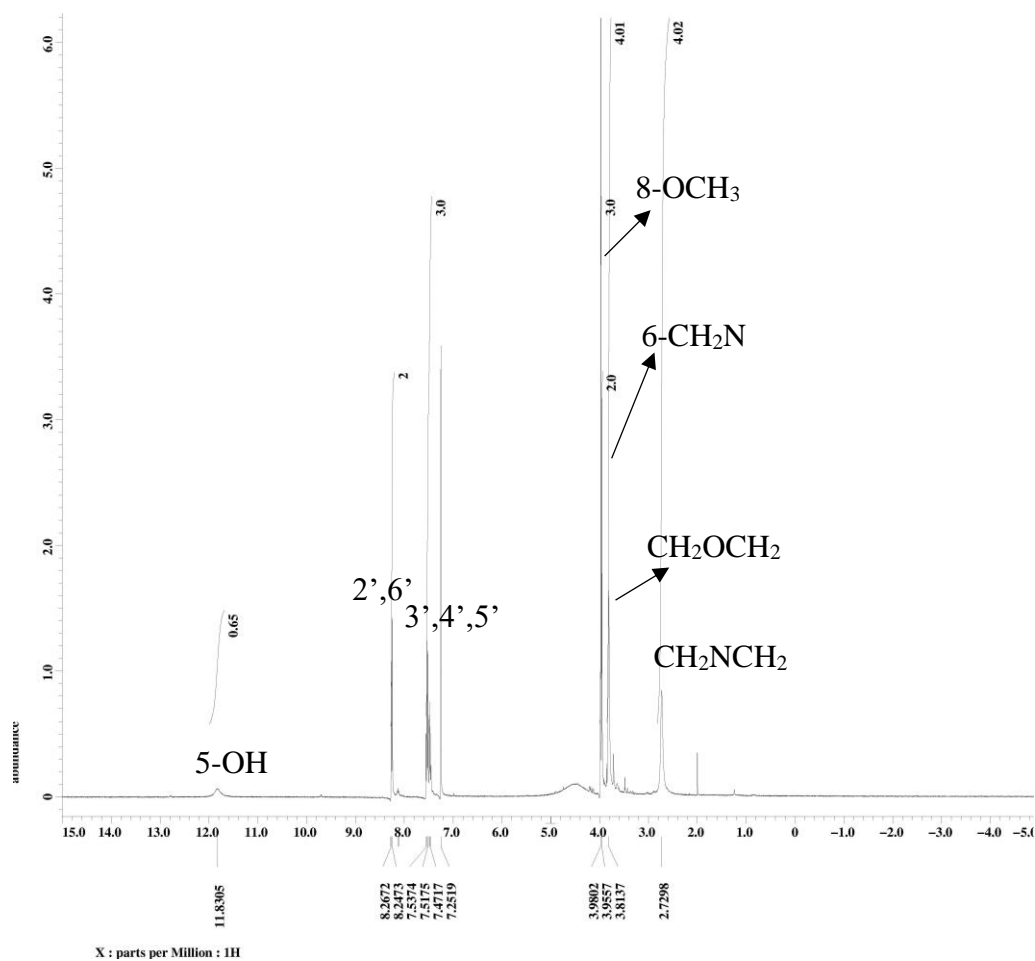
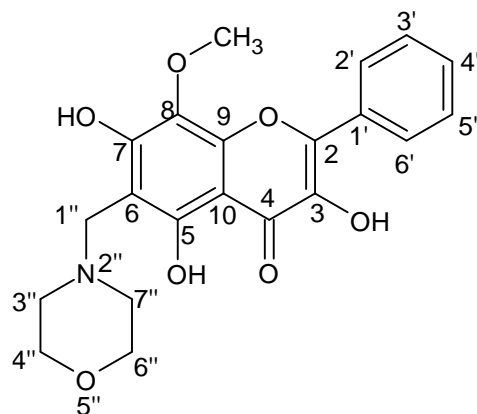


Figure 4.73: ^1H NMR (400 MHz, CDCl_3) of 3,5,7-trihydroxy-8-methoxy-6-(morpholinomethyl)-2-phenyl-4H-chromen-4-one (M5d)



(M5d)

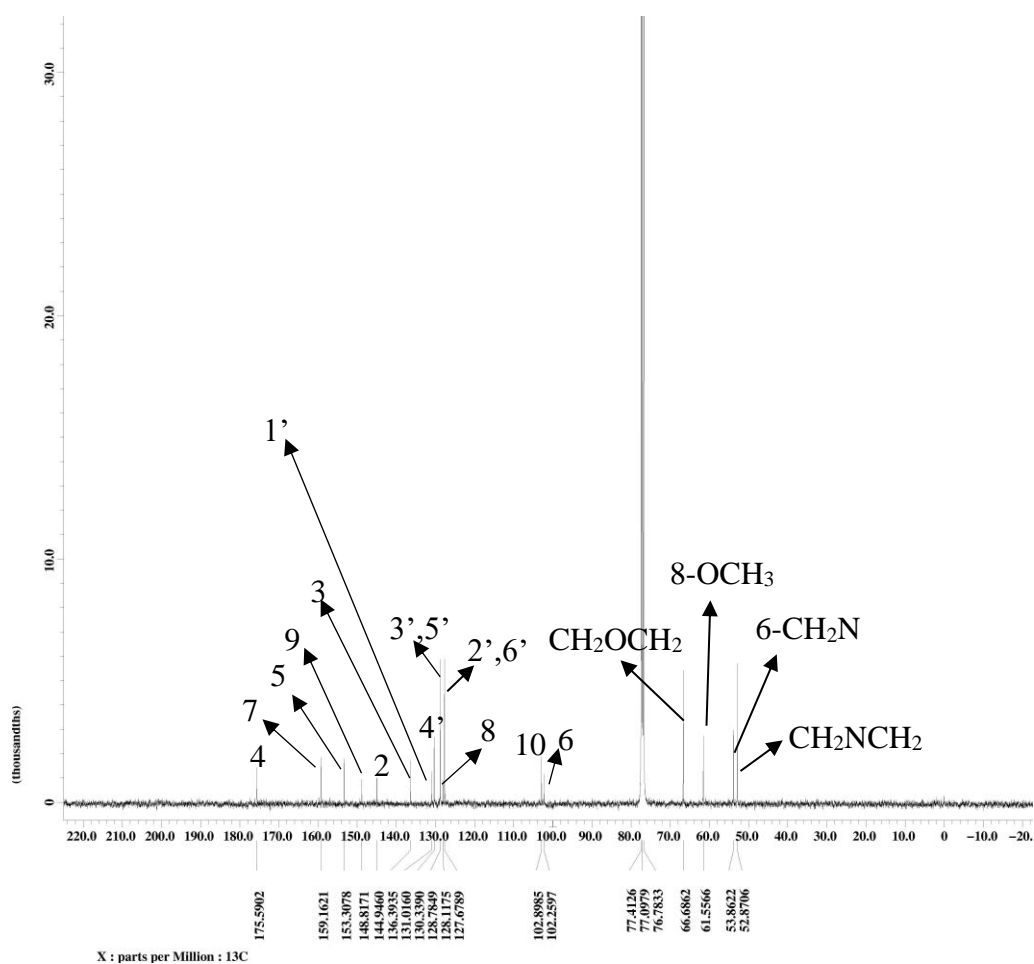


Figure 4.74: ^{13}C NMR (100 MHz, CDCl_3) of 3,5,7-trihydroxy-8-methoxy-6-(morpholinomethyl)-2-phenyl-4H-chromen-4-one (M5d)

Table 4.34: ¹H, ¹³C and HMBC spectral data of M5 (acetone-d₆) and M5d (CDCl₃)

| | M5 | M5d | M5 | M5d | M5d |
|----------------------------------|-------------------------------|-------------------------------|----------------------------|----------------------------|---------------------|
| Proton | δ _H (Multiplicity) | δ _H (Multiplicity) | δ _c (Type of C) | δ _c (Type of C) | HMBC |
| 2 | - | - | 145.2 (C) | 144.9 (C) | - |
| 3 | - | - | 137.2 (C) | 136.3 (C) | - |
| 4 | - | - | 176.3 (C) | 175.5 (C) | - |
| 5 | - | - | 156.5 (C) | 153.3 (C) | - |
| 6 | 6.30 (1H, s) | - | 98.4 (C) | 102.2 (C) | - |
| 7 | - | - | 157.0 (C) | 159.1 (C) | - |
| 8 | - | - | 127.8 (C) | 128.1 (C) | - |
| 9 | - | - | 149.1 (C) | 148.8 (C) | - |
| 10 | - | - | 103.5 (C) | 102.8 (C) | - |
| 1' | - | - | 131.4 (C) | 131.0 (C) | - |
| 2',6' | 8.28 (2H, m) | 8.24 (2H, m) | 127.6 (CH) | 127.6 (CH) | C-2, 3', 4', 5' |
| 3',5' | 7.57 (2H, m) | 7.47 (2H, m) | 128.7 (CH) | 128.7 (CH) | C-2', 6', 4' |
| 4' | 7.51 (1H, m) | 7.51 (1H, m) | 130.1(CH) | 130.3 (CH) | C- 2', 6' |
| 5-OH | 11.77 (1H, s) | 11.79 (1H, s) | - | - | C-6, 10, 5 |
| 8-OCH ₃ | 3.93 (3H, s) | 3.97 (3H, s) | 61.1(CH ₃) | 61.5 (CH ₃) | C-8 |
| 3-OH | 8.35 (1H, s) | - | - | - | - |
| 7-OH | 9.47 (1H, s) | - | - | - | - |
| 6-CH ₂ N | - | 3.91 (2H, s) | - | 53.8 (CH ₂) | C-3'', 7'', 6, 5, 7 |
| CH ₂ NCH ₂ | - | 2.72 (4H, s) | - | 52.8 (CH ₂) | - |
| CH ₂ OCH ₂ | - | 3.81 (4H, m) | - | 66.6 (CH ₂) | - |

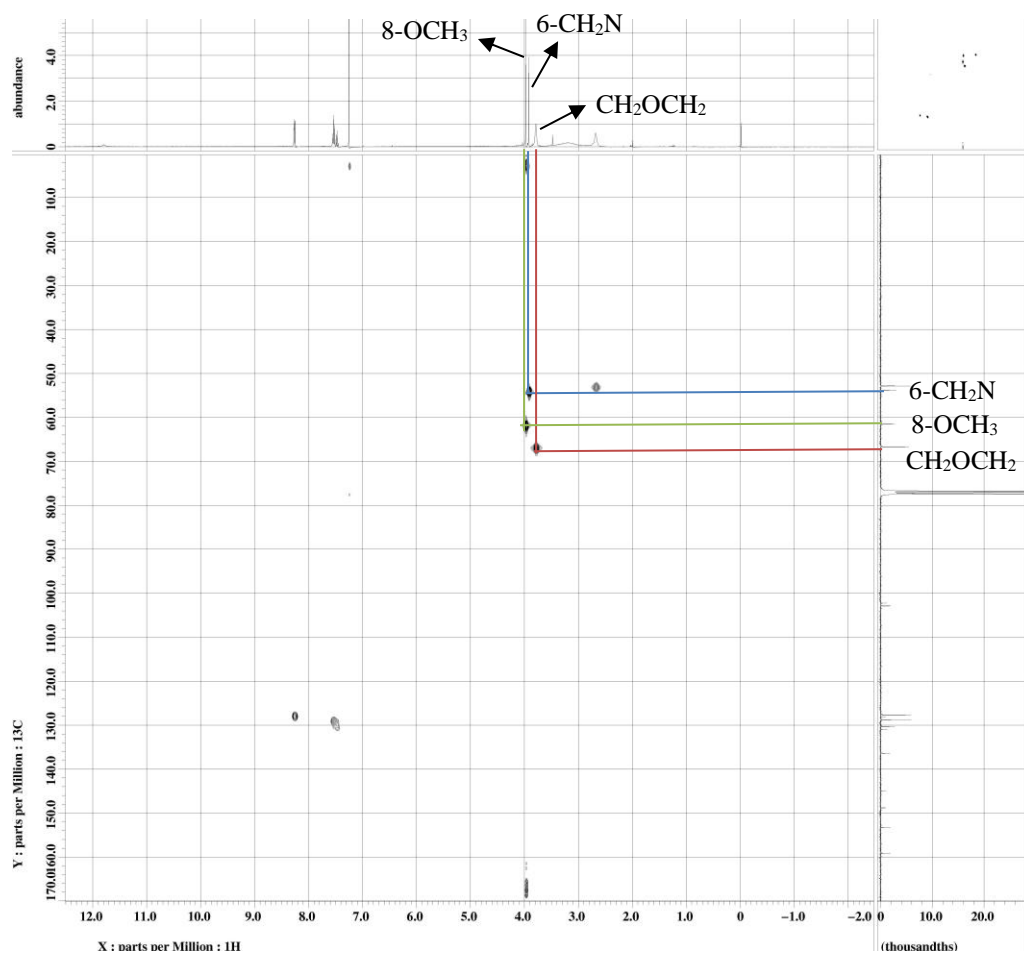
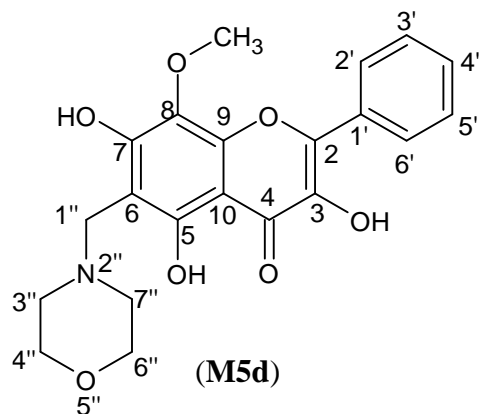
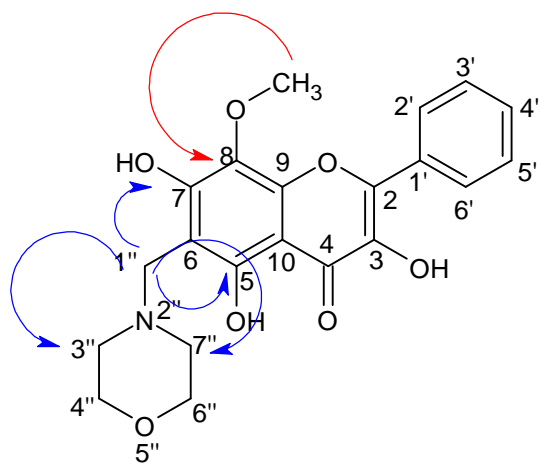


Figure 4.75: HMBC Spectrum of 3,5,7-trihydroxy-8-methoxy-6-(morpholinomethyl)-2-phenyl-4H-chromen-4-one (M5d)



(M5d)

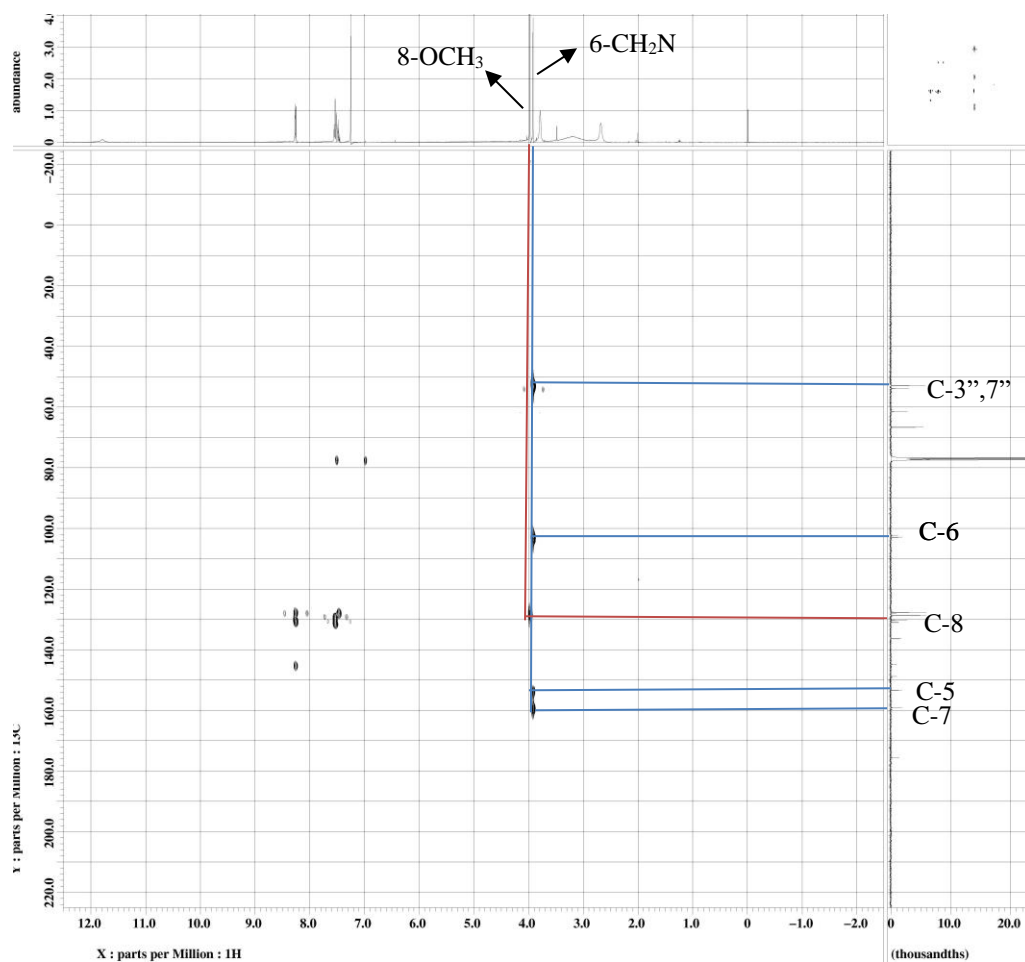
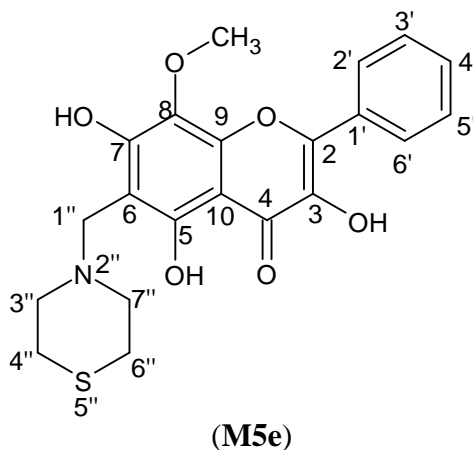


Figure 4.76: HMBC Spectrum of 3,5,7-trihydroxy-8-methoxy-6-(morpholinomethyl)-2-phenyl-4H-chromen-4-one (M5d)

4.3.3.5 Characterization of 3,5,7-trihydroxy-8-methoxy-6-(thiomorpholinomethyl)-2-phenyl-4H-chromen-4-one (M5e)



Compound **M5e** was obtained as yellow solid, mp 239-240 °C. It gave R_f value of 0.42 on a TLC plate in mobile phase hexane:acetone 6:3. The percentage yield of **M5e** was obtained at 43.6%. The HRESIMS (Appendix A27) gave a pseudomolecular ion peak at $m/z = 416.1162$ $[M+H]^+$ which analysed for $C_{21}H_{21}NO_6S$ (found 415.1090; calculated 415.1089). Table 4.35 shows the summary physical properties of **M5e**.

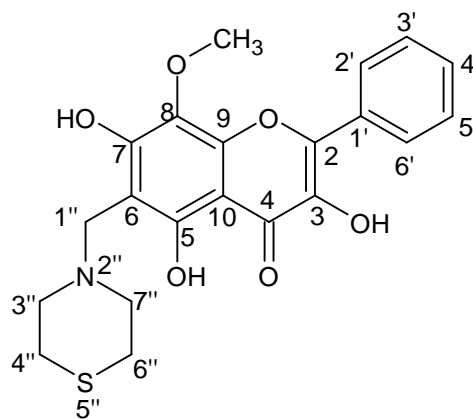
The IR spectrum of **M5e** (Appendix C27) shows absorption bands at 3436 (OH stretch), 1636 (C=O stretch), 1625 (C=C stretch), 1180 (C-N stretch), 1143 (C-O stretch), 1055 (C-O-C stretch) cm^{-1} .

Table 4.35: Summary Physical Properties of M5e

| Compound | M5e |
|-------------------------|---|
| IUPAC Name | 3,5,7-trihydroxy-8-methoxy-6-(thiomorpholinomethyl)-2-phenyl-4H-chromen-4-one |
| Molecular formula | C ₂₁ H ₂₁ NO ₆ S |
| Molecular weight, g/mol | 415.1090 |
| Physical appearance | Yellow solid |
| Percentage yield, % | 43.6 |
| Obtained Mass, mg | 18.1 |
| R _f value | 0.42 |
| Melting point, °C | 239-240 |

In the ¹H NMR of compound **M5e** (Figure 4.77), the presence of multiplets signals at δ_{H} 2.76 (CH₂SCH) and δ_{H} 2.92 (CH₂NCH₂) were the characteristic peaks of thiomorpholine. The methylene protons signal was shown at signal δ_{H} 3.91. The disappearance singlet at δ_{H} 6.30 (H-6) in compound **M5e** showed that the aminomethylation was occurred at C-6. In ¹³C NMR (Figure 4.78) of compound **M5e**, signal at δ_{C} 54.3 was the methylene carbon and the signals at δ_{C} 27.8 and δ_{C} 54.4 were the characteristic peaks of CH₂SCH₂ and CH₂NCH₂, respectively. In the HMBC spectrum (Figure 4.80), methylene protons displayed two bonds correlations with C-6 (δ_{C} 102.2), and three bonds correlations with C-5 (δ_{C} 153.2), C-7 (δ_{C} 159.3). Furthermore, methylene protons also show three-bond correlations with C-3'', 7'' (δ_{C} 54.4) which belong to thiomorpholine moiety. The structure was further confirmed by using DEPT

(Appendix D63) and HMQC (Figure 4.79) spectra. Table 4.36 shows the summary NMR data of compounds **M5** and **M5e**.



(M5e)

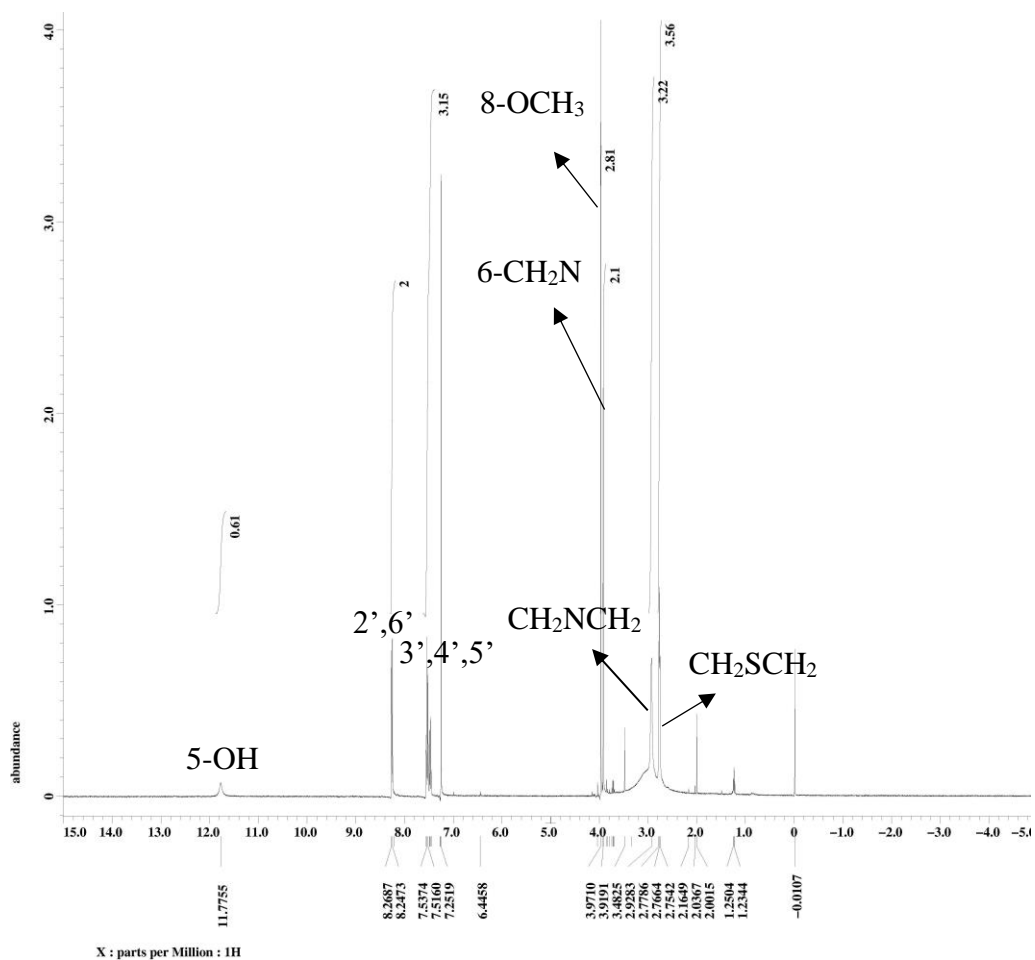
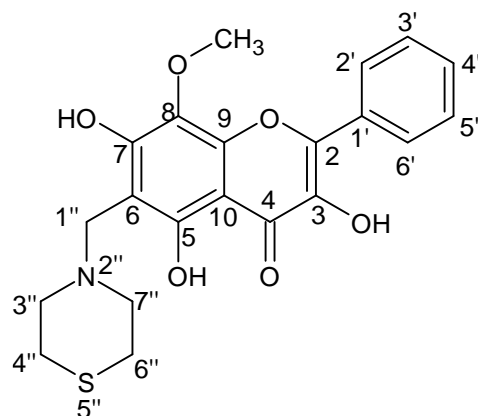


Figure 4.77: ¹H NMR (400 MHz, CDCl₃) of 3,5,7-trihydroxy-8-methoxy-6-(thiomorpholinomethyl)-2-phenyl-4*H*-chromen-4-one (M5e)



(M5e)

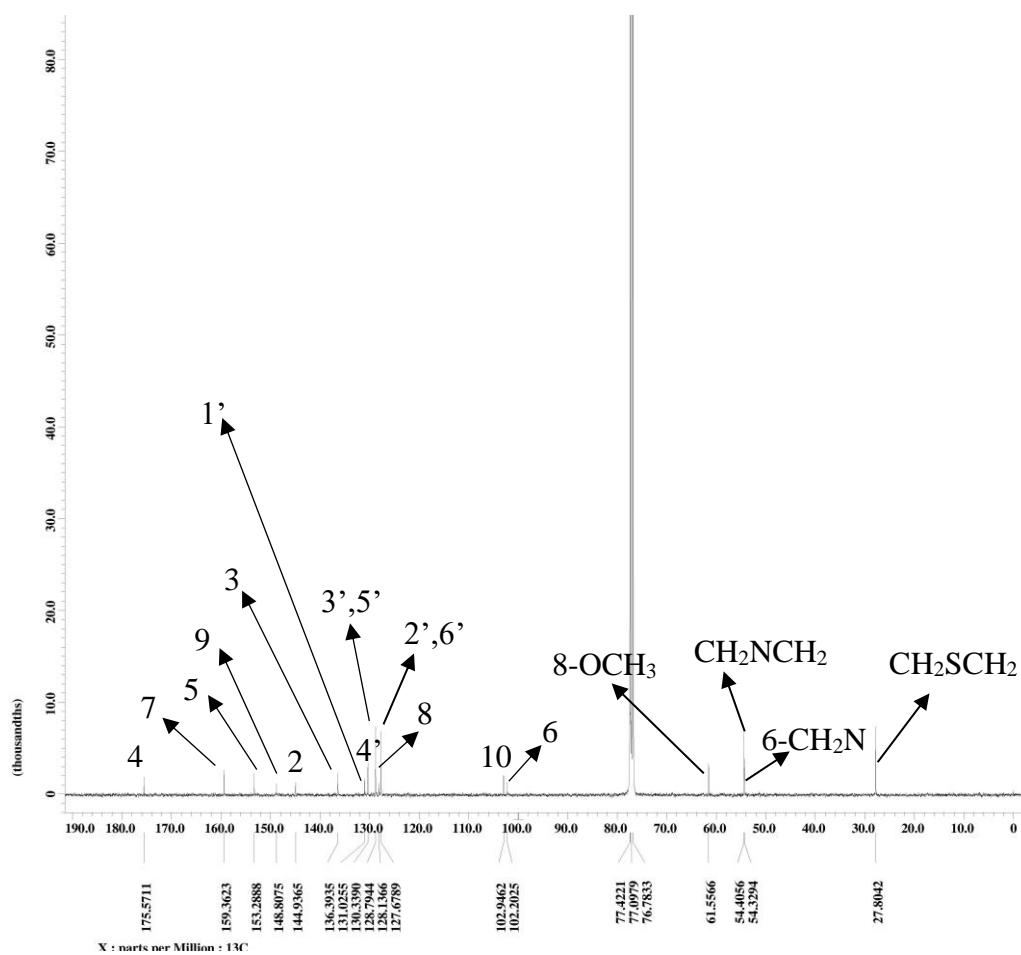


Figure 4.78: ¹³C NMR (100 MHz, CDCl₃) of 3,5,7-trihydroxy-8-methoxy-6-(thiomorpholinomethyl)-2-phenyl-4*H*-chromen-4-one (M5e)

Table 4.36: ¹H, ¹³C and HMBC spectral data of M5 (acetone-d₆) and M5e (CDCl₃)

| | M5 | M5e | M5 | M5e | M5e |
|----------------------------------|-------------------------------|-------------------------------|----------------------------|----------------------------|---------------------|
| Proton | δ _H (Multiplicity) | δ _H (Multiplicity) | δ _c (Type of C) | δ _c (Type of C) | HMBC |
| 2 | - | - | 145.2 (C) | 144.9 (C) | - |
| 3 | - | - | 137.2 (C) | 136.3 (C) | - |
| 4 | - | - | 176.3 (C) | 175.5 (C) | - |
| 5 | - | - | 156.5 (C) | 153.2 (C) | - |
| 6 | 6.30 (1H, s) | - | 98.4 (C) | 102.2 (C) | - |
| 7 | - | - | 157.0 (C) | 159.3 (C) | - |
| 8 | - | - | 127.8 (C) | 128.1 (C) | - |
| 9 | - | - | 149.1 (C) | 148.8 (C) | - |
| 10 | - | - | 103.5 (C) | 102.9 (C) | - |
| 1' | - | - | 131.4 (C) | 131.0 (C) | - |
| 2',6' | 8.28 (2H, m) | 8.26 (2H, m) | 127.6 (CH) | 127.6 (CH) | C-2, 3', 4', 5' |
| 3',5' | 7.57 (2H, m) | 7.51 (2H, m) | 128.7 (CH) | 128.7 (CH) | C-2', 6', 4' |
| 4' | 7.51 (1H, m) | 7.53 (1H, m) | 130.1(CH) | 130.3 (CH) | C- 2', 6' |
| 5-OH | 11.77 (1H, s) | 11.77 (1H, s) | - | - | C-6, 10, 5 |
| 8-OCH ₃ | 3.93 (3H, s) | 3.97 (3H, s) | 61.1(CH ₃) | 61.5 (CH ₃) | C-8 |
| 3-OH | 8.35 (1H, s) | - | - | - | - |
| 7-OH | 9.47 (1H, s) | - | - | - | - |
| 6-CH ₂ N | - | 3.91 (2H, s) | - | 54.3 (CH ₂) | C-3'', 7'', 6, 5, 7 |
| CH ₂ NCH ₂ | - | 2.92 (4H, s) | - | 54.4 (CH ₂) | - |
| CH ₂ SCH ₂ | - | 2.76 (4H, s) | - | 27.8 (CH ₂) | - |

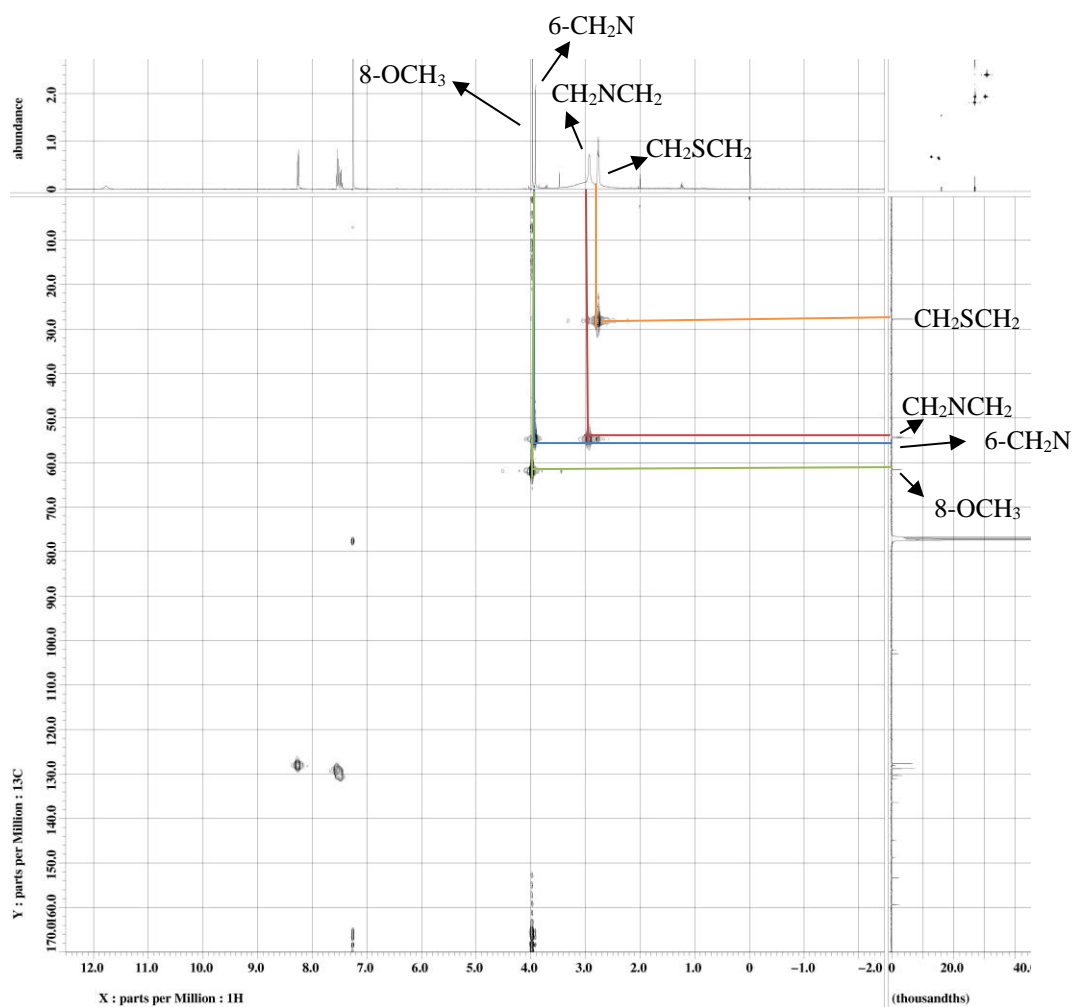
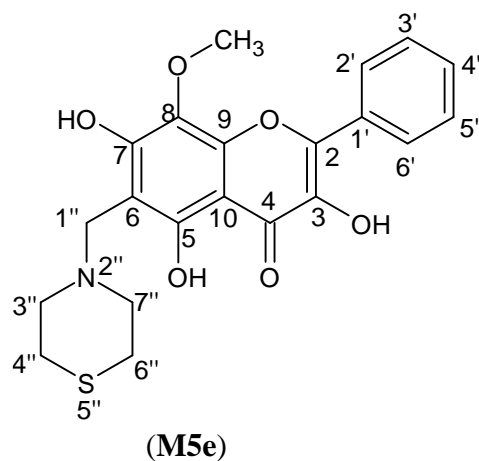
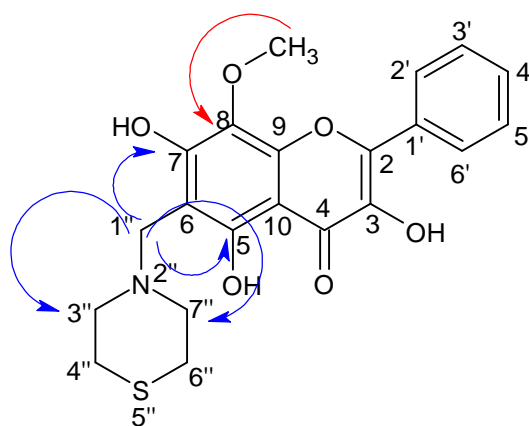


Figure 4.79: HMBC Spectrum of 3,5,7-trihydroxy-8-methoxy-6-(thiomorpholinomethyl)-2-phenyl-4H-chromen-4-one (M5e)



(M5e)

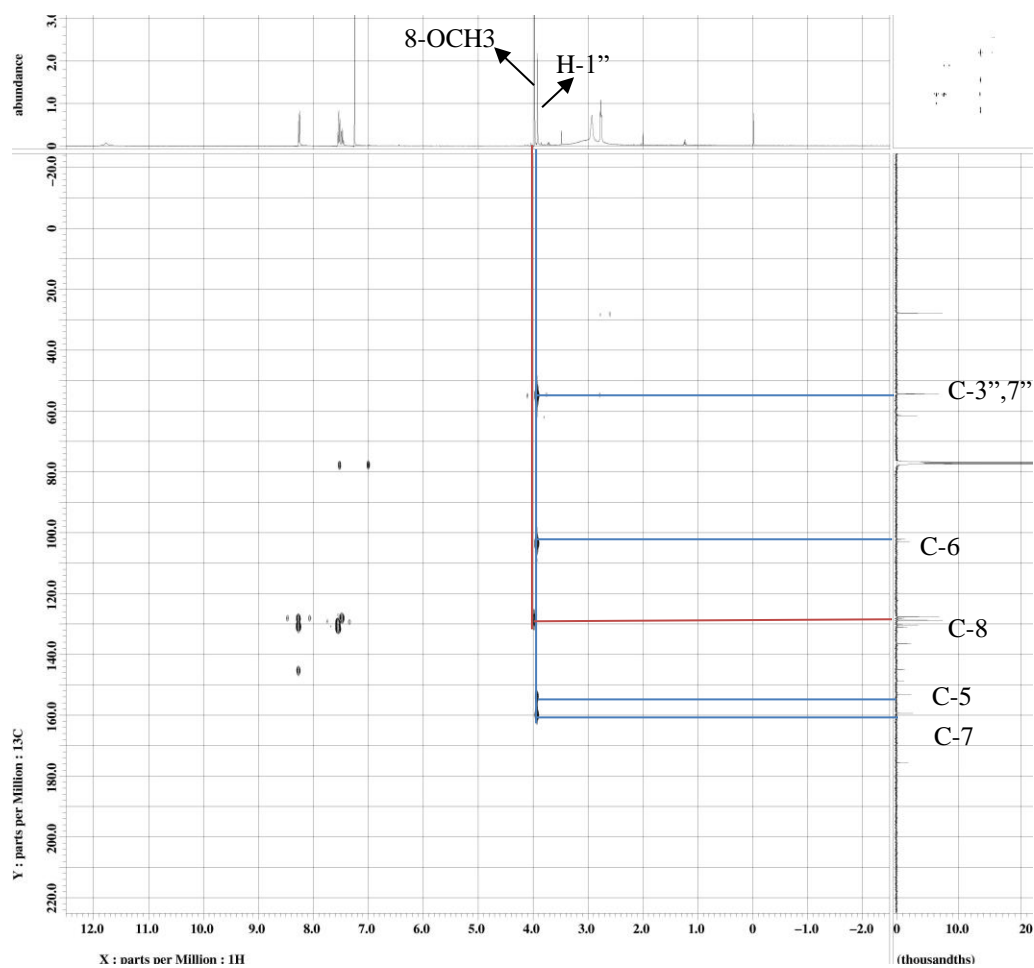


Figure 4.80: HMBC Spectrum of 3,5,7-trihydroxy-8-methoxy-6-(thiomorpholinomethyl)-2-phenyl-4H-chromen-4-one (M5e)

4.3.4 Synthesis of 5,7-dihydroxyflavone (M14) Monoamine Mannich Bases

Isolate 5,7-dihydroxyflavone (**M14**) was used to synthesize flavone Mannich bases via Mannich reaction. The reaction route was shown in Figure 4.81.

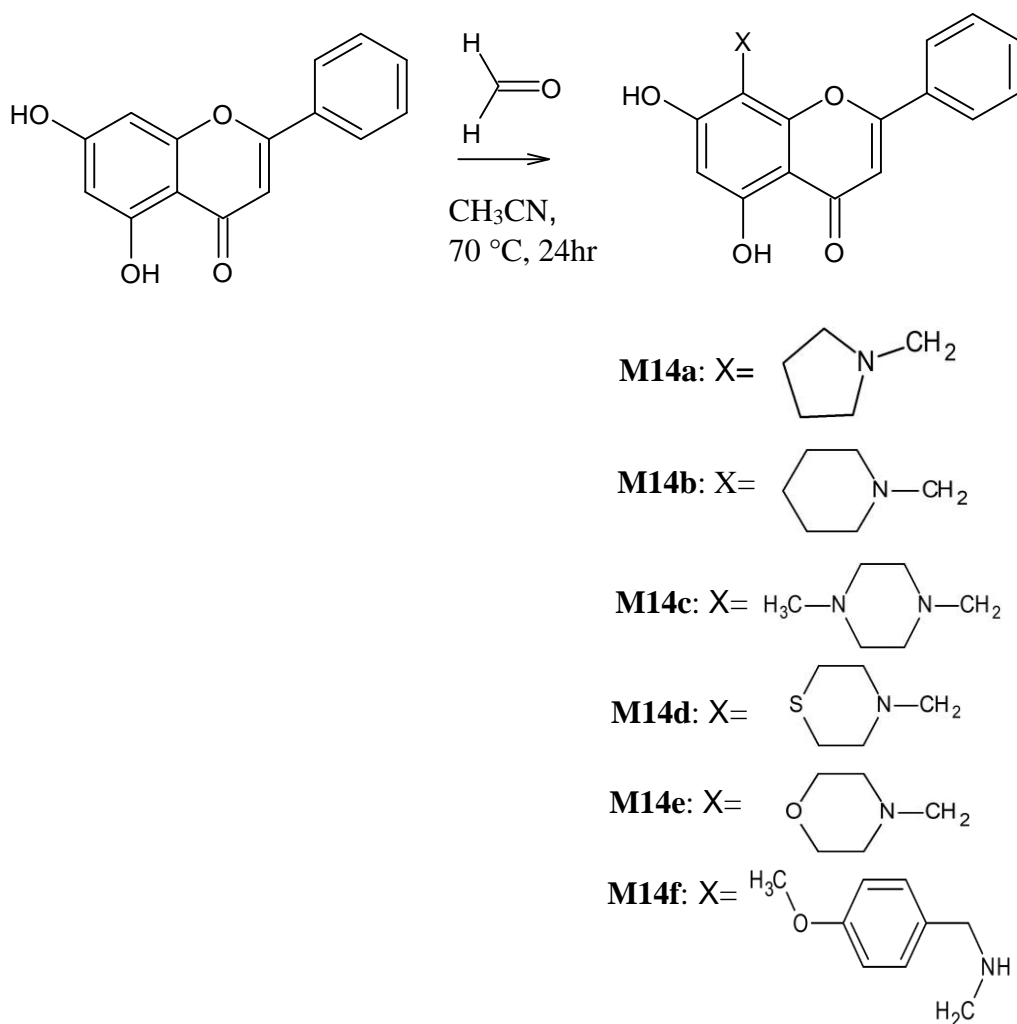


Figure 4.81: Synthesis route of flavone M14 monoamine Mannich bases with mol ratio flavone: formaldehyde: amine 1:2:2

Mannich flavones (**M14a-M14f**) were prepared by reaction of **M14** flavone with formaldehyde, secondary amine (pyrrolidine in **M14a**; piperidine in **M14b**; 1-methylpiperazine in **M14c**; thiomorpholine in **M14d**; morpholine in **M14e**; 4-methoxybenzylamine in **M14f**) in mol ratio 1:2:2, respectively, and stirred under reflux in acetonitrile for 24 hr at 70 °C.

The reaction mechanism involves the formation of iminium ion (Figure 4.39) which is the condensation between formaldehyde and secondary amine. Then, followed by the electrophilic attack of the iminium ion on the aromatic A-ring of the flavone substrate at C8 which is ortho to hydroxyl group. The reaction mechanism was shown in Figure 4.82.

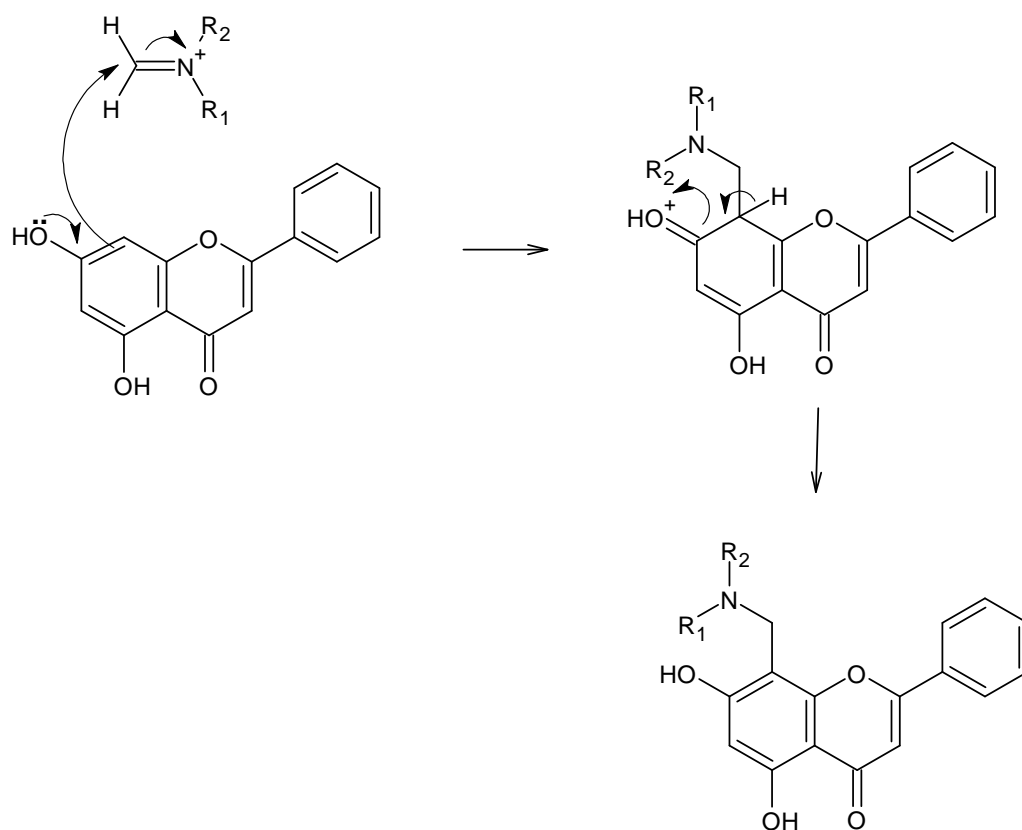
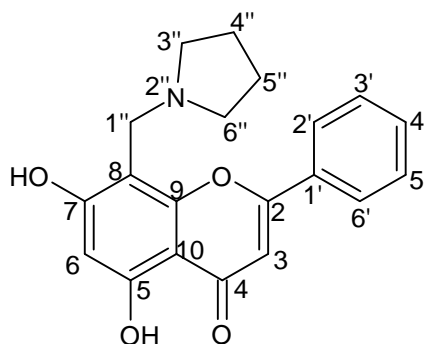


Figure 4.82: Reaction mechanism of flavone M14 monoamine Mannich bases

4.3.4.1 Characterization of 5,7-dihydroxy-8-(pyrrolidine-1-ylmethyl)-2-phenyl-4*H*-chromen-4-one (M14a)



(M14a)

Compound **M14a** was obtained as yellow solid, mp 163-166 °C. In TLC plate, R_f value of 0.08 was obtained in mobile phase hexane:acetone 6:3. The percentage yield of **M14a** was obtained at 75.4%. The HRESIMS (Appendix A28) gave a pseudomolecular ion peak at $m/z = 338.1390$ $[M+H]^+$ which analysed for $C_{20}H_{19}NO_4$ (found 337.1317; calculated 337.1314). Table 4.37 shows the summary physical properties of **M14a**.

The IR spectrum of **M14a** (Appendix C28) shows absorption bands at 3414 (OH stretch), 1638 (C=O stretch), 1616 (C=C stretch), 1287 (C-N stretch), 1165 (C-O stretch) cm^{-1} .

Table 4.37: Summary Physical Properties of M14a

| Compound | M14a |
|-------------------------|--|
| IUPAC Name | 5,7-dihydroxy-8-(pyrrolidine-1-ylmethyl)-2-phenyl-4H-chromen-4-one |
| Molecular formula | C ₂₀ H ₁₉ NO ₄ |
| Molecular weight, g/mol | 337.1317 |
| Physical appearance | Yellow solid |
| Percentage yield, % | 75.4 |
| Obtained Mass, mg | 30.5 |
| R _f value | 0.08 |
| Melting point, °C | 163-166 |

In the ¹H NMR of compound **M14a** (Figure 4.83), the signals were similar to parent compound **M14** (Figure 4.32) except the appearance signals in up field region. Signal at δ_H 4.14 (s) indicate the presence of methylene protons. Signals at δ_H 1.91 (s, CH₂CH₂) and δ_H 2.79 (s, CH₂NCH₂) were the characteristic peaks of pyrrolidine. The disappearance of doublet at δ_H 6.47 (H-8, *J*=1.8 Hz) in compound **M14a** showed that the aminomethylation was occurred at C-8. In ¹³C NMR (Figure 4.84) of compound **M14a**, signal at δ_c 51.3 was the methylene carbon and the signals at δ_c 23.7 (C-3'',5'') and δ_c 53.7 (C-2'',6'') were the characteristic peaks of pyrrolidine moiety. In the HMBC spectrum (Figure 4.86), methylene protons displayed two bonds correlations with C-8 (δ_c 99.3), and three bonds correlations with C-7 (δ_c 166.7) and C-9 (δ_c 154.3). In addition, methylene protons also displayed three-bond correlations with C-3'', 6'' (δ_c 51.3) which belong to pyrrolidine moiety. Liu et. al. (2012) reported that as the 5-OH

and 7-OH that present in the ring A causing p- π conjugative effect, this has increased the hydrogen atom activity at C-8 position. The structure was further confirmed by using DEPT (Appendix D64) and HMQC (Figure 4.85) spectra.

Table 4.38 shows the summary NMR data of compounds **M14** and **M14a**.

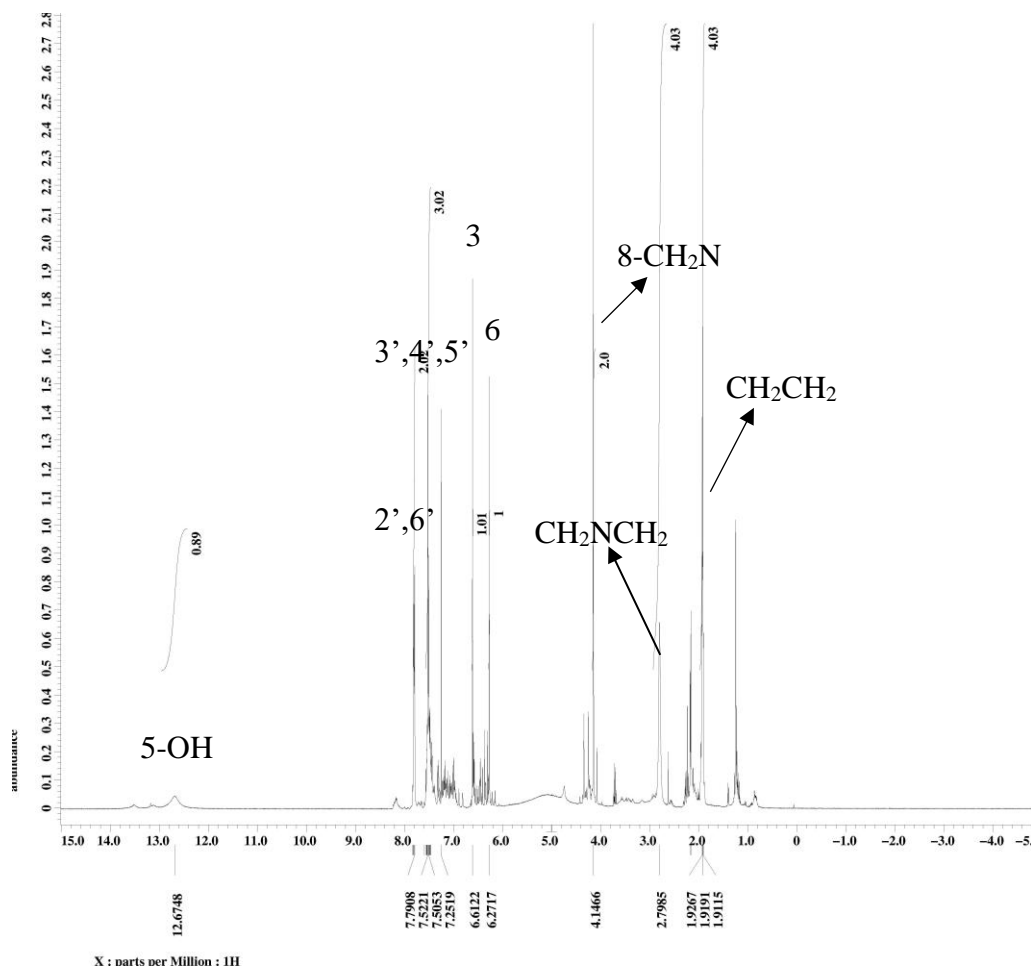
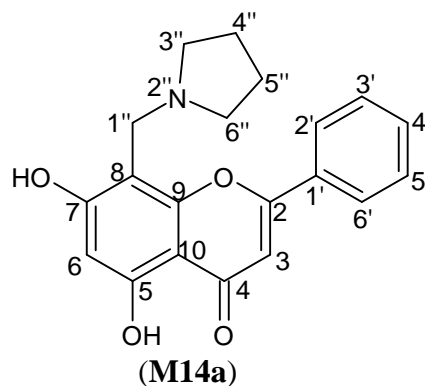
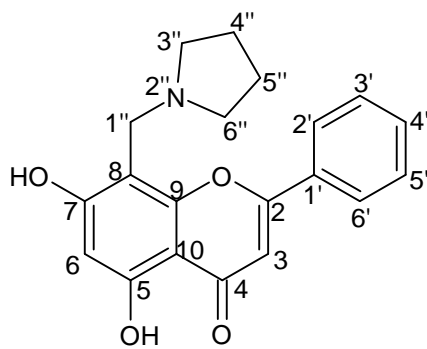


Figure 4.83: ^1H NMR (400 MHz, CDCl_3) of 5,7-dihydroxy-8-(pyrrolidine-1-ylmethyl)-2-phenyl-4H-chromen-4-one (**M14a**)



(M14a)

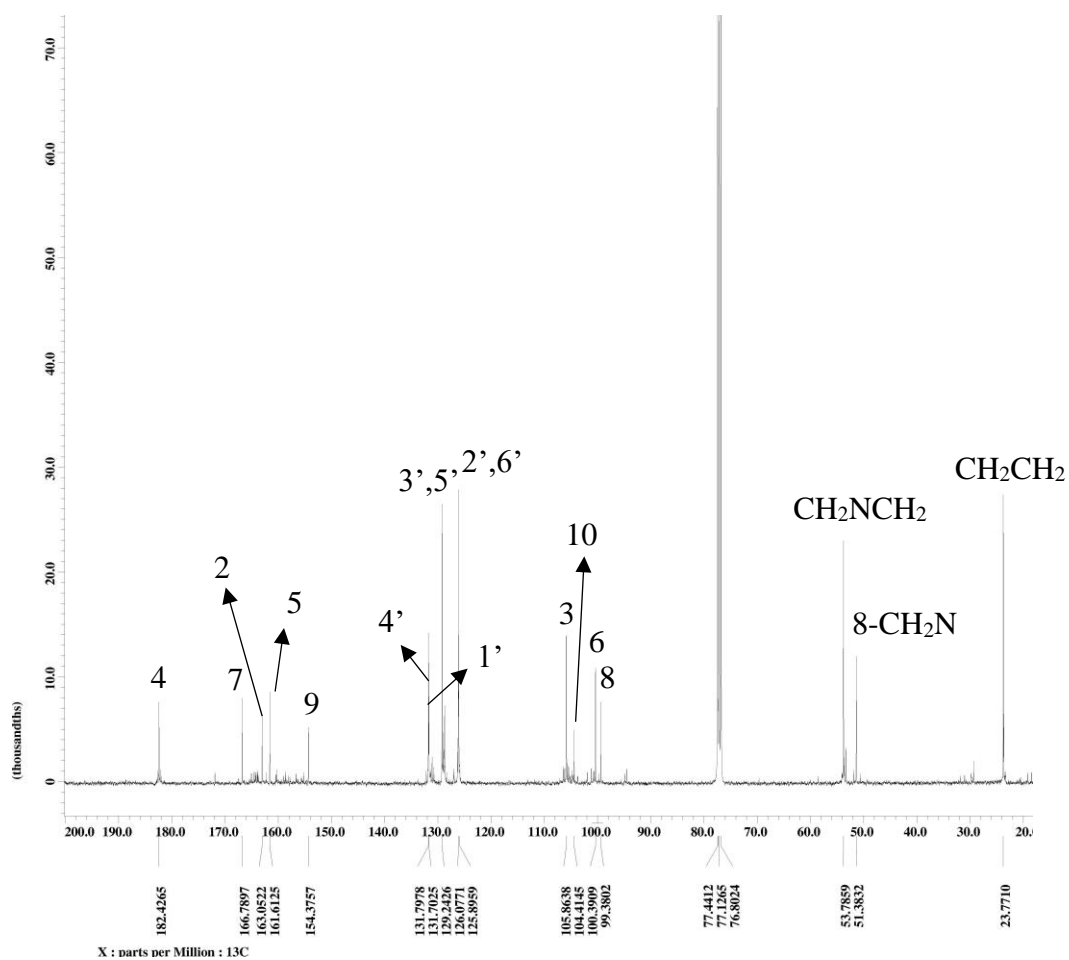
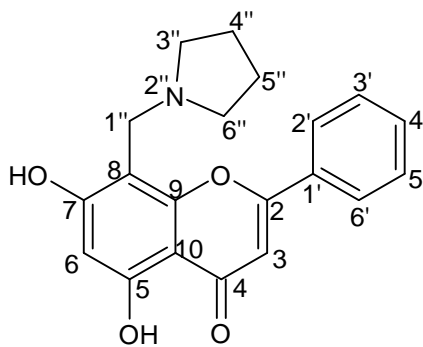


Figure 4.84: ¹³C NMR (100 MHz, CDCl₃) of 5,7-dihydroxy-8-(pyrrolidine-1-ylmethyl)-2-phenyl-4H-chromen-4-one (M14a)

Table 4.38: ¹H, ¹³C and HMBC spectral data of M14 (DMSO-d₆) and M14a (CDCl₃)

| | M14 | M14a | M14 | M14a | M14a |
|----------------------------------|--------------------------------|--------------------------------|-------------------------|-------------------------|---------------------|
| Position | δ _H (multiplicity) | δ _H (multiplicity) | δ _C (C-type) | δ _C (C-type) | HMBC |
| 2 | - | - | 163.6 (C) | 163.0 (C) | - |
| 3 | 6.91 (1H, s) | 6.61 (1H, s) | 105.6 (CH) | 105.8 (CH) | C-2, 1', 10, 4 |
| 4 | - | - | 182.3 (C) | 182.4 (C) | - |
| 5 | - | - | 161.9 (C) | 161.6 (C) | - |
| 6 | 6.17 (1H, d, <i>J</i> =1.8 Hz) | 6.28 (1H, d, <i>J</i> =1.8 Hz) | 99.5 (CH) | 100.3 (CH) | C-5, 7, 8, 10 |
| 7 | - | - | 164.9 (C) | 166.7 (C) | - |
| 8 | 6.47 (1H, d, <i>J</i> =1.8 Hz) | - | 94.6 (CH) | 99.3 (CH) | - |
| 9 | - | - | 157.9 (C) | 154.3 (C) | - |
| 10 | - | - | 104.5 (C) | 104.4 (C) | - |
| 1' | - | - | 131.2 (C) | 131.7 (C) | - |
| 2', 6' | 8.03 (2H, m) | 7.79 (2H, m) | 126.9 (CH) | 126.1 (CH) | C-2, 1', 3', 5', |
| 3', 5' | 7.53 (2H, m) | 7.52 (2H, m) | 129.6 (CH) | 129.0 (CH) | C-2', 6' |
| 4' | 7.53 (1H, m) | 7.48 (1H, m) | 133.5 (CH) | 131.7 (CH) | C-3', 5' |
| 5-OH | 12.78 (1H, s) | 12.67 (1H, s) | - | - | - |
| 8-CH ₂ N | - | 4.14 (2H, s) | - | 51.3 (CH ₂) | C-3'', 6'', 8, 9, 7 |
| CH ₂ CH ₂ | - | 1.91 (4H, s) | - | 23.7 (CH ₂) | - |
| CH ₂ NCH ₂ | - | 2.79 (4H, s) | - | 53.7 (CH ₂) | - |



(M14a)

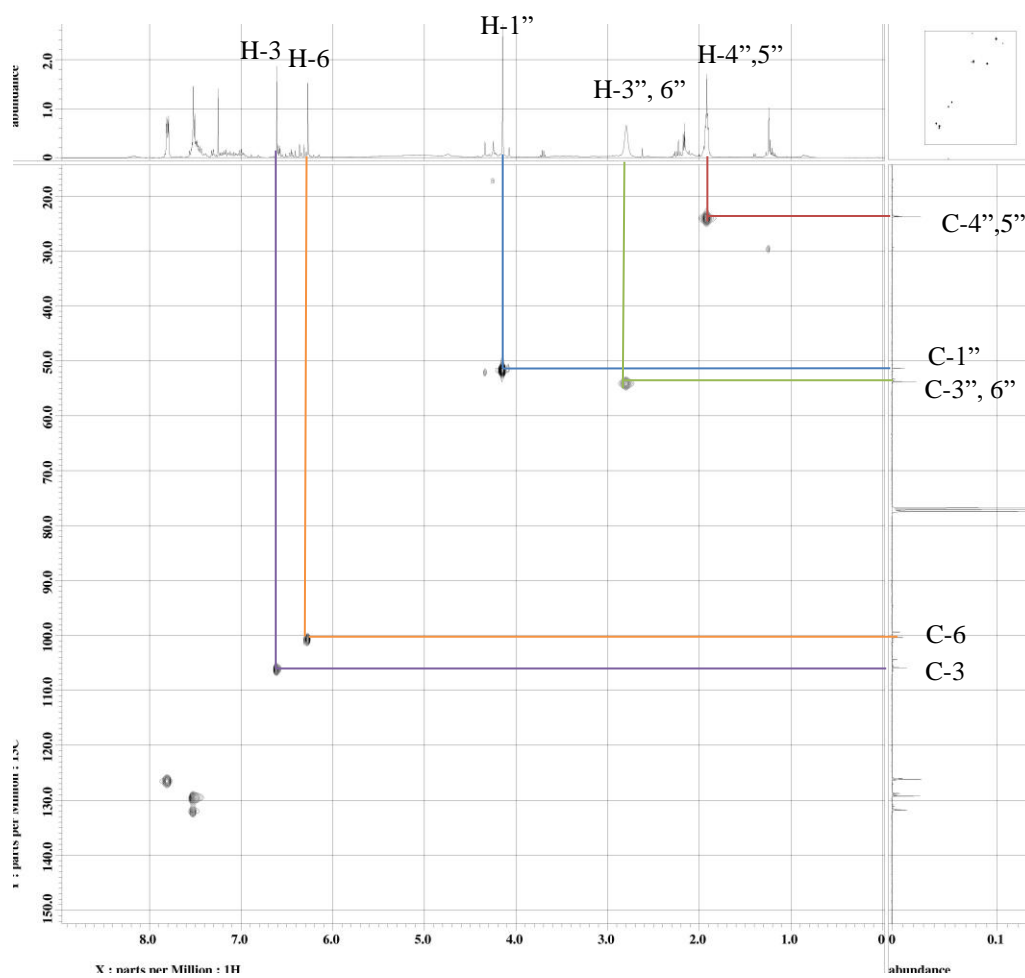
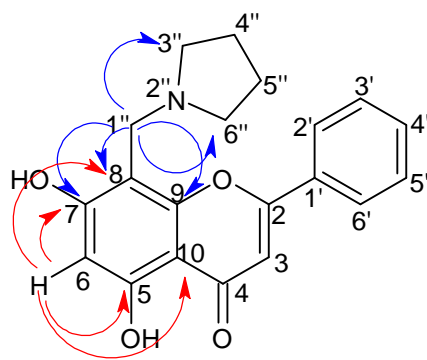


Figure 4.85: HMBC Spectrum of 5,7-dihydroxy-8-(pyrrolidine-1-ylmethyl)-2-phenyl-4H-chromen-4-one (M14a)



(M14a)

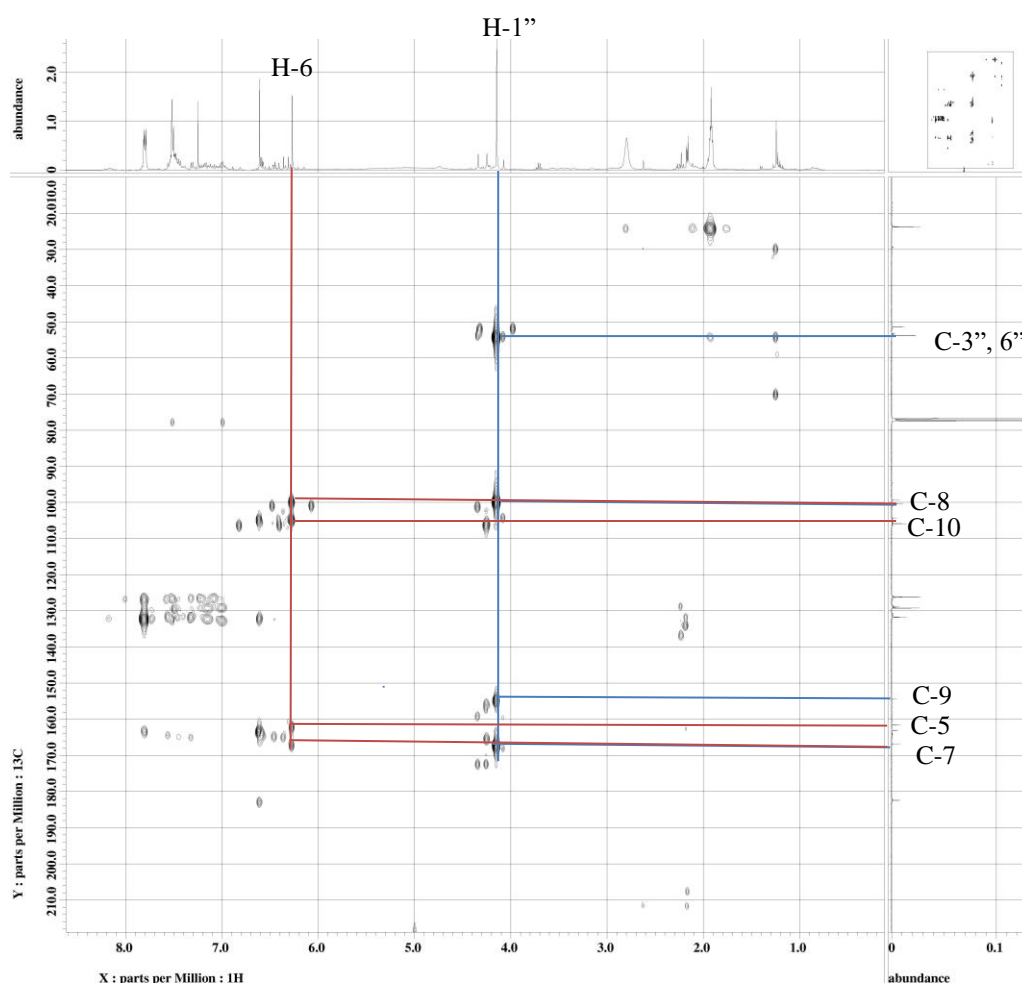
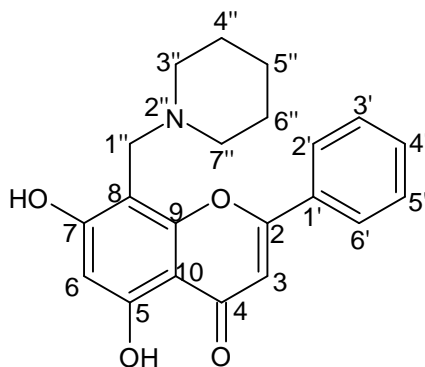


Figure 4.86: HMBC Spectrum of 5,7-dihydroxy-8-(pyrrolidine-1-ylmethyl)-2-phenyl-4H-chromen-4-one (M14a)

4.3.4.2 Characterization of 5,7-dihydroxy-8-(piperidin-1-ylmethyl)-2-phenyl-4*H*-chromen-4-one (M14b)



(M14b)

Compound **M14b** was obtained as yellow solid, mp 168-170 °C. In TLC plate, R_f value of 0.13 was obtained in mobile phase hexane:acetone 6:3. The percentage yield of **M14b** was obtained at 80.3%. The HRESIMS (Appendix A29) gave a pseudomolecular ion peak at $m/z = 352.1547 [M+H]^+$ which analysed for $C_{21}H_{21}NO_4$ (found 351.1474; calculated 351.1470). Table 4.39 shows the summary physical properties of **M14b**.

The IR spectrum of **M14b** (Appendix C29) shows absorption bands at 3436 (OH stretch), 2947, 2920 (CH_3 stretch), 1635 (C=O stretch), 1448 (C=C stretch), 1285 (C-N stretch), 1177 (C-O stretch) cm^{-1} .

Table 4.39: Summary Physical Properties of M14b

| Compound | M14b |
|-------------------------|---|
| IUPAC Name | 5,7-dihydroxy-8-(piperidin-1-ylmethyl)-2-phenyl-4 <i>H</i> -chromen-4-one |
| Molecular formula | C ₂₁ H ₂₁ NO ₄ |
| Molecular weight, g/mol | 351.1474 |
| Physical appearance | Yellow solid |
| Percentage yield, % | 80.3 |
| Obtained Mass, mg | 33.9 |
| R _f value | 0.13 |
| Melting point, °C | 163-166 |

In the ¹H NMR of compound **M14b** (Figure 4.87), signal at δ_H 4.14 (s) indicate the presence of methylene protons. Signals at δ_H 1.43 (CH₂), δ_H 1.68 (s, CH₂CH₂) and δ_H 2.63 (s, CH₂NCH₂) were the characteristic peaks of piperidine. In ¹³C NMR (Figure 4.88) of compound **M14b**, signal at δ_c 54.6 was the methylene carbon and the signals at δ_c 23.8 (C-5''), δ_c 25.7 (C-4'',6'') and δ_c 54.0 (C-3'', 7'') were the characteristic peaks of piperidine moiety. In the HMBC spectrum (Figure 4.90), methylene protons displayed two bonds correlations with C-8 (δ_c 98.5), and three bonds correlations with C-7 (δ_c 166.6) and C-9 (δ_c 154.8). In addition, methylene protons also displayed three bonds correlations with C-3'', 7'' (δ_c 54.0) which belong to piperidine moiety. This confirmed the aminomethylation was occurred at C-8 of ring A. The structure was further confirmed by using DEPT (Appendix D65) and HMQC (Figure 4.89) spectrums. Table 4.40 shows the summary NMR data of compounds **M14** and **M14b**.

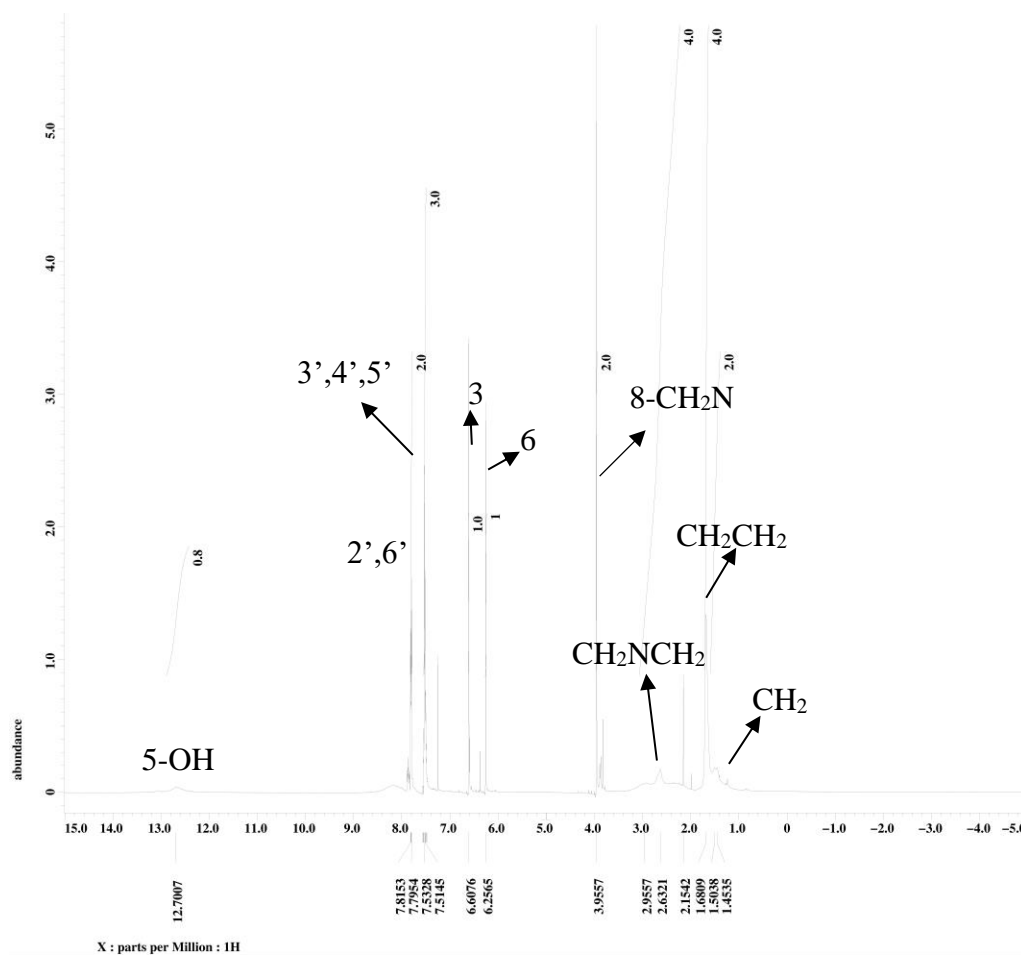
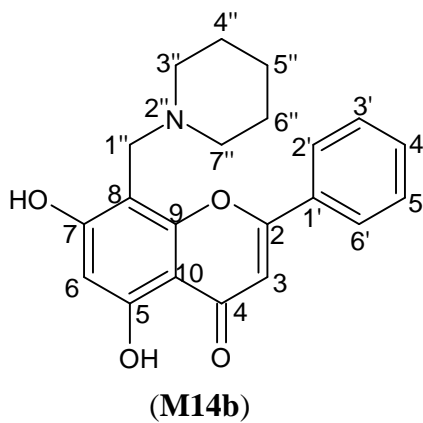


Figure 4.87: ¹H NMR (400 MHz, CDCl₃) of 5,7-dihydroxy-8-(piperidin-1-ylmethyl)-2-phenyl-4*H*-chromen-4-one (M14b)

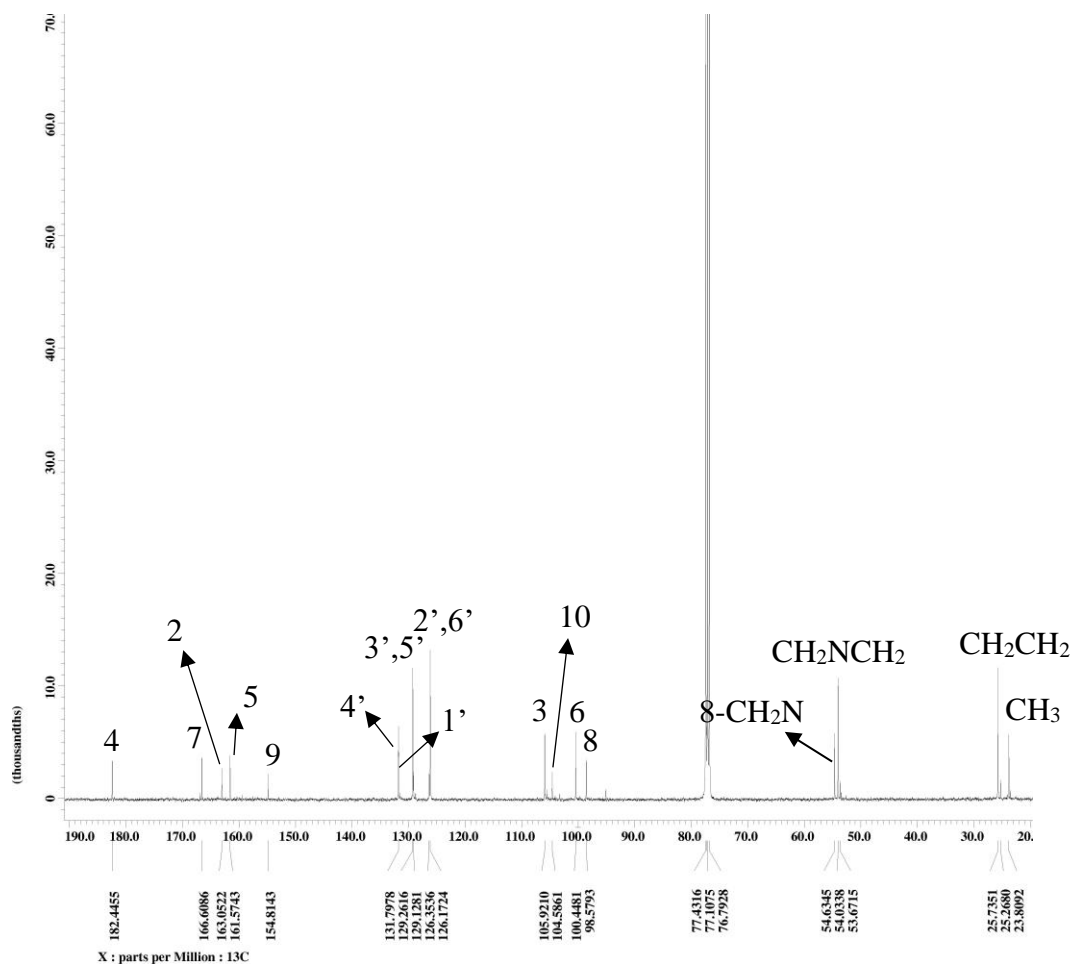
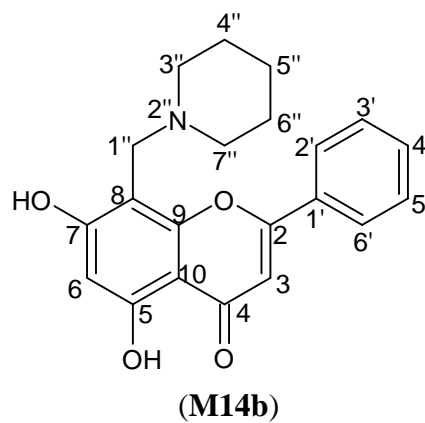
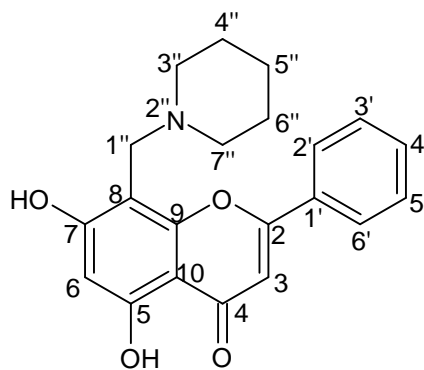


Figure 4.88: ¹³C NMR (100 MHz, CDCl₃) of 5,7-dihydroxy-8-(piperidin-1-ylmethyl)-2-phenyl-4H-chromen-4-one (M14b)

Table 4.40: ¹H, ¹³C and HMBC spectral data of M14 (DMSO-d₆) and M14b (CDCl₃)

| | M14 | M14b | M14 | M14b | M14b |
|----------------------------------|--------------------------------|--------------------------------|-------------------------|-------------------------|---------------------|
| Position | δ _H (multiplicity) | δ _H (multiplicity) | δ _C (C-type) | δ _C (C-type) | HMBC |
| 2 | - | - | 163.6 (C) | 163.0 (C) | - |
| 3 | 6.91 (1H, s) | 6.61 (s) | 105.6 (CH) | 105.9 (CH) | C-2, 1', 10, 4 |
| 4 | - | - | 182.3 (C) | 182.4 (C) | - |
| 5 | - | - | 161.9 (C) | 161.5 (C) | - |
| 6 | 6.17 (1H, d, <i>J</i> =1.8 Hz) | 6.28 (1H, d, <i>J</i> =1.8 Hz) | 99.5 (CH) | 100.4 (CH) | C-5, 8, 10, 7 |
| 7 | - | - | 164.9 (C) | 166.6 (C) | - |
| 8 | 6.47 (1H, d, <i>J</i> =1.8 Hz) | - | 94.6 (CH) | 98.5 (CH) | - |
| 9 | - | - | 157.9 (C) | 154.8 (C) | - |
| 10 | - | - | 104.5 (C) | 104.5 (C) | - |
| 1' | - | - | 131.2 (C) | 131.7 (C) | - |
| 2', 6' | 8.03 (2H, m) | 7.79 (2H, m) | 126.9 (CH) | 126.3 (CH) | C-2, 1', 3', 5', |
| 3', 5' | 7.53 (2H, m) | 7.53 (2H, m) | 129.6 (CH) | 129.1 (CH) | C-2',6' |
| 4' | 7.53 (1H, m) | 7.51 (1H, m) | 133.5 (CH) | 131.7 (CH) | C-3', 5' |
| 5-OH | 12.78 (1H, s) | 12.70 (1H, s) | - | - | - |
| 8-CH ₂ N | - | 4.14 (2H, s) | - | 54.6 (CH ₂) | C-3'', 7'', 8, 9, 7 |
| CH ₂ | - | 1.43 (2H, s) | - | 23.8 (CH ₂) | - |
| CH ₂ CH ₂ | - | 1.68 (4H, s) | - | 25.7 (CH ₂) | - |
| CH ₂ NCH ₂ | - | 2.63 (4H, s) | - | 54.0 (CH ₂) | - |



(M14b)

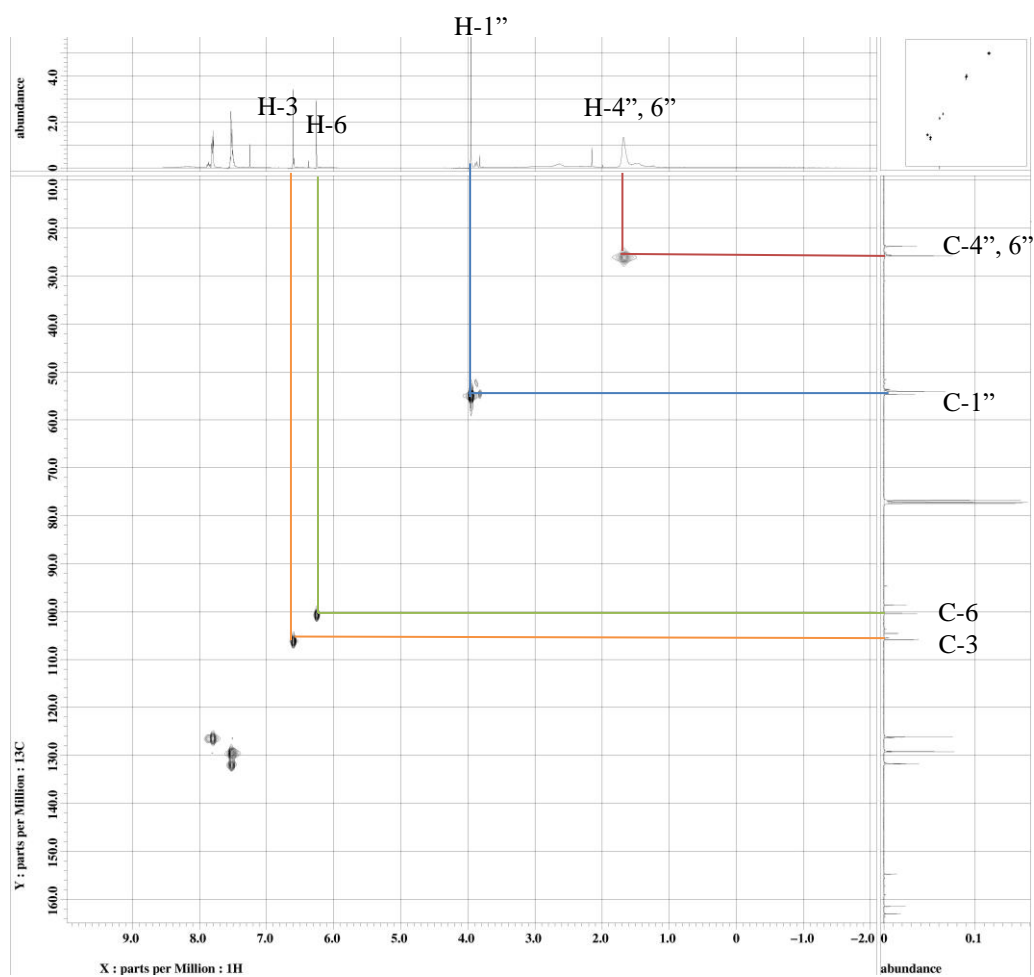
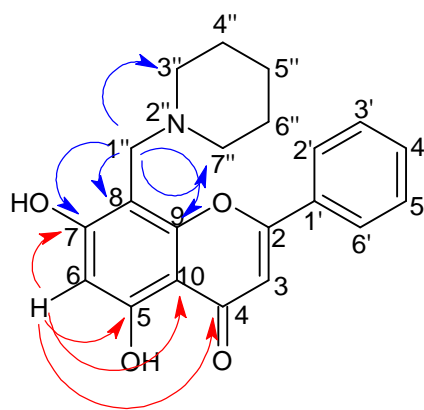


Figure 4.89: HMBC Spectrum of 5,7-dihydroxy-8-(piperidin-1-ylmethyl)-2-phenyl-4H-chromen-4-one (M14b)



(M14b)

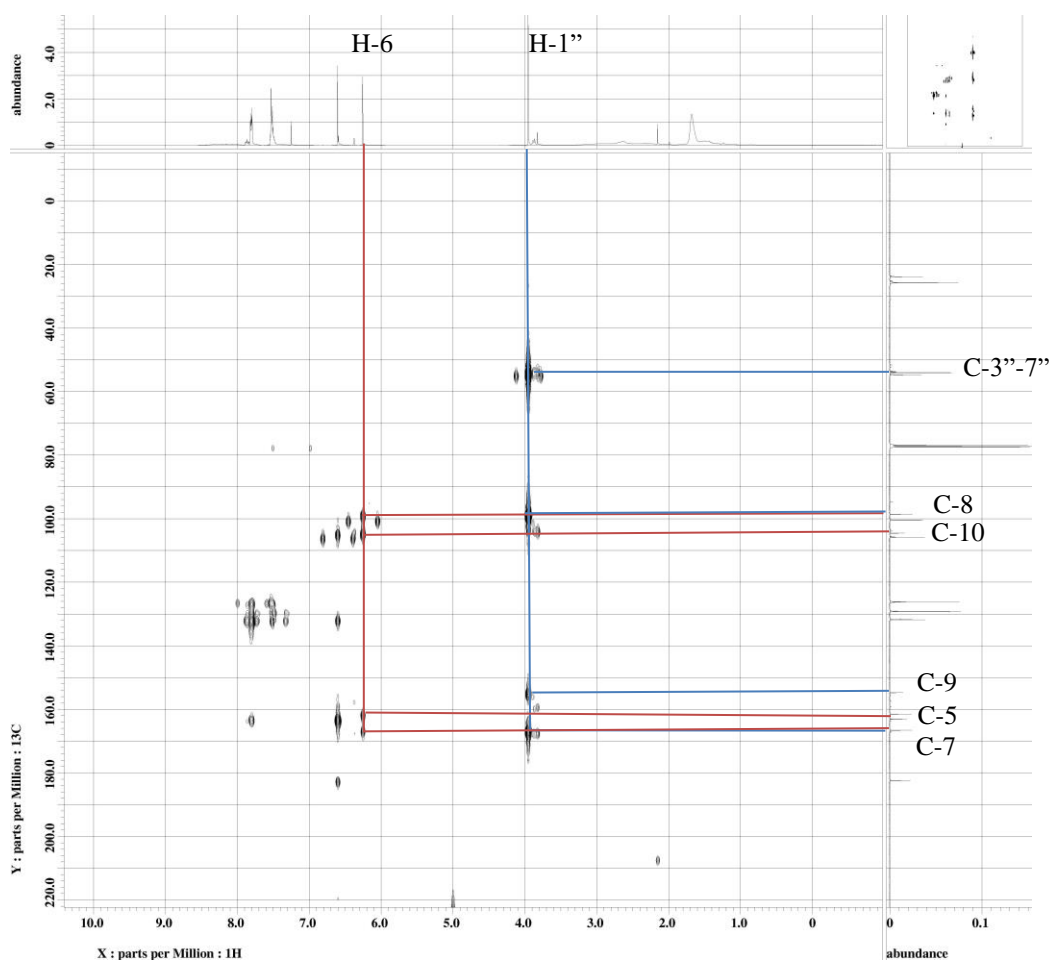
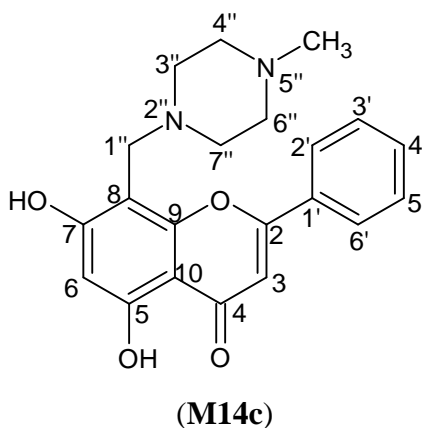


Figure 4.90: HMBC Spectrum of 5,7-dihydroxy-8-(piperidin-1-ylmethyl)-2-phenyl-4H-chromen-4-one (M14b)

4.3.4.3 Characterization of 5,7-dihydroxy-8-(4-methylpiperazin-1-ylmethyl)-2-phenyl-4*H*-chromen-4-one (M14c)



Compound **M14c** was obtained as yellow solid, mp 177-178 °C. In TLC plate, R_f value of 0.12 was obtained in mobile phase hexane:acetone 6:4. The percentage yield of **M14c** was obtained at 81.4%. The HRESIMS (Appendix A30) gave a pseudomolecular ion peak at $m/z = 367.1658$ $[M+H]^+$ which analysed for $C_{21}H_{22}N_2O_4$ (found 366.1585; calculated 366.1579). Table 4.41 shows the summary physical properties of **M14c**.

The IR spectrum of **M14c** (Appendix C30) shows absorption bands at 3413 (OH stretch), 1637 (C=O stretch), 1618 (C=C stretch), 1282 (C-N stretch), 1163 (C-O stretch) cm^{-1} .

Table 4.41: Summary Physical Properties of M14c

| Compound | M14c |
|-------------------------|--|
| IUPAC Name | 5,7-dihydroxy-8-(4-methylpiperazin-1-ylmethyl)-2-phenyl-4H-chromen-4-one |
| Molecular formula | C ₂₁ H ₂₂ N ₂ O ₄ |
| Molecular weight, g/mol | 351.1474 |
| Physical appearance | Yellow solid |
| Percentage yield, % | 81.4 |
| Obtained Mass, mg | 35.8 |
| R _f value | 0.12 |
| Melting point, °C | 177-178 |

In the ¹H NMR of compound **M14c** (Figure 4.91), signal at δ_H 3.99 (s) indicate the presence of methylene protons. Signals at δ_H 2.15 (N-CH₃), δ_H 2.25 (s, CH₂NCH₂) and δ_H 2.60 (s, CH₂NCH₂) were the characteristic peaks of 1-methylpiperazine. In ¹³C NMR (Figure 4.92) of compound **M14c**, signal at δ_c 53.7 was the methylene carbon and the signals at δ_c 45.8 (C-5''), δ_c 52.6 (C-4'',6'') and δ_c 54.7 (C3'', 7'') were the characteristic peaks of 1-methylpiperazine moiety. In the HMBC spectrum (Figure 4.94), methylene protons displayed two bonds correlations with C-8 (δ_c 98.4), and three bonds correlations with C-7 (δ_c 165.7) and C-9 (δ_c 154.8). In addition, methylene protons also displayed three bonds correlations with C-3'', 7'' (δ_c 54.7) which belong to 1-methylpiperazine moiety. This confirmed the aminomethylation was occurred at C-8 of ring A. The structure was further confirmed by using DEPT (Appendix D66) and

HMQC (Figure 4.93) spectra. Table 4.42 shows the summary NMR data of compounds **M14** and **M14c**.

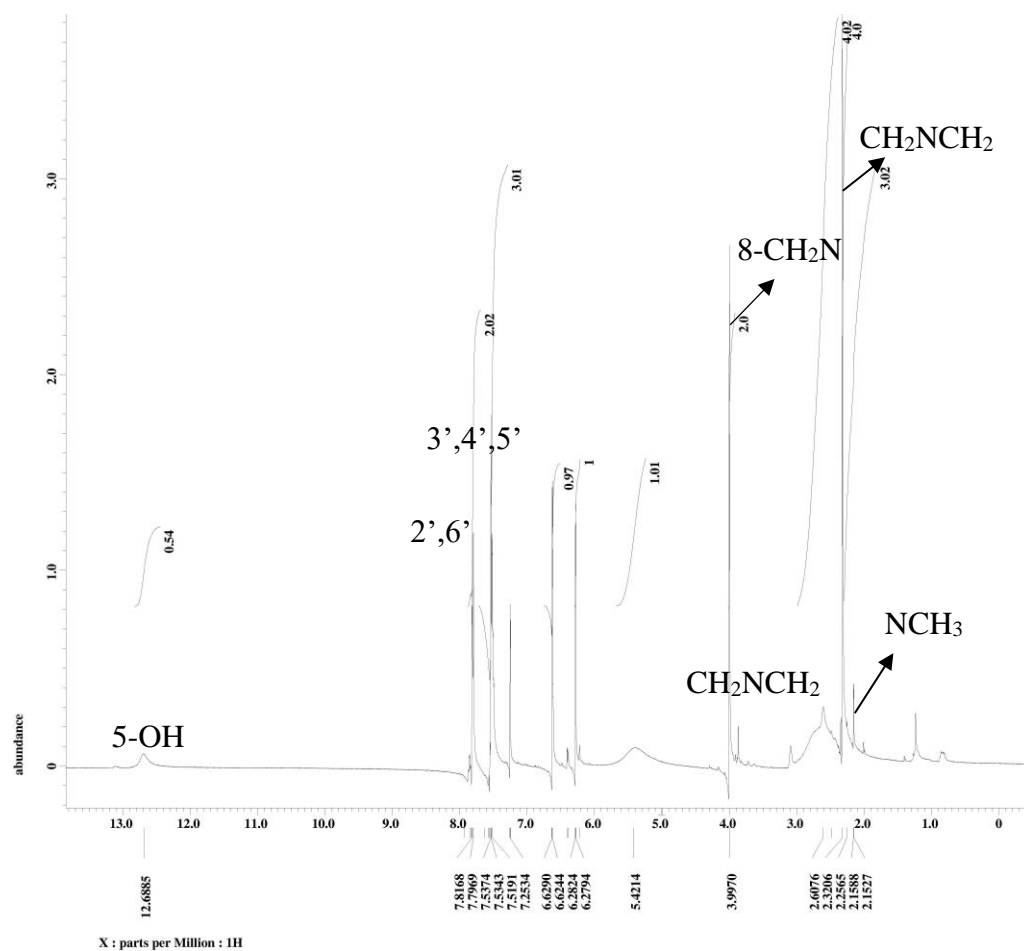
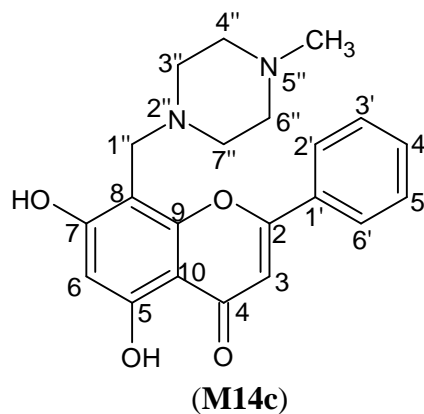
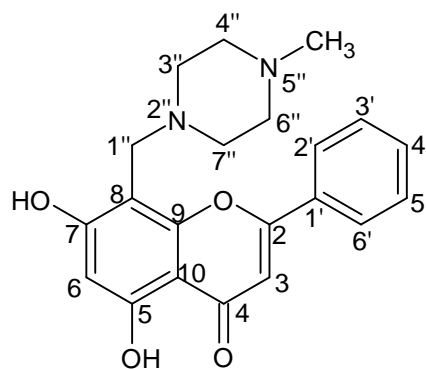


Figure 4.91: ^1H NMR (400 MHz, CDCl_3) of 5,7-dihydroxy-8-(4-methylpiperazin-1-ylmethyl)-2-phenyl-4H-chromen-4-one (**M14c**)



(M14c)

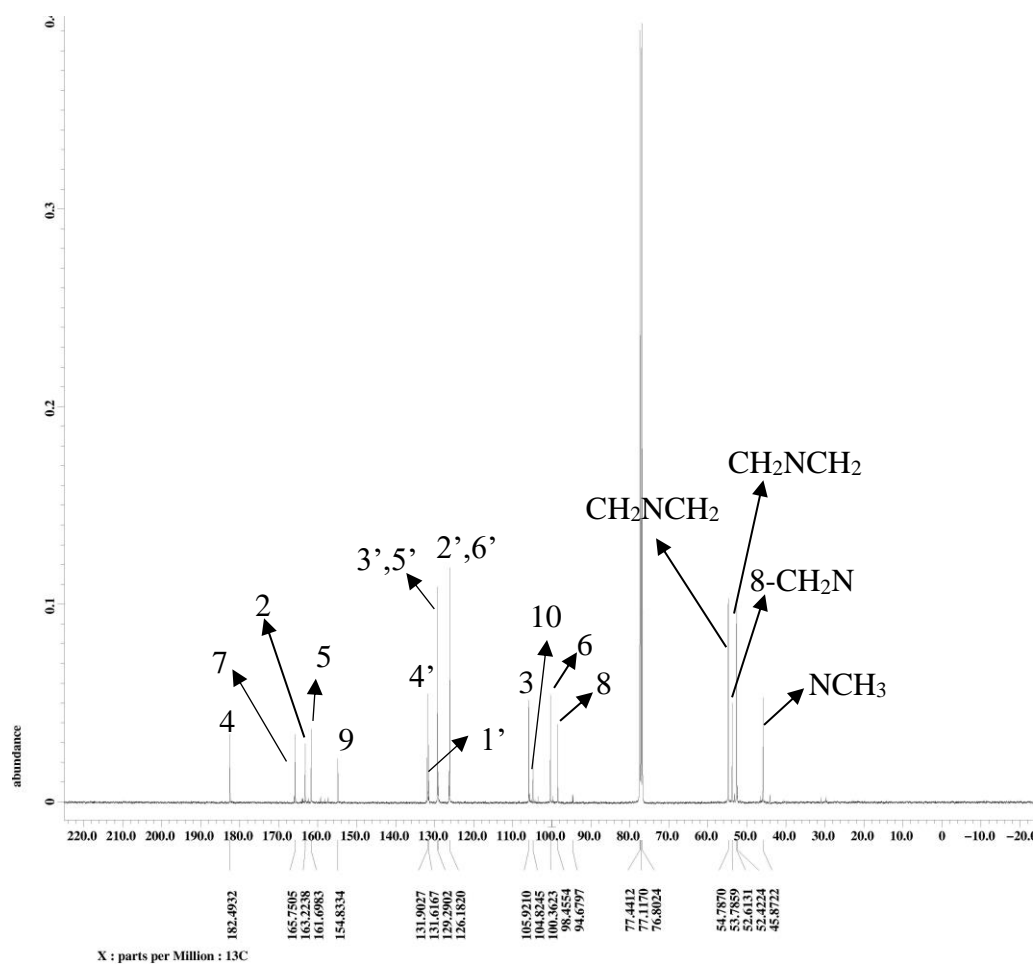
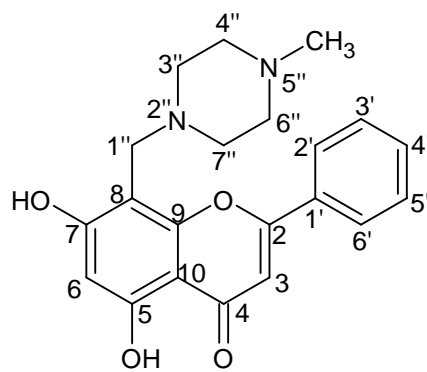


Figure 4.92: ¹³C NMR (100 MHz, CDCl₃) of 5,7-dihydroxy-8-(4-methylpiperazin-1-ylmethyl)-2-phenyl-4H-chromen-4-one (M14c)

Table 4.42: ¹H, ¹³C and HMBC spectral data of M14 (DMSO-d₆) and M14c (CDCl₃)

| | M14 | M14c | M14 | M14c | M14c |
|----------------------------------|--------------------------------|--------------------------------|-------------------------|-------------------------|---------------------|
| Position | δ _H (multiplicity) | δ _H (multiplicity) | δ _C (C-type) | δ _C (C-type) | HMBC |
| 2 | - | - | 163.6 (C) | 163.2 (C) | - |
| 3 | 6.91 (1H, s) | 6.62 (1H, s) | 105.6 (CH) | 105.9 (CH) | C-2, 1', 10, 4 |
| 4 | - | - | 182.3 (C) | 182.4 (C) | - |
| 5 | - | - | 161.9 (C) | 161.6 (C) | - |
| 6 | 6.17 (1H, d, <i>J</i> =1.8 Hz) | 6.28 (1H, d, <i>J</i> =1.8 Hz) | 99.5 (CH) | 100.3 (CH) | C-5, 7, 8, 10 |
| 7 | - | - | 164.9 (C) | 165.7 (C) | - |
| 8 | 6.47 (1H, d, <i>J</i> =1.8 Hz) | - | 94.6 (CH) | 98.4 (CH) | - |
| 9 | - | - | 157.9 (C) | 154.8 (C) | - |
| 10 | - | - | 104.5 (C) | 104.8 (C) | - |
| 1' | - | - | 131.2 (C) | 131.6 (C) | - |
| 2', 6' | 8.03 (2H, m) | 7.81 (2H, m) | 126.9 (CH) | 126.1 (CH) | C-2, 1', 3', 5', |
| 3', 5' | 7.53 (2H, m) | 7.53 (2H, m) | 129.6 (CH) | 129.2 (CH) | C-2', 6' |
| 4' | 7.53 (1H, m) | 7.53 (1H, m) | 133.5 (CH) | 131.9 (CH) | C-3', 5' |
| 5-OH | 12.78 (1H, s) | 12.68 (1H, s) | - | - | - |
| 8-CH ₂ N | - | 3.99 (2H, s) | - | 53.7 (CH ₂) | C-3'', 7'', 8, 9, 7 |
| NCH ₃ | - | 2.15 (3H, s) | - | 45.8 (CH ₃) | C-4'', 6'' |
| CH ₂ NCH ₂ | - | 2.25 (4H, s) | - | 52.6 (CH ₂) | - |
| CH ₂ NCH ₂ | - | 2.60 (4H, s) | - | 54.7 (CH ₂) | - |



(M14c)

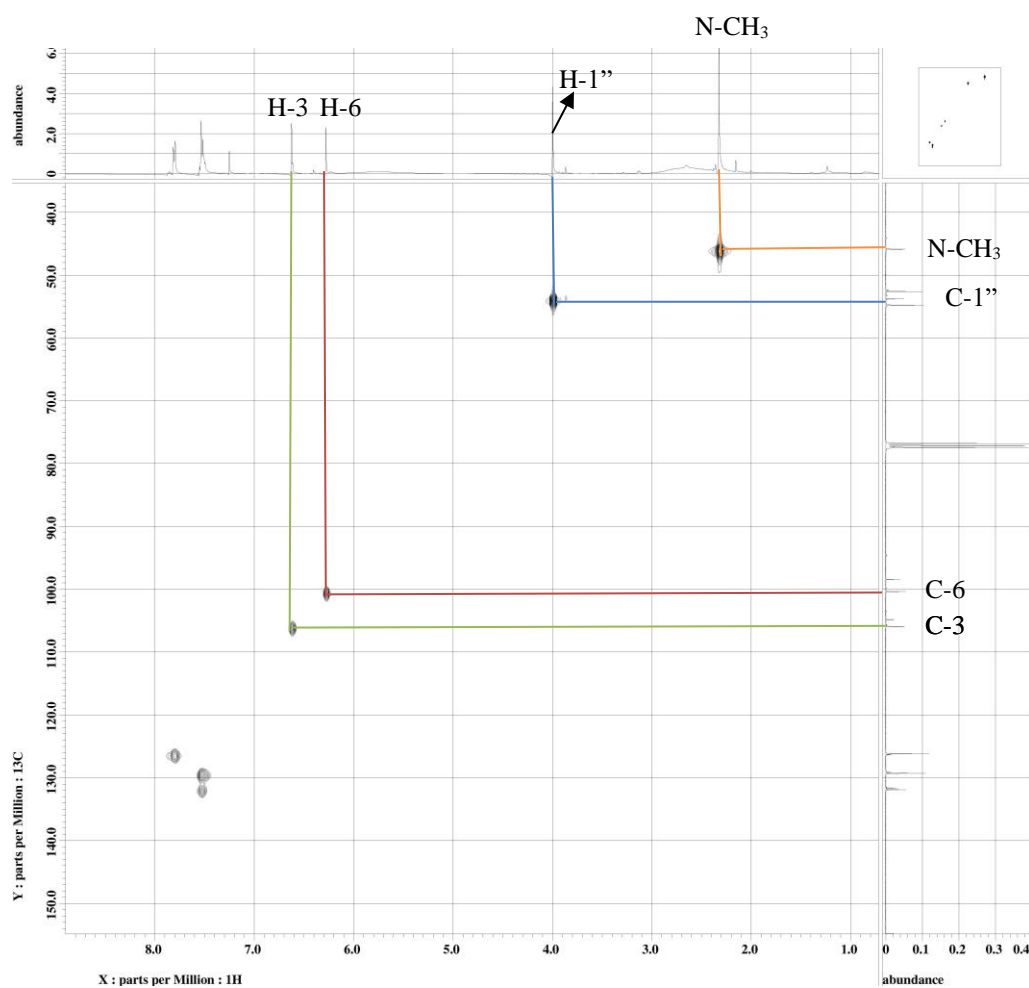


Figure 4.93: HMQC Spectrum of 5,7-dihydroxy-8-(4-methylpiperazin-1-ylmethyl)-2-phenyl-4H-chromen-4-one (M14c)

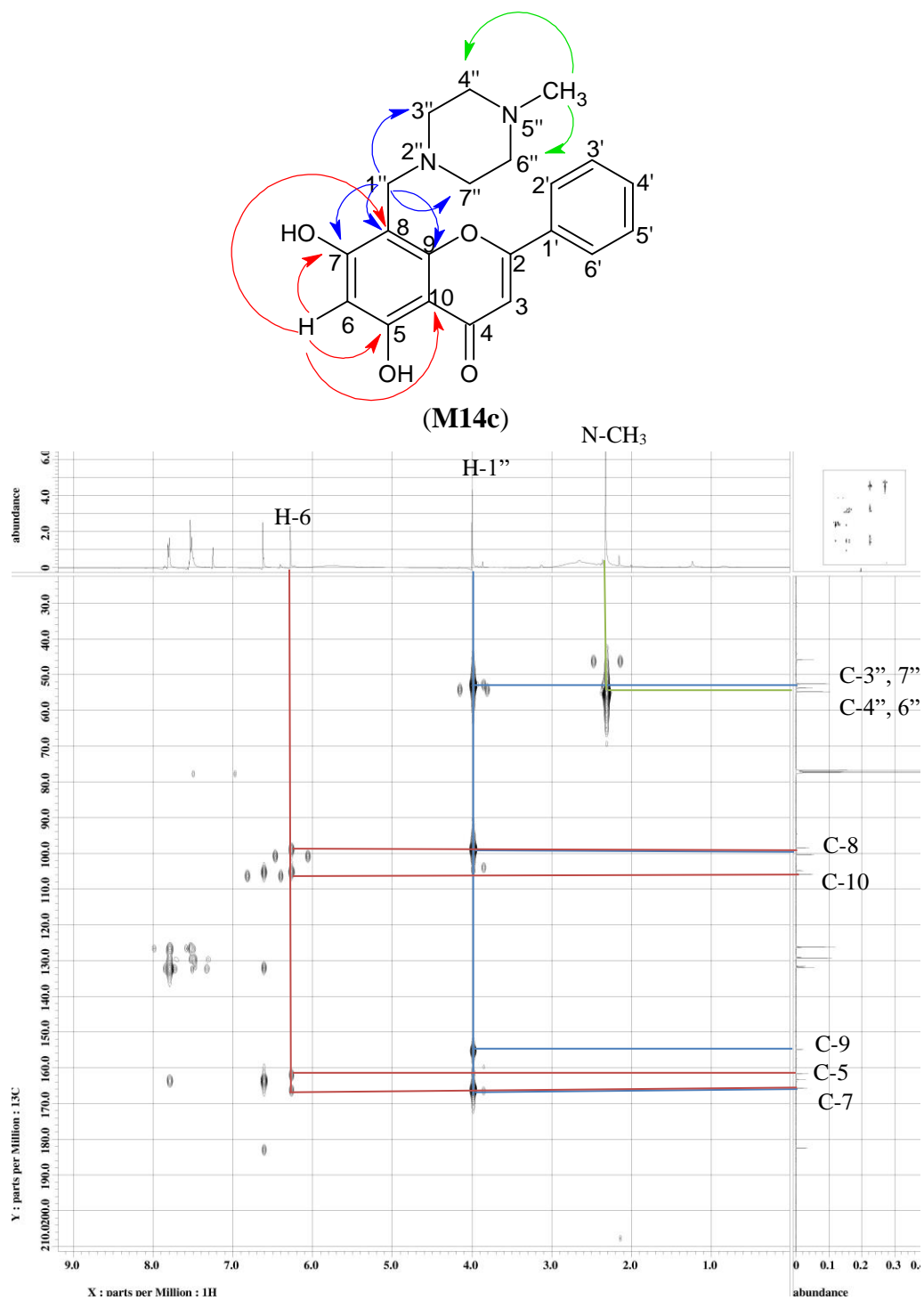
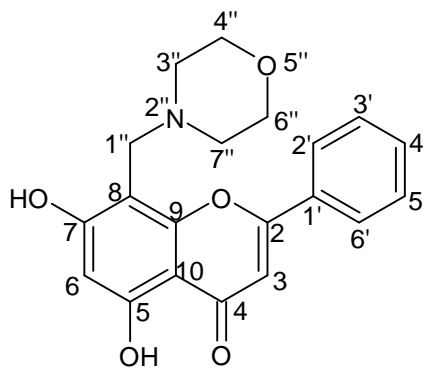


Figure 4.94: HMBC Spectrum of 5,7-dihydroxy-8-(4-methylpiperazin-1-ylmethyl)-2-phenyl-4H-chromen-4-one (M14c)

4.3.4.4 Characterization of 5,7-dihydroxy-8-(morpholinomethyl)-2-phenyl-4*H*-chromen-4-one (M14d)



(M14d)

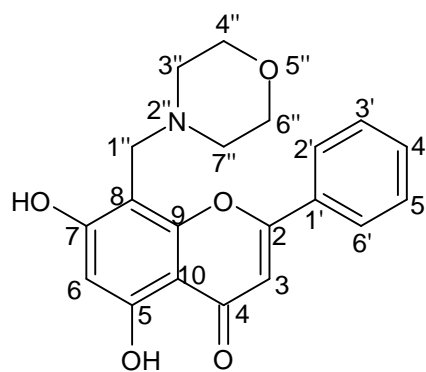
Compound **M14d** was obtained as yellow solid, mp 186-188 °C. In TLC plate, R_f value of 0.14 was obtained in mobile phase hexane:acetone 6:3. The percentage yield of **M14d** was obtained at 77.5%. The HRESIMS (Appendix A31) gave a pseudomolecular ion peak at $m/z = 354.1337$ $[M+H]^+$ which analysed for $C_{20}H_{19}NO_5$ (found 353.1264; calculated 354.1263). Table 4.43 shows the summary physical properties of **M14d**.

The IR spectrum of **M14d** (Appendix C31) shows absorption bands at 3467 (OH stretch), 2964, 2896 (CH_3 stretch), 1653 (C=O stretch), 1618 (C=C stretch), 1286 (C-N stretch), 1118 (C-O stretch), 1032 (C-O-C stretch) cm^{-1} .

Table 4.43: Summary Physical Properties of M14d

| Compound | M14d |
|-------------------------|---|
| IUPAC Name | 5,7-dihydroxy-8-(morpholinomethyl)-2-phenyl-4 <i>H</i> -chromen-4-one |
| Molecular formula | C ₂₀ H ₁₉ NO ₅ |
| Molecular weight, g/mol | 353.1264 |
| Physical appearance | Yellow solid |
| Percentage yield, % | 77.5 |
| Obtained Mass, mg | 32.9 |
| R _f value | 0.14 |
| Melting point, °C | 186-188 |

In the ¹H NMR of compound **M14d** (Figure 4.95), signal at δ_H 4.00 (s) indicate the presence of methylene protons. Signals at δ_H 2.25 (s, CH₂NCH₂) and δ_H 2.60 (s, CH₂OCH₂) were the characteristic peaks of morpholine. In ¹³C NMR (Figure 4.96) of compound **M14d**, signal at δ_c 54.2 was the methylene carbon and the signals at δ_c 53.0 (C-3'', 7'') and δ_c 66.7 (C4'', 6'') were the characteristic peaks of morpholine moiety. In the HMBC spectrum (Figure 4.98), methylene protons displayed two bonds correlations with C-8 (δ_c 98.0), and three bonds correlations with C-7 (δ_c 165.4) and C-9 (δ_c 154.9). In addition, methylene protons also displayed three bonds correlations with C-3'', 7'' (δ_c 53.0) which belong to morpholine moiety. This confirmed the aminomethylation was occurred at C-8 of ring A. The structure was further confirmed by using DEPT (Appendix D67) and HMQC (Figure 4.97) spectra. Table 4.44 shows the summary NMR data of compounds **M14** and **M14d**.



(M14d)

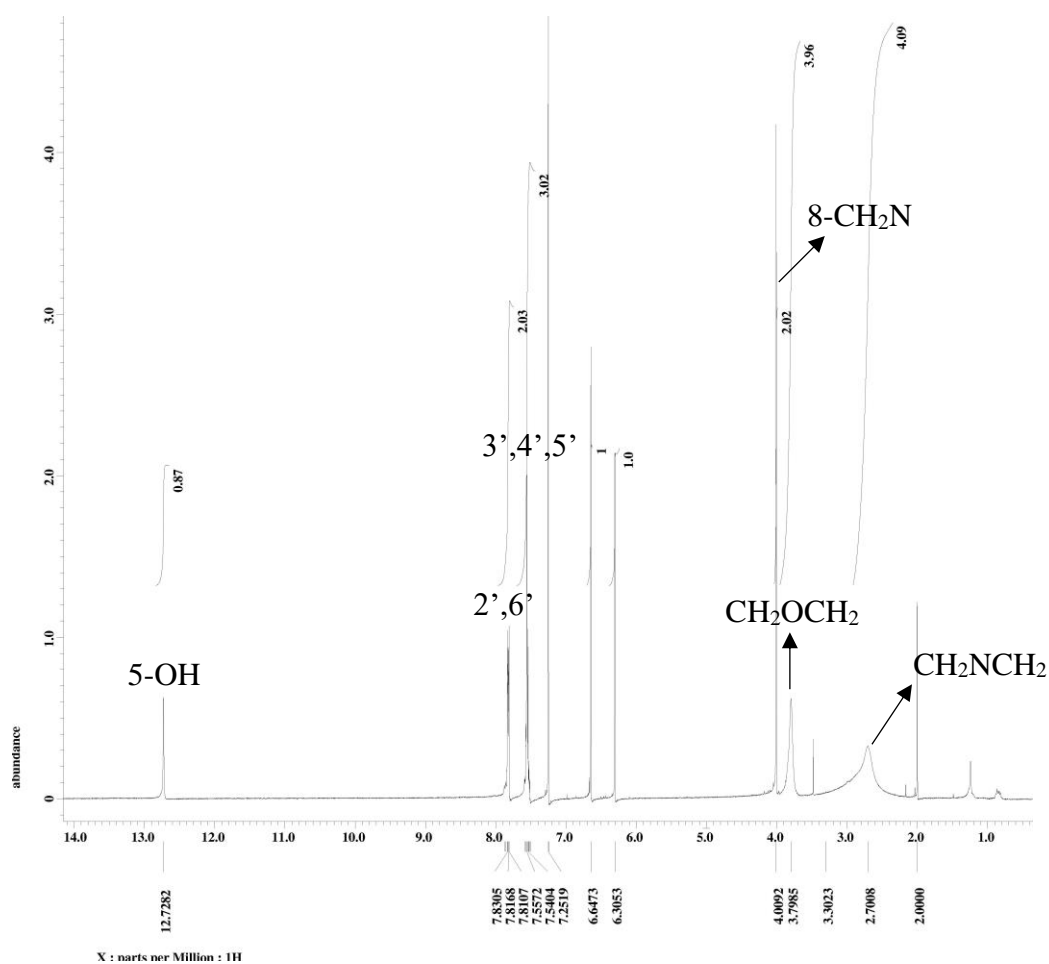
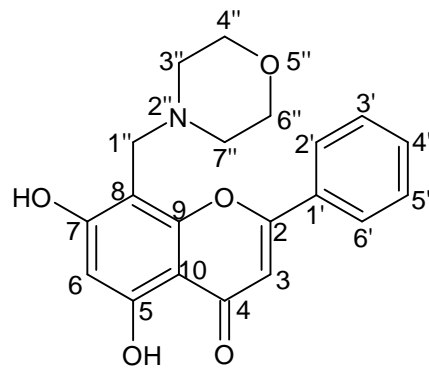


Figure 4.95: ^1H NMR (400 MHz, CDCl_3) of 5,7-dihydroxy-8-(morpholinomethyl)-2-phenyl-4H-chromen-4-one (M14d)



(M14d)

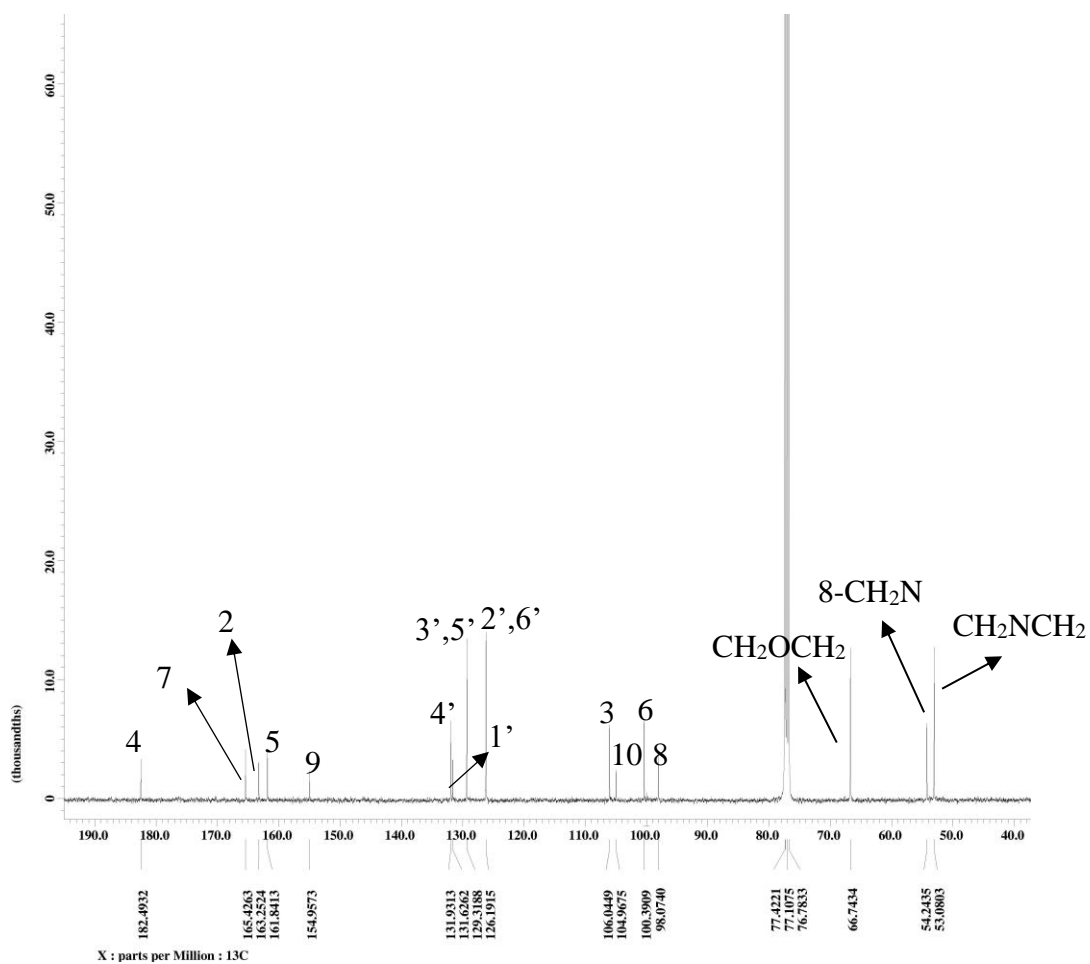
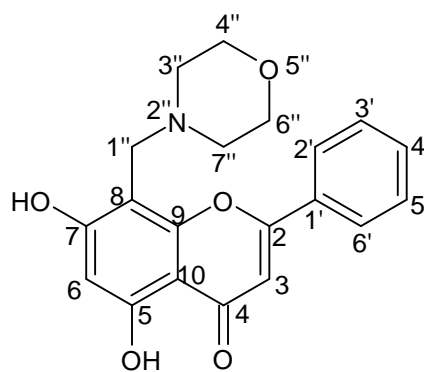


Figure 4.96: ¹³C NMR (100 MHz, CDCl₃) of 5,7-dihydroxy-8-(morpholinomethyl)-2-phenyl-4H-chromen-4-one (M14d)

Table 4.44: ¹H, ¹³C and HMBC spectral data of M14 (DMSO-d₆) and M14d (CDCl₃)

| | M14 | M14d | M14 | M14d | M14d |
|----------------------------------|--------------------------------|--------------------------------|-------------------------|-------------------------|---------------------|
| Position | δ _H (multiplicity) | δ _H (multiplicity) | δ _C (C-type) | δ _C (C-type) | HMBC |
| 2 | - | - | 163.6 (C) | 163.2 (C) | - |
| 3 | 6.91 (1H, s) | 6.62 (s) | 105.6 (CH) | 106.0 (CH) | C-2, 1', 10, 4 |
| 4 | - | - | 182.3 (C) | 182.4 (C) | - |
| 5 | - | - | 161.9 (C) | 161.8 (C) | - |
| 6 | 6.17 (1H, d, <i>J</i> =1.8 Hz) | 6.28 (1H, d, <i>J</i> =1.8 Hz) | 99.5 (CH) | 100.3 (CH) | C-5, 7, 8, 10 |
| 7 | - | - | 164.9 (C) | 165.4 (C) | - |
| 8 | 6.47 (1H, d, <i>J</i> =1.8 Hz) | - | 94.6 (CH) | 98.0 (CH) | - |
| 9 | - | - | 157.9 (C) | 154.9 (C) | - |
| 10 | - | - | 104.5 (C) | 104.9 (C) | - |
| 1' | - | - | 131.2 (C) | 131.6 (C) | - |
| 2', 6' | 8.03 (2H, m) | 7.81 (2H, m) | 126.9 (CH) | 126.1 (CH) | C-2, 1', 3', 5', |
| 3', 5' | 7.53 (2H, m) | 7.53 (2H, m) | 129.6 (CH) | 129.3 (CH) | C-2', 6' |
| 4' | 7.53 (1H, m) | 7.53 (1H, m) | 133.5 (CH) | 131.9 (CH) | C-3', 5' |
| 5-OH | 12.78 (1H, s) | 12.72 (1H, s) | - | - | - |
| 8-CH ₂ N | - | 4.00 (2H, s) | - | 54.2 (CH ₂) | C-3'', 7'', 8, 9, 7 |
| CH ₂ NCH ₂ | - | 2.70 (4H, s) | - | 53.0 (CH ₂) | - |
| CH ₂ OCH ₂ | - | 3.79 (4H, s) | - | 66.7 (CH ₂) | - |



(M14d)

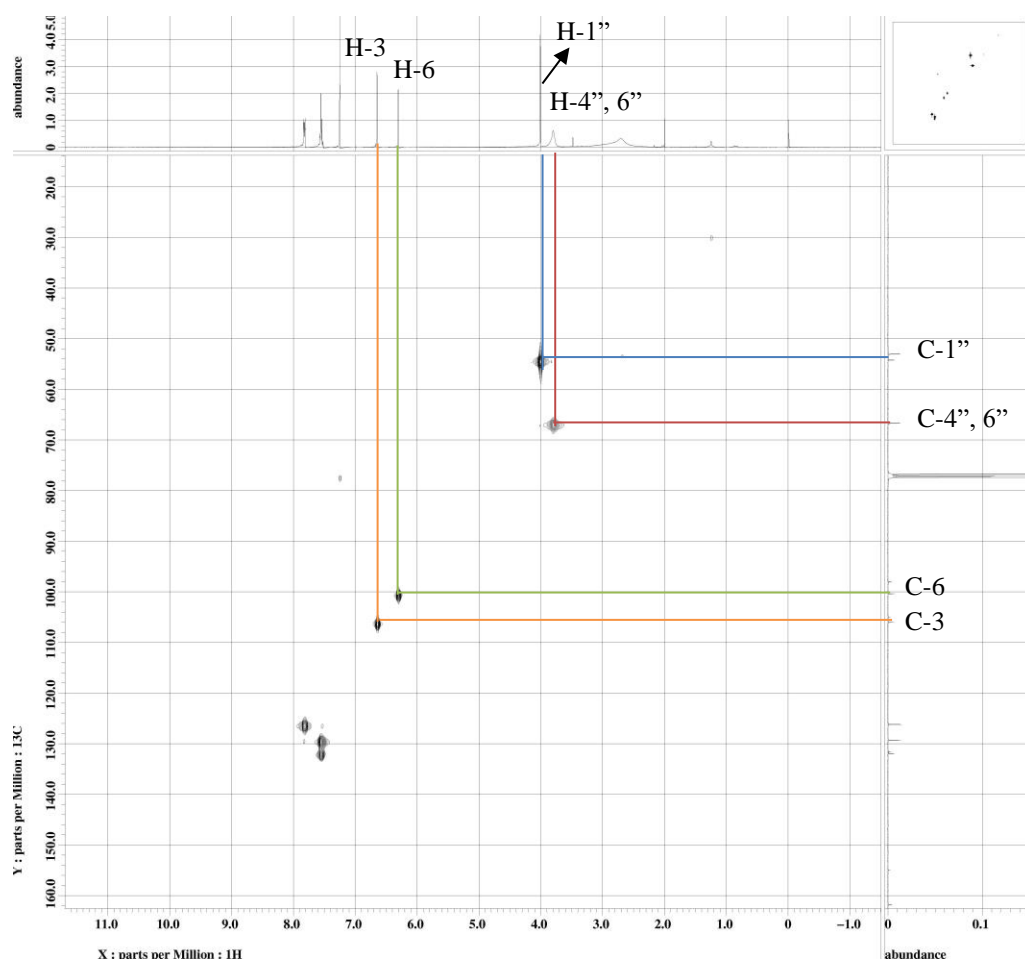
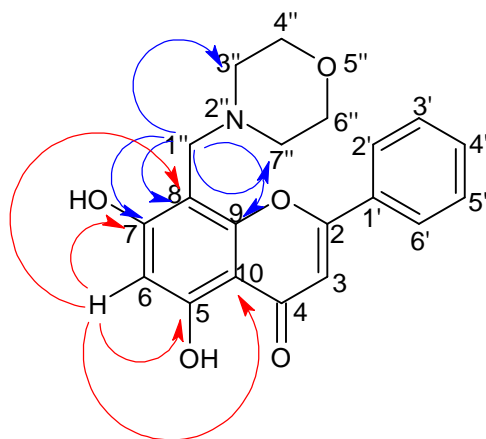


Figure 4.97: HMQC Spectrum of 5,7-dihydroxy-8-(morpholinomethyl)-2-phenyl-4H-chromen-4-one (M14d)



(M14d)

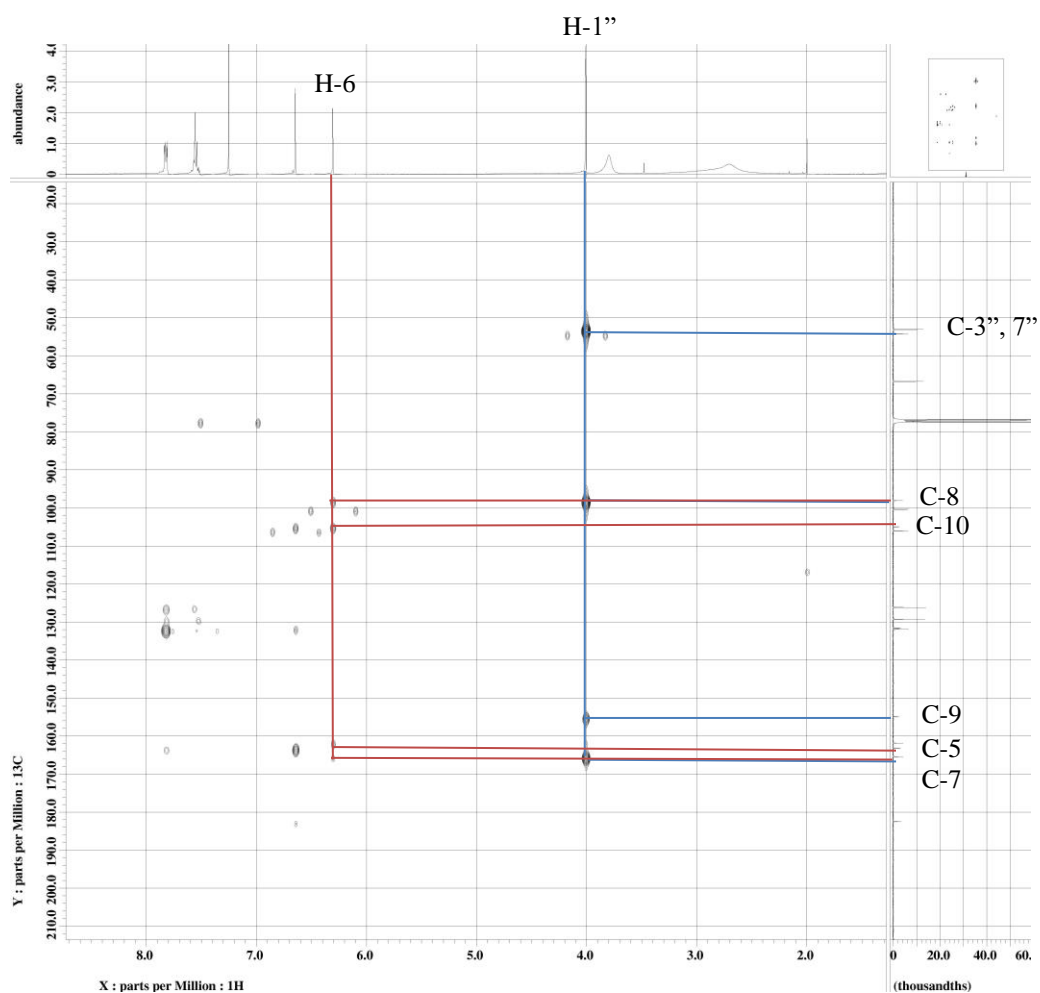
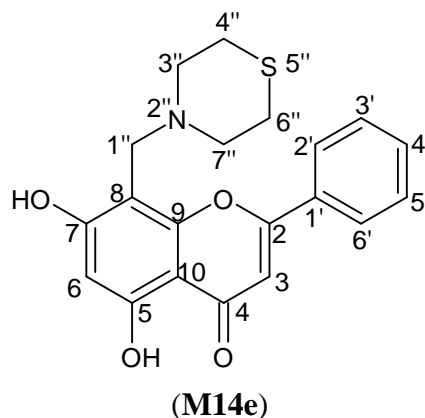


Figure 4.98: HMBC Spectrum of 5,7-dihydroxy-8-(morpholinomethyl)-2-phenyl-4H-chromen-4-one (M14d)

4.3.4.5 Characterization of 5,7-dihydroxy-8-(thiomorpholinomethyl)-2-phenyl-4*H*-chromen-4-one (M14e)



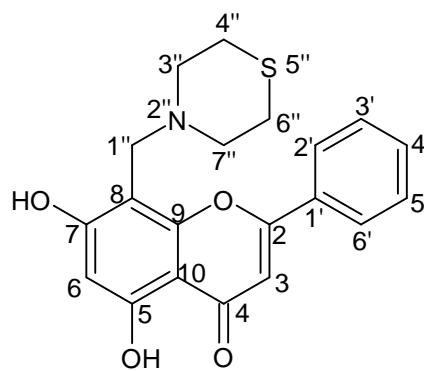
Compound **M14e** was obtained as yellow solid, mp 196-198 °C. In TLC plate, R_f value of 0.26 was obtained in mobile phase hexane:acetone 6:3. The percentage yield of **M14e** was obtained at 70.1%. The HRESIMS (Appendix A32) gave a pseudomolecular ion peak at $m/z = 354.1337 [M+H]^+$ which analysed for $C_{20}H_{19}NO_4S$ (found 369.1036; calculated 369.1035). Table 4.45 shows the summary physical properties of **M14e**.

The IR spectrum of **M14e** (Appendix C32) shows absorption bands at 3413 (OH stretch), 2901, 2838 (CH_3 stretch), 1638 (C=O stretch), 1617 (C=C stretch), 1287 (C-N stretch), 1105 (C-O stretch) cm^{-1} .

Table 4.45: Summary Physical Properties of M14e

| Compound | M14e |
|-------------------------|--|
| IUPAC Name | 5,7-dihydroxy-8-(thiomorpholinomethyl)-2-phenyl-4H-chromen-4-one |
| Molecular formula | C ₂₀ H ₁₉ NO ₄ S |
| Molecular weight, g/mol | 369.1036 |
| Physical appearance | Bright yellow solid |
| Percentage yield, % | 70.1 |
| Obtained Mass, mg | 31.1 |
| R _f value | 0.26 |
| Melting point, °C | 196-198 |

In the ¹H NMR of compound **M14e** (Figure 4.99), signal at δ_H 4.05 (s) indicate the presence of methylene protons. Signals at δ_H 2.80 (s, CH₂NCH₂) and δ_H 3.00 (s, CH₂SCH₂) were the characteristic peaks of thiomorpholine. In ¹³C NMR (Figure 4.100) of compound **M14e**, signal at δ_c 54.6 was the methylene carbon and the signals at δ_c 27.8 (C-3'', 7'') and δ_c 54.7 (C4'', 6'') were the characteristic peaks of thiomorpholine moiety. In the HMBC spectrum (Figure 4.102), methylene protons displayed two bonds correlations with C-8 (δ_c 98.1), and three bonds correlations with C-7 (δ_c 165.5) and C-9 (δ_c 154.9). In addition, methylene protons also displayed three bonds correlations with C-3'', 7'' (δ_c 27.8) which belong to thiomorpholine moiety. This confirmed the aminomethylation was occurred at C-8 of ring A. The structure was further confirmed by using DEPT (Appendix D68) and HMQC (Figure 4.101) spectra. Table 4.46 shows the summary NMR data of compounds **M14** and **M14e**.



(M14e)

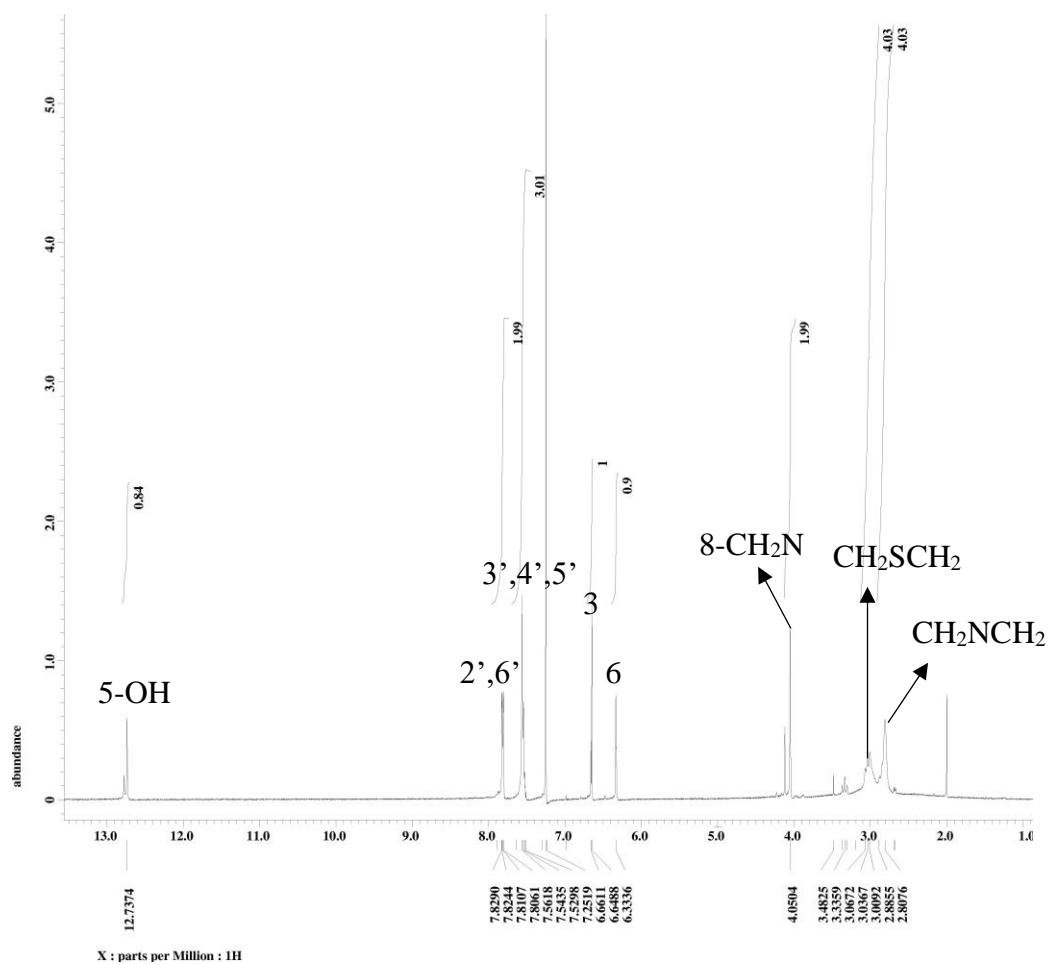
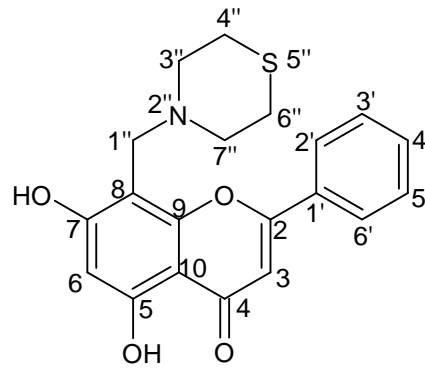


Figure 4.99: ^1H NMR (400 MHz, CDCl_3) of 5,7-dihydroxy-8-(thiomorpholinomethyl)-2-phenyl-4*H*-chromen-4-one (M14e)



(M14e)

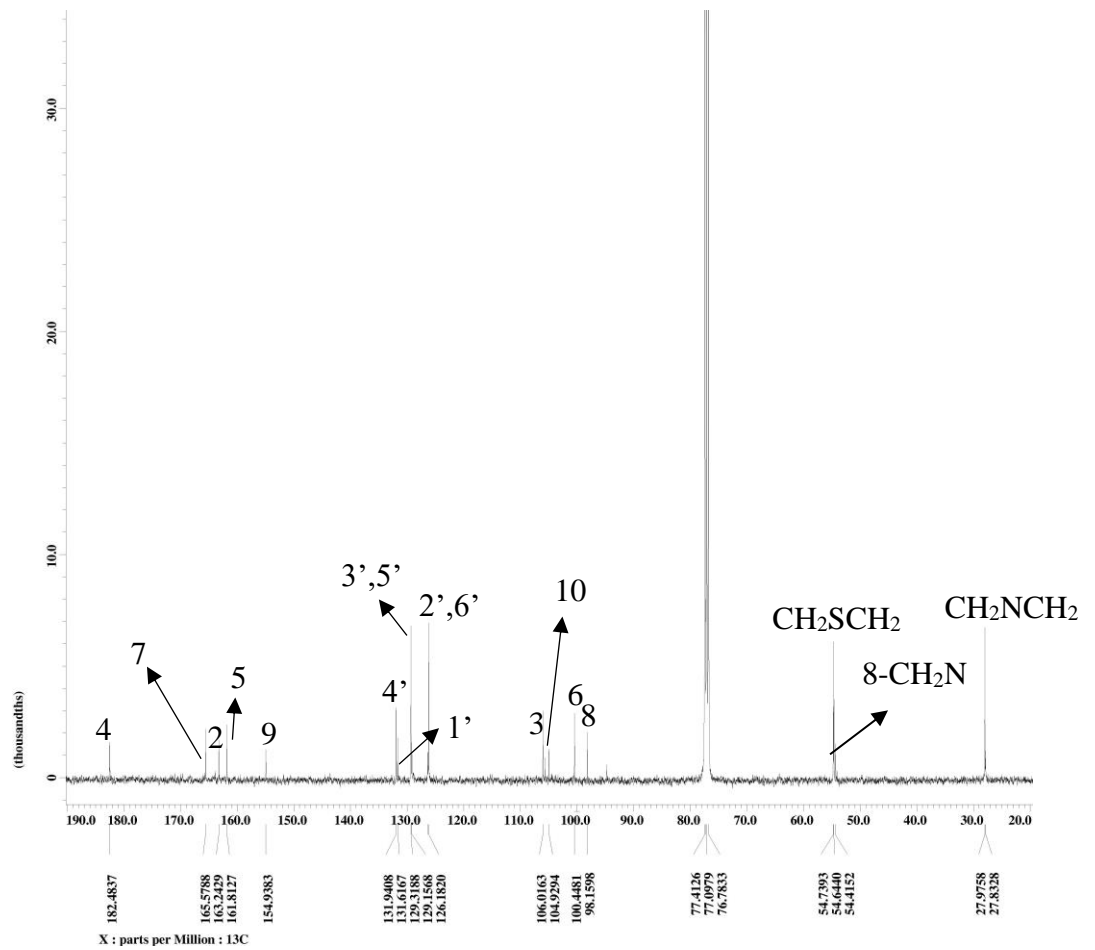
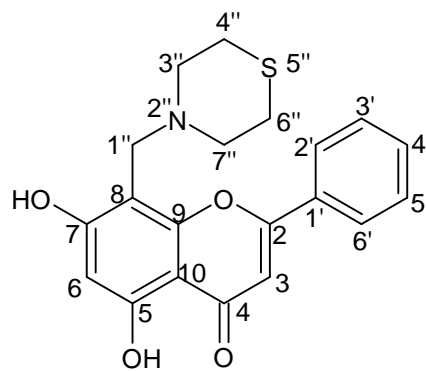


Figure 4.100: ¹³C NMR (100 MHz, CDCl₃) of 5,7-dihydroxy-8-(thiomorpholinomethyl)-2-phenyl-4H-chromen-4-one (M14e)

Table 4.46: ¹H, ¹³C and HMBC spectral data of M14 (DMSO-d₆) and M14e (CDCl₃)

| | M14 | M14e | M14 | M14e | M14e |
|----------------------------------|--------------------------------|--------------------------------|-------------------------|-------------------------|---------------------|
| Position | δ _H (multiplicity) | δ _H (multiplicity) | δ _C (C-type) | δ _C (C-type) | HMBC |
| 2 | - | - | 163.6 (C) | 163.2 (C) | - |
| 3 | 6.91 (1H, s) | 6.64 (s) | 105.6 (CH) | 106.0 (CH) | C-2, 1', 10, 4 |
| 4 | - | - | 182.3 (C) | 182.4 (C) | - |
| 5 | - | - | 161.9 (C) | 161.8 (C) | - |
| 6 | 6.17 (1H, d, <i>J</i> =1.8 Hz) | 6.33 (1H, d, <i>J</i> =1.8 Hz) | 99.5 (CH) | 100.4 (CH) | C-5, 7, 8, 10 |
| 7 | - | - | 164.9 (C) | 165.5 (C) | - |
| 8 | 6.47 (1H, d, <i>J</i> =1.8 Hz) | - | 94.6 (CH) | 98.1 (C) | - |
| 9 | - | - | 157.9 (C) | 154.9 (C) | - |
| 10 | - | - | 104.5 (C) | 104.9 (C) | - |
| 1' | - | - | 131.2 (C) | 131.6 (C) | - |
| 2', 6' | 8.03 (2H, m) | 7.82 (2H, m) | 126.9 (CH) | 126.1 (CH) | C-2, 1', 3', 5', |
| 3', 5' | 7.53 (2H, m) | 7.52 (2H, m) | 129.6 (CH) | 129.3 (CH) | C-2', 6' |
| 4' | 7.53 (1H, m) | 7.52 (1H, m) | 133.5 (CH) | 131.9 (CH) | C-3', 5' |
| 5-OH | 12.78 (1H, s) | 12.73 (1H, s) | - | - | - |
| 8-CH ₂ N | - | 4.05 (2H, s) | - | 54.6 (CH ₂) | C-3'', 7'', 8, 9, 7 |
| CH ₂ NCH ₂ | - | 2.80 (4H, s) | - | 27.8 (CH ₂) | - |
| CH ₂ SCH ₂ | - | 3.00 (4H, m) | - | 54.7 (CH ₂) | - |



(M14e)

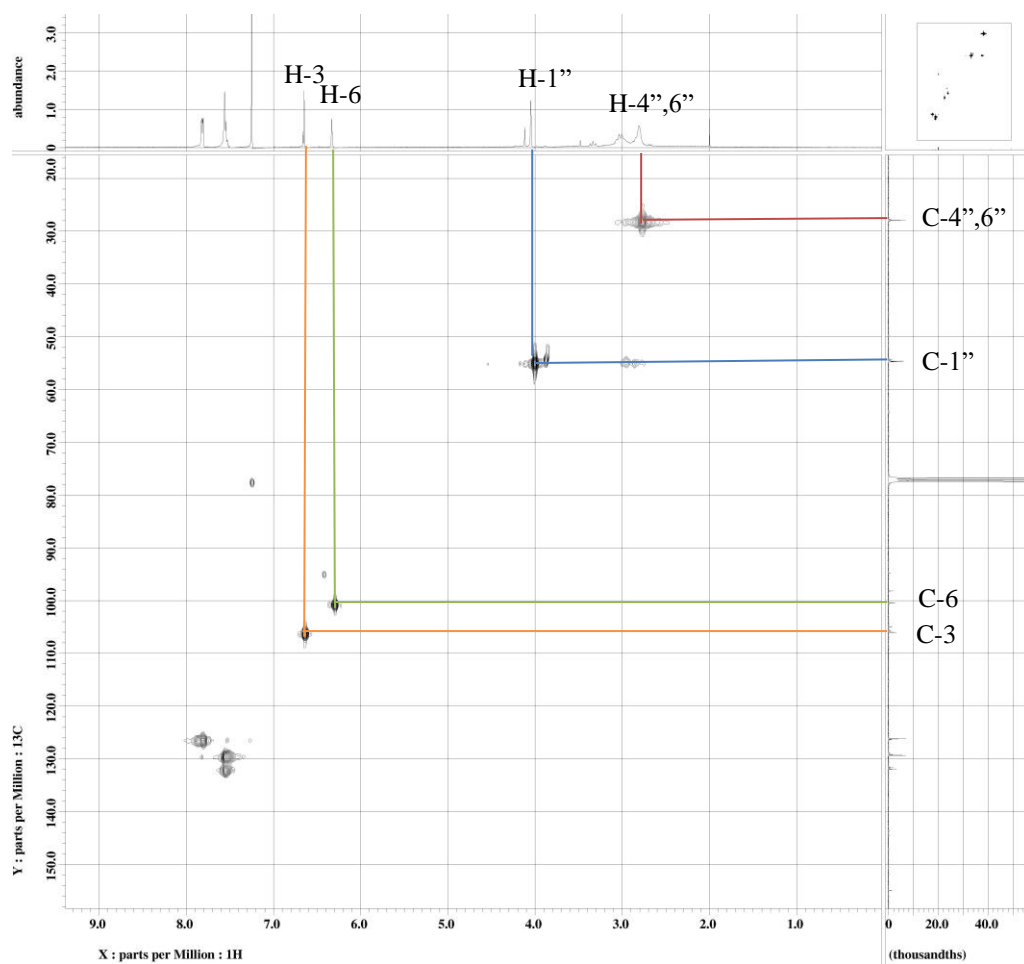
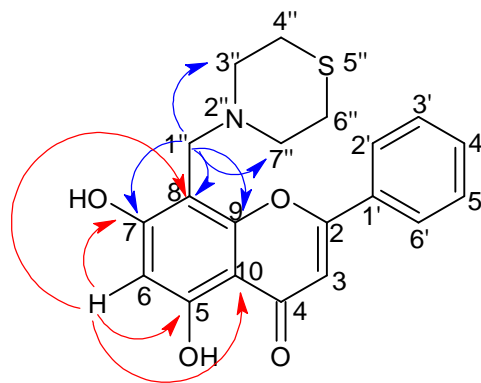


Figure 4.101: HMBC Spectrum of 5,7-dihydroxy-8-(thiomorpholinomethyl)-2-phenyl-4H-chromen-4-one (M14e)



(M14e)

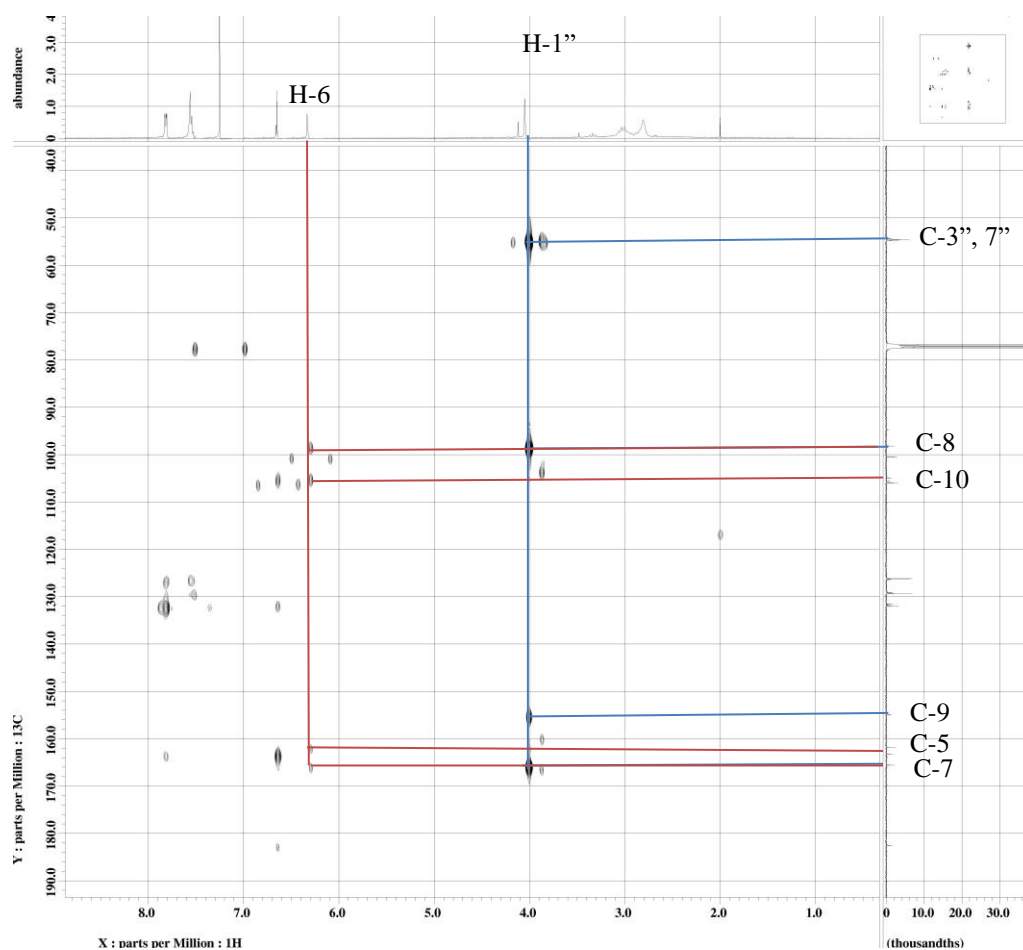
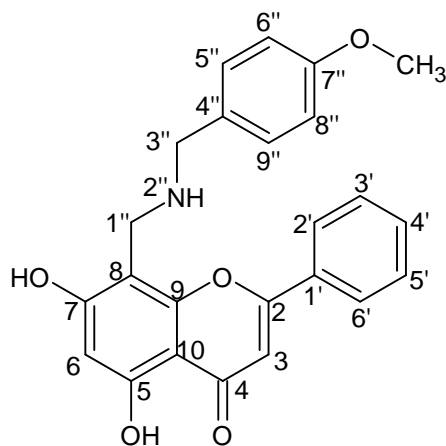


Figure 4.102: HMBC Spectrum of 5,7-dihydroxy-8-(thiomorpholinomethyl)-2-phenyl-4H-chromen-4-one (M14e)

4.3.4.6 Characterization of 5,7-dihydroxy-8-(4-methoxybenzylamine)-2-phenyl-4H-chromen-4-one (M14f)



(M14f)

Compound **M14f** was obtained as yellow solid, mp 183-184 °C. In TLC plate, R_f value of 0.07 was obtained in mobile phase hexane:acetone 6:3. The percentage yield of **M14f** was obtained at 47.1%. The HRESIMS (Appendix A33) gave a pseudomolecular ion peak at $m/z = 404.1479$ $[M+H]^+$ which analysed for $C_{24}H_{21}NO_5$ (found 403.1425; calculated 403.1419). Table 4.47 shows the summary physical properties of **M14f**.

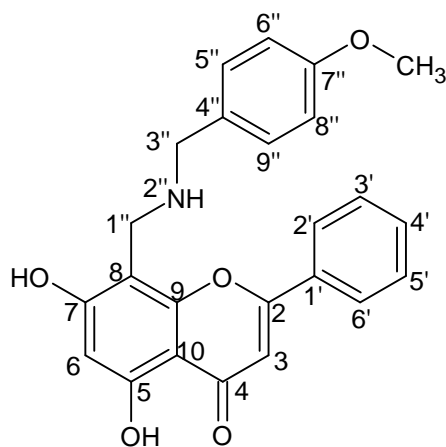
The IR spectrum of **M14f** (Appendix C33) shows absorption bands at 3433 (OH/NH stretch), 1640 (C=O stretch), 1619 (C=C stretch), 1254 (C-N stretch), 1186 (C-O stretch), 1105 (C-O-C stretch) cm^{-1} . As the OH stretch is broad, NH stretch is overlapped with OH stretch.

Table 4.47: Summary Physical Properties of M14f

| Compound | M14f |
|-------------------------|--|
| IUPAC Name | 5,7-dihydroxy-8-(4-methoxybenzylamine)-2-phenyl-4H-chromen-4-one |
| Molecular formula | C ₂₄ H ₂₁ NO ₅ |
| Molecular weight, g/mol | 403.1425 |
| Physical appearance | Yellow solid |
| Percentage yield, % | 70.1 |
| Obtained Mass, mg | 19.0 |
| R _f value | 0.07 |
| Melting point, °C | 183-184 |

Signals of C8-NCH₂ (δ_{H} 3.86, δ_{C} 50.1) indicate the presence of aminomethyl group in the ¹H NMR of compound **M14f** (Figure 4.103). Signal at δ_{H} 4.06 and δ_{H} 3.67 (s) were the signals for the methylene protons and methoxy group of 4-methoxybenzylamine in **M14f**. A pair of doublets at δ_{H} 6.81 (d, $J = 8.5$ Hz) and δ_{H} 7.27 (d, $J = 8.5$ Hz) due to ortho-coupled protons were assigned to H-6'', 8'' and H-5'', 9'', respectively. In ¹³C NMR (Figure 4.104) of compound **M14f**, signal at δ_{C} 41.7 (3''-CH₂N) was the methylene carbon that attached to 4-methoxybenzylamine. The methoxy group signal was shown at δ_{C} 55.5. In the HMBC spectrum (Figure 4.106), methylene protons (C8-CH₂N) displayed two bonds correlations with C-8 (δ_{C} 99.6), and three bonds correlations with C-7 (δ_{C} 170.6) and C-9 (δ_{C} 155.4). This confirmed the aminomethylation was occurred at C-8 of ring A. The structure was further confirmed by using DEPT (Appendix

D69) and HMQC (Figure 4.105) spectra. Table 4.48 shows the summary NMR data of compounds **M14** and **M14f**.



(M14f)

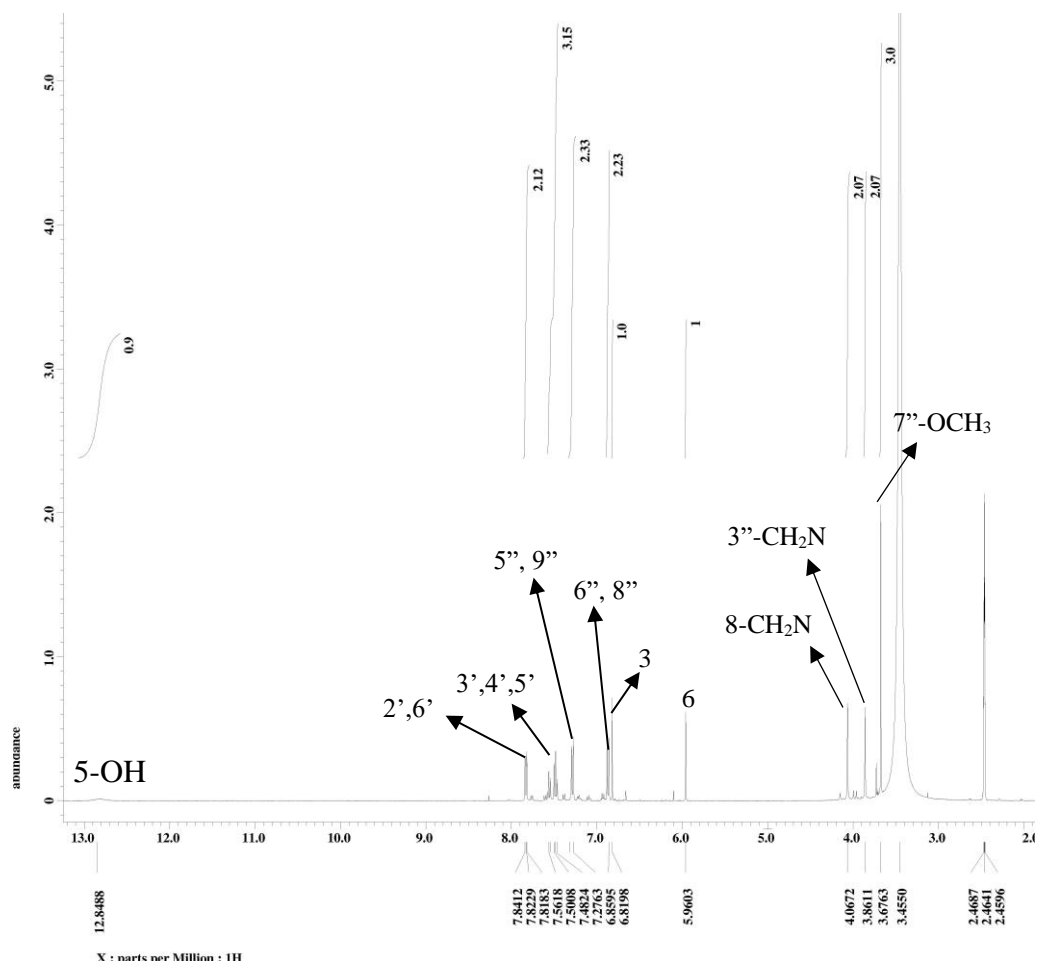


Figure 4.103: ¹H NMR (400 MHz, CDCl₃) of 5,7-dihydroxy-8-(4-methoxybenzylamine)-2-phenyl-4H-chromen-4-one (M14f)

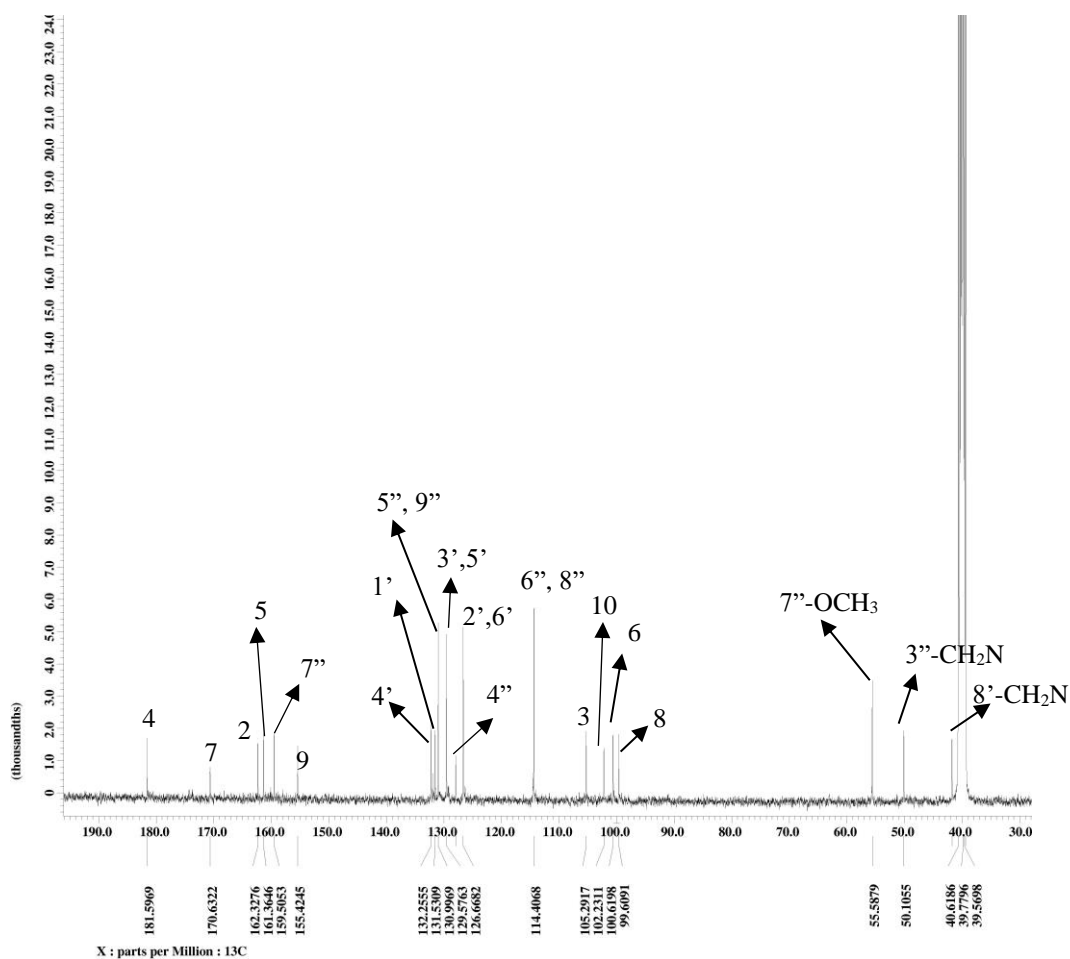
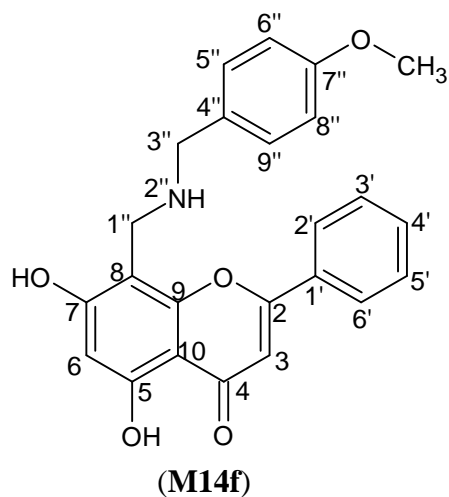
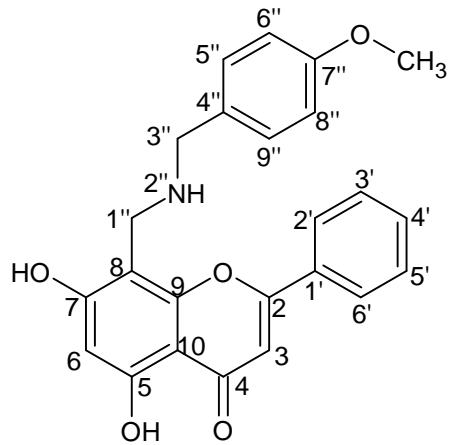


Figure 4.104: ¹³C NMR (100 MHz, CDCl₃) of 5,7-dihydroxy-8-(4-methoxybenzylamine)-2-phenyl-4H-chromen-4-one (M14f)

Table 4.48: ¹H, ¹³C and HMBC spectral data of M14 (DMSO-d₆) and M14f (DMSO-d₆)

| | M14 | M14f | M14 | M14f | M14f |
|---------------------------|--------------------------------|---------------------------------|-------------------------|-------------------------|----------------------|
| Position | δ _H (multiplicity) | δ _H (multiplicity) | δ _C (C-type) | δ _C (C-type) | HMBC |
| 2 | - | - | 163.6 (C) | 162.3 (C) | - |
| 3 | 6.91 (1H, s) | 6.64 (s) | 105.6 (CH) | 105.2 (CH) | C-2, 10, 4 |
| 4 | - | - | 182.3 (C) | 181.5 (C) | - |
| 5 | - | - | 161.9 (C) | 161.3 (C) | - |
| 6 | 6.17 (1H, d, <i>J</i> =1.8 Hz) | 6.33 (1H, d, <i>J</i> =1.8 Hz) | 99.5 (CH) | 100.6 (CH) | C-5, 8, 10 |
| 7 | - | - | 164.9 (C) | 170.6 (C) | - |
| 8 | 6.47 (1H, d, <i>J</i> =1.8 Hz) | - | 94.6 (CH) | 99.6 (CH) | - |
| 9 | - | - | 157.9 (C) | 155.4 (C) | - |
| 10 | - | - | 104.5 (C) | 102.2 (C) | - |
| 1' | - | - | 131.2 (C) | 131.5 (C) | - |
| 2', 6' | 8.03 (2H, m) | 7.82 (2H, m) | 126.9 (CH) | 126.6 (CH) | C-2, 1', 3', 5', |
| 3', 5' | 7.53 (2H, m) | 7.48 (2H, m) | 129.6 (CH) | 129.5 (CH) | C-2', 6' |
| 4' | 7.53 (1H, m) | 7.48 (1H, m) | 133.5 (CH) | 132.2 (CH) | C-3', 5' |
| 5-OH | 12.78 (1H, s) | 12.84 (1H, s) | - | - | - |
| 8-CH ₂ N (1'') | - | 3.86 (2H, s) | - | 50.1 (CH ₂) | C-3'', 8, 9, 7 |
| 3''-CH ₂ N | - | 3.67 (2H, s) | - | 41.7 (CH ₂) | C-1'', 4'', 5'', 9'' |
| 7''-OCH ₃ | - | 4.06 (3H, s) | - | 55.5 (CH ₂) | C-7'' |
| 7'' | - | - | - | 159.5 (CH) | - |
| 5'', 9'' | - | 7.27 (2H, d, <i>J</i> =8.5 Hz) | - | 130.9 (CH) | C-1'', 4'', 7'' |
| 6'', 8'' | - | 6.81 (2H, d, <i>J</i> = 8.5 Hz) | - | 114.4 (CH) | C-4'', |



(M14f)

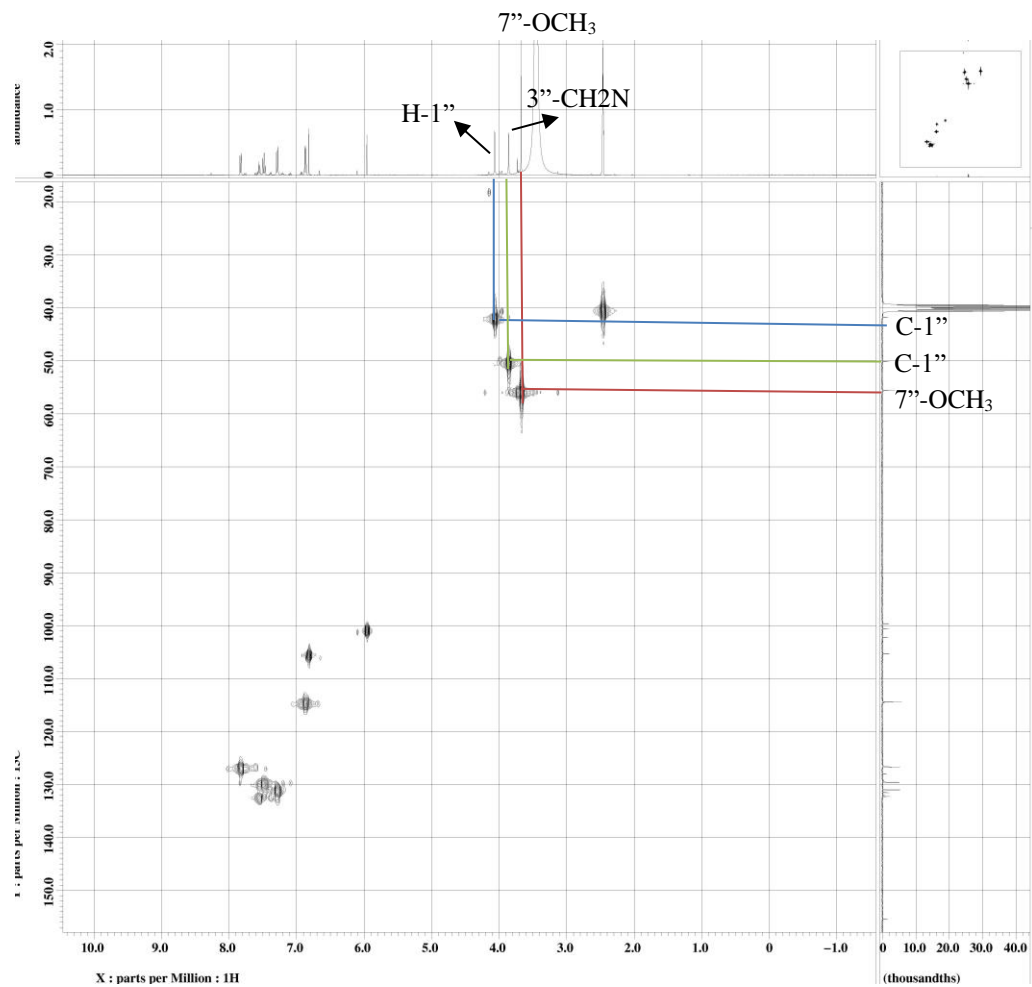
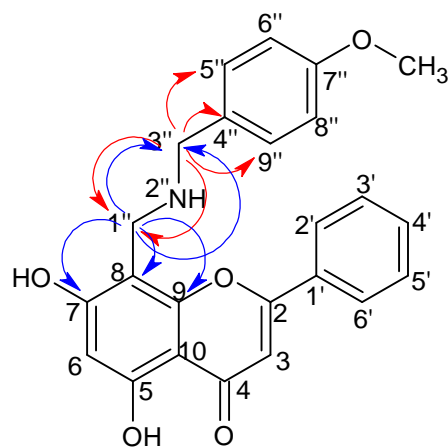


Figure 4.105: HMBC Spectrum of 5,7-dihydroxy-8-(4-methoxybenzylamine)-2-phenyl-4H-chromen-4-one (M14f)



(M14f)

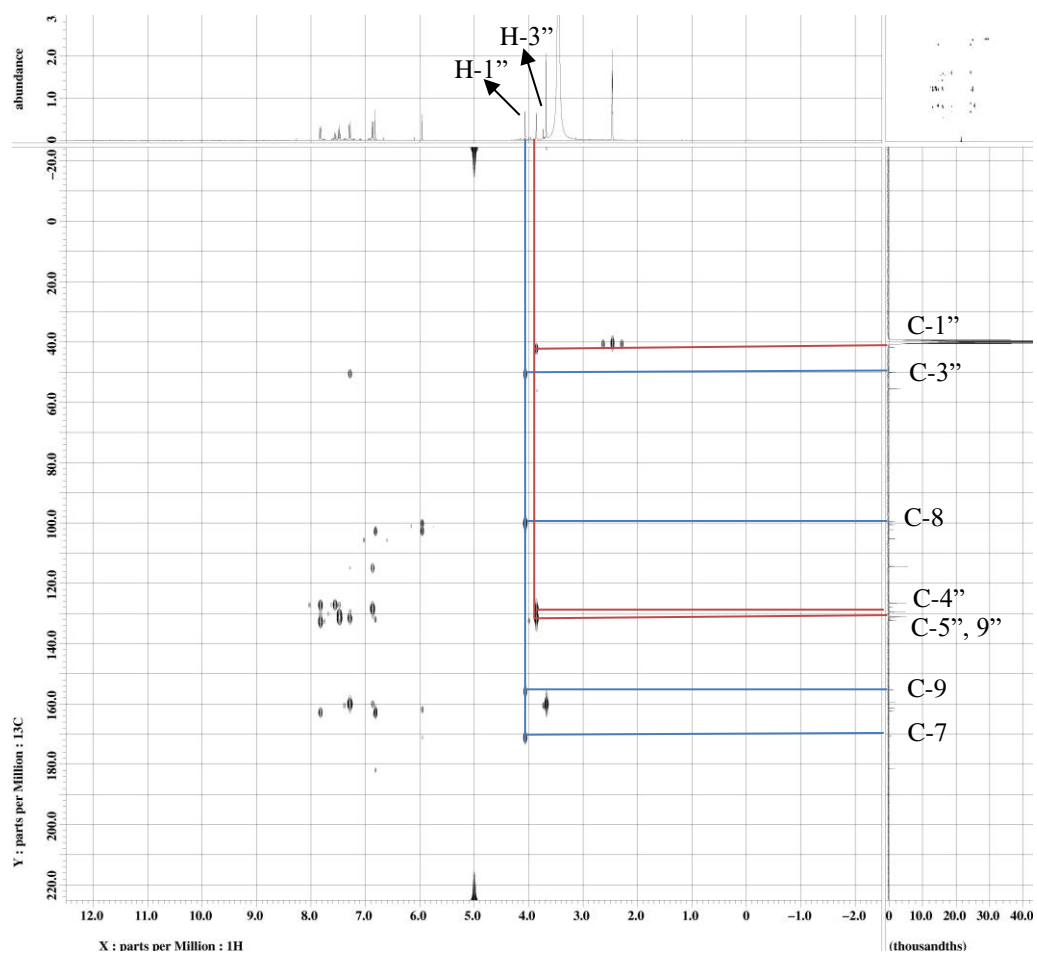


Figure 4.106: HMBC Spectrum of 5,7-dihydroxy-8-(4-methoxybenzylamine)-2-phenyl-4H-chromen-4-one (M14f)

4.3.5 Synthesis of 5,7-dihydroxyflavone (M14) Diamine Mannich Bases

Isolate 5,7-dihydroxyflavone (**M14**) was used to synthesis diamine Mannich bases via Mannich reaction. The reaction route was shown in Figure 4.107.

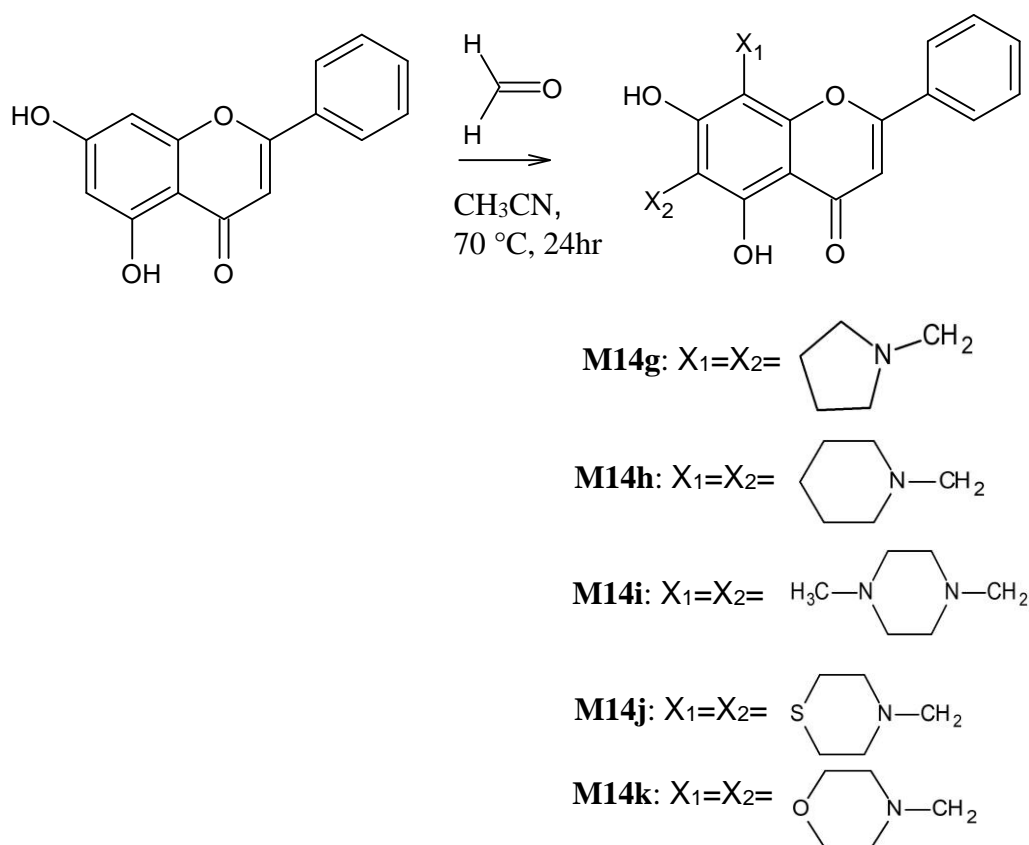


Figure 4.107: Synthesis route of flavone M14 diamine Mannich bases with mol ratio flavone: formaldehyde: amine 1:3:3

Mannich flavones (**M14g-M14k**) were prepared by reaction of **M14** flavone with formaldehyde, secondary amine (pyrrolidine in **M14g**; piperidine in **M14h**; 1-methylpiperazine in **M14i**; thiomorpholine in **M14j**; morpholine in **M14k**) in mol ratio 1:3:3, respectively, and stirred under reflux in acetonitrile for 24 hr at $70\text{ }^\circ\text{C}$.

The reaction mechanism involves the formation of iminium ion (Figure 4.39) which is the condensation between formaldehyde and secondary amine. Then, followed by the electrophilic attack of the iminium ion on the aromatic A-ring of the flavone substrate at C8 and C6. The reaction mechanism was shown in Figure 4.108.

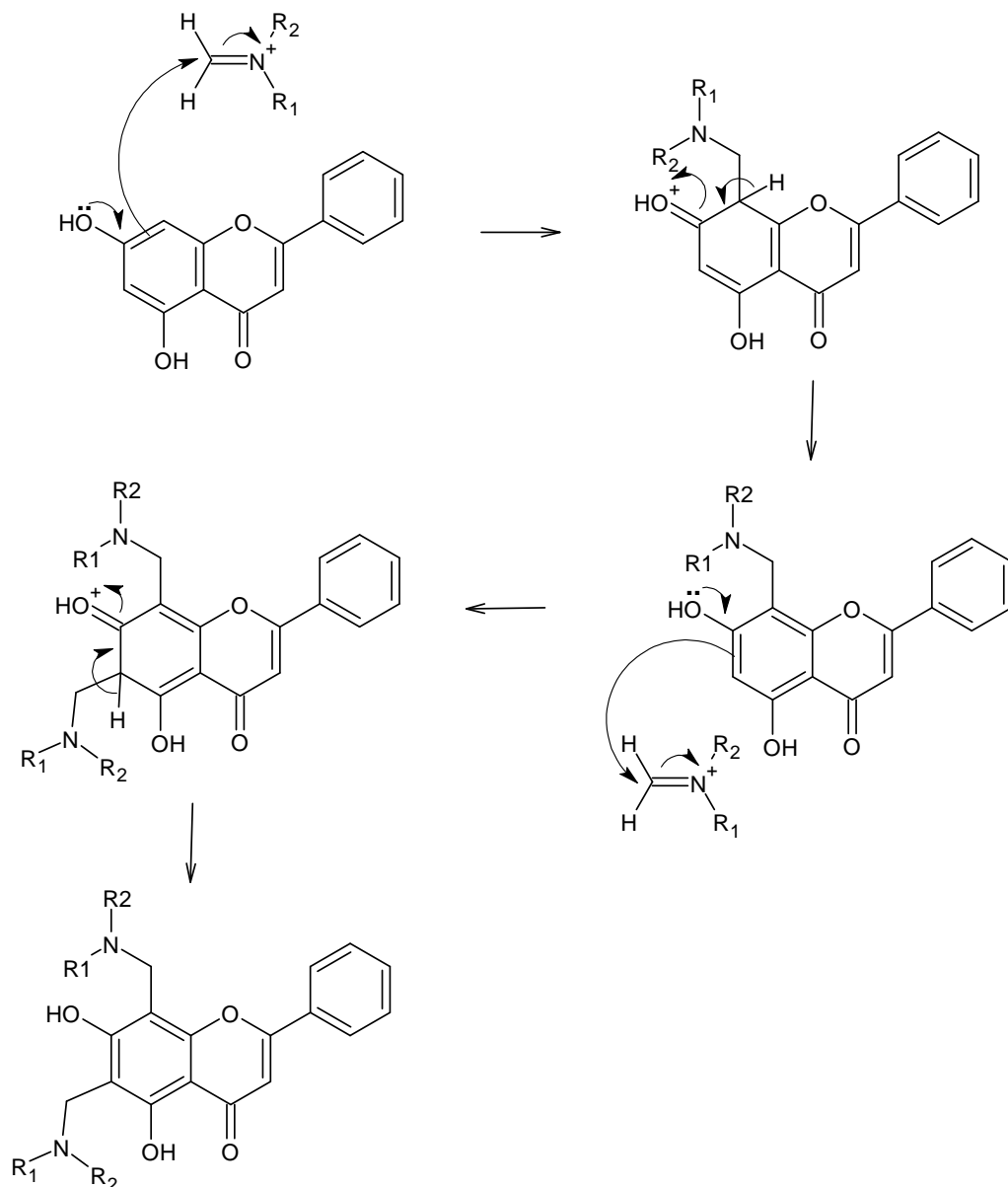
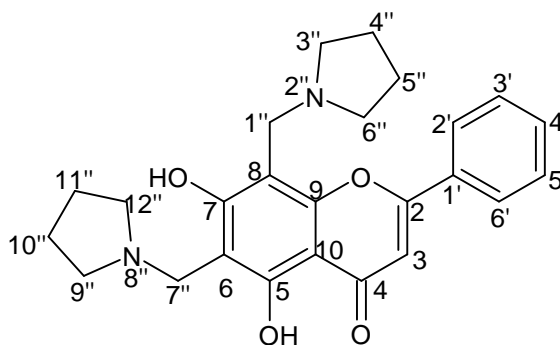


Figure 4.108: Reaction mechanism of flavone M14 diamine Mannich bases

4.3.5.1 Characterization of 5,7-dihydroxy-6,8-bis(pyrrolidine-1-ylmethyl)-2-phenyl-4H-chromen-4-one (**M14g**)



(**M14g**)

Compound **M14g** was obtained as yellow solid, mp 174-176 °C. In TLC plate, R_f value of 0.10 was obtained in mobile phase hexane:acetone 10:3. The percentage yield of **M14g** was obtained at 61.2%. The HRESIMS (Appendix A34) gave a pseudomolecular ion peak at $m/z = 421.2126 [M+H]^+$ which analysed for $C_{25}H_{28}N_2O_4$ (found 420.2053; calculated 420.2049). Table 4.49 shows the summary physical properties of **M14g**.

The IR spectrum of **M14g** (Appendix C34) shows absorption bands at 3434 (OH stretch), 2965, 2947 (CH_3 stretch), 1636 (C=O stretch), 1584 (C=C stretch), 1257 (C-N stretch), 1131 (C-O stretch) cm^{-1} .

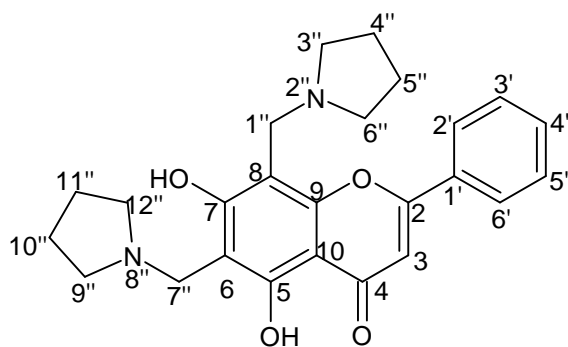
Table 4.49: Summary Physical Properties of M14g

| Compound | M14g |
|-------------------------|---|
| IUPAC Name | 5,7-dihydroxy-6,8-bis(pyrrolidine-1-ylmethyl)-2-phenyl-4H-chromen-4-one |
| Molecular formula | C ₂₅ H ₂₈ N ₂ O ₄ |
| Molecular weight, g/mol | 420.2053 |
| Physical appearance | Yellow solid |
| Percentage yield, % | 61.2 |
| Obtained Mass, mg | 30.9 |
| R _f value | 0.10 |
| Melting point, °C | 174-176 |

In comparison ¹H NMR of compound **M14g** (Figure 4.109) with ¹H NMR of compound **M14** (Figure 4.32), the disappearance of H-6 and H-8 resonances in ¹H NMR of flavone **M14g** and the occurrence of two methylenes signals and amine signals showed that the amine group was attached to C-6 and C-8 to formed bis-aminomethyl flavone **M14**. Methylene signals were shown at δ_{H} 3.96 and δ_{H} 3.98 which belong to 6-CH₂N and 8-CH₂N, respectively. Pyrrolidine peaks were appeared at δ_{H} 1.78 (H-10'', 11''), δ_{H} 1.81 (H-4'', 5''), δ_{H} 2.66 (H-9'', 12''), δ_{H} 2.72 (H-3'', 6'').

In ¹³C NMR (Figure 4.110) of compound **M14g**, signal at δ_{C} 47.6 and δ_{C} 49.9 were the methylene C-8 and methylene C-6, respectively. Methylene C-8 in lower chemical shift as increased electron density from the resonance effect of oxygen atom at ring C. Signals at δ_{C} 23.6 (C-4'', 5''), δ_{C} 23.7 (C-10'', 11''), δ_{C}

53.6 (C-3'',6''), and δ_c 53.9 (C-9'', 12'') were the characteristic peaks of pyrrolidine moiety. In the HMBC spectrum (Figure 4.112), methylene H-6 displayed two bonds correlations with C-6 (δ_c 103.6), and three bonds correlations with C-5 (δ_c 158.2), C-7 (δ_c 166.1) and C-9'', 12'' (δ_c 53.9). Whereas, methylene H-8 displayed two bonds correlations with C-8 (δ_c 102.7), three bonds correlations with C-7 (δ_c 166.1), C-9 (δ_c 155.0) and C-2'', 6'' (δ_c 53.6) which belong to pyrrolidine moiety. The structure was further confirmed by using DEPT (Appendix D70) and HMQC (Figure 4.111) spectra. Table 4.50 shows the summary NMR data of compounds **M14** and **M14g**.



(M14g)

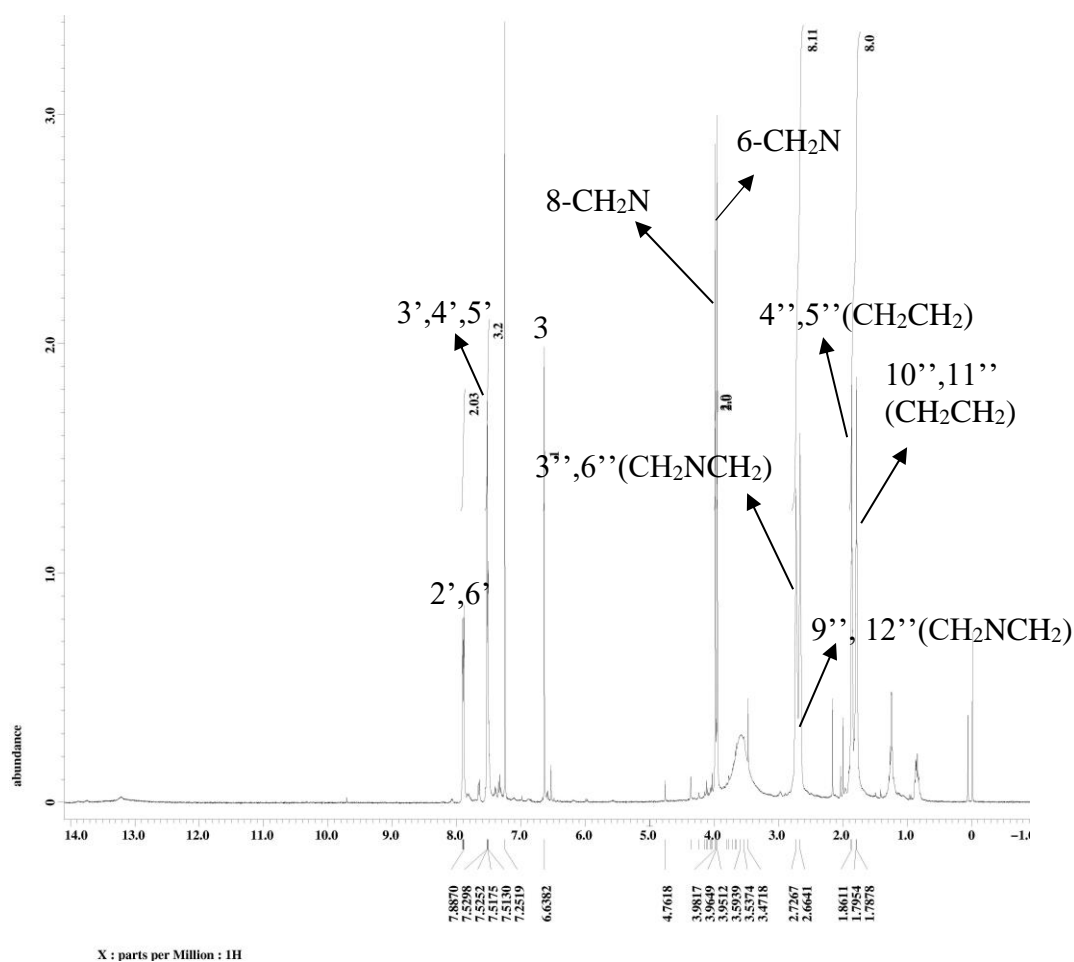


Figure 4.109: ^1H NMR (400 MHz, CDCl_3) of 5,7-dihydroxy-6,8-bis(pyrrolidine-1-ylmethyl)-2-phenyl-4H-chromen-4-one (M14g)

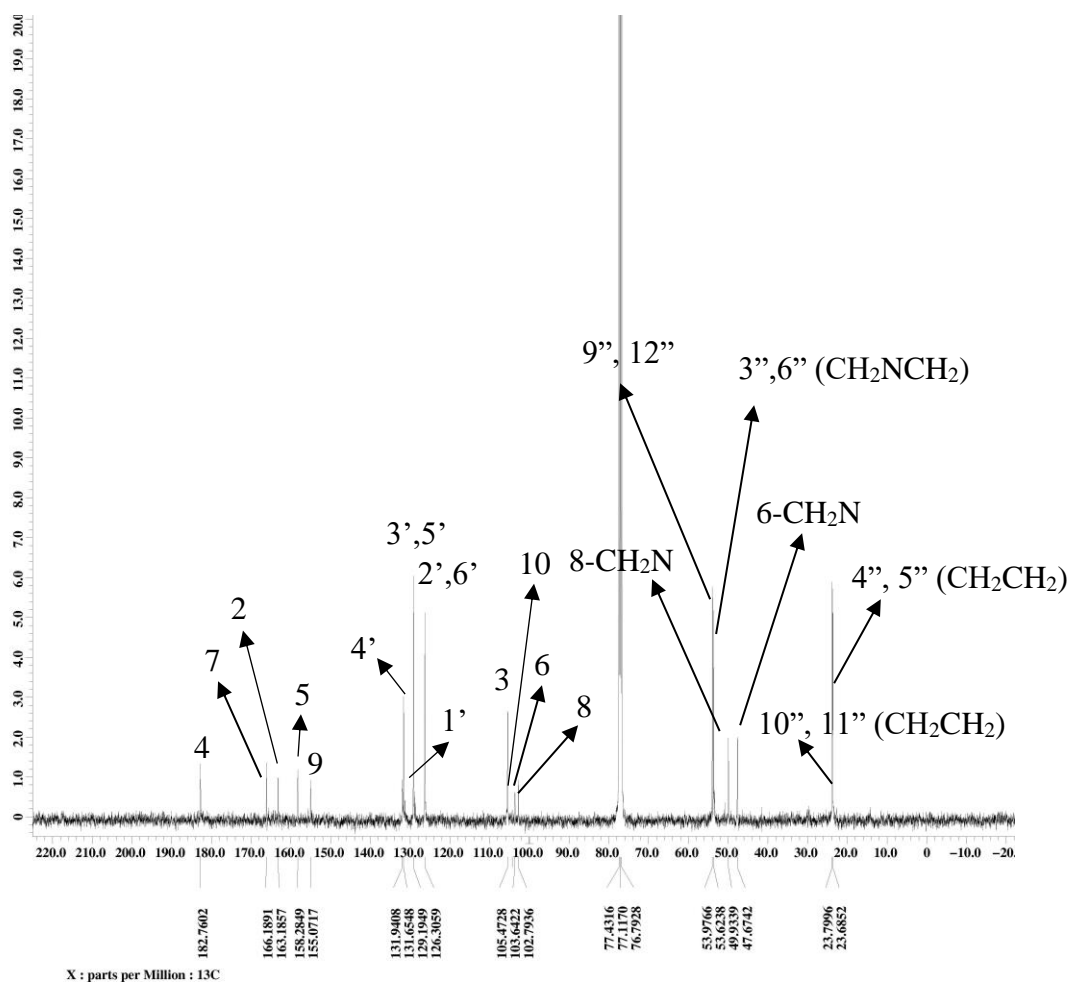
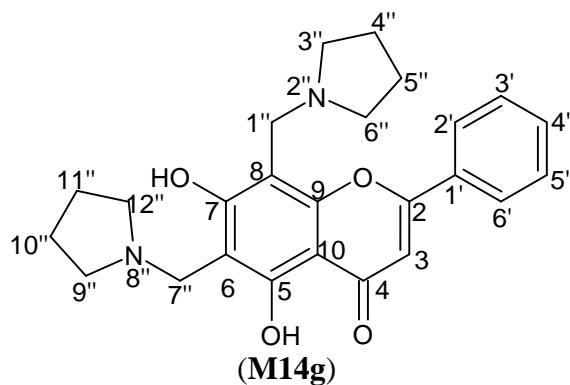
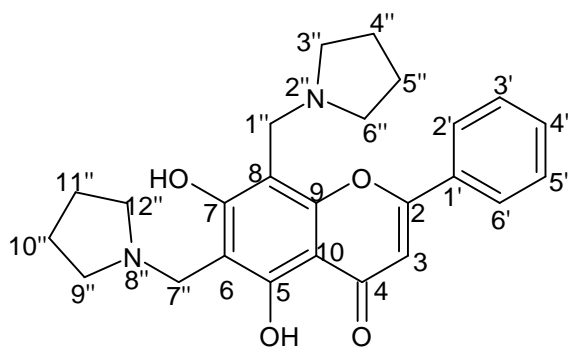


Figure 4.110: ^{13}C NMR (100 MHz, CDCl_3) of 5,7-dihydroxy-6,8-bis(pyrrolidine-1-ylmethyl)-2-phenyl-4H-chromen-4-one (M14g)

Table 4.50: ¹H, ¹³C and HMBC spectral data of M14 (DMSO-d₆) and M14g (CDCl₃)

| | M14 | M14g | M14 | M14g | M14g |
|---------------------|-------------------------------|-------------------------------|-------------------------|-------------------------|----------------------|
| Position | δ _H (multiplicity) | δ _H (multiplicity) | δ _C (C-type) | δ _C (C-type) | HMBC |
| 2 | - | - | 163.6 (C) | 163.1(C) | - |
| 3 | 6.91 (1H, s) | 6.61 (1H, s) | 105.6 (CH) | 105.4 (CH) | C-2, 1', 10, 4 |
| 4 | - | - | 182.3 (C) | 182.7 (C) | - |
| 5 | - | - | 161.9 (C) | 158.2 (C) | - |
| 6 | 6.17 (1H, d, J=1.8 Hz) | - | 99.5 (CH) | 103.6 (C) | - |
| 7 | - | - | 164.9 (C) | 166.1 (C) | - |
| 8 | 6.47 (1H, d, J=1.8 Hz) | - | 94.6 (CH) | 102.7 (C) | - |
| 9 | - | - | 157.9 (C) | 155.0 (C) | - |
| 10 | - | - | 104.5 (C) | 104.3 (C) | - |
| 1' | - | - | 131.2 (C) | 131.9 (C) | - |
| 2', 6' | 8.03 (2H, m) | 8.09 (2H, m) | 126.9 (CH) | 126.3 (CH) | C-2, 1', 3', 5', |
| 3', 5' | 7.53 (2H, m) | 7.60 (2H, m) | 129.6 (CH) | 129.1 (CH) | C-2',6', 4' |
| 4' | 7.53 (1H, m) | 7.60 (1H, m) | 133.5 (CH) | 131.6 (CH) | C-3', 5' |
| 5-OH | 12.78 (1H, s) | - | - | - | - |
| 8-CH ₂ N | - | 3.98 (2H, s) | - | 47.6 (CH ₂) | C-3'', 6'', 8, 9, 7 |
| 6-CH ₂ N | - | 3.96 (2H, s) | - | 49.9 (CH ₂) | C-9'', 12'', 6, 5, 7 |
| 3'', 6'' | - | 2.72 (4H, s) | - | 53.6 (CH ₂) | C-4'', 5'' |
| 9'', 12'' | - | 2.66 (4H, s) | - | 53.9 (CH ₂) | C-10'', 11'' |
| 4'', 5'' | - | 1.81 (4H, s) | - | 23.6 (CH ₂) | C-4'', 5'' |
| 10'', 11'' | - | 1.78 (4H, s) | - | 23.7 (CH ₂) | C-10'', 11'' |



(M14g)

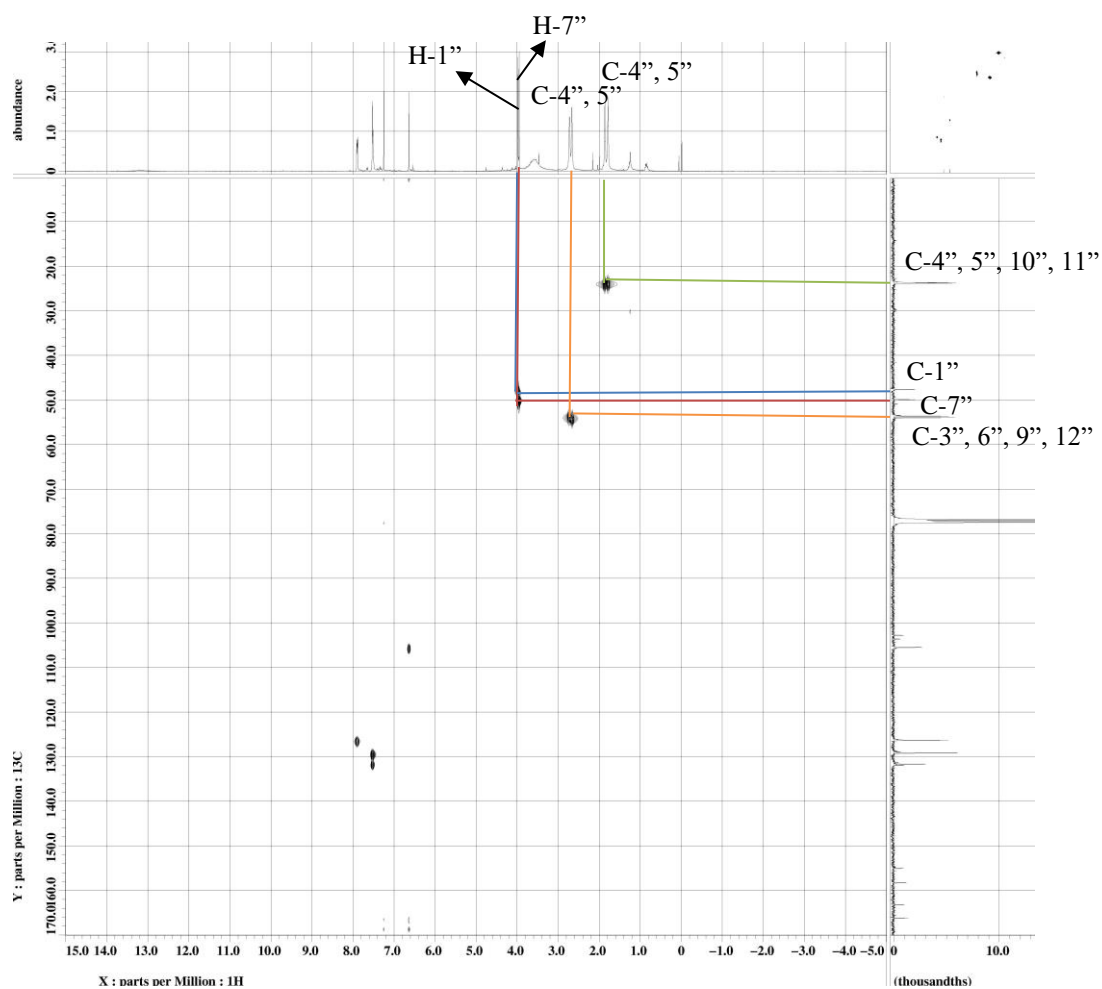


Figure 4.111: HMQC Spectrum of 5,7-dihydroxy-6,8-bis(pyrrolidine-1-ylmethyl)-2-phenyl-4H-chromen-4-one (M14g)

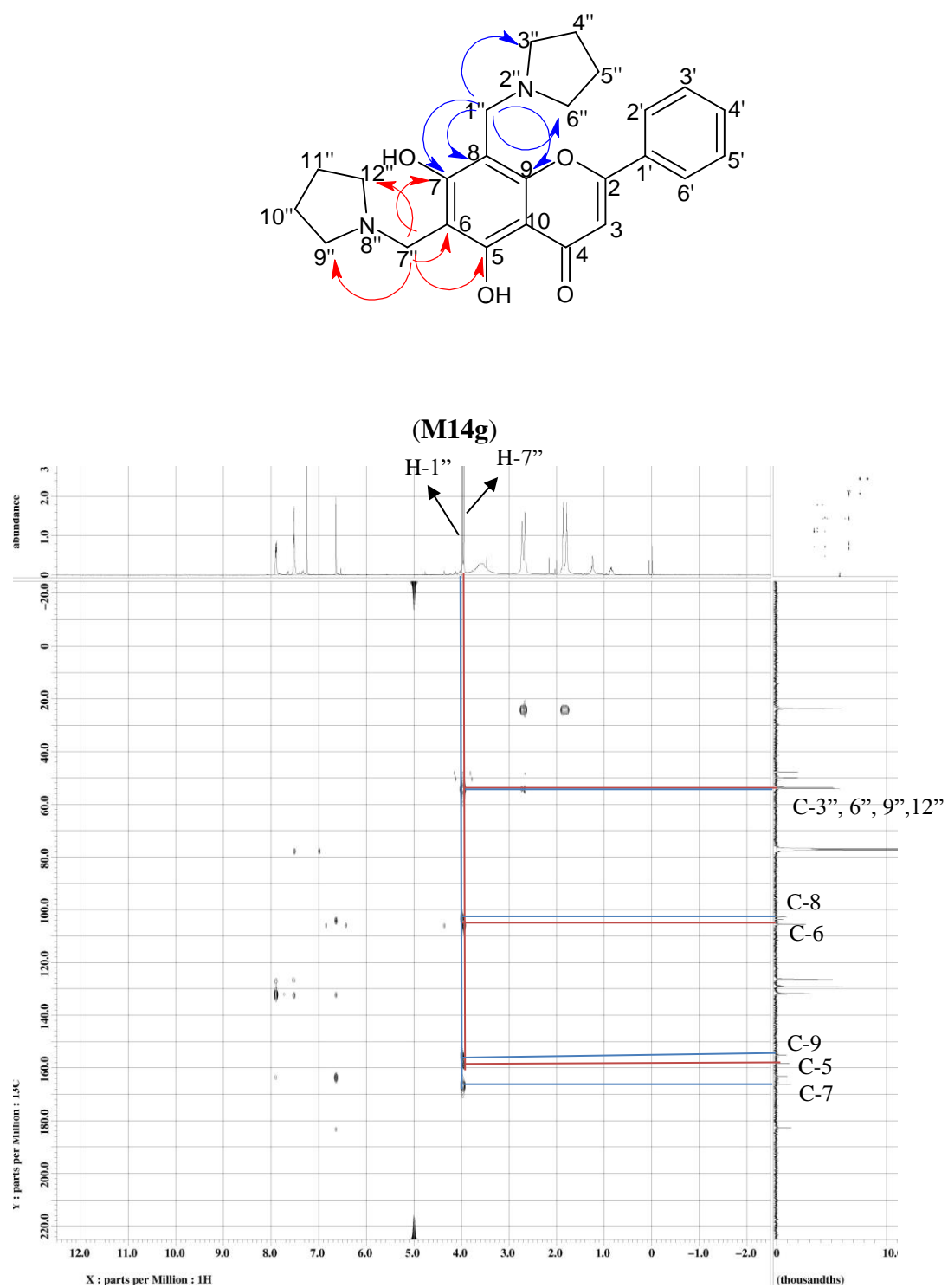
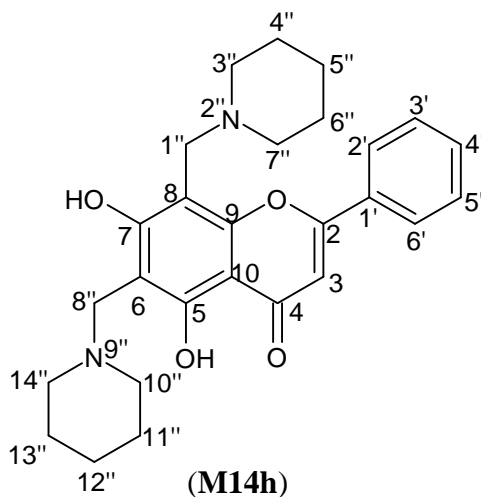


Figure 4.112: HMBC Spectrum of 5,7-dihydroxy-6,8-bis(pyrrolidine-1-ylmethyl)-2-phenyl-4H-chromen-4-one (M14g)

4.3.5.2 Characterization of 5,7-dihydroxy-6,8-bis(piperidin-1-ylmethyl)-2-phenyl-4*H*-chromen-4-one (M14h)



Compound **M14h** was obtained as yellow solid, mp 179-182 °C. In TLC plate, R_f value of 0.25 was obtained in mobile phase hexane:acetone 6:4. The percentage yield of **M14h** was obtained at 87.1%. The HRESIMS (Appendix A35) gave a pseudomolecular ion peak at $m/z = 449.2438 [M+H]^+$ which analysed for $C_{27}H_{32}N_2O_4$ (found 448.2365; calculated 448.2362). Table 4.51 shows the summary physical properties of **M14h**.

The IR spectrum of **M14h** (Appendix C35) shows absorption bands at 3435 (OH stretch), 2938, 2850 (CH_3 stretch), 1638 (C=O stretch), 1590 (C=C stretch), 1214 (C-N stretch), 1151 (C-O stretch) cm^{-1} .

Table 4.51: Summary Physical Properties of M14h

| Compound | M14h |
|-------------------------|---|
| IUPAC Name | 5,7-dihydroxy-6,8-bis(piperidin-1-ylmethyl)-2-phenyl-4H-chromen-4-one |
| Molecular formula | C ₂₇ H ₃₂ N ₂ O ₄ |
| Molecular weight, g/mol | 448.2365 |
| Physical appearance | Yellow solid |
| Percentage yield, % | 87.1 |
| Obtained Mass, mg | 46.9 |
| R _f value | 0.25 |
| Melting point, °C | 179-182 |

The ¹H NMR of compound **M14h** (Figure 4.113) showed methylene proton signals at δ_H 3.80 (s) which belong to 6-CH₂N and 8-CH₂N. Signals at δ_H 1.41 (H-12''), δ_H 1.49 (H-5''), δ_H 1.63 (H-11'', 13''), δ_H 1.64 (H-4'', 6''), δ_H 2.55 (H-3'', 6'' and H-9'', 12'') were the characteristic peaks of piperidine moiety at C-6 and C-8.

In ¹³C NMR (Figure 4.114) of compound **M14h**, signal at δ_c 51.4 and δ_c 52.9 were the methylene C-8 and methylene C-6, respectively. Signals at δ_c 23.9 (C-5''), δ_c 24.2 (C-12''), δ_c 25.5 (C-4'', 6''), δ_c 25.9 (C-11'', 13''), δ_c 53.8 (C-3'', 7''), and δ_c 54.3 (C-10'', 14'') were the characteristic peaks of piperidine moieties. In the HMBC spectrum (Figure 4.116), methylene H-6 displayed two bonds correlations with C-6 (δ_c 103.7), and three bonds correlations with C-5 (δ_c 158.7), C-7 (δ_c 166.1) and C-10'', 14'' (δ_c 54.3). Whereas, methylene H-8

displayed two bonds correlations with C-8 (δ_c 102.2), three bonds correlations with C-7 (δ_c 166.1), C-9 (δ_c 155.4) and C-3'', 7'' (δ_c 53.8) which belong to piperidine moiety. The structure was further confirmed by using DEPT (Appendix D71) and HMQC (Figure 4.115) spectra. Table 4.52 shows the summary NMR data of compounds **M14** and **M14h**.

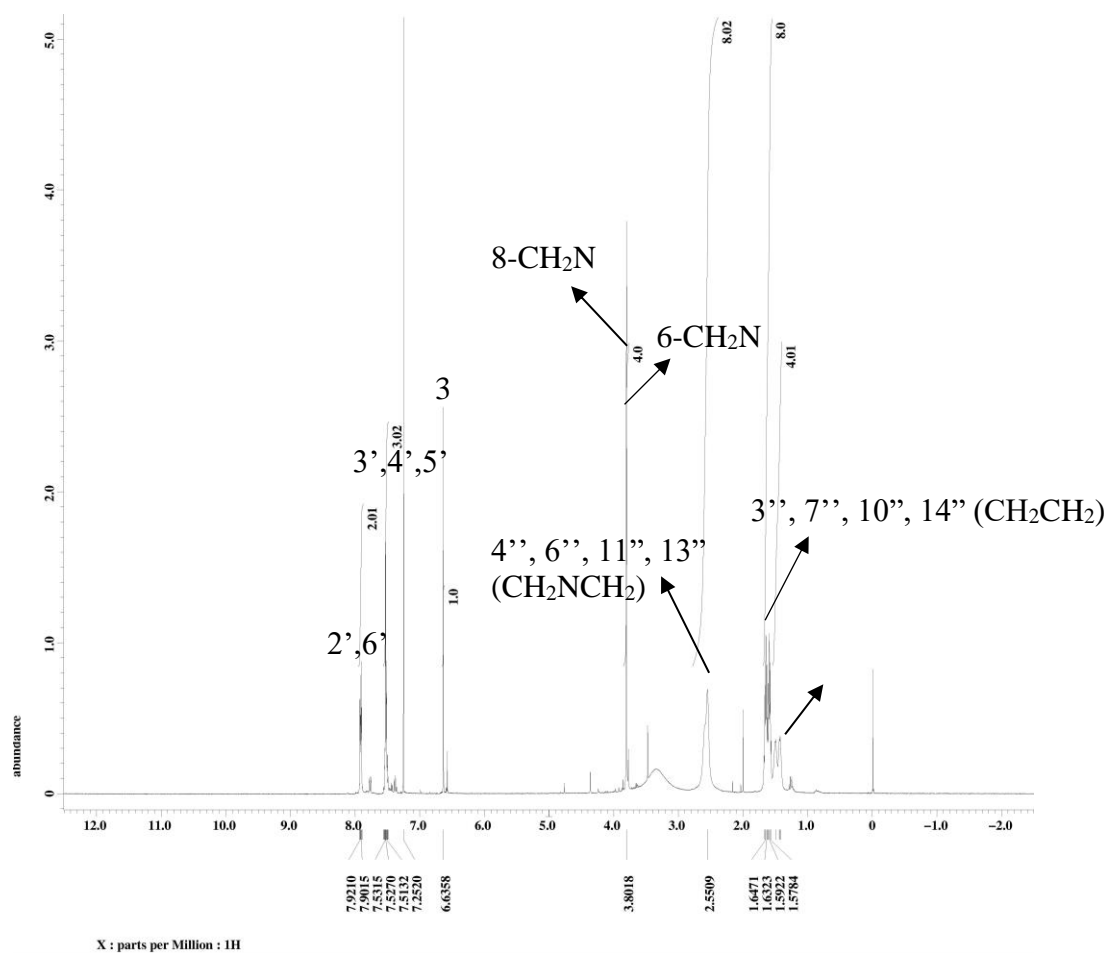
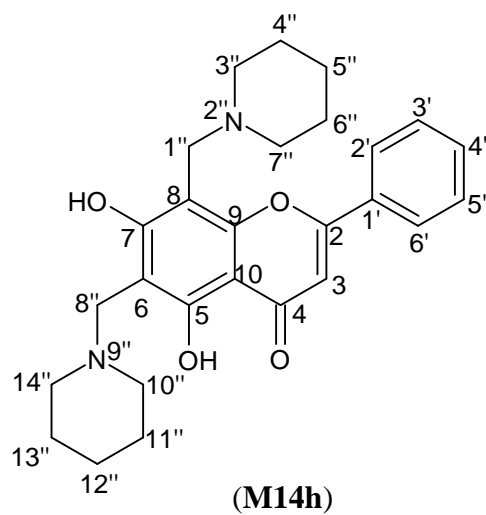
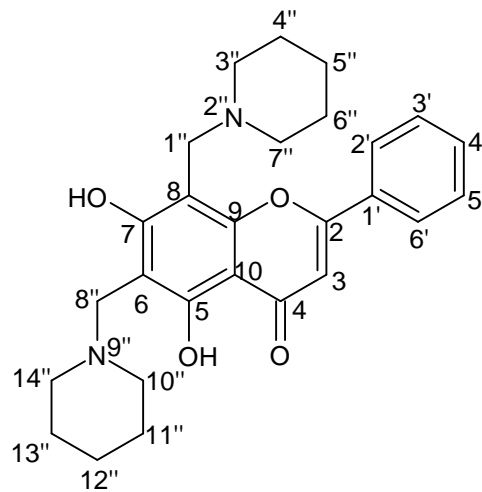


Figure 4.113: ^1H NMR (400 MHz, CDCl_3) of 5,7-dihydroxy-6,8-bis(piperidin-1-ylmethyl)-2-phenyl-4H-chromen-4-one (M14h)



(M14h)

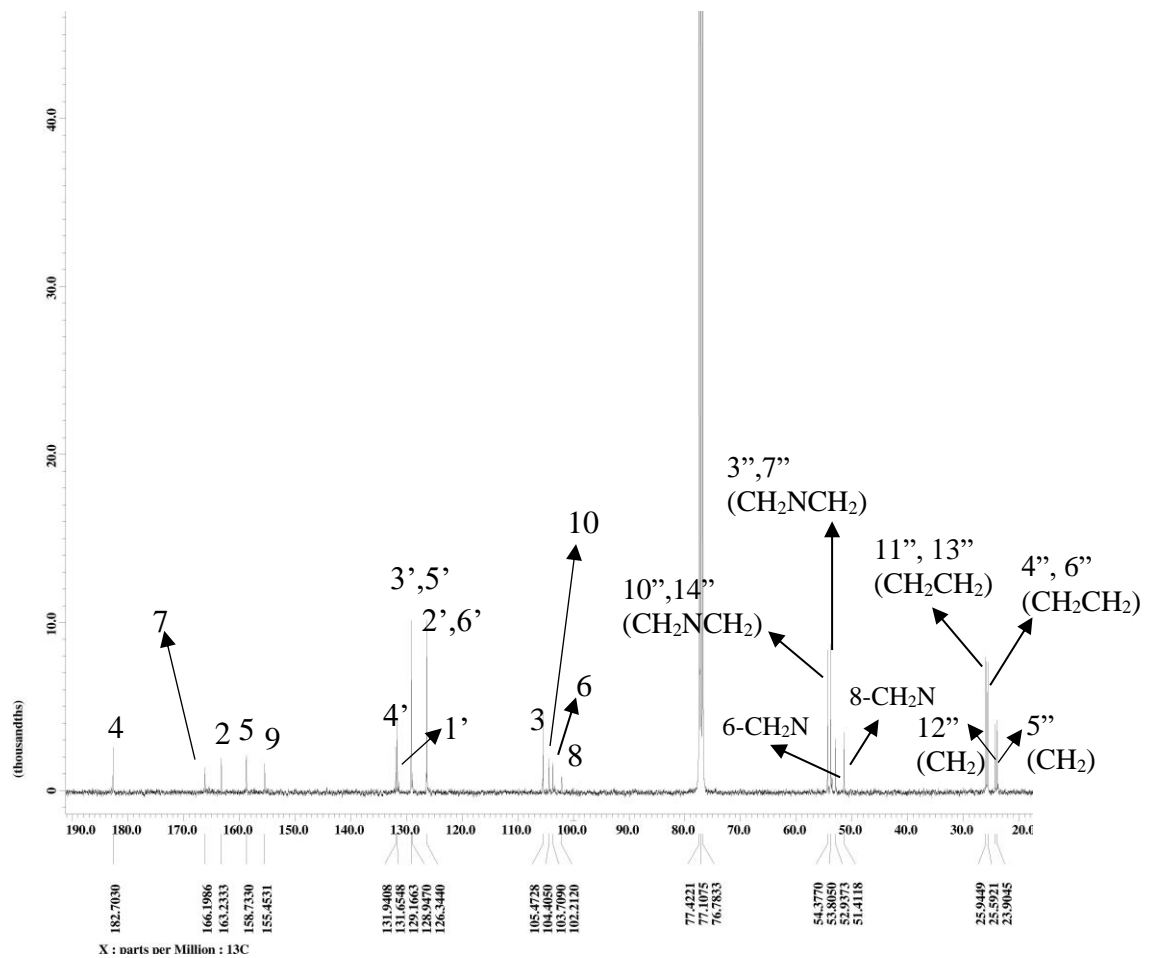


Figure 4.114: ^{13}C NMR (100 MHz, CDCl_3) of 5,7-dihydroxy-6,8-bis(piperidin-1-ylmethyl)-2-phenyl-4H-chromen-4-one (M14h)

Table 4.52: ¹H, ¹³C and HMBC spectral data of M14 (DMSO-d₆) and M14h (CDCl₃)

| Position | M14 δ _H (multiplicity) | M14h δ _H (multiplicity) | M14 δ _C (C-type) | M14h δ _C (C-type) | M14h HMBC |
|---------------------|--------------------------------------|---------------------------------------|--------------------------------|---------------------------------|-----------------------|
| 2 | - | - | 163.6 (C) | 163.1 (C) | - |
| 3 | 6.91 (1H, s) | 6.63 (s) | 105.6 (CH) | 105.4 (CH) | C-2, 1', 10, 4 |
| 4 | - | - | 182.3 (C) | 182.7 (C) | - |
| 5 | - | - | 161.9 (C) | 158.7 (C) | - |
| 6 | 6.17 (1H, d, <i>J</i> =1.8 Hz) | - | 99.5 (CH) | 103.7 (C) | - |
| 7 | - | - | 164.9 (C) | 166.1 (C) | - |
| 8 | 6.47 (1H, d, <i>J</i> =1.8 Hz) | - | 94.6 (CH) | 102.2 (C) | - |
| 9 | - | - | 157.9 (C) | 155.4 (C) | - |
| 10 | - | - | 104.5 (C) | 104.4 (C) | - |
| 1' | - | - | 131.2 (C) | 131.9 (C) | - |
| 2', 6' | 8.03 (2H, m) | 7.92 (2H, m) | 126.9 (CH) | 126.3 (CH) | C-2, 1', 3', 5', |
| 3', 5' | 7.53 (2H, m) | 7.52 (2H, m) | 129.6 (CH) | 129.1 (CH) | C-2', 6', 4' |
| 4' | 7.53 (1H, m) | 7.52 (1H, m) | 133.5 (CH) | 131.6 (CH) | C-3', 5' |
| 5-OH | 12.78 (1H, s) | - | - | - | - |
| 8-CH ₂ N | - | 3.80 (2H, s) | - | 51.4 (CH ₂) | C-3'', 7'', 8, 9, 7 |
| 6-CH ₂ N | - | 3.80 (2H, s) | - | 52.9 (CH ₂) | C-10'', 14'', 6, 5, 7 |
| 3'', 7'' | - | 2.55 (4H, s) | - | 53.8 (CH ₂) | C-4'', 6'' |
| 10'', 14'' | - | 2.55 (4H, s) | - | 54.3 (CH ₂) | - |
| 4'', 6'' | - | 1.64 (4H, m) | - | 25.5 (CH ₂) | C-3'', 7'' |
| 11'', 13'' | - | 1.63 (4H, m) | - | 25.9 (CH ₂) | - |
| 5'' | - | 1.49 (2H, m) | - | 23.9 (CH ₂) | - |
| 12'' | - | 1.41 (2H, m) | - | 24.2 (CH ₂) | - |

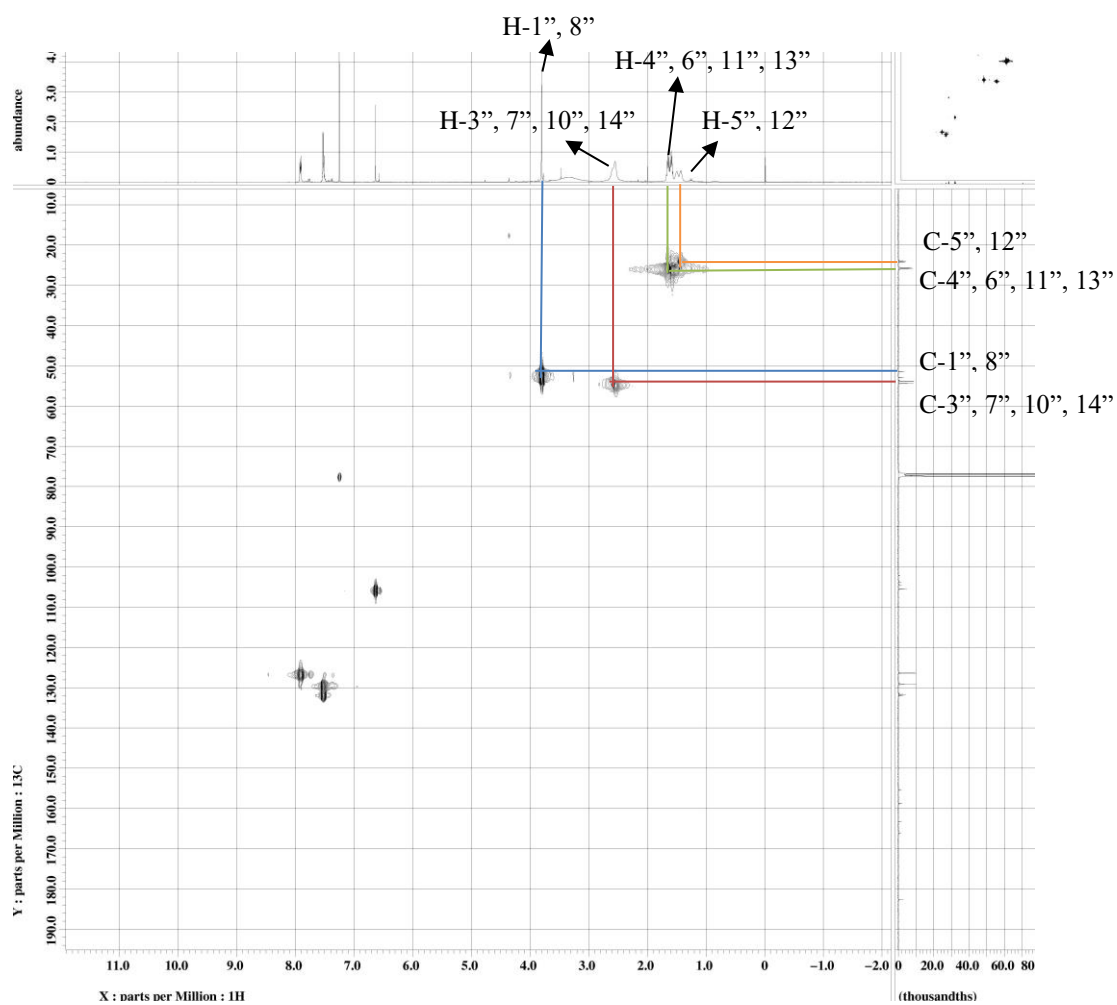
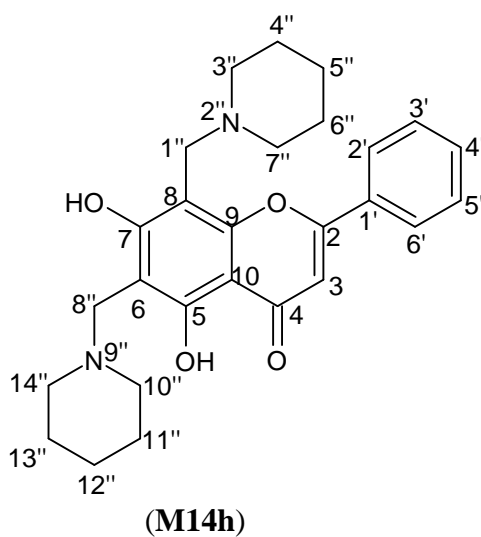
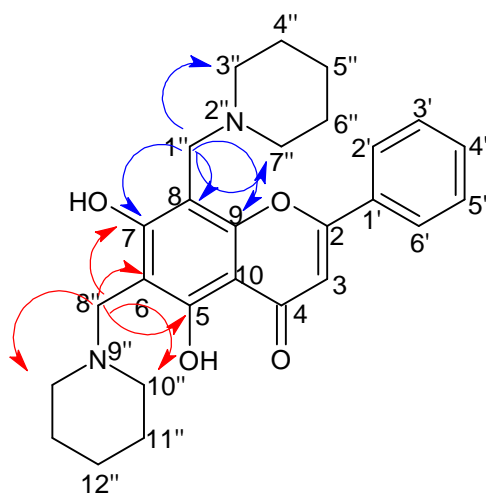


Figure 4.115: HMBC Spectrum of 5,7-dihydroxy-6,8-bis(piperidin-1-ylmethyl)-2-phenyl-4H-chromen-4-one (M14h)



(M14h)

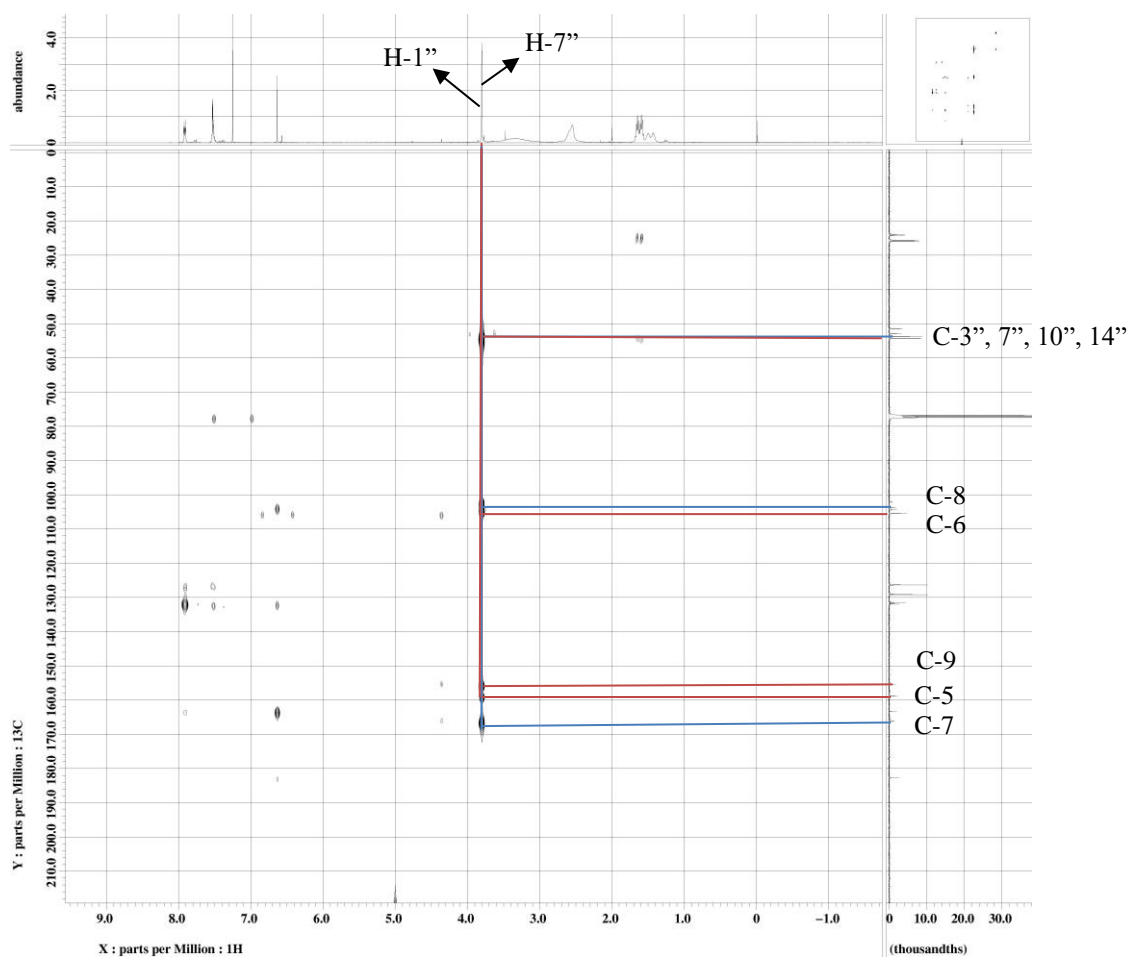
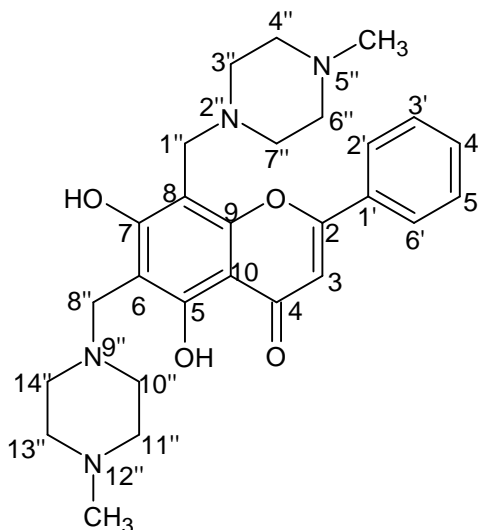


Figure 4.116: HMBC Spectrum of 5,7-dihydroxy-6,8-bis(piperidin-1-ylmethyl)-2-phenyl-4H-chromen-4-one (M14h)

4.3.5.3 Characterization of 5,7-dihydroxy-6,8-bis(4-methylpiperazin-1-ylmethyl)-2-phenyl-4*H*-chromen-4-one (M14i)



(M14i)

Compound **M14i** was obtained as yellow solid, mp 203-204 °C. In TLC plate, R_f value of 0.08 was obtained in mobile phase hexane:acetone 6:4. The percentage yield of **M14i** was obtained at 91.1%. The HRESIMS (Appendix A36) gave a pseudomolecular ion peak at $m/z = 479.2650$ $[M+H]^+$ which analysed for $C_{27}H_{34}N_4O_4$ (found 478.2577; calculated 478.2580). Table 4.53 shows the summary physical properties of **M14i**.

The IR spectrum of **M14i** (Appendix C36) shows absorption bands at 3435 (OH stretch), 2935, 2838 (CH_3 stretch), 1635 (C=O stretch), 1589 (C=C stretch), 1217 (C-N stretch), 1159 (C-O stretch) cm^{-1} .

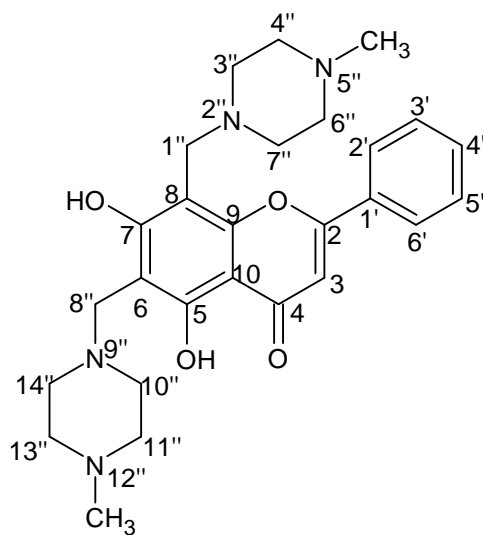
Table 4.53: Summary Physical Properties of M14i

| Compound | M14i |
|-------------------------|--|
| IUPAC Name | 5,7-dihydroxy-6,8-bis(4-methylpiperazin-1-ylmethyl)-2-phenyl-4 <i>H</i> -chromen-4-one |
| Molecular formula | C ₂₇ H ₃₄ N ₄ O ₄ |
| Molecular weight, g/mol | 478.2577 |
| Physical appearance | Yellow solid |
| Percentage yield, % | 91.1 |
| Obtained Mass, mg | 52.3 |
| R _f value | 0.08 |
| Melting point, °C | 203-204 |

The ¹H NMR of compound **M14i** (Figure 4.117) showed methylene proton signals at δ_H 3.83 (s) which belong to 6-CH₂N and 8-CH₂N. Signals at δ_H 2.26 (H-5''), δ_H 2.29 (H-12''), δ_H 2.33 (H-3'', 7'' and H-10'', 14'') and δ_H 2.65 (H-4'', 6'' and H-11'', 13'') were the characteristic peaks of 1-methylpiperazine moiety at C-6 and C-8. The rest of the peaks remain same with ¹H NMR of **M14** (Figure 4.23).

In ¹³C NMR (Figure 4.118) of compound **M14i**, signal at δ_c 50.5 and δ_c 52.0 were the methylene C-8 and methylene C-6, respectively. Signals at δ_c 45.8 (C-5''), δ_c 45.9 (C-12''), δ_c 52.4 (C-4'', 6''), δ_c 54.9 (C-10'', 14''), δ_c 54.7 (C-3'', 7''), and δ_c 54.9 (C-10'', 14'') were the characteristic peaks of 1-methylpiperazine moieties. In the HMBC spectrum (Figure 4.120), methylene H-6 showed two-bond correlations with C-6 (δ_c 100.4), and three-bond

correlations with C-5 (δ_c 161.5), C-7 (δ_c 166.6) and C-10'', 14'' (δ_c 54.9). Whereas, methylene H-8 displayed two bonds correlations with C-8 (δ_c 98.5), three bonds correlations with C-7 (δ_c 166.6), C-9 (δ_c 154.8) and C-3'', 7'' (δ_c 54.7) which belong to 1-methylpiperazine moiety. The structure was further confirmed by using DEPT (Appendix D72) and HMQC (Figure 4.119) spectra. Table 4.54 shows the summary NMR data of compounds **M14** and **M14i**.



(M14i)

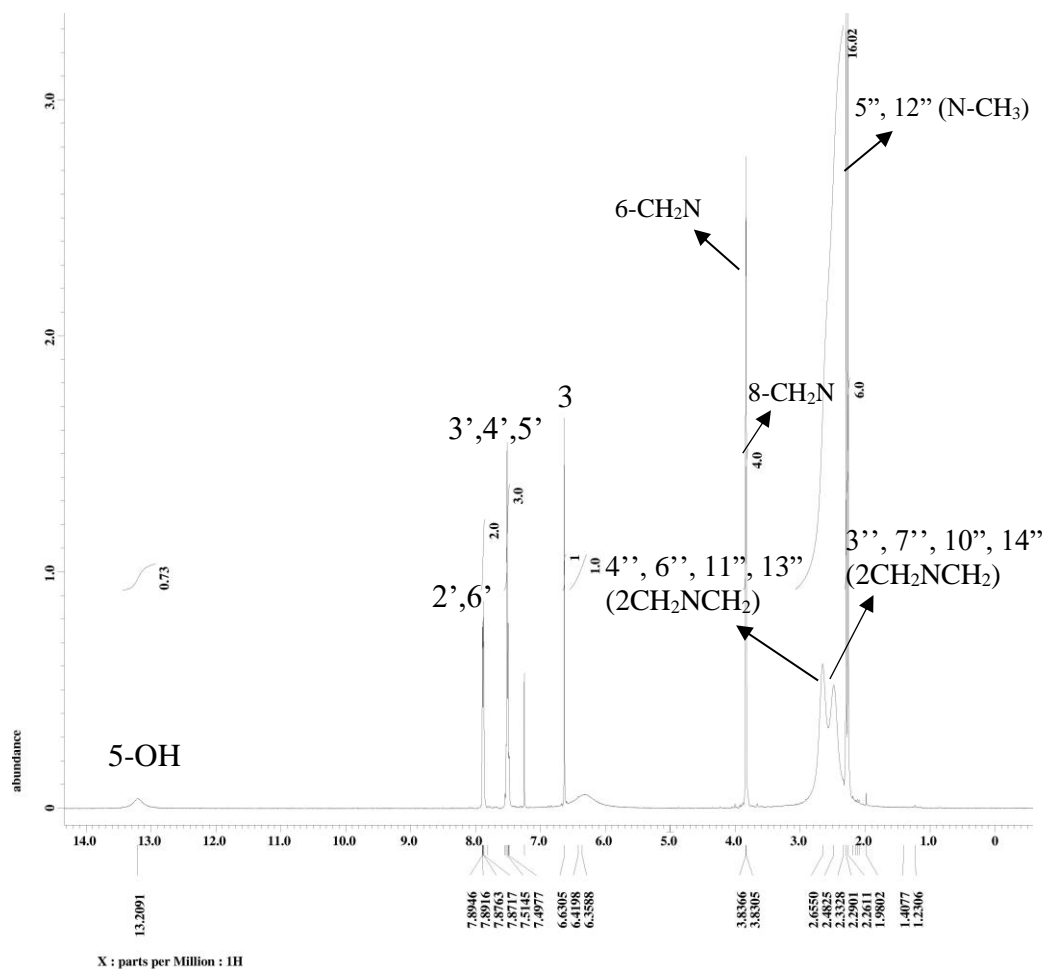
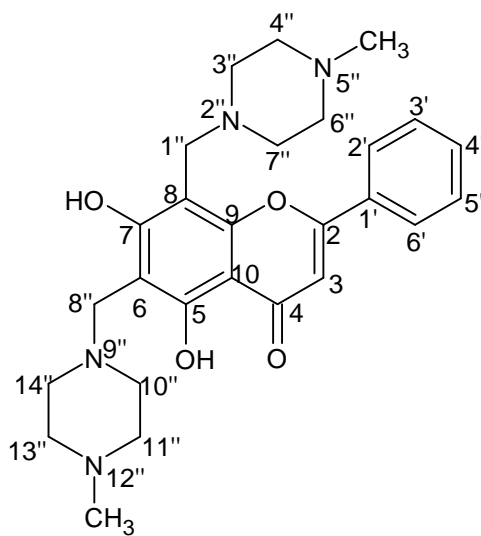


Figure 4.117: ^1H NMR (400 MHz, CDCl_3) of 5,7-dihydroxy-6,8-bis(4-methylpiperazin-1-ylmethyl)-2-phenyl-4H-chromen-4-one (M14i)



(M14i)

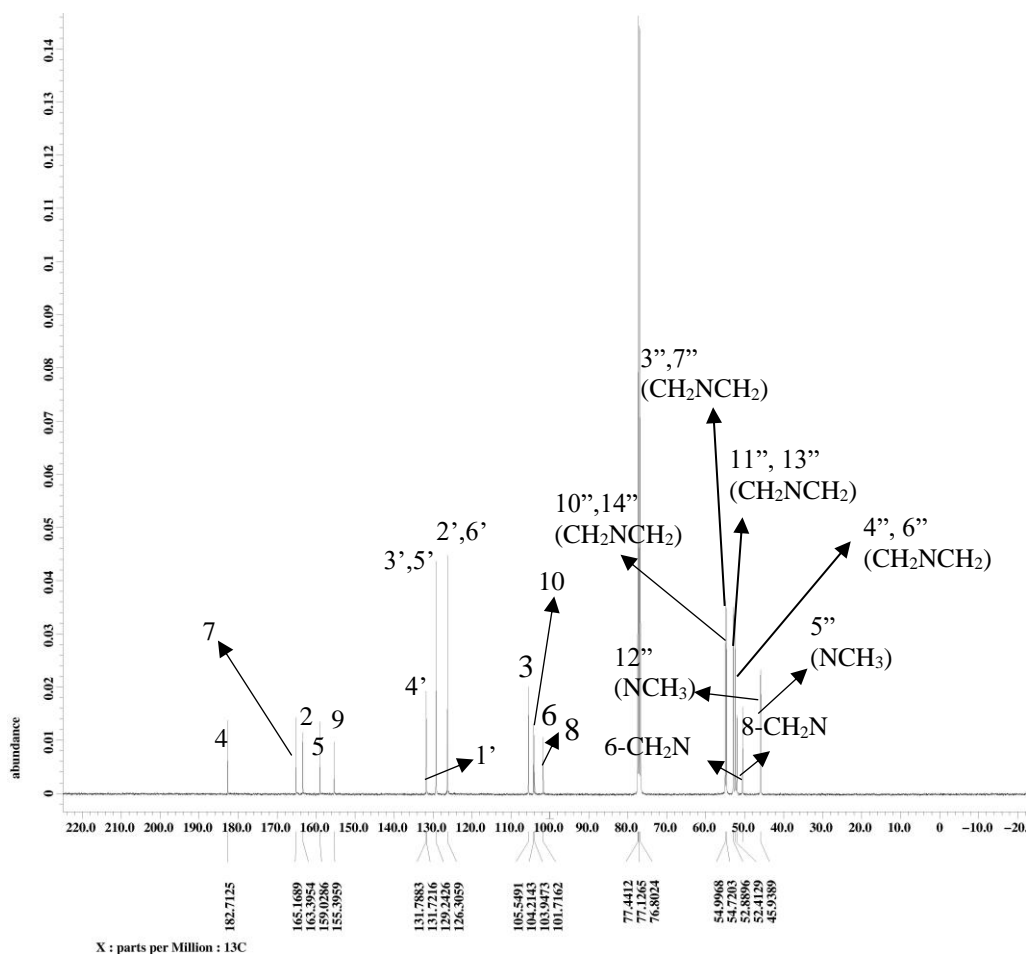
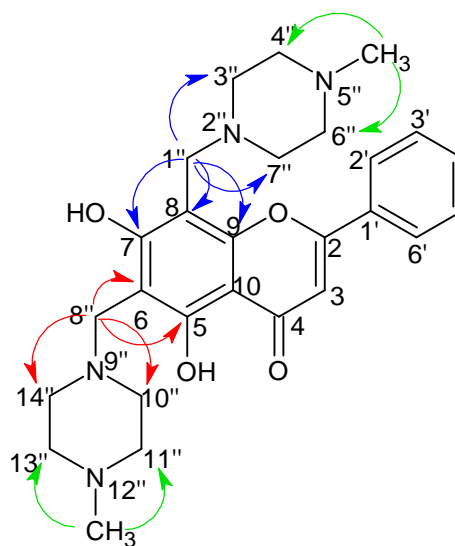


Figure 4.118: ¹³C NMR (100 MHz, CDCl₃) of 5,7-dihydroxy-6,8-bis(4-methylpiperazin-1-ylmethyl)-2-phenyl-4H-chromen-4-one (M14i)

Table 4.54: ¹H, ¹³C and HMBC spectral data of M14 (DMSO-d₆) and M14i (CDCl₃)

| Position | M14 δ _H (multiplicity) | M14i δ _H (multiplicity) | M14 δ _C (C-type) | M14i δ _C (C-type) | M14i HMBC |
|---------------------|--------------------------------------|---------------------------------------|--------------------------------|---------------------------------|---------------------|
| 2 | - | - | 163.6 (C) | 163.0 (C) | - |
| 3 | 6.91 (1H, s) | 6.63 (1H, s) | 105.6 (CH) | 105.9 (CH) | C-2, 1', 10, 4 |
| 4 | - | - | 182.3 (C) | 182.4 (C) | - |
| 5 | - | - | 161.9 (C) | 161.5 (C) | - |
| 6 | 6.17 (1H, d, <i>J</i> =1.8 Hz) | - | 99.5 (CH) | 100.4 (C) | - |
| 7 | - | - | 164.9 (C) | 166.6 (C) | - |
| 8 | 6.47 (1H, d, <i>J</i> =1.8 Hz) | - | 94.6 (CH) | 98.5 (C) | - |
| 9 | - | - | 157.9 (C) | 154.8 (C) | - |
| 10 | - | - | 104.5 (C) | 104.5 (C) | - |
| 1' | - | - | 131.2 (C) | 131.7 (C) | - |
| 2', 6' | 8.03 (2H, m) | 7.89 (2H, m) | 126.9 (CH) | 126.3 (CH) | C-2, 1', 3', 5' |
| 3', 5' | 7.53 (2H, m) | 7.51 (2H, m) | 129.6 (CH) | 129.1 (CH) | C-2', 6' |
| 4' | 7.53 (1H, m) | 7.51 (1H, m) | 133.5 (CH) | 131.7 (CH) | C-3', 5' |
| 5-OH | 12.78 (1H, s) | 13.20 (1H, s) | - | - | - |
| 8-CH ₂ N | - | 3.83 (2H, s) | - | 50.5 (CH ₂) | C-3'', 7'', 8, 9, 7 |
| 6-CH ₂ N | - | 3.83 (2H, s) | - | 52.0 (CH ₂) | C-10'', 14'', 6, 5 |
| 3'', 7'' | - | 2.33 (4H, s) | - | 54.7 (CH ₂) | - |
| 10'', 14'' | - | 2.33 (4H, s) | - | 54.9 (CH ₂) | - |
| 4'', 6'' | - | 2.65 (4H, s) | - | 52.4 (CH ₂) | - |
| 11'', 13'' | - | 2.65 (4H, s) | - | 52.8 (CH ₂) | - |
| 5'' | - | 2.29 (3H, s) | - | 45.8 (CH ₃) | - |
| 12'' | - | 2.26 (3H, s) | - | 45.9 (CH ₃) | - |



(M14i)

5''-NCH₃ / 12''-NCH₃

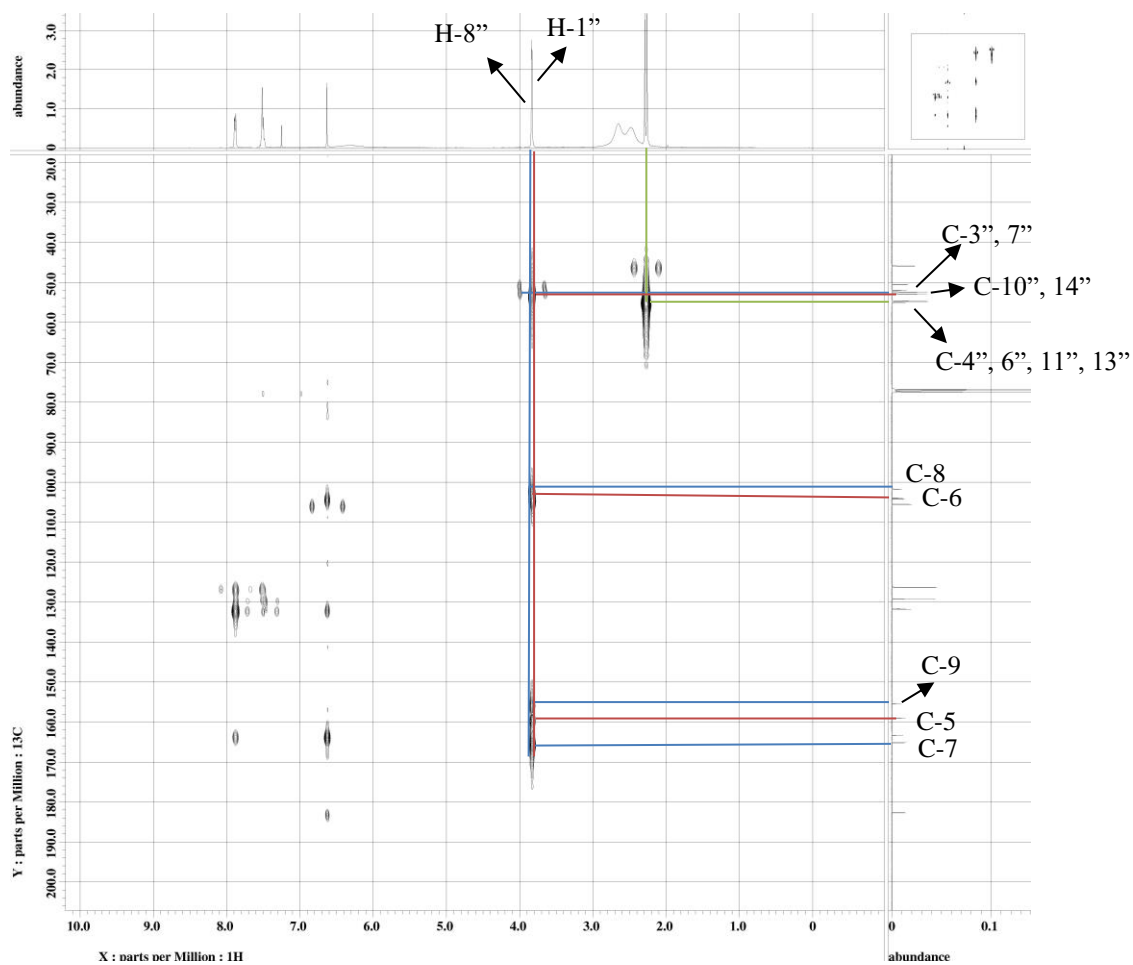
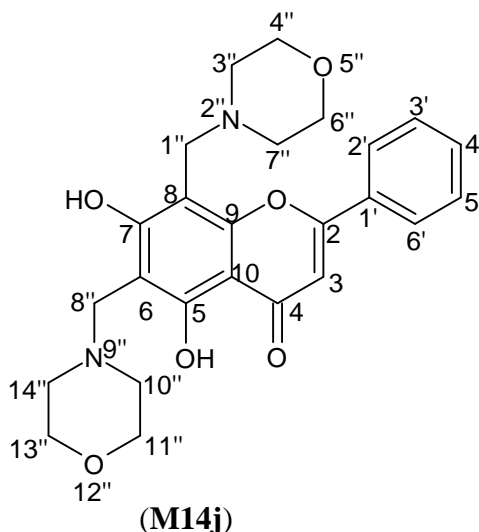


Figure 4.120: HMBC Spectrum of 5,7-dihydroxy-6,8-bis(4-methylpiperazin-1-ylmethyl)-2-phenyl-4H-chromen-4-one (M14i)

4.3.5.4 Characterization of 5,7-dihydroxy-6,8-bis(morpholinomethyl)-2-phenyl-4H-chromen-4-one (M14j)



Compound **M14j** was obtained as bright yellow solid, mp 186-188 °C. In TLC plate, R_f value of 0.14 was obtained in mobile phase hexane:acetone 6:3. The percentage yield of **M14j** was obtained at 77.5%. The HRESIMS (Appendix A37) gave a pseudomolecular ion peak at $m/z = 453.2021 [M+H]^+$ which analysed for $C_{25}H_{28}N_2O_6$ (found 452.1948; calculated 452.1947). Table 4.55 shows the summary physical properties of **M14j**.

The IR spectrum of **M14j** (Appendix C37) shows absorption bands at 3435 (OH stretch), 2937, 2838 (CH_3 stretch), 1635 (C=O stretch), 1587 (C=C stretch), 1285 (C-N stretch), 1114 (C-O stretch), 1006 (C-O-C stretch) cm^{-1} .

Table 4.55: Summary Physical Properties of M14j

| Compound | M14j |
|-------------------------|---|
| IUPAC Name | 5,7-dihydroxy-6,8-bis(morpholinomethyl)-2-phenyl-4H-chromen-4-one |
| Molecular formula | C ₂₅ H ₂₈ N ₂ O ₆ |
| Molecular weight, g/mol | 452.1948 |
| Physical appearance | Bright yellow solid |
| Percentage yield, % | 77.5 |
| Obtained Mass, mg | 32.9 |
| R _f value | 0.14 |
| Melting point, °C | 186-188 |

The ¹H NMR of compound **M14j** (Figure 4.121) showed methylene proton signals at δ_{H} 3.83 (s) and δ_{H} 3.84 (s) which belong to 6-CH₂N and 8-CH₂N. Signals at δ_{H} 2.60 (H-10'', 14''), δ_{H} 2.63 (H-3'', 7''), δ_{H} 3.72 (H-4'', 6'' and H-11'', 13'') were the characteristic peaks of morpholine moiety at C-6 and C-8. The rest of the peaks remain same with ¹H NMR of **M14** (Figure 4.23).

In ¹³C NMR (Figure 4.122) of compound **M14j**, signal at δ_{C} 51.1 and δ_{C} 52.1 were the methylene C-8 and methylene C-6, respectively. Signals at δ_{C} 52.4 (C-3'', 7''), δ_{C} 53.5 (C-10'', 14''), δ_{C} 66.7 (C-4'', 6'') and δ_{C} 67.0 (C-11'', 13'') were the characteristic peaks of morpholine moieties. In the HMBC spectrum (Figure 4.124), methylene H-6 displayed two bonds correlations with C-6 (δ_{C} 100.4), and three bonds correlations with C-5 (δ_{C} 159.2), C-7 (δ_{C} 164.7) and C-10'', 14'' (δ_{C} 53.5). Whereas, methylene H-8 displayed two bonds correlations

with C-8 (δ_c 101.3), three bonds correlations with C-7 (δ_c 164.7), C-9 (δ_c 155.4) and C-3'', 7'' (δ_c 52.4) which belong to morpholine moiety. The structure was further confirmed by using DEPT (Appendix D73) and HMQC (Figure 4.123) spectra. Table 4.56 shows the summary NMR data of compounds **M14** and **M14j**.

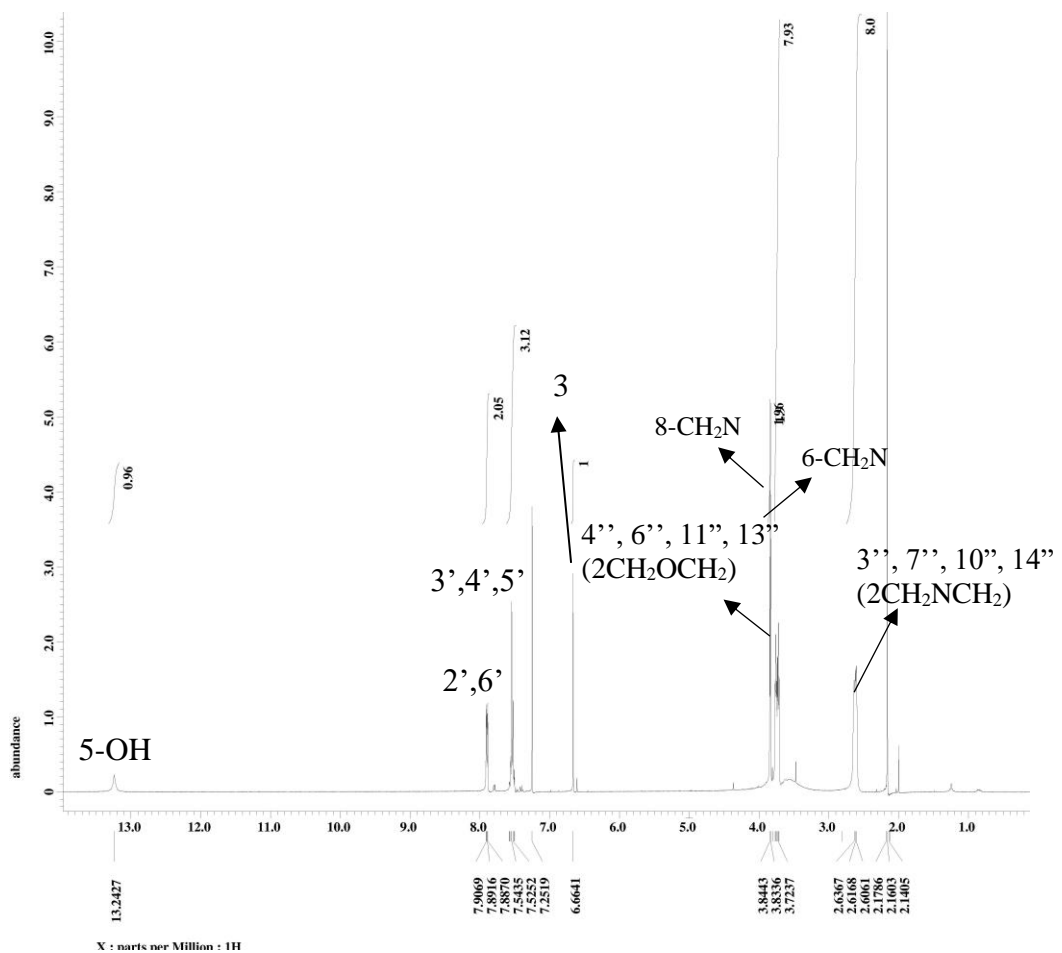
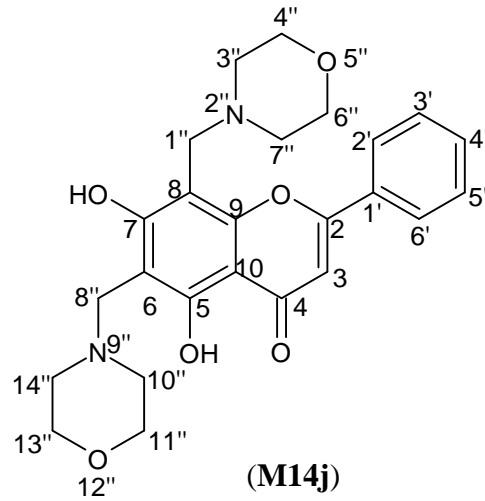


Figure 4.121: ¹H NMR (400 MHz, CDCl₃) of 5,7-dihydroxy-6,8-bis(morpholinomethyl)-2-phenyl-4H-chromen-4-one (M14j)

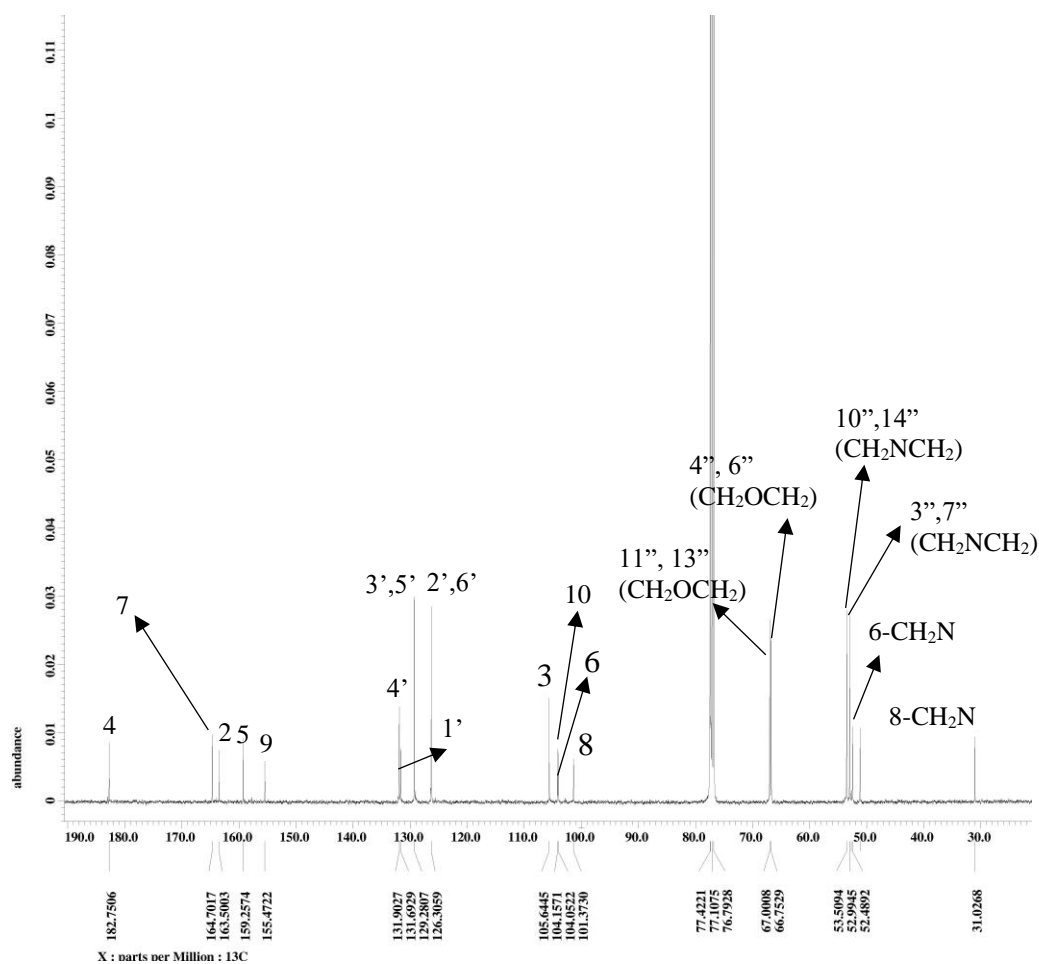
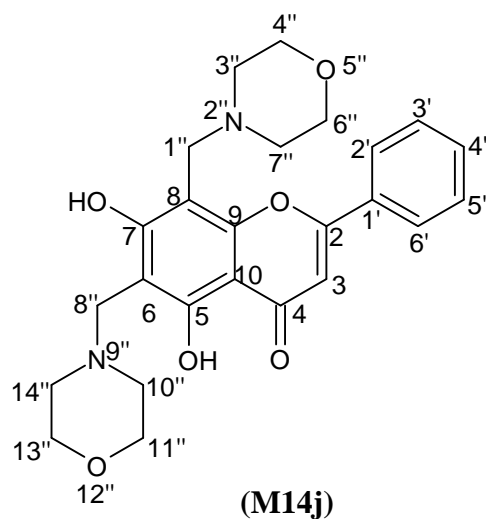
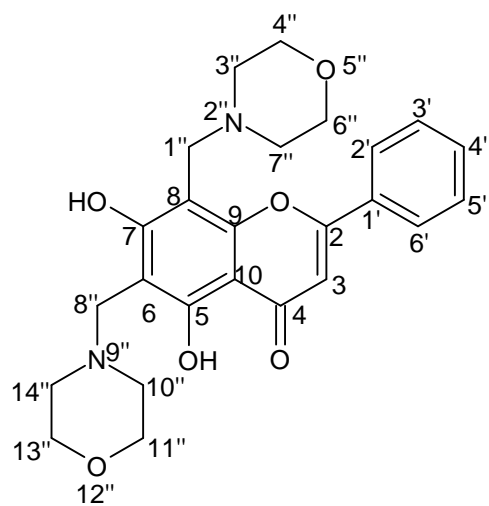


Figure 4.122: ¹³C NMR (100 MHz, CDCl₃) of 5,7-dihydroxy-6,8-bis(morpholinomethyl)-2-phenyl-4H-chromen-4-one (M14j)

Table 4.56: ^1H , ^{13}C and HMBC spectral data of M14 (DMSO- d_6) and M14j (CDCl_3)

| | M14 | M14j | M14 | M14j | M14j |
|--------------------------|------------------------------------|------------------------------------|------------------------------|------------------------------|---------------------|
| Position | δ_{H} (multiplicity) | δ_{H} (multiplicity) | δ_{C} (C-type) | δ_{C} (C-type) | HMBC |
| 2 | - | - | 163.6 (C) | 163.5 (C) | - |
| 3 | 6.91 (1H, s) | 6.66 (1H, s) | 105.6 (CH) | 105.6 (CH) | C-2, 1', 10, 4 |
| 4 | - | - | 182.3 (C) | 182.7 (C) | - |
| 5 | - | - | 161.9 (C) | 159.2 (C) | - |
| 6 | 6.17 (1H, d, $J=1.8$ Hz) | - | 99.5 (CH) | 104.0 (C) | - |
| 7 | - | - | 164.9 (C) | 164.7 (C) | - |
| 8 | 6.47 (1H, d, $J=1.8$ Hz) | - | 94.6 (CH) | 101.3 (C) | - |
| 9 | - | - | 157.9 (C) | 155.4 (C) | - |
| 10 | - | - | 104.5 (C) | 104.1 (C) | - |
| 1' | - | - | 131.2 (C) | 131.6 (C) | - |
| 2', 6' | 8.03 (2H, m) | 7.89 (2H, m) | 126.9 (CH) | 126.3 (CH) | C-2, 1', 3', 5' |
| 3', 5' | 7.53 (2H, m) | 7.54 (2H, m) | 129.6 (CH) | 129.2 (CH) | C-2', 6' |
| 4' | 7.53 (1H, m) | 7.54 (1H, m) | 133.5 (CH) | 131.9 (CH) | C-3', 5' |
| 5-OH | 12.78 (1H, s) | 13.24 (1H, s) | - | - | - |
| 8- CH_2N | - | 3.84 (2H, s) | - | 51.1 (CH_2) | C-3'', 7'', 8, 9, 7 |
| 6- CH_2N | - | 3.83 (2H, s) | - | 52.1 (CH_2) | C-10'', 14'', 6, 5 |
| 3'', 7'' | - | 2.63 (4H, s) | - | 52.4 (CH_2) | C-3'', 7'' |
| 10'', 14'' | - | 2.60 (4H, s) | - | 53.5 (CH_2) | C-10'', 14'' |
| 4'', 6'' | - | 3.72 (4H, s) | - | 66.7 (CH_2) | - |
| 11'', 13'' | - | 3.75 (4H, s) | - | 67.0 (CH_2) | - |



(M14j)

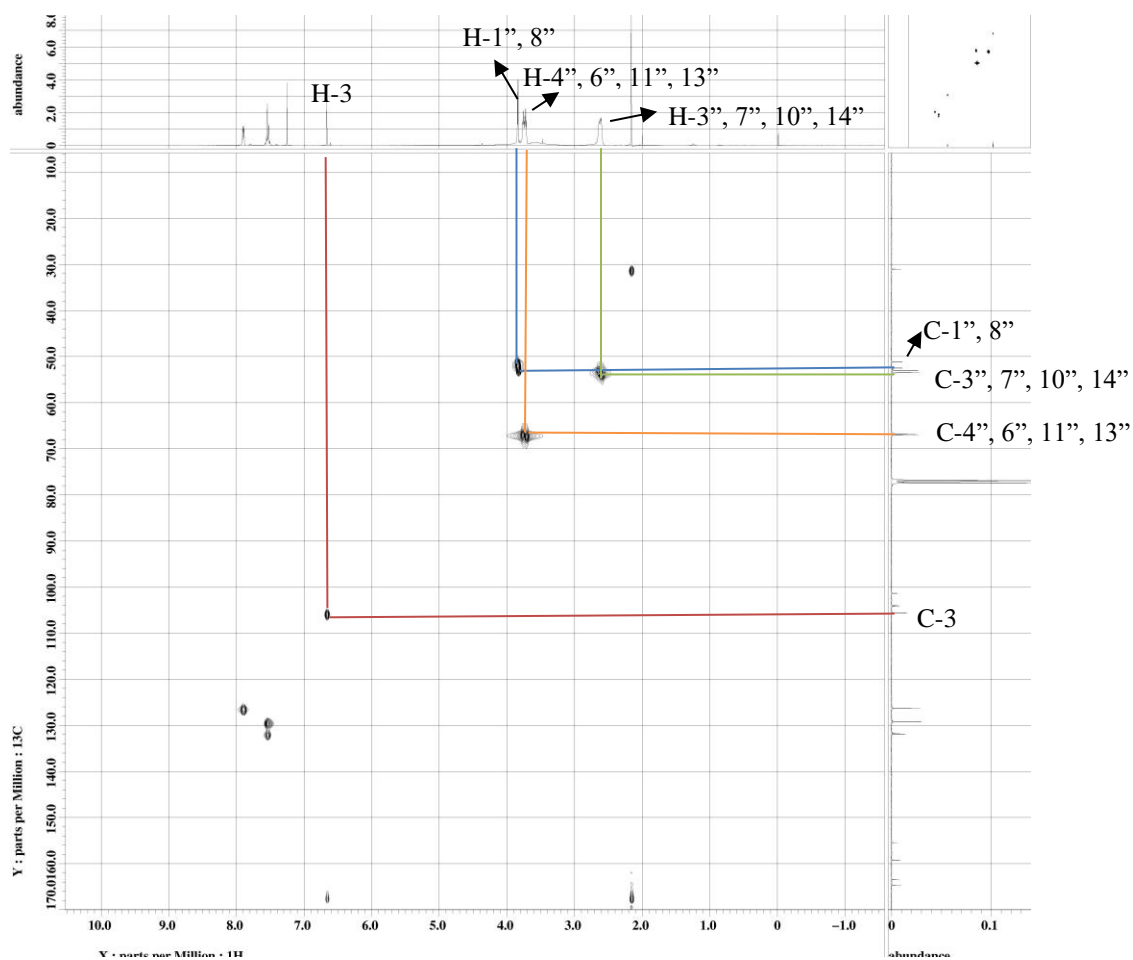
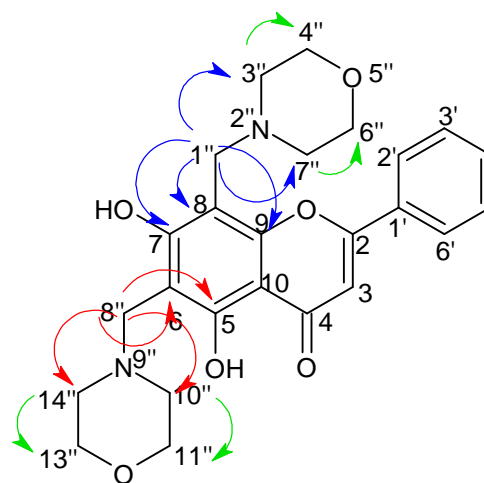


Figure 4.123: HMQC Spectrum of 5,7-dihydroxy-6,8-bis(morpholinomethyl)-2-phenyl-4H-chromen-4-one (M14j)



(M14j)

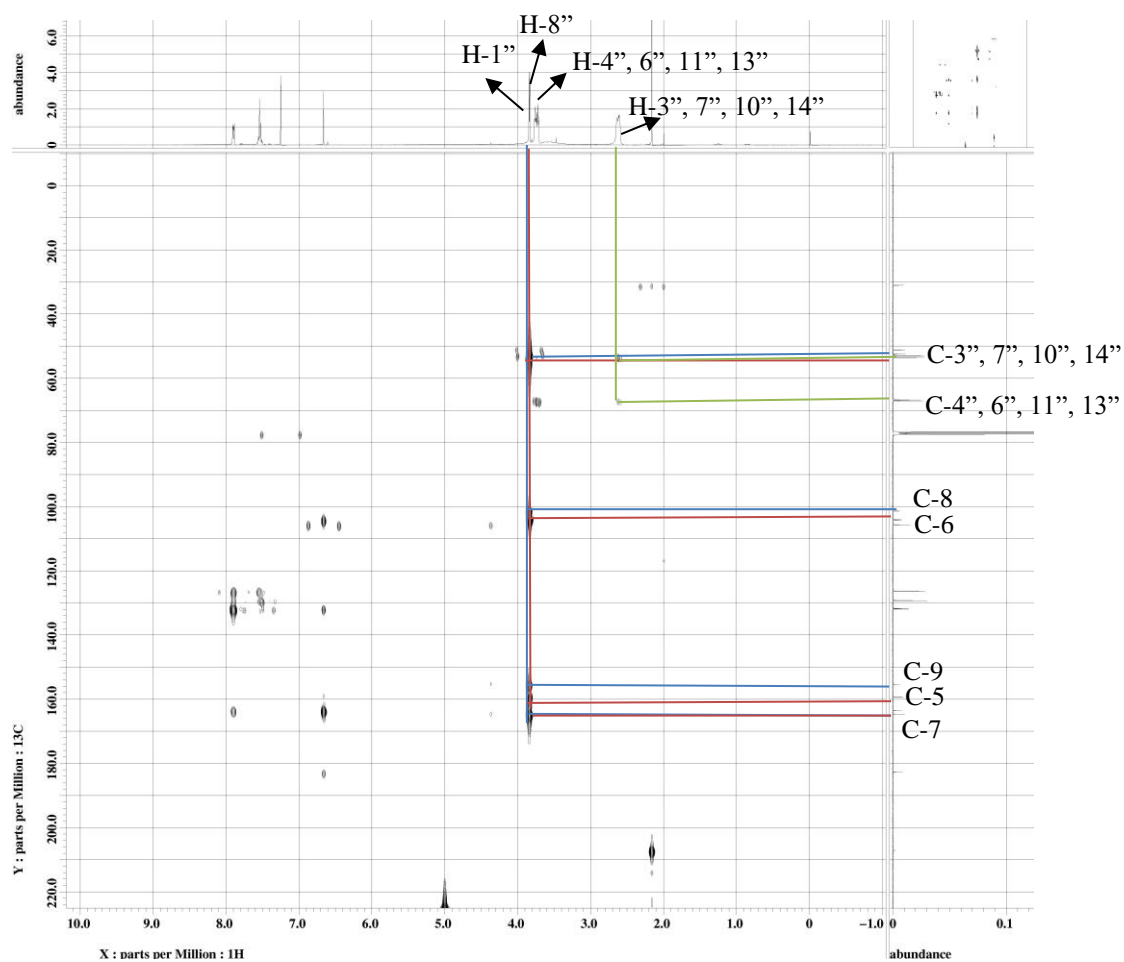
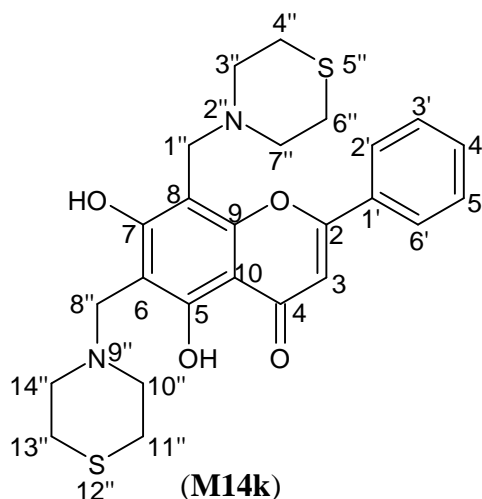


Figure 4.124: HMBC Spectrum of 5,7-dihydroxy-6,8-bis(morpholinomethyl)-2-phenyl-4H-chromen-4-one (M14j)

4.3.5.5 Characterization of 5,7-dihydroxy-6,8-bis(thiomorpholinomethyl)-2-phenyl-4H-chromen-4-one (M14k)



Compound **M14k** was obtained as bright yellow solid, mp 208-210 °C. In TLC plate, R_f value of 0.20 was obtained in mobile phase hexane:acetone 6:3. The percentage yield of **M14k** was obtained at 92.2%. The HRESIMS (Appendix A38) gave a pseudomolecular ion peak at $m/z = 485.1568$ $[M+H]^+$ which analysed for $C_{25}H_{28}N_2O_4S_2$ (found 484.1495; calculated 484.1490). Table 4.57 shows the summary physical properties of **M14k**.

The IR spectrum of **M14k** (Appendix C38) shows absorption bands at 3467 (OH stretch), 2925, 2831 (CH_3 stretch), 1635 (C=O stretch), 1586 (C=C stretch), 1286 (C-N stretch), 1131 (C-O stretch) cm^{-1} .

Table 4.57: Summary Physical Properties of M14k

| Compound | M14k |
|-------------------------|--|
| IUPAC Name | 5,7-dihydroxy-6,8-bis(thiomorpholinomethyl)-2-phenyl-4H-chromen-4-one |
| Molecular formula | C ₂₅ H ₂₈ N ₂ O ₄ S ₂ |
| Molecular weight, g/mol | 484.1495 |
| Physical appearance | Bright yellow solid |
| Percentage yield, % | 94.9 |
| Obtained Mass, mg | 55.2 |
| R _f value | 0.20 |
| Melting point, °C | 186-188 |

The ¹H NMR of compound **M14k** (Figure 4.125) showed methylene proton signals at δ_{H} 3.83 (s) which belong to 6-CH₂N and 8-CH₂N. Signals at δ_{H} 2.69 (H-10'', 14''), δ_{H} 2.72 (H-3'', 7''), δ_{H} 2.86 (H-11'', 13''), δ_{H} 2.87 (H-4'', 6'') were the characteristic peaks of thiomorpholine moiety at C-6 and C-8. The rest of the peaks remain same with ¹H NMR of **M14** (Figure 4.23).

In ¹³C NMR (Figure 4.126) of compound **M14k**, signal at δ_{C} 51.5 and δ_{C} 52.8 were the methylene C-8 and methylene C-6, respectively. Signals at δ_{C} 27.7 (C-3'', 7''), δ_{C} 28.0 (C-10'', 14''), δ_{C} 54.3 (C-4'', 6'') and δ_{C} 54.8 (C-11'', 13'') were the characteristic peaks of thiomorpholine moieties. In the HMBC spectrum (Figure 4.128), methylene H-6 displayed two bonds correlations with C-6 (δ_{C} 104.1), and three bonds correlations with C-5 (δ_{C} 159.2), C-7 (δ_{C} 164.8)

and C-10'', 14'' (δ_c 28.0). Whereas, methylene H-8 displayed two bonds correlations with C-8 (δ_c 101.6), three bonds correlations with C-7 (δ_c 164.8), C-9 (δ_c 155.4) and C-3'', 7'' (δ_c 27.7) which belong to morpholine moiety. The structure was further confirmed by using DEPT (Appendix D74) and HMQC (Figure 4.127) spectra. Table 4.58 shows the summary NMR data of compounds **M14** and **M14k**.

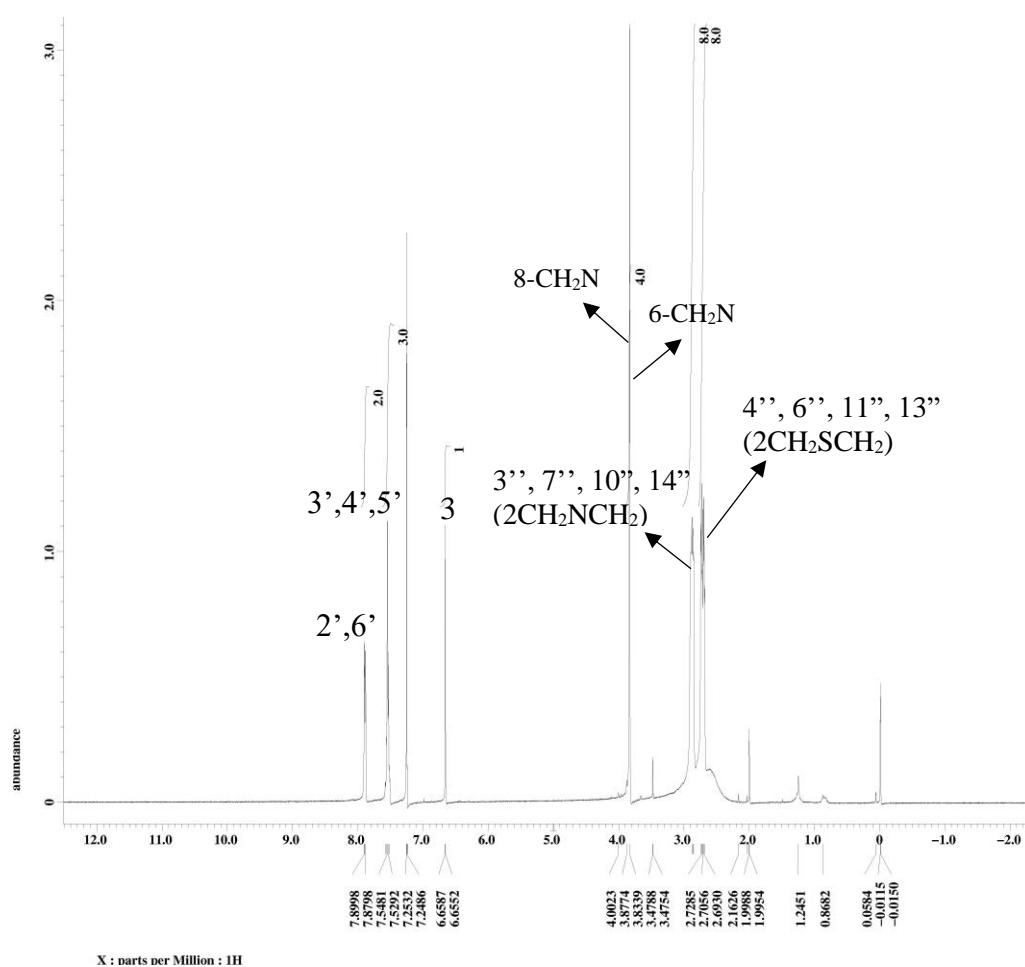
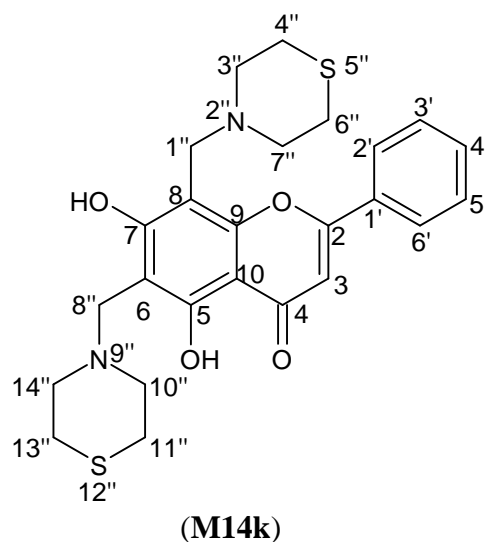
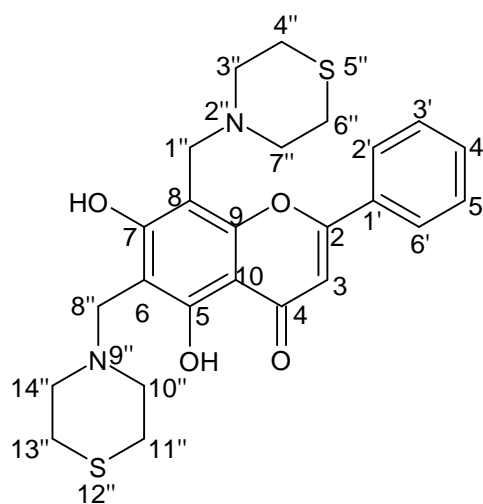


Figure 4.125: ¹H NMR (400 MHz, CDCl₃) of 5,7-dihydroxy-6,8-bis(thiomorpholinomethyl)-2-phenyl-4H-chromen-4-one (M14k)



(M14k)

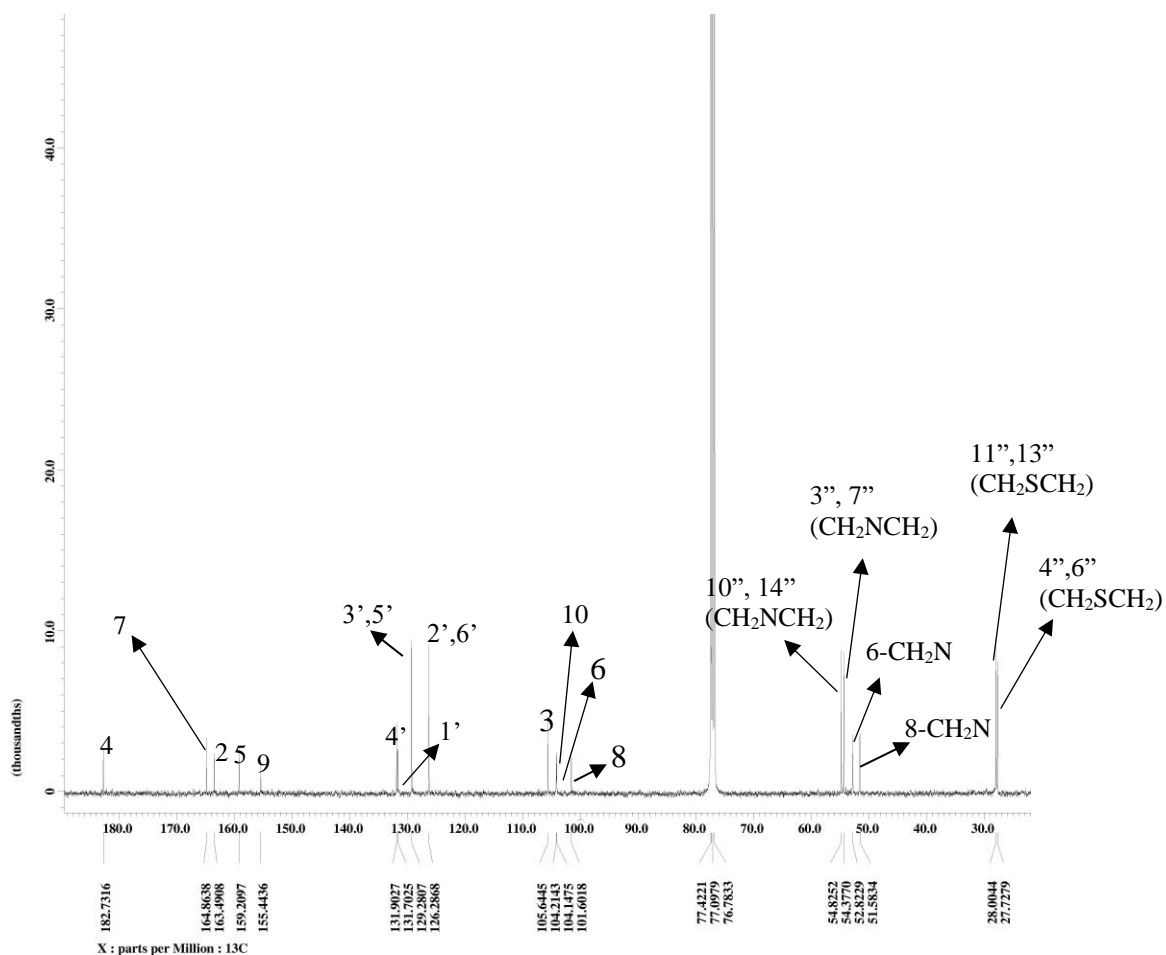
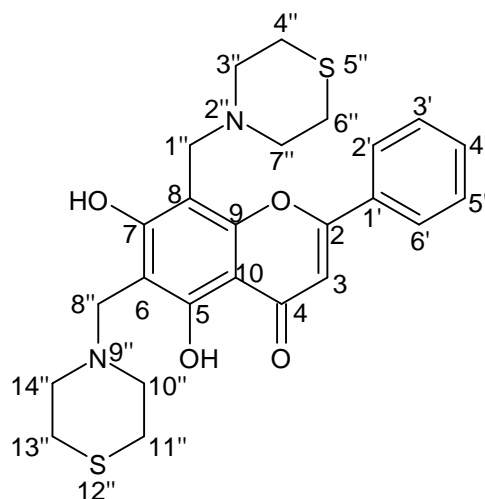


Figure 4.126: ¹³C NMR (100 MHz, CDCl₃) of 5,7-dihydroxy-6,8-bis(thiomorpholinomethyl)-2-phenyl-4H-chromen-4-one (M14k)

Table 4.58: ¹H, ¹³C and HMBC spectral data of M14 (DMSO-d₆) and M14k (CDCl₃)

| | M14 | M14k | M14 | M14k | M14k |
|---------------------|--------------------------------|-------------------------------|-------------------------|-------------------------|--------------------------|
| Position | δ _H (multiplicity) | δ _H (multiplicity) | δ _C (C-type) | δ _C (C-type) | HMBC |
| 2 | - | - | 163.6 (C) | 163.4 (C) | - |
| 3 | 6.91 (1H, s) | 6.65 (s) | 105.6 (CH) | 105.6 (CH) | C-2, 1', 10, 4 |
| 4 | - | - | 182.3 (C) | 182.7 (C) | - |
| 5 | - | - | 161.9 (C) | 159.2 (C) | - |
| 6 | 6.17 (1H, d, <i>J</i> =1.8 Hz) | - | 99.5 (CH) | 104.1 (C) | - |
| 7 | - | - | 164.9 (C) | 164.8 (C) | - |
| 8 | 6.47 (1H, d, <i>J</i> =1.8 Hz) | - | 94.6 (CH) | 101.6 (C) | - |
| 9 | - | - | 157.9 (C) | 155.4 (C) | - |
| 10 | - | - | 104.5 (C) | 104.2 (C) | - |
| 1' | - | - | 131.2 (C) | 131.7 (C) | - |
| 2', 6' | 8.03 (2H, m) | 7.89 (2H, m) | 126.9 (CH) | 126.2 (CH) | C-2, 1', 3', 5' |
| 3', 5' | 7.53 (2H, m) | 7.54 (2H, m) | 129.6 (CH) | 129.2 (CH) | C-2', 6' |
| 4' | 7.53 (1H, m) | 7.54 (1H, m) | 133.5 (CH) | 131.9 (CH) | C-3', 5' |
| 5-OH | 12.78 (1H, s) | 13.24 (1H, s) | - | - | - |
| 8-CH ₂ N | - | 3.83 (2H, s) | - | 51.5 (CH ₂) | C-3'', 7'', 8, 9, 7 |
| 6-CH ₂ N | - | 3.83 (2H, s) | - | 52.8 (CH ₂) | C-10'', 14'', 6, 5 |
| 3'', 7'' | - | 2.72 (4H, s) | - | 27.7 (CH ₂) | C-3'', 7'', 4'', 6'' |
| 10'', 14'' | - | 2.69 (4H, s) | - | 28.0 (CH ₂) | C-10'', 14'' |
| 4'', 6'' | - | 2.87 (4H, s) | - | 54.3 (CH ₂) | C-4'', 6'' |
| 11'', 13'' | - | 2.86 (4H, s) | - | 54.8 (CH ₂) | C-11'', 13'', 10'', 14'' |



(M14k)

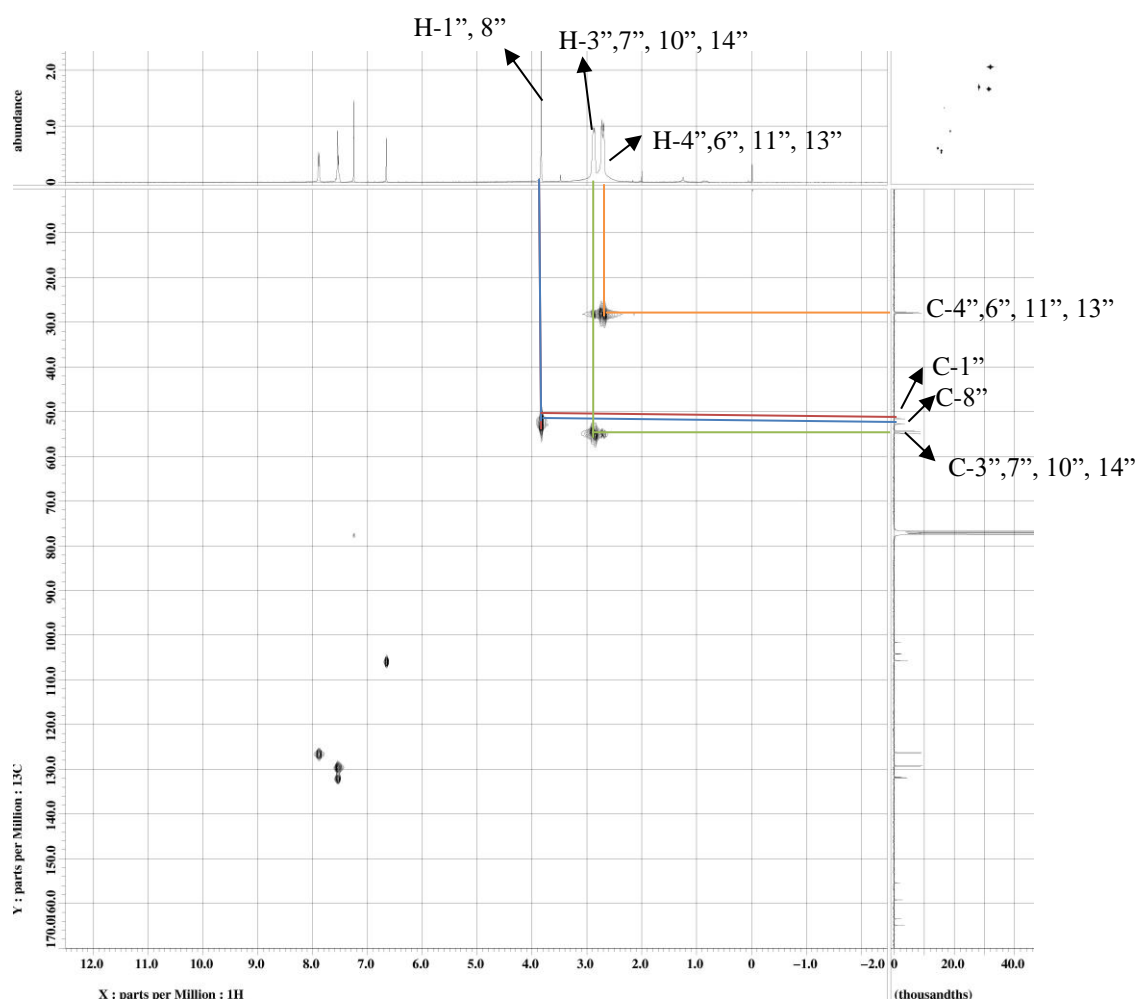
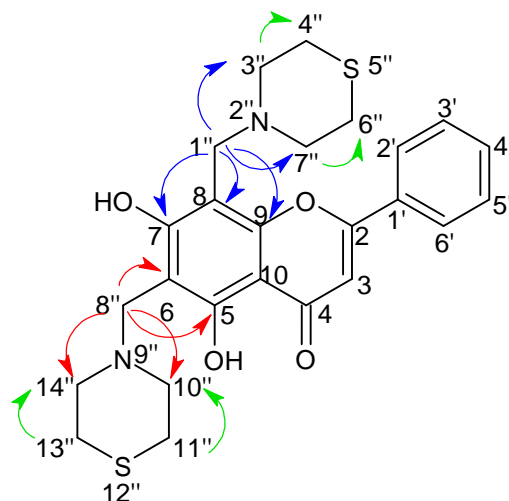


Figure 4.127: HMBC Spectrum of 5,7-dihydroxy-6,8-bis(thiomorpholinomethyl)-2-phenyl-4H-chromen-4-one (M14k)



(M14k)

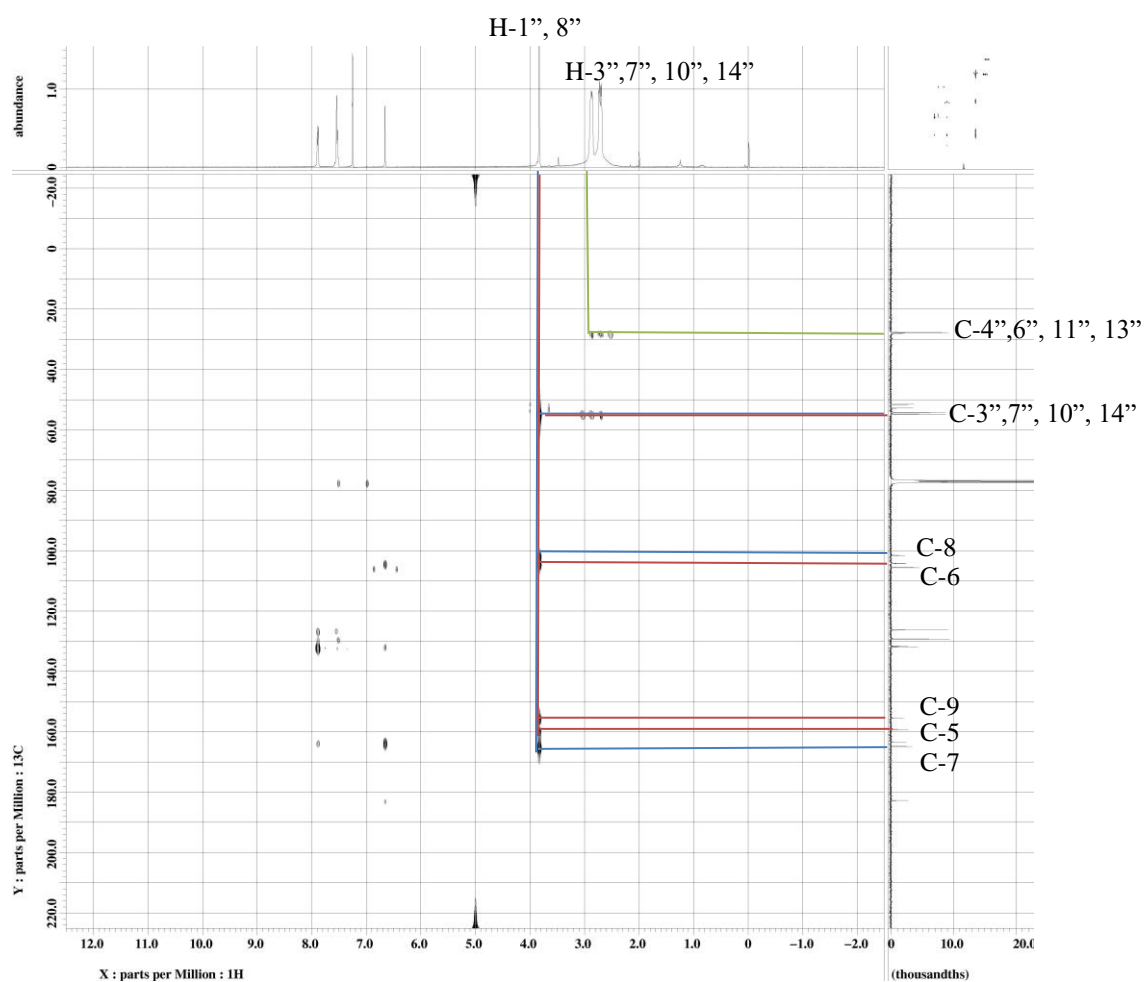


Figure 4.128: HMBC Spectrum of 5,7-dihydroxy-6,8-bis(thiomorpholinomethyl)-2-phenyl-4H-chromen-4-one (M14k)

4.4 Cytotoxic Activity

Cytotoxic activity of parent compounds and synthesized Mannich bases were evaluated against two breast cancer cell lines i.e. MCF-7, MDA-MB-231, and one normal breast cell line, MCF-10A via MTT assay. The cytotoxic results were shown in Table 4.59.

For MCF-7 cell line, the parent compounds and all the Mannich bases showed moderate activity with the IC₅₀ range of 9.17-68.5 μ M. For statistical analysis, in the case of chalcones (**M2**, **M2a-b**, **M4**, **M4a-b**), ‘*’ indicates the anticancer activity of **M2a-b** and **M4a-b** is significantly different from **M4**. Compounds with the same alphabets indicate no difference in the anticancer activity, whereas compounds with the different alphabets indicate their anticancer activity are significantly different from each other. The anticancer activity on MCF-7 cells for the following set of compounds is the same. i) **M2**, **M2a**, **M2b**, **M5** and **M5a** ; ii) **M4a**, **M14a**, **M14b**, **M14e**, **M14f**, **M14g**, **M14h** and **M14j** ; iii) **M4b**, **M14c**, **M14d**, **M14i** and **M14k** ; iv) **M5b**, **M5c**, **M5d**, and **M5e**. In the case of flavonoids (**M5**, **M5a-e**, **M14**, **M14a-k**), ‘*’ indicates the anticancer activity of (**M5**, **M14a-k**) is significantly different from **M14**. The anticancer activity of flavonoids (**M5**, **M14a-k**) is lower than that of **M14**.

Table 4.59: Cytotoxic results of parent compounds and synthesized Mannich Bases against cancer and normal cell lines

| Compounds | (IC ₅₀), μM | | |
|--------------------|-------------------------------|------------------------------------|---------------------------------|
| | MCF-7 (IC ₅₀), μM | MDA-MB-231 (IC ₅₀), μM | MCF-10A (IC ₅₀), μM |
| M2 | 68.5 ± 1.66 ^{*,c} | >100 | >100 |
| M2a | 62.44 ± 1.84 ^{*,c} | 66.66 ± 1.52 ^c | >100 |
| M2b | 67.83 ± 1.88 ^{*,c} | 44.12 ± 1.25 ^d | >100 |
| M4 | 52.21 ± 4.83 | >100 | 31.56 ± 0.97 |
| M4a | 43.27 ± 2.42 ^{*,a} | 87.27 ± 3.82 ^a | >100 |
| M4b | 31.86 ± 3.27 ^{*,b} | 56.43 ± 4.61 ^b | >100 |
| M5 | 28.16 ± 1.73 ^{*,c} | >100 | 30.65 ± 1.59 [*] |
| M5a | 27.11 ± 1.77 ^{*,c} | 51.04 ± 2.41 [*] | >100 |
| M5b | 37.40 ± 0.91 ^{*,d} | 51.34 ± 2.20 [*] | >100 |
| M5c | 34.32 ± 0.19 ^{*,d} | 36.61 ± 1.08 | >100 |
| M5d | 32.38 ± 1.21 ^{*,d} | 15.25 ± 1.11 [*] | >100 |
| M5e | 37.62 ± 2.47 ^{*,d} | 30.14 ± 1.52 [*] | >100 |
| M14 | 9.17 ± 1.21 | 40.27 ± 2.14 | 10.55 ± 1.05 |
| M14a | 14.54 ± 3.08 ^{*,a} | 37.35 ± 1.25 | >100 |
| M14b | 12.84 ± 1.94 ^{*,a} | 39.11 ± 1.05 | >100 |
| M14c | 18.12 ± 1.71 ^{*,b} | 24.45 ± 1.55 [*] | >100 |
| M14d | 16.33 ± 0.82 ^{*,b} | 33.67 ± 1.03 [*] | >100 |
| M14e | 13.52 ± 0.48 ^{*,a} | 34.23 ± 0.90 [*] | >100 |
| M14f | 14.08 ± 1.97 ^{*,a} | 5.75 ± 0.82 [*] | >100 |
| M14g | 11.45 ± 2.06 ^{*,a} | 34.04 ± 1.48 [*] | >100 |
| M14h | 11.44 ± 1.42 ^{*,a} | 35.68 ± 2.88 [*] | >100 |
| M14i | 17.66 ± 1.42 ^{*,b} | 38.74 ± 3.08 | >100 |
| M14j | 12.18 ± 0.61 ^{*,a} | 12.06 ± 0.17 [*] | >100 |
| M14k | 18.76 ± 1.72 ^{*,b} | 22.73 ± 1.52 [*] | >100 |
| Doxorubicin | 1.52 ± 0.06 | 2.86 ± 0.25 | 3.92 ± 0.11 |

Note: The ‘*’ indicates significant difference (P<0.05).

Cytotoxic activity against MDA-MB-231 cancer cell line showed that chalcone and flavone based Mannich bases exhibited greater cytotoxic activity than parent compounds. Chalcone Mannich bases **M2a** and **M2b** showed inhibition towards MDA-MB-231 cell line with IC_{50} of 66.66 and 44.12 μM , respectively. Whereas parent compound **M2** showed IC_{50} of $>100 \mu\text{M}$ towards MDA-MB-231 cell line. For **M4a** and **M4b**, these compounds exhibited IC_{50} of 87.27 and 56.43 μM towards MDA-MB-231 cell line, respectively which showed better cytotoxic activity than parent compound **M4** ($IC_{50} > 100 \mu\text{M}$). In the case of compounds (**M2**, **M2a-b**, **M4**, and **M4a-b**), the statistical significance of differences in the activity of compounds (**M2a-b**, **M4a-b**, **M2**) with respect to that of **M4** cannot be calculated because the IC_{50} value of **M4** is greater than 100 μM , the highest concentration used in this study. In general, the compounds (**M2**, **M2a-b**, **M4a-b**, except **M2a**) are found to be more active than **M4**.

From the results, it supported the hypothesis that biological activity of nitrogen containing flavonoids were improved compared to the naturally flavonoids without the presence of nitrogen atom (Wilhelm et al., 2015). For cytotoxicities of the chalcone Mannich bases, **M2b** and **M4b** which incorporate with morpholine showed higher improvement on cytotoxicity toward MDA-MB-231 compared to **M2a** and **M4a** which incorporate with piperidine moiety. For **M2b** and **M4b**, they exhibited cytotoxicity activity against MDA-MB-231 with IC_{50} values of 44.12 μM , and 56.43 μM , respectively. Whereas for **M2a** and **M4a**, they exhibited cytotoxicity against MDA-MB-231 with IC_{50} values of 66.66 μM and 87.27 μM , respectively. **M2b** with methoxy group at 3'-position

showed higher toxicity against MDA-MB-231 compared to **M4b** without the presence of methoxy group. This showed that the potency of the compound will increase as the lipophilicity increases (Hieu et al., 2012).

According to Hieu et al. (2012), the improved activity that shown by chalcone Mannich bases were due to the deamination of chalcone Mannich bases into the corresponding cyclohexadienones. This will create a further site for cellular thiols to attack as nucleophile.

For flavone **M5** Mannich bases, **M5a-e** displayed inhibition towards MDA-MB-231 cell line with the IC_{50} ranged from 15.25 – 51.34 μ M which showed improved activity than parent compound **M5** which $IC_{50} > 100 \mu$ M. Among flavone **M5** Mannich bases, **M5d** which incorporate with morpholine also showed the highest improvement on cytotoxicity toward MDA-MB-231 compared to others amine moiety. **M5d** exhibited cytotoxicity against MDA-MB-231 with IC_{50} values of 15.25 μ M.

For flavone **M14**, Mannich based **M14a-k** also exhibited improved activity towards MDA-MB-231 cell line than parent compound **M14** ($IC_{50} = 40.27 \mu$ M) with IC_{50} ranged from 5.75-39.11 μ M. Among them, Mannich bases **M14f** showed the highest cytotoxic activity against MDA-MB-231 cell with IC_{50} of $5.75 \pm 0.82 \mu$ M. It was due to the presence of the benzylamine moiety in the structure which will increase the hydrophobicity of molecule. It was reported

that the cytotoxicity will be enhanced with the increase in the general hydrophobicity of the molecule (Roman, 2015). In the case of compounds (**M5**, **M5a-b**, **M14**, **M14a-k**), ‘*’ indicates the anticancer activity of **M5**, **M5a-b**, **M14a-b** is significantly different from **M14**. Out of the compounds **M5**, **M5a-d**, **M14a-k**, only **M5d-e**, **M14c-h**, **M14j-k** are found to be more active than **M14**. The compounds **M5a-b** are less active than **M14**. The compound **M5** was found to be inactive. Compounds without ‘*’ indicates no significant difference in activity to that of **M14**.

According to Nguyen et al. (2015), biological potency may increase due to the presence of amine moiety in flavonoid molecule. The presence of amine moiety has greater number of molecular sites for electrophilic attack by cellular constituents and the cascade effect of preferential chemosensitization. Liu et al. (2012) found out that apigenin with the piperazin-1-yl-ethoxy group that present at C-8 position, highest potency was obtained. The antiproliferative activity of apigenin analogs was critical when the nitrogen atom at the C-8 position of apigenin.

For cytotoxic activity against MCF-10A cell line, parent compounds (**M2**, **M4**, **M5**, and **M14**) showed more toxic effect than Mannich bases. Parent compound **M14** showed highest toxicity against MCF-10A with IC_{50} of $10.55 \pm 1.05 \mu\text{M}$, however all the Mannich bases showed less toxicity with $IC_{50} > 100 \mu\text{M}$. The results suggest that synthetic modifications have produced the compounds with improved anticancer activity and selectivity against breast

cancer cells. In the case of compounds (**M2**, **M2a-b**, **M4**, **M4a-b**), **M4** is cytotoxic, whereas other compounds (**M2**, **M2a-b**, **M4a-b**) are not. The statistics cannot be calculated because the IC_{50} values of (**M2**, **M2a-b**, **M4a-b**) is more than 100 μ M (the highest concentration used in this study).

CHAPTER 5

CONCLUSIONS

5.1 Conclusion

A total of eighteen compounds were isolated from the leaves of *Muntingia calabura* which consists of five flavanones {(2*R*,3*R*)3,5-dihydroxy-7-methoxyflavanone (**M1**), (2*R*,3*R*) 3,5-dihydroxy-6,7-dimethoxyflavanone (**M12**), (2*R*,3*R*) 3,5,7-trihydroxyflavanone (**M13**), (2*S*) 7,8-dihydroxyflavanone (**M17**), (2*R*, 3*R*) 3,5,7-trihydroxy-8-methoxyflavanone (**M18**)}, three chalcones {2',4'-dihydroxy-3'-methoxychalcone (**M2**), 2', 4'-dihydroxychalcone (**M4**), 2', 3', 4'-trihydroxychalcone (**M6**)} and ten flavones {3,5-dihydroxy-7,8-dimethoxyflavone (**M3**), 3, 5, 7-trihydroxy-8-methoxyflavone (**M5**), 5-hydroxy-3,7-dimethoxyflavone (**M7**), 3, 5-dihydroxy-7-methoxyflavone (**M8**), 5-hydroxy-7-methoxyflavone (**M9**), 5-hydroxy-3,7,8-trimethoxyflavone (**M10**), 5,7-dihydroxy-3,8-dimethoxyflavone (**M11**), 5,7-dihydroxyflavone (**M14**), 5-hydroxy-6,7-dimethoxyflavone (**M15**), 5,4'-dihydroxy-3,7-dimethoxyflavone (**M16**)}. Among the isolates, 3,5-dihydroxy-7-methoxyflavanone (**M1**), 7,8-dihydroxyflavanone (**M4**) and 2',3',4'-trihydroxychalcone (**M6**) were first isolated from the leaves of *Muntingia calabura*.

For Mannich bases, four chalcone Mannich bases namely 1-[3-methoxy-5-(piperidin-4-yl) methyl-2,4-dihydroxyphenyl]-3-phenyl-2-propen-1-one (**M2a**), 1-[3-methoxy-5-(morpholino-4-yl) methyl-2,4-dihydroxyphenyl]-3-phenyl-2-propen-1-one (**M2b**), 1-[3-(piperidin-1-yl)methyl-2,4-dihydroxyphenyl]-3-phenyl-2-propen-1-one (**M4a**), and 1-[3-(morpholino-4-yl) methyl-2,4-dihydroxyphenyl]-3-phenyl-2-propen-1-one (**M4b**) and sixteen flavone Mannich bases were synthesized and characterized. The synthesized flavone **M5** Mannich bases are 3,5,7-trihydroxy-8-methoxy-6-(pyrrolidin-1-ylmethyl)-2-phenyl-4H-chromen-4-one (**M5a**), 3,5,7-trihydroxy-8-methoxy-6-(piperidin-1-ylmethyl)-2-phenyl-4H-chromen-4-one (**M5b**), 3,5,7-trihydroxy-8-methoxy-6-(4-methylpiperazin-1-ylmethyl)-2-phenyl-4H-chromen-4-one (**M5c**), 3,5,7-trihydroxy-8-methoxy-6-(morpholinomethyl)-2-phenyl-4H-chromen-4-one (**M5d**), 3,5,7-trihydroxy-8-methoxy-6-(thiomorpholinomethyl)-2-phenyl-4H-chromen-4-one (**M5e**).

The synthesized monoamine **M14** flavone Mannich bases are 5,7-dihydroxy-8-(pyrrolidine-1-ylmethyl)-2-phenyl-4H-chromen-4-one (**M14a**), 5,7-dihydroxy-8-(piperidin-1-ylmethyl)-2-phenyl-4H-chromen-4-one (**M14b**), 5,7-dihydroxy-8-(4-methylpiperazin-1-ylmethyl)-2-phenyl-4H-chromen-4-one (**M14c**), 5,7-dihydroxy-8-(morpholinomethyl)-2-phenyl-4H-chromen-4-one (**M14d**), 5,7-dihydroxy-8-(thiomorpholinomethyl)-2-phenyl-4H-chromen-4-one (**M14e**) and 5,7-dihydroxy-8-(4-methoxybenzylamine)-2-phenyl-4H-chromen-4-one (**M14f**). The synthesized diamine **M14** flavone Mannich bases are 5,7-dihydroxy-6,8-bis(pyrrolidine-1-ylmethyl)-2-phenyl-4H-chromen-4-one (**M14g**), 5,7-dihydroxy-6,8-bis(piperidin-1-ylmethyl)-2-phenyl-4H-chromen-4-

one (**M14h**), 5,7-dihydroxy-6,8-bis(4-methylpiperazin-1-ylmethyl)-2-phenyl-4H-chromen-4-one (**M14i**), 5,7-dihydroxy-6,8-bis(morpholinomethyl)-2-phenyl-4H-chromen-4-one (**M14j**) and 5,7-dihydroxy-6,8-bis(thiomorpholinomethyl)-2-phenyl-4H-chromen-4-one (**M14k**).

For cytotoxicity screening, chalcone and flavone based Mannich bases exhibited greater activity and selectivity than their parent compounds against MDA-MB-231 cell. Mannich base **M14f** showed the highest activity against MDA-MB-231 cell with the IC_{50} of $5.75 \pm 0.82 \mu\text{M}$. Parent compounds and Mannich bases showed moderate activity against MCF-7 cell with the IC_{50} range of 9.17-68.5 μM and there is no difference in the activity of parent compounds and their derivatives. The synthesised Mannich bases were found to be less toxic to normal breast cancer cells, MCF-10A, with the IC_{50} of the parent compounds are in the range of 10.55 – 31.56 μM and for Mannich bases is more than 100 μM . The mechanism of cytotoxic action of the synthesized compounds towards breast cancer cell line is unknown and it can be conducted in future studies.

5.2 Future Studies

In future, the relationship between the compounds structure and the cytotoxic activity can be determined through molecular docking study. The chalcone based Mannich bases with moderate cytotoxic activity can be modified by introduction of different amino groups on the chalcone scaffold, in order to

obtain chalcone derivatives with better activity. The synthesized Mannich bases can be further assess for different biological activities.

REFERENCES

- Aziz, D., 2014. Isolation, structural elucidation and biological activity of the flavonoid from the leaves of *Juniperus phoenicea*. *World Journal of Pharmaceutical Research*, 3(10), pp. 951-965.
- Boghrati, Z. et al., 2016. Tyrosinase inhibitory properties of phenylpropanoid glycosides and flavonoids from *Teucrium polium L. var. gnaphalodes*, *Iranian Journal of Basic Medical Sciences*, 19, pp. 804-811.
- Buckingham, J., and Munasinghe, V. R. N., 2015. *Dictionary of Flavonoids with CD ROM*, 1st Ed. United States: CRC Press.
- Buhian, W.P.C., Rubio, R.O., Valle, D.L. and Martin-Puzon, J.J., 2016. Bioactive metabolite profiles and antimicrobial activity of ethanolic extracts from *Muntingia calabura L.* leaves and stems. *Asian Pacific Journal of Tropical Biomedicine*, 6 (8), pp.682–685.
- Che, C.T. and Zhang, H., 2019. Plant natural products for human health. *International Journal of Molecular Sciences*, 20 (4), pp. 830-833.
- Chen, J.-J. et al., 2004. Flavones and cytotoxic constituents from the stem bark of *Muntingia calabura*. *Journal of the Chinese Chemical Society*, 51 (3), pp. 665–670.
- Chen, J.-J. et al., 2007. New dihydrochalcones and anti-platelet aggregation constituents from the leaves of *Muntingia calabura*. *Planta Medica*, 73, pp. 572-577.
- Chen, J.J., Lee, H.H., Duh, C.Y. and Chen, I.S., 2005. Cytotoxic chalcones and flavonoids from the leaves of *Muntingia calabura*. *Planta Medica*, 71 (10), pp. 970–973.

- Crayn, D.M., Rossetto, M. and Maynard, D.J., 2006. Molecular phylogeny and dating reveals an Oligomiocene radiation of dry-adapted shrubs (former *Tremandraceae*) from rainforest tree progenitors (Elaeocarpaceae) in Australia. *American Journal of Botany*, 93 (9), pp. 1328–1342.
- Dias, D.A., Urban, S. and Roessner, U., 2012. A Historical overview of natural products in drug discovery. *Metabolites*, 2(2), pp.303–336.
- Ekalu, A. and Habila, J.D., 2020. Flavonoids: isolation, characterization, and health benefits. *Beni-Suef University Journal of Basic and Applied Sciences*, 9 (45). pp. 1-14.
- Fu, H. et al., 2014. Synthesis and anti-tumor activity of novel aminomethylated derivatives of isoliquiritigenin. *Molecules*, 19(11), pp.17715–17726.
- Ghani, N.A., Ahmat, N., Ismail, N.H., Zakaria, I. and Zawawi N.K.N.A., 2012. Chemical constituents and cytotoxic activity of *Polyalthia cauliflora* var. *cauliflora*. *Research Journal of Medicinal Plants*, 6, pp. 74-82.
- Gul, H.I. et al., 2007. Synthesis of 4'-hydroxy-3'-piperidinomethylchalcone derivatives and their cytotoxicity against PC-3 cell lines. *Archiv der Pharmazie*, 340 (4), pp.195–201.
- Hahm, E.R., Park, S. and Yang, C.H., 2003. 7,8-dihydroxyflavonone as an inhibitor for Jun-Fos-DNA complex formation and its cytotoxic effect on cultured human cancer cells. *Natural Product Research*, 17(6), pp.431–436.
- Hieu, B.T. et al., 2012. Design, synthesis and *in vitro* cytotoxic activity evaluation of new mannich bases. *Bulletin of the Korean Chemical Society*, 33(5), pp.1586–1592.
- Hoang, T.K.D., Huynh, T.K.C., Do, T.H.T. and Nguyen, T.D., 2018. Mannich aminomethylation of flavonoids and anti-proliferative activity against breast cancer cell. *Chemical Papers*, 72 (6), pp. 1399–1406.

- Jing, L. et al., 2016. Chemical constituents of *Saussurea involucrata* with anti-hypoxia activity. *Chemistry of Natural Compounds*, 52 (3), pp. 487–489.
- Kandaswami, C.C. and Hwang, J.-J., 2005. The antitumor activities of flavonoids. *In vivo*, 19 (5), pp. 895-909.
- Kaneda, N. et al., 1991. Plant anticancer agents, xlviii. new cytotoxic flavonoids from *Muntingia calabura* roots, *Journal of Natural Products*, 54 (1), pp. 196-206.
- Kuo, W.L., Liao, H.R. and Chen, J.J., 2014. Biflavans, flavonoids, and a dihydrochalcone from the stem wood of *Muntingia calabura* and their inhibitory activities on neutrophil pro-inflammatory responses. *Molecules*, 19(12), pp. 20521–20535.
- Kurkin, V.A. et al., 1994. Flavonoids of the buds of *Populus laurifolia*, *Chemistry of Natural Compounds*, 30 (6), pp. 778-779.
- Liu, R. et al., 2012. Nitrogen-containing apigenin analogs: Preparation and biological activity. *Molecules*, 17(12), pp. 14748–14764.
- Mahmood, N.D. et al., 2014. *Muntingia calabura*: A review of its traditional uses, chemical properties, and pharmacological observations. *Pharmaceutical Biology*, 52(12), pp.1598–1623.
- McChesney, J.D., Venkataraman, S.K. and Henri, J.T., 2007. Plant natural products: Back to the future or into extinction? *Phytochemistry*, 68(14), pp.2015–2022.
- Mohamad Yusof, M.I. et al., 2013. Activity-guided isolation of bioactive constituents with antinociceptive activity from *Muntingia calabura* L. Leaves using the formalin test. *Evidence-based Complementary and Alternative Medicine*, 2013 (2013), pp. 1-9.

- Mohammed, H.A. et al., 2011. Facile synthesis of chrysin-derivatives with promising activities as aromatase inhibitors. *Natural Product Communications*, 6 (1), pp.31–34.
- Mortan, J., 1987. Jamaica Cherry. In: J.F. Mortan. Fruits of warm climates. Miami, FL. pp. 65-69.
- Newman, D.J. and Cragg, G.M., 2012. Natural products as sources of new drugs over the 30 years from 1981 to 2010. *Journal of Natural Products*, 75 (3), pp. 311–335.
- Nguyen, V.S., Shi, L., Luan, F.Q. and Wang, Q.A., 2015. Synthesis of kaempferide Mannich base derivatives and their antiproliferative activity on three human cancer cell. *Acta Biochimica Polonica*, 62 (3), pp. 547–552.
- Nor-Eljaleel, A. et al., 2015. Synthesis of Nitrogen-Containing Chalcone Via One-Pot Three-Component Reaction: Part IV. *International Research Journal of Pure and Applied Chemistry*, 5(1), pp. 106–112.
- Nshimo, C.M., 1991. *Phytochemical and Biological Studies on Muntingia calabura* L. PhD. University of Illinois at Chicago.
- Nshimo, C.M., Pezzuto, J.M., Kinghorn, A.D. and Farns Worth, N.R., 1993. Cytotoxic constituents of *Muntingia calabura* leaves and stems Collected in Thailand, *International Journal of Pharmacognosy*, 31 (1), pp. 77-81.
- Ouyang, L. et al., 2014. Plant natural products: From traditional compounds to new emerging drugs in cancer therapy. *Cell Proliferation*, 47(6), pp.506–515.
- Peña-Morán, O.A. et al., 2016. Cytotoxicity, post-treatment recovery, and selectivity analysis of naturally occurring podophyllotoxins from *Bursera fagaroides* var. *fagaroides* on breast cancer cell lines. *Molecules*, 21(8), pp. 1-15.

- Ragasa, C.Y. et al., 2015. Chemical constituents of *Muntingia calabura* L. *Der Pharma Chemica*, 7(5), pp. 136-141.
- Roman, G., 2015. Mannich bases in medicinal chemistry and drug design. *European Journal of Medicinal Chemistry*, 89, pp.743–816.
- Rosandy, A.R., Laily B. D., Yaacob, W.A., Yusof, N.I., Sahidin, I., Jalifah, L., Syarul, N. and Normah, M.N., 2013. Isolation and characterization of compounds from the stem bark of *Uvaria rufa* (Annonaceae). *The Malaysian Journal of Analytical Sciences*, 17(1), pp. 50-58.
- Su, B.N. et al., 2003. Activity-guided isolation of the chemical constituents of *Muntingia calabura* using a quinone reductase induction assay. *Phytochemistry*, 63 (3), pp. 335–341.
- Subramaniapillai, S.G., 2013. Mannich reaction: a versatile and convenient approach to bioactive skeletons. *Journal of Chemical Sciences*, 125 (3), pp. 467-482.
- Sufian, A.S. et al., 2013. Isolation and identification of antibacterial and cytotoxic compounds from the leaves of *Muntingia calabura* L. *Journal of Ethnopharmacology*, 146 (1), pp. 198–204.
- Sujith, K. v., Rao, J.N., Shetty, P. and Kalluraya, B., 2009. Regioselective reaction: Synthesis and pharmacological study of Mannich bases containing ibuprofen moiety. *European Journal of Medicinal Chemistry*, 44 (9), pp. 3697–3702.
- Surjowardojo, P., Thohari, I. and Ridhowi, A., 2014. Quantitative and qualitative phytochemicals analysis of *Muntingia calabura*. *Journal of Biology, Agriculture and Healthcare*, 4(16), pp. 84-88.
- Tapas, A.R., Sakarkar, D.M. and Kakde, R.B., 2008. Flavonoids as nutraceuticals: A Review. *Tropical Journal of Pharmaceutical Research*, 7(3), pp. 1089-1099.

- Urzúa, A., Mendoza, L., Tojo, E. and Rial, M.E., 1999. Acylated flavonoids from *Pseudognaphalium* species. *Journal of Natural Products*, 62 (2), pp. 381–382.
- Urzúa, A. et al., 2000. External flavonoids from *Heliotropium Megalanthum* and *H. Huascoense* (Boraginaceae). Chemotaxonomic considerations. *Boletín de la Sociedad Chilena de Química*, 45(1), pp.023–029.
- Valenzuela, B., Rodríguez, F.E., Modak, B. and Imarai, M., 2018. Alpinone exhibited immunomodulatory and antiviral activities in Atlantic salmon. *Fish and Shellfish Immunology*, 74, pp. 76–83.
- Wilhelm, A. et al., 2015. Syntheses and *in Vitro* antiplasmodial activity of aminoalkylated chalcones and analogues. *Journal of Natural Products*, 78(8), pp.1848–1858.
- Yamali, C., Gul, H.I., Sakagami, H. and Supuran, C.T., 2016. Synthesis and bioactivities of halogen bearing phenolic chalcones and their corresponding bis Mannich bases. *Journal of Enzyme Inhibition and Medicinal Chemistry*, 31, pp. 125–131.
- Yun, B.W. et al., 2012. Plant natural products: History, limitations and the potential of cambial meristematic cells. *Biotechnology and Genetic Engineering Reviews*, 28, pp. 47–60.
- Zakaria, Z.A., Hassan, M. H., Aqmar, N.M.N.H., (2007). Effects of various nonopioid receptor antagonist on the antinociceptive activity of *Muntingia calabura* extracts in mice. *Methods and Findings in Experimental and Clinical Pharmacology*, 29, pp. 515-520.
- Zhang, X. et al., 2019. Design, synthesis and evaluation of chalcone Mannich base derivatives as multifunctional agents for the potential treatment of Alzheimer's disease. *Bioorganic Chemistry*, 87, pp. 395–408.

APPENDIX A

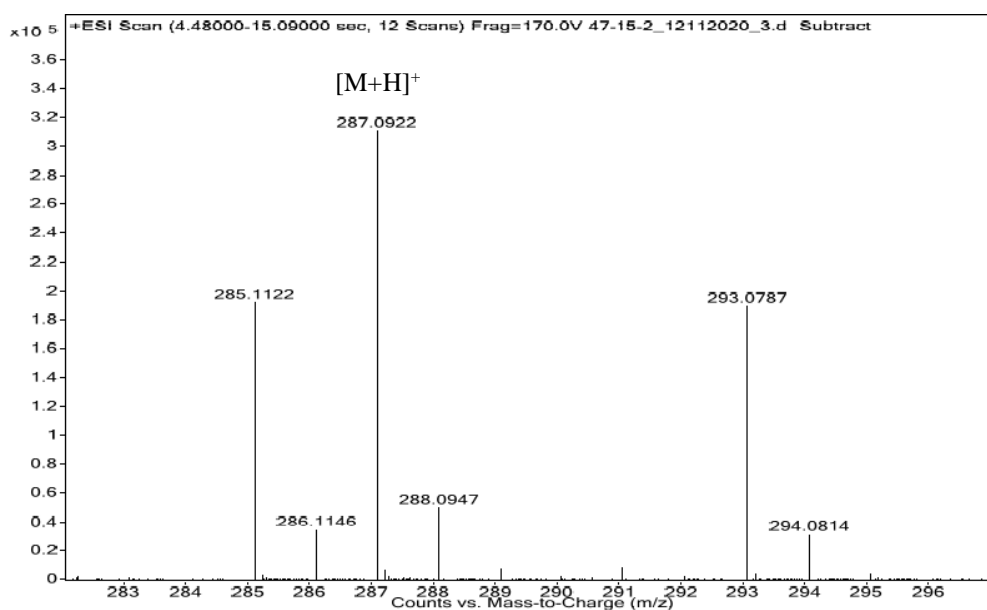


Figure A1: HRESIMS of (2*S*,3*S*) 3,5-dihydroxy-7-methoxyflavanone (M1)

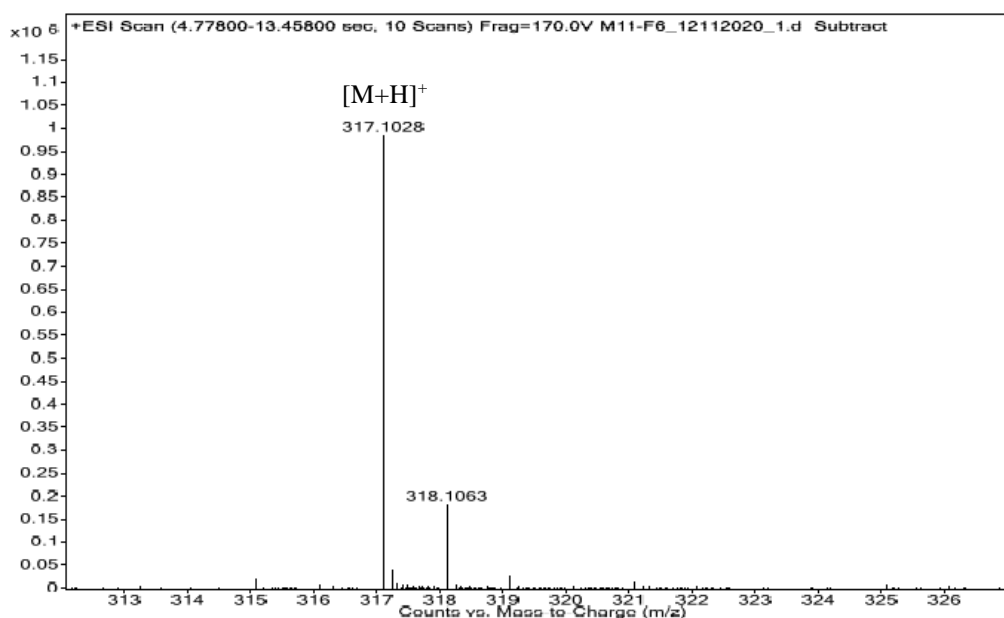


Figure A2: HRESIMS of (2*R*,3*R*) 3,5-dihydroxy-6,7-dimethoxyflavanone (M12)

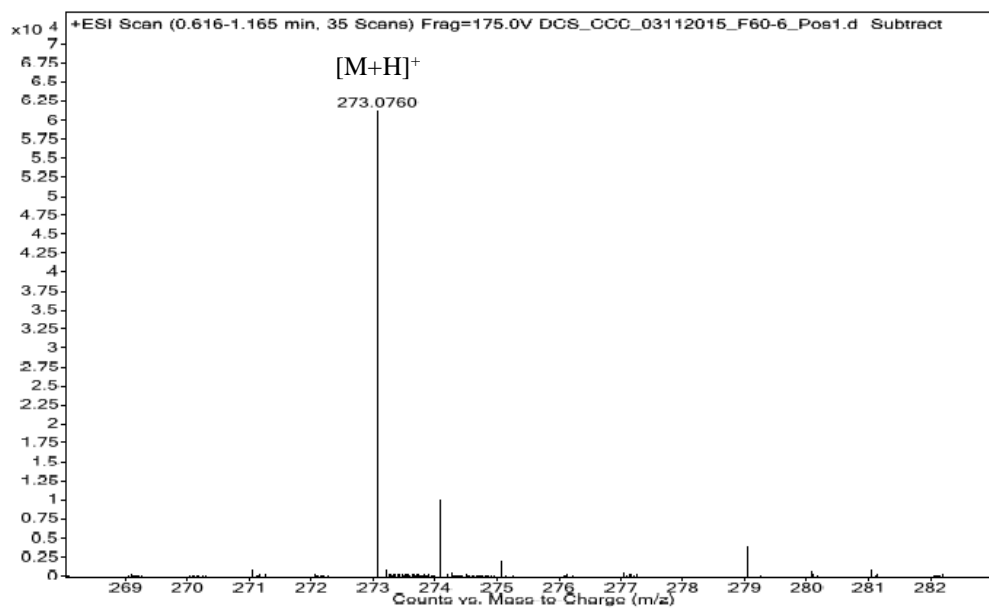


Figure A3: HRESIMS of (2*R*,3*R*) 3,5-dihydroxy-6,7-dimethoxyflavanone (M13)

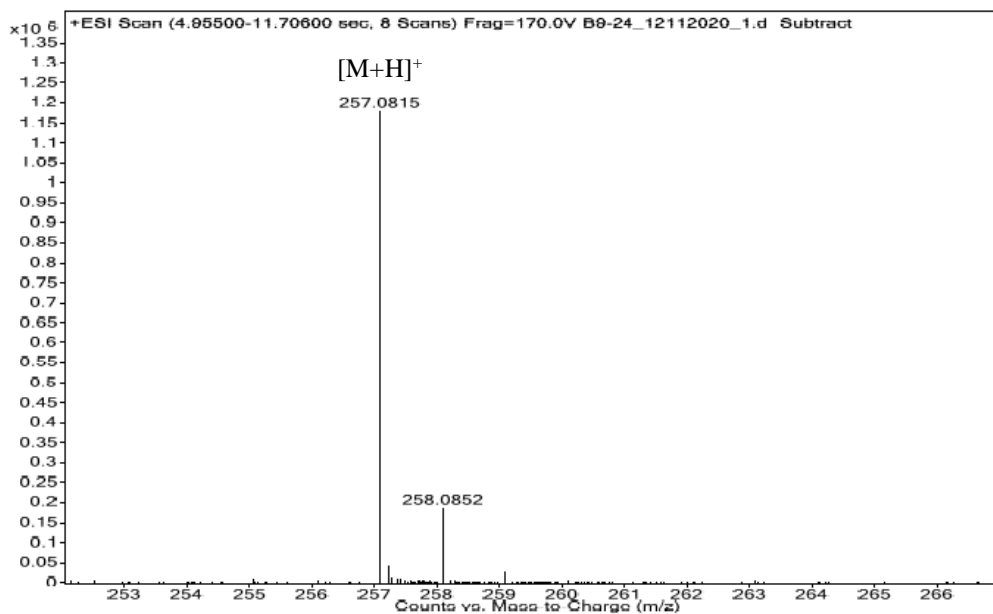


Figure A4: HRESIMS of (2*S*) 7,8-dihydroxyflavanone (M17)

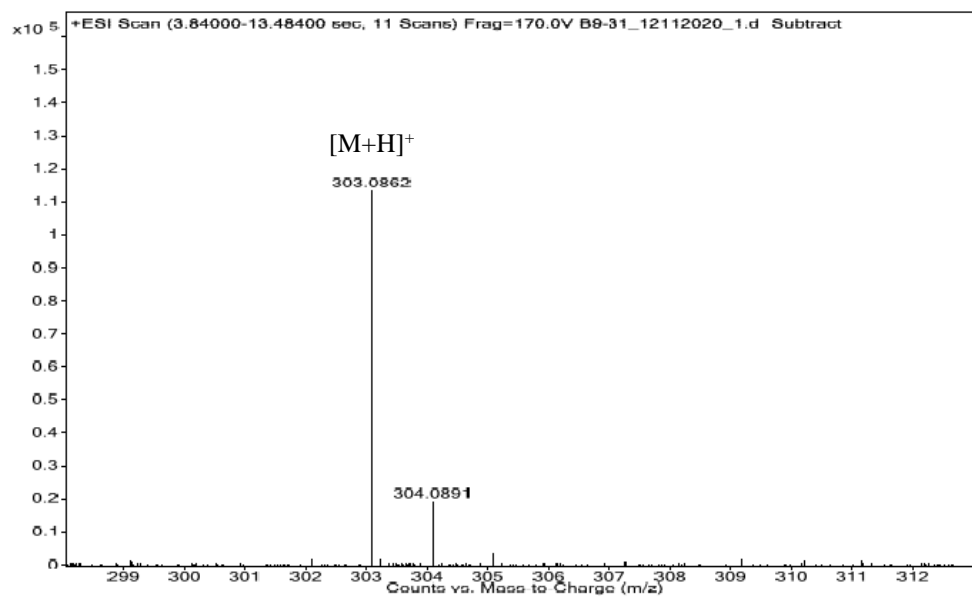


Figure A5: HRESIMS of (2R,3R) 3,5,7-trihydroxy-8-methoxyflavanone (M18)

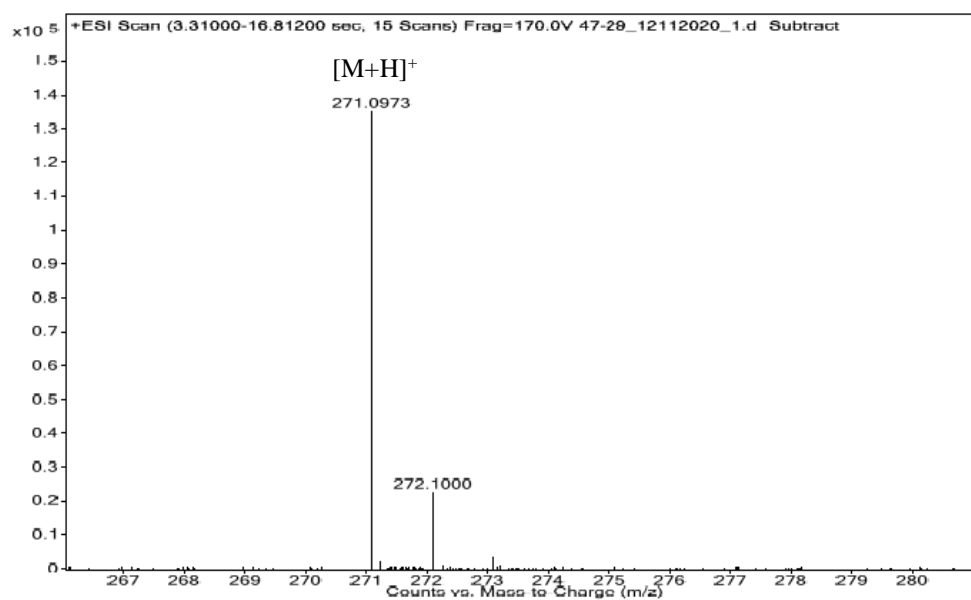


Figure A6: HRESIMS of 2',4'-dihydroxy-3'-methoxychalcone (M2)

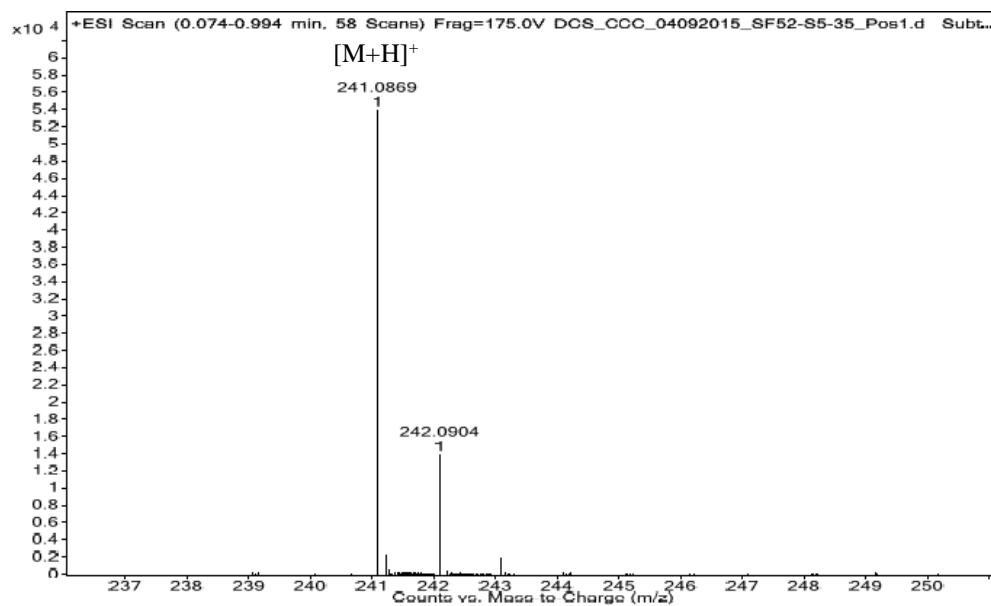


Figure A7: HRESIMS of 2', 4'-dihydroxychalcone (M4)

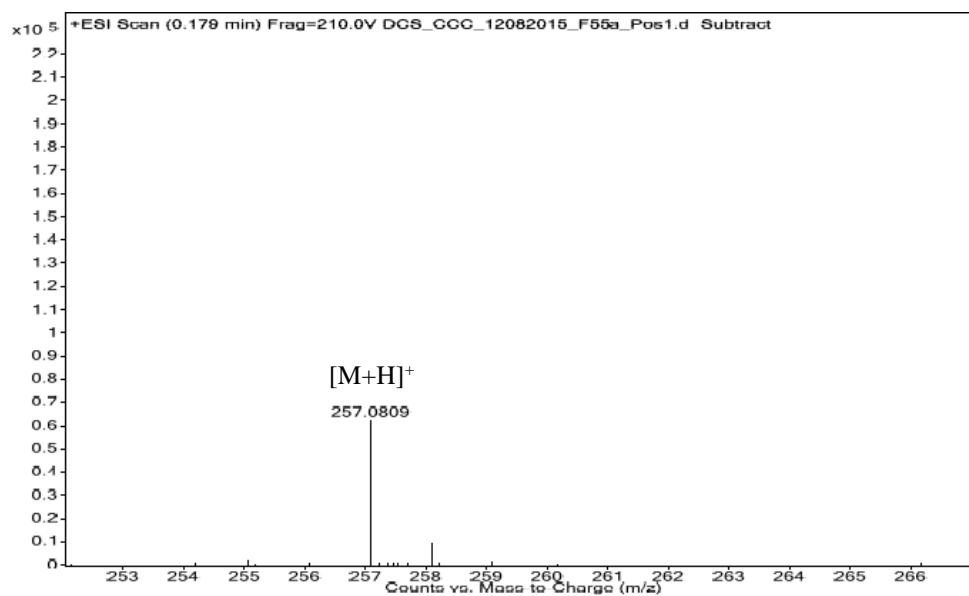


Figure A8: HRESIMS of 2', 3', 4'-trihydroxychalcone (M6)

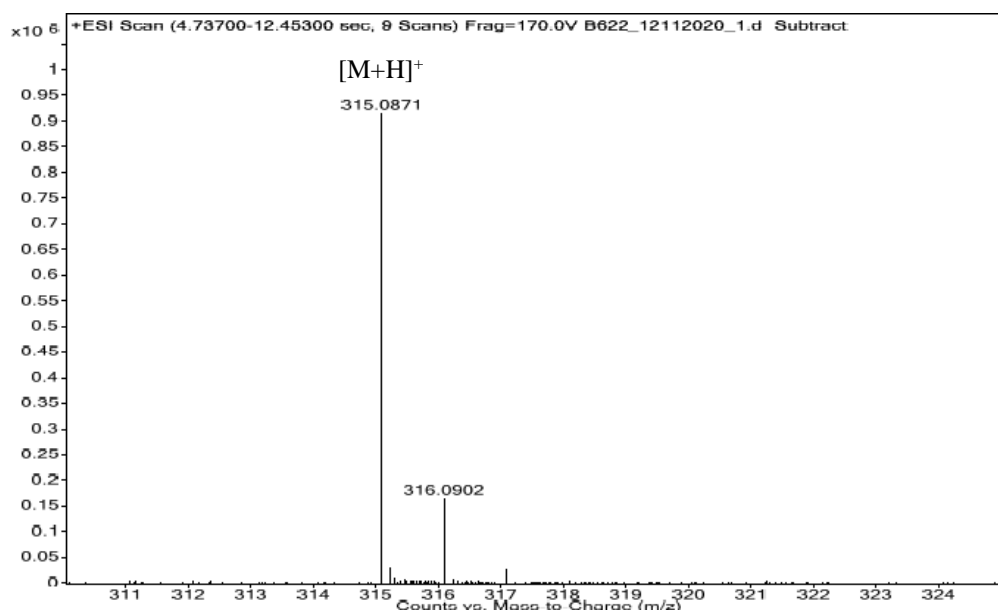


Figure A9: HRESIMS of 3,5-dihydroxy-7,8-dimethoxyflavone (M3)

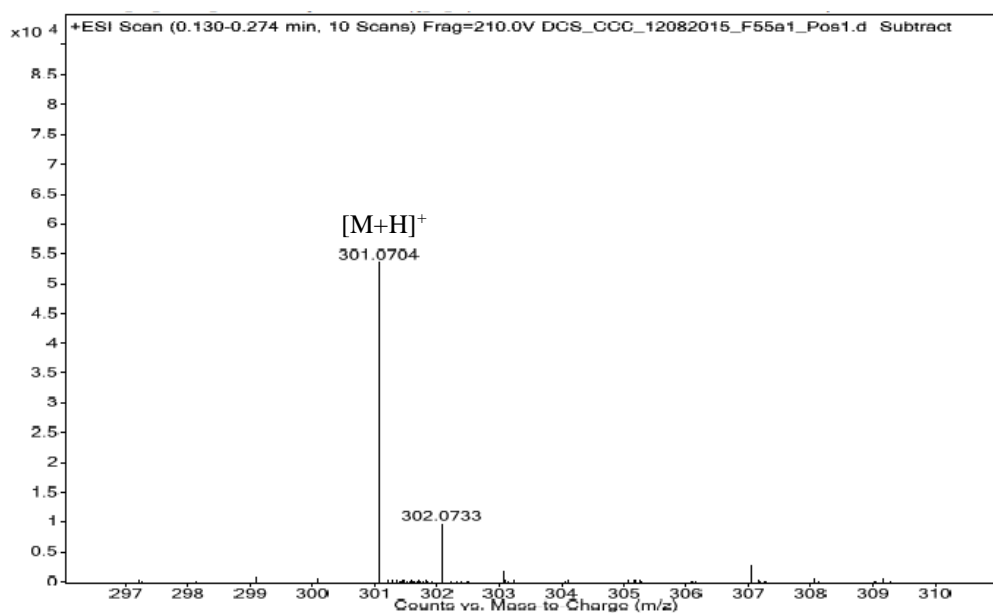


Figure A10: HRESIMS of 3,5,7-trihydroxy-8-methoxyflavone (M5)

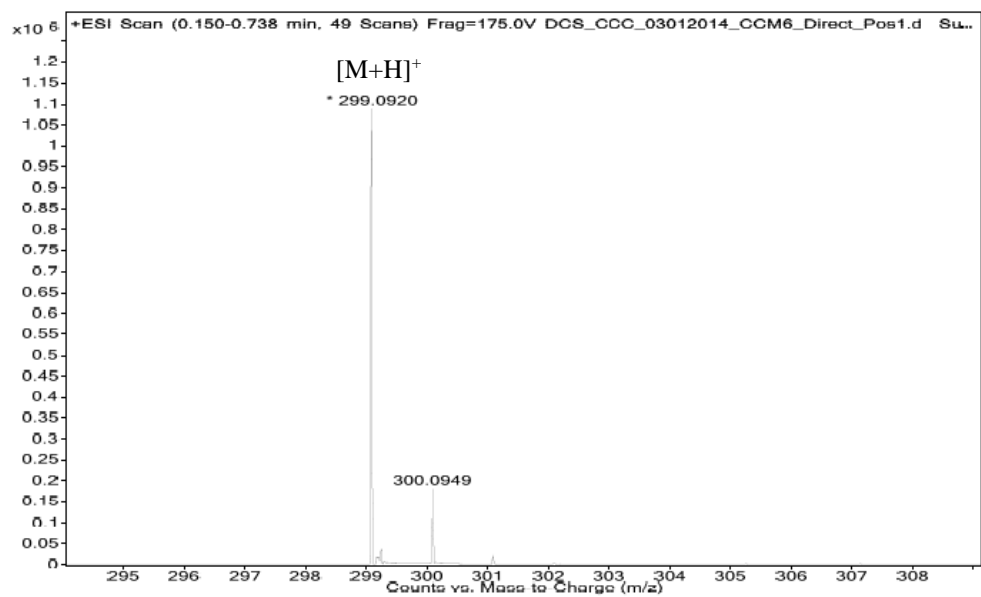


Figure A11: HRESIMS of 5-hydroxy-3,7-dimethoxyflavone (M7)

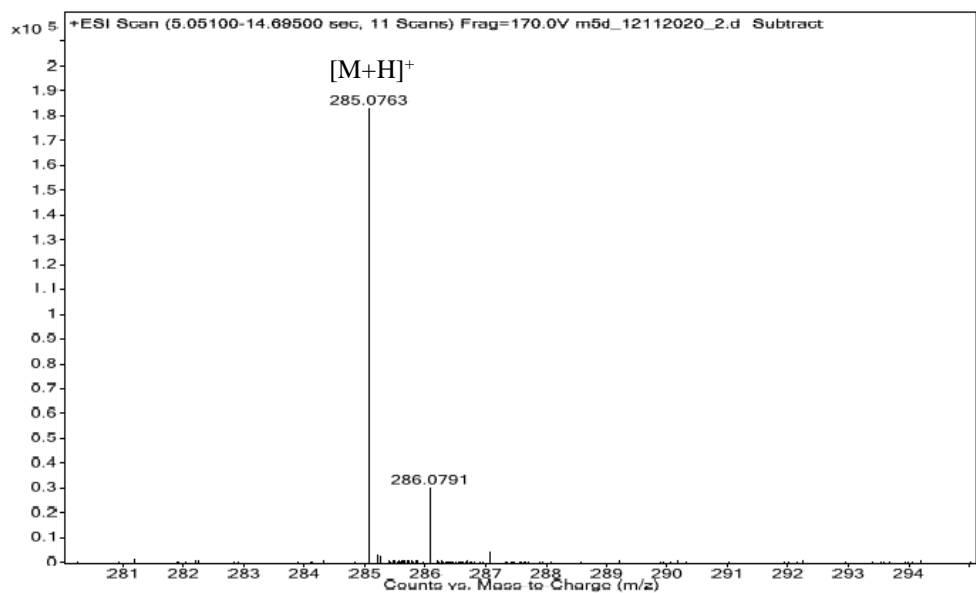


Figure A12: HRESIMS of 3,5-dihydroxy-7-methoxyflavone (M8)

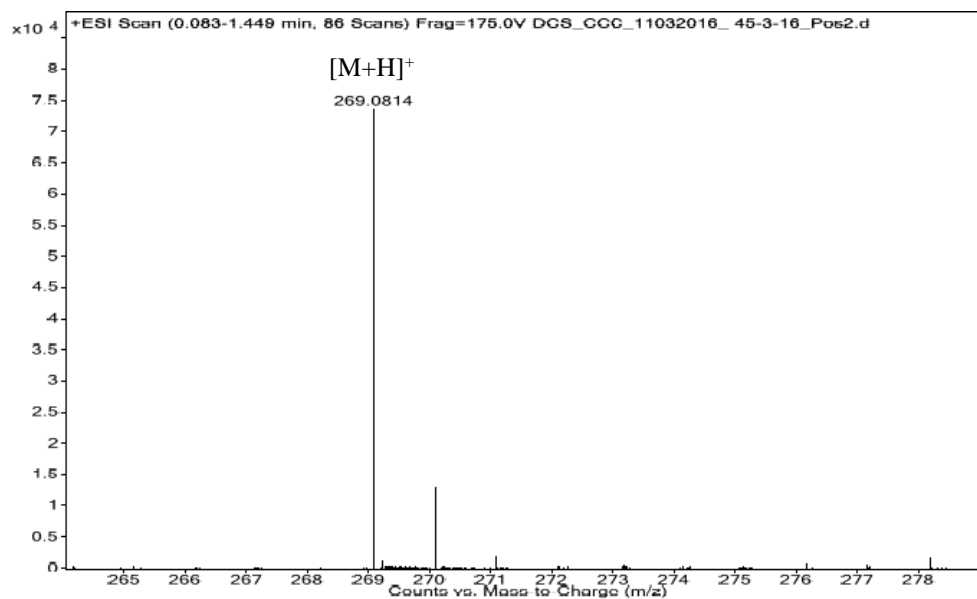


Figure A13: HRESIMS of 5-hydroxy-7-methoxyflavone (M9)

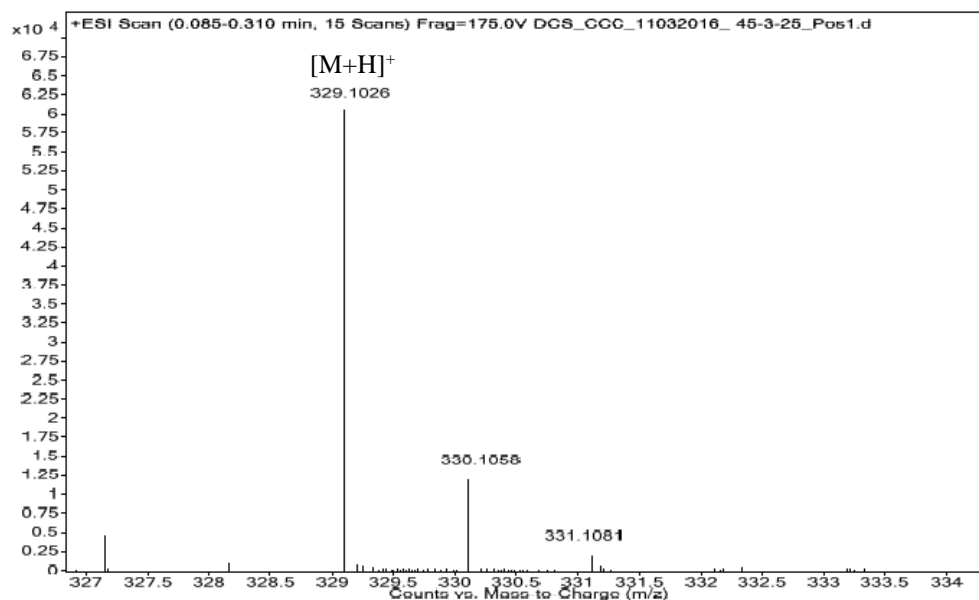


Figure A14: HRESIMS of 5-hydroxy-3,7,8-trimethoxyflavone (M10)

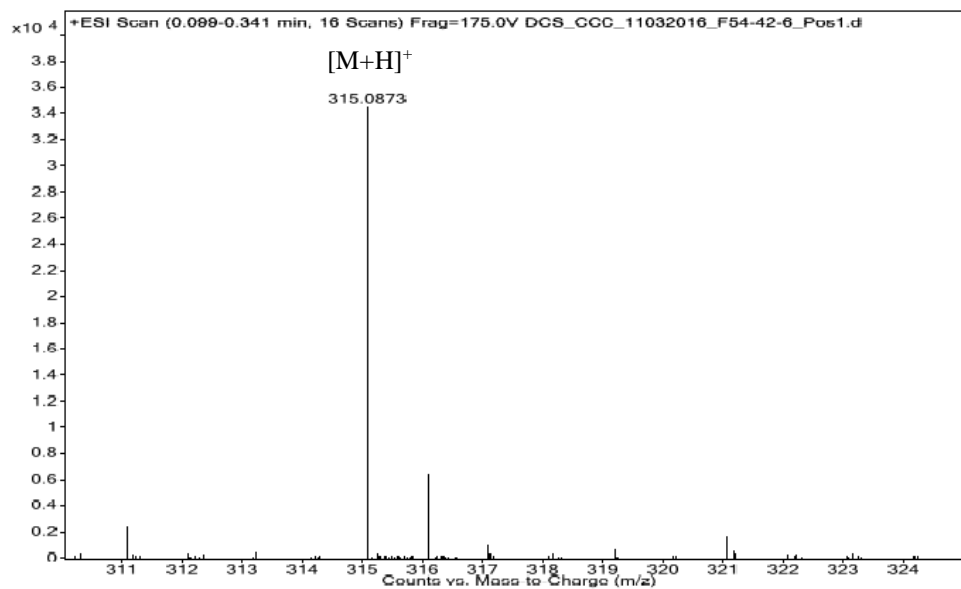


Figure A15: HRESIMS of 5,7-dihydroxy-3,8-dimethoxyflavone (M11)

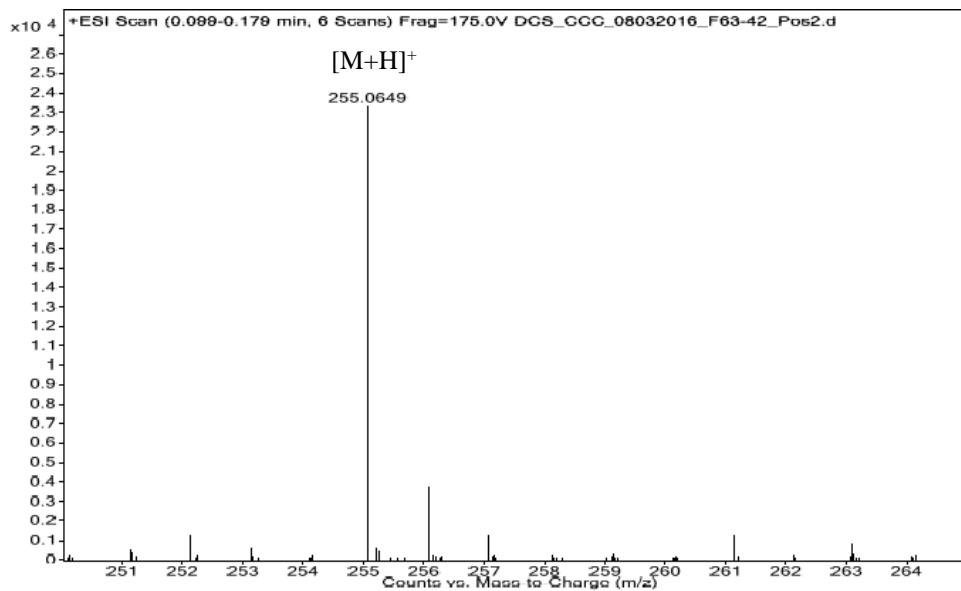


Figure A16: HRESIMS of 5,7-dihydroxyflavone (M14)

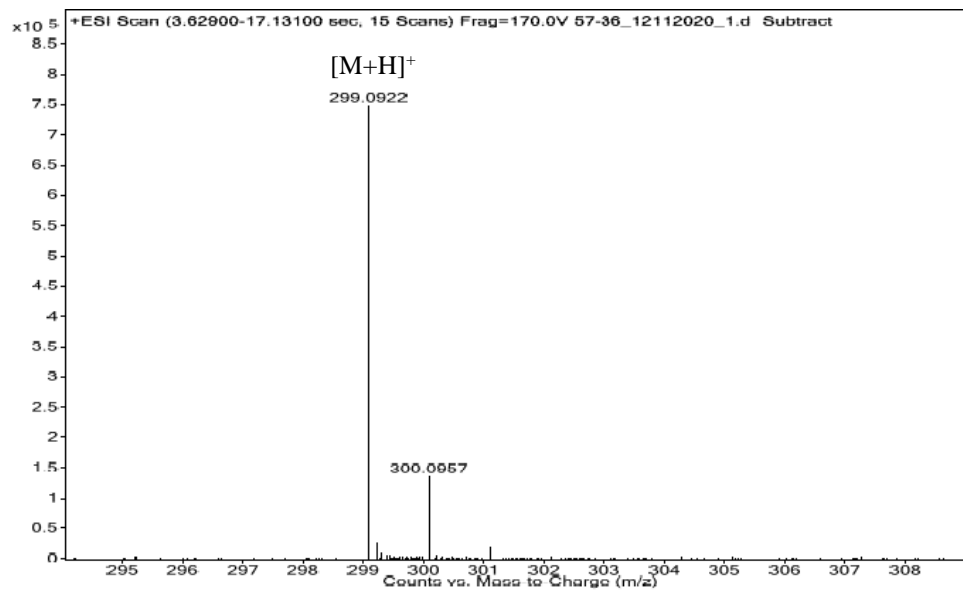


Figure A17: HRESIMS of 5-hydroxy-6,7-dimethoxyflavone (M15)

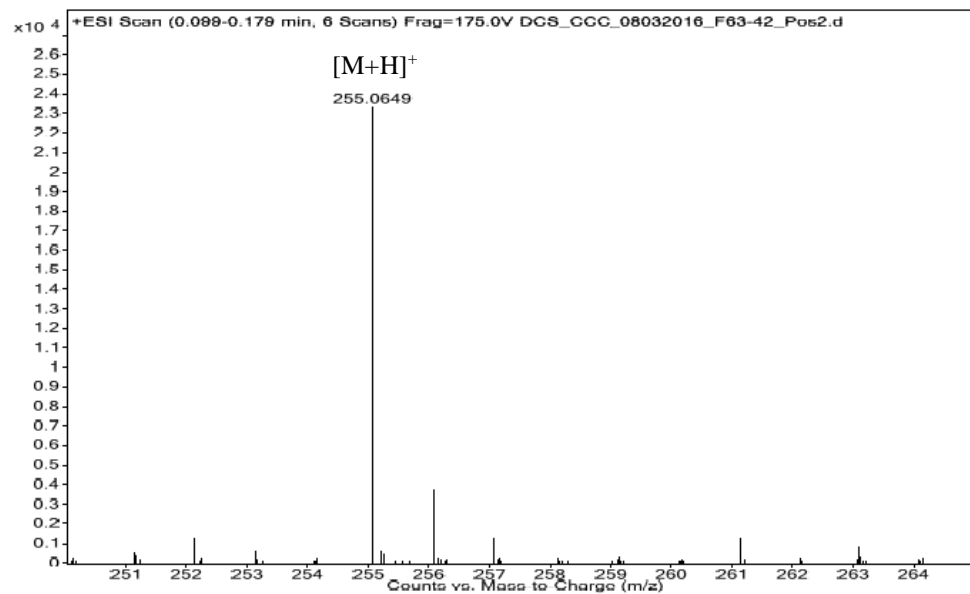


Figure A18: HRESIMS of 5,4'-dihydroxy-3,7-dimethoxyflavone (M16)

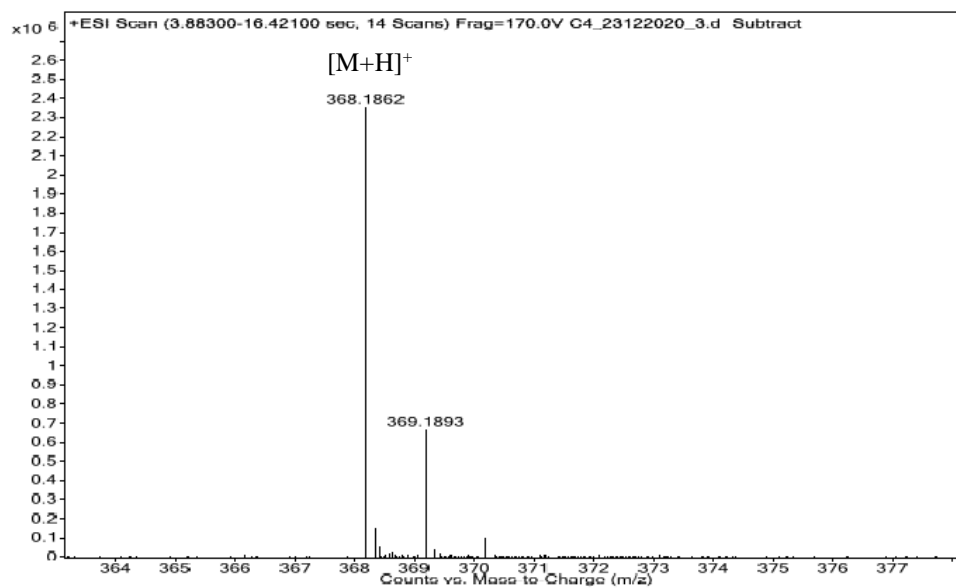


Figure A19: HRESIMS of 1-[3-methoxy-5-(piperidin-4-yl) methyl-2,4-dihydroxyphenyl]-3-phenyl-2-propen-1-one (M2a)

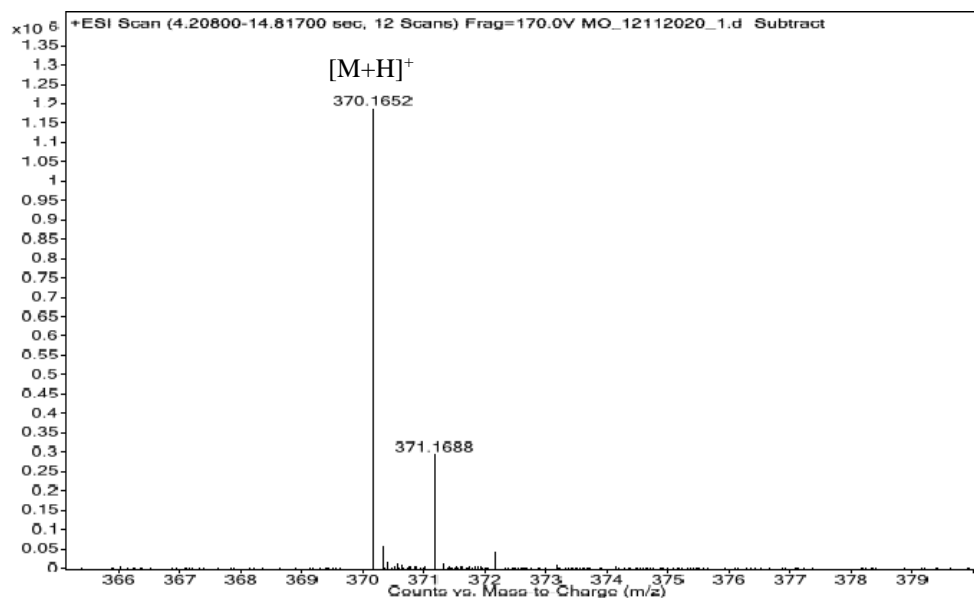


Figure A20: HRESIMS of 1-[3-methoxy-5-(morpholino-4-yl) methyl-2,4-dihydroxyphenyl]-3-phenyl-2-propen-1-one (M2b)

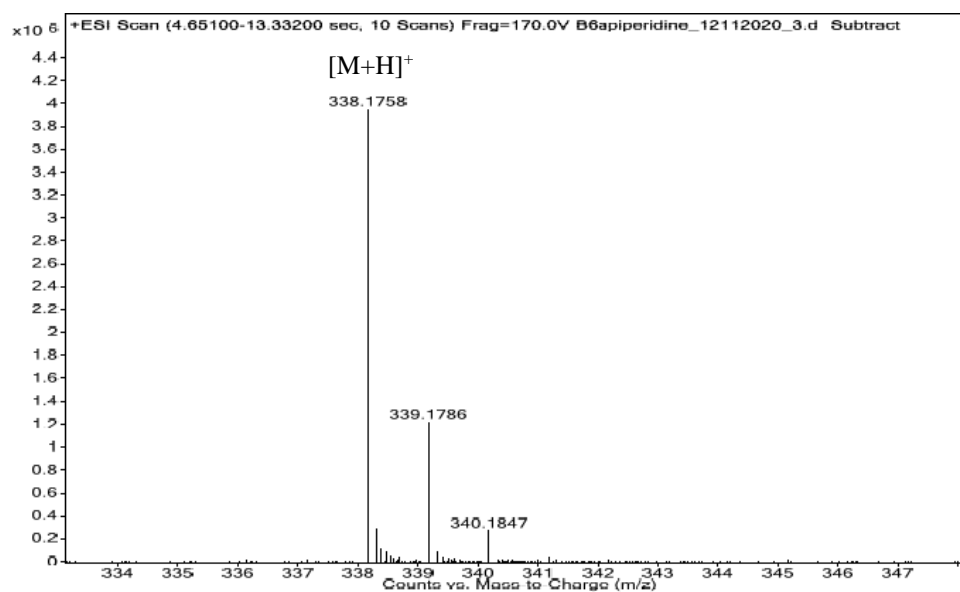


Figure A21: HRESIMS of 1-[3-(piperidin-1-yl)methyl-2,4-dihydroxyphenyl]-3-phenyl-2-propen-1-one (M4a)

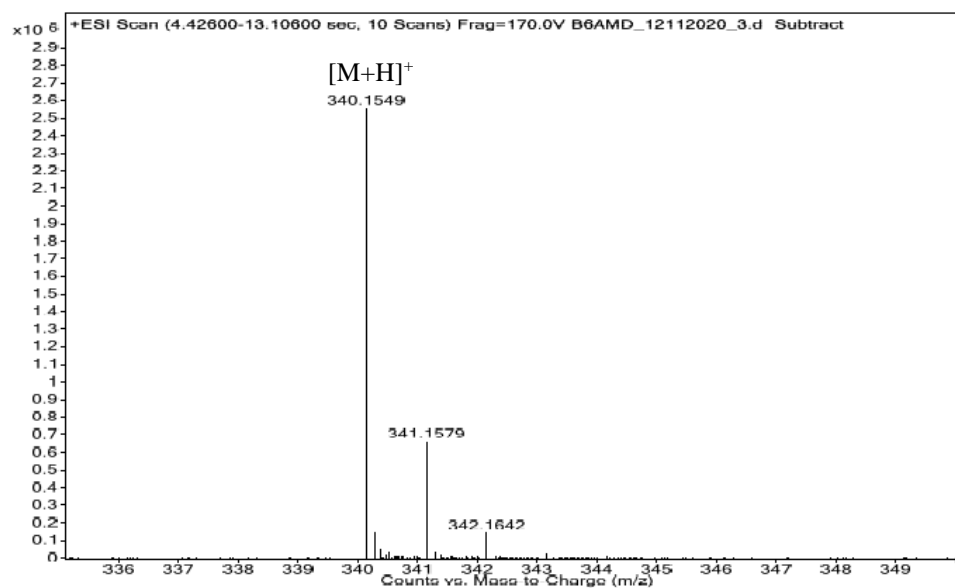


Figure A22: HRESIMS of 1-[3-(morpholino-4-yl) methyl-2,4-dihydroxyphenyl]-3-phenyl-2-propen-1-one (M4b)

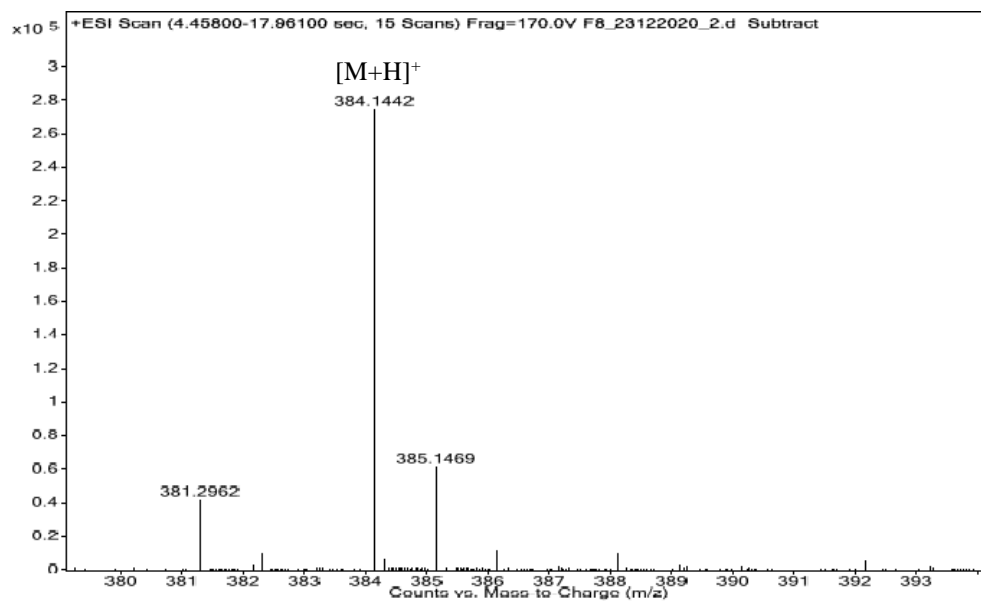


Figure A23: HRESIMS of 3,5,7-trihydroxy-8-methoxy-6-(pyrrolidin-1-ylmethyl)-2-phenyl-4H-chromen-4-one (M5a)

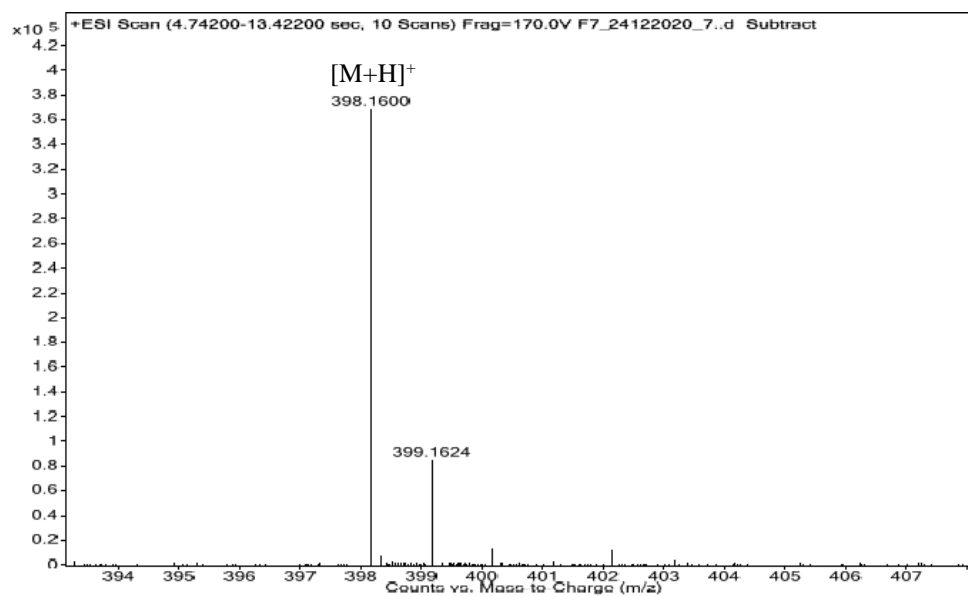


Figure A24: HRESIMS of 3,5,7-trihydroxy-8-methoxy-6-(piperidin-1-ylmethyl)-2-phenyl-4H-chromen-4-one (M5b)

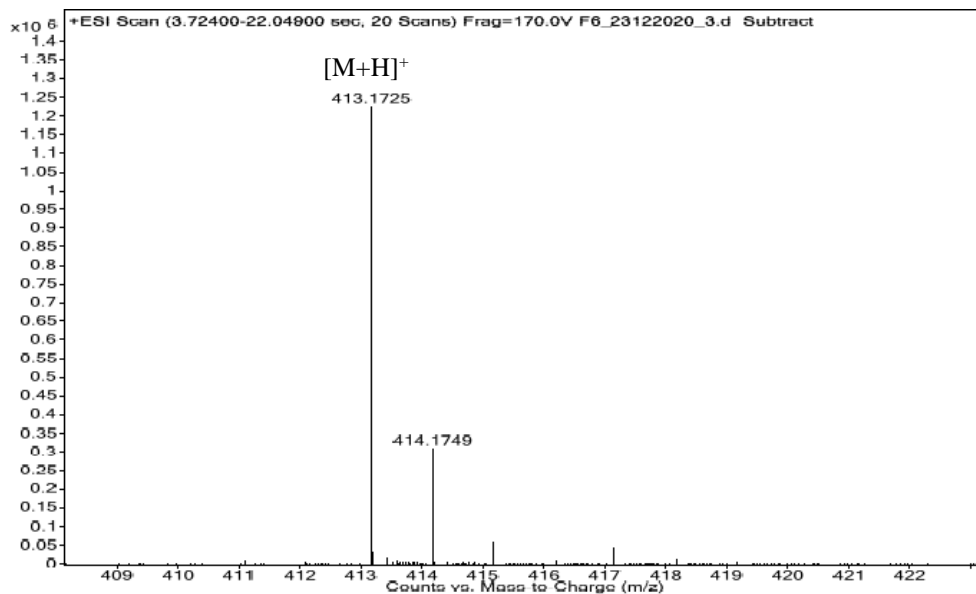


Figure A25: HRESIMS of 3,5,7-trihydroxy-8-methoxy-6-(4-methylpiperazin-1-ylmethyl)-2-phenyl-4H-chromen-4-one (M5c)

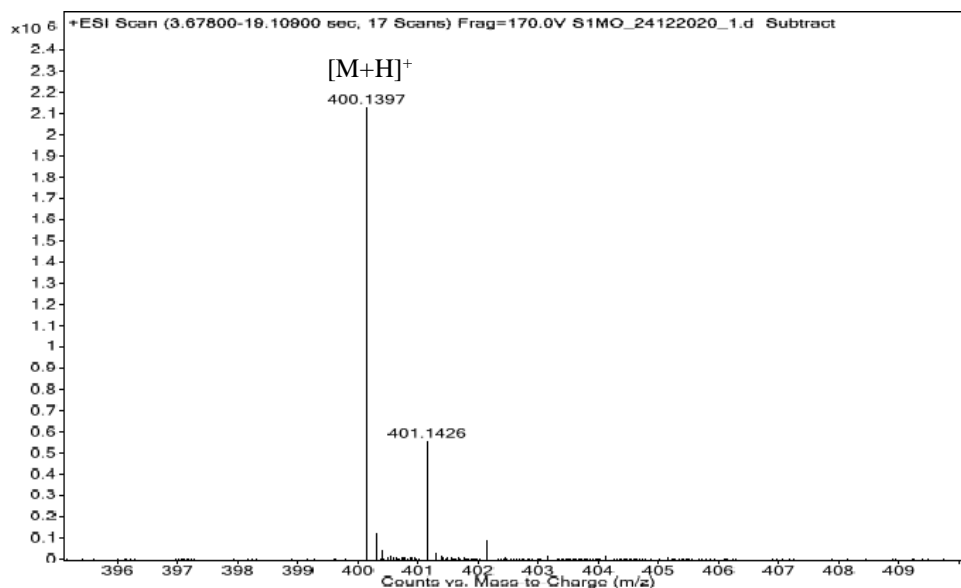


Figure A26: HRESIMS of 3,5,7-trihydroxy-8-methoxy-6-(morpholinomethyl)-2-phenyl-4H-chromen-4-one (M5d)

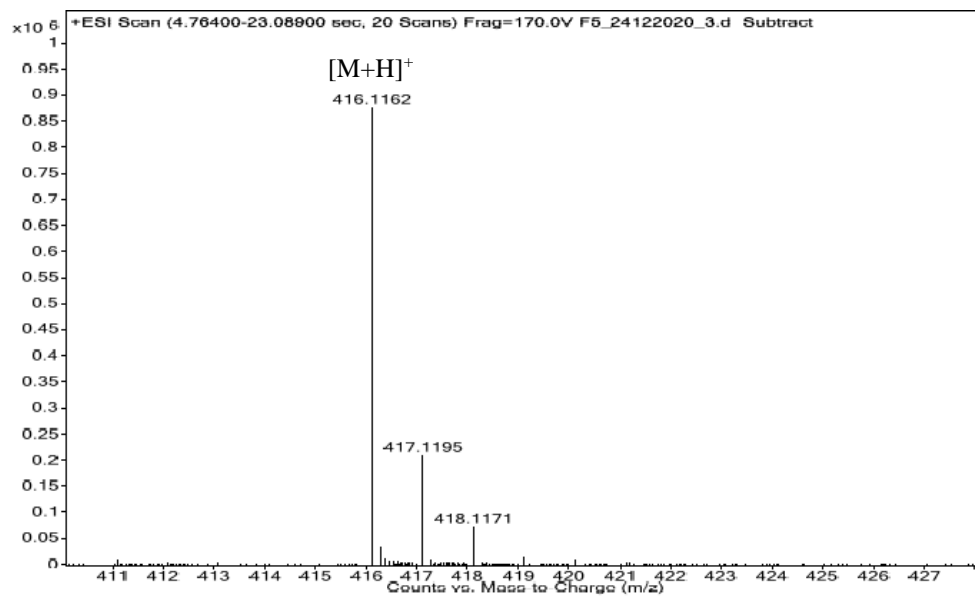


Figure A27: HRESIMS of 3,5,7-trihydroxy-8-methoxy-6-(thiomorpholinomethyl)-2-phenyl-4H-chromen-4-one (M5e)

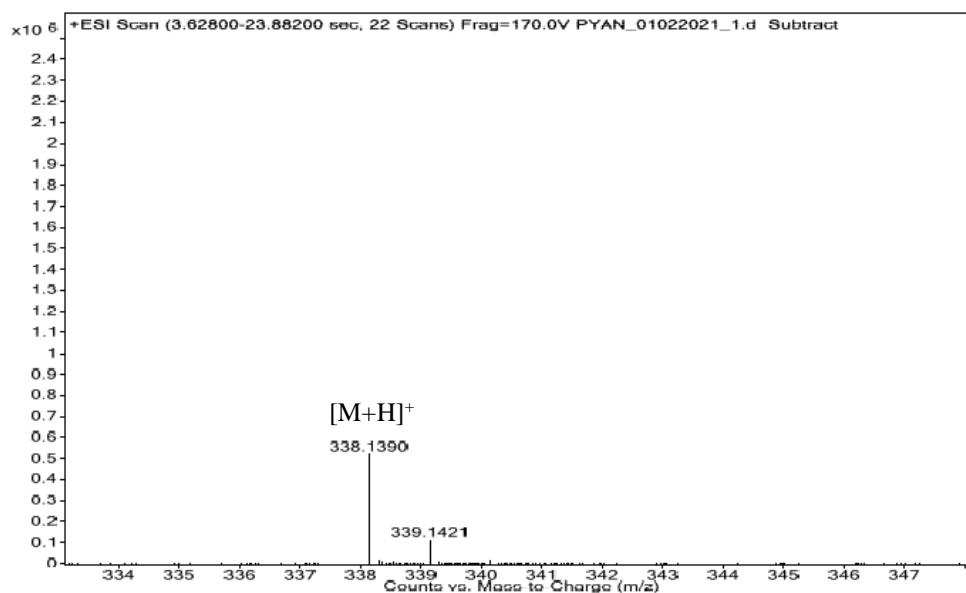


Figure A28: HRESIMS of 5,7-dihydroxy-8-(pyrrolidine-1-ylmethyl)-2-phenyl-4H-chromen-4-one (M14a)

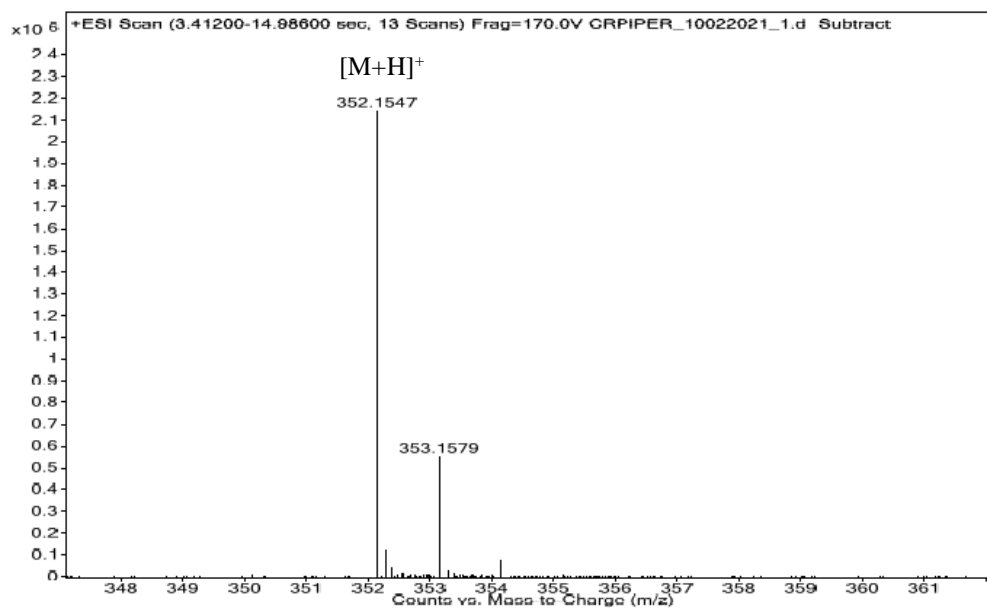


Figure A29: HRESIMS of 5,7-dihydroxy-8-(piperidin-1-ylmethyl)-2-phenyl-4H-chromen-4-one (M14b)

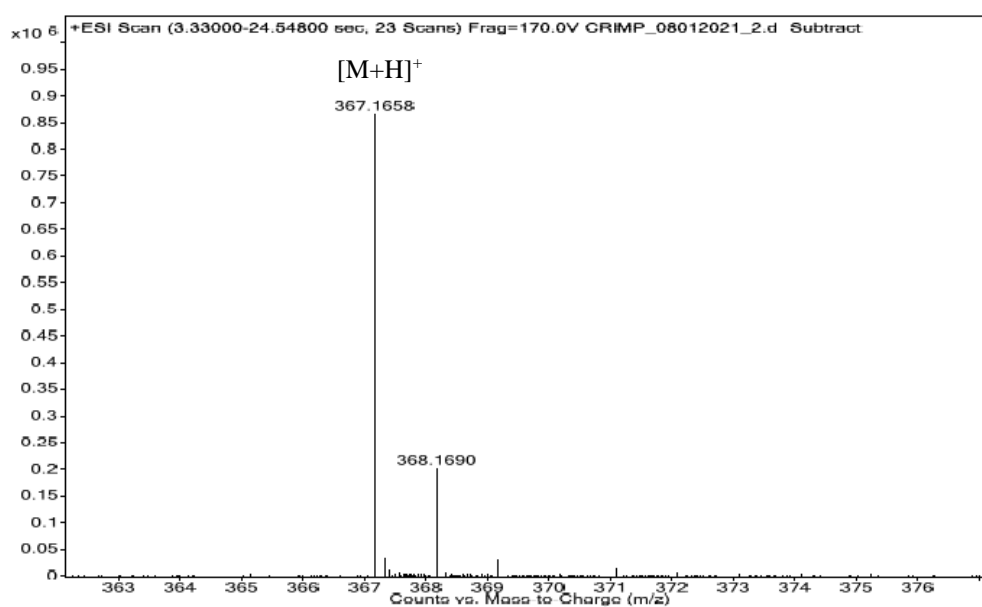


Figure A30: HRESIMS of 5,7-dihydroxy-8-(4-methylpiperazin-1-ylmethyl)-2-phenyl-4H-chromen-4-one (M14c)

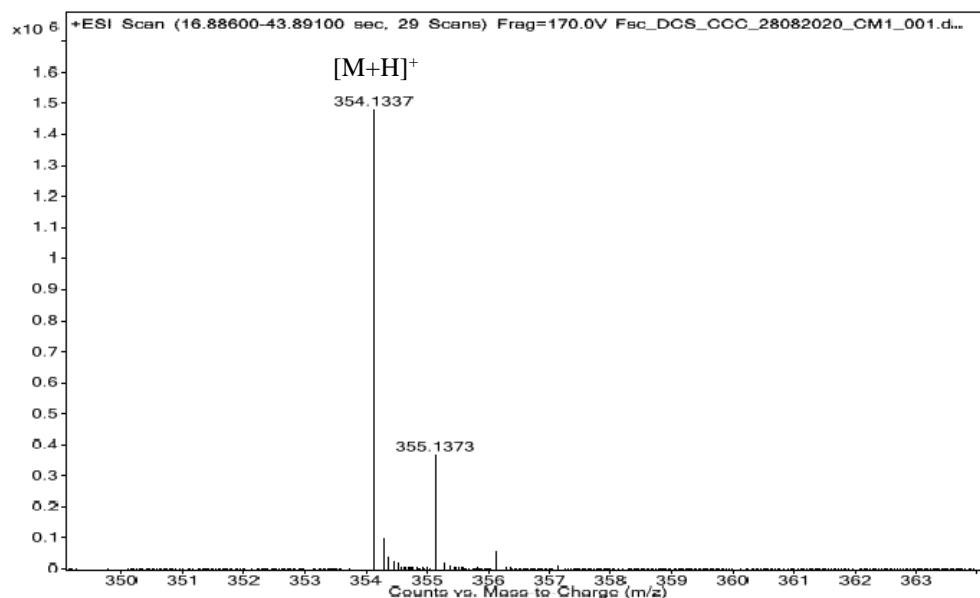


Figure A31: HESIMS of 5,7-dihydroxy-8-(morpholinomethyl)-2-phenyl-4H-chromen-4-one (M14d)

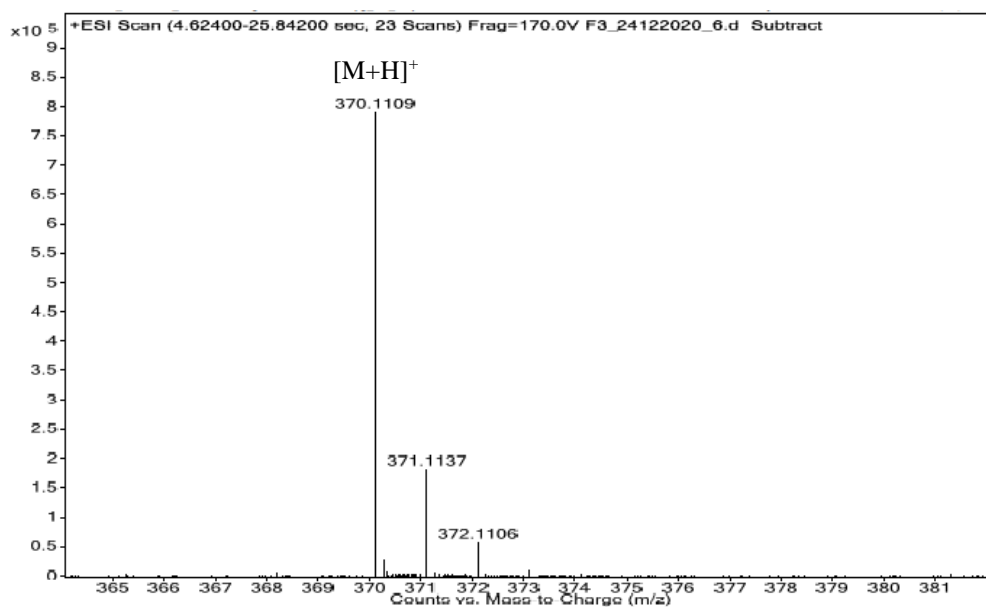


Figure A32: HRESIMS of 5,7-dihydroxy-8-(thiomorpholinomethyl)-2-phenyl-4H-chromen-4-one (M14e)

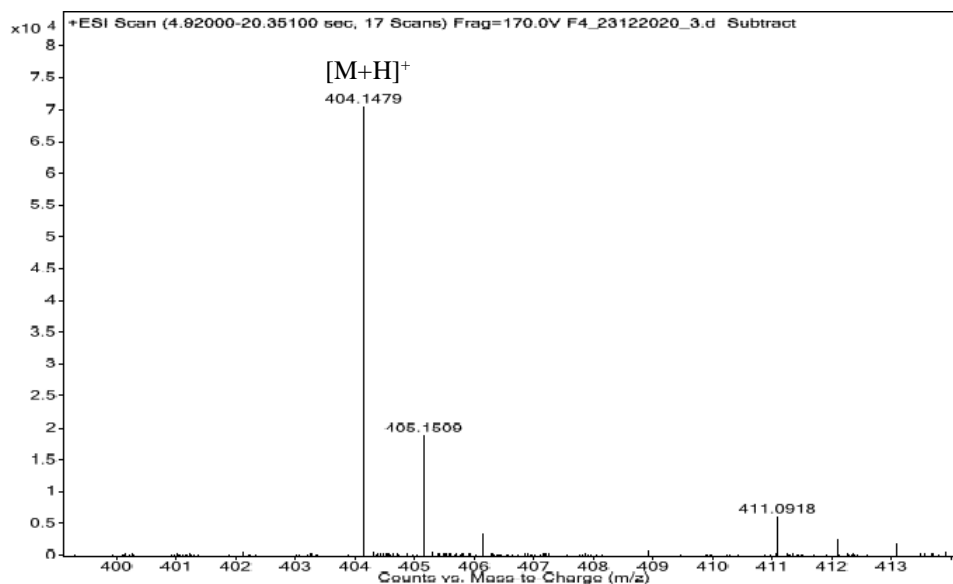


Figure A33: HRESIMS of 5,7-dihydroxy-8-(4-methoxybenzylamine)-2-phenyl-4H-chromen-4-one (M14f)

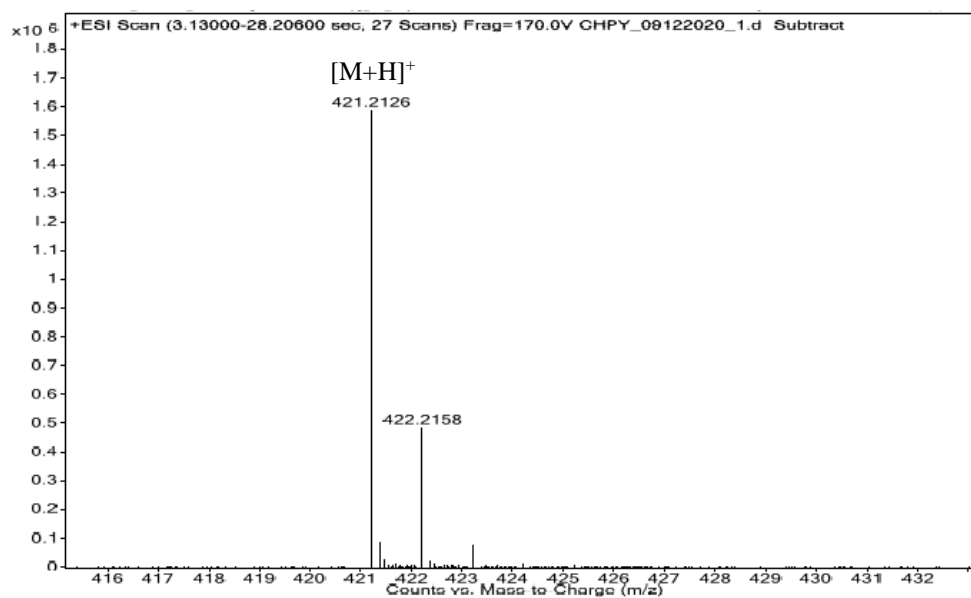


Figure A34: HRESIMS of 5,7-dihydroxy-6,8-bis(pyrrolidine-1-ylmethyl)-2-phenyl-4H-chromen-4-one (M14g)

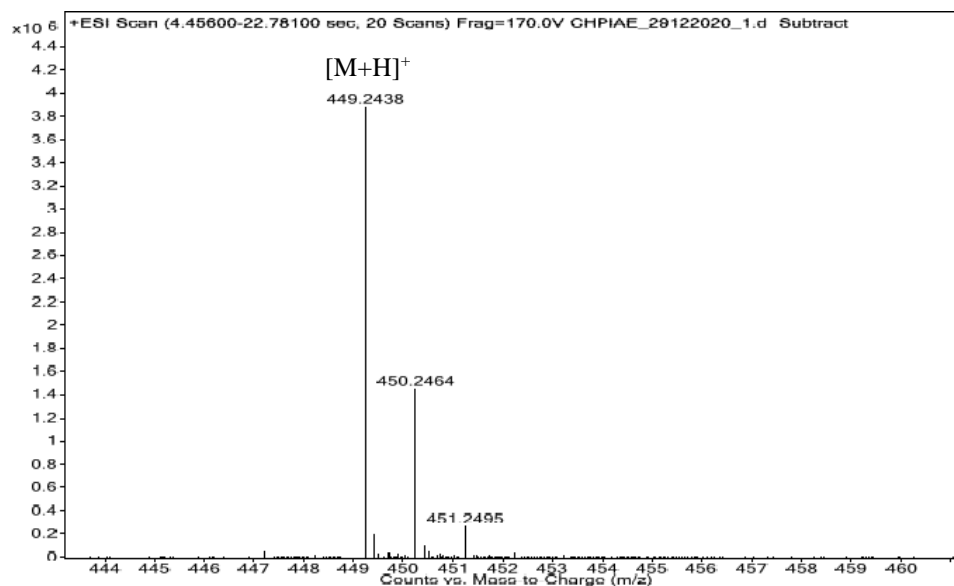


Figure A35: HRESIMS of 5,7-dihydroxy-6,8-bis(piperidin-1-ylmethyl)-2-phenyl-4H-chromen-4-one (M14h)

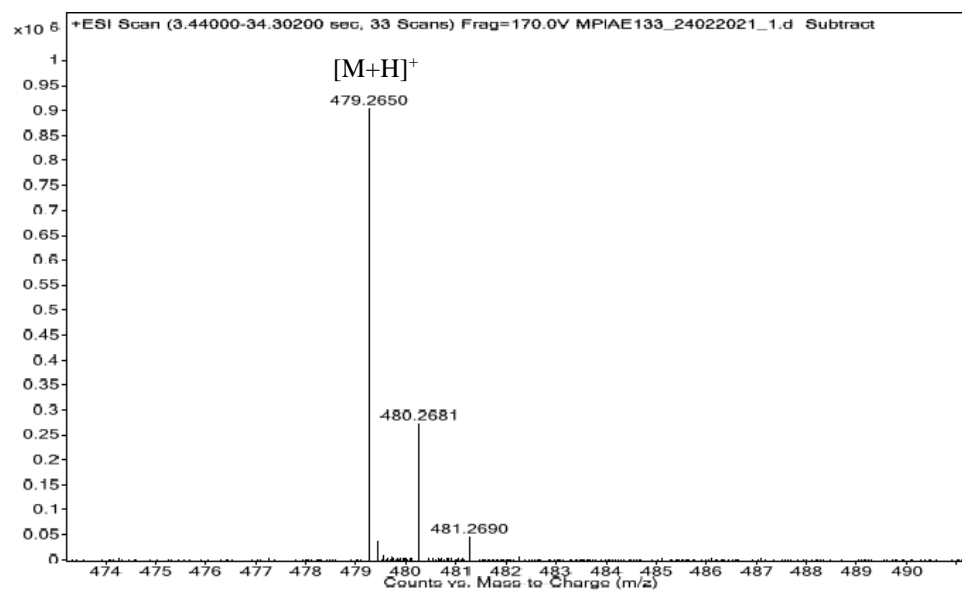


Figure A36: HRESIMS of 5,7-dihydroxy-6,8-bis(4-methylpiperazin-1-ylmethyl)-2-phenyl-4H-chromen-4-one (M14i)

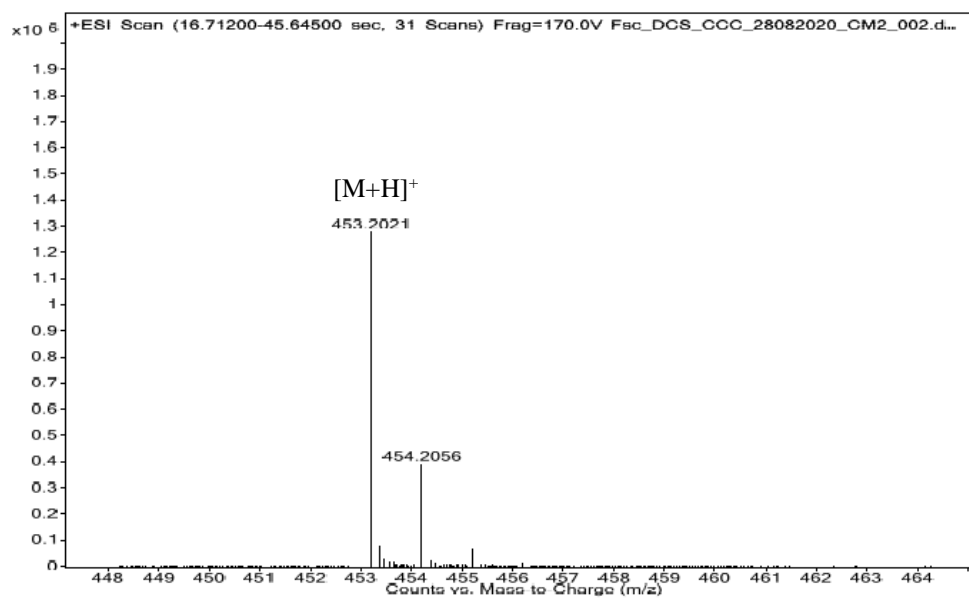


Figure A37: HRESIMS of 5,7-dihydroxy-6,8-bis(morpholinomethyl)-2-phenyl-4H-chromen-4-one (M14j)

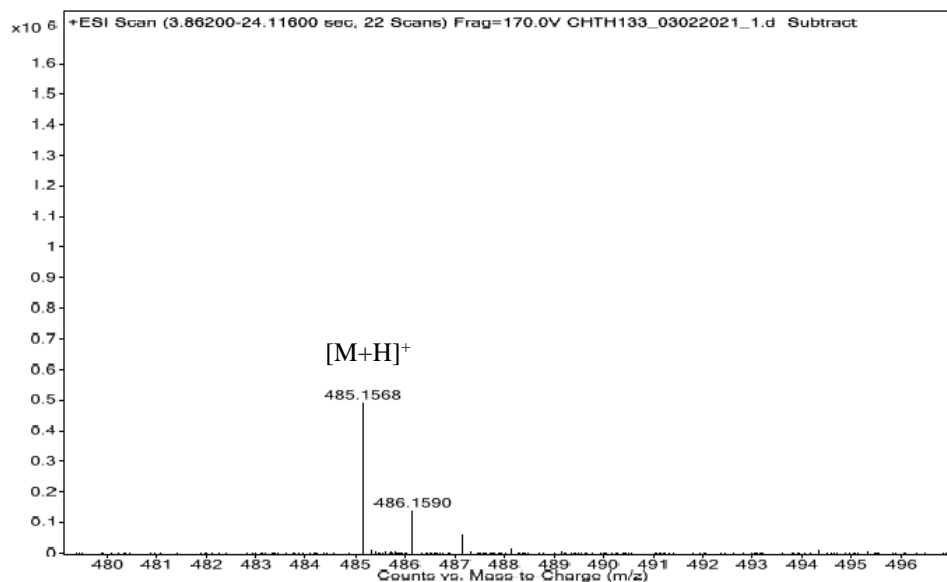


Figure A38: HRESIMS of 5,7-dihydroxy-6,8-bis(thiomorpholinomethyl)-2-phenyl-4H-chromen-4-one (M14k)

APPENDIX B

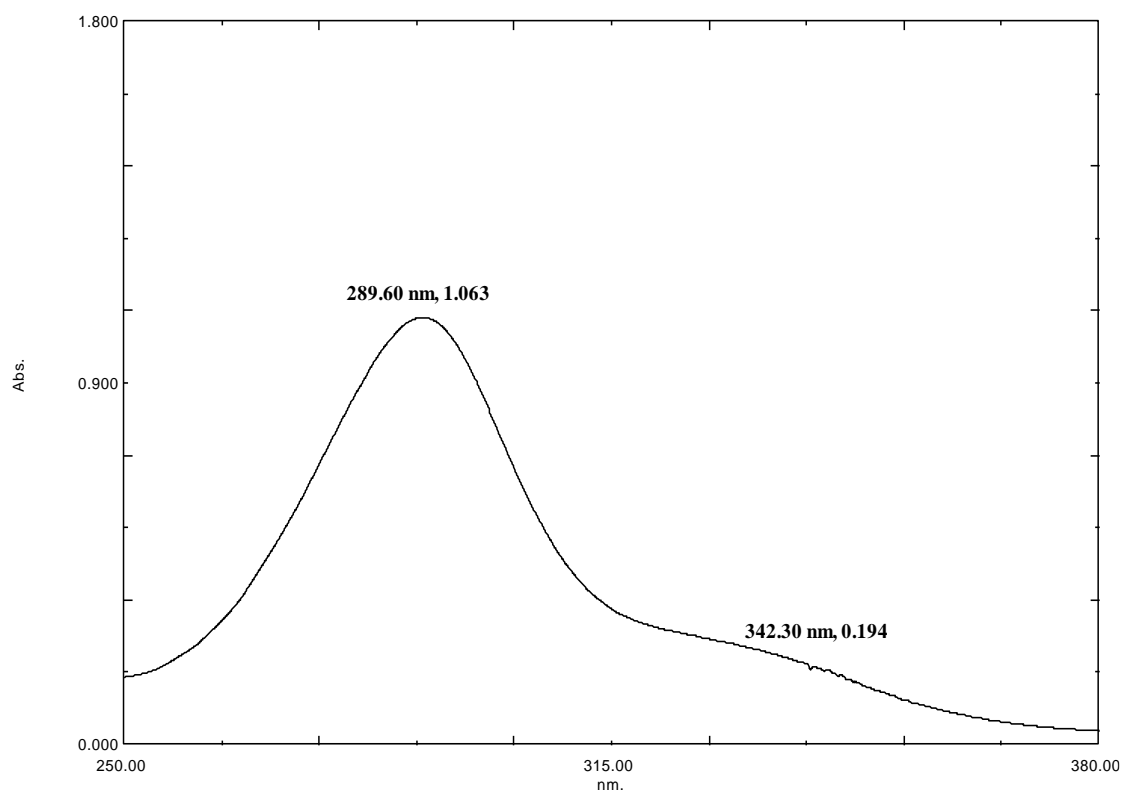


Figure B1: UV-vis spectrum of (2S, 3S)3,5-dihydroxy-7-methoxyflavaone (M1)

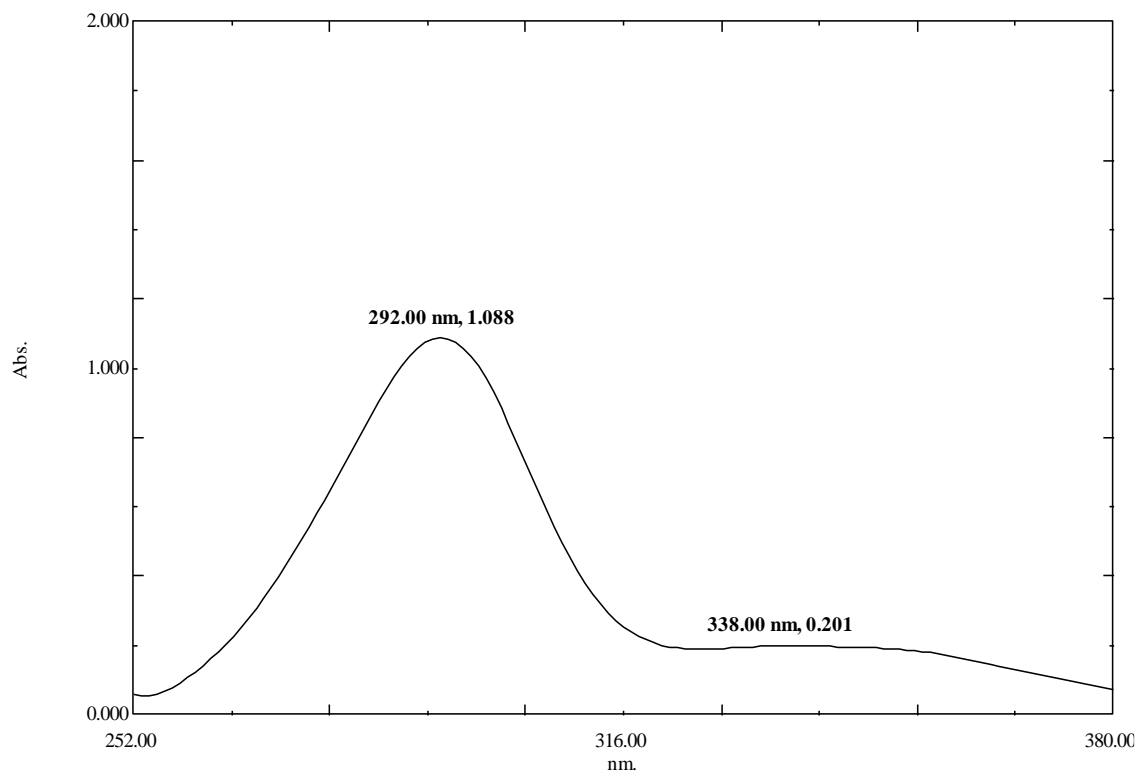


Figure B2: UV-vis spectrum of 3,5-dihydroxy-6,7-methoxyflavanone (M12)

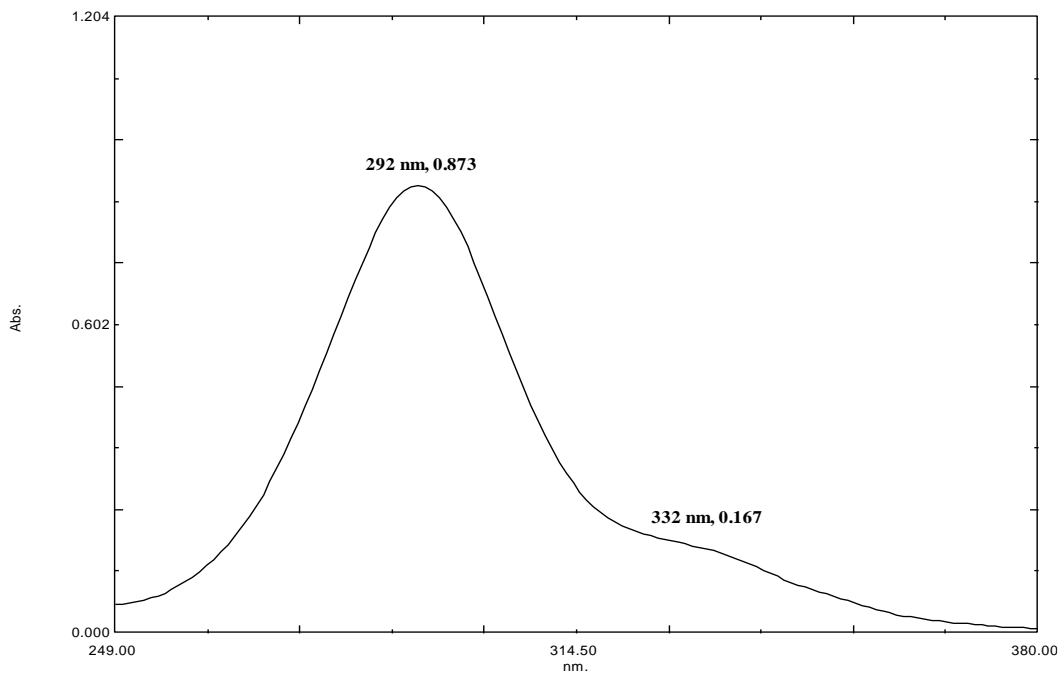


Figure B3: UV-vis spectrum of 3,5,7-trihydroxyflavanone (M13)

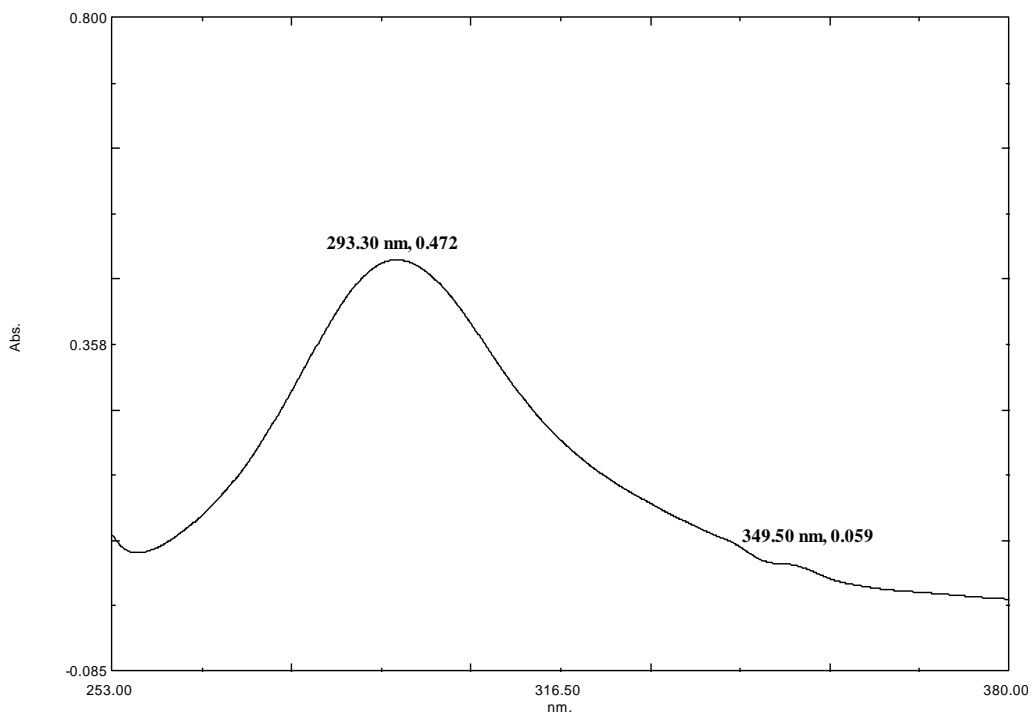


Figure B4: UV-vis spectrum of 7,8-dihydroxyflavanone (M17)

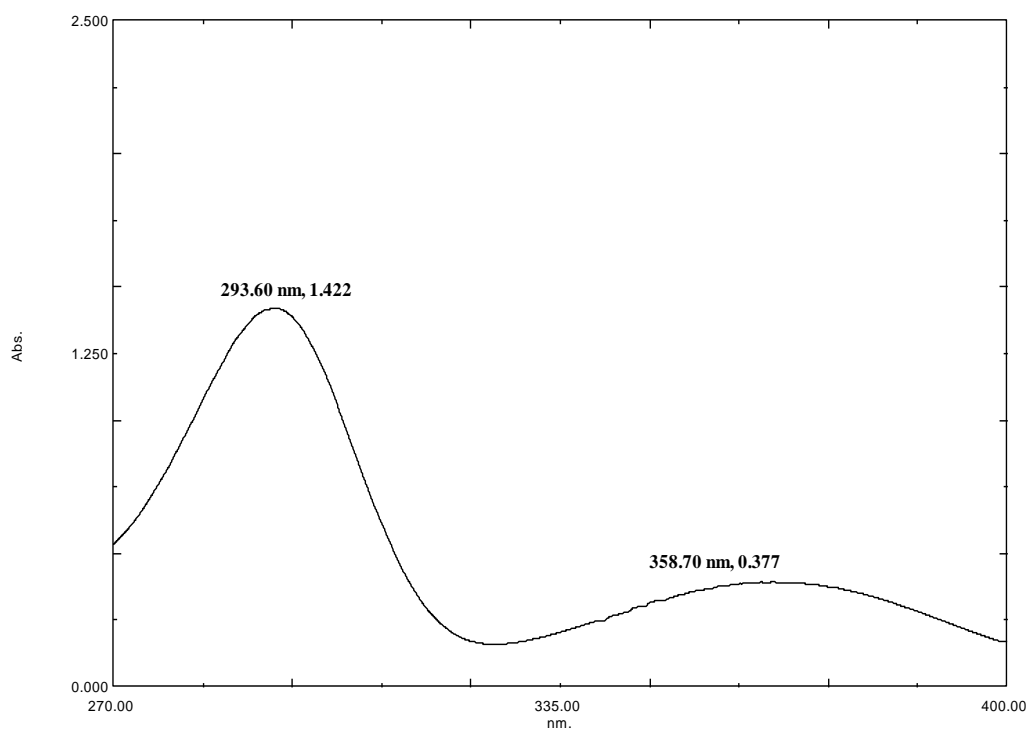


Figure B5: UV-vis spectrum of 3,5,7-trihydroxy-7-methoxyflavanone (M18)

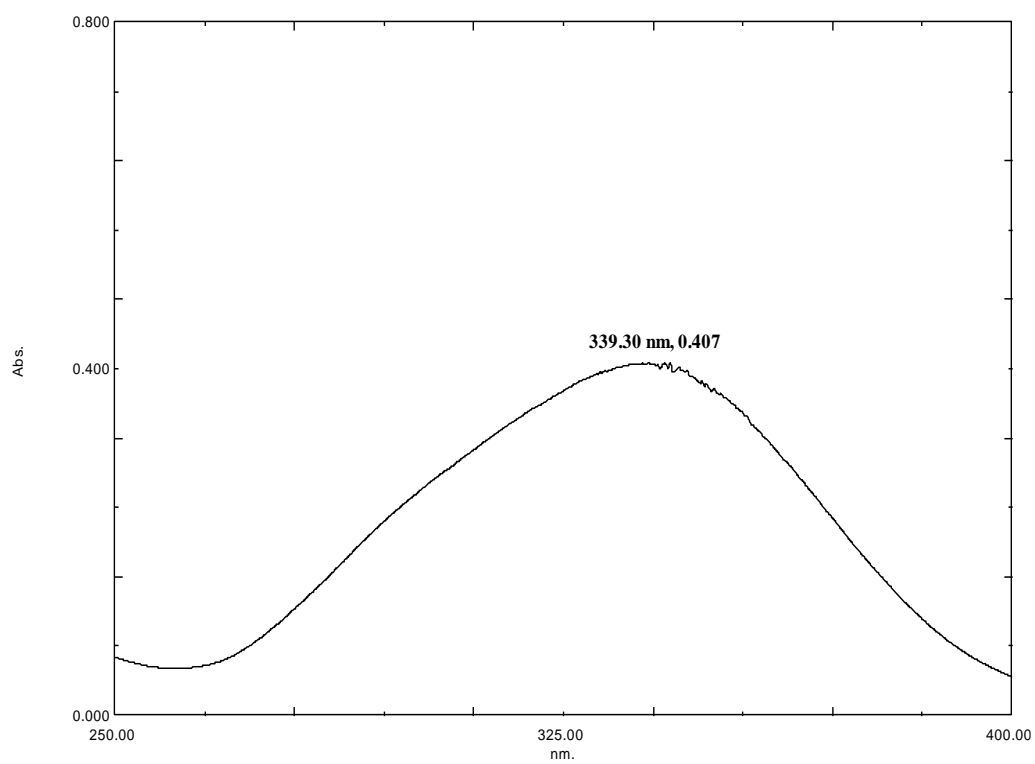


Figure B6: UV-vis spectrum of 2',4'-dihydroxy-3'-methoxychalcone (M2)

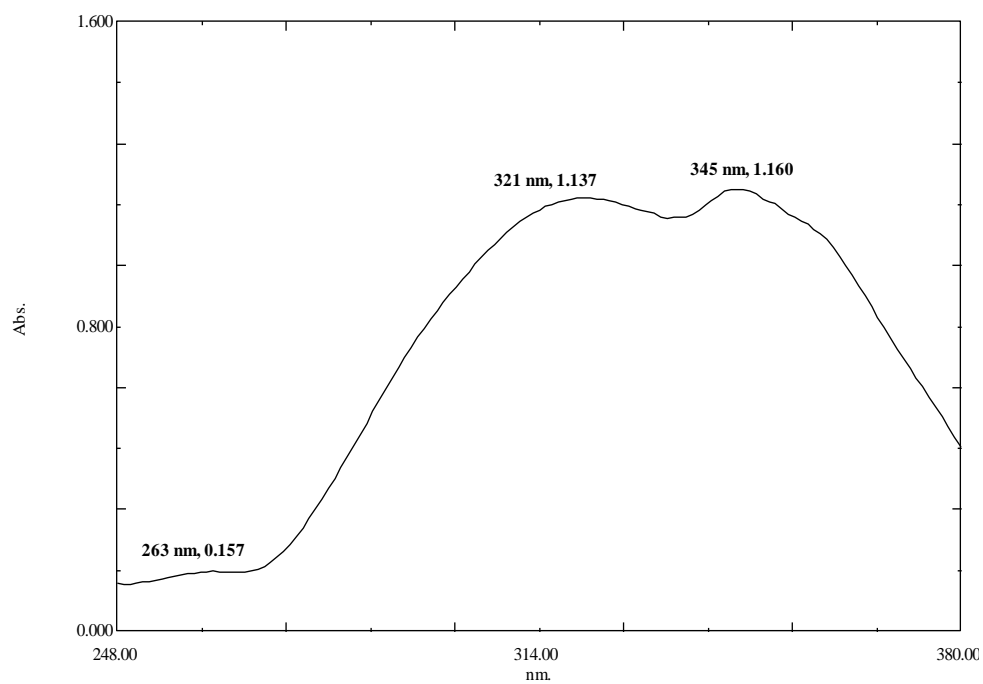


Figure B7: UV-vis spectrum of 2',4'-dihydroxychalcone (M4)

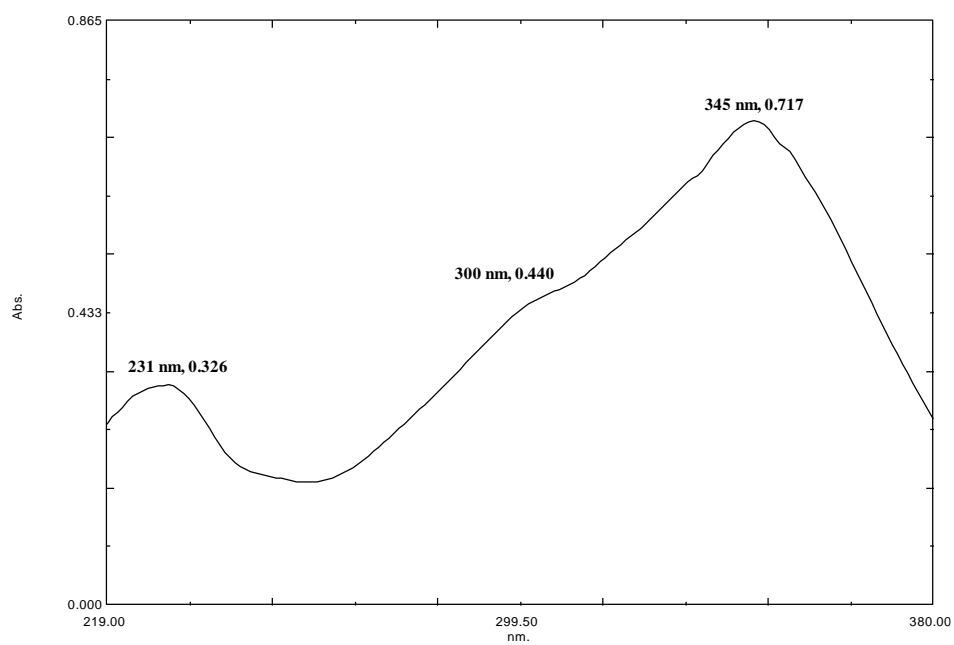


Figure B8: UV-vis spectrum of 2',3',4'-trihydroxychalcone (M6)

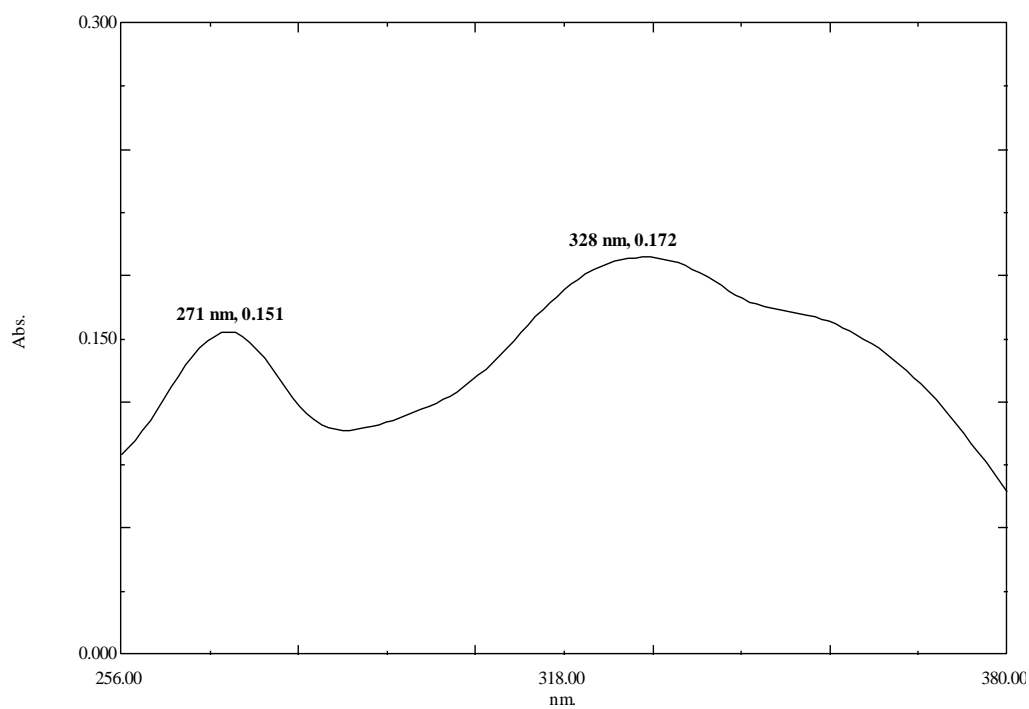


Figure B9: UV-vis spectrum of 3,5-dihydroxy-6,7-dimethoxyflavone (M3)

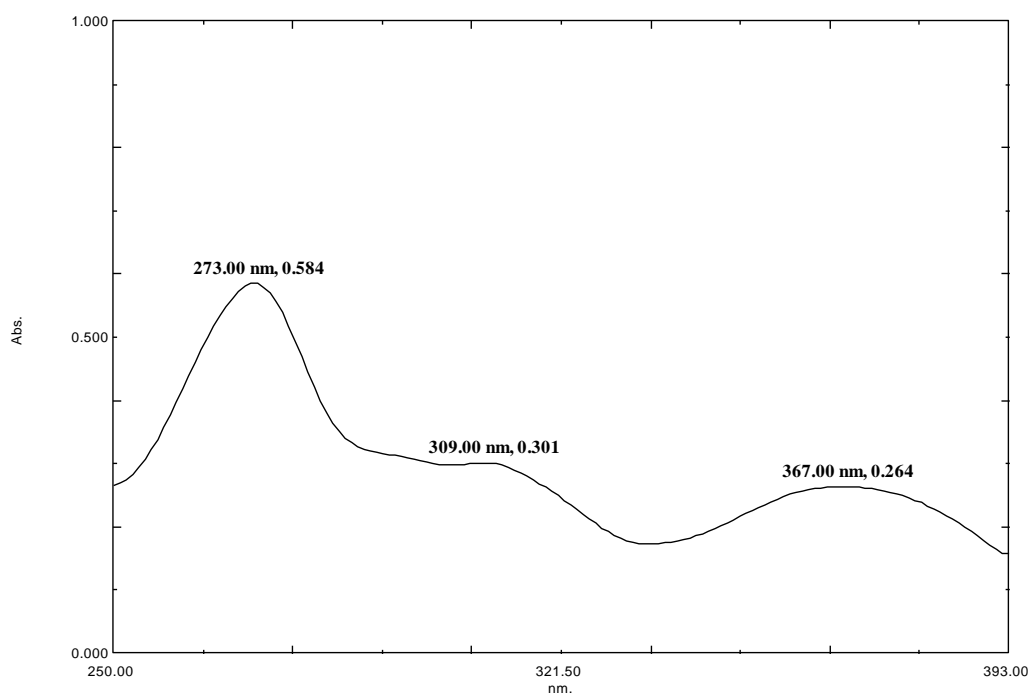


Figure B10: UV-vis spectrum of 3,5,7-trihydroxy-8-methoxyflavone (M5)

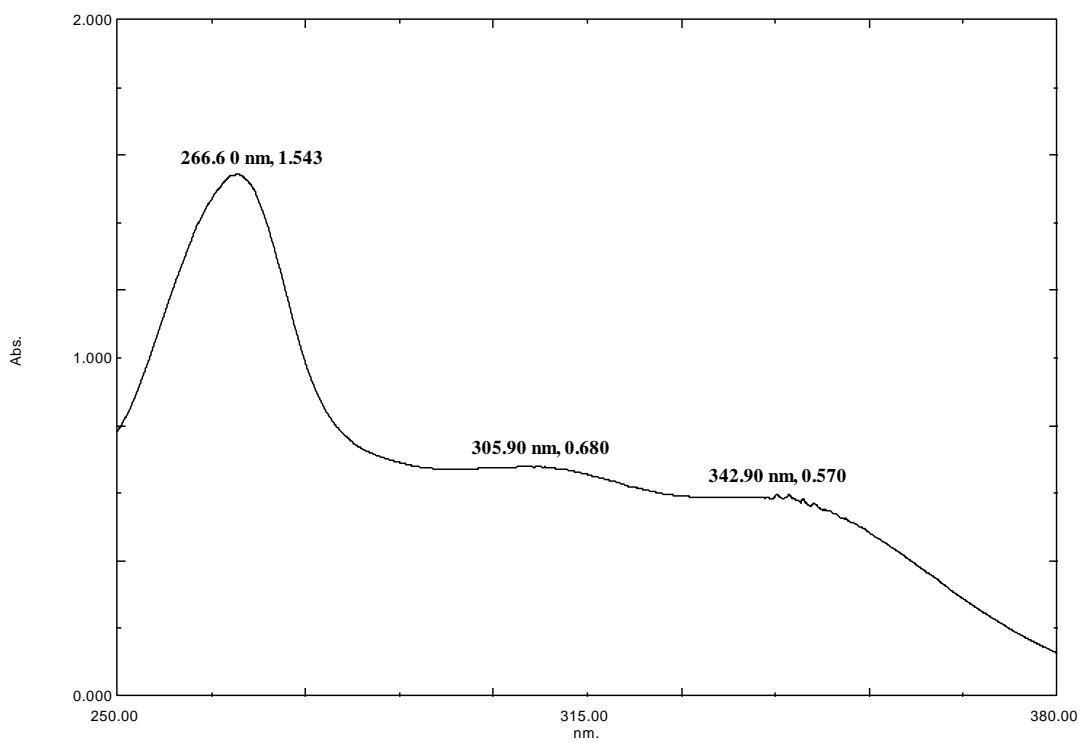


Figure B11: UV-vis spectrum of 5-hydroxy-3,7-dimethoxyflavone (M7)

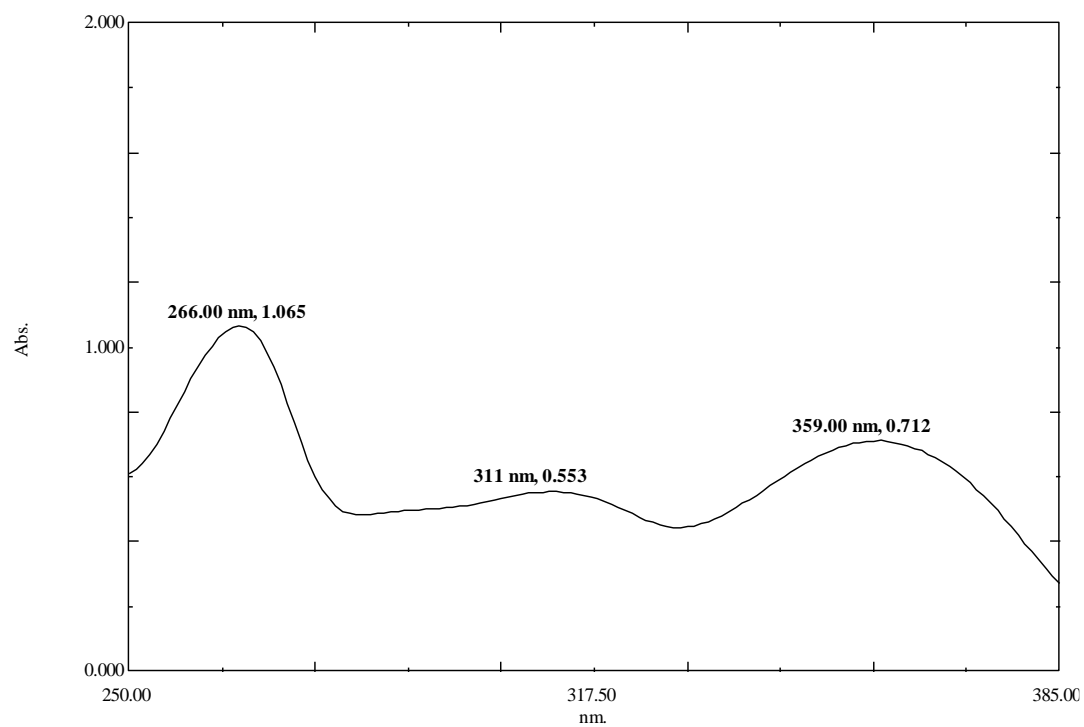


Figure B12: UV-vis spectrum of 3,5-dihydroxy-7-methoxyflavone (M8)

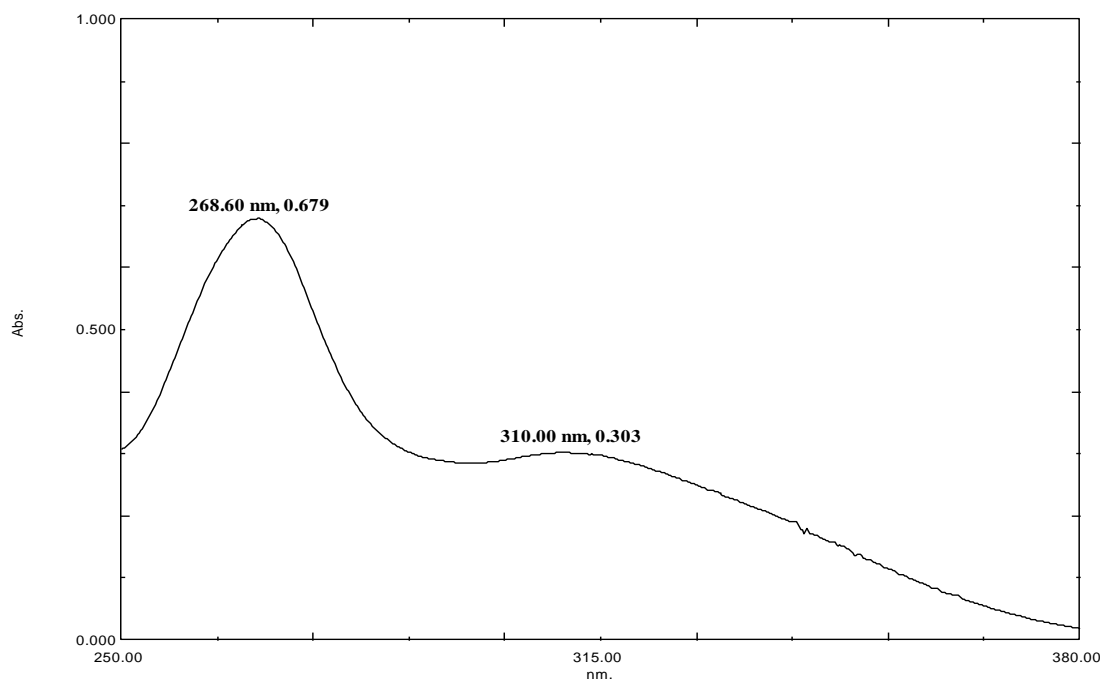


Figure B13: UV-vis spectrum of 5-hydroxy-7-methoxyflavone (M9)

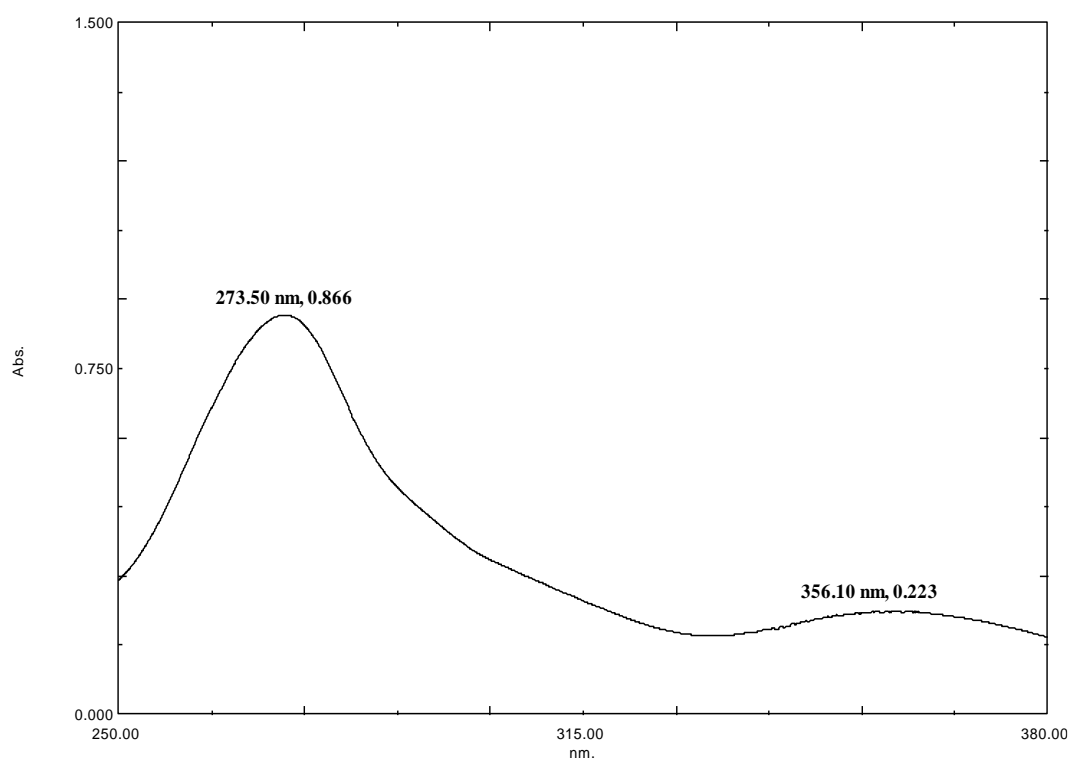


Figure B14: UV-vis spectrum of 5-hydroxy-3,7,8-trimethoxyflavone (M10)

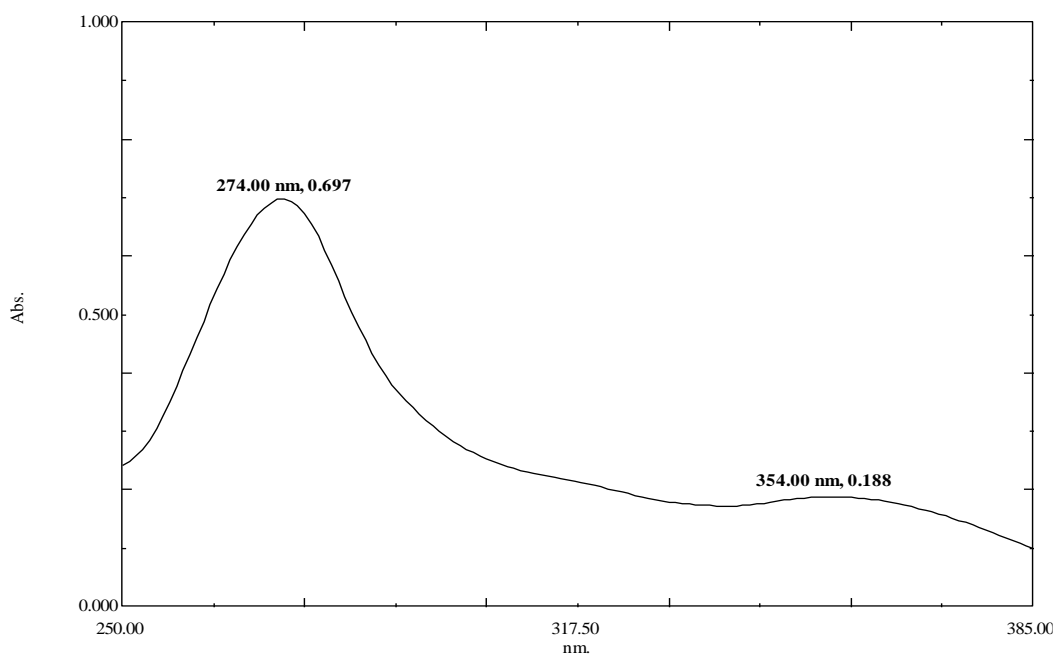


Figure B15: UV-vis spectrum of 5,7-dihydroxy-3,8-dimethoxyflavone (M11)

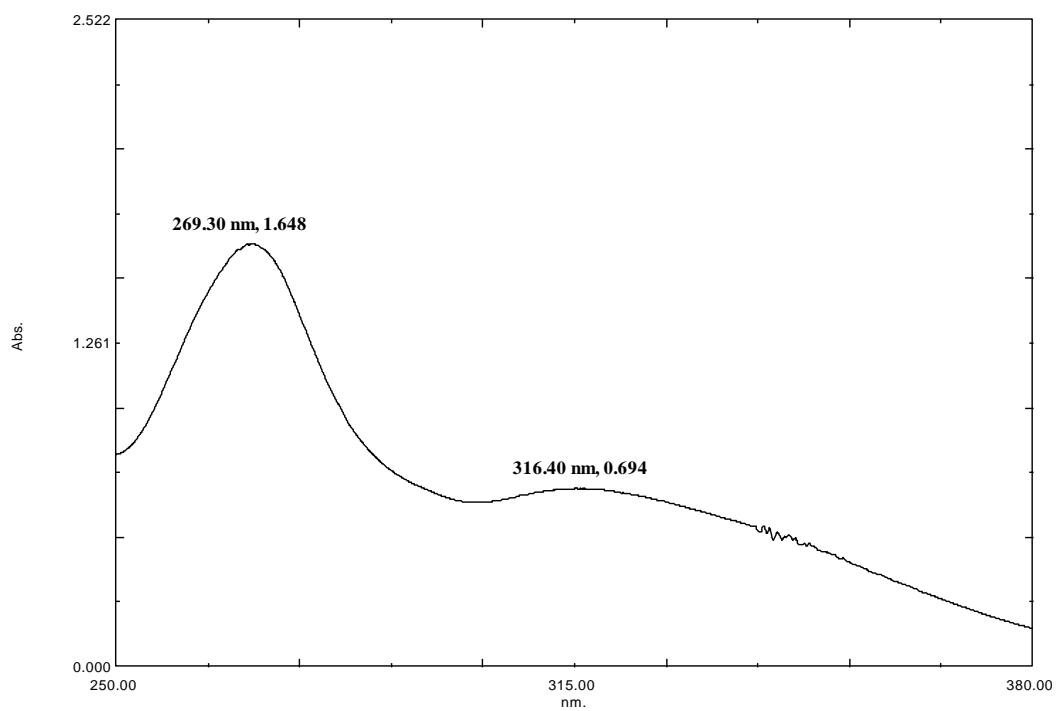


Figure B16: UV-vis spectrum of 5,7-dihydroxyflavone (M14)

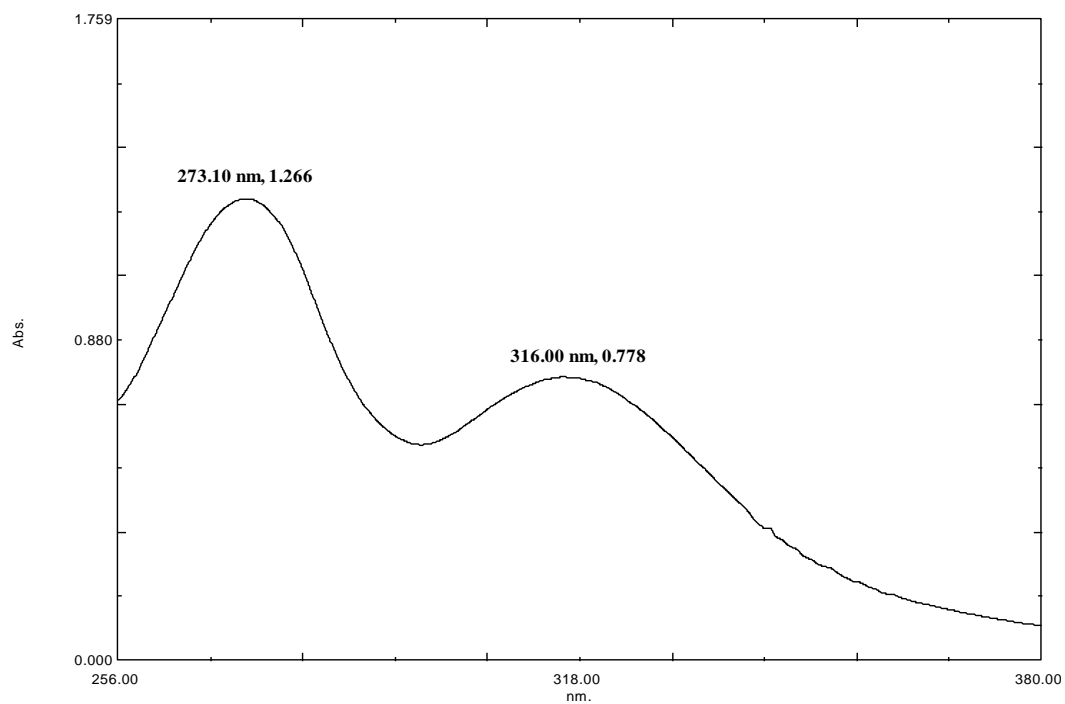


Figure B17: UV-vis spectrum of 5-hydroxy-6,7-dimethoxyflavone (M15)

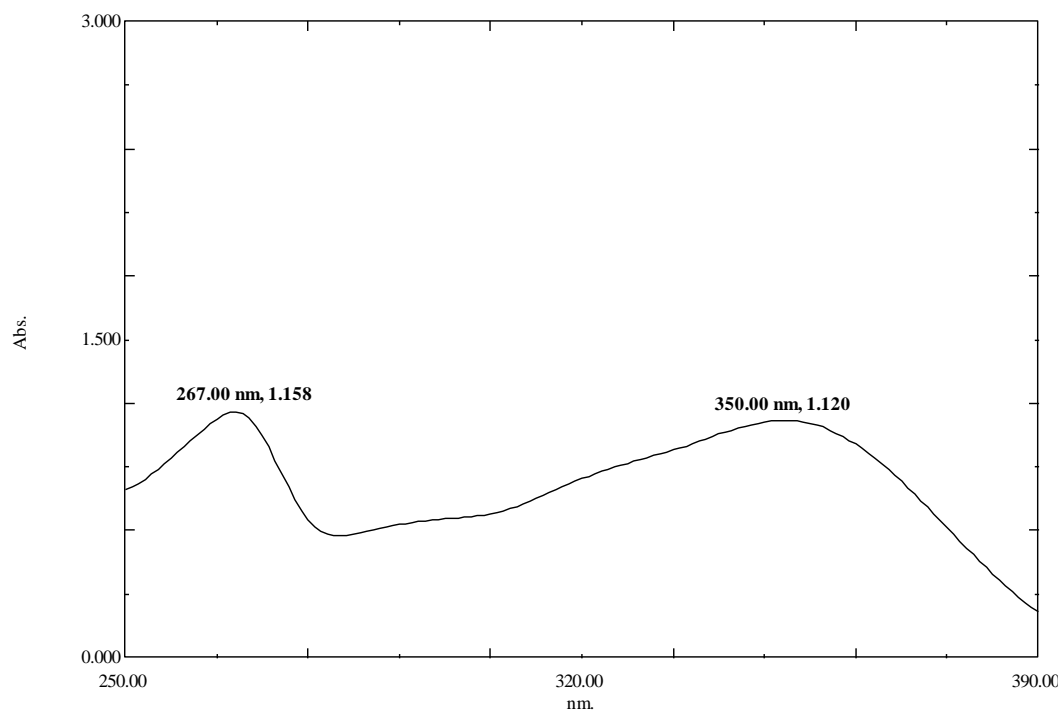


Figure B18: UV-vis spectrum of 5,4'-dihydroxy-3,7-dimethoxyflavone (M16)

APPENDIX C

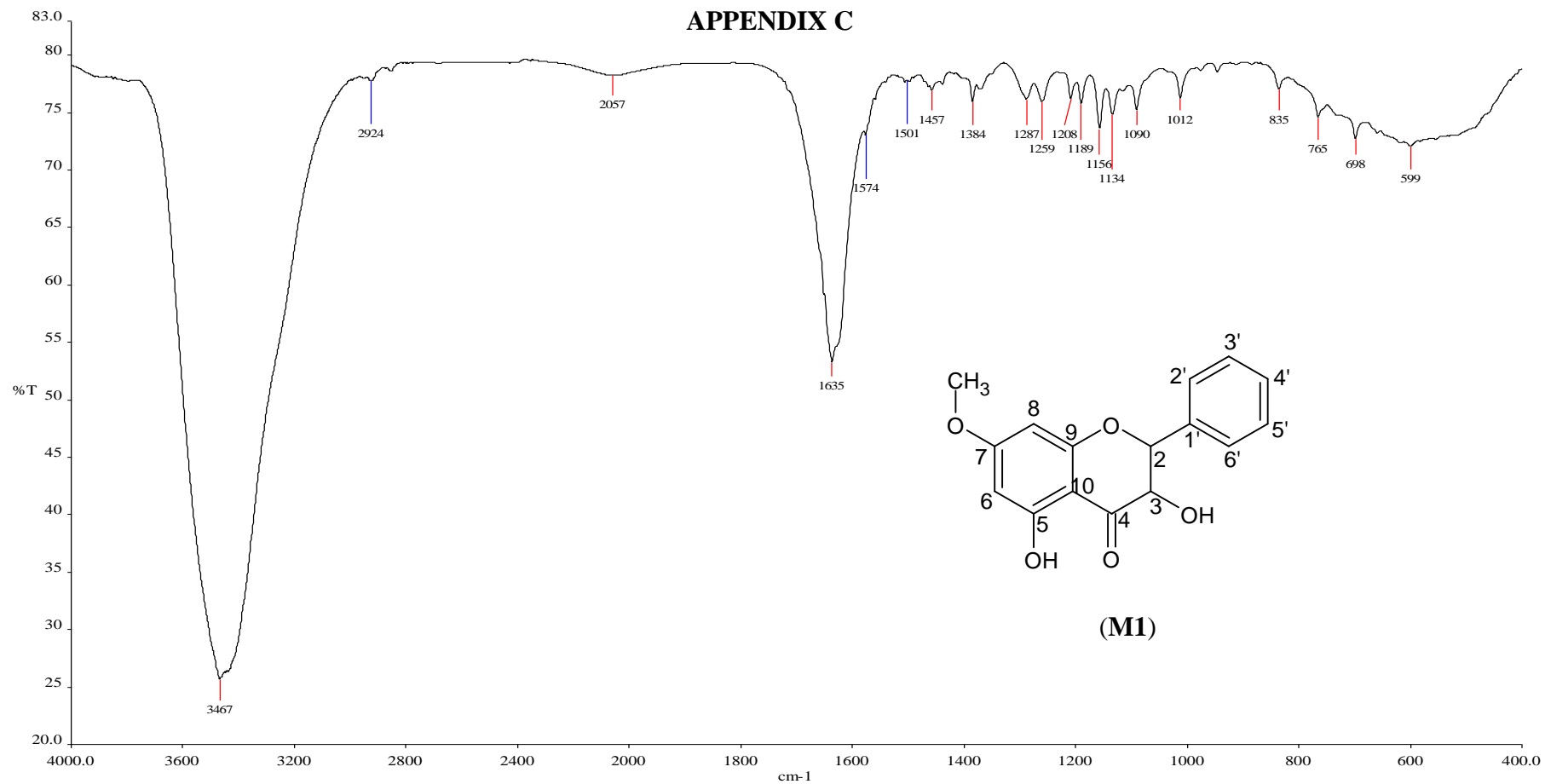


Figure C1: FTIR (KBr) of (2S,3S) 3,5-dihydroxy-7-methoxyflavanone (M1)

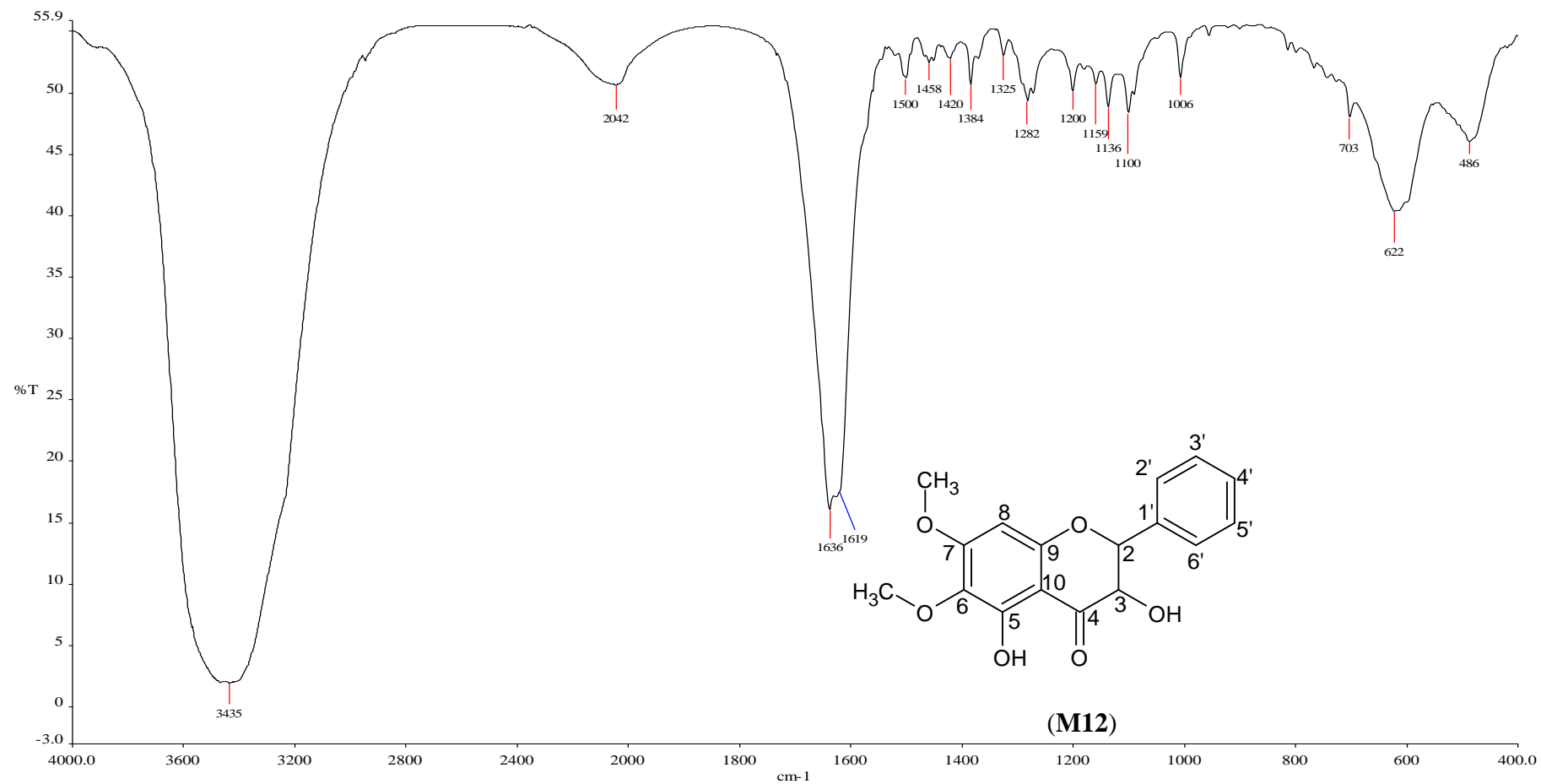


Figure C2: FTIR (KBr) of (2R,3R) 3,5-dihydroxy-6,7-dimethoxyflavanone (M12)

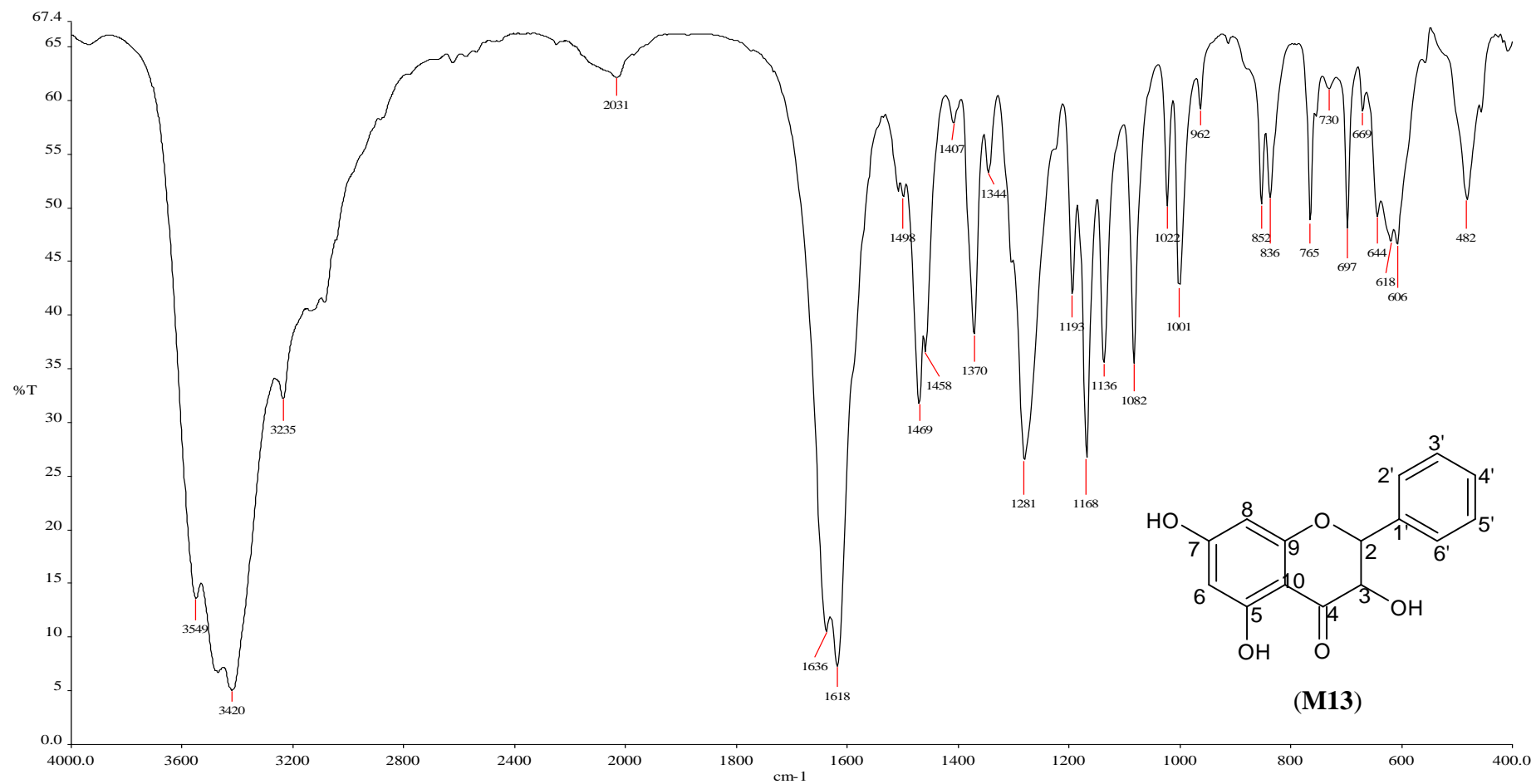


Figure C3: FTIR (KBr) of (2R,3R) 3,5,7-trihydroxyflavanone (M13)

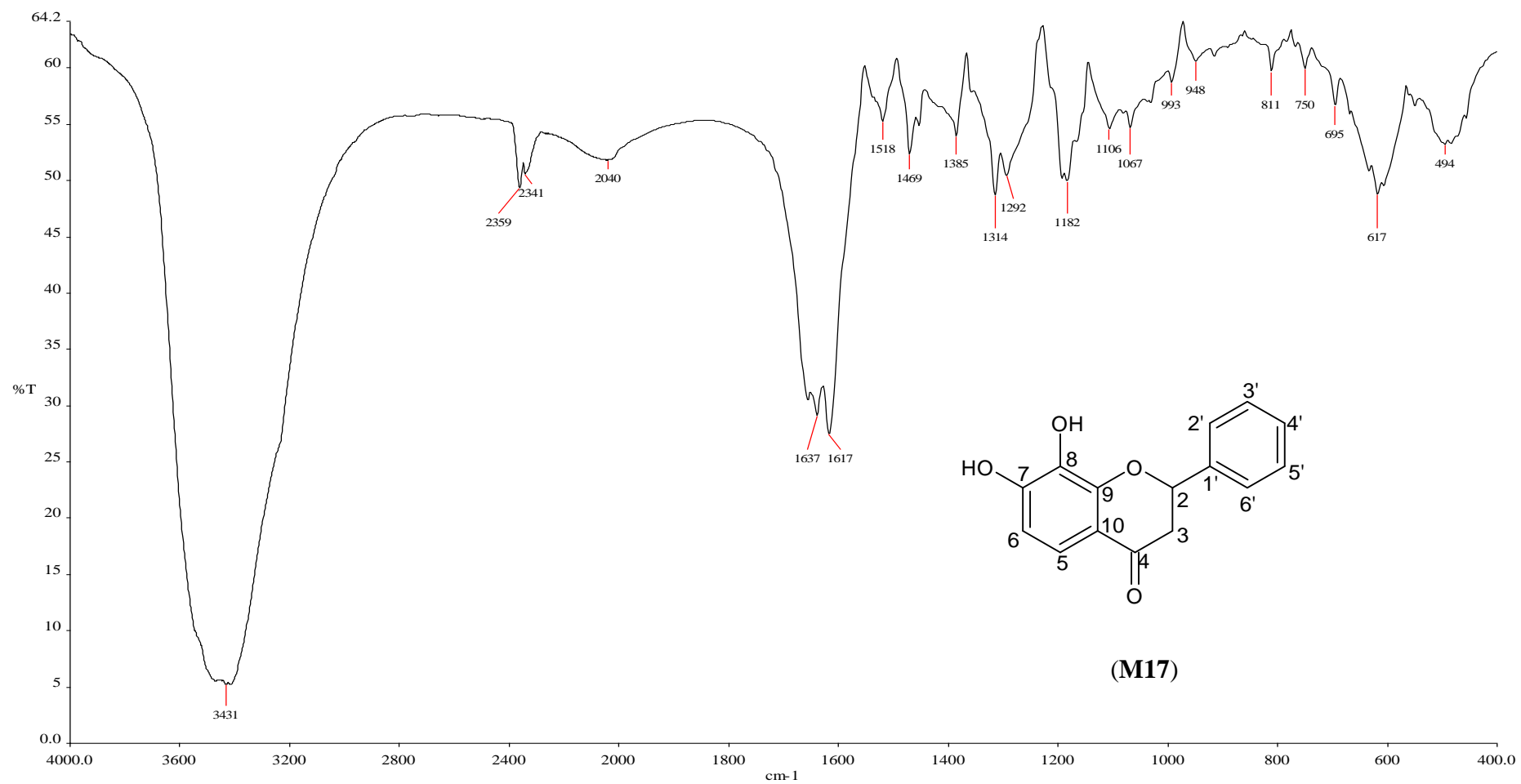


Figure C4: FTIR (KBr) of (2S) 7,8-dihydroxyflavanone (M17)

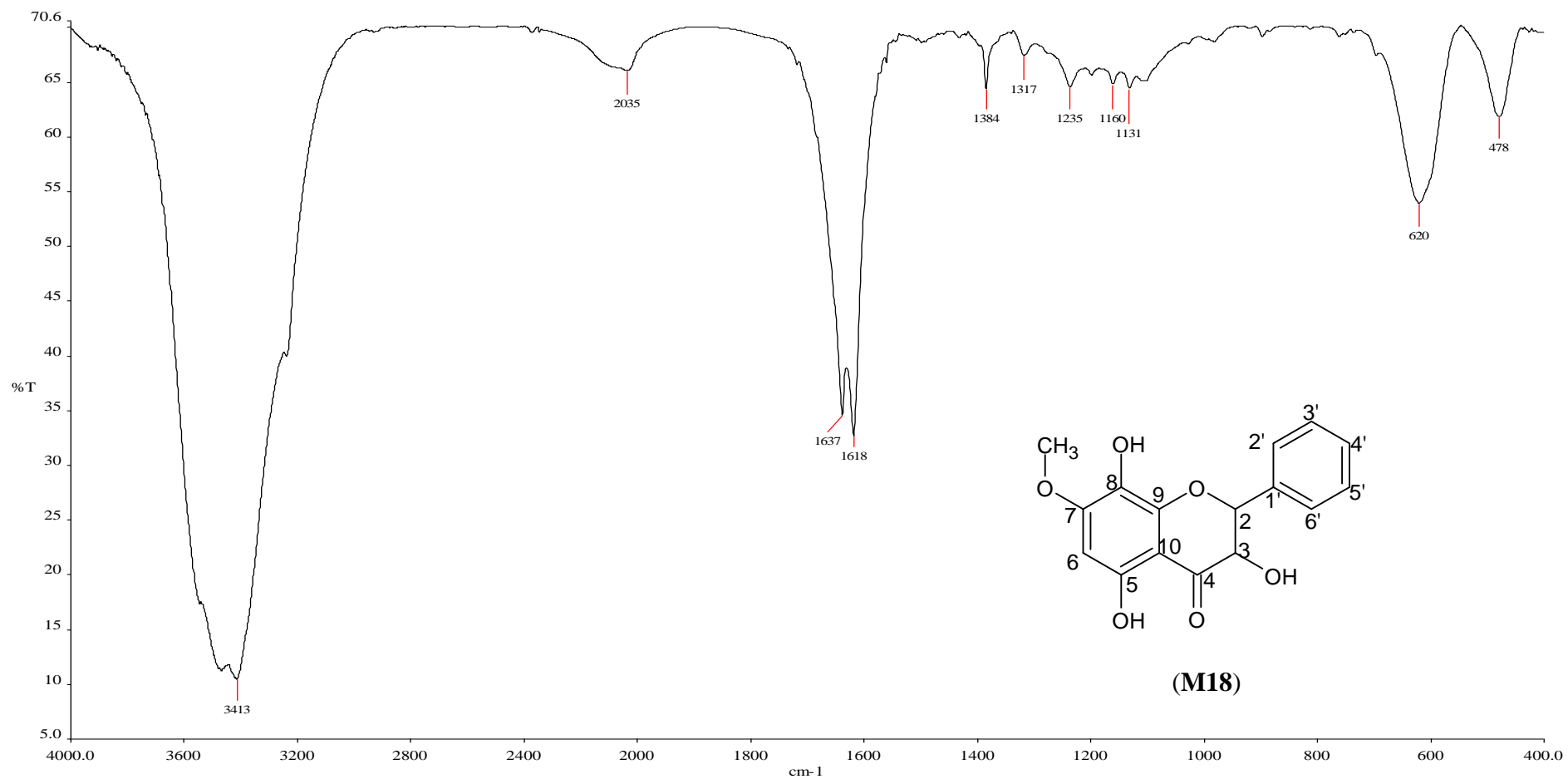


Figure C5: FTIR (KBr) of (2R,3R) 3,5,8-trihydroxy-7-methoxyflavanone (M18)

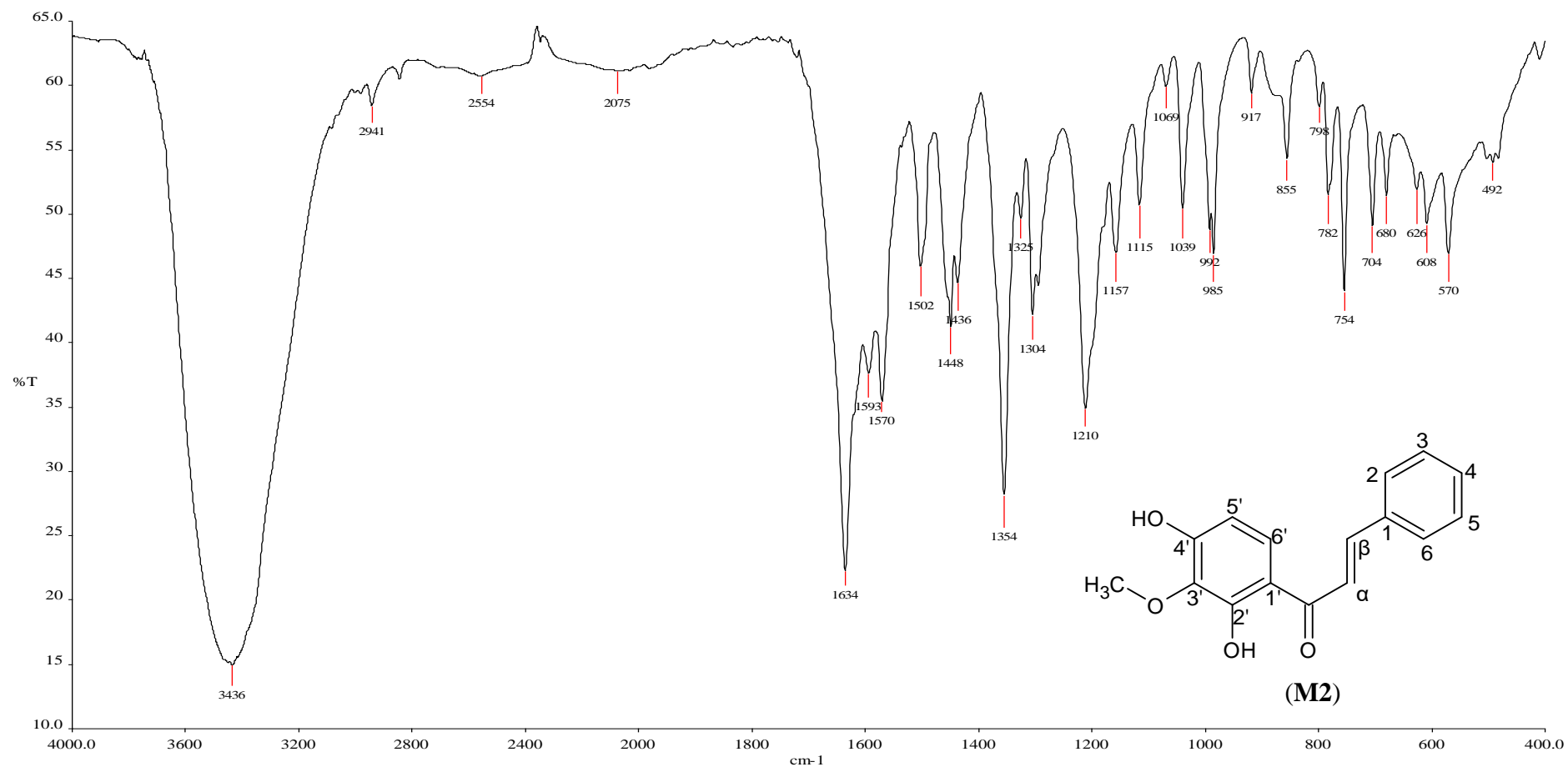


Figure C6: FTIR (KBr) of 2',4'-dihydroxy-3'-methoxychalcone (M2)

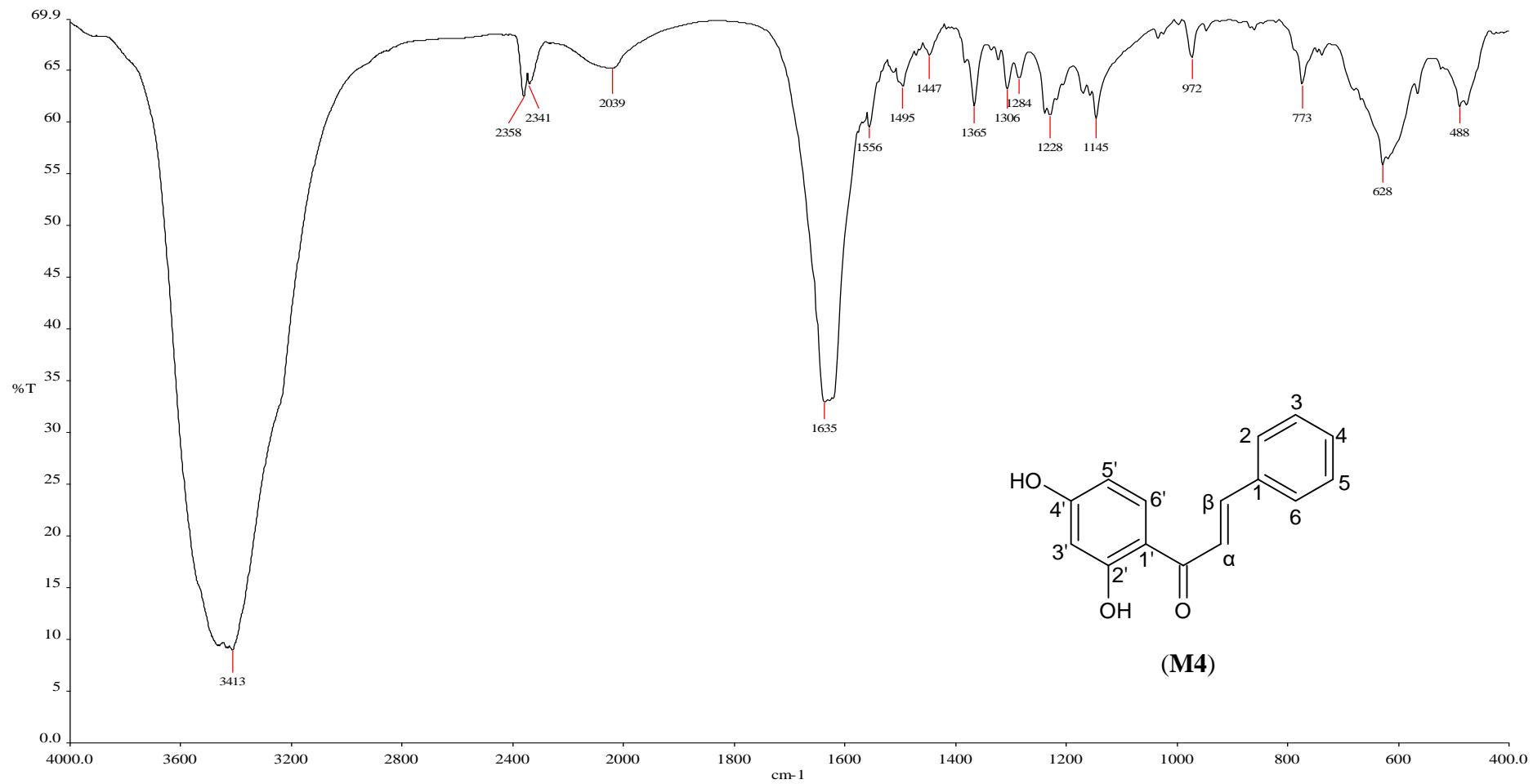


Figure C7: FTIR (KBr) of 2',4'-dihydroxychalcone (M4)

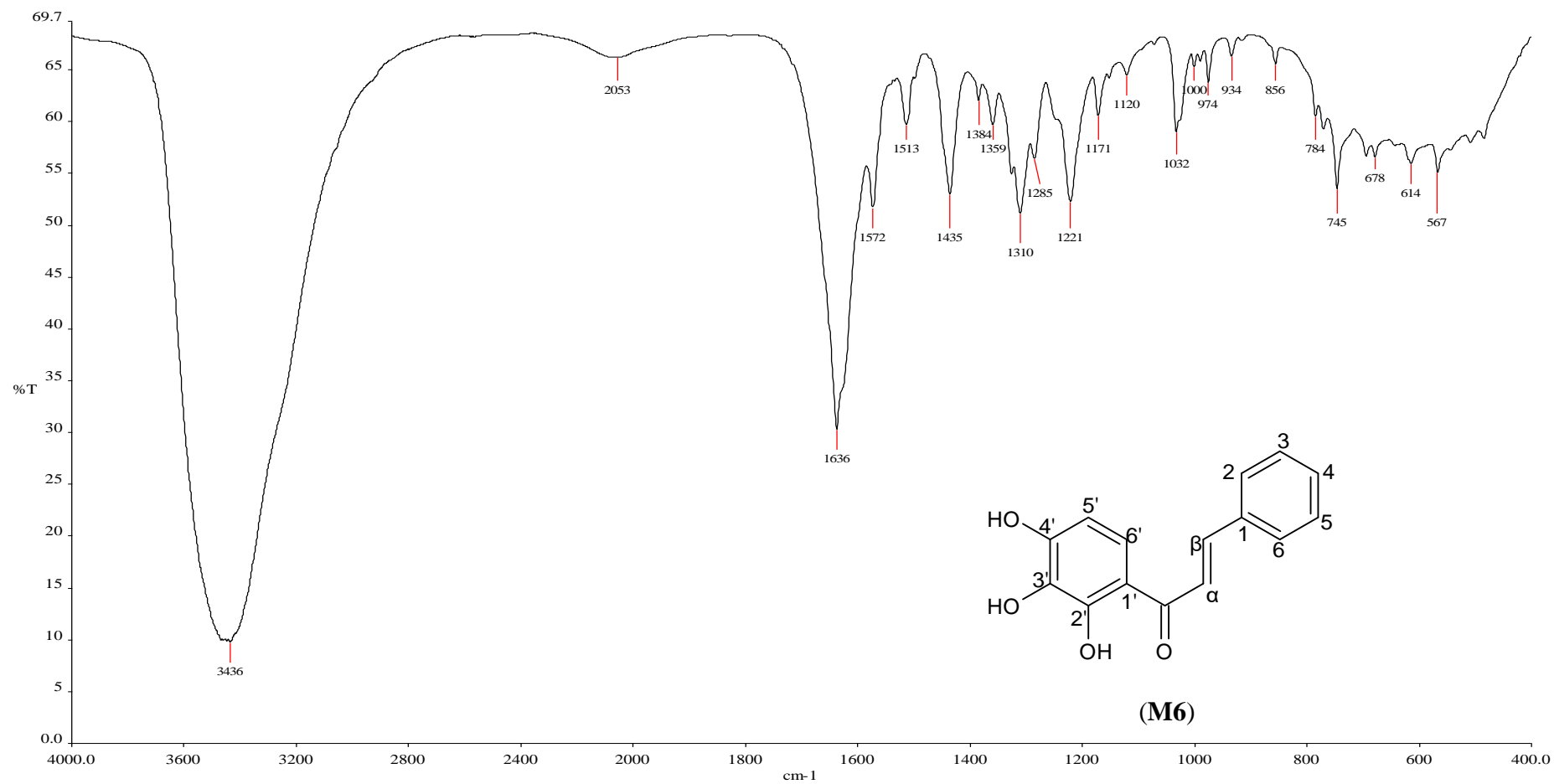


Figure C8: FTIR (KBr) of 2',3',4'-trihydroxychalcone (M6)

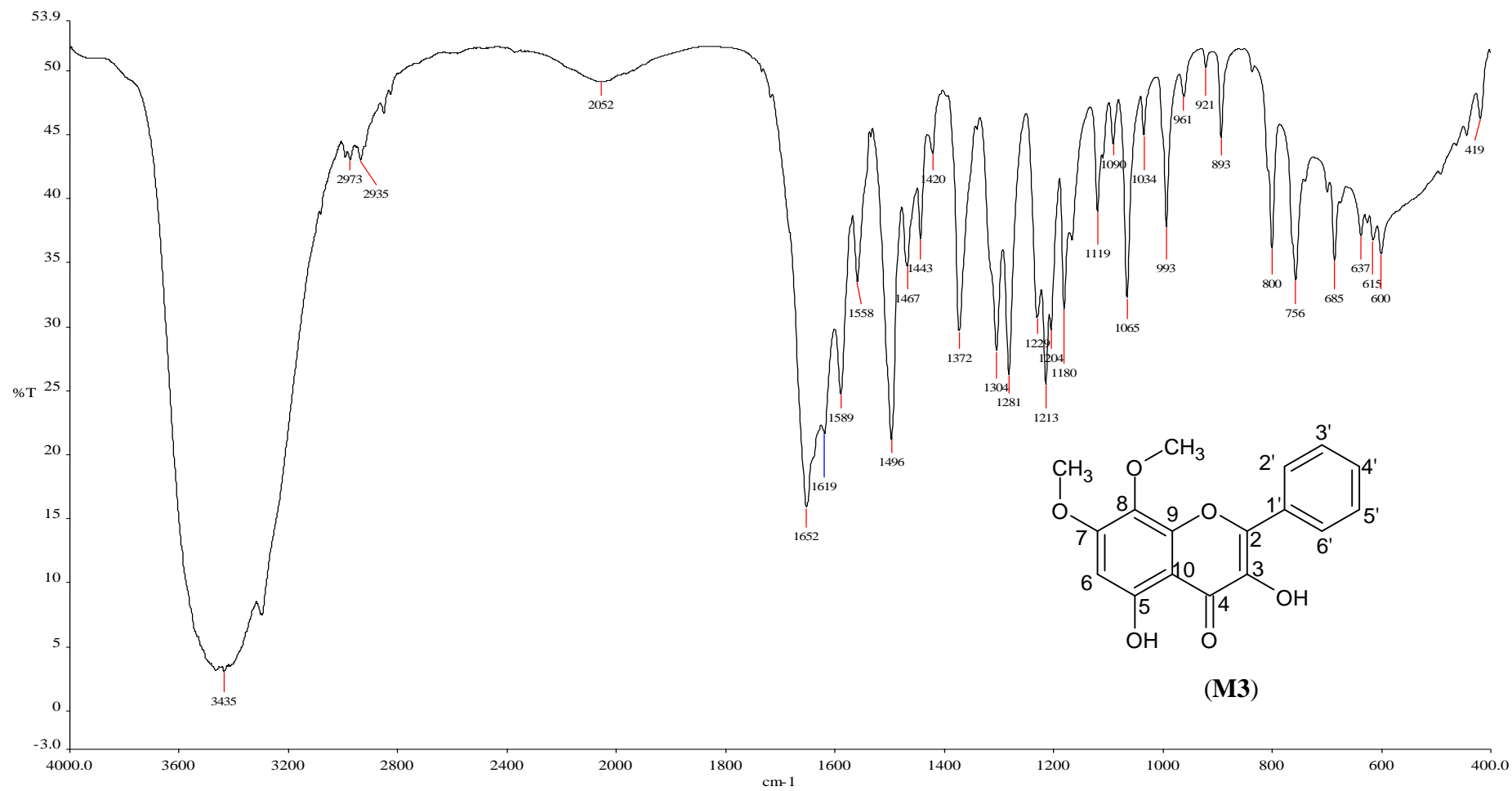


Figure C9: FTIR (KBr) of 3,5-dihydroxy-7,8-dimethoxyflavone (M3)

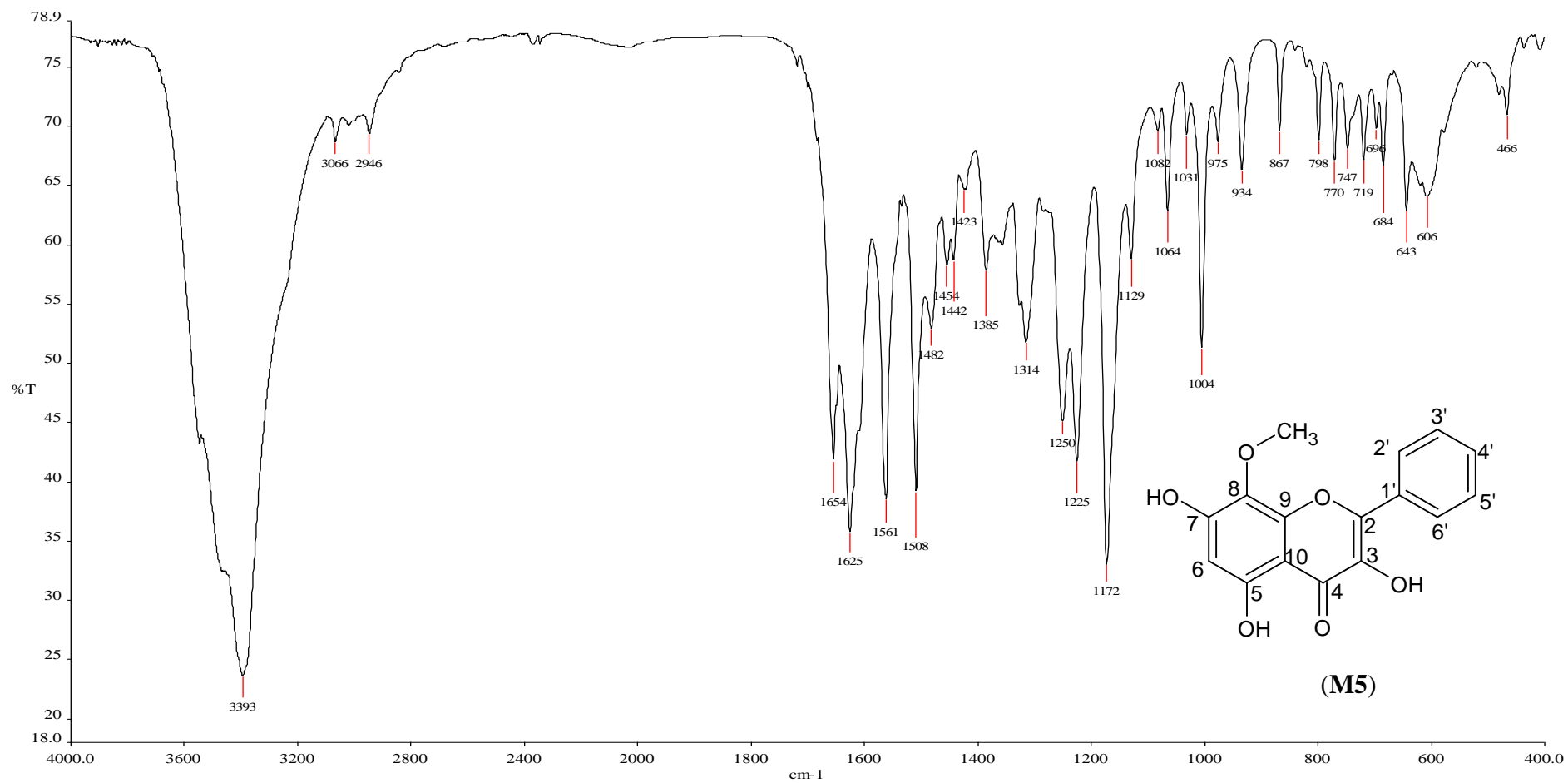


Figure C10: FTIR (KBr) of 3, 5, 7-trihydroxy-8-methoxyflavone (M5)

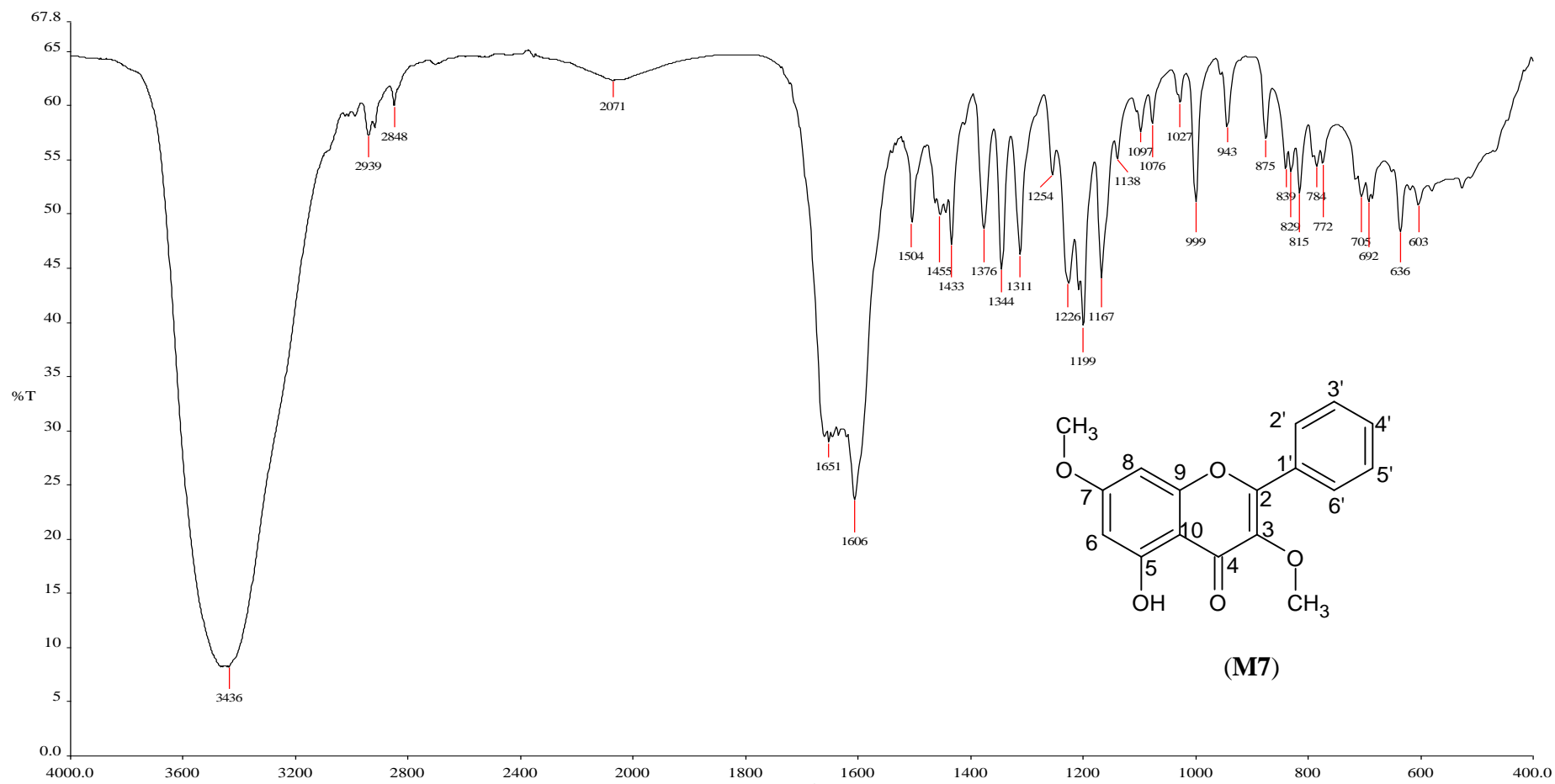


Figure C11: FTIR (KBr) of 5-hydroxy-3,7-dimethoxyflavone (M7)

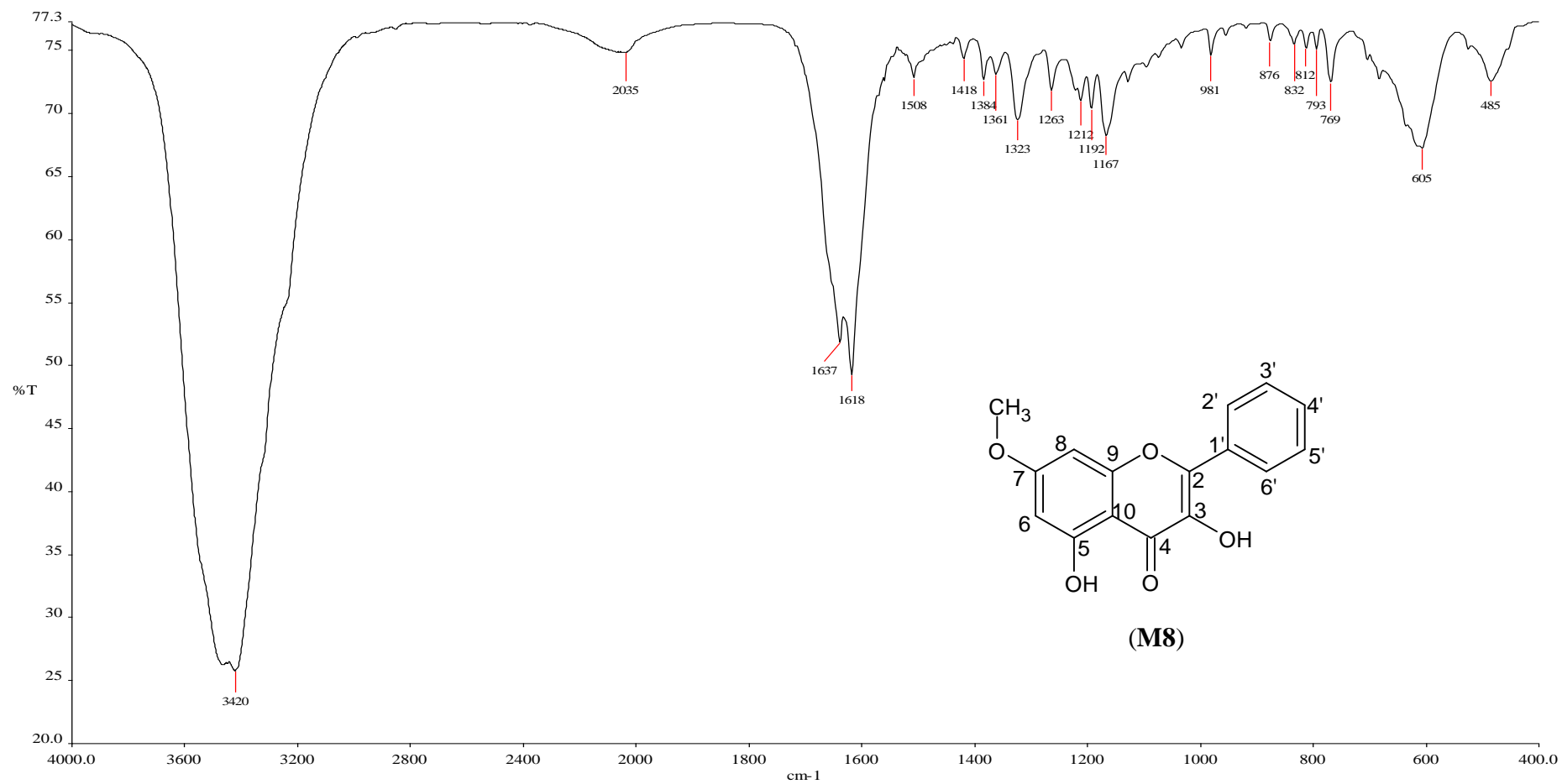


Figure C12: FTIR (KBr) of 3, 5-dihydroxy-7-methoxyflavone (M8)

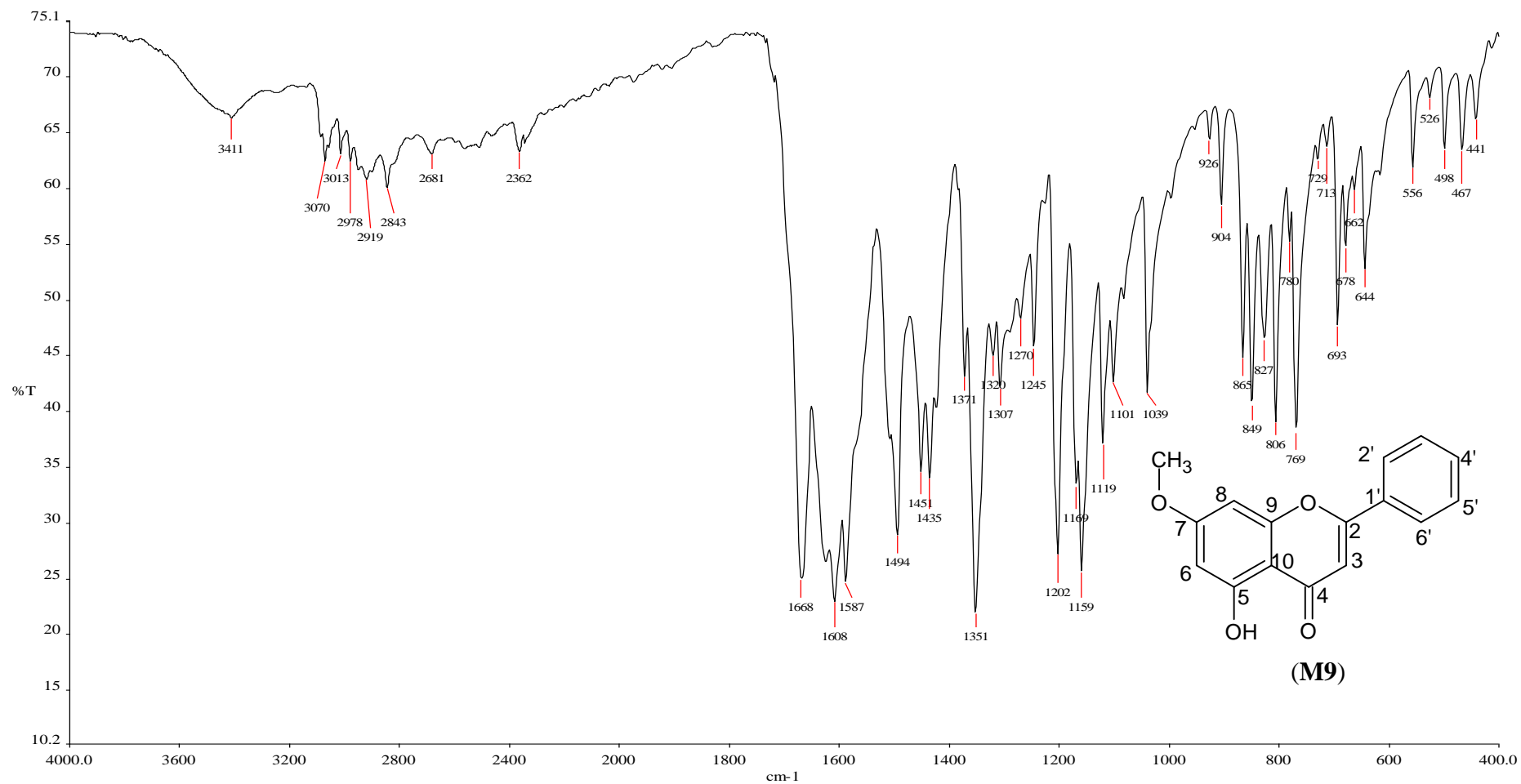


Figure C13: FTIR (KBr) of 5-hydroxy-7-methoxyflavone (M9)

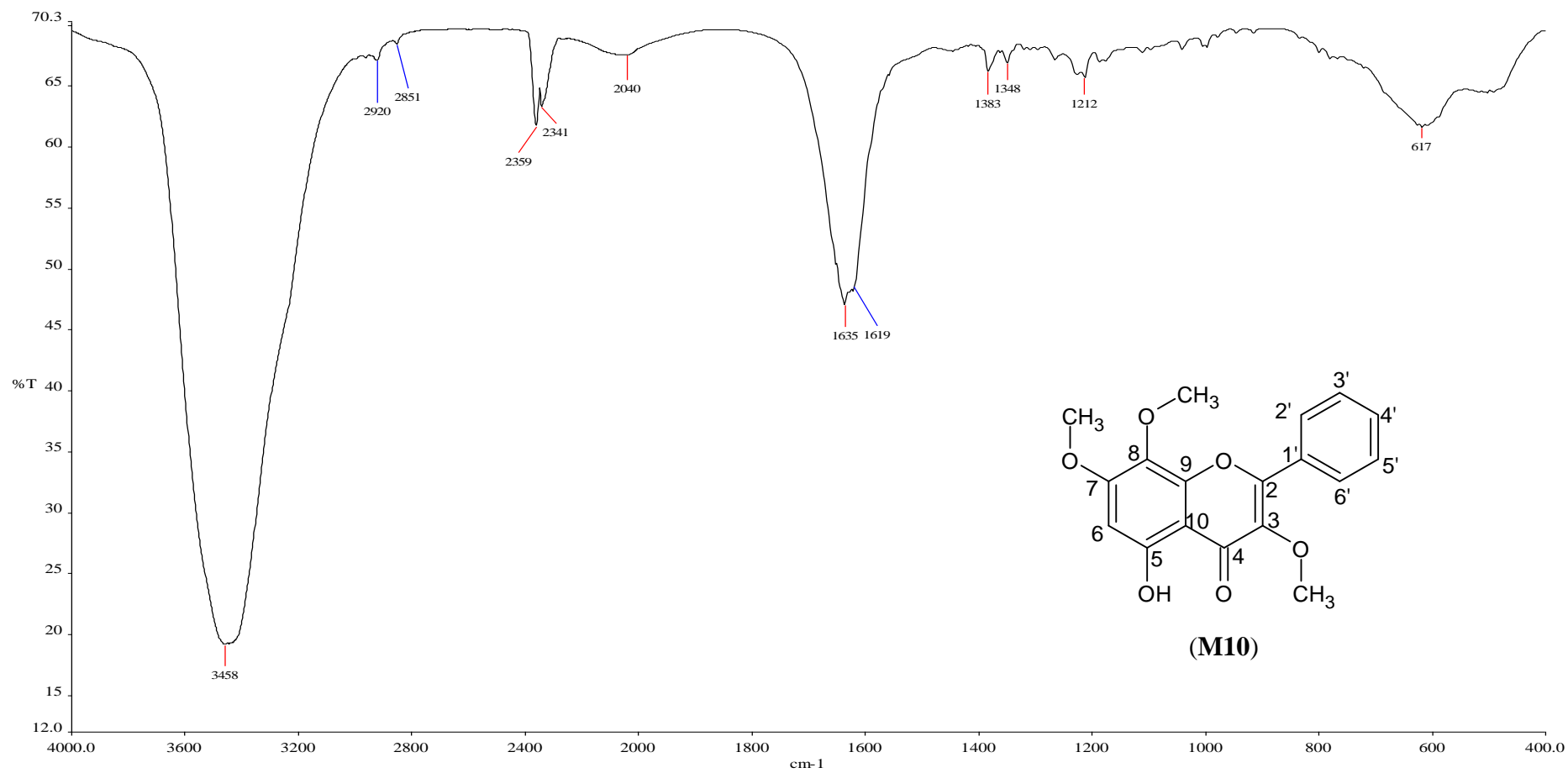


Figure C14: FTIR (KBr) of 5-hydroxy-3,7,8-trimethoxyflavone (M10)

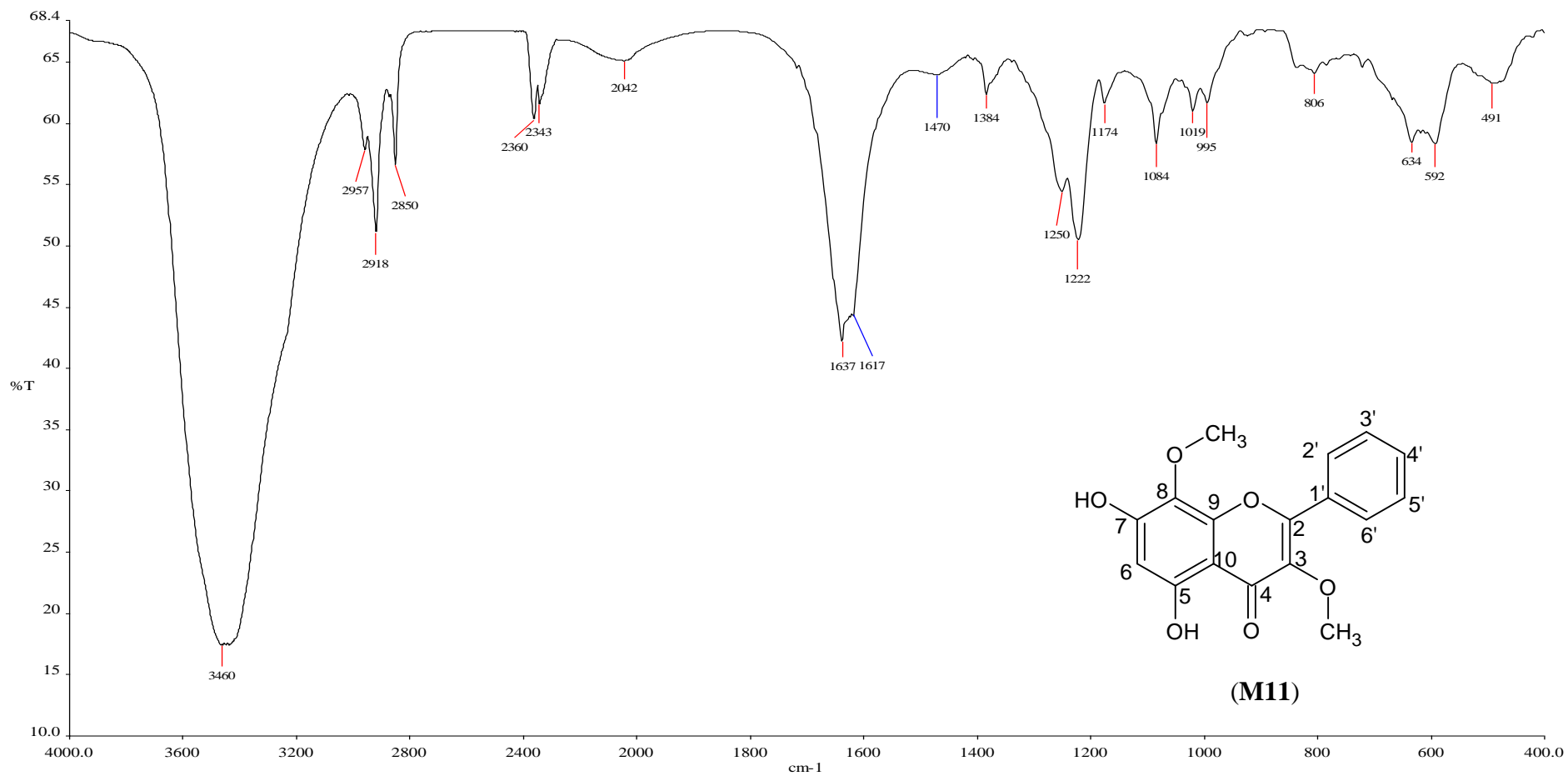


Figure C15: FTIR (KBr) of 5,7-dihydroxy-3,8-dimethoxyflavone (M11)

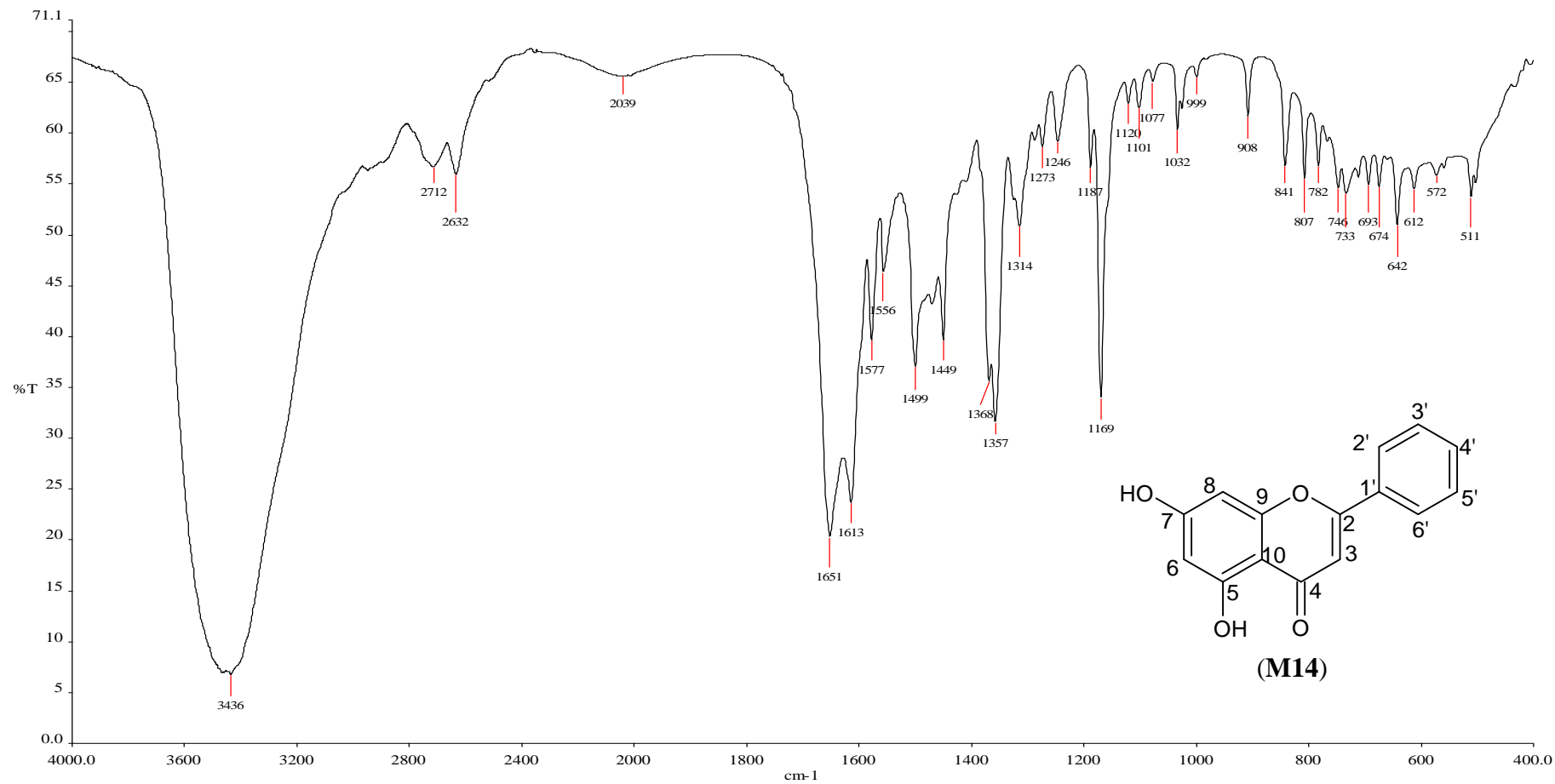


Figure C16: FTIR (KBr) of 5,7-dihydroxyflavone (M14)

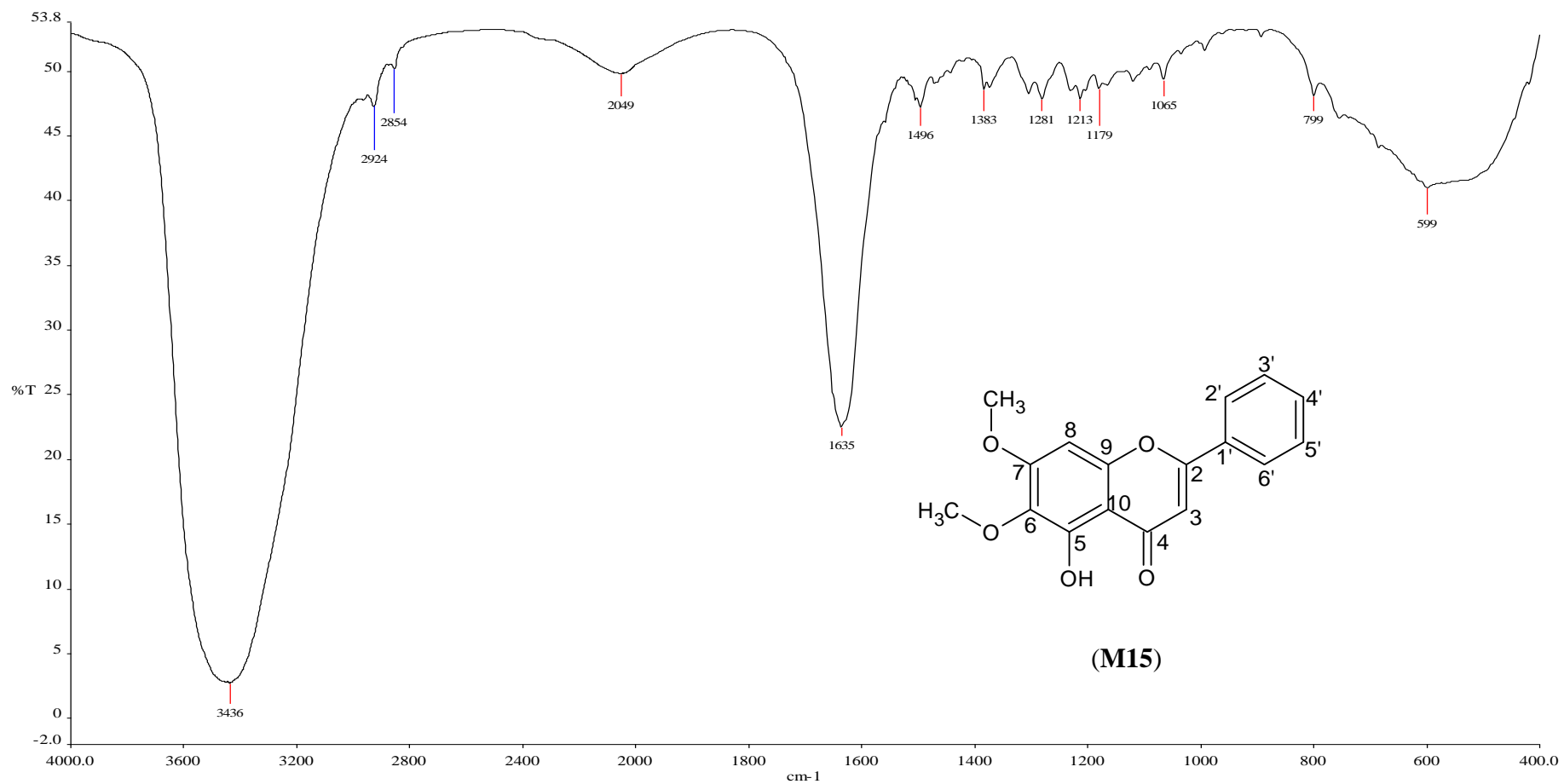


Figure C17: FTIR (KBr) of 5-hydroxy-6,7-dimethoxyflavone (M15)

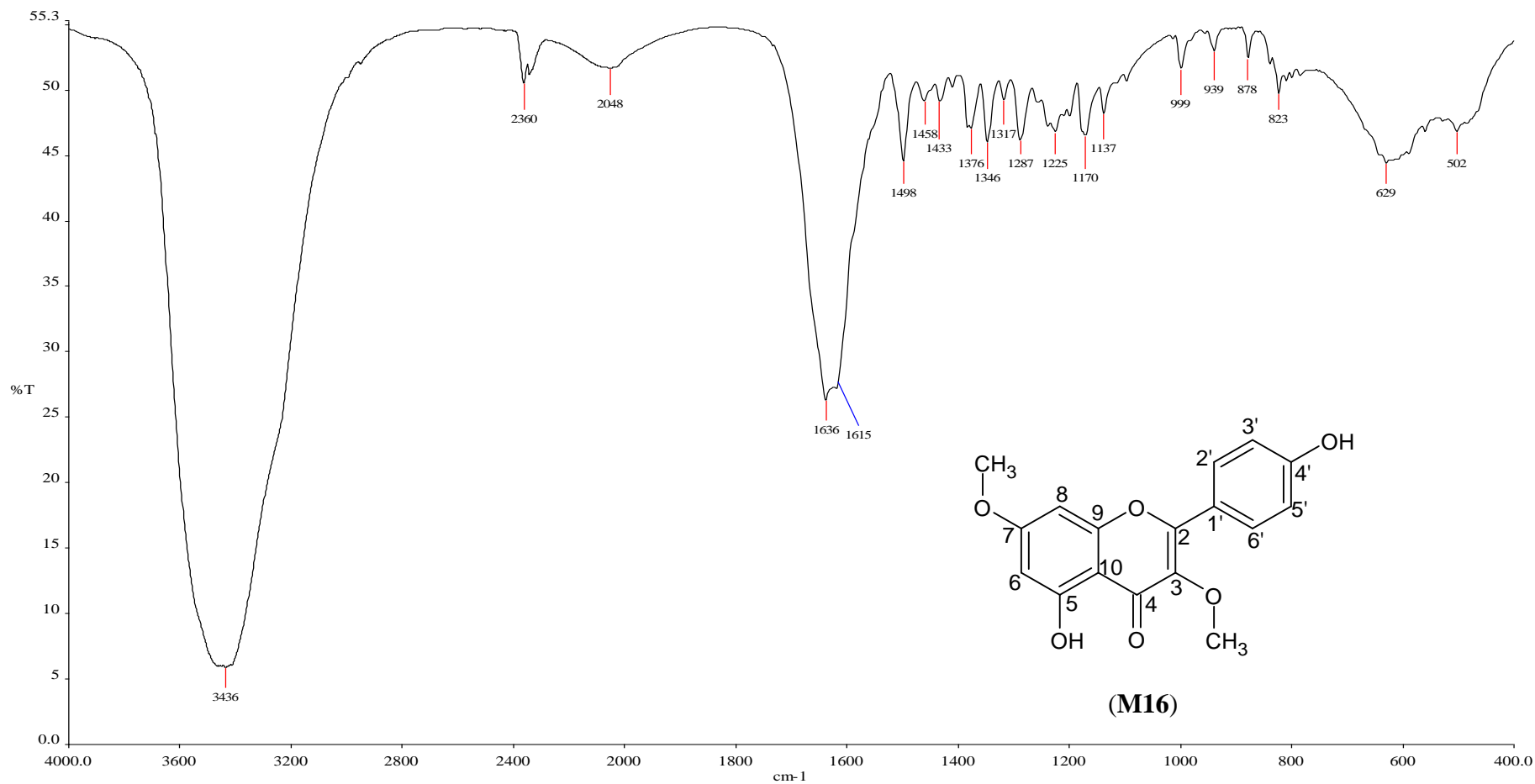


Figure C18: FTIR (KBr) of 5,4'-dihydroxy-7-methoxyflavone (M16)

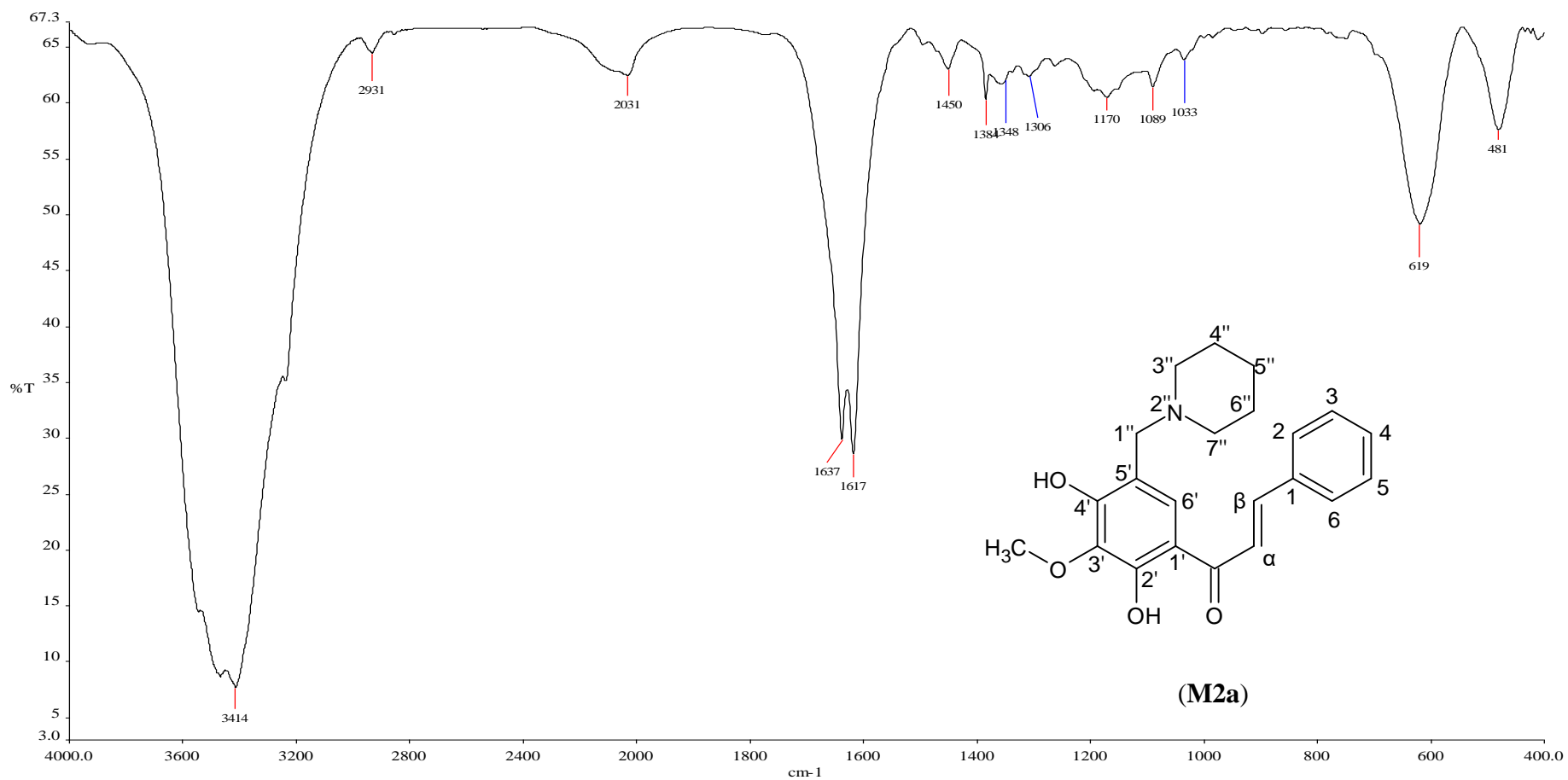


Figure C19: FTIR (KBr) of 1-[3-methoxy-5-(piperidin-4-yl) methyl-2,4-dihydroxyphenyl]-3-phenyl-2-propen-1-one (M2a)

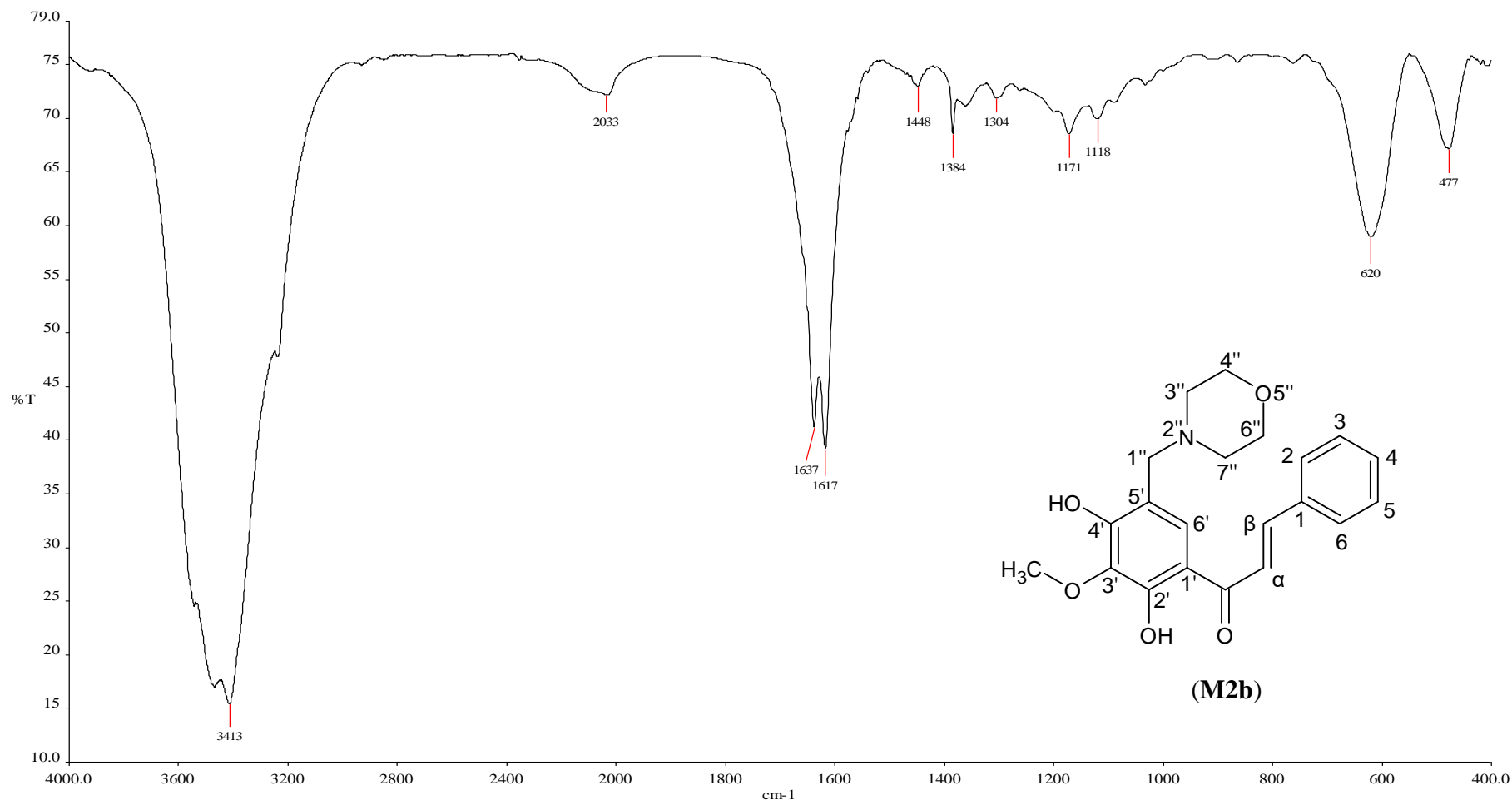


Figure C20: FTIR (KBr) of 1-[3-methoxy-5-(morpholino-4-yl) methyl-2,4-dihydroxyphenyl]-3-phenyl-2-propen-1-one (M2b)

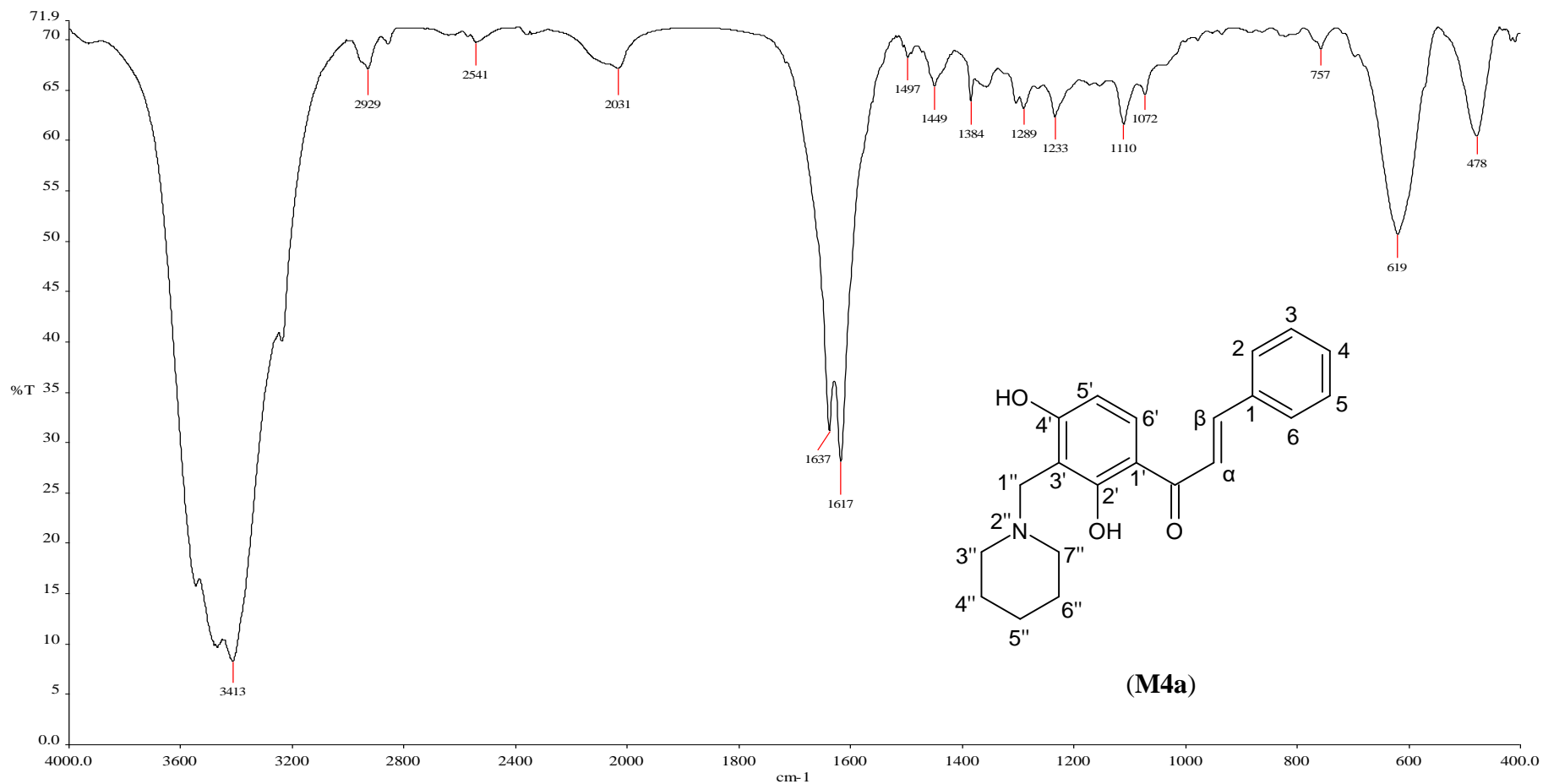


Figure C21: FTIR (KBr) of 1-[3-(piperidin-1-yl) methyl-2,4-dihydroxyphenyl]-3-phenyl-2-propen-1-one (M4a)

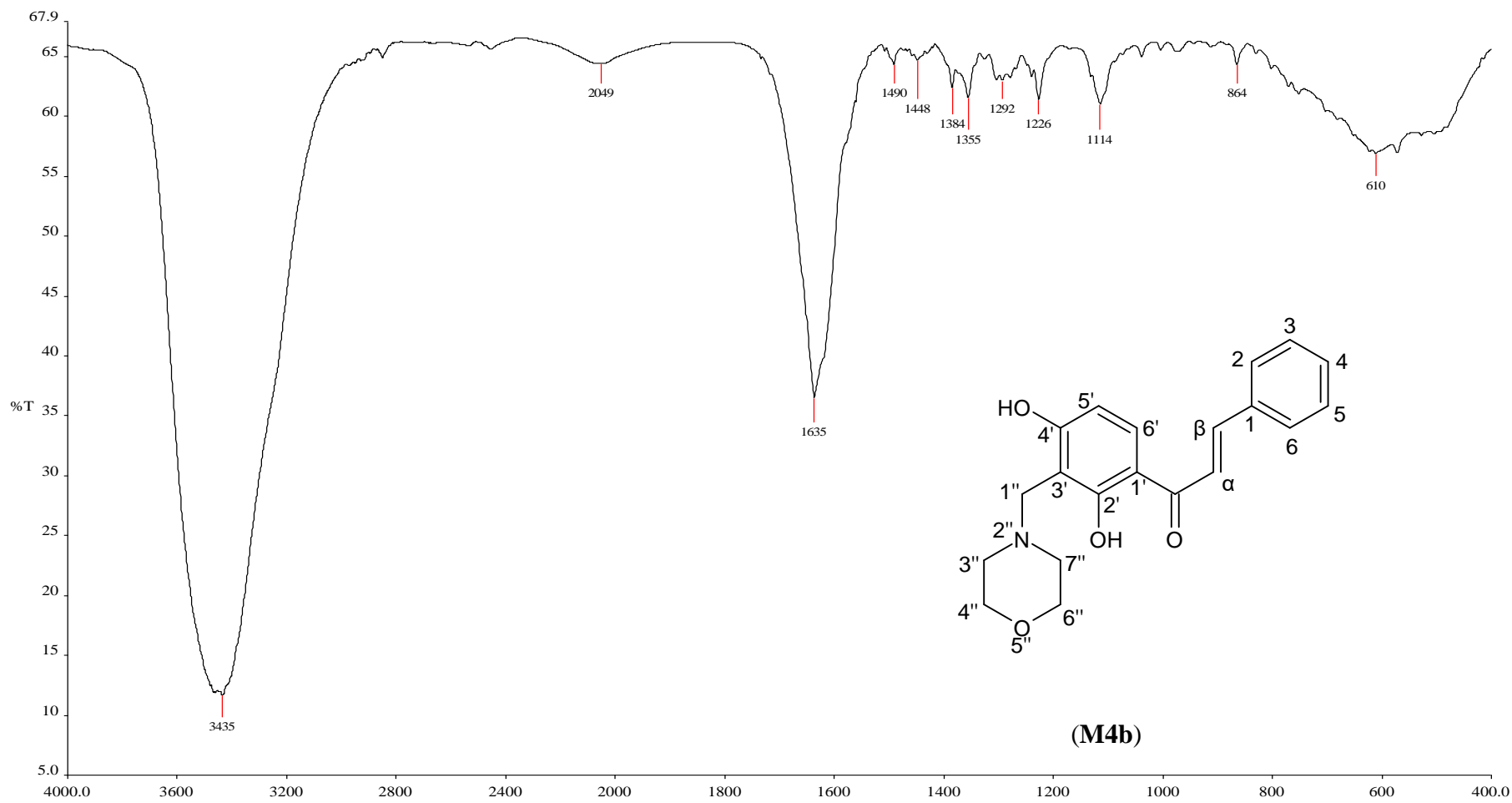


Figure C22: FTIR (KBr) of 1-[3-(morpholino-4-yl) methyl-2,4-dihydroxyphenyl]-3-phenyl-2-propen-1-one (M4b)

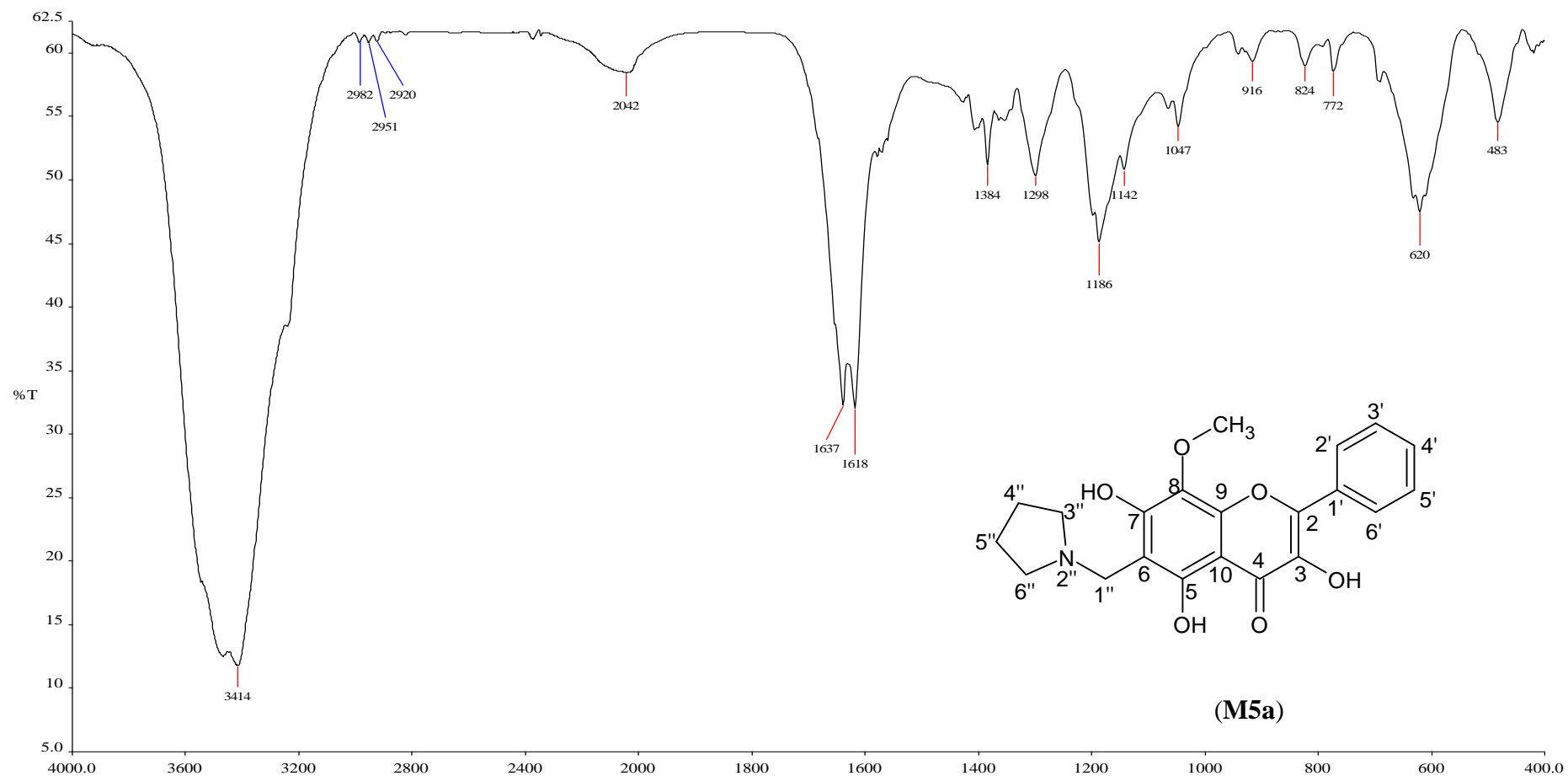


Figure C23: FTIR (KBr) of 3,5,7-trihydroxy-8-methoxy-6-(pyrrolidin-1-ylmethyl)-2-phenyl-4H-chromen-4-one (M5a)

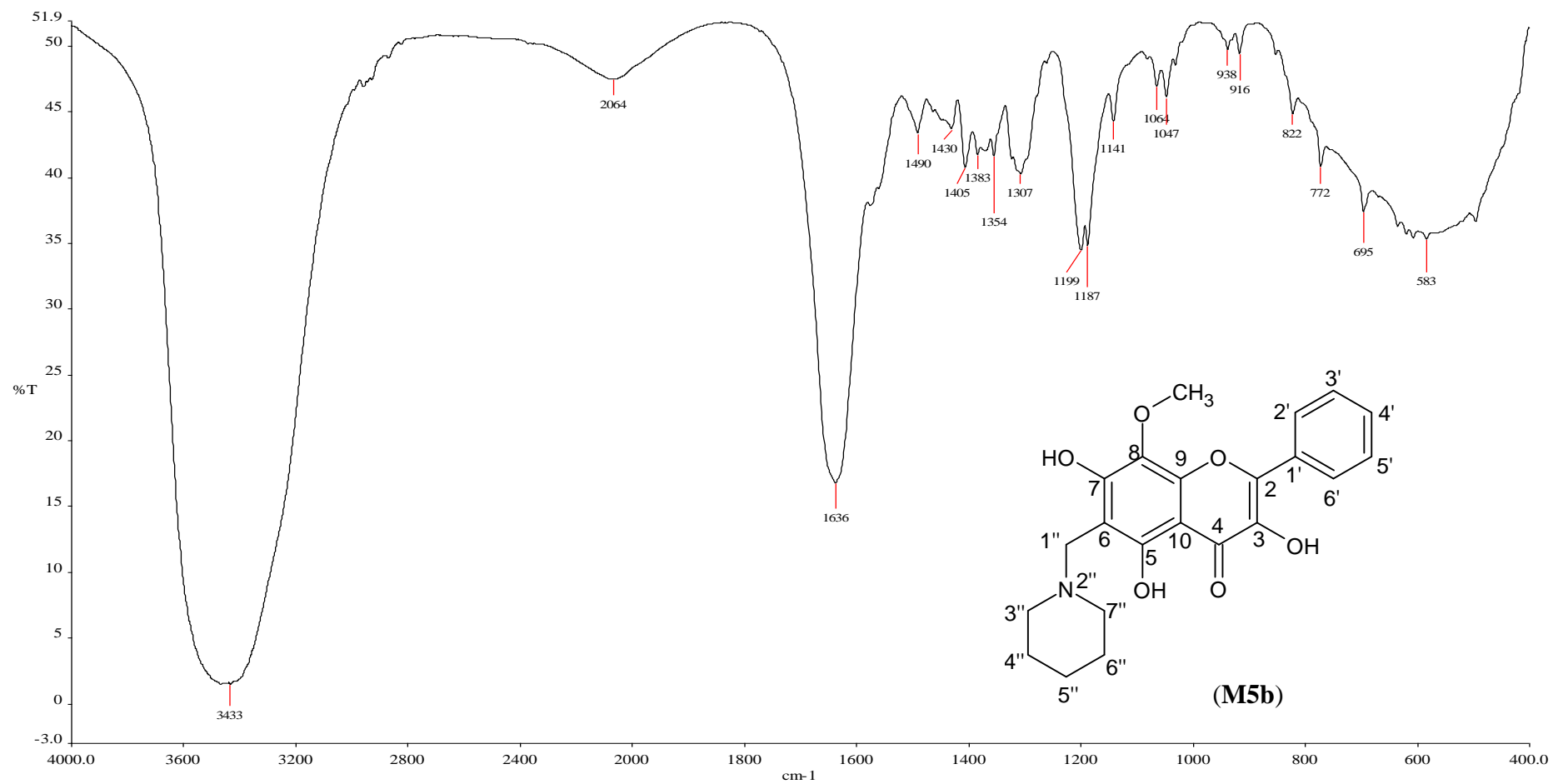


Figure C24: FTIR (KBr) of 3,5,7-trihydroxy-8-methoxy-6-(piperidin-1-ylmethyl)-2-phenyl-4H-chromen-4-one (M5b)

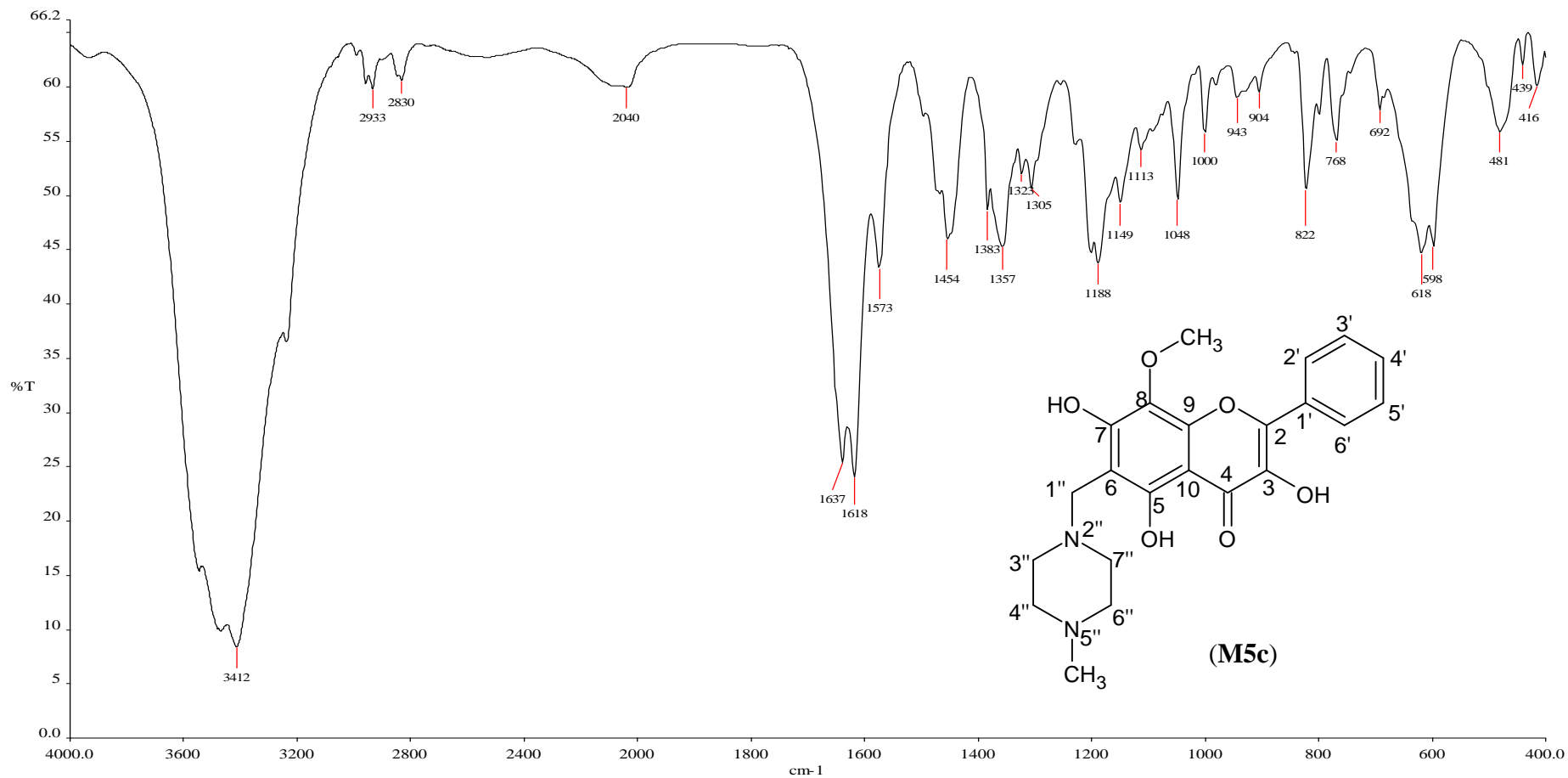


Figure C25: FTIR (KBr) of 3,5,7-trihydroxy-8-methoxy-6-(4-methylpiperazin-1-ylmethyl)-2-phenyl-4H-chromen-4-one (M5c)

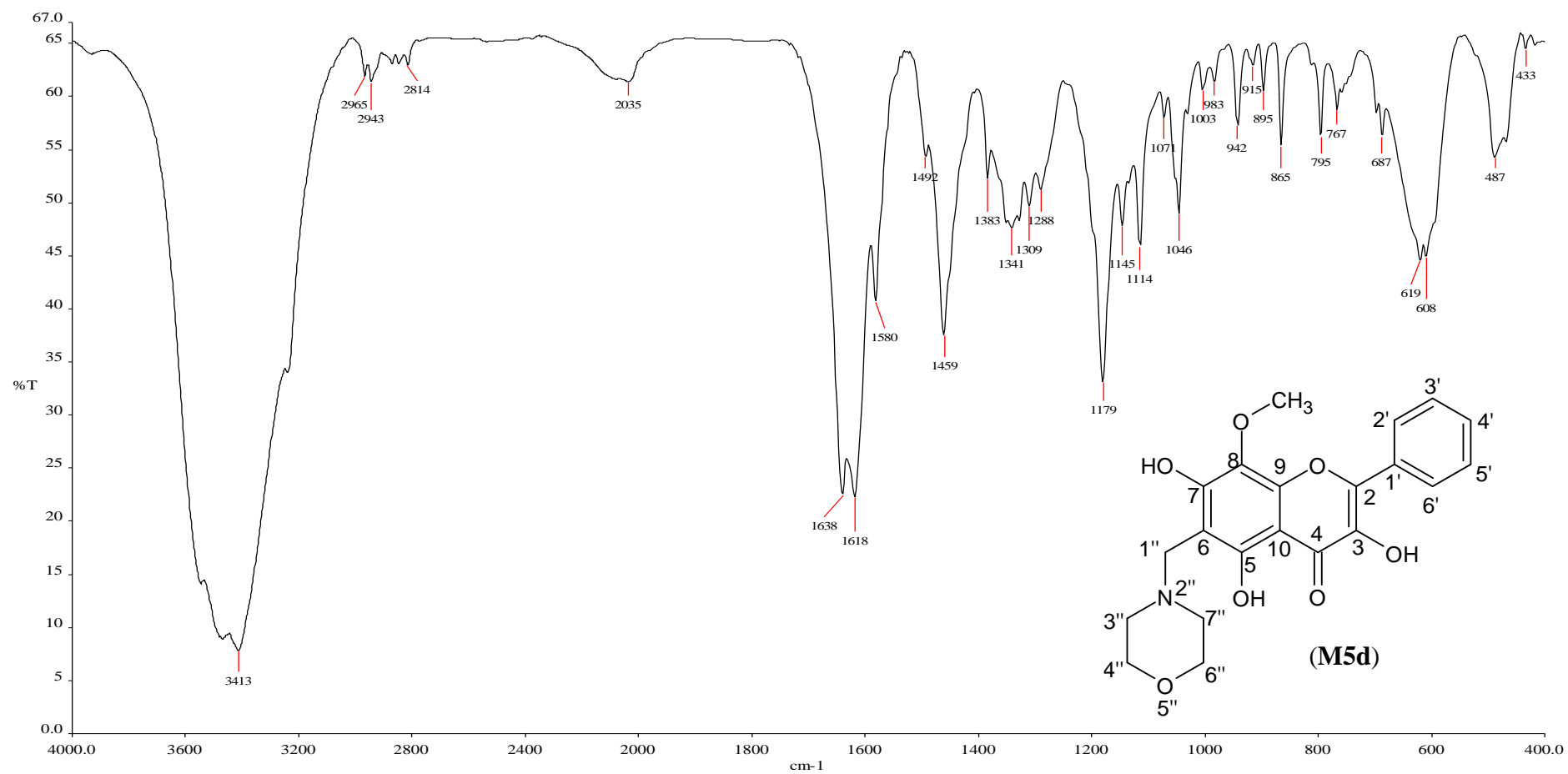


Figure C26: FTIR (KBr) of 3,5,7-trihydroxy-8-methoxy-6-(morpholinomethyl)-2-phenyl-4H-chromen-4-one (M5d)

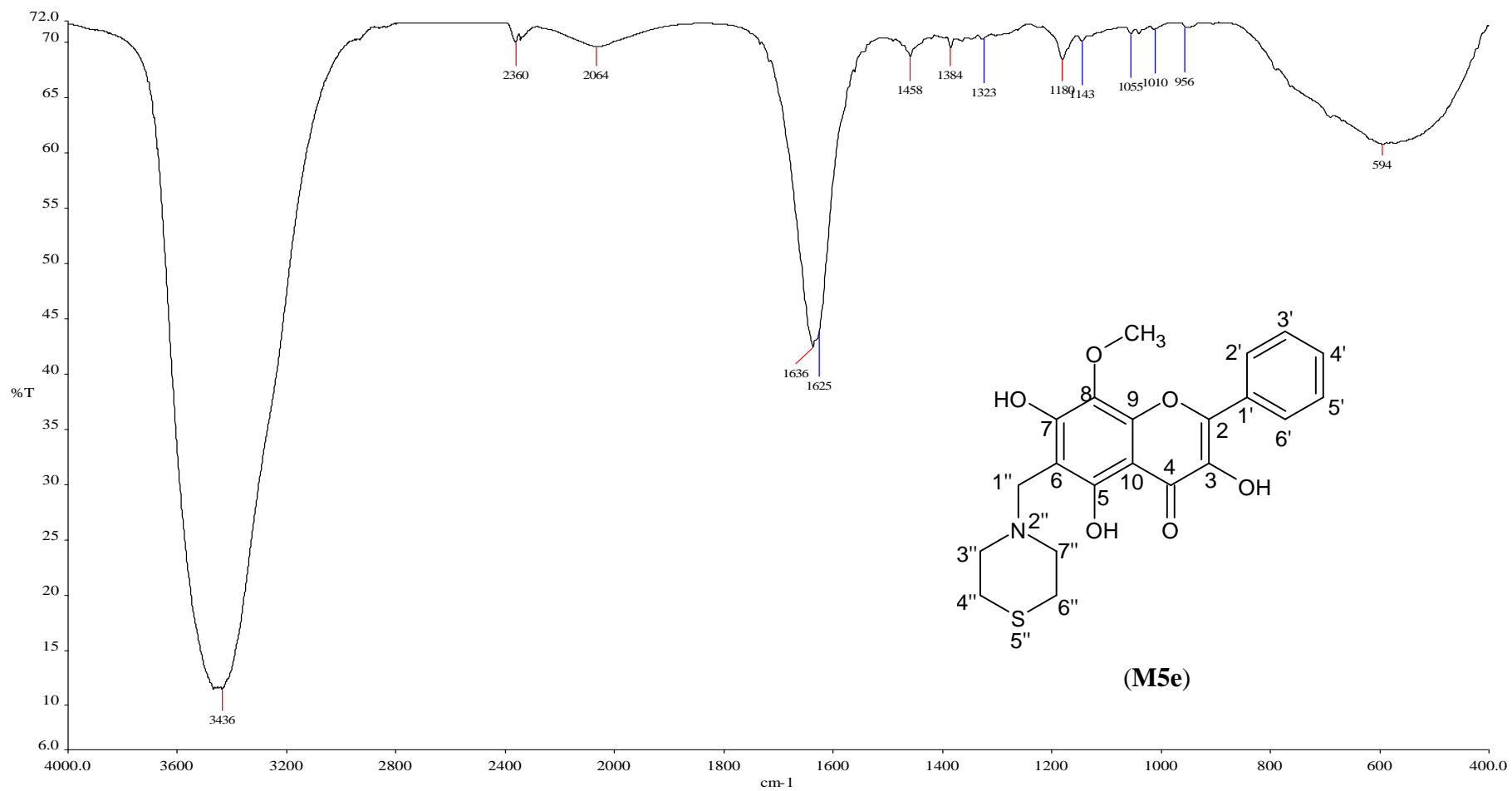


Figure C27: FTIR (KBr) of 3,5,7-trihydroxy-8-methoxy-6-(thiomorpholinomethyl)-2-phenyl-4H-chromen-4-one (M5e)

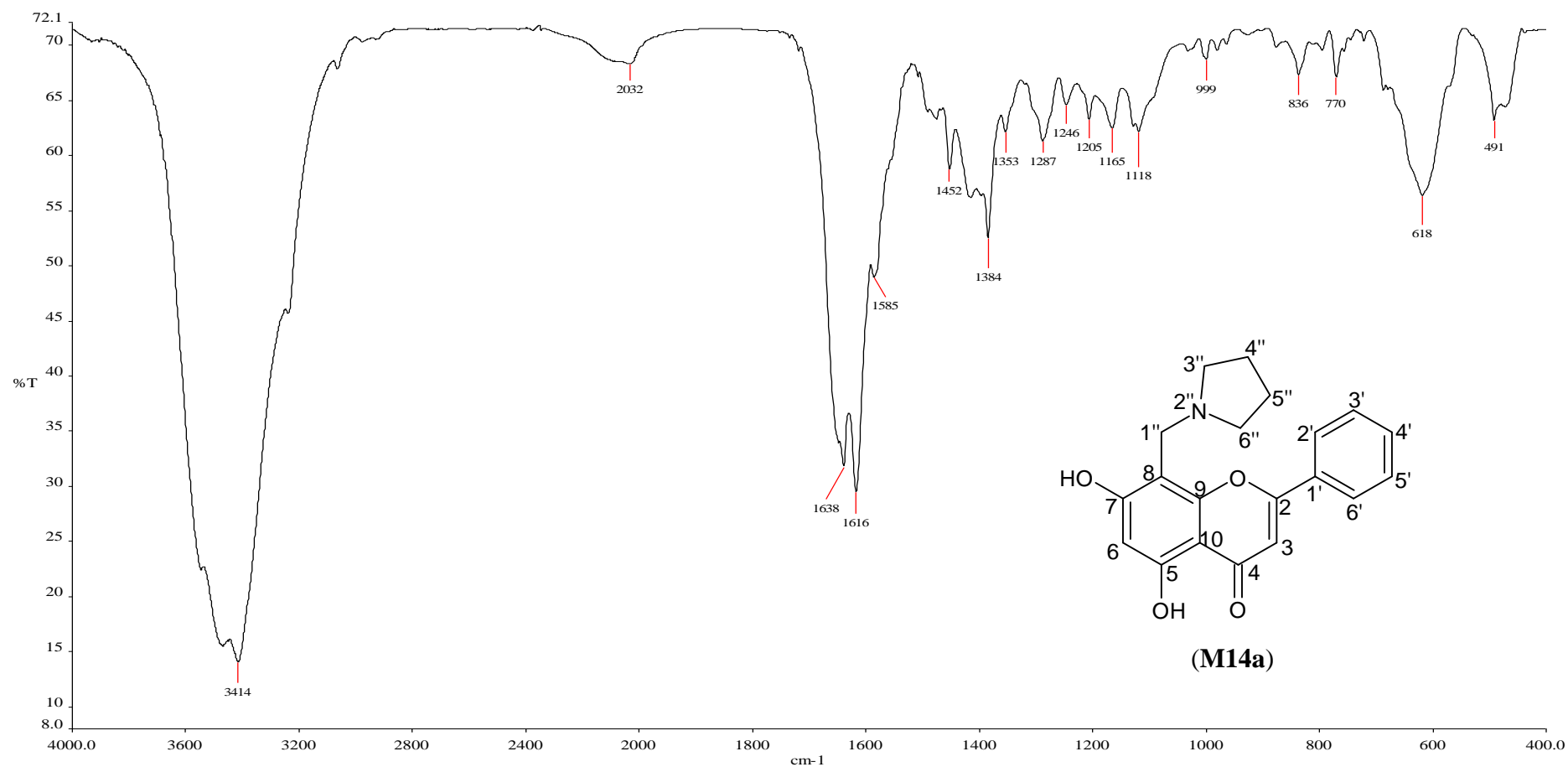


Figure C28: FTIR (KBr) of 5,7-dihydroxy-8-(pyrrolidine-1-ylmethyl)-2-phenyl-4H-chromen-4-one (M14a)

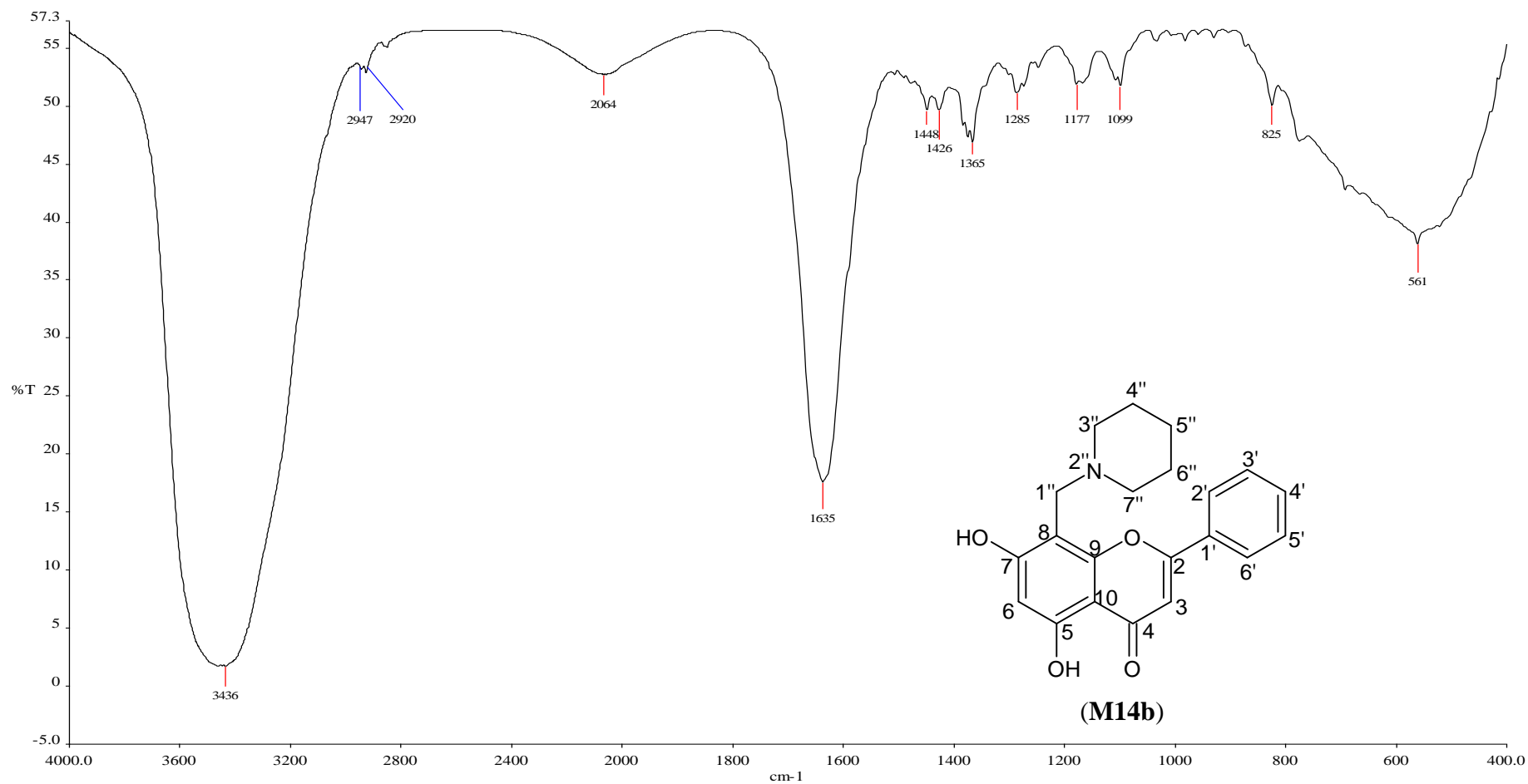


Figure C29: FTIR (KBr) of 5,7-dihydroxy-8-(piperidin-1-ylmethyl)-2-phenyl-4H-chromen-4-one (M14b)

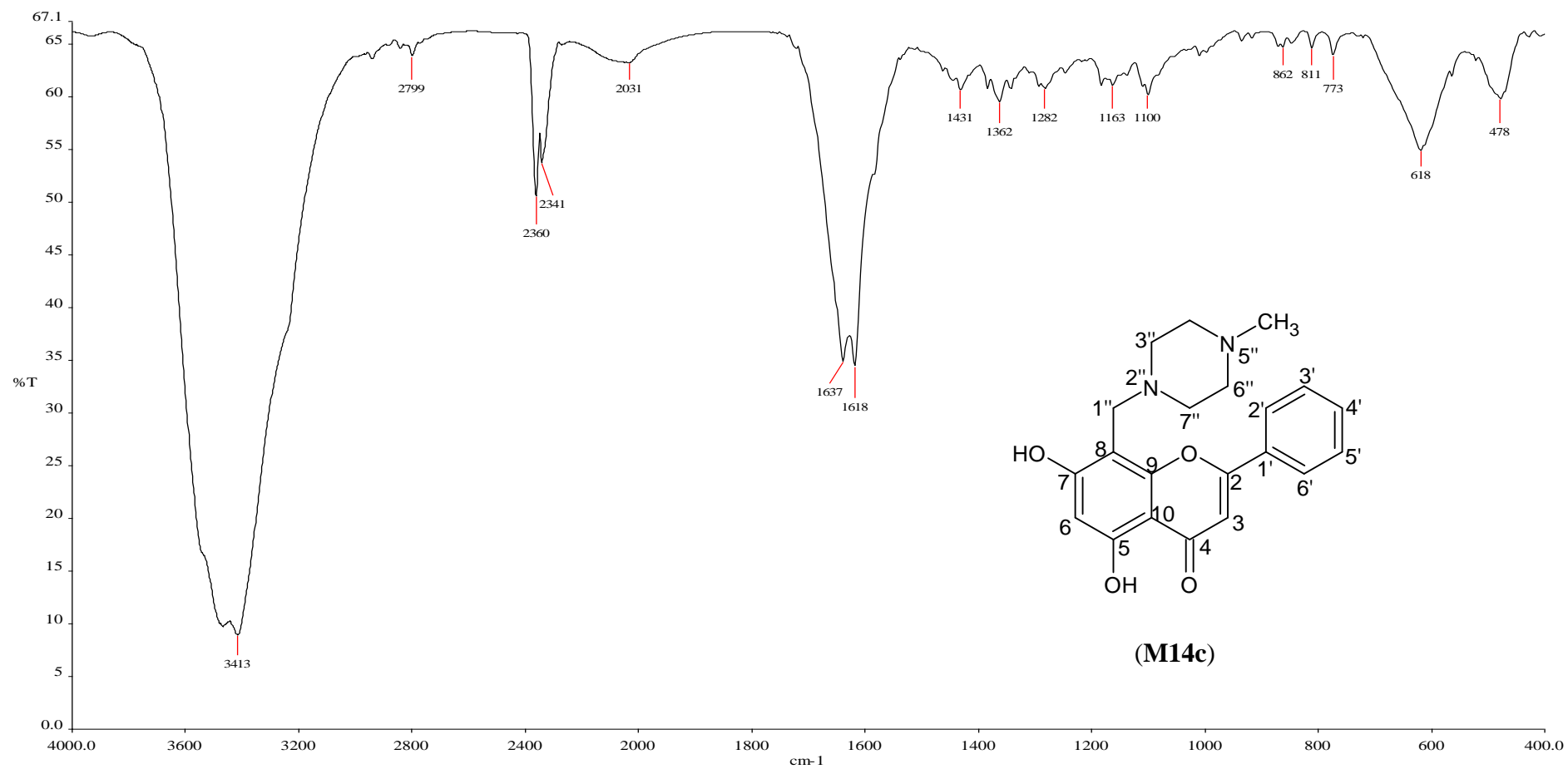


Figure C30: FTIR (KBr) of 5,7-dihydroxy-8-(4-methylpiperazin-1-ylmethyl)-2-phenyl-4H-chromen-4-one (M14c)

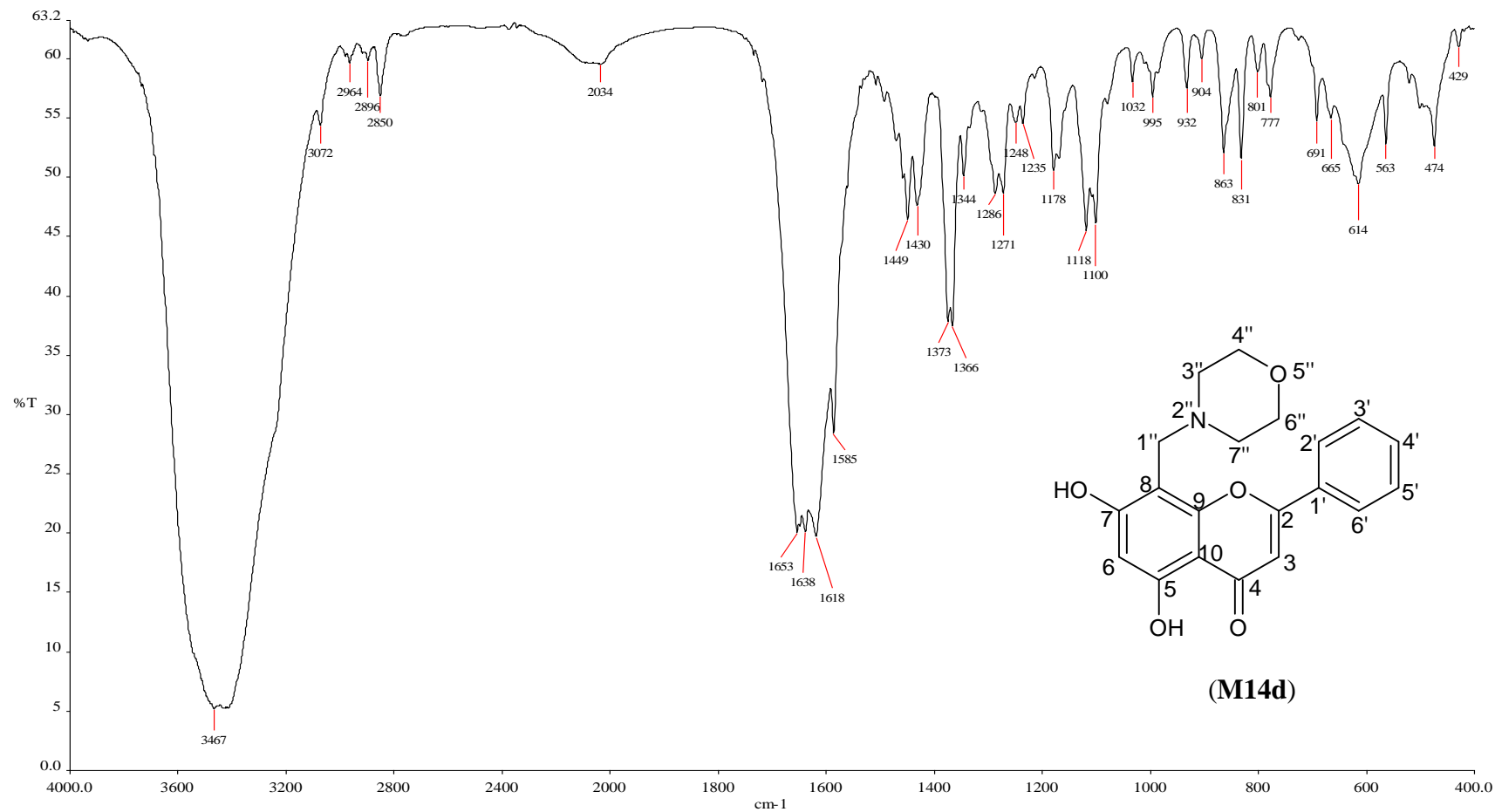


Figure C31: FTIR (KBr) of 5,7-dihydroxy-8-(morpholinomethyl)-2-phenyl-4H-chromen-4-one (M14d)

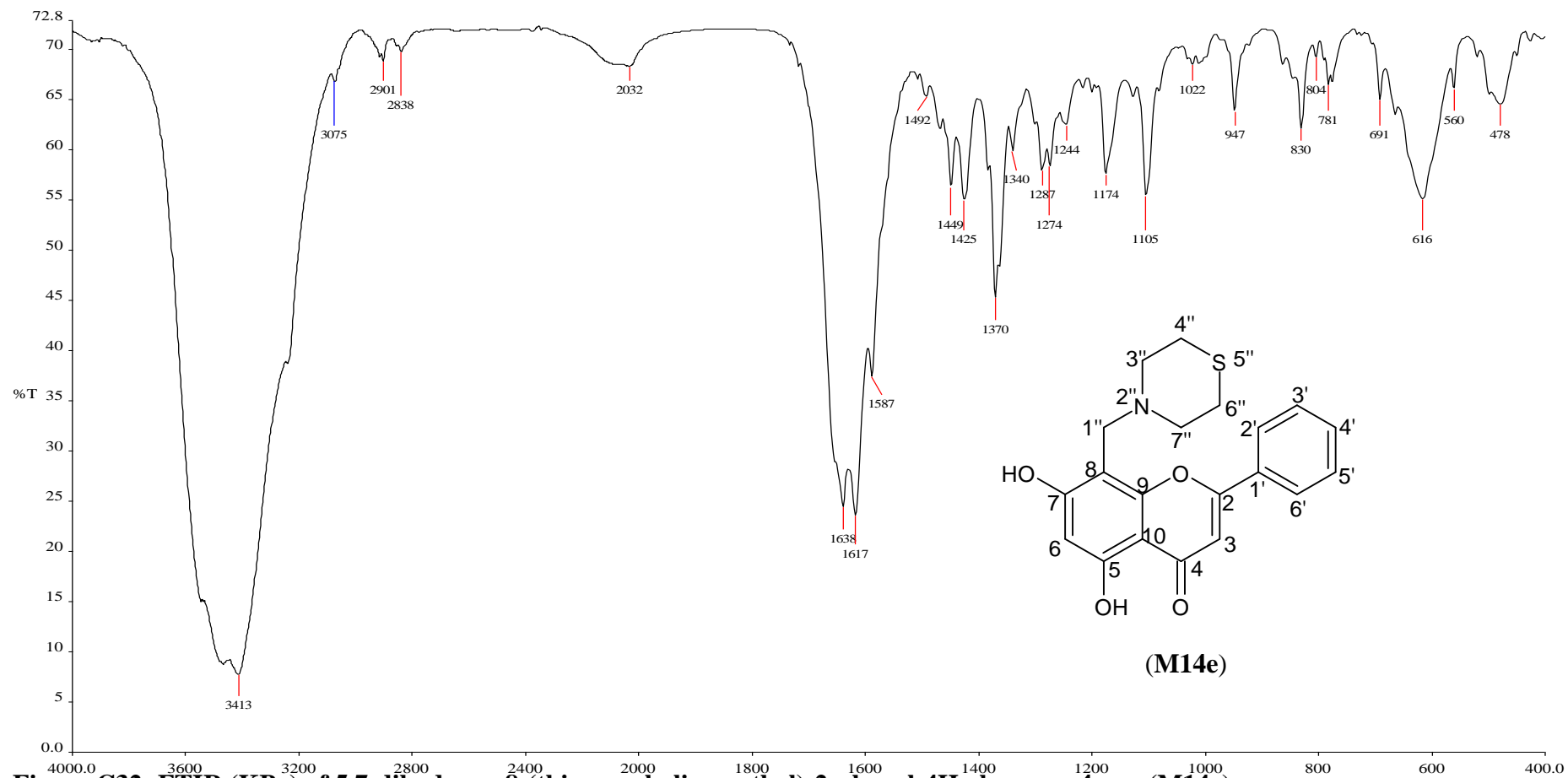


Figure C32: FTIR (KBr) of 5,7-dihydroxy-8-(thiomorpholinomethyl)-2-phenyl-4H-chromen-4-one (M14e)

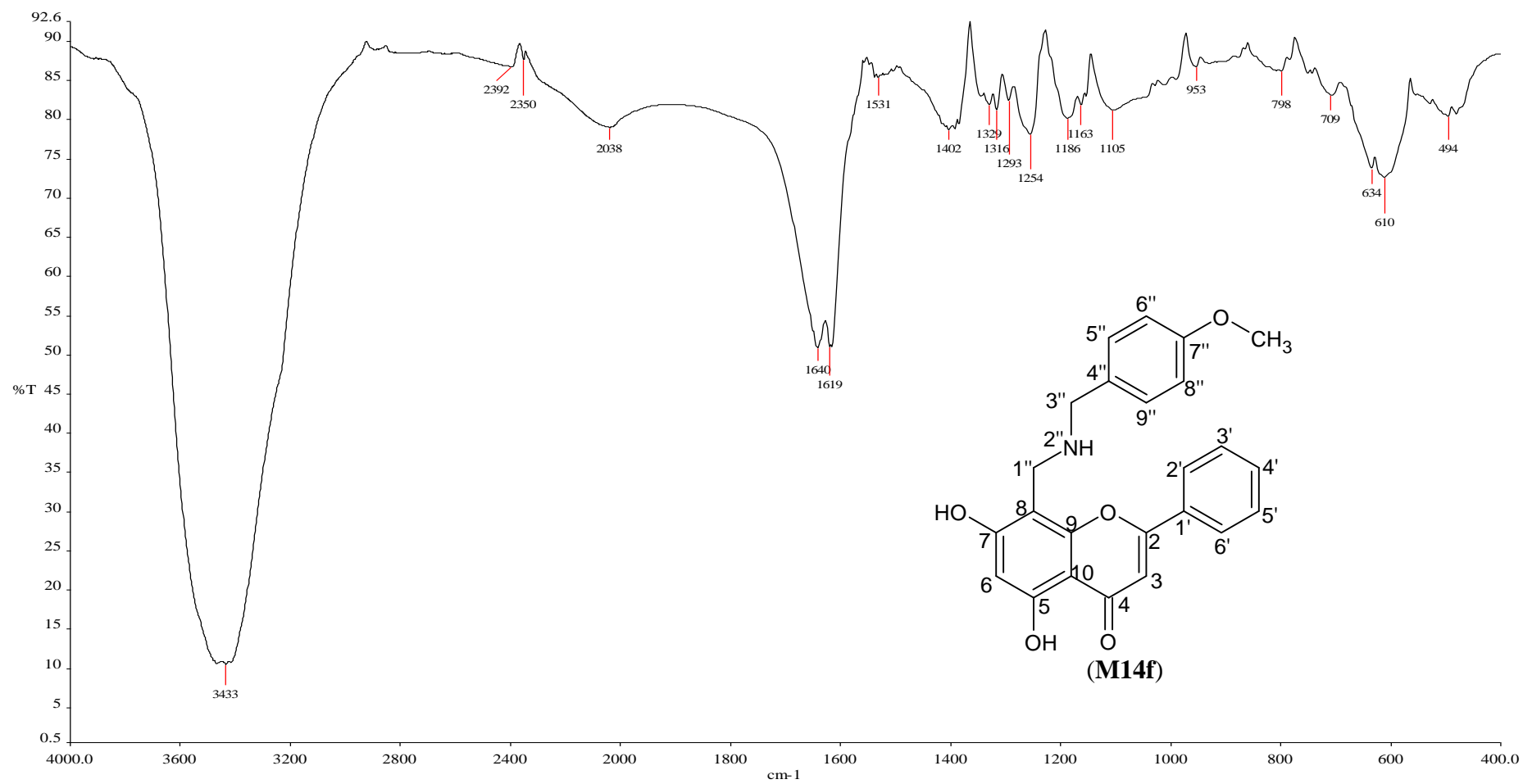


Figure C33: FTIR (KBr) of 5,7-dihydroxy-8-(4-methoxybenzylamine)-2-phenyl-4H-chromen-4-one (M14f)

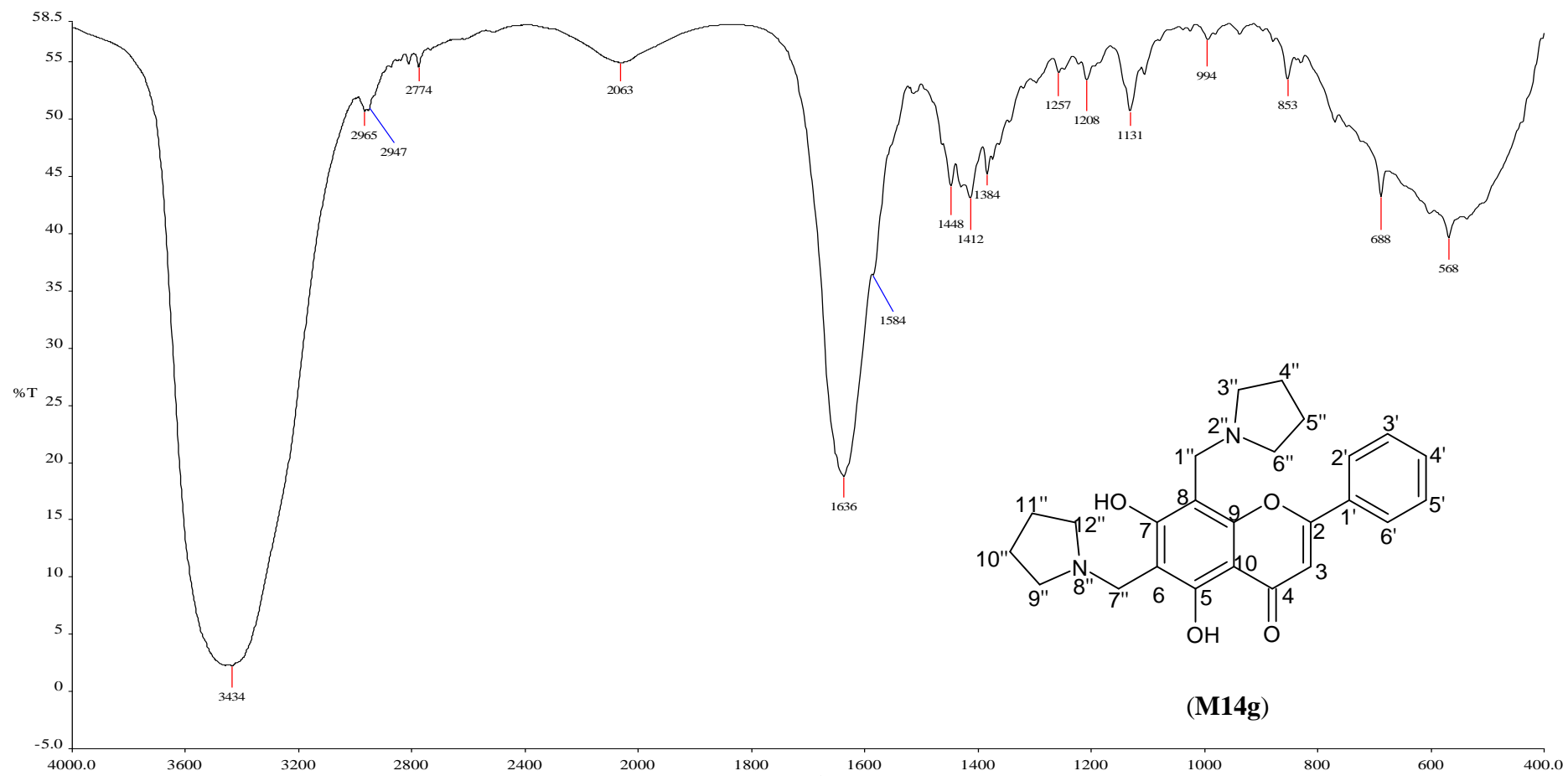


Figure C34: FTIR (KBr) of 5,7-dihydroxy-6,8-bis(pyrrolidine-1-ylmethyl)-2-phenyl-4H-chromen-4-one (M14g)

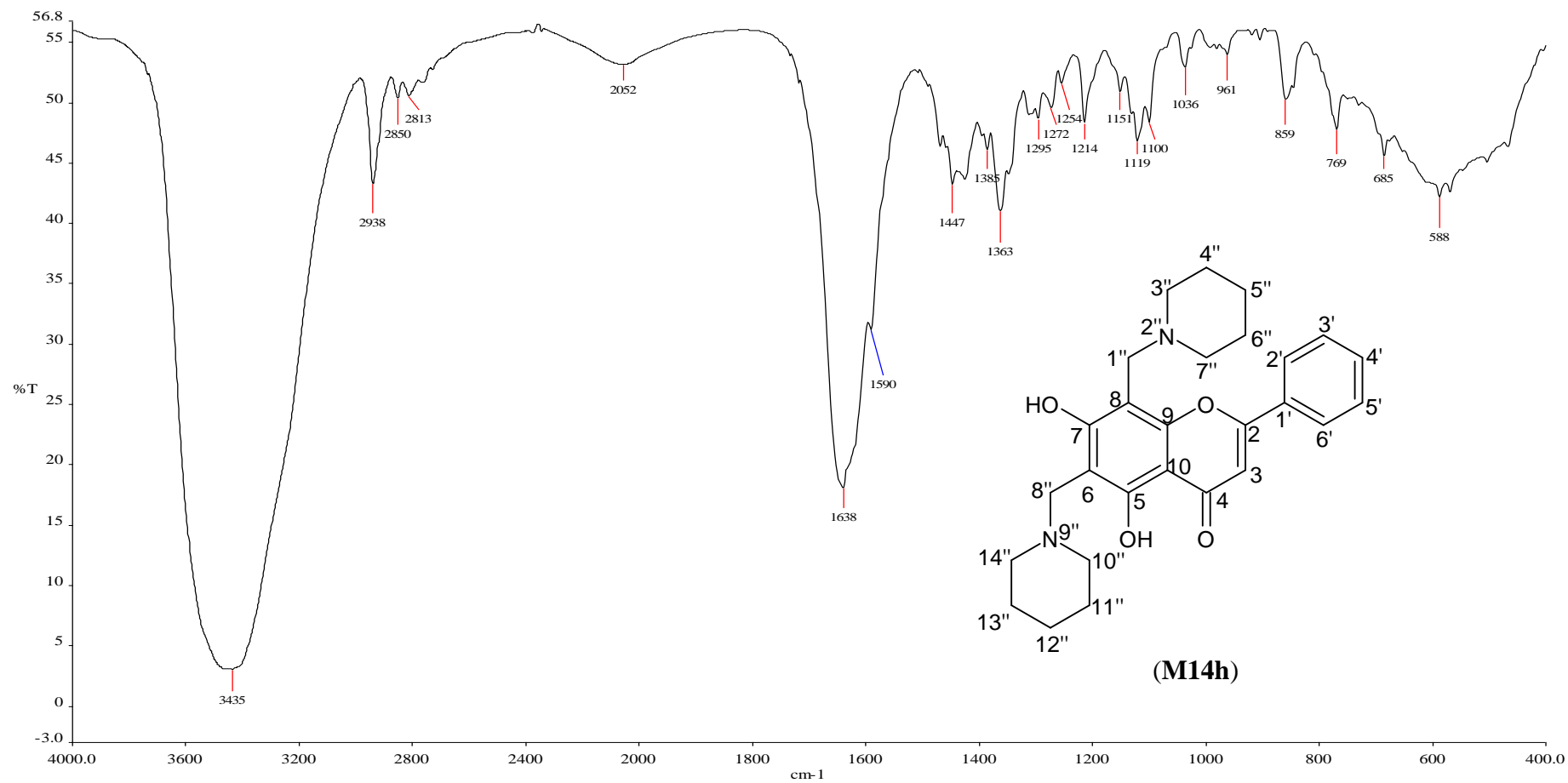


Figure C35: FTIR (KBr) of 5,7-dihydroxy-6,8-bis(piperidin-1-ylmethyl)-2-phenyl-4H-chromen-4-one (M14h)

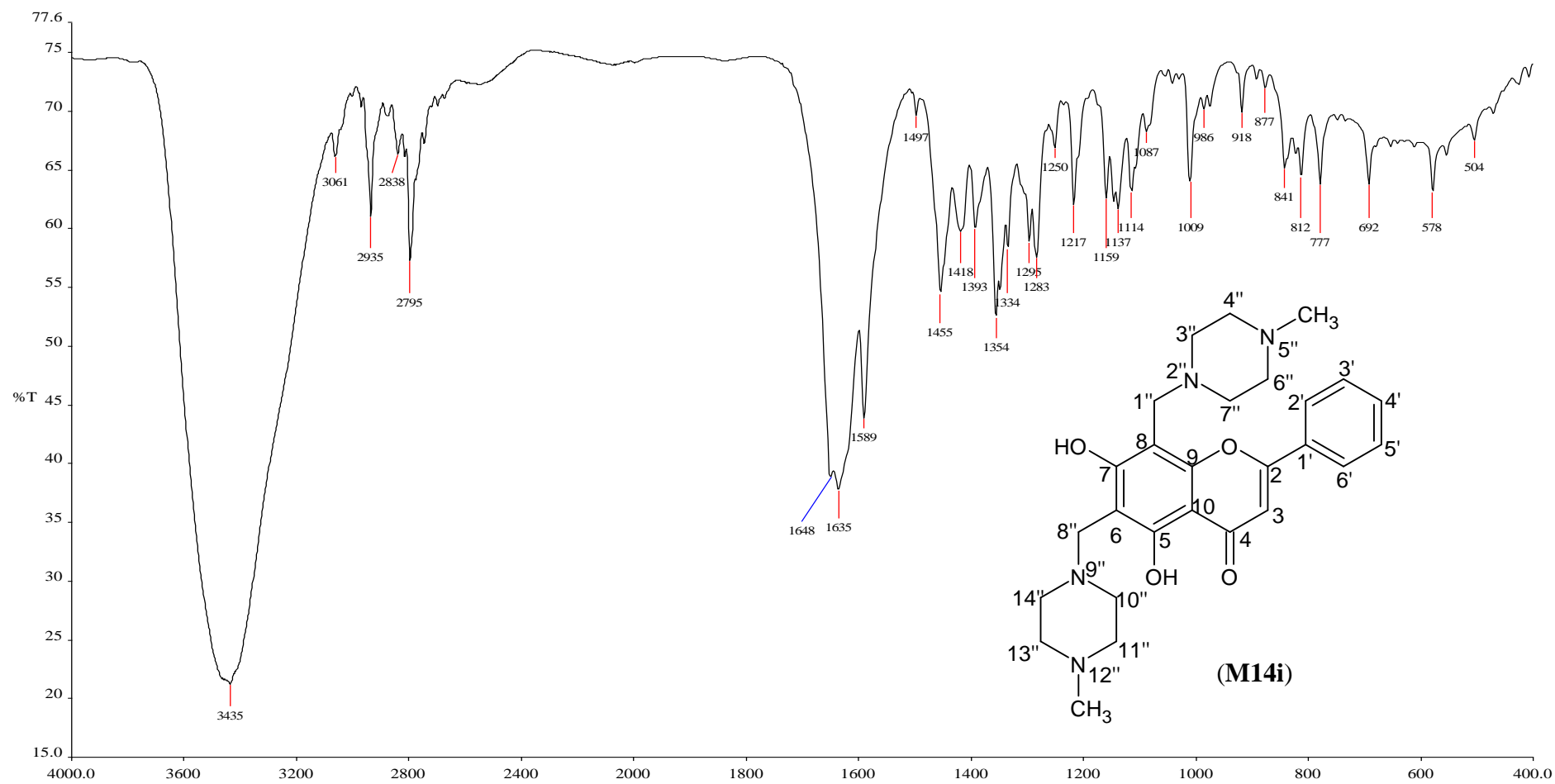


Figure C36: FTIR (KBr) of 5,7-dihydroxy-6,8-bis(4-methylpiperazin-1-ylmethyl)-2-phenyl-4H-chromen-4-one (M14i)

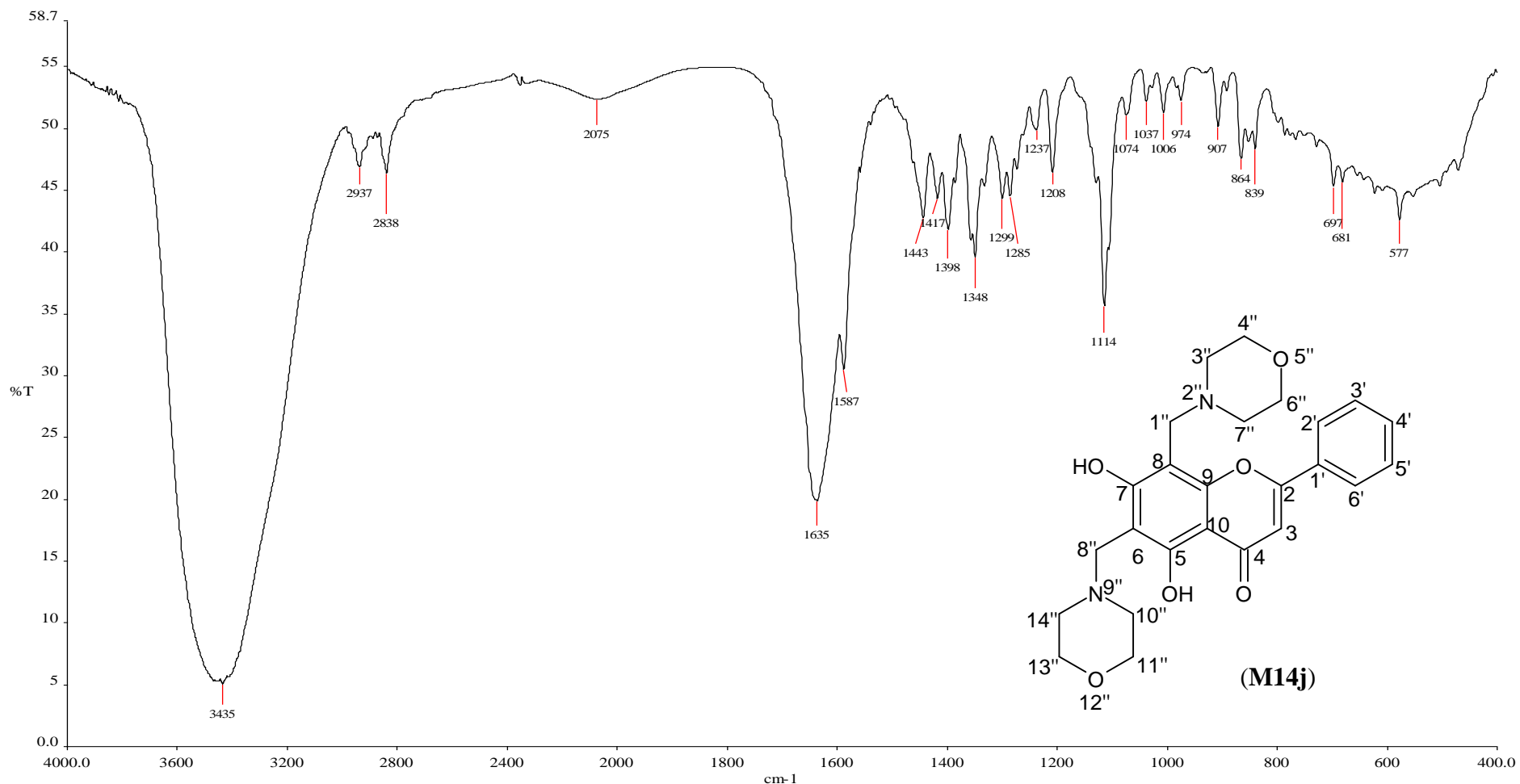


Figure C37: FTIR (KBr) of 5,7-dihydroxy-6,8-bis(morpholinomethyl)-2-phenyl-4H-chromen-4-one (M14j)

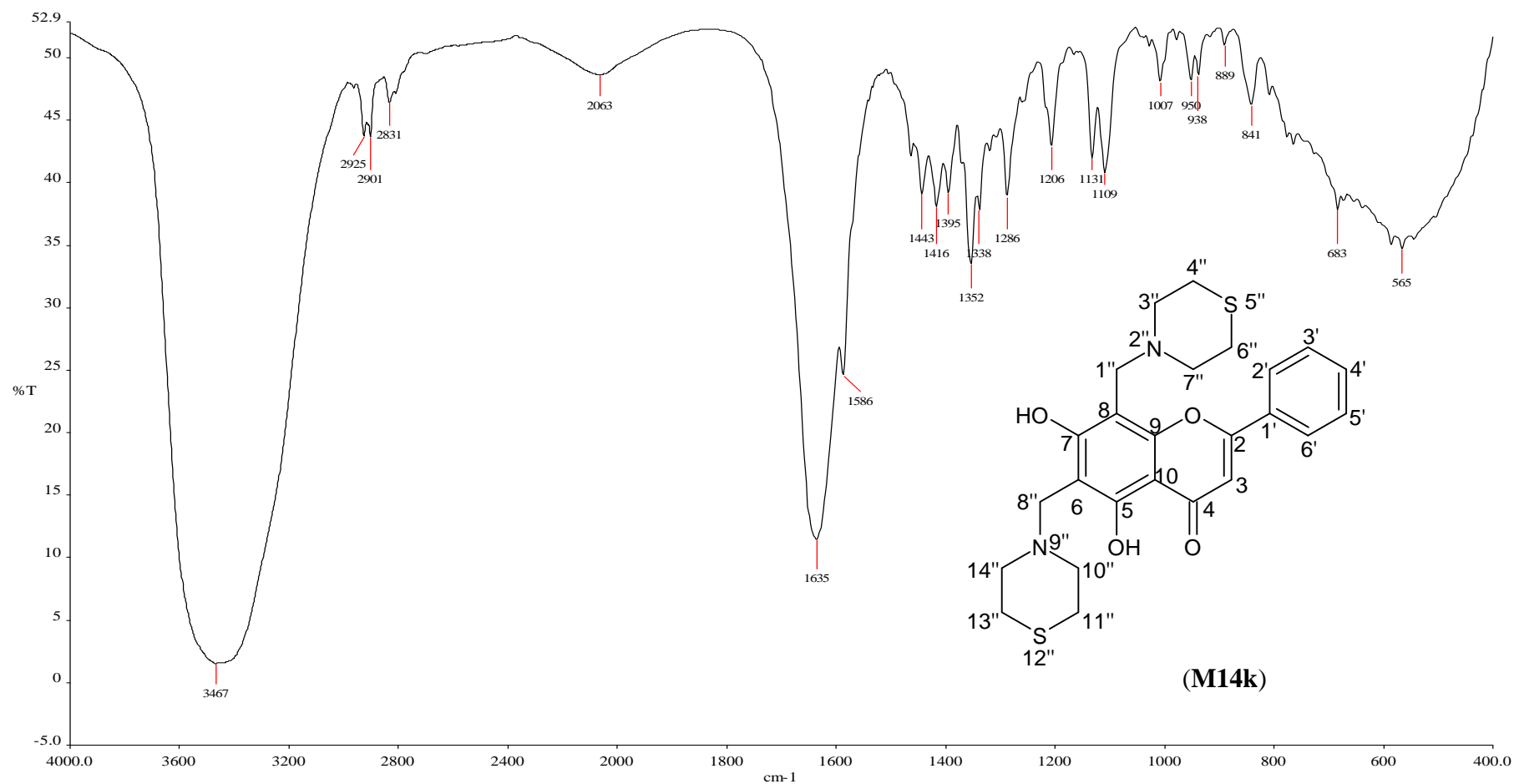
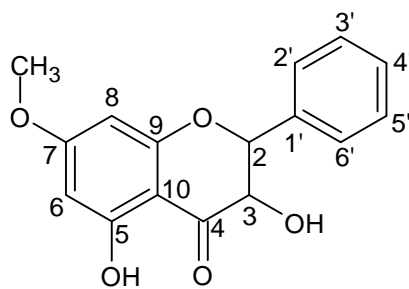
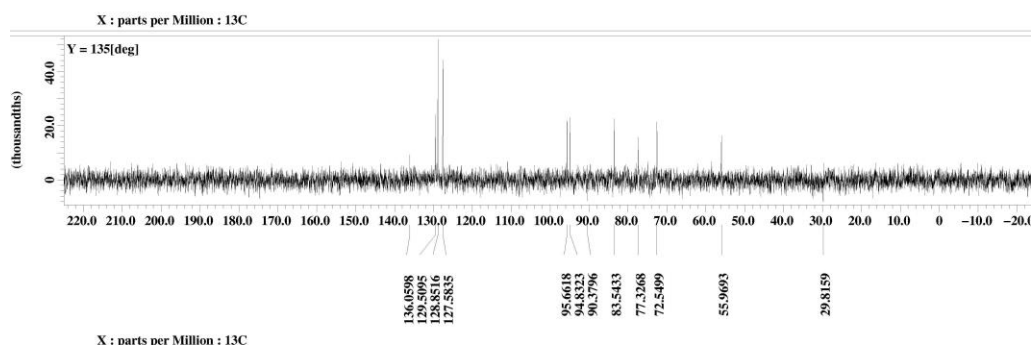
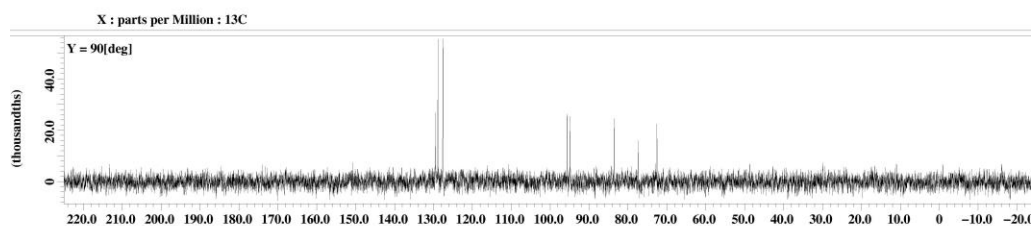
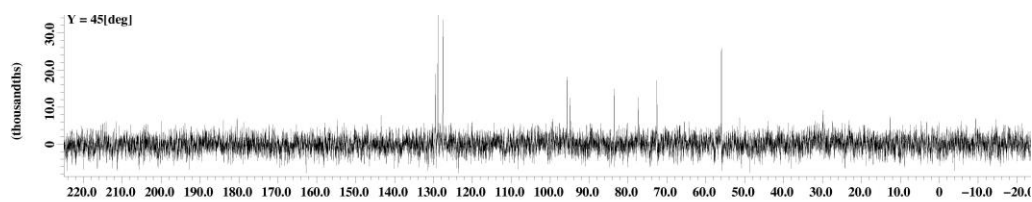


Figure C38: FTIR (KBr) of 5,7-dihydroxy-6,8-bis(thiomorpholinomethyl)-2-phenyl-4H-chromen-4-one (M14k)

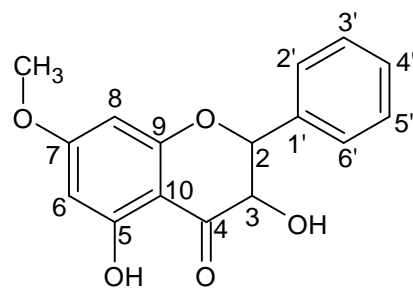
APPENDIX D



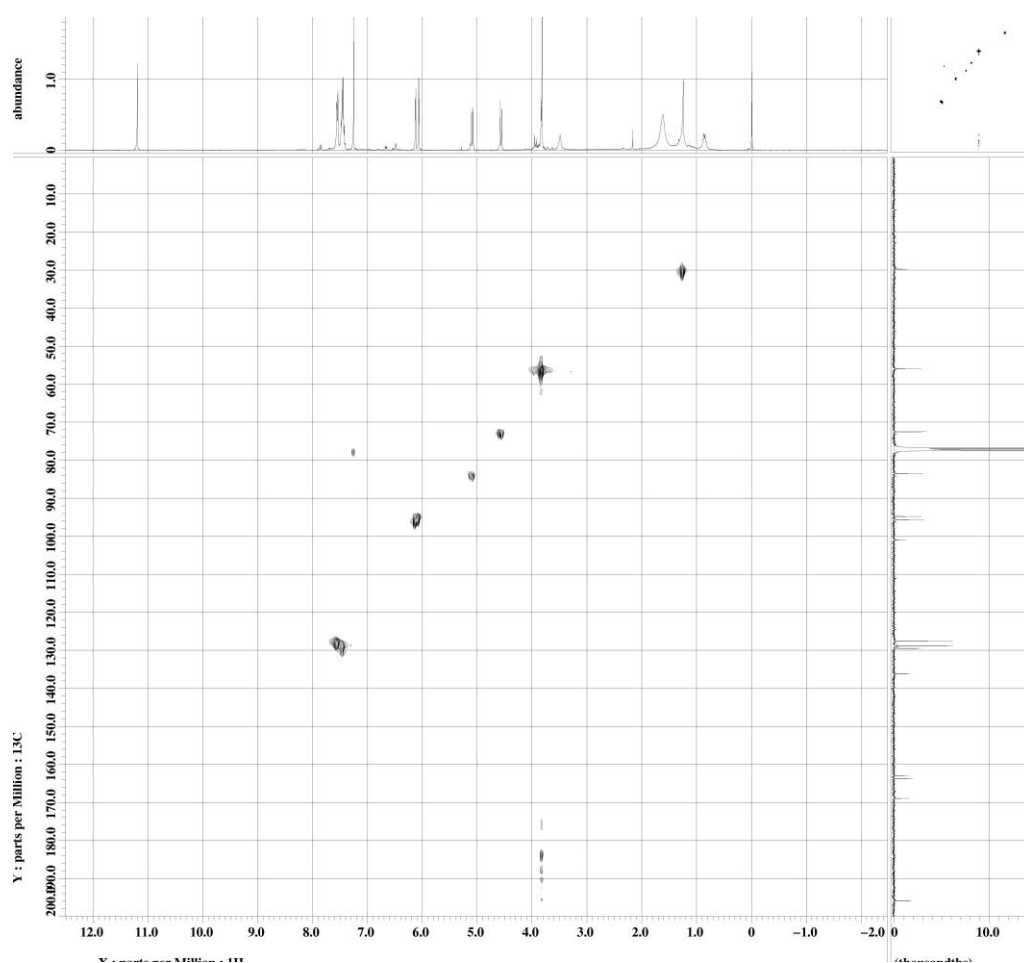
(M1)



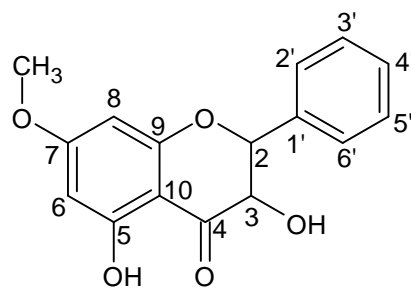
Appendix D1: DEPT Spectrum of (2*S*,3*S*) 3,5-dihydroxy-7-methoxyflavanone (M1)



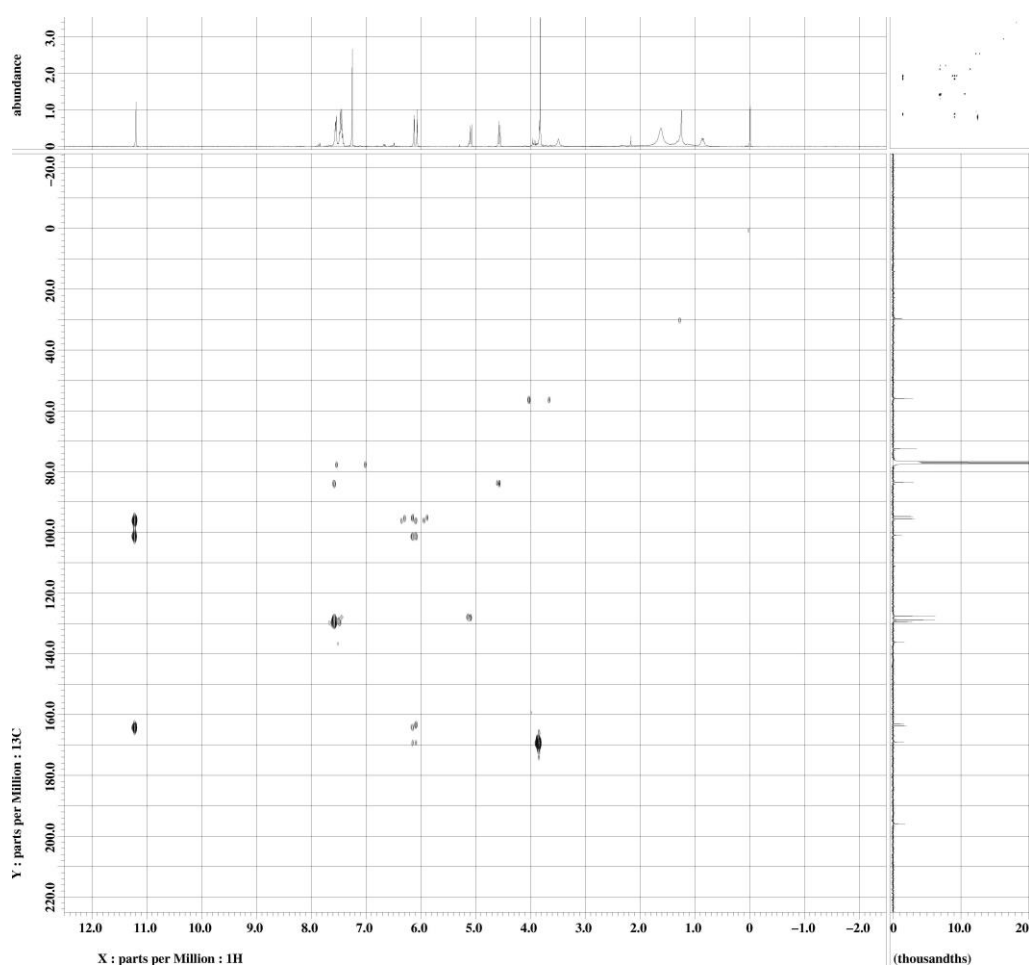
(M1)



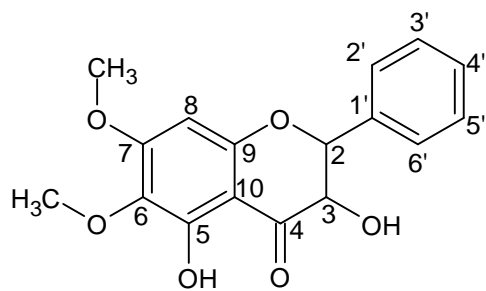
Appendix D2: HMQC Spectrum of (2*S*,3*S*) 3,5-dihydroxy-7-methoxyflavanone (M1)



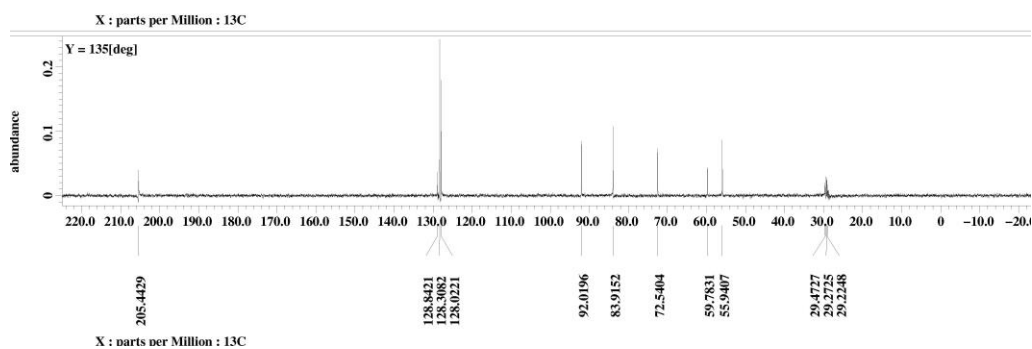
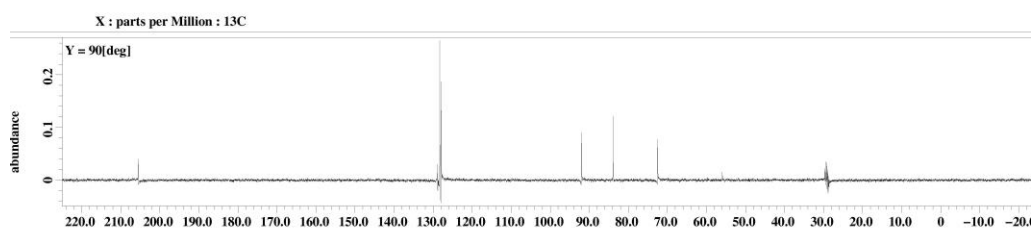
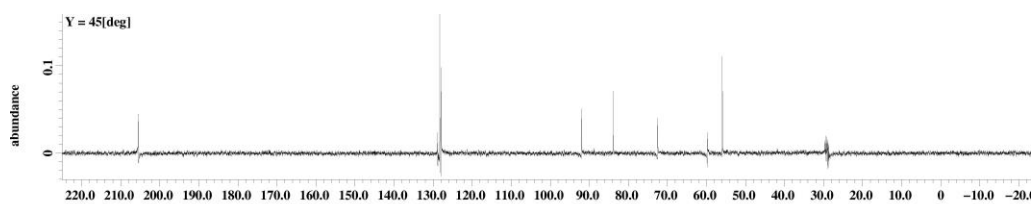
(M1)



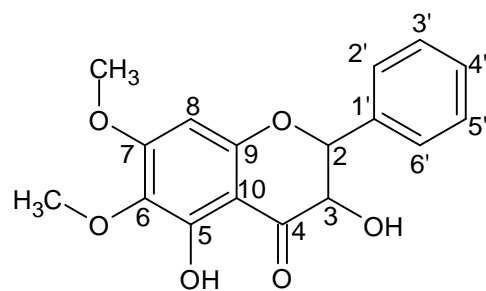
Appendix D3: HMBC Spectrum of (2*S*,3*S*) 3,5-dihydroxy-7-methoxyflavanone (M1)



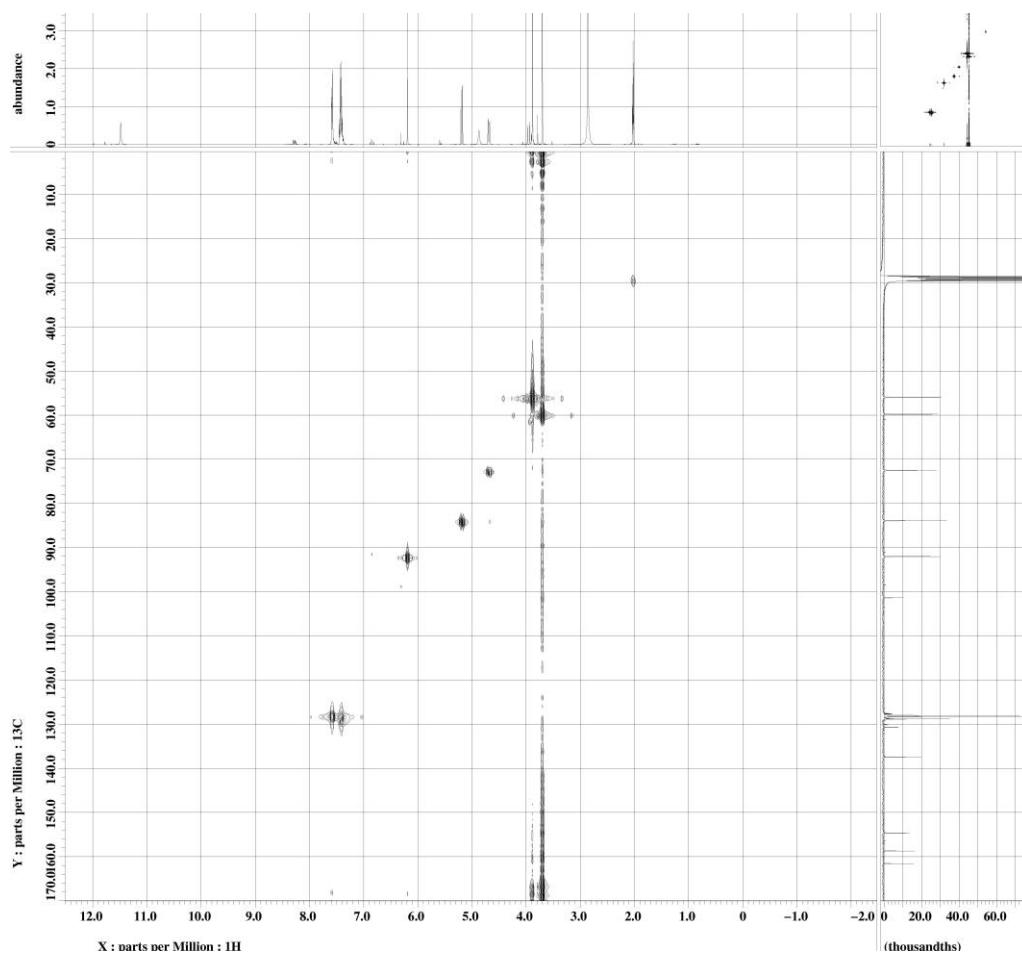
(M12)



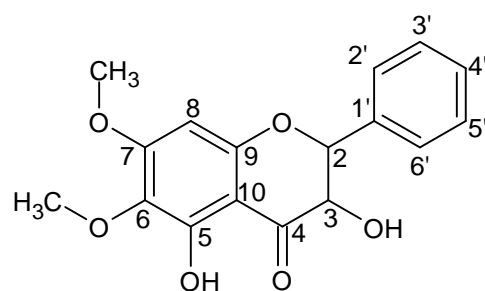
Appendix D4: DEPT Spectrum of (2R,3R) 3,5-dihydroxy-6,7-dimethoxyflavanone (M12)



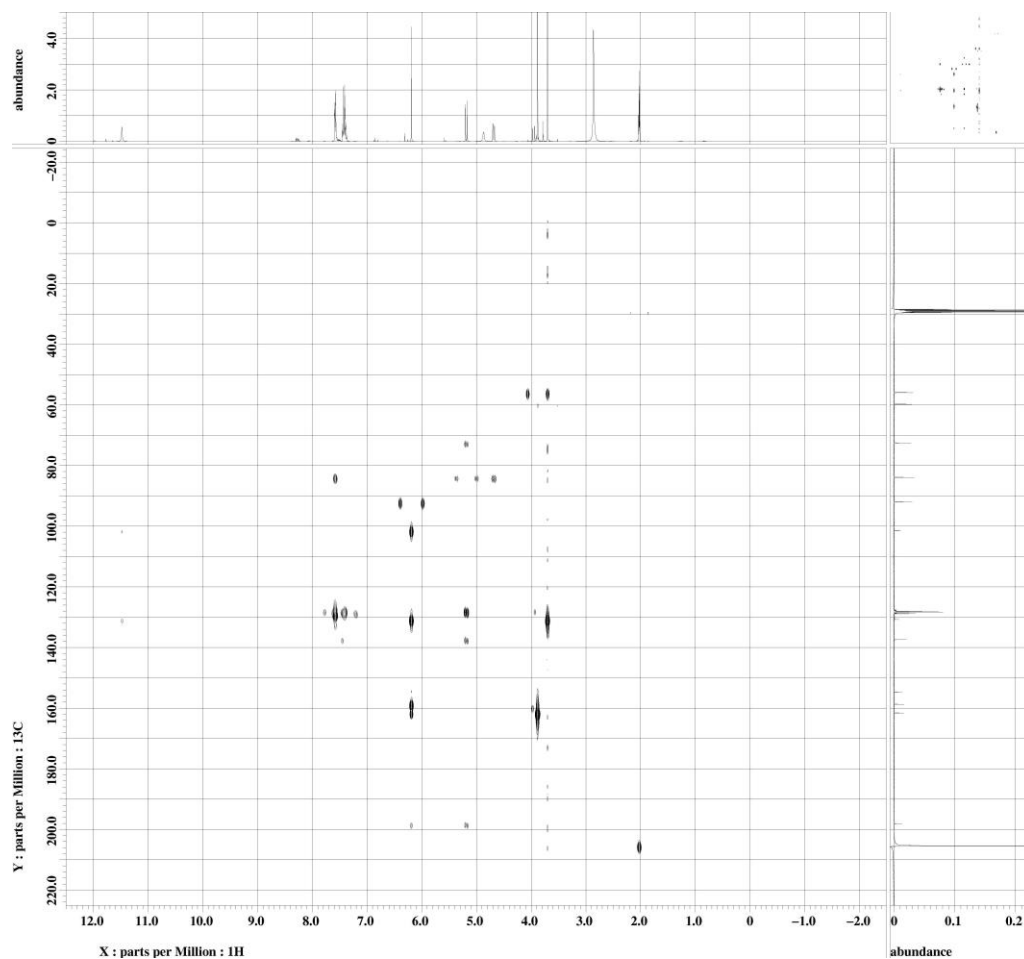
(M12)



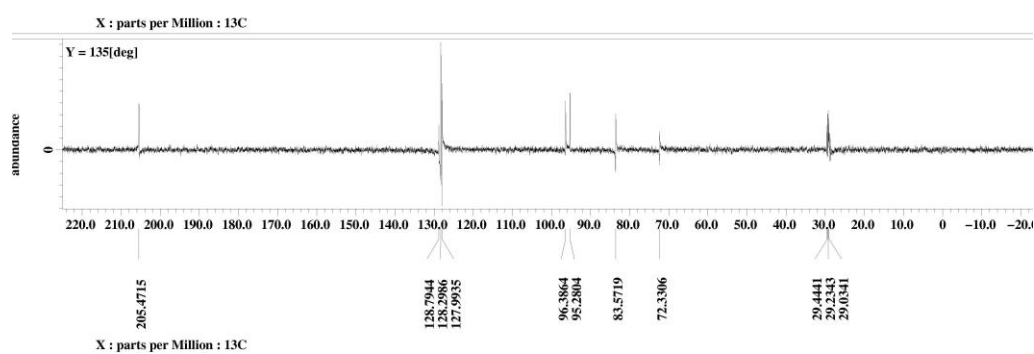
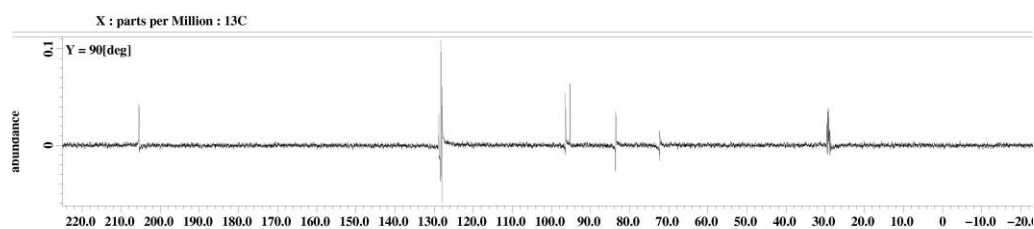
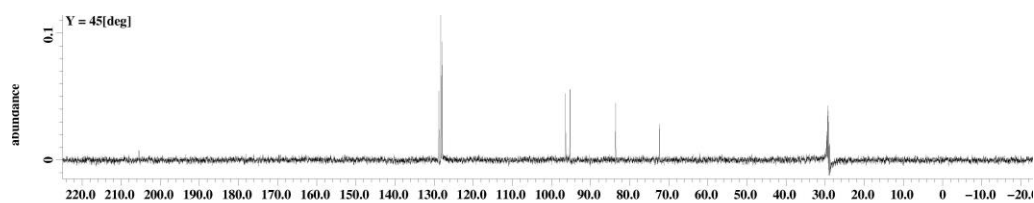
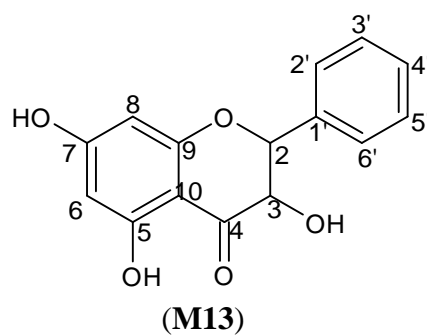
Appendix D5: HMQC Spectrum of (2*R*,3*R*) 3,5-dihydroxy-6,7-dimethoxyflavanone (M12)



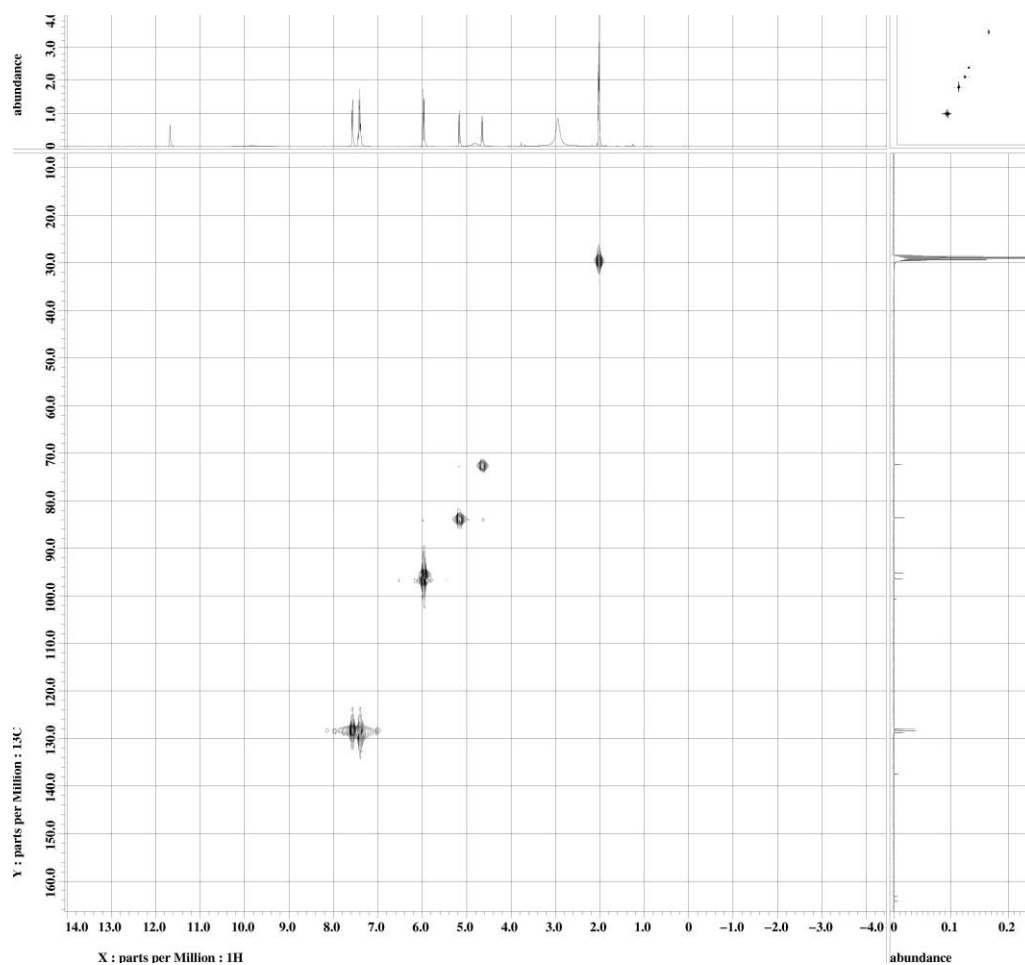
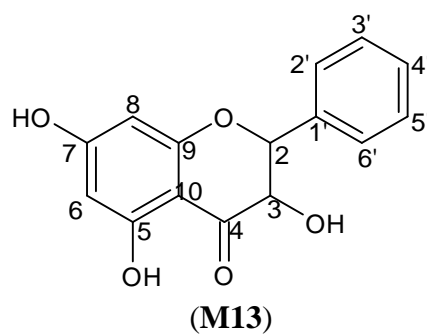
(M12)



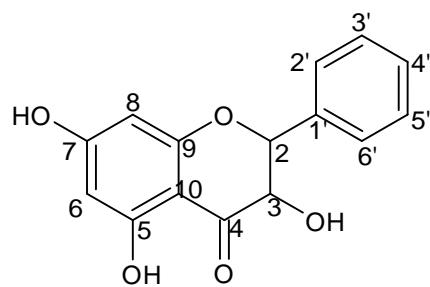
Appendix D6: HMBC Spectrum of (2*R*,3*R*) 3,5-dihydroxy-6,7-dimethoxyflavanone (M12)



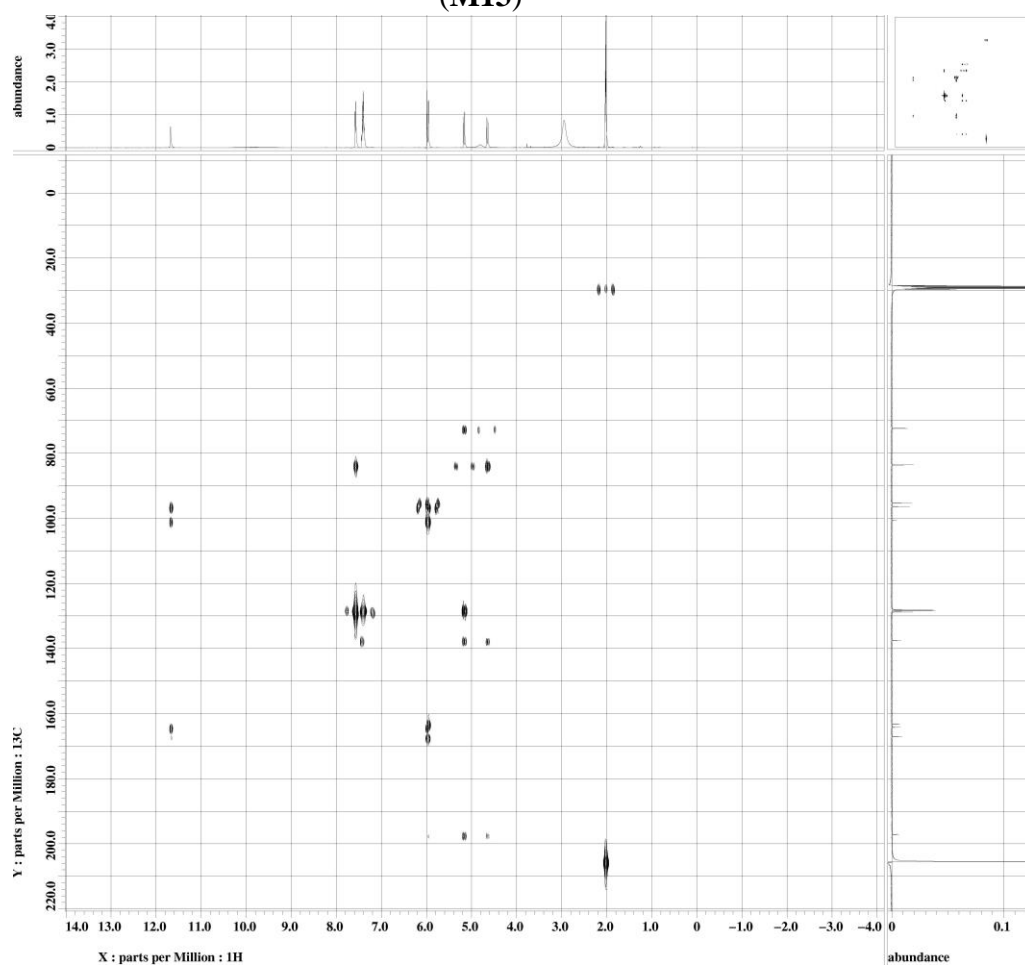
Appendix D7: DEPT Spectrum of (2R,3R) 3,5,7-trihydroxyflavanone (M13)



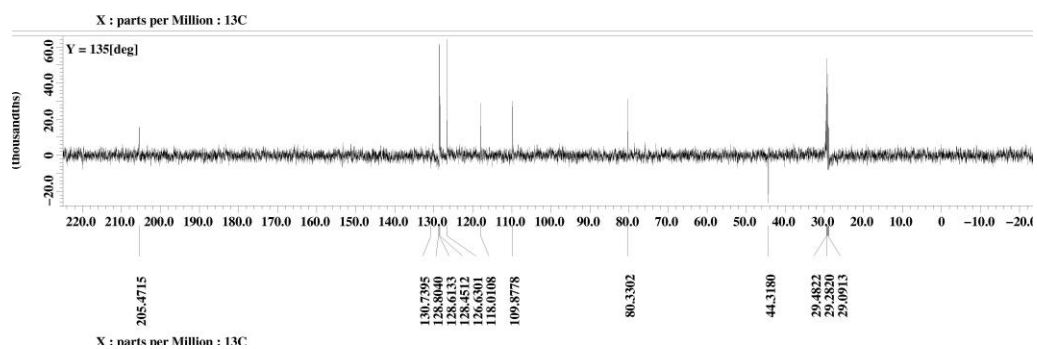
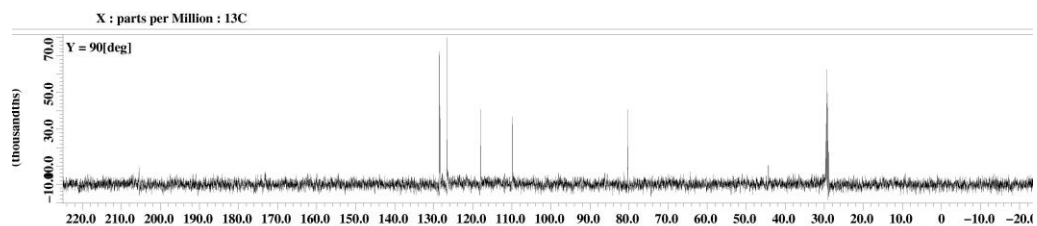
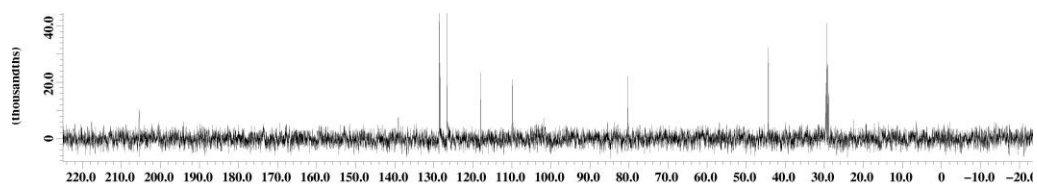
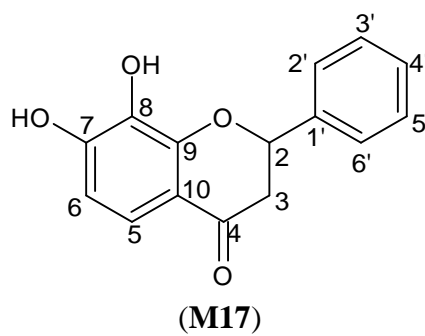
Appendix D8: HMQC Spectrum of (2*R*,3*R*) 3,5,7-trihydroxyflavanone (M13)



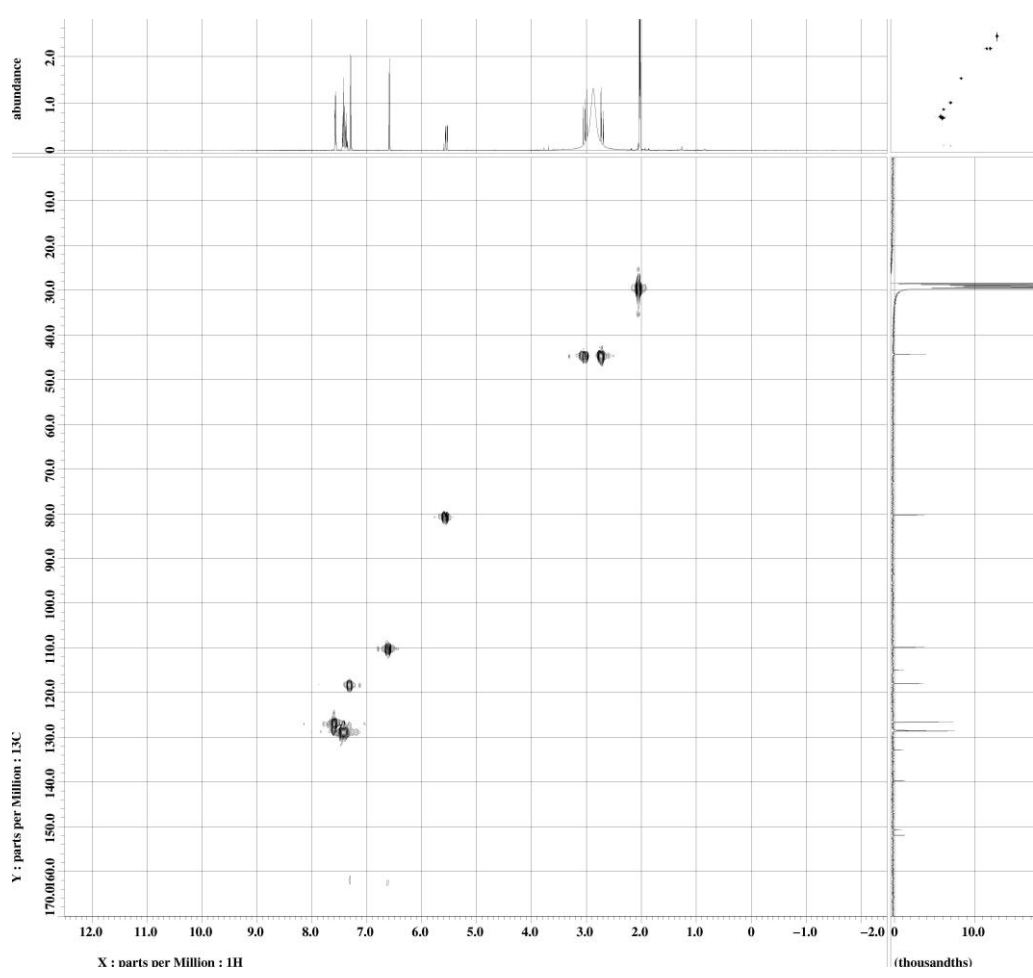
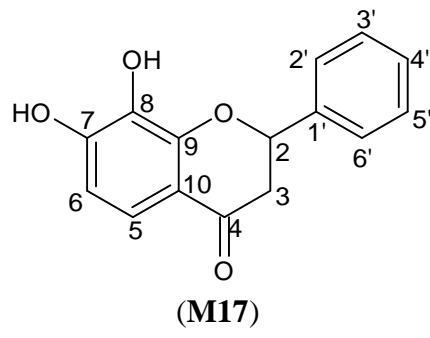
(M13)



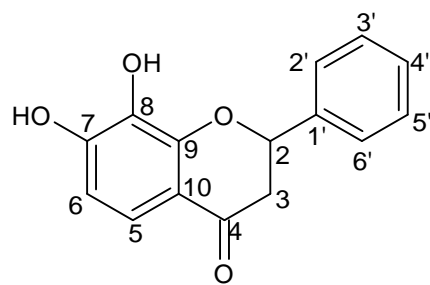
Appendix D9: HMBC Spectrum of (2*R*,3*R*) 3,5,7-trihydroxyflavanone (M13)



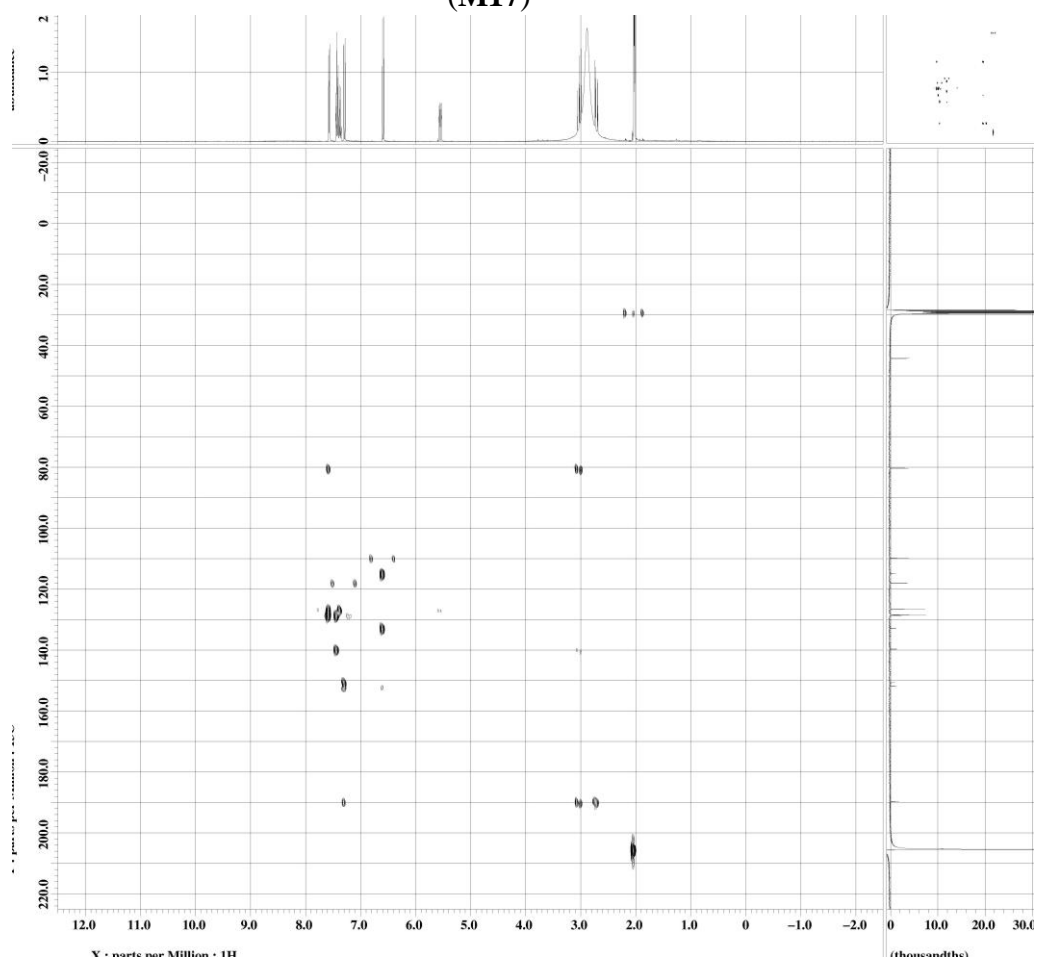
Appendix D10: DEPT Spectrum of (2S)-7,8-dihydroxyflavanone (M17)



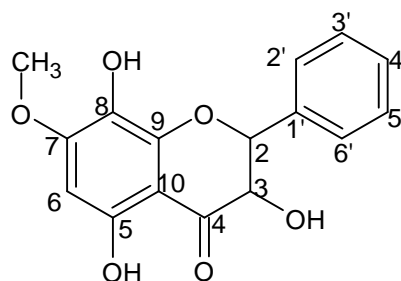
Appendix D11: HMQC Spectrum of (2S) 7,8-dihydroxyflavanone (M17)



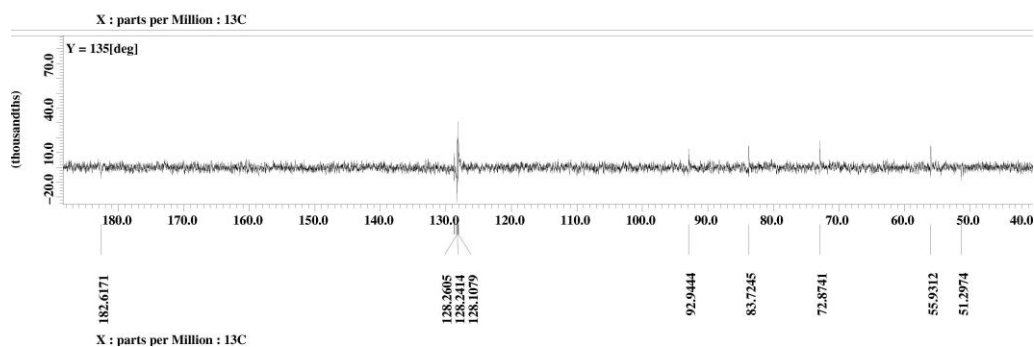
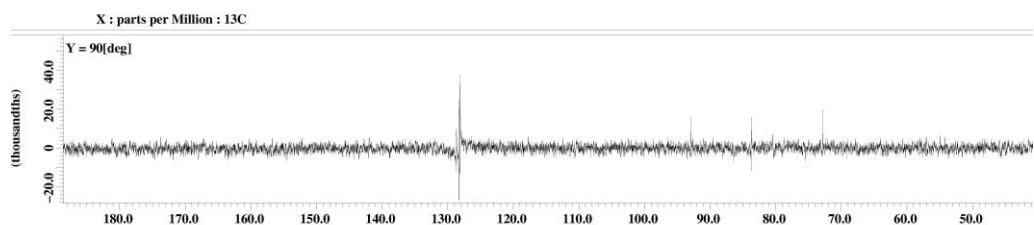
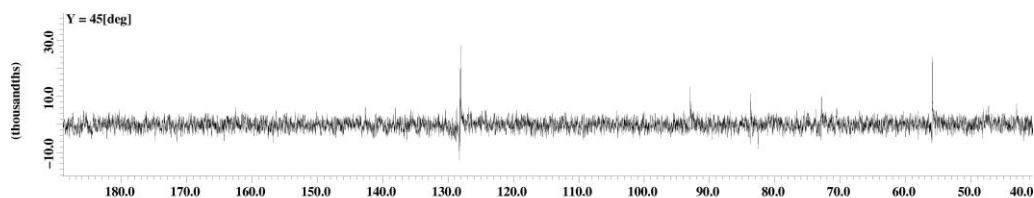
(M17)



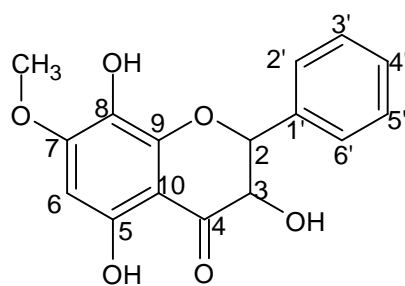
Appendix D12: HMBC Spectrum of (2S)-7,8-dihydroxyflavanone (M17)



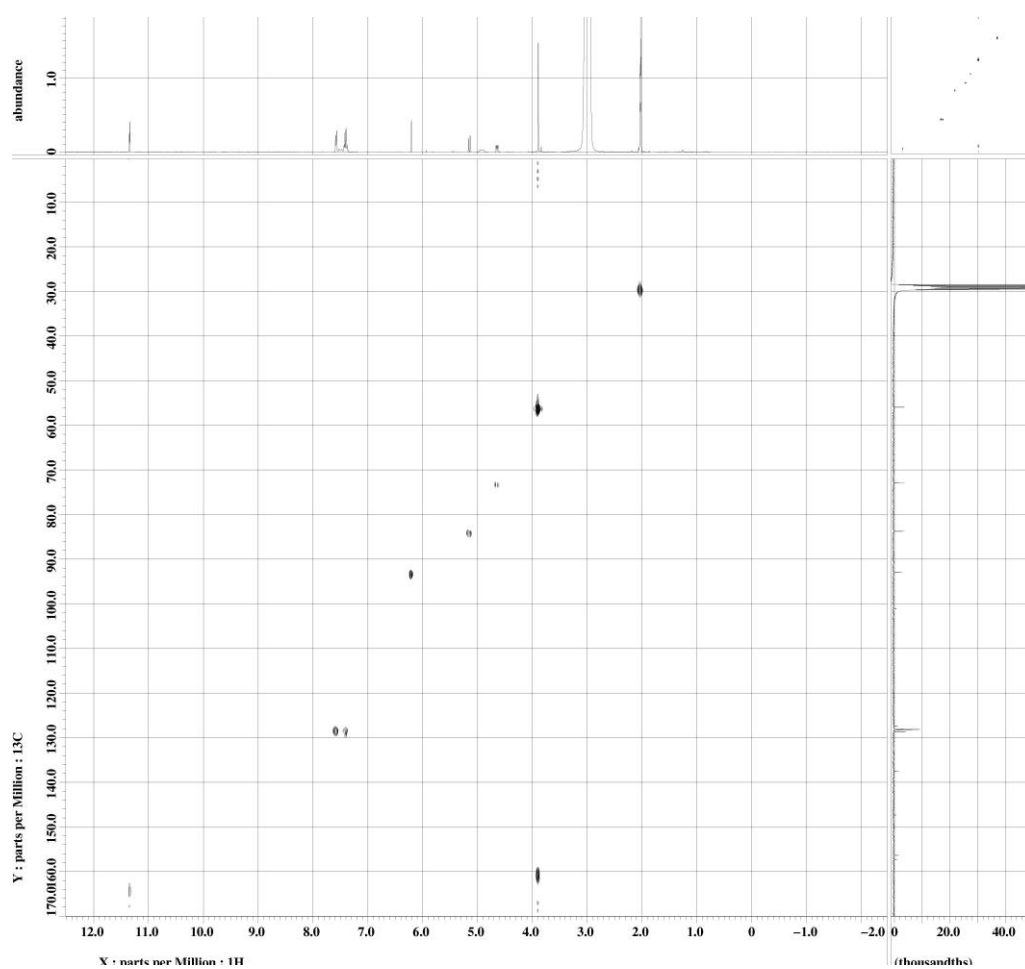
(M18)



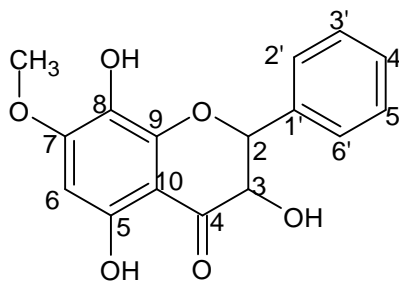
Appendix D13: DEPT Spectrum of (2R, 3R) 3,5,7-trihydroxy-8-methoxyflavanone (M18)



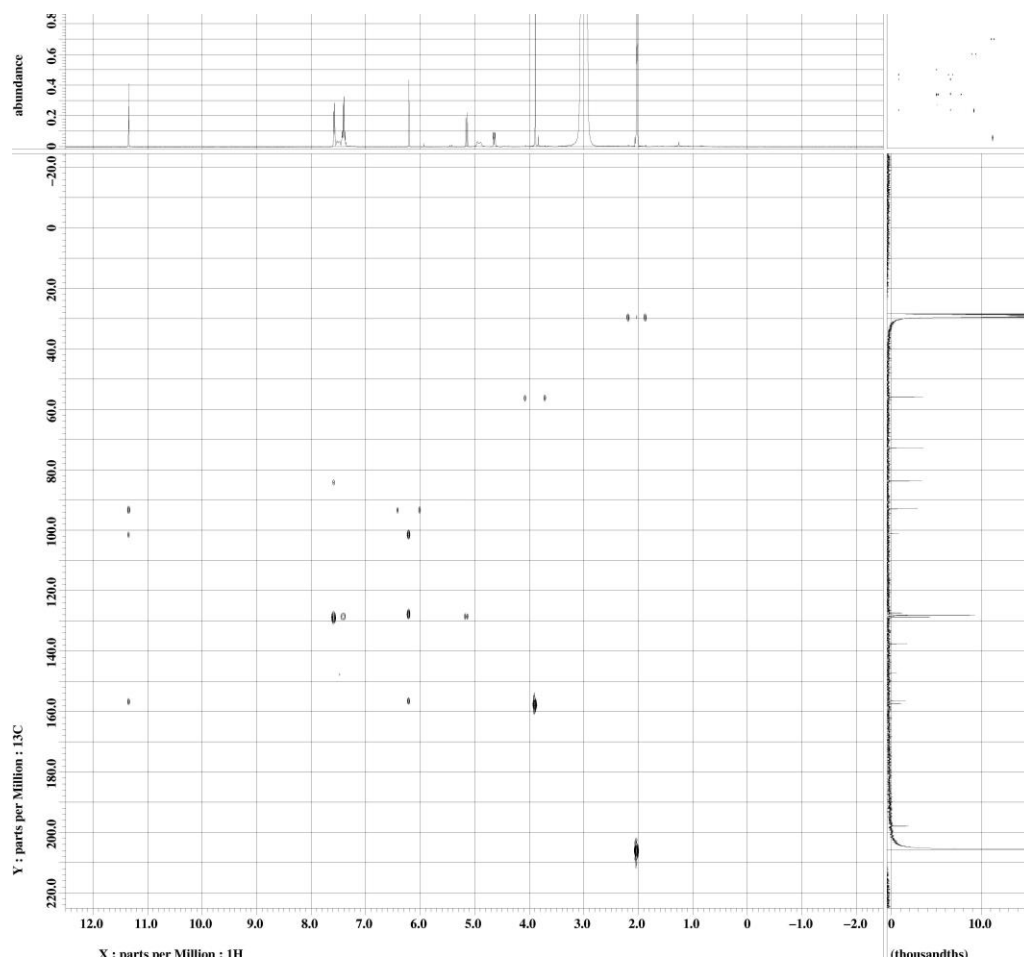
(M18)



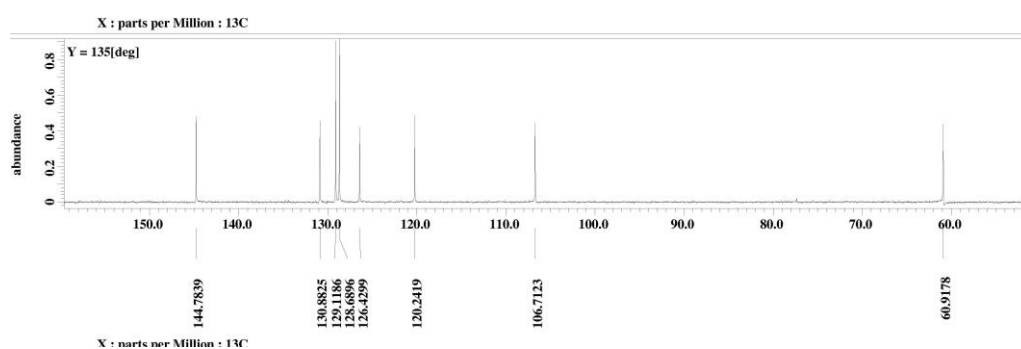
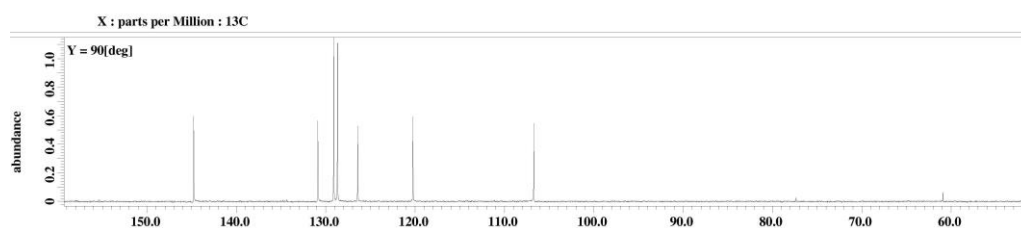
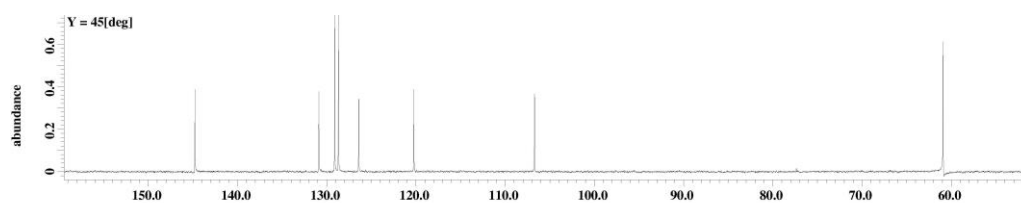
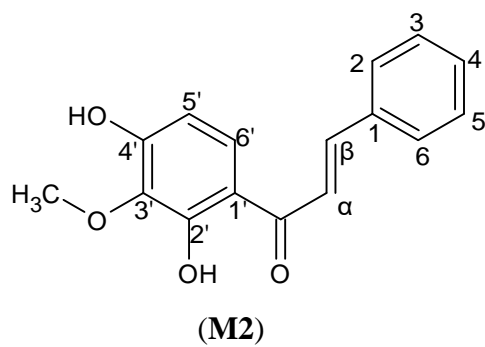
Appendix D14: HMQC Spectrum of (2*R*, 3*R*) 3,5,7-trihydroxy-8-methoxyflavanone (M18)



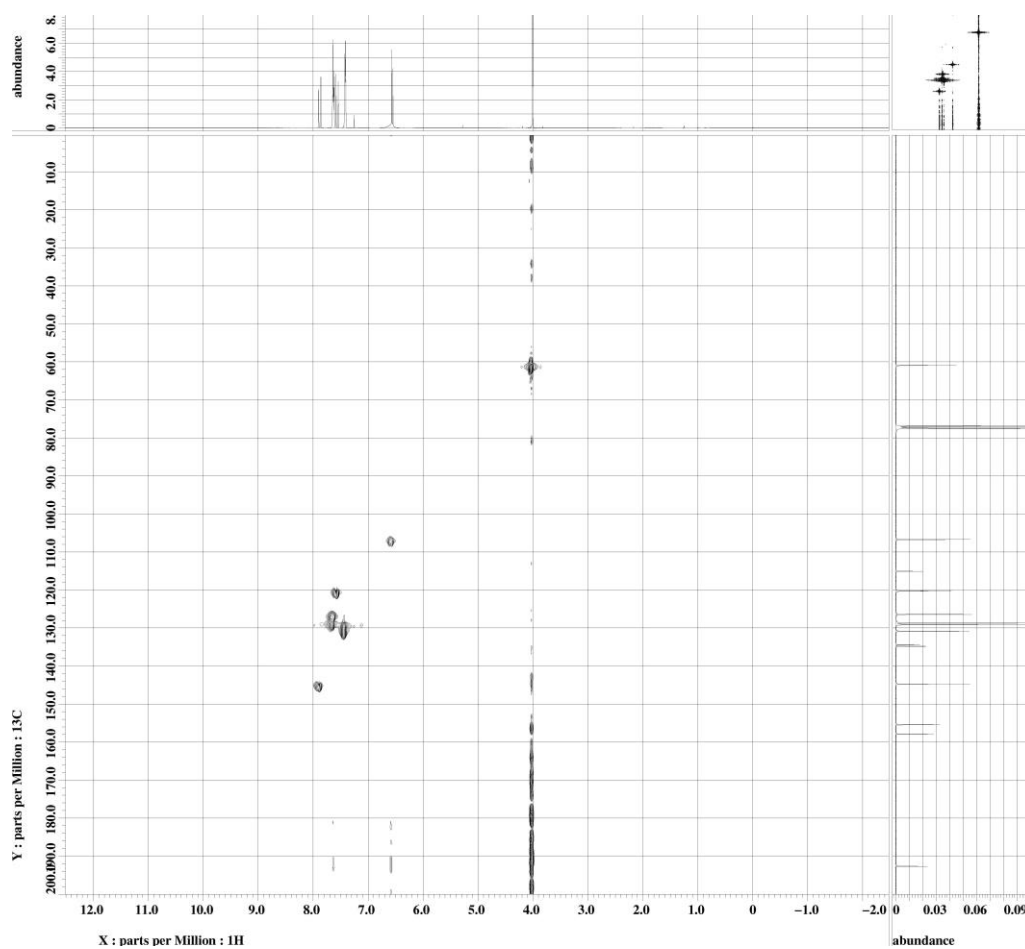
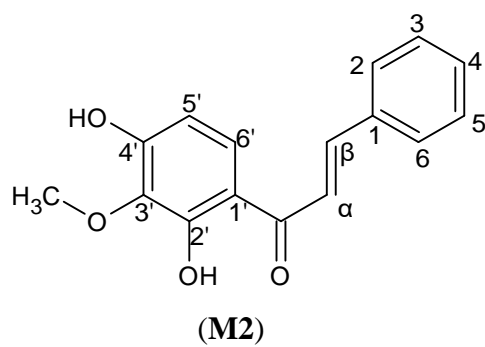
(M18)



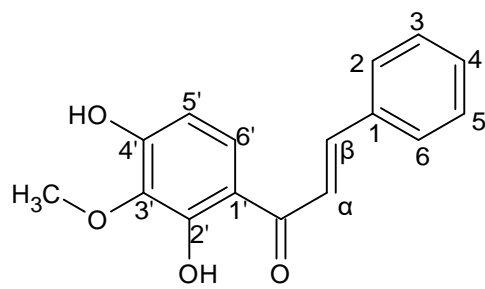
Appendix D15: HMBC Spectrum of (2R, 3R) 3,5,7-trihydroxy-8-methoxyflavanone (M18)



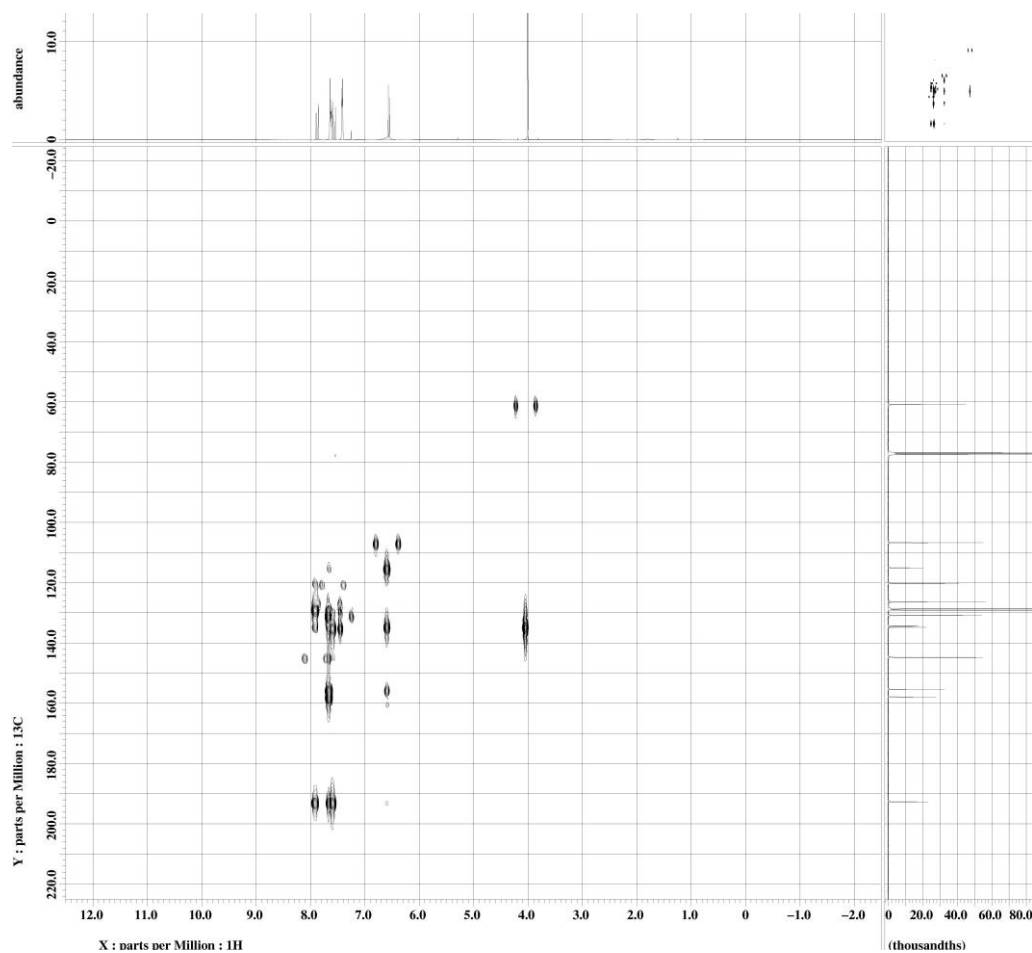
Appendix D16: DEPT Spectrum of 2',4'-dihydroxy-3'-methoxychalcone (M2)



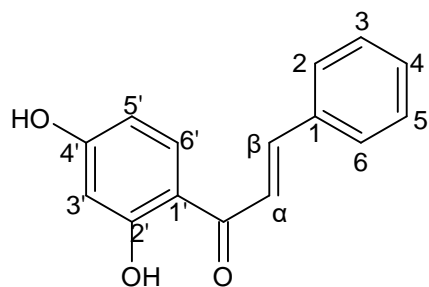
Appendix D17: HMQC Spectrum of 2',4'-dihydroxy-3'-methoxychalcone (M2)



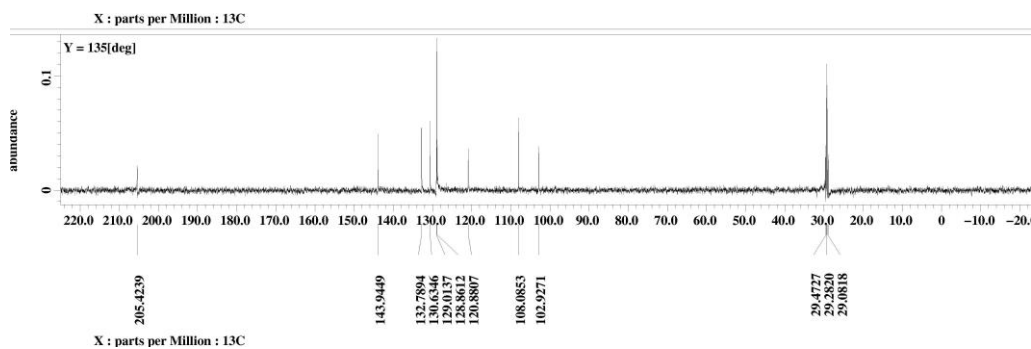
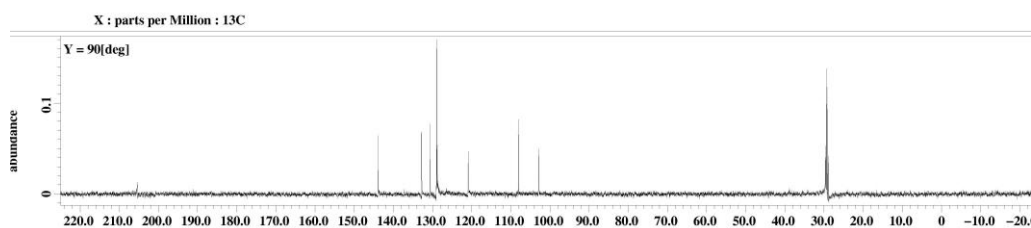
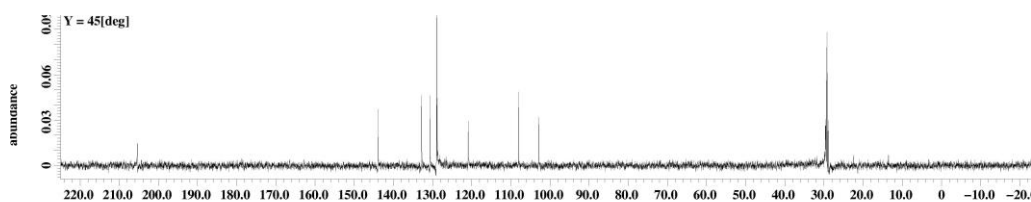
(M2)



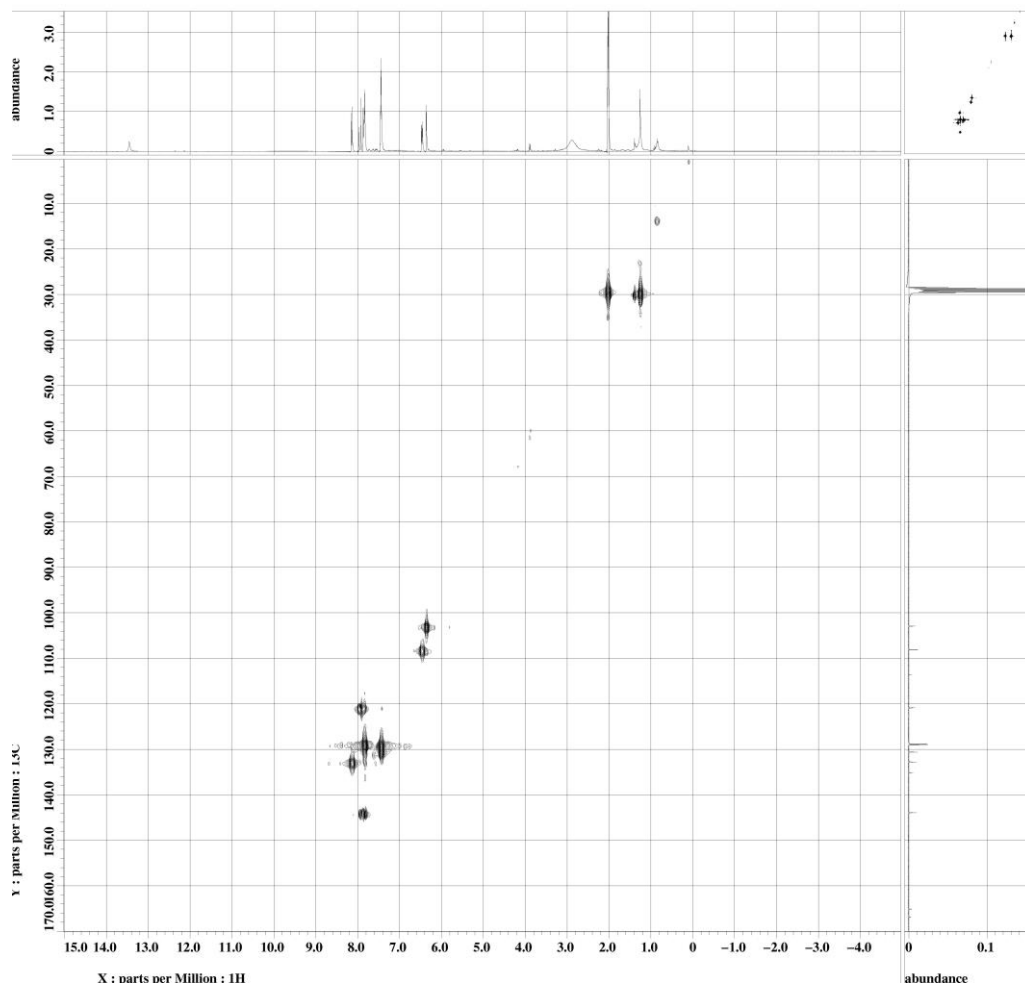
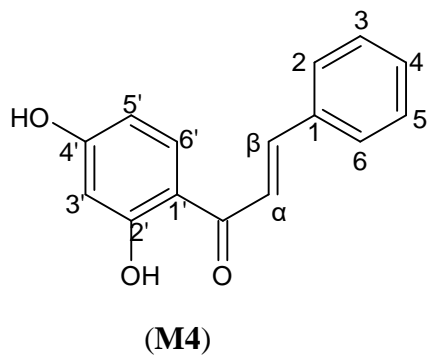
Appendix D18: HMBC Spectrum of 2',4'-dihydroxy-3'-methoxychalcone (M2)



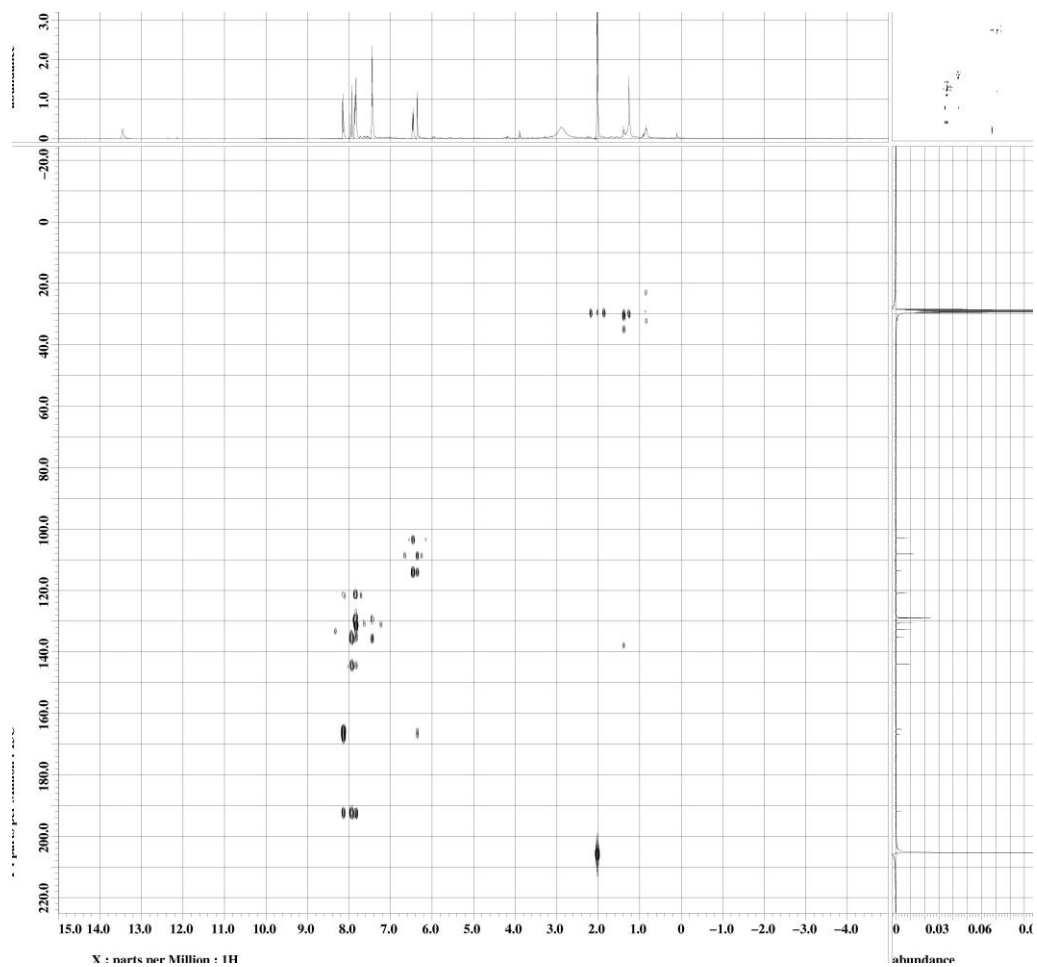
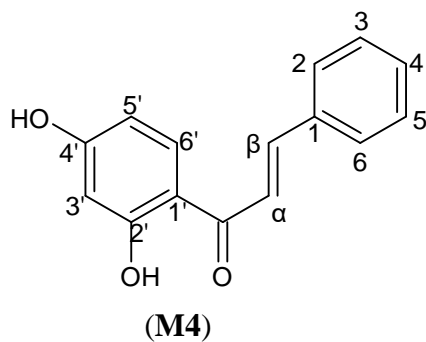
(M4)



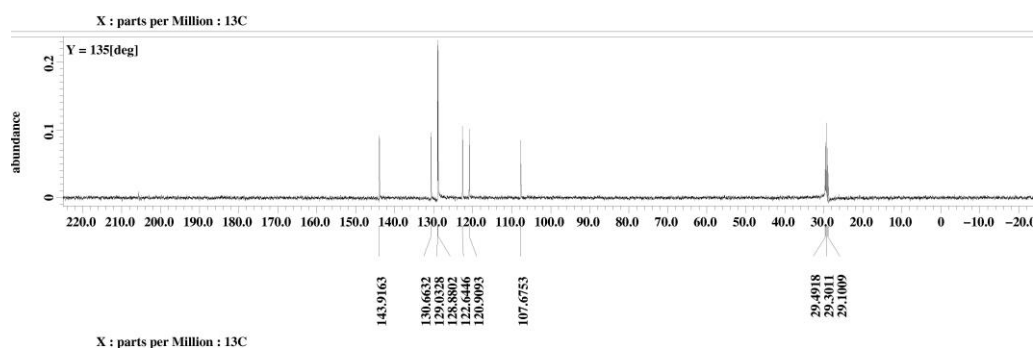
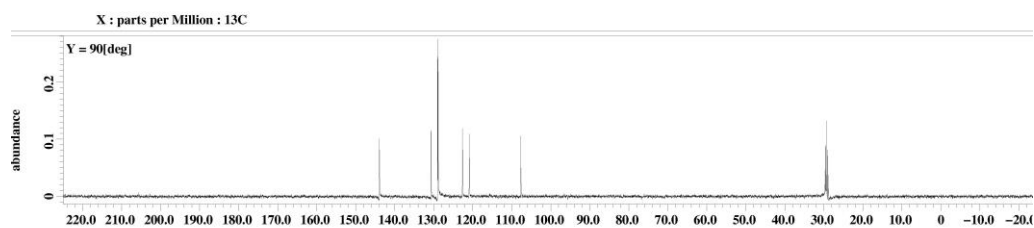
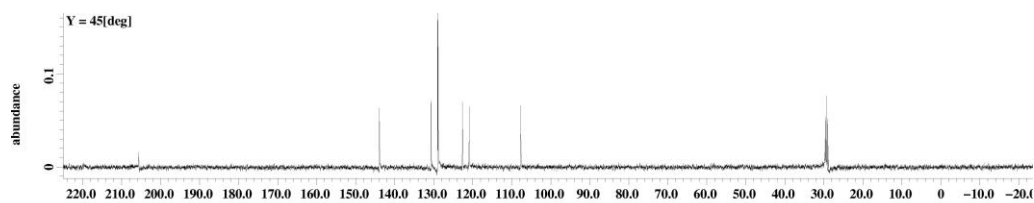
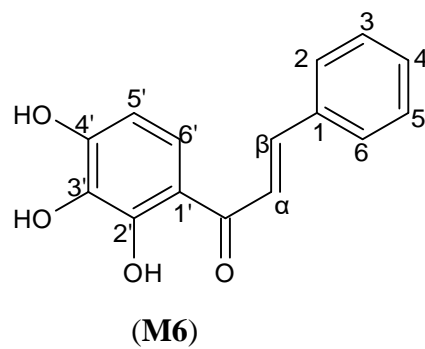
Appendix D19: DEPT Spectrum of 2',4'-dihydroxychalcone (M4)



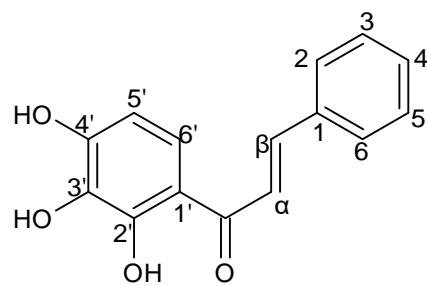
Appendix D20: HMQC Spectrum of 2',4'-dihydroxychalcone (M4)



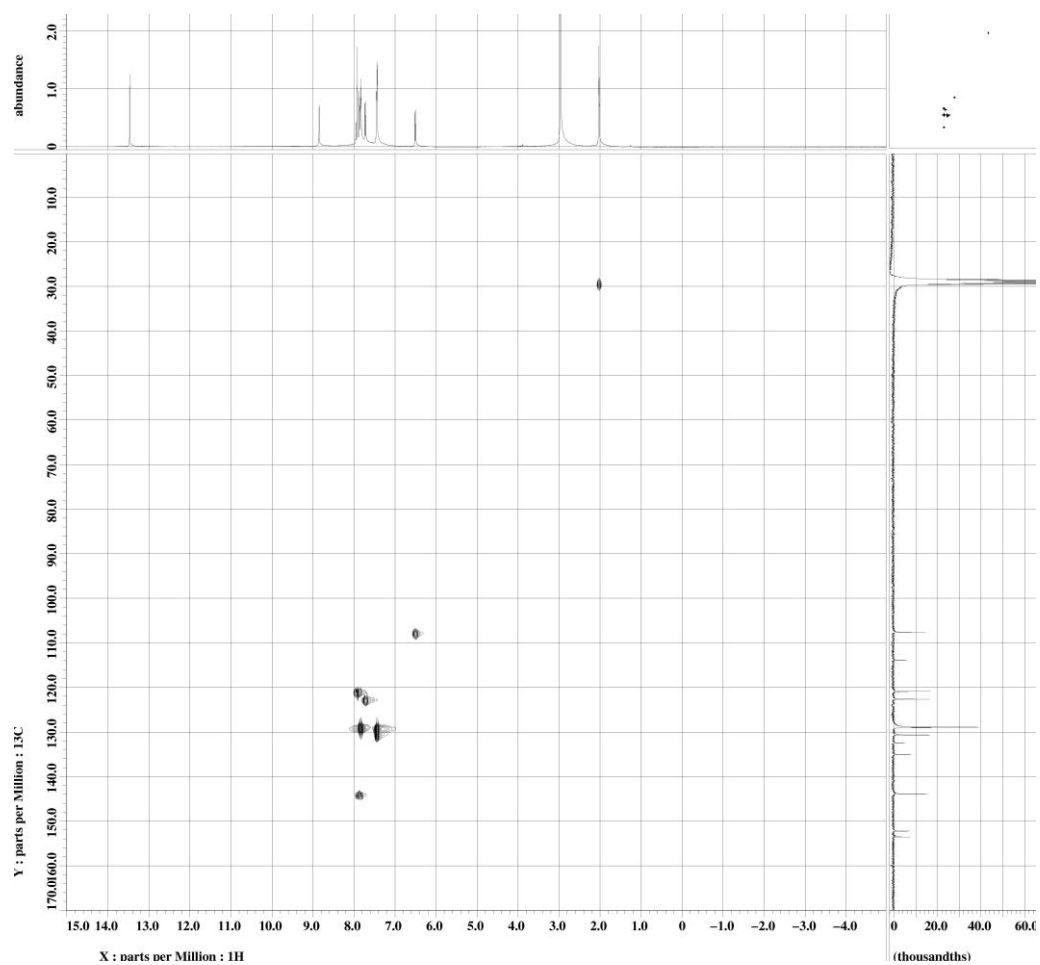
Appendix D21: HMBC Spectrum of 2',4'-dihydroxychalcone (M4)



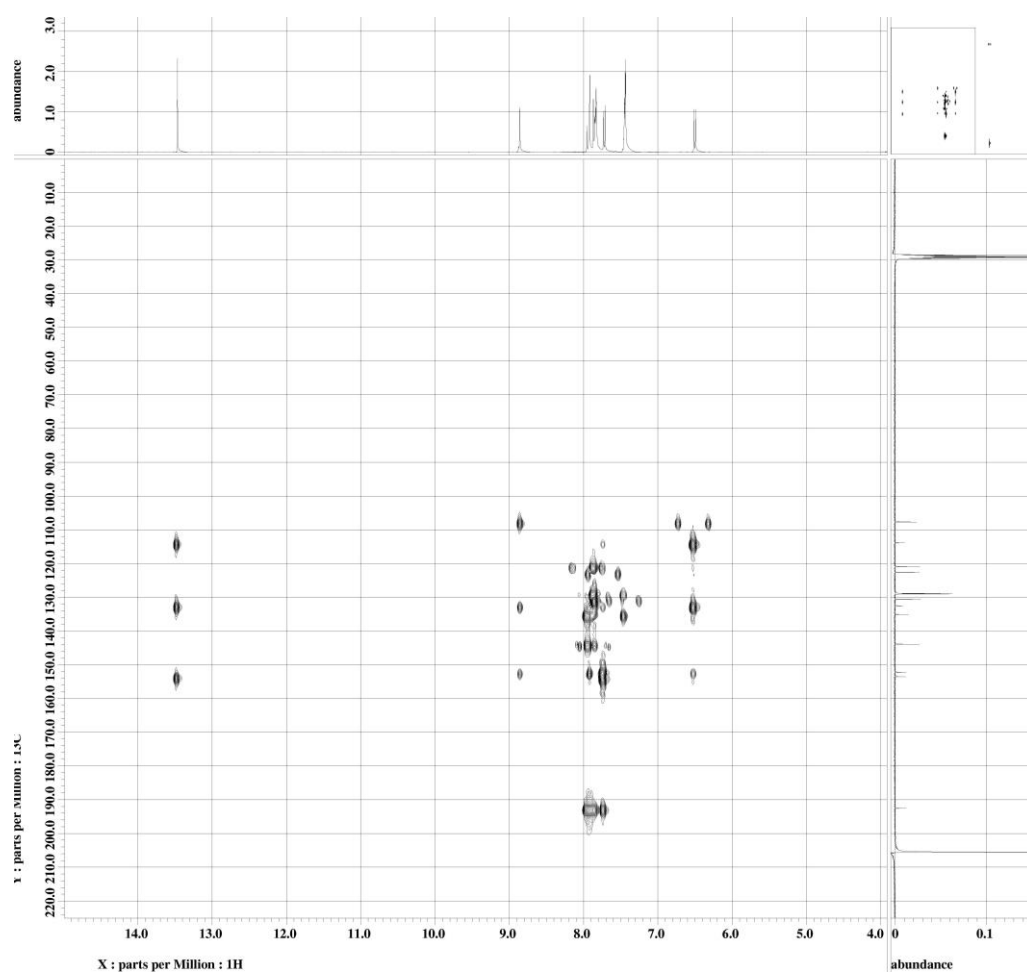
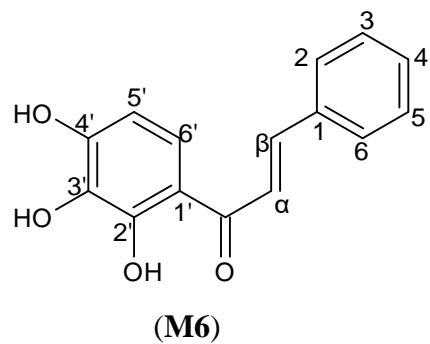
Appendix D22: DEPT Spectrum of 2',3',4'-trihydroxychalcone (M6)



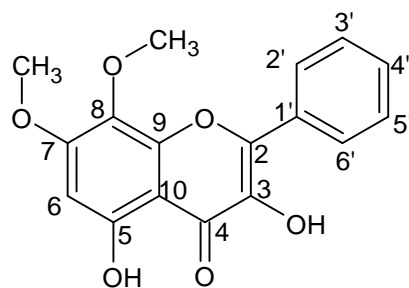
(M6)



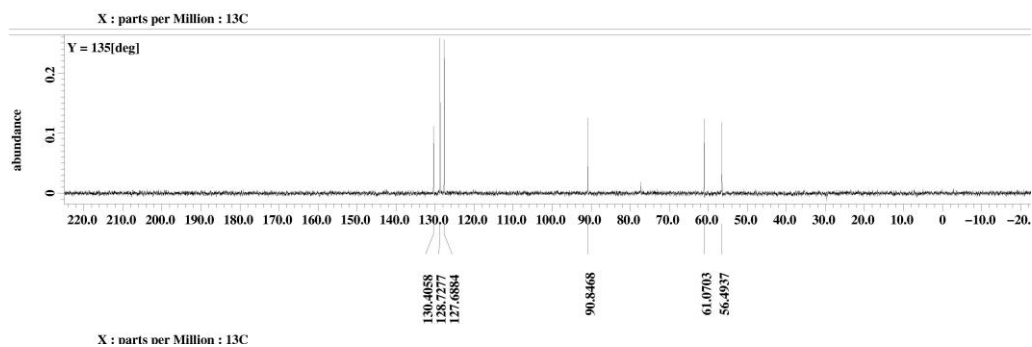
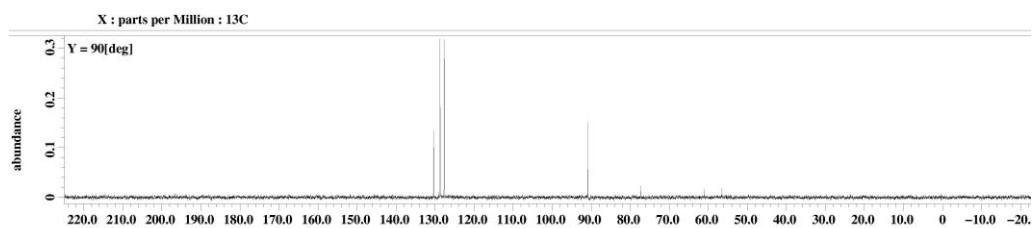
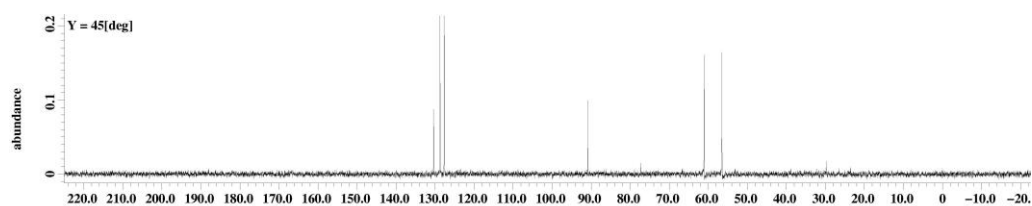
Appendix D23: HMQC Spectrum of 2', 3', 4'-trihydroxychalcone (M6)



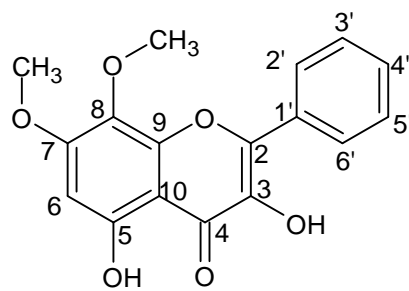
Appendix D24: HMBC Spectrum of 2', 3', 4'-trihydroxychalcone (M6)



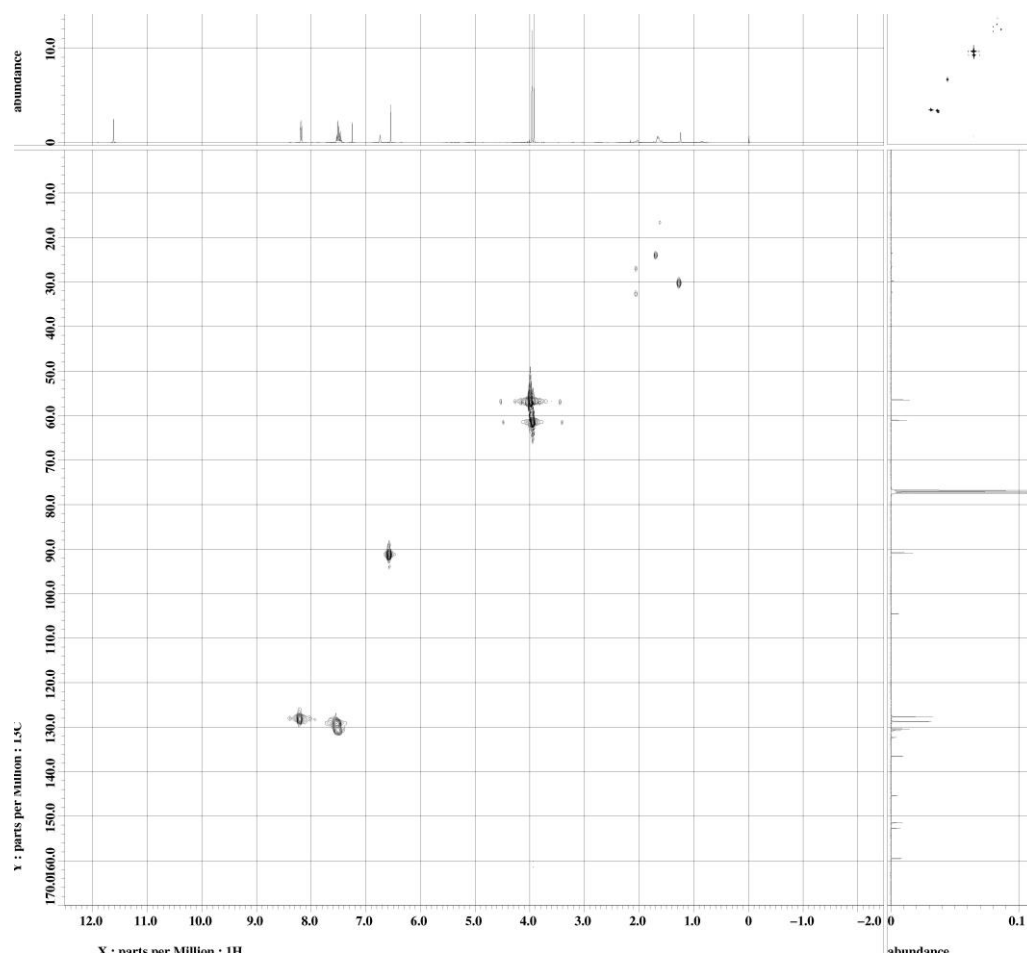
(M3)



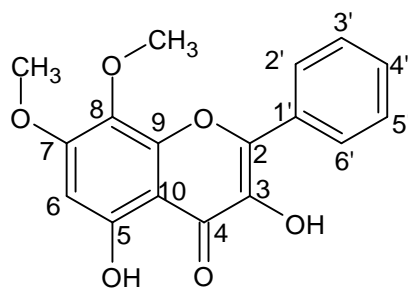
Appendix D25: DEPT Spectrum of 3,5-dihydroxy-7,8-dimethoxyflavone (M3)



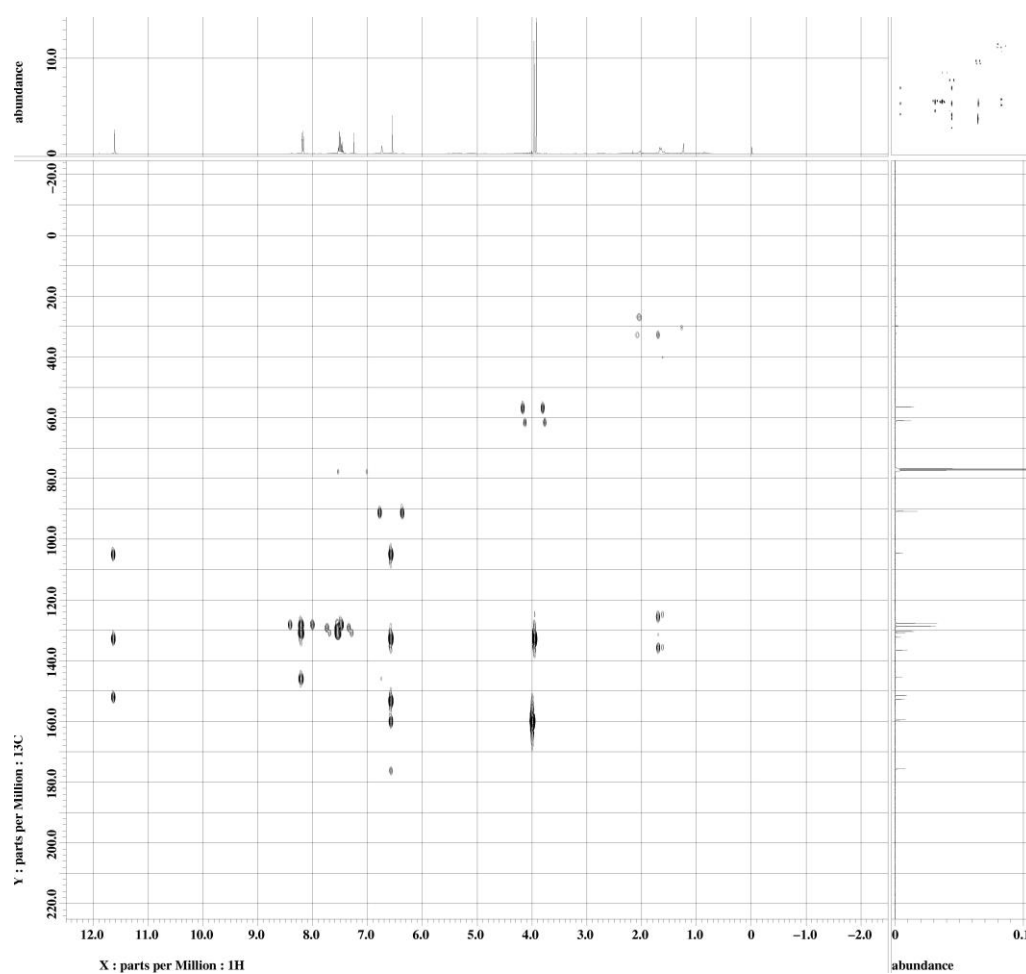
(M3)



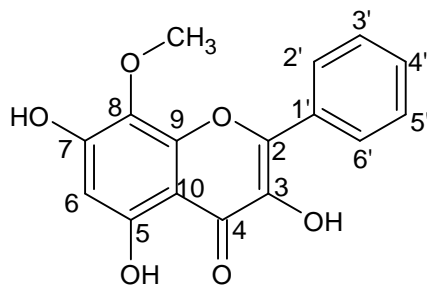
Appendix D26: HMQC Spectrum of 3,5-dihydroxy-7,8-dimethoxyflavone (M3)



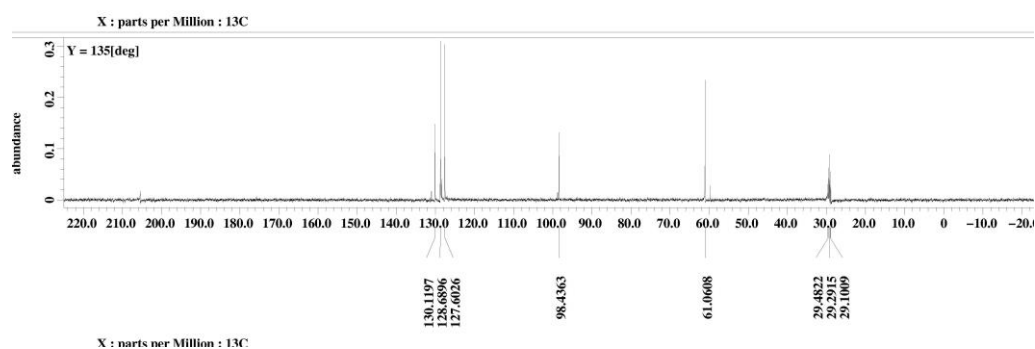
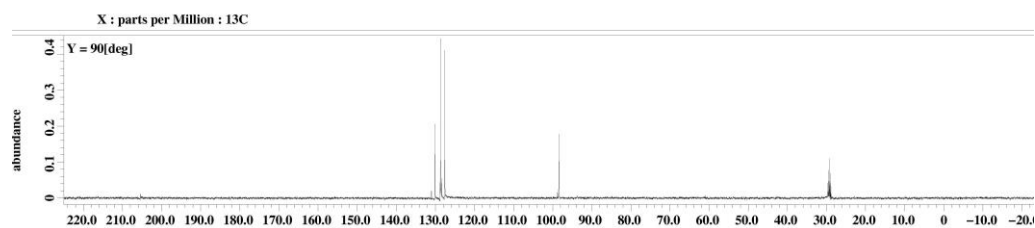
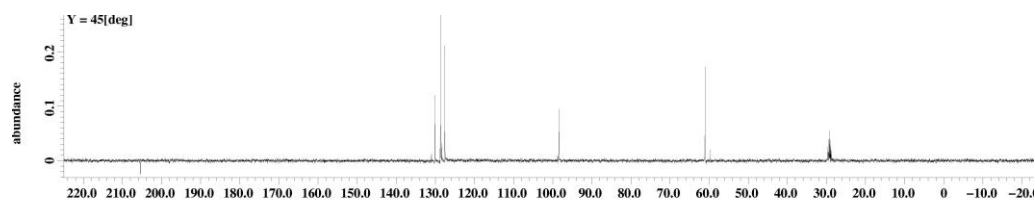
(M3)



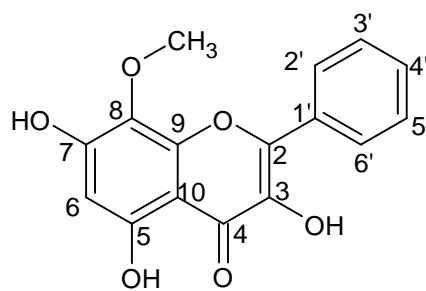
Appendix D27: HMBC Spectrum of 3,5-dihydroxy-7,8-dimethoxyflavone (M3)



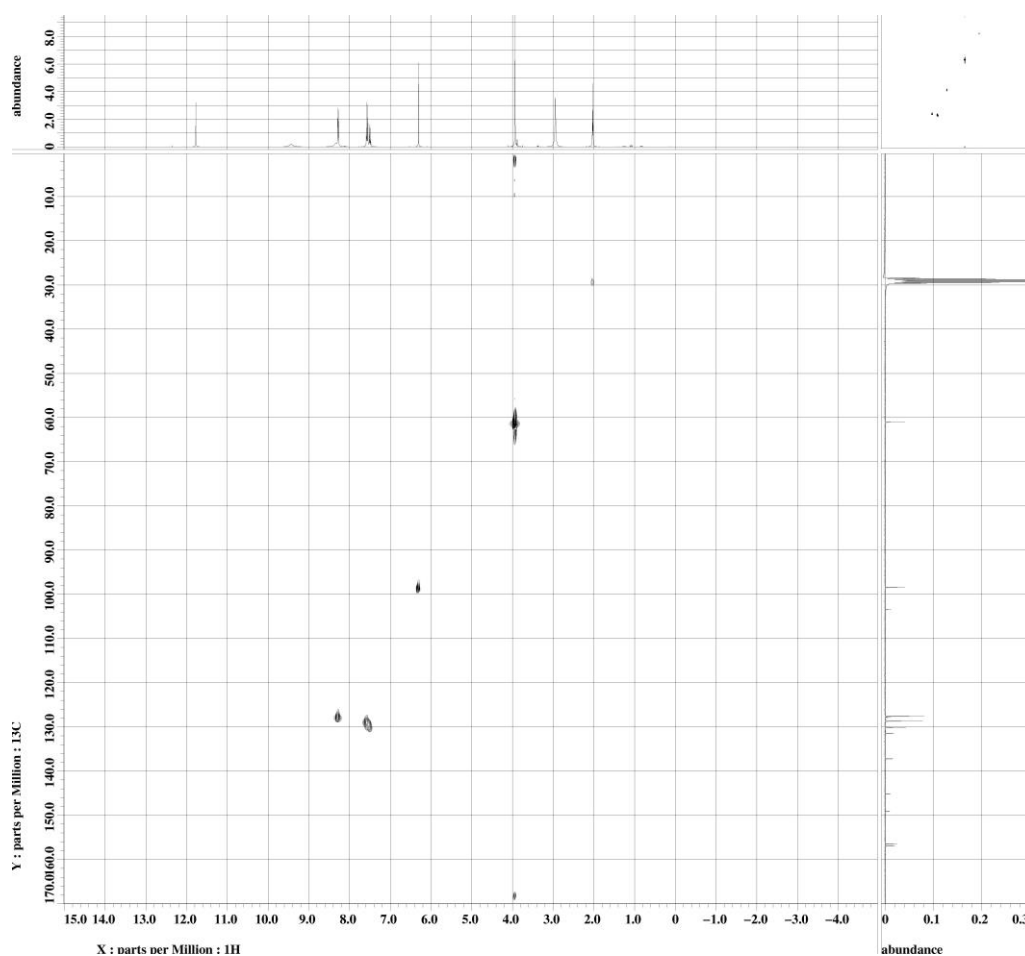
(M5)



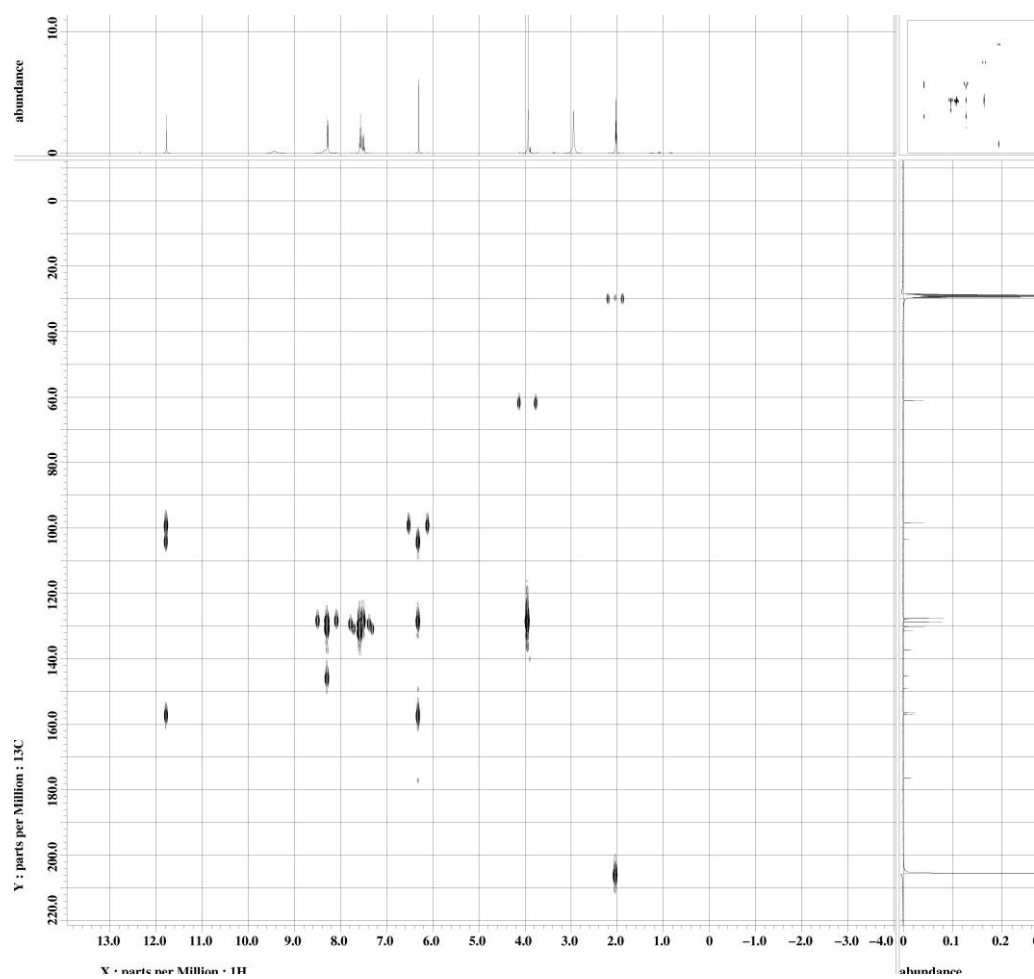
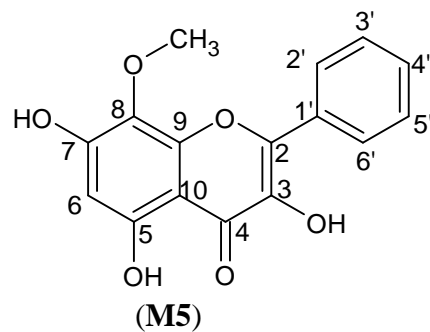
Appendix D28: DEPT Spectrum of 3,5,7-trihydroxy-8-methoxyflavone (M5)



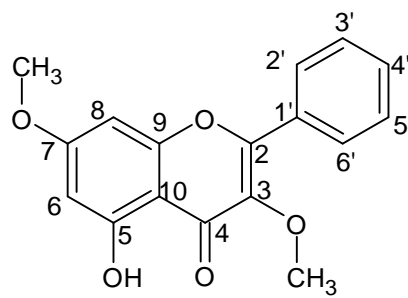
(M5)



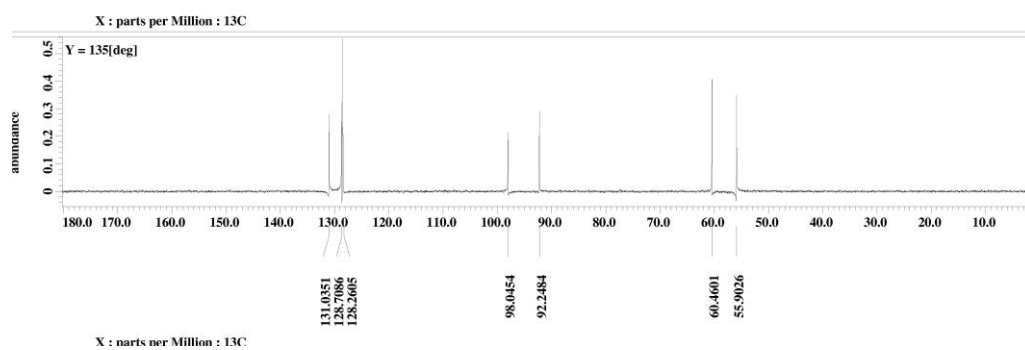
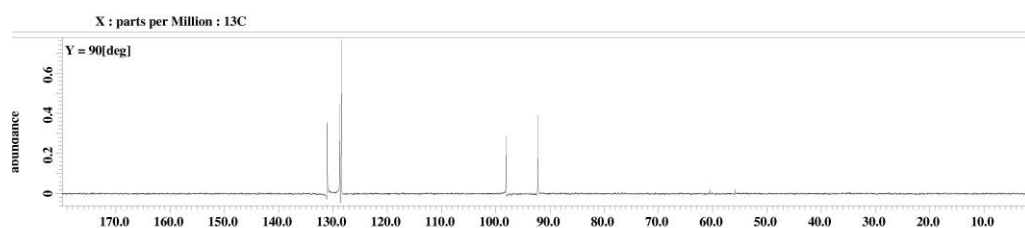
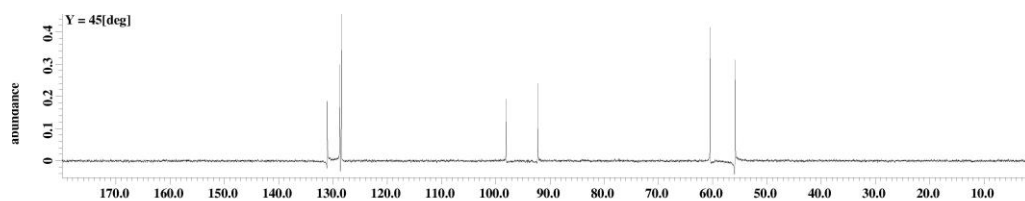
Appendix D29: HMQC Spectrum of 3,5,7-trihydroxy-8-methoxyflavone (M5)



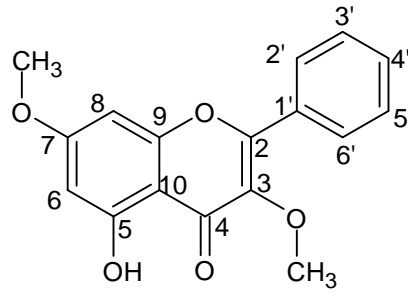
Appendix D30: HMBC Spectrum of 3,5,7-trihydroxy-8-methoxyflavone (M5)



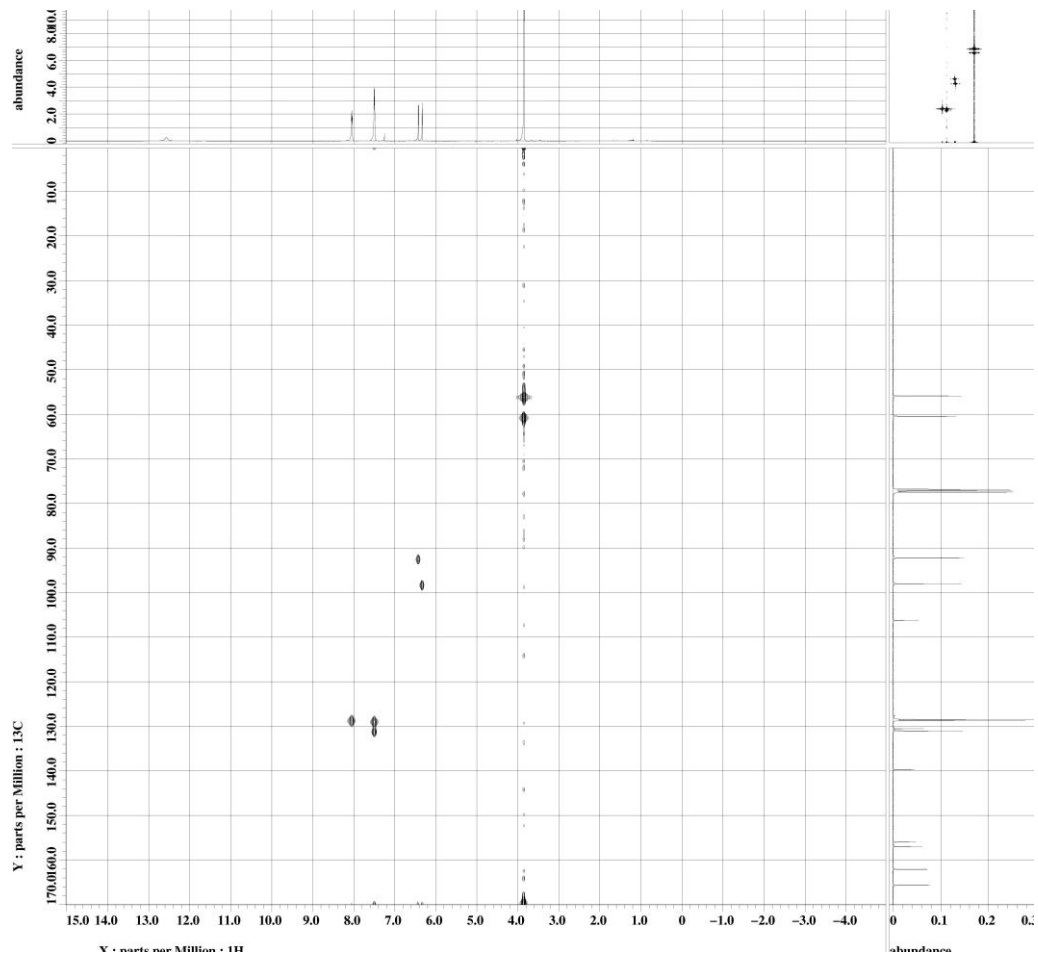
(M7)



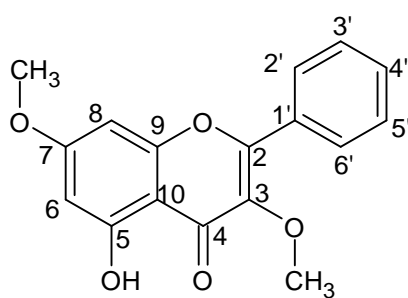
Appendix D31: DEPT Spectrum of 5-hydroxy-3,7-dimethoxyflavone (M7)



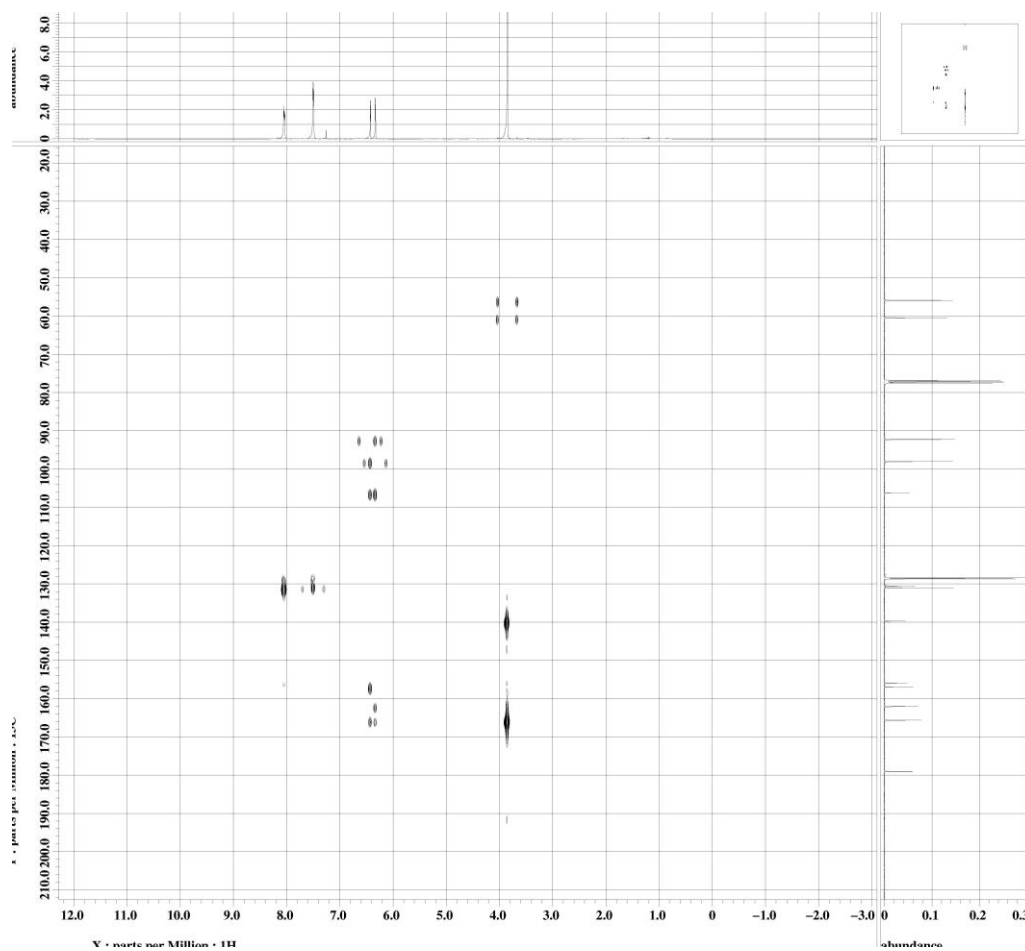
(M7)



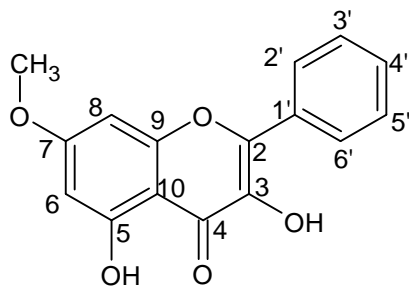
Appendix D32: HMQC Spectrum of 5-hydroxy-3,7-dimethoxyflavone (M7)



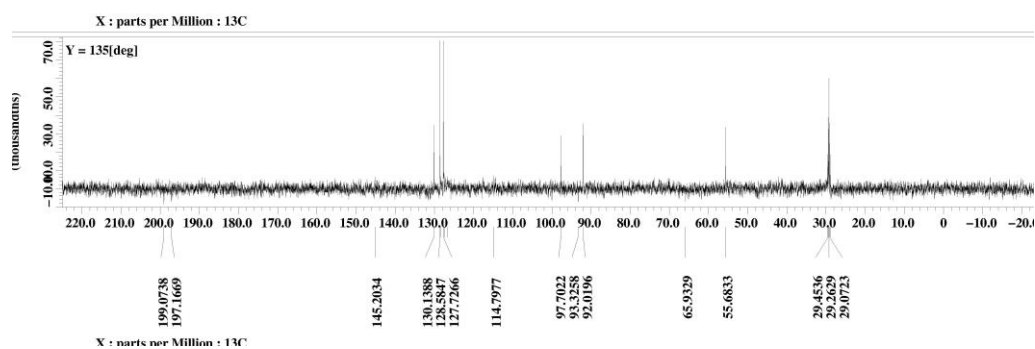
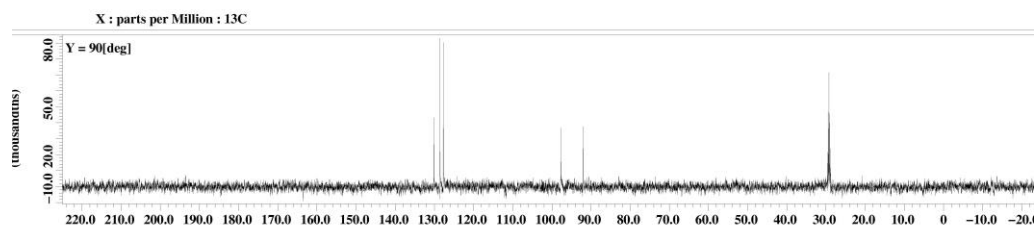
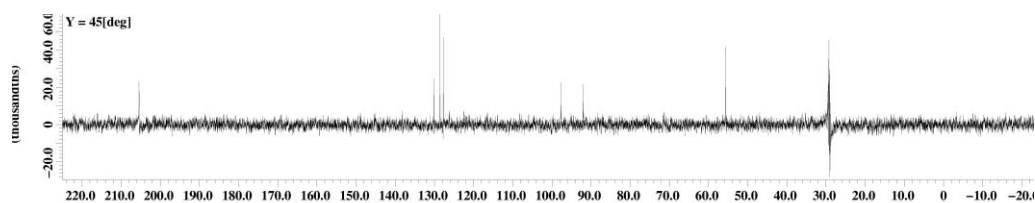
(M7)



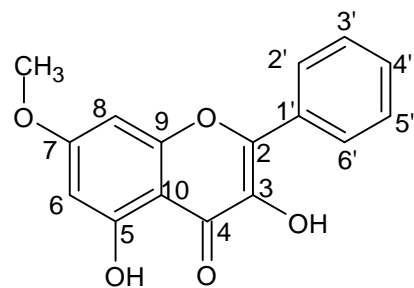
Appendix D33: HMBC Spectrum of 5-hydroxy-3,7-dimethoxyflavone (M7)



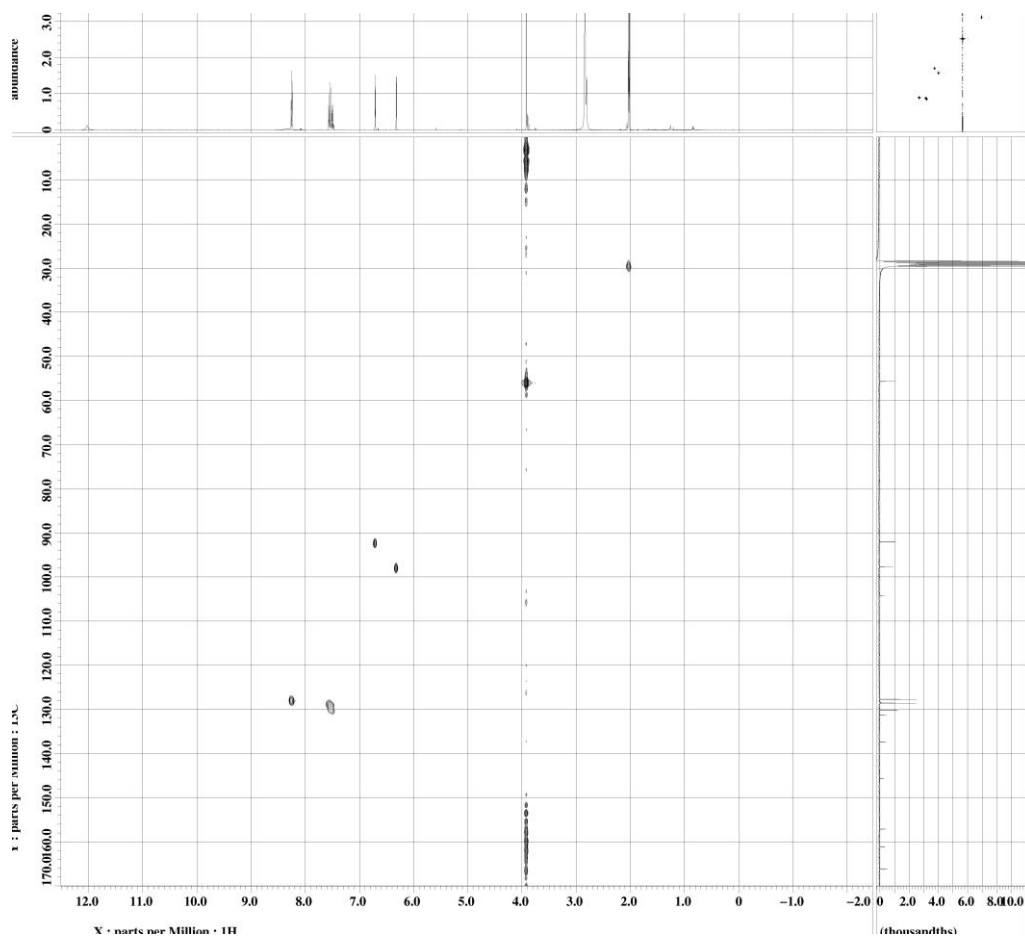
(M8)



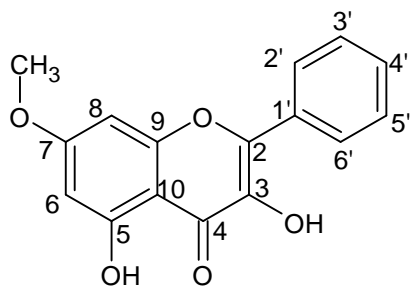
Appendix D34: DEPT Spectrum of 3,5-dihydroxy-7-methoxyflavone (M8)



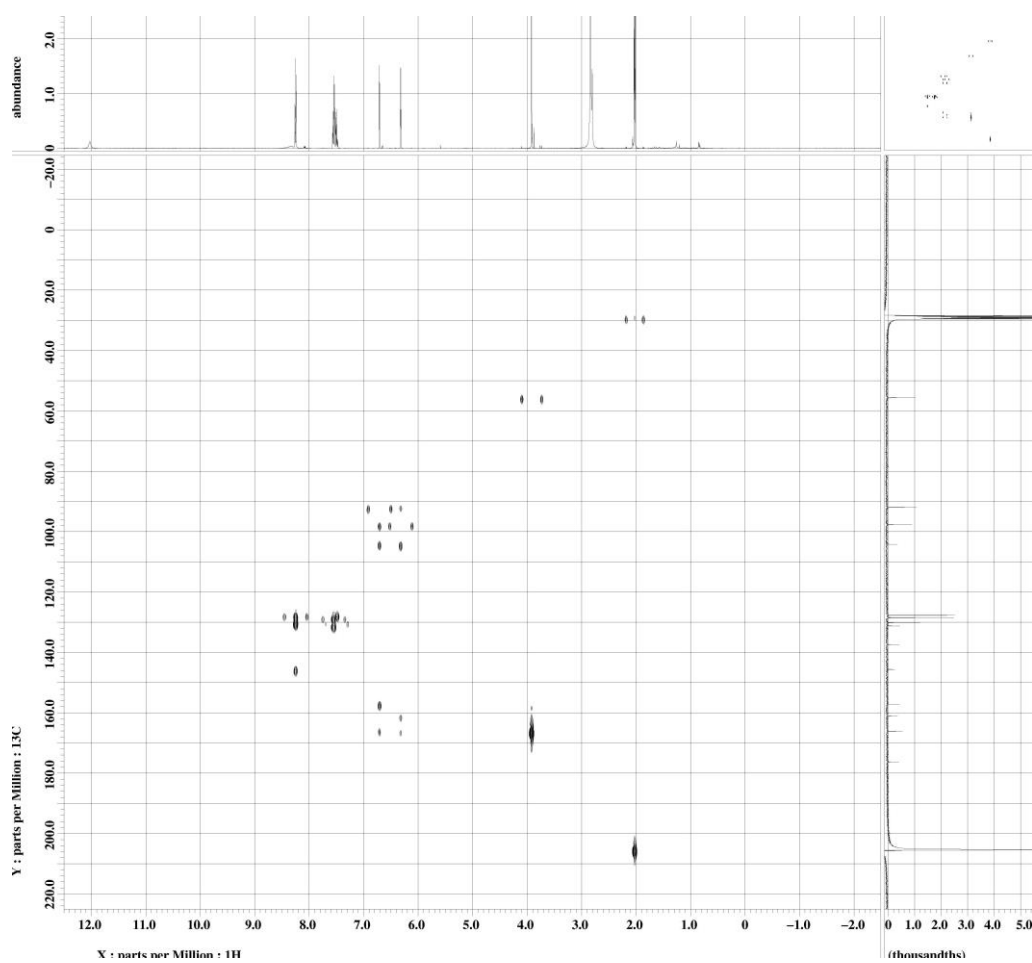
(M8)



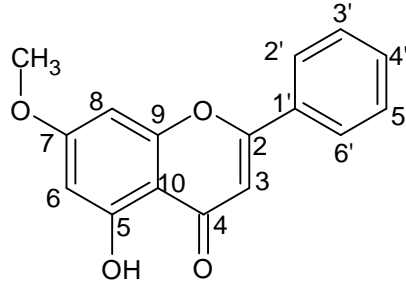
Appendix D35: HMQC Spectrum of 3,5-dihydroxy-7-methoxyflavone (M8)



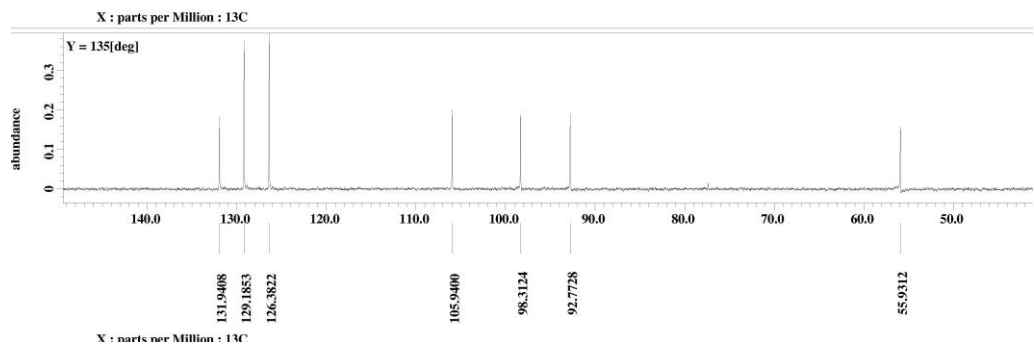
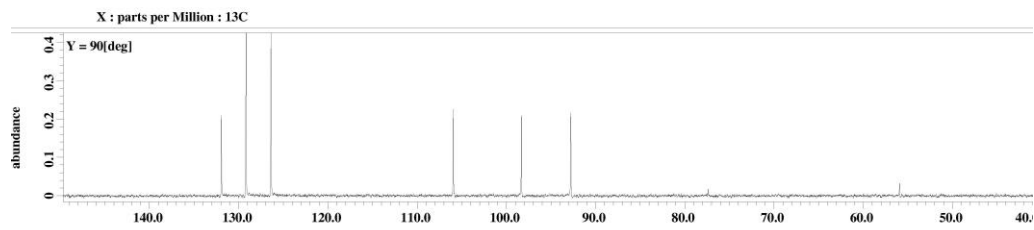
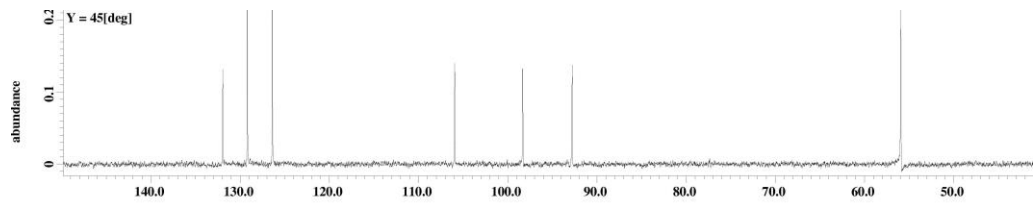
(M8)



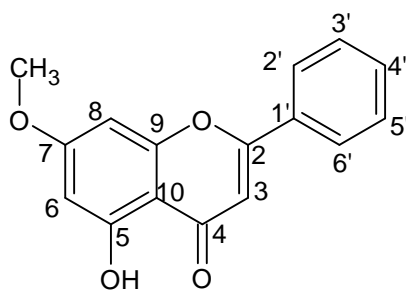
Appendix D36: HMBC Spectrum of 3,5-dihydroxy-7-methoxyflavone (M8)



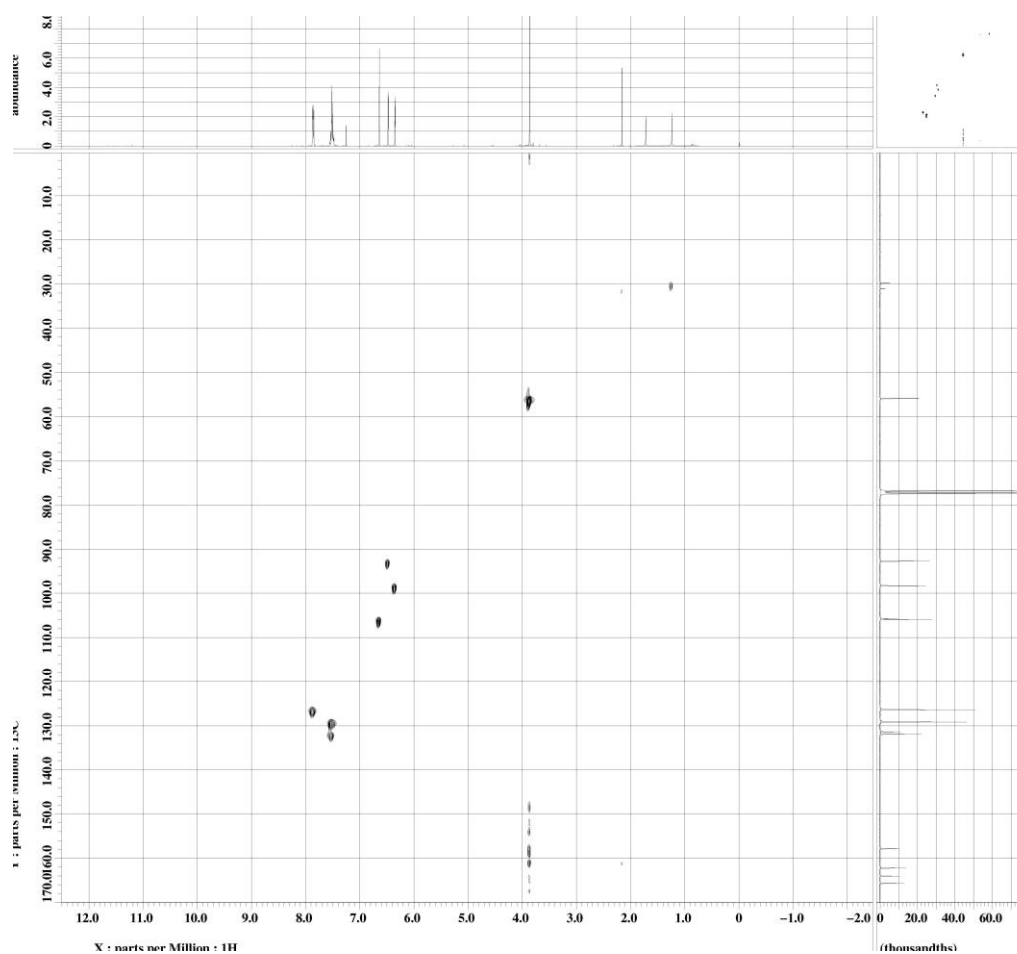
(M9)



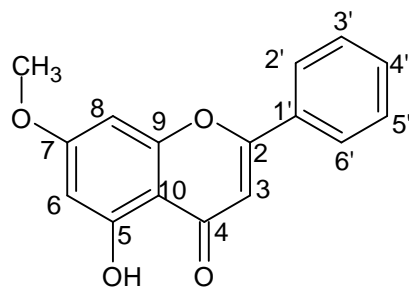
Appendix D37: DEPT Spectrum of 5-hydroxy-7-methoxyflavone (M9)



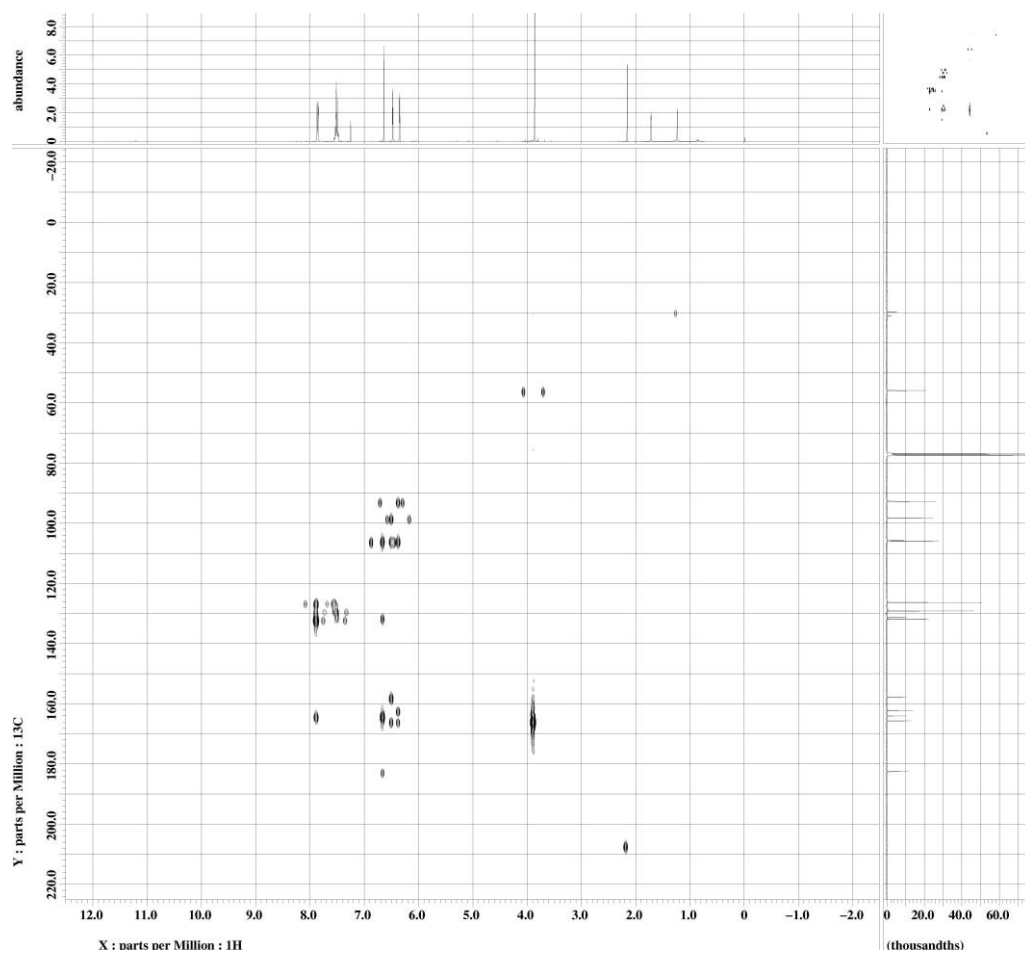
(M9)



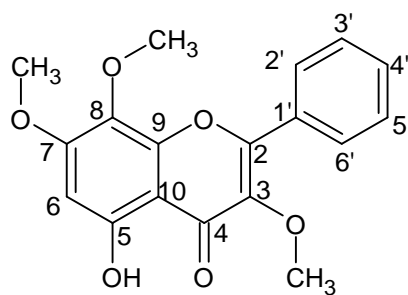
Appendix D38: HMQC Spectrum of 5-hydroxy-7-methoxyflavone (M9)



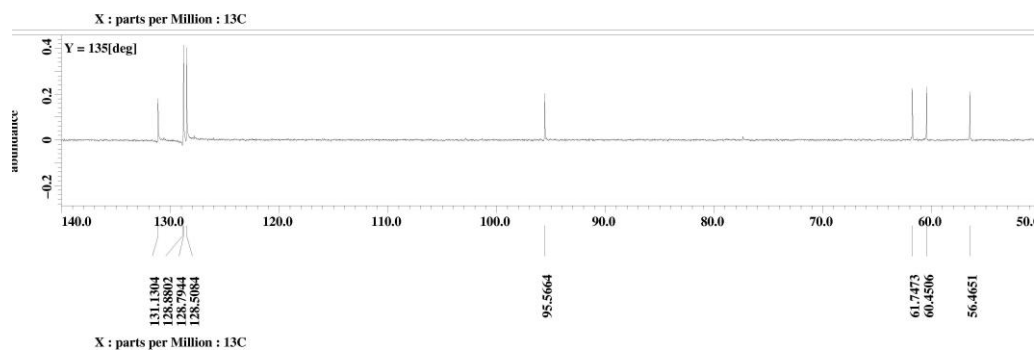
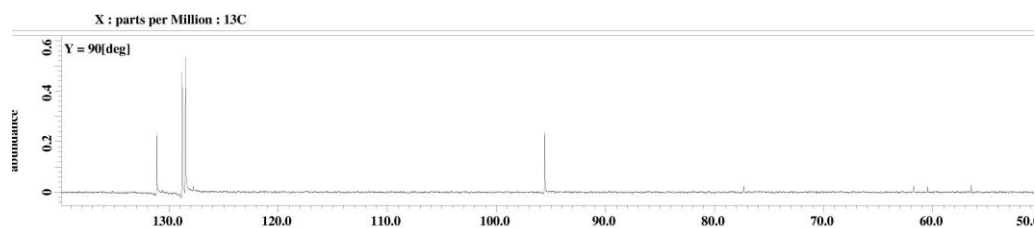
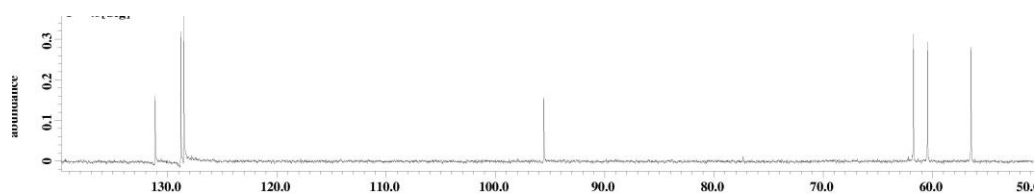
(M9)



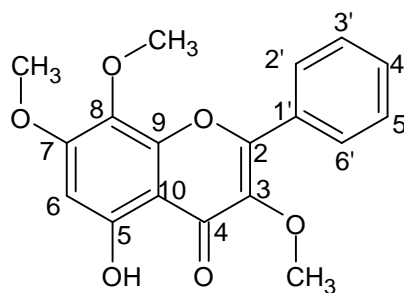
Appendix D39: HMBC Spectrum of 5-hydroxy-7-methoxyflavone (M9)



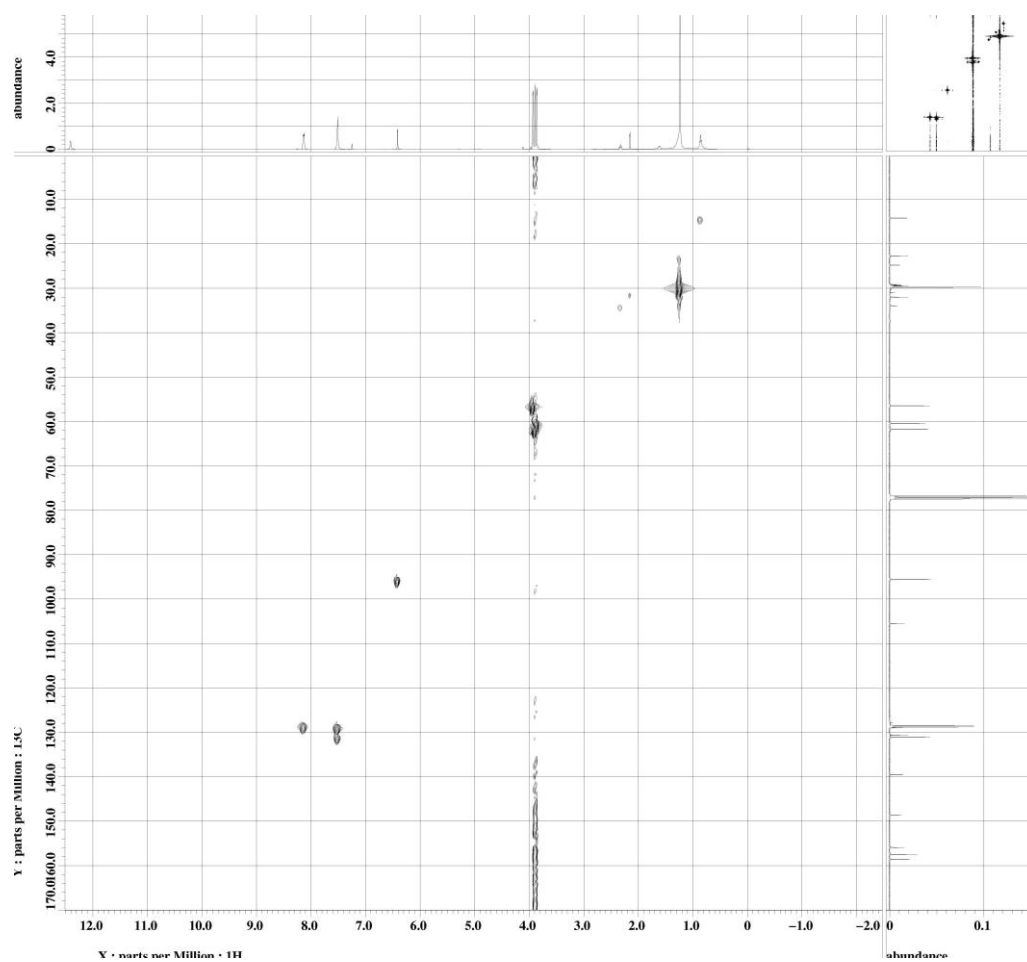
(M10)



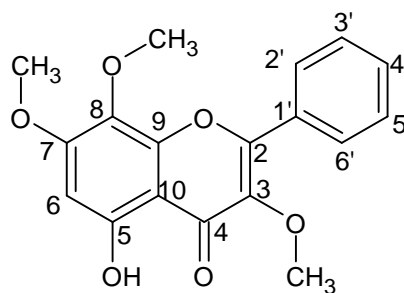
Appendix D40: DEPT Spectrum of 5-hydroxy-3,7,8-trimethoxyflavone (M10)



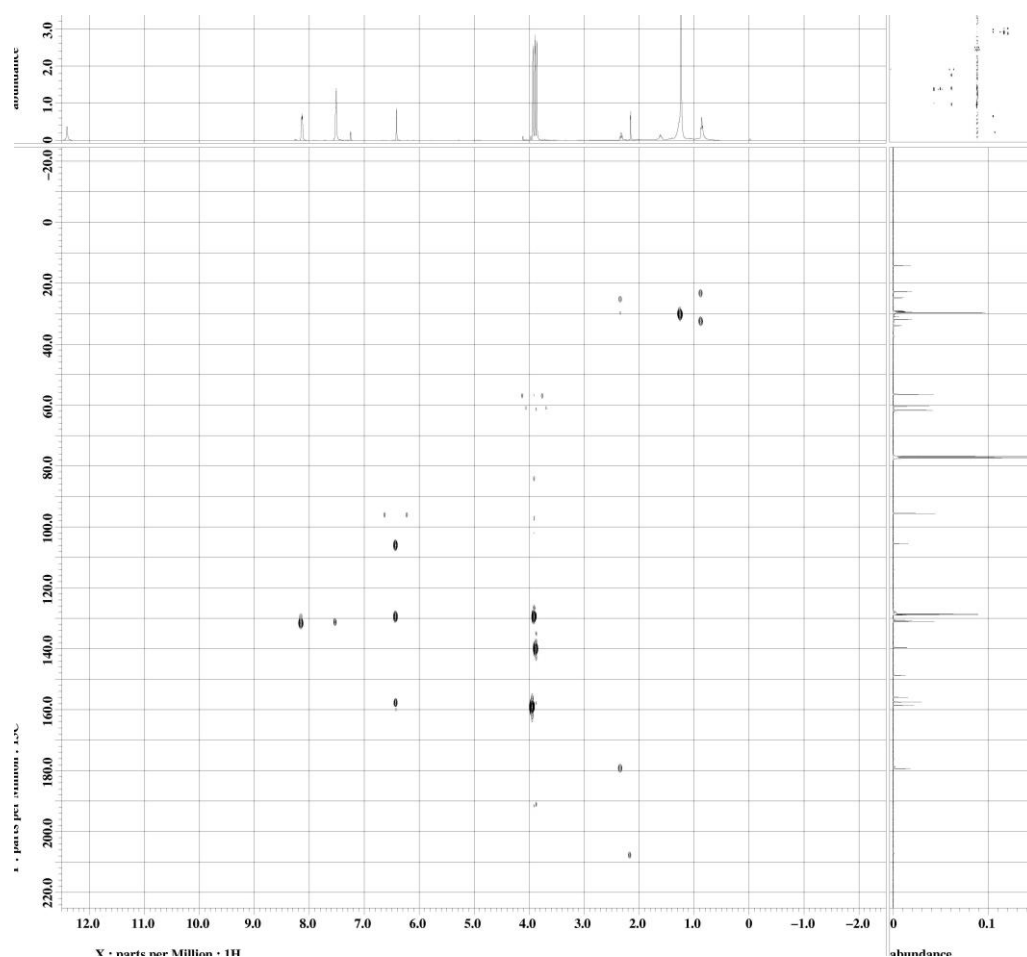
(M10)



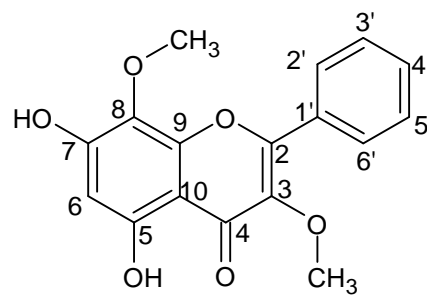
Appendix D41: HMBC Spectrum of 5-hydroxy-3,7,8-trimethoxyflavone (M10)



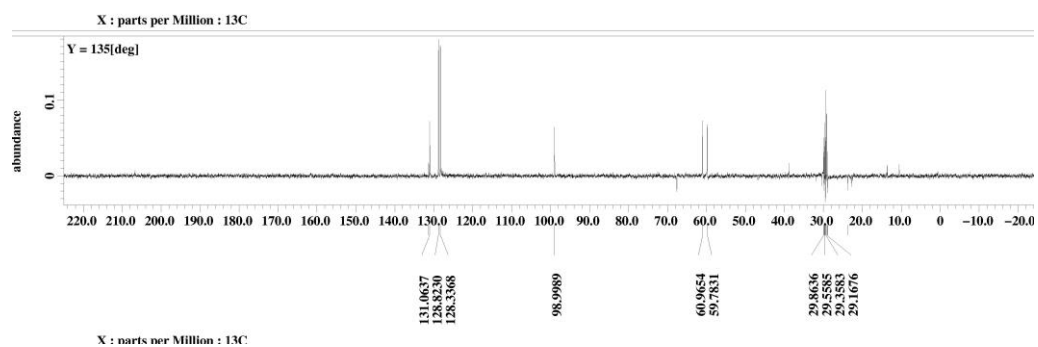
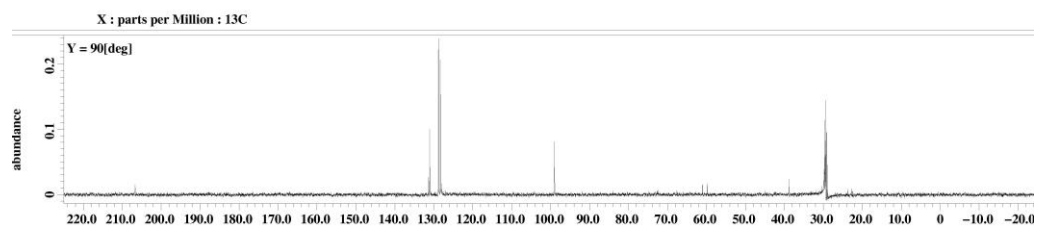
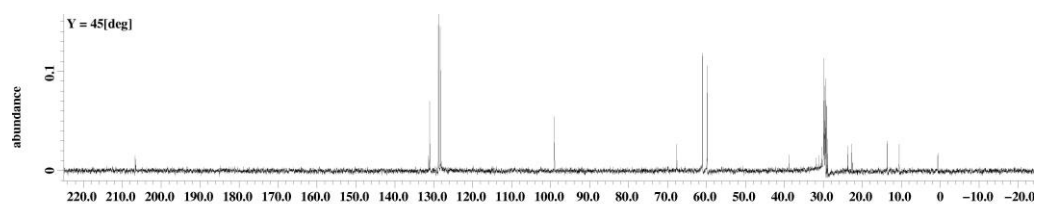
(M10)



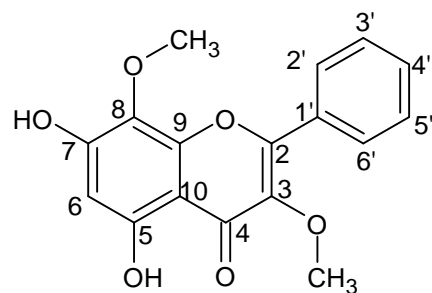
Appendix D42: HMBC Spectrum of 5-hydroxy-3,7,8-trimethoxyflavone (M10)



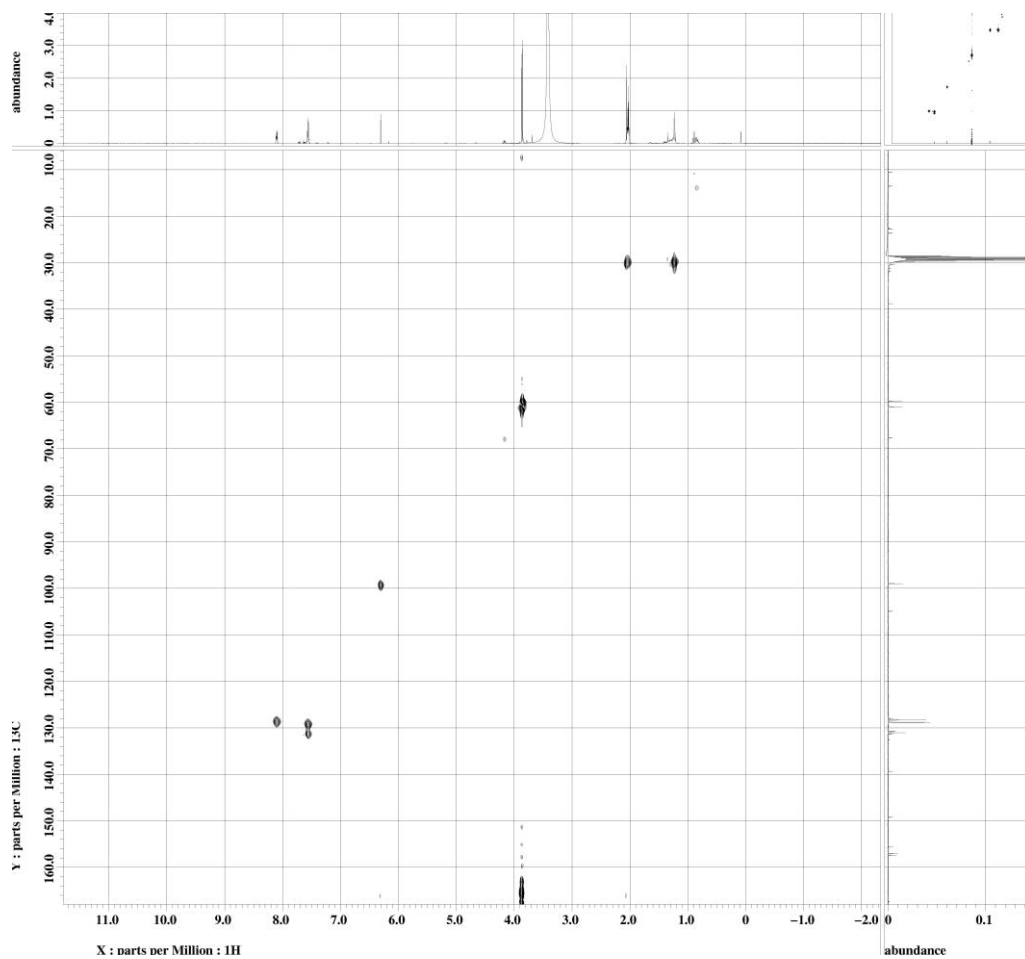
(M11)



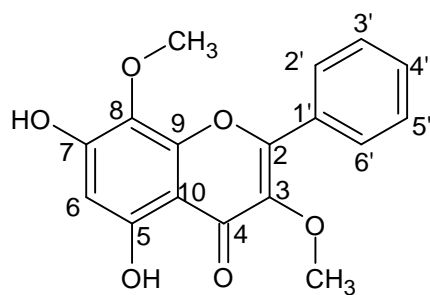
Appendix D43: DEPT Spectrum of 5,7-dihydroxy-3,8-dimethoxyflavone (M11)



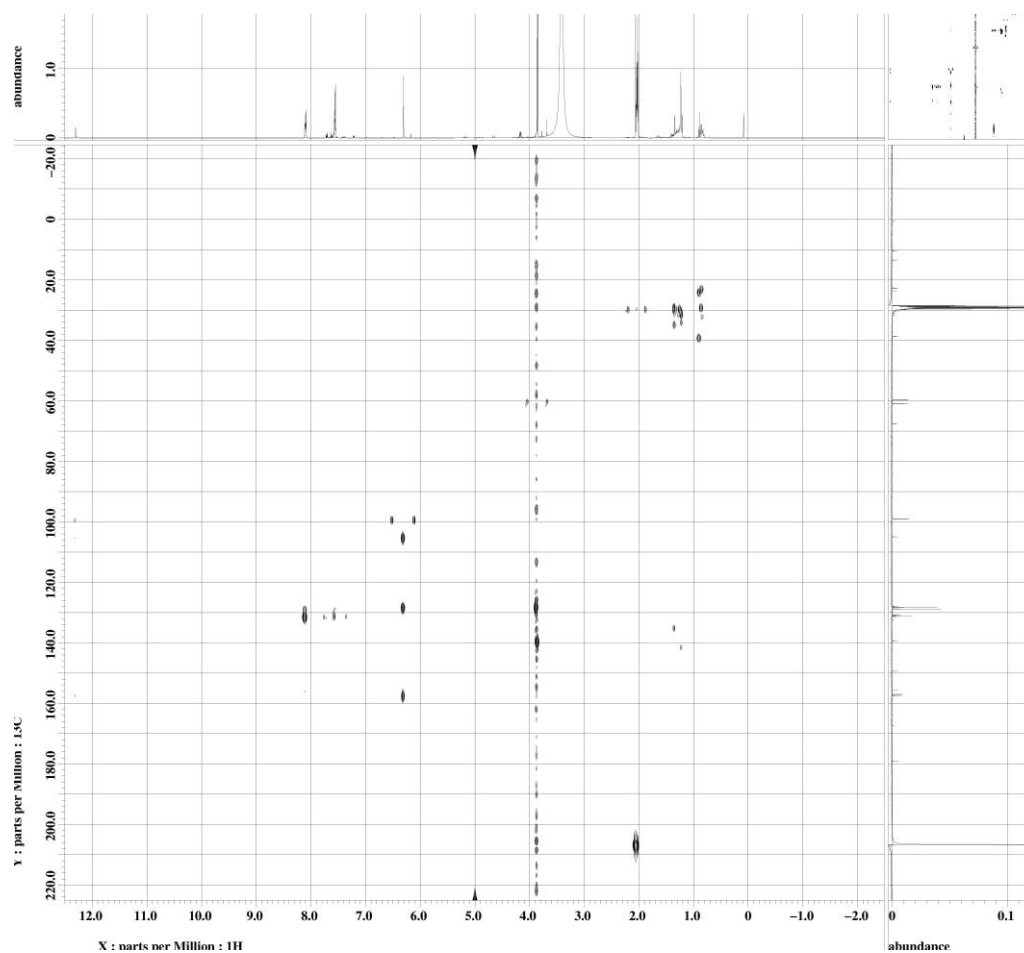
(M11)



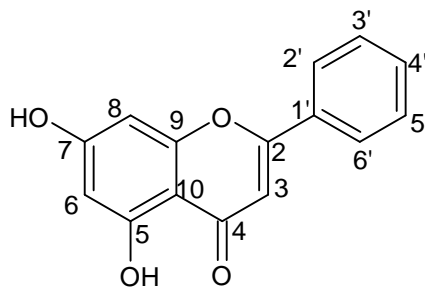
Appendix D44: HMQC Spectrum of 5,7-dihydroxy-3,8-dimethoxyflavone (M11)



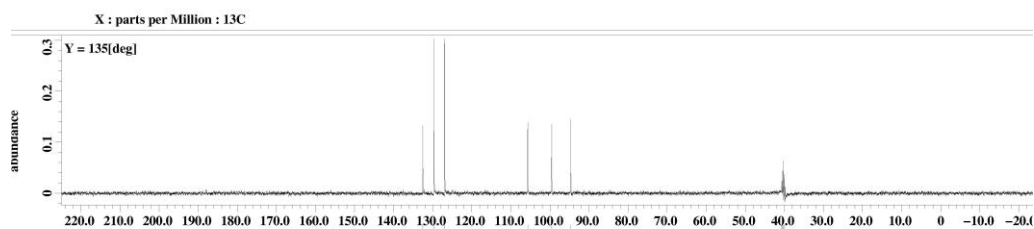
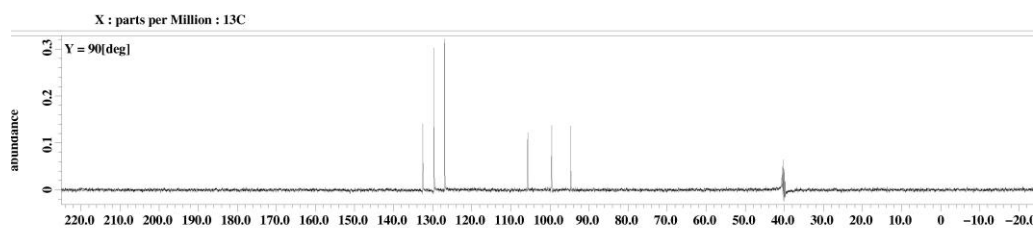
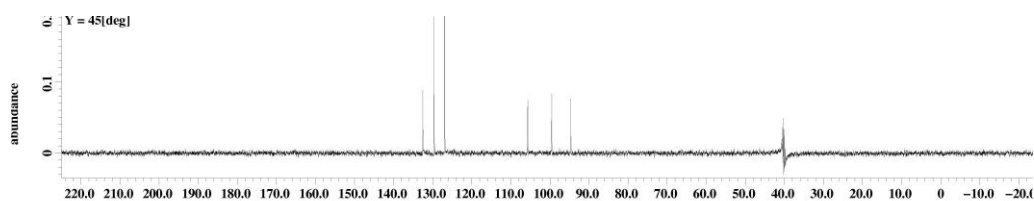
(M11)



Appendix D45: HMBC Spectrum of 5,7-dihydroxy-3,8-dimethoxyflavone (M11)



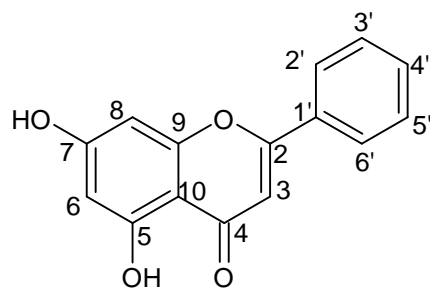
(M14)



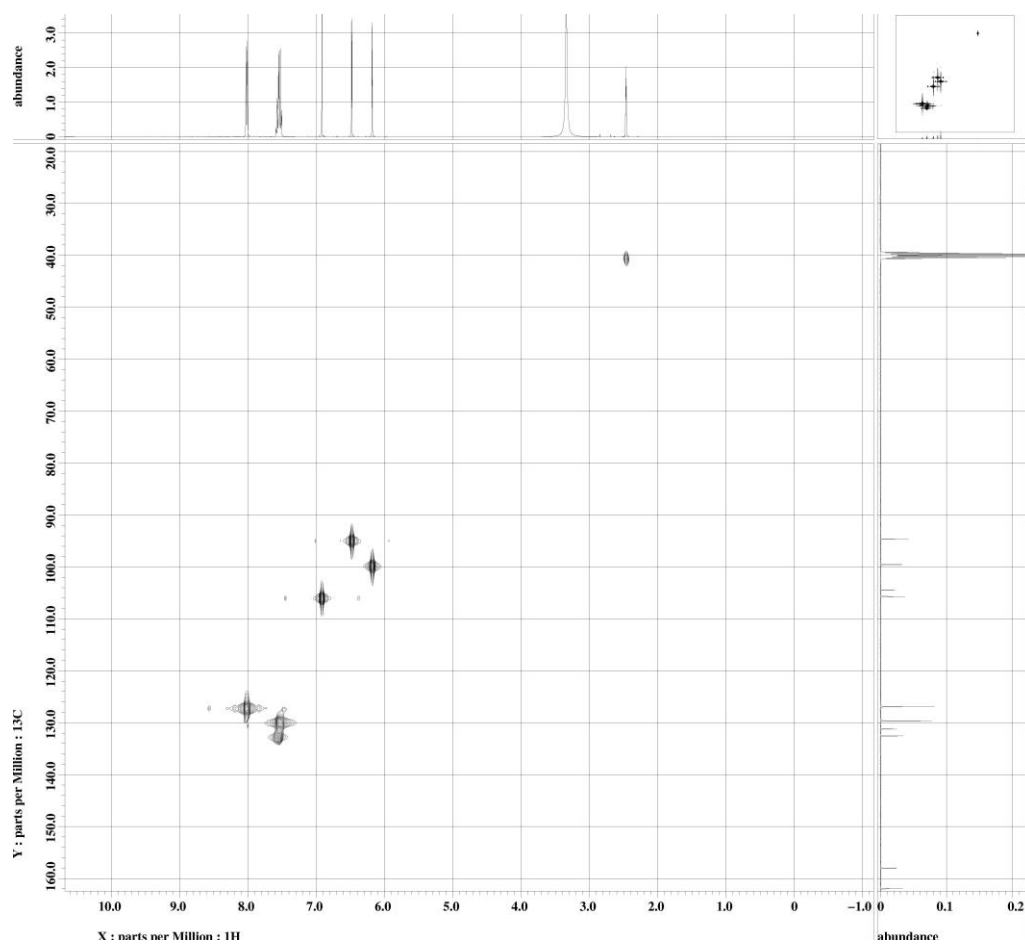
137.5415
129.6621
126.9257
105.6921
99.5519
94.6511
40.4851
40.2754
40.0656

X : parts per Million : 13C

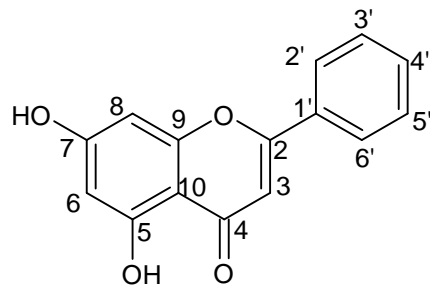
Appendix D46: DEPT Spectrum of 5,7-dihydroxyflavone (M14)



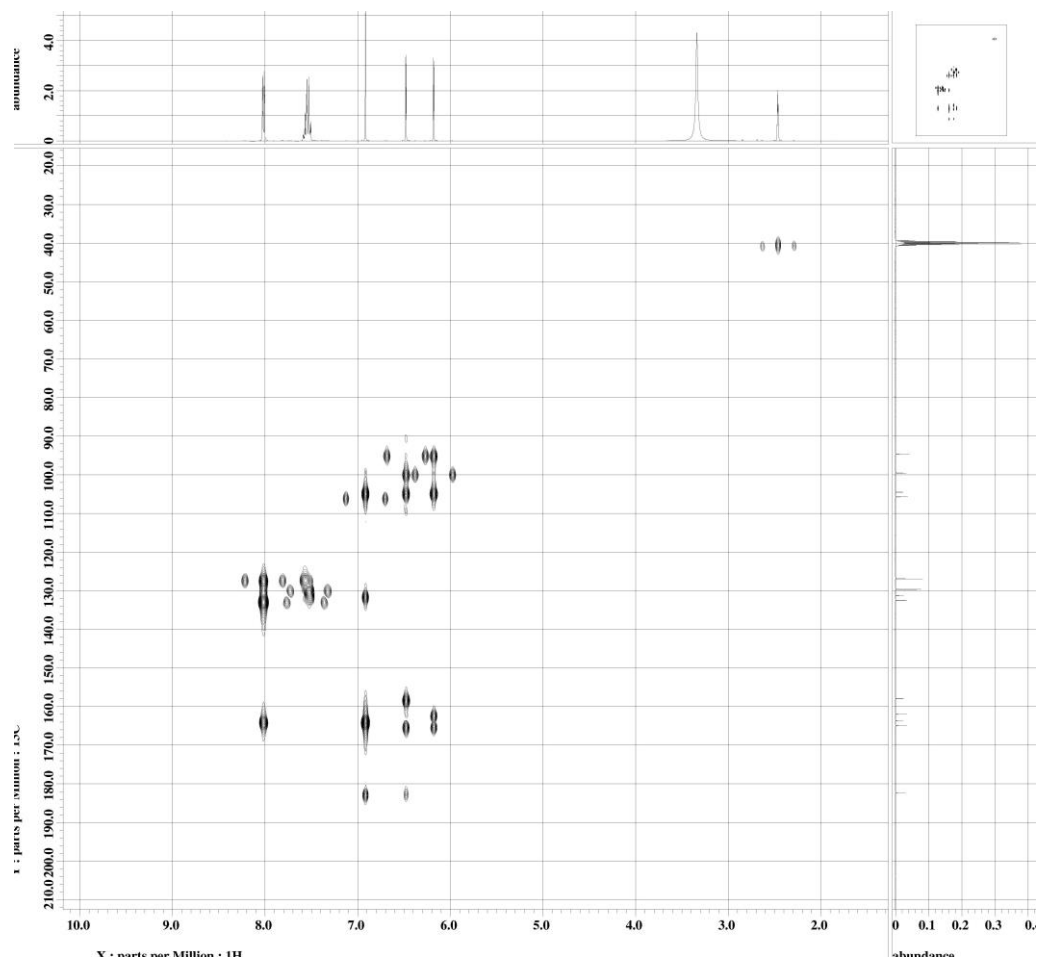
(M14)



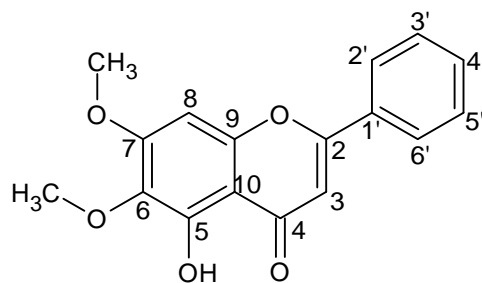
Appendix D47: HMQC Spectrum of 5,7-dihydroxyflavone (M14)



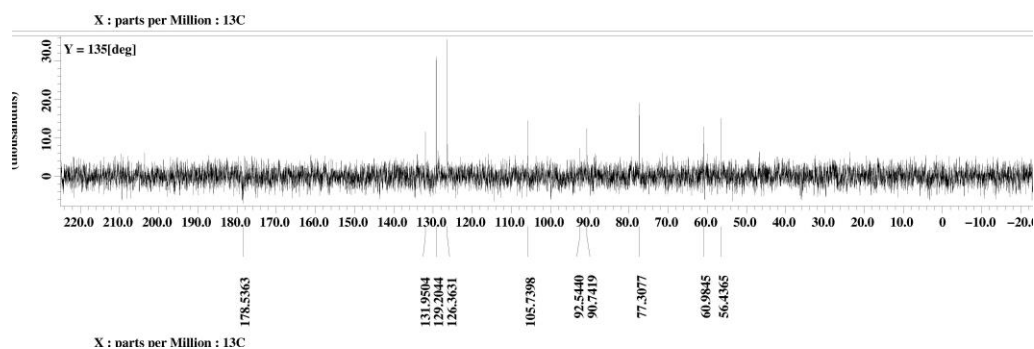
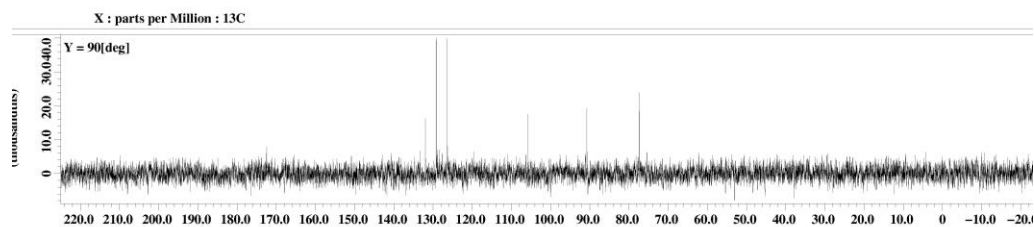
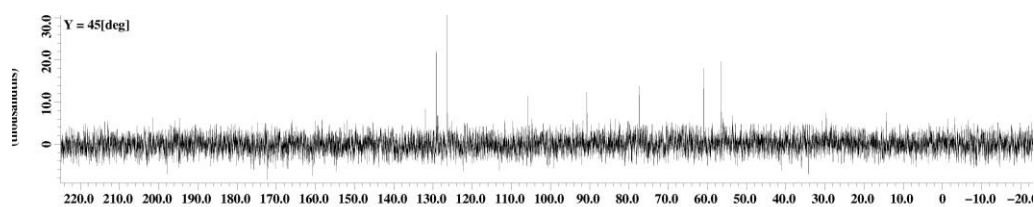
(M14)



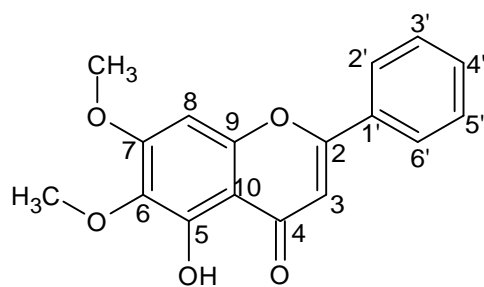
Appendix D48: HMBC Spectrum of 5,7-dihydroxyflavone (M14)



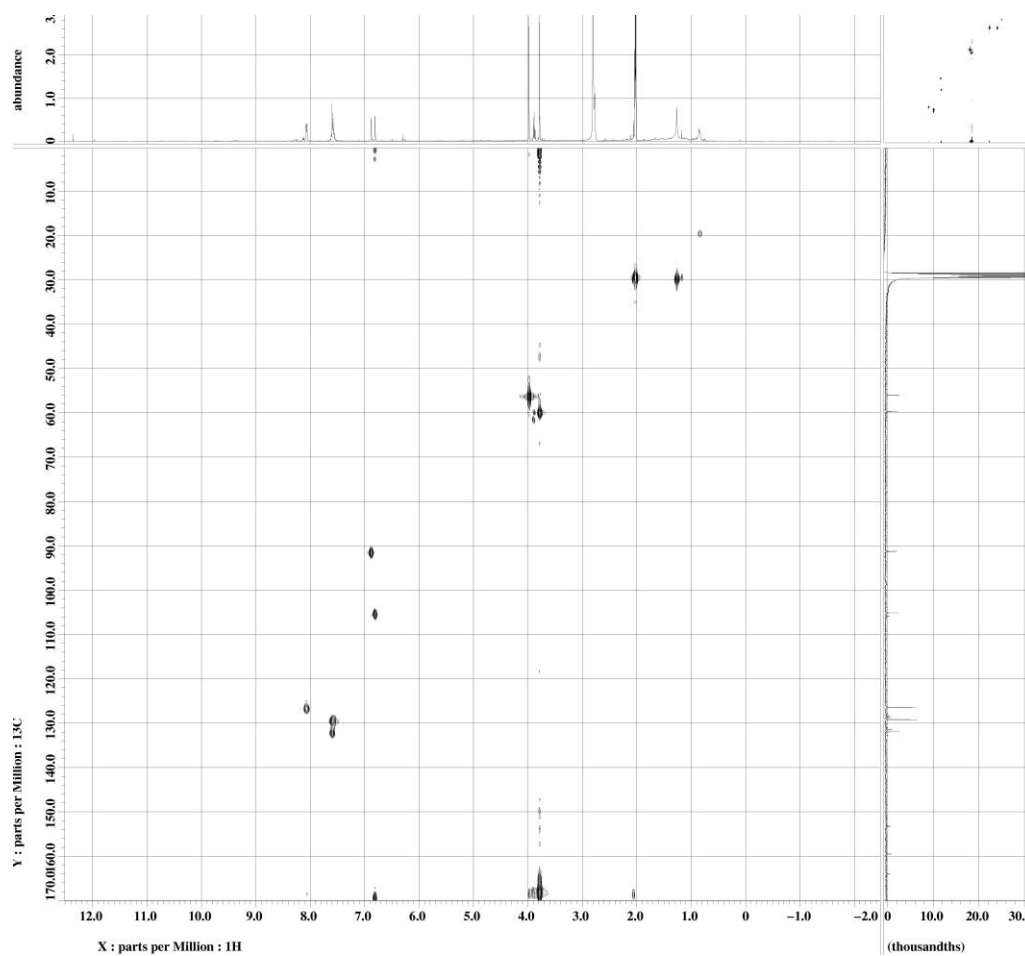
(M15)



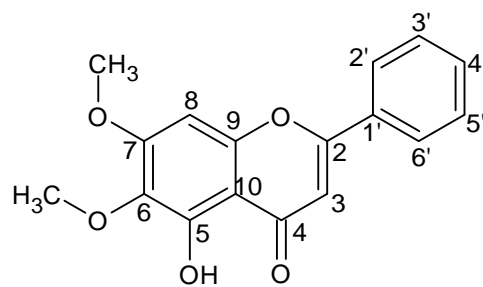
Appendix D49: DEPT Spectrum of 5-hydroxy-6,7-dimethoxyflavone (M15)



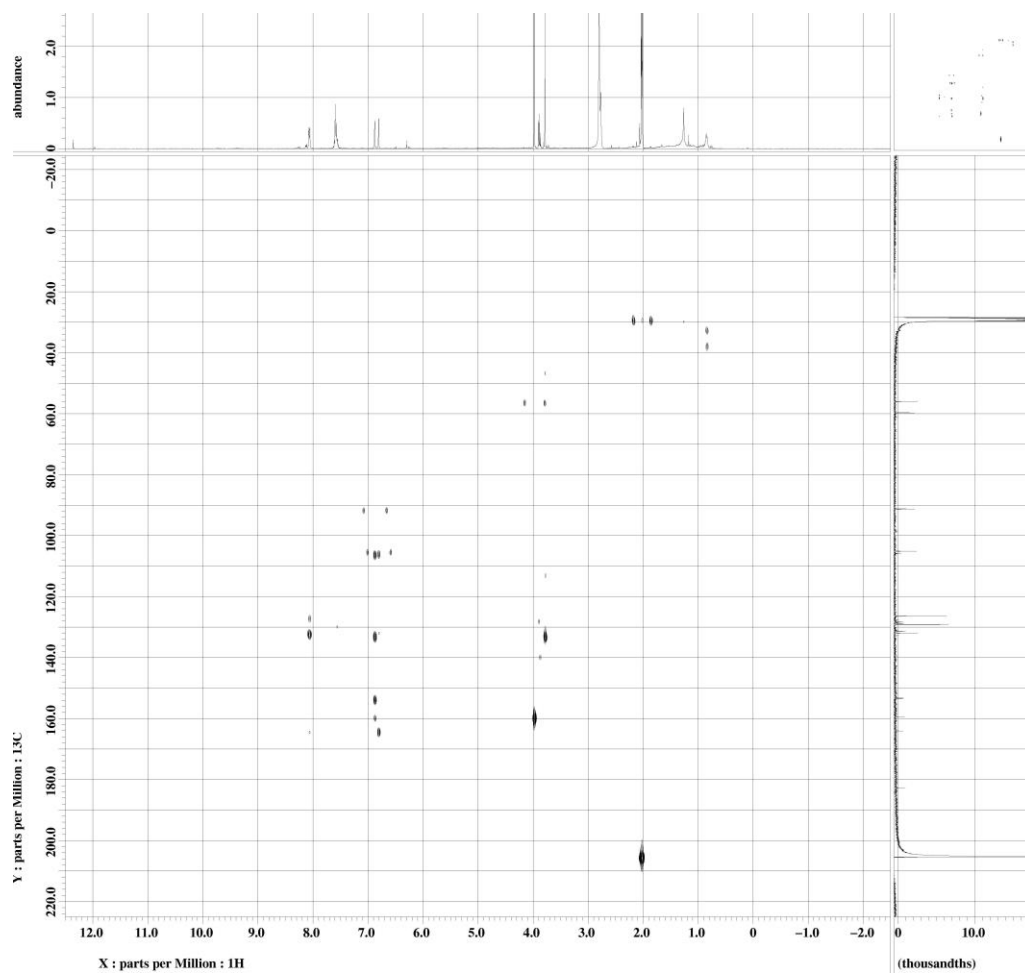
(M15)



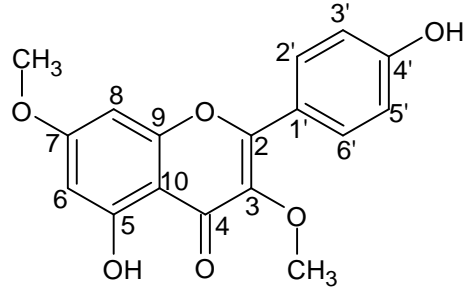
Appendix D50: HMQC Spectrum of 5-hydroxy-6,7-dimethoxyflavone (M15)



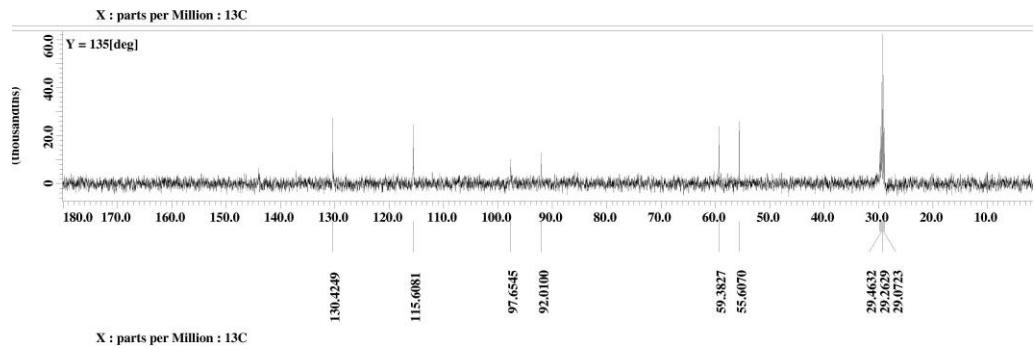
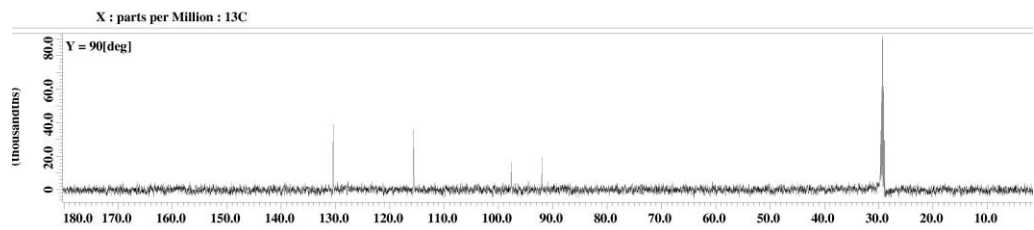
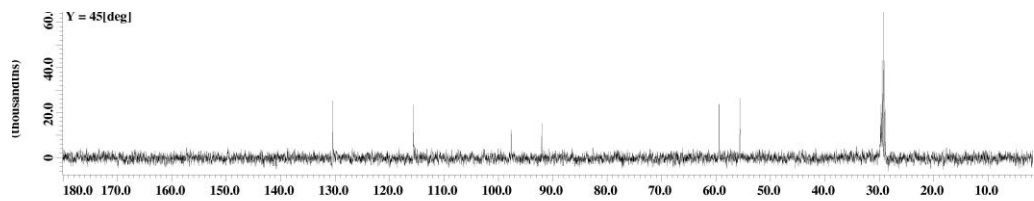
(M15)



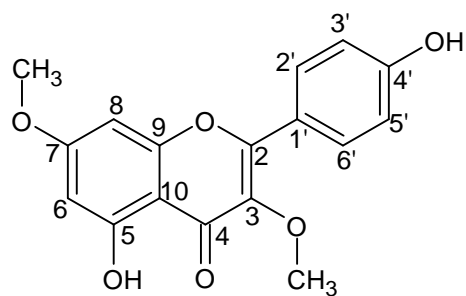
Appendix D51: HMBC Spectrum of 5-hydroxy-6,7-dimethoxyflavone (M15)



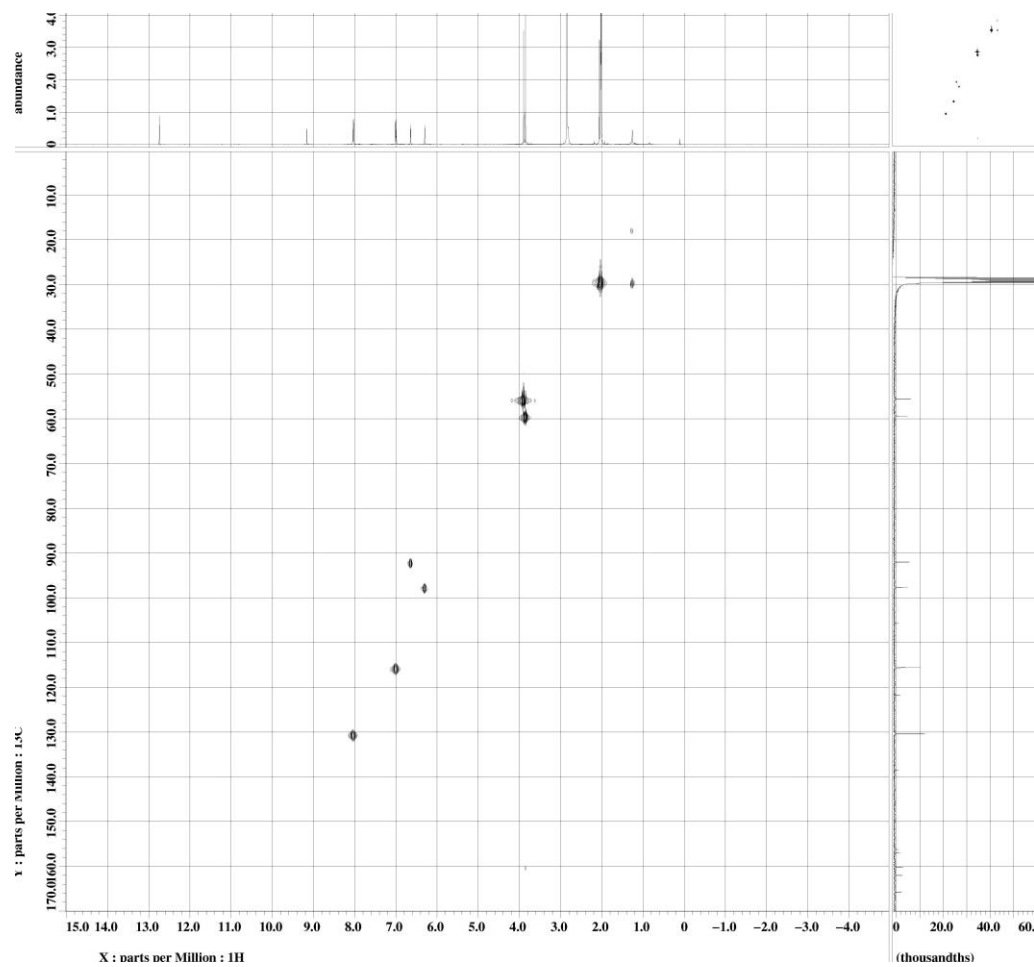
(M16)



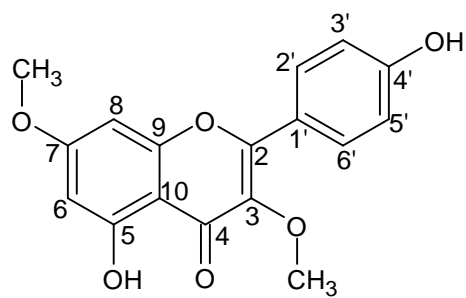
Appendix D52: DEPT Spectrum of 5,4'-dihydroxy-3,7-dimethoxyflavone (M16)



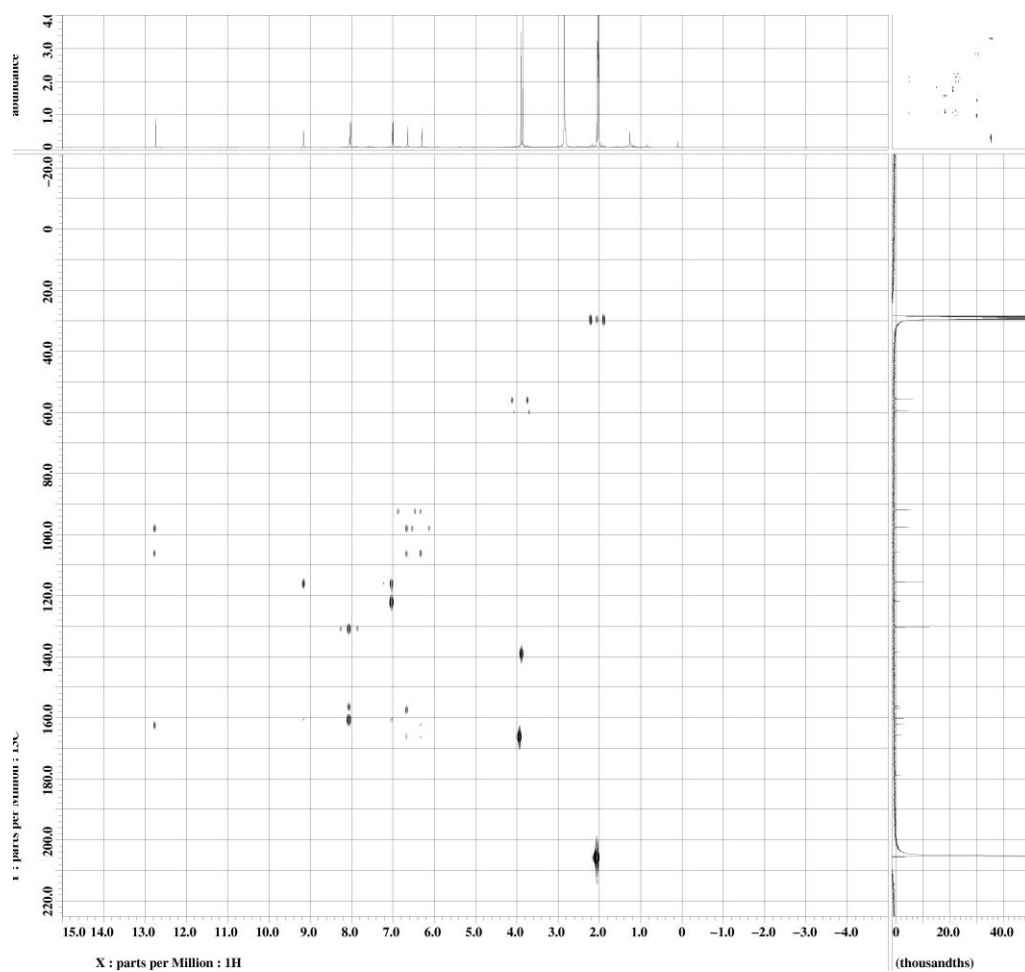
(M16)



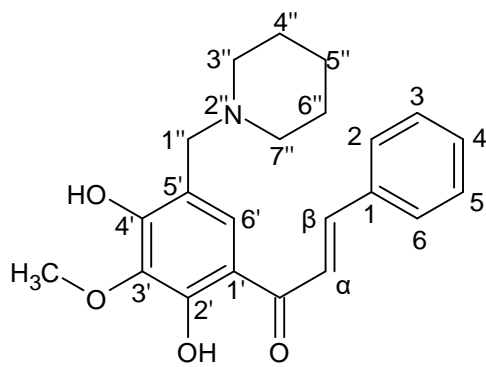
Appendix D53: HMQC Spectrum of 5,4'-dihydroxy-3,7-dimethoxyflavone (M16)



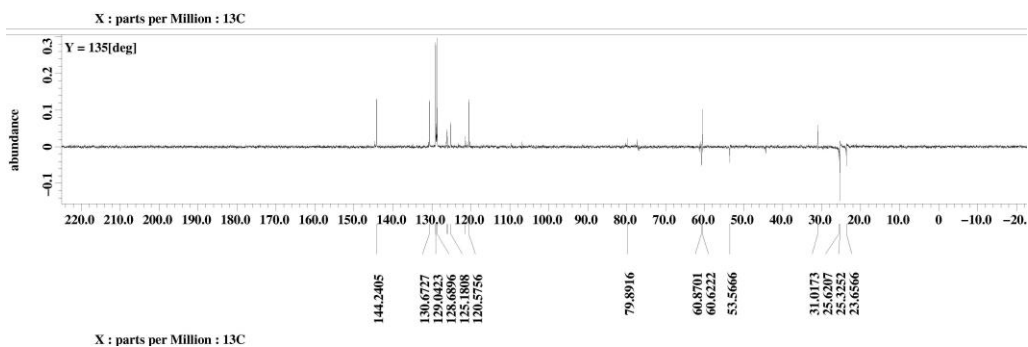
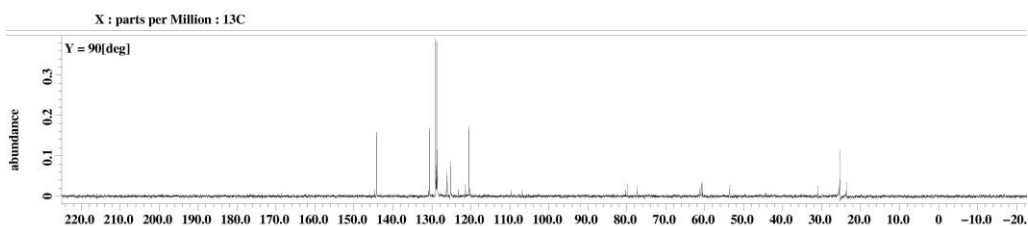
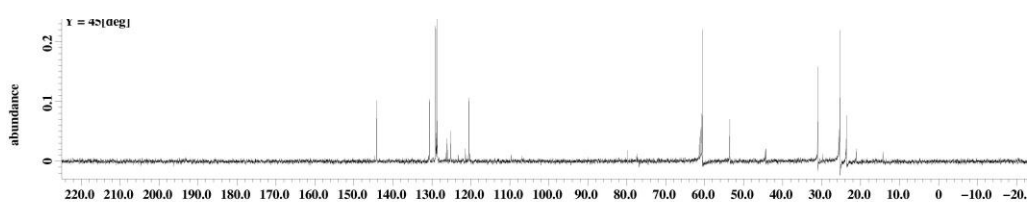
(M16)



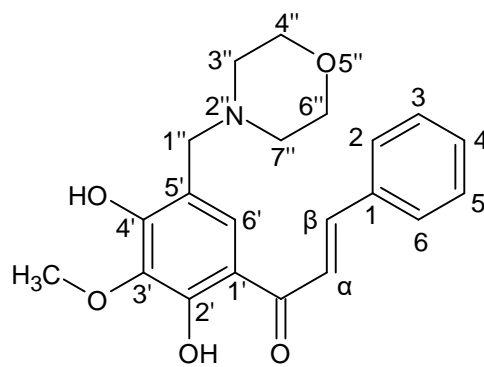
Appendix D54: HMBC Spectrum of 5,4'-dihydroxy-3,7-dimethoxyflavone (M16)



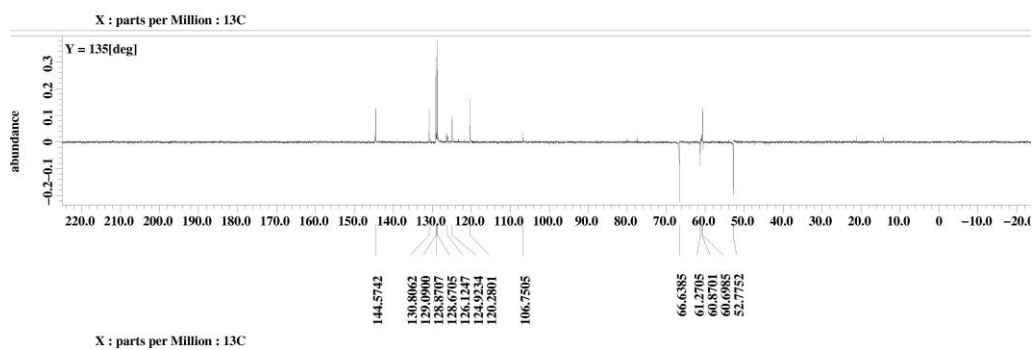
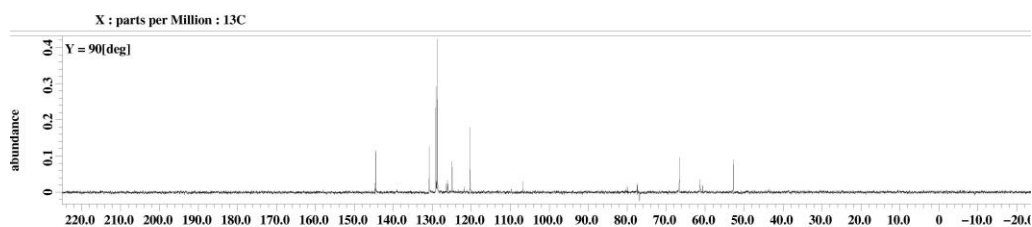
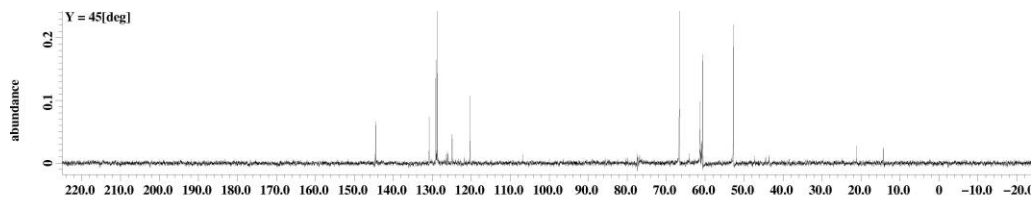
(M2a)



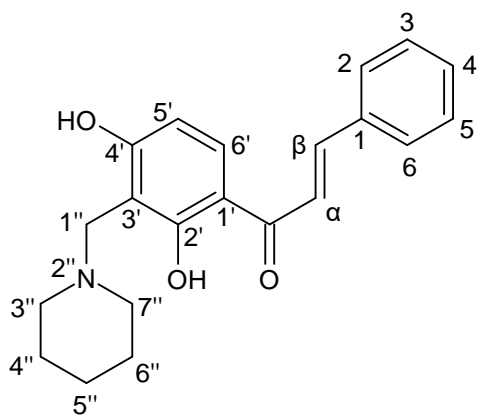
Appendix D55: DEPT Spectrum of 1-[3-methoxy-5-(piperidin-4-yl) methyl-2,4-dihydroxyphenyl]-3-phenyl-2-propen-1-one (M2a)



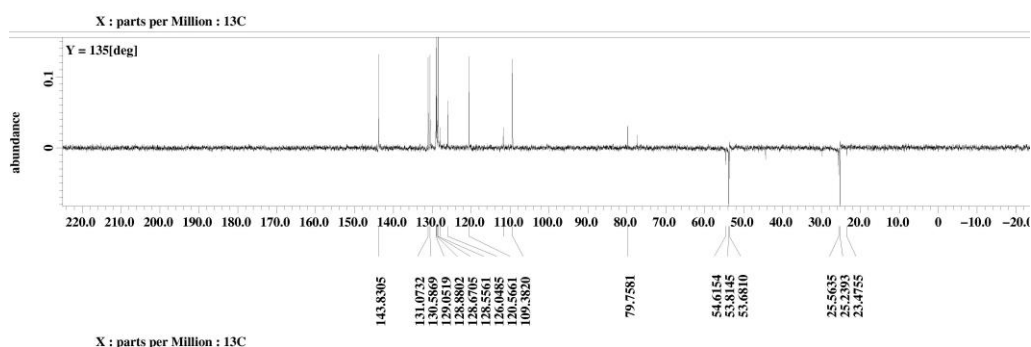
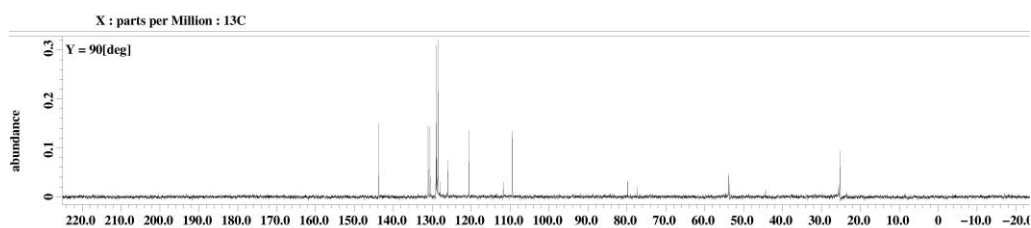
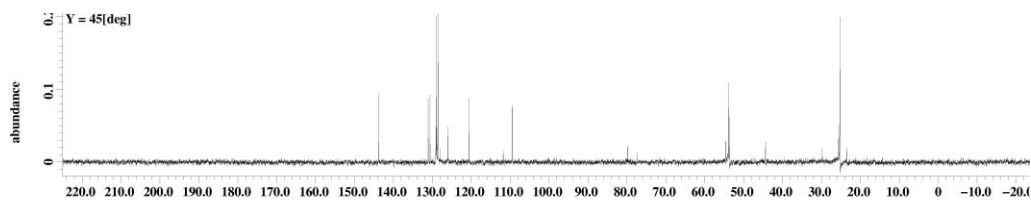
(M2b)



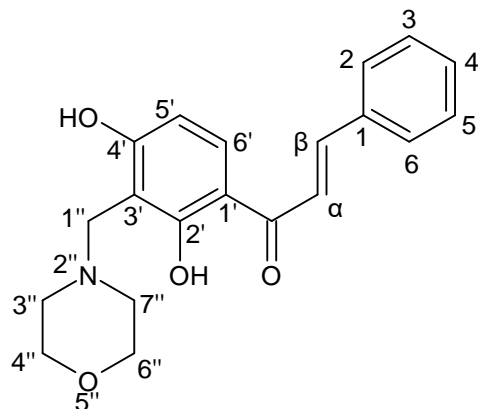
Appendix D56: DEPT Spectrum of 1-[3-methoxy-5-(morpholino-4-yl) methyl-2,4-dihydroxyphenyl]-3-phenyl-2-propen-1-one (M2b)



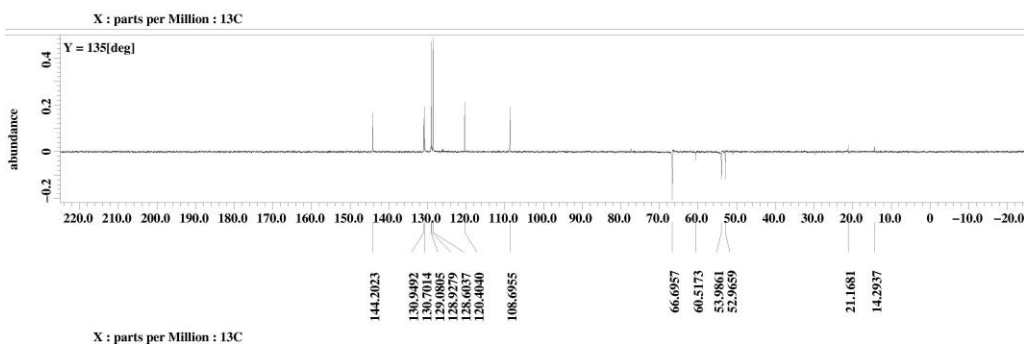
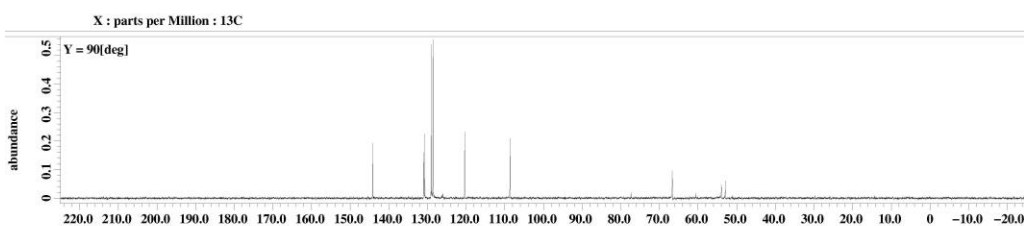
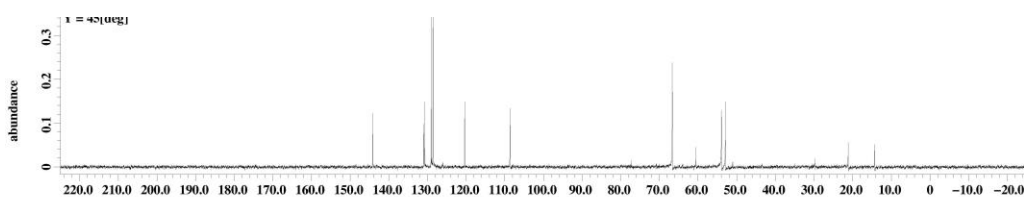
(M4a)



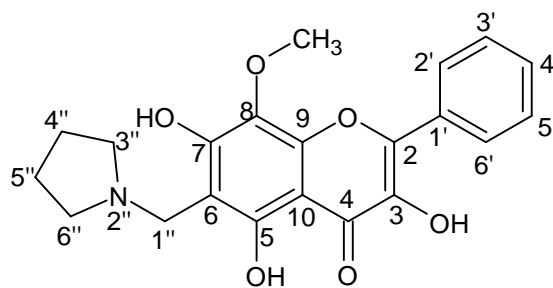
Appendix D57: DEPT Spectrum of 1-[3-(piperidin-1-yl)methyl]-2,4-dihydroxyphenyl]-3-phenyl-2-propen-1-one (M4a)



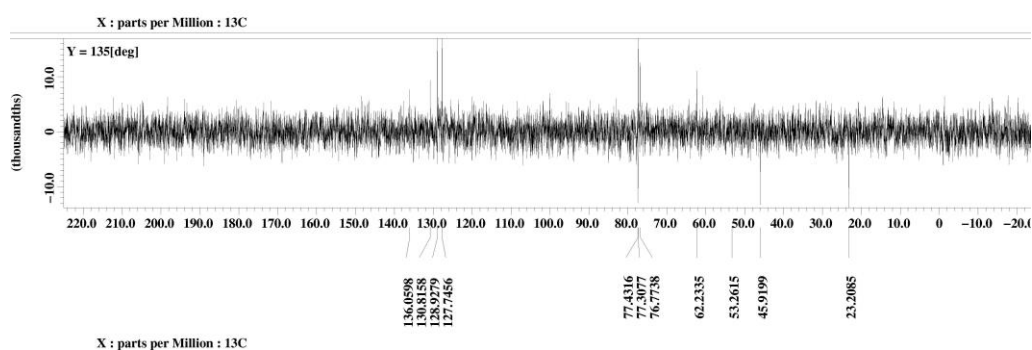
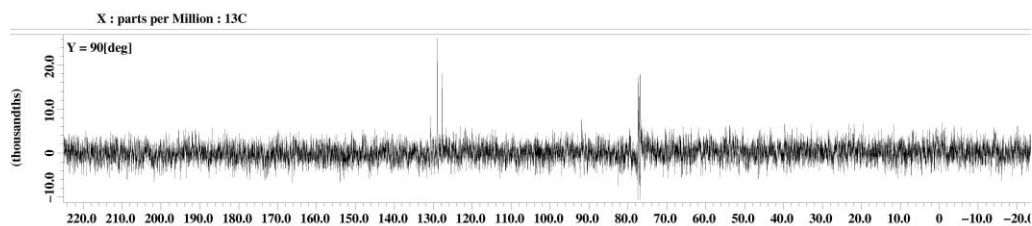
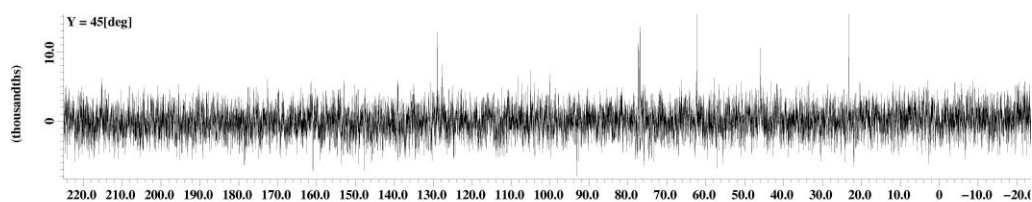
(M4b)



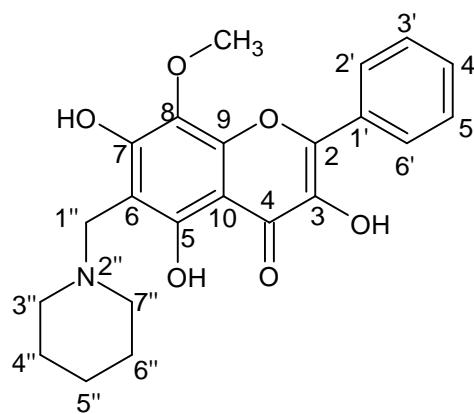
Appendix D58: DEPT Spectrum of 1-[3-(morpholino-4-yl)methyl-2,4-dihydroxyphenyl]-3-phenyl-2-propen-1-one (M4b)



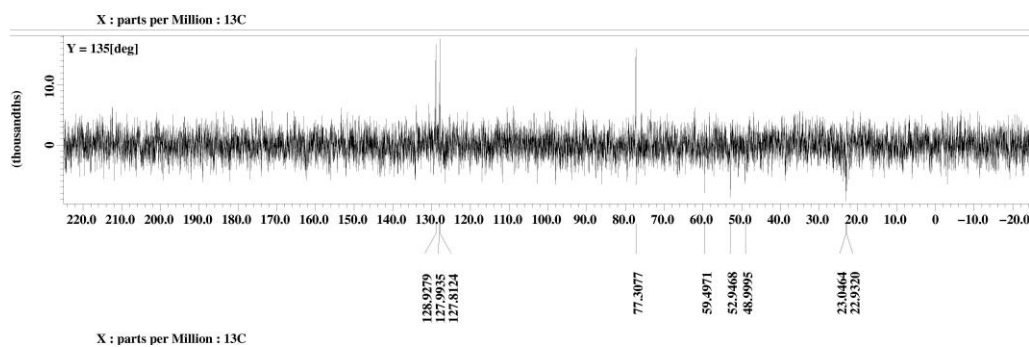
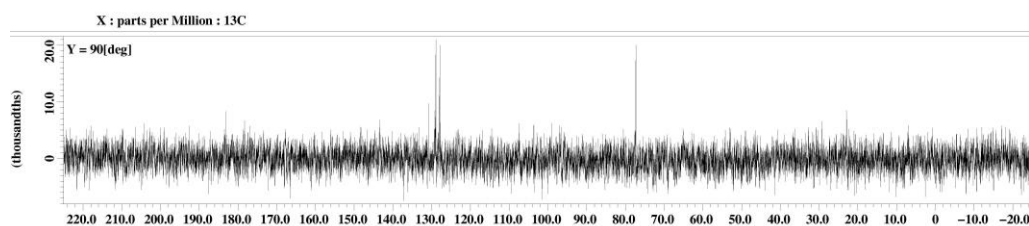
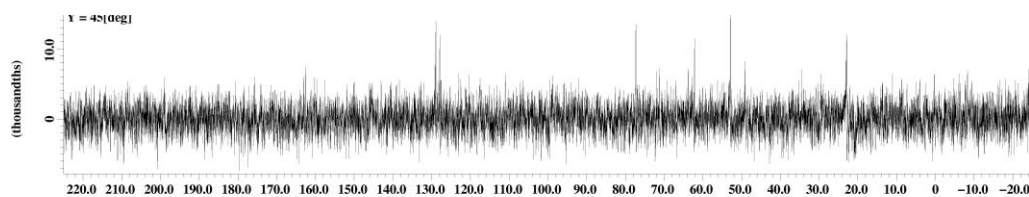
(M5a)



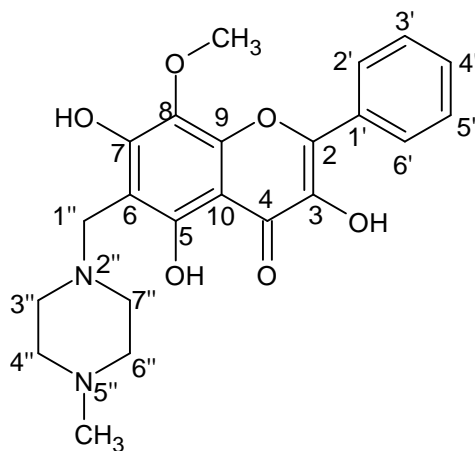
Appendix D59: DEPT Spectrum of 3,5,7-trihydroxy-8-methoxy-6-(pyrrolidin-1-ylmethyl)-2-phenyl-4H-chromen-4-one (M5a)



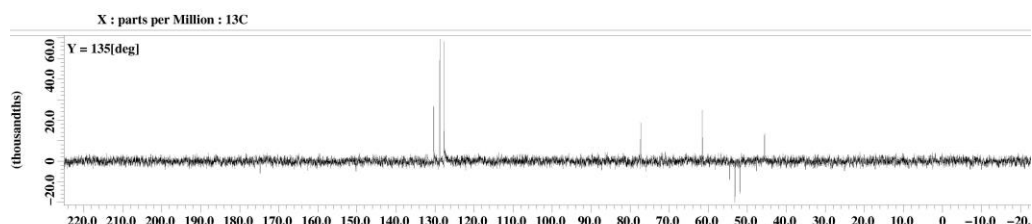
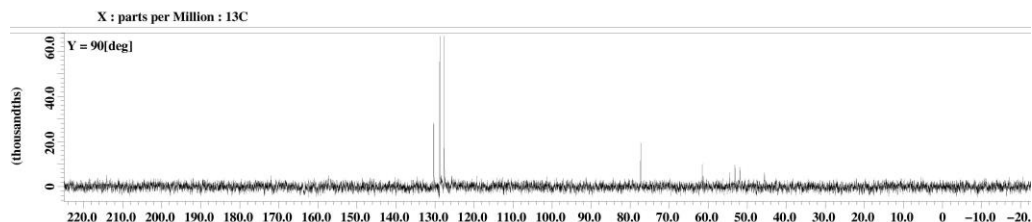
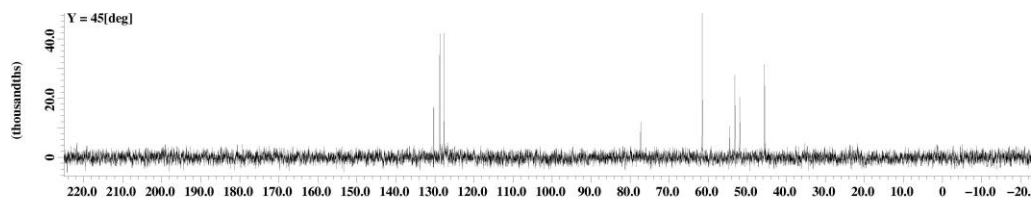
(M5b)



Appendix D60: DEPT Spectrum of 3,5,7-trihydroxy-8-methoxy-6-(piperidin-1-ylmethyl)-2-phenyl-4H-chromen-4-one (M5b)

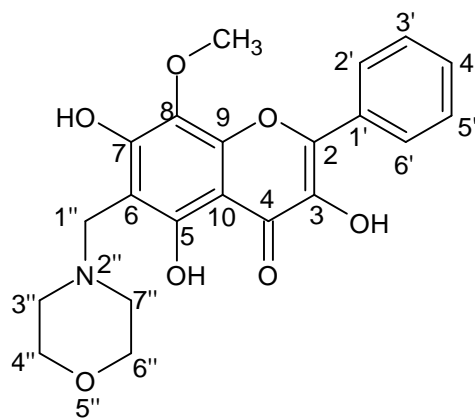


(M5c)

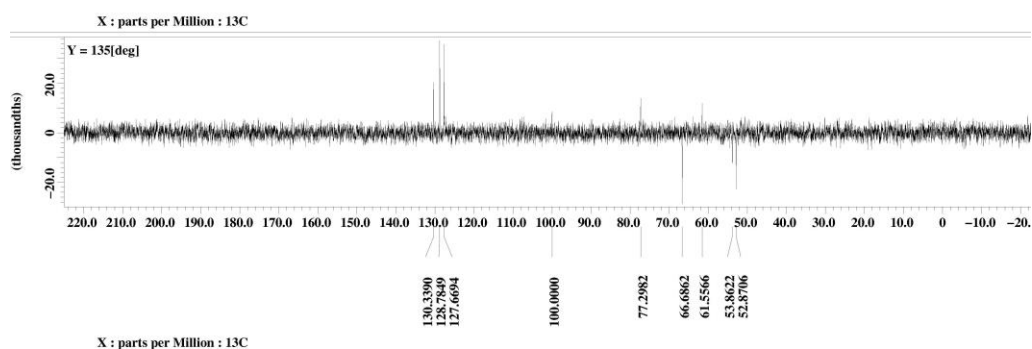
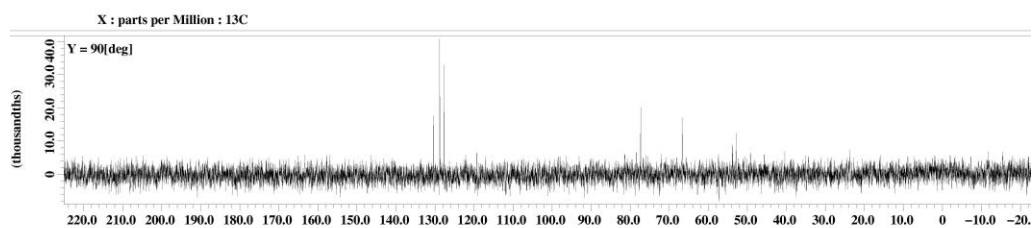
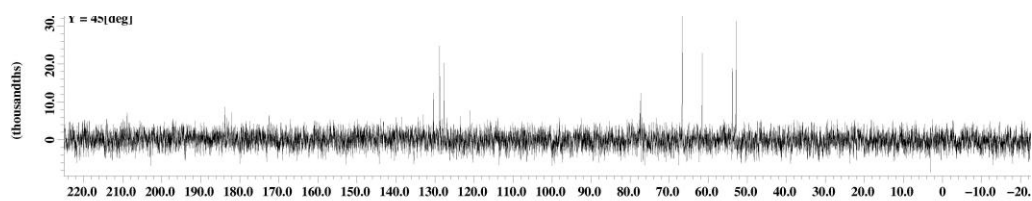


130.2914
128.7658
127.6598
77.2982
61.5375
54.4628
51.9076
45.5575

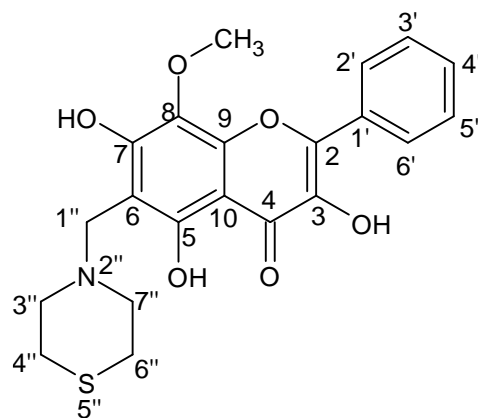
Appendix D61: DEPT Spectrum of 3,5,7-trihydroxy-8-methoxy-6-(4-methylpiperazin-1-ylmethyl)-2-phenyl-4H-chromen-4-one (M5c)



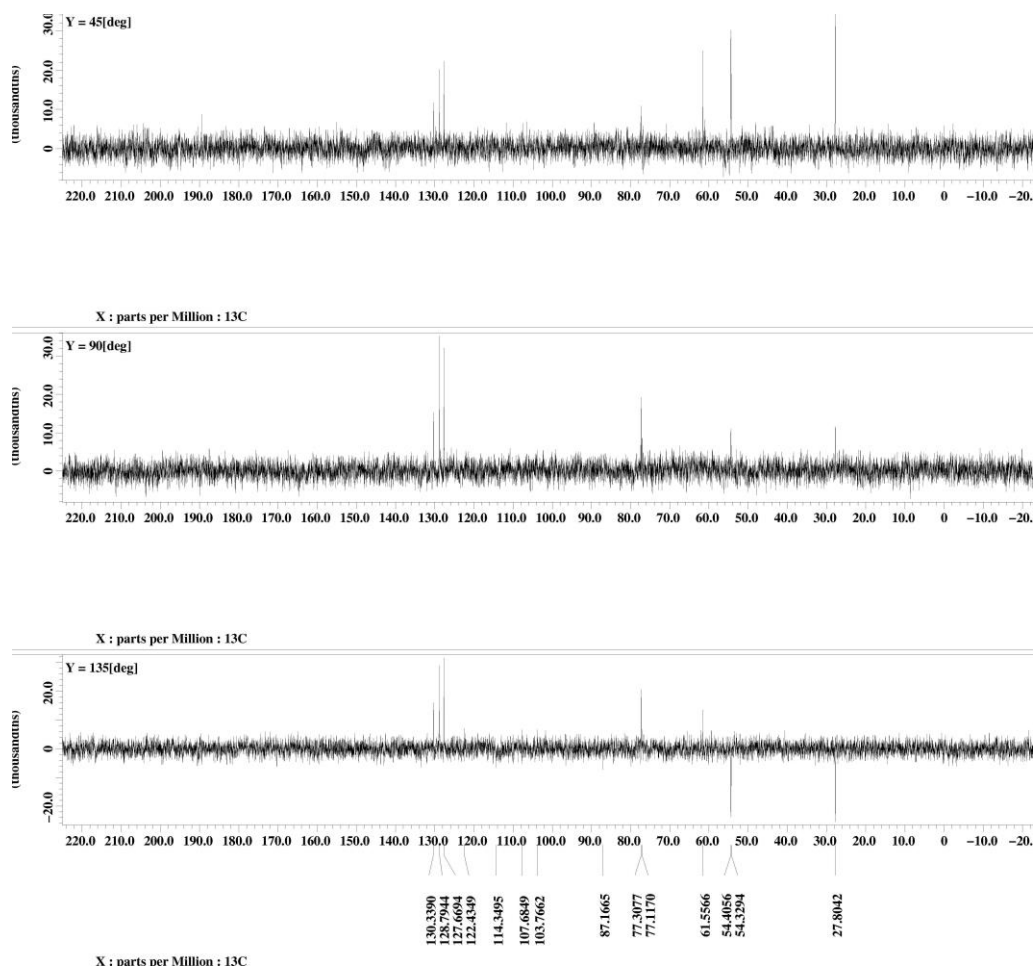
(M5d)



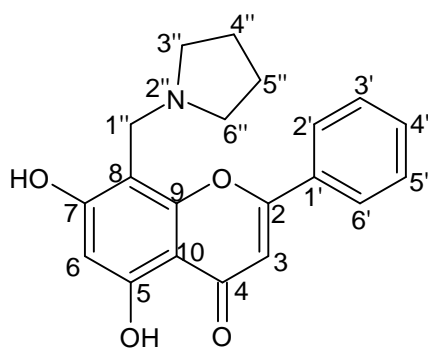
Appendix D62: DEPT Spectrum of 3,5,7-trihydroxy-8-methoxy-6-(morpholinomethyl)-2-phenyl-4H-chromen-4-one (M5d)



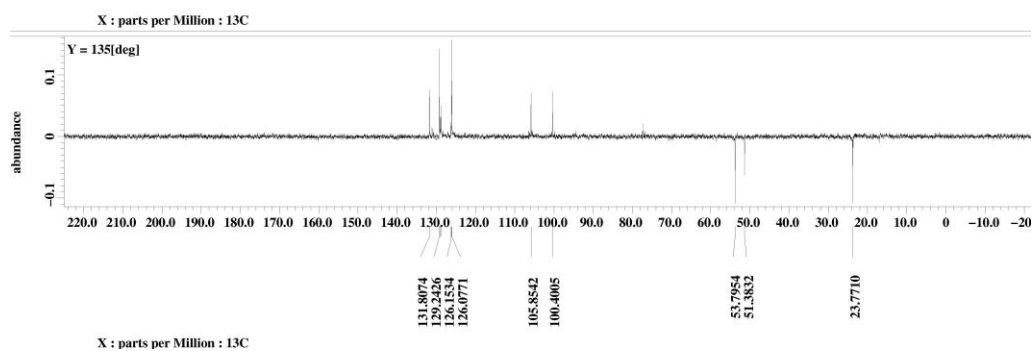
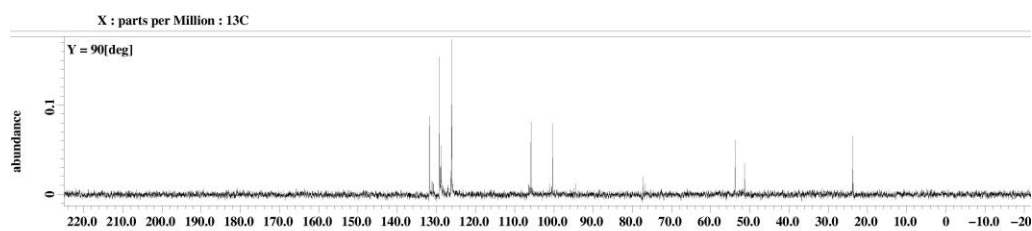
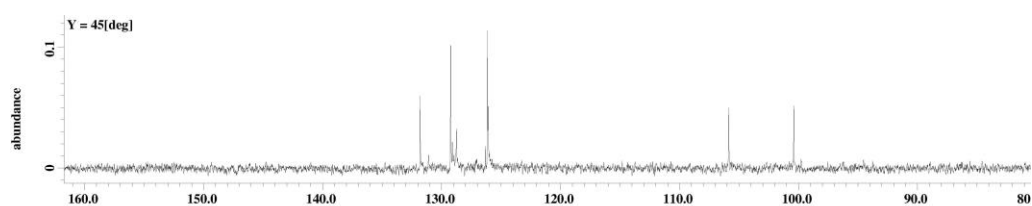
(M5e)



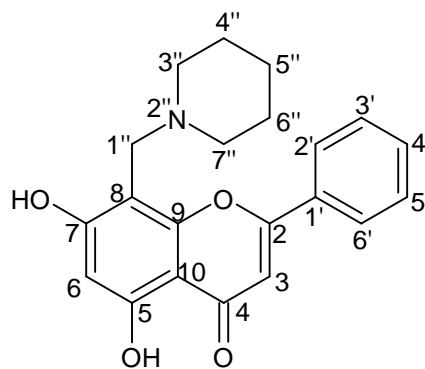
Appendix D63: DEPT Spectrum of 3,5,7-trihydroxy-8-methoxy-6-(thiomorpholinomethyl)-2-phenyl-4H-chromen-4-one (M5e)



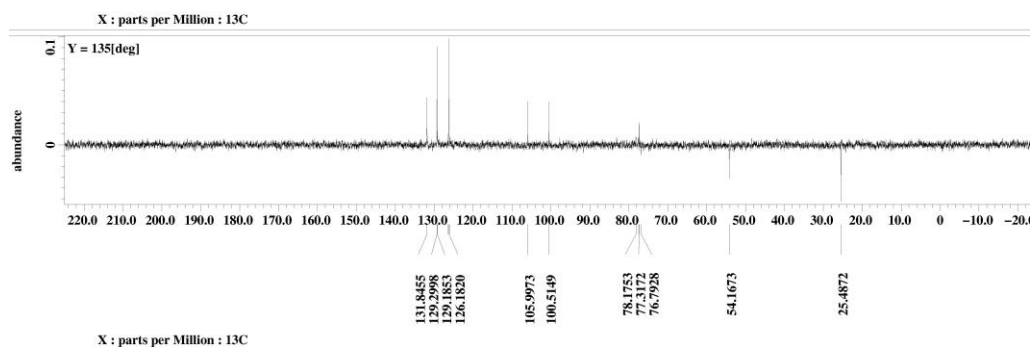
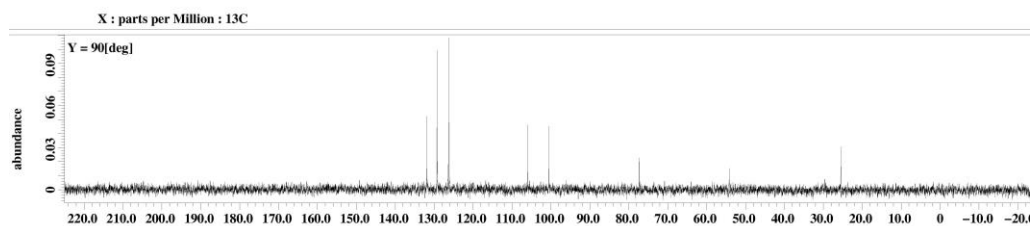
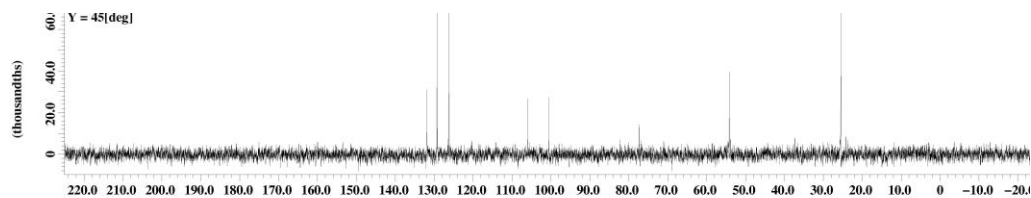
(M14a)



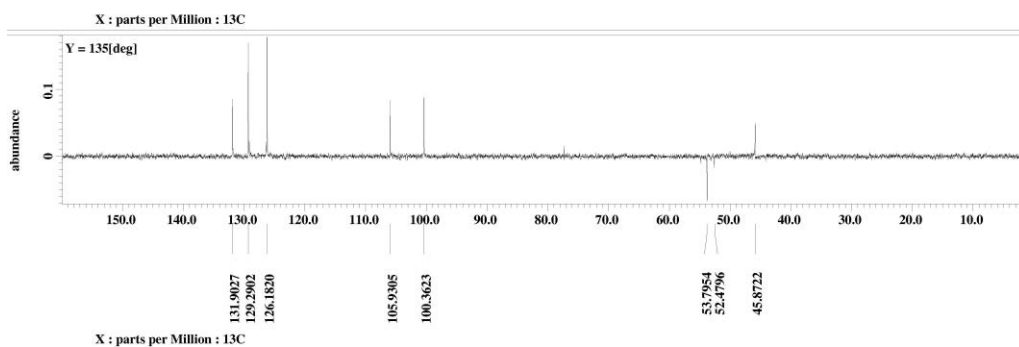
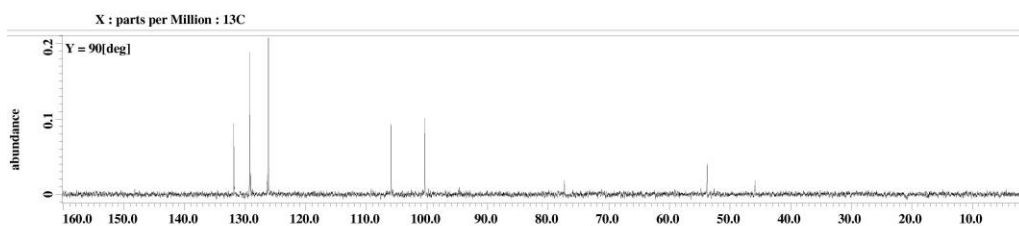
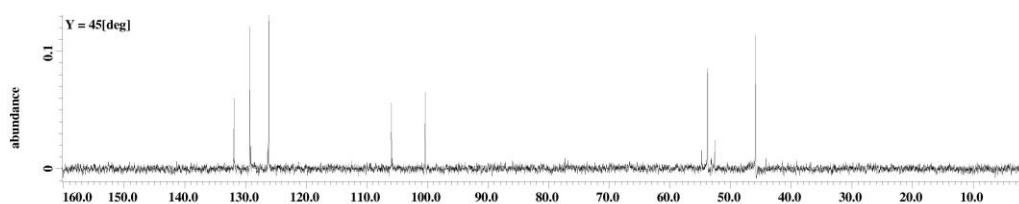
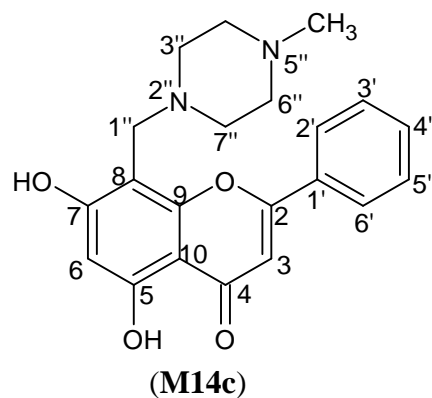
Appendix D64: DEPT Spectrum of 5,7-dihydroxy-8-(pyrrolidine-1-ylmethyl)-2-phenyl-4H-chromen-4-one (M14a)



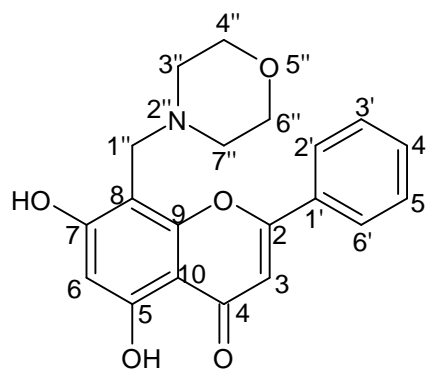
(M14b)



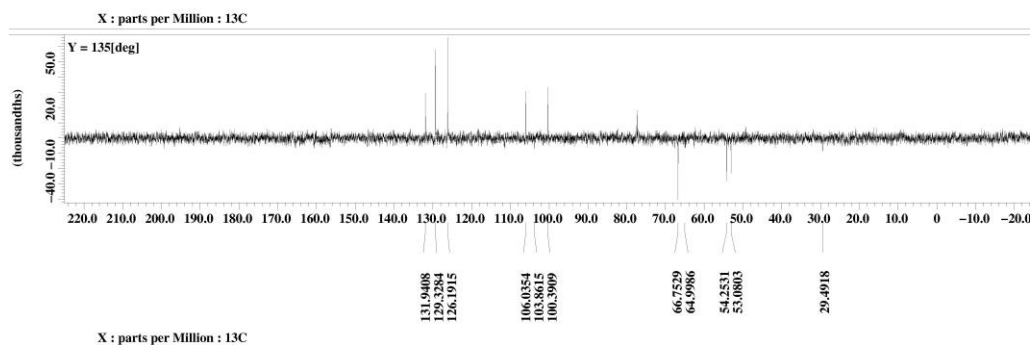
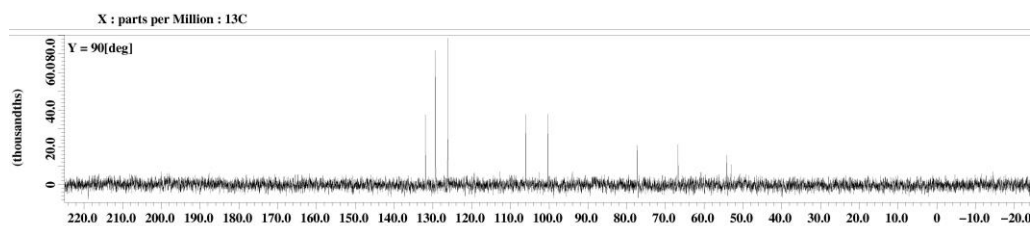
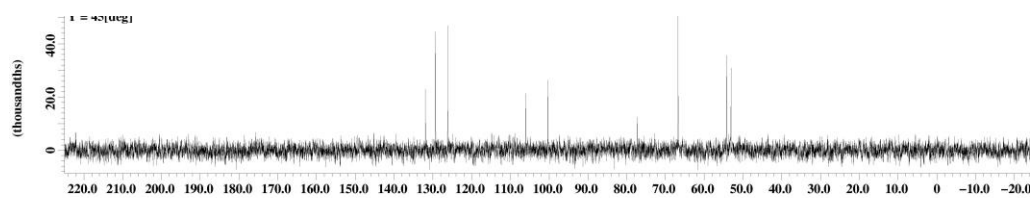
Appendix D65: DEPT Spectrum of 5,7-dihydroxy-8-(piperidin-1-ylmethyl)-2-phenyl-4H-chromen-4-one (M14b)



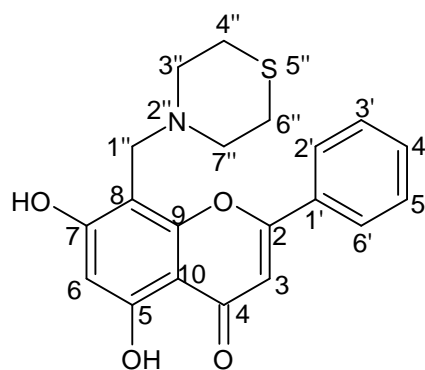
Appendix D66: DEPT Spectrum of 5,7-dihydroxy-8-(4-methylpiperazin-1-ylmethyl)-2-phenyl-4H-chromen-4-one (M14c)



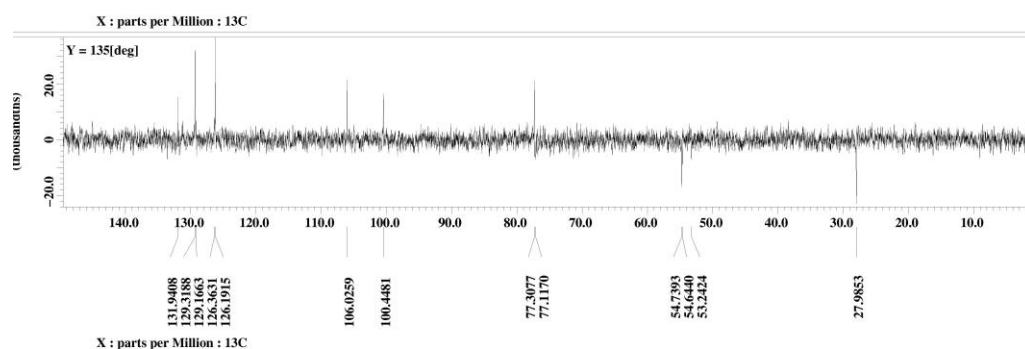
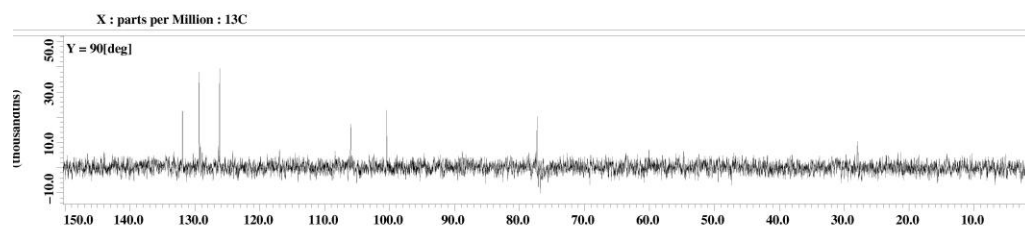
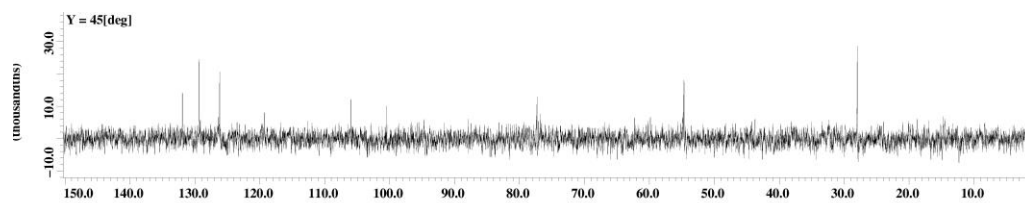
(M14d)



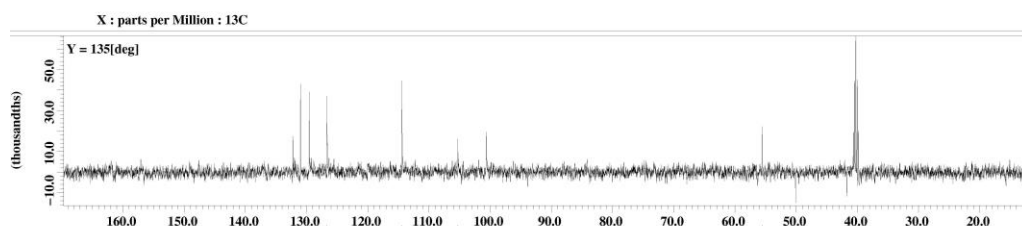
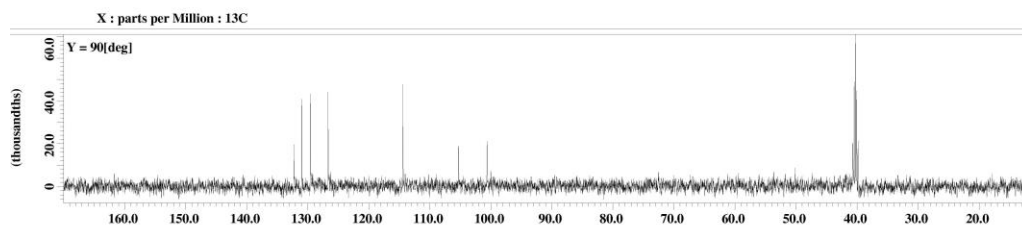
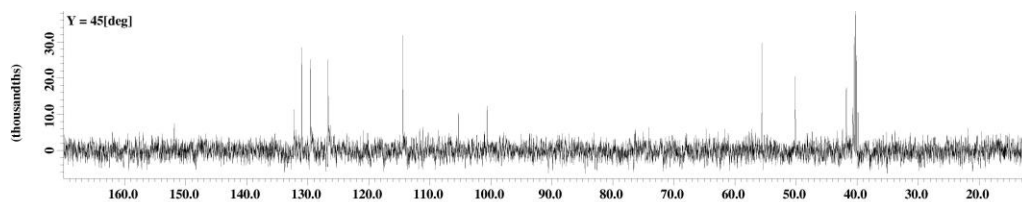
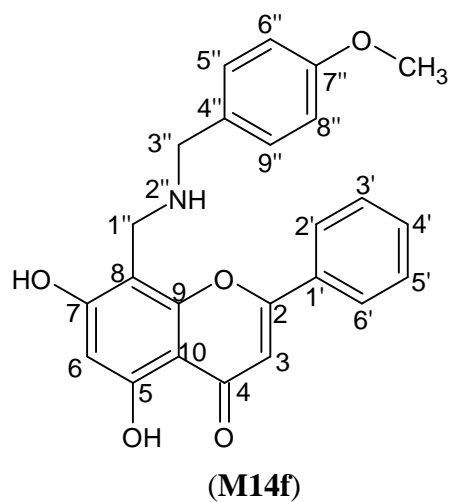
Appendix D67: DEPT Spectrum of 5,7-dihydroxy-8-(morpholinomethyl)-2-phenyl-4H-chromen-4-one (M14d)



(M14e)



Appendix D68: DEPT Spectrum of 5,7-dihydroxy-8-(thiomorpholinomethyl)-2-phenyl-4H-chromen-4-one (M14e)

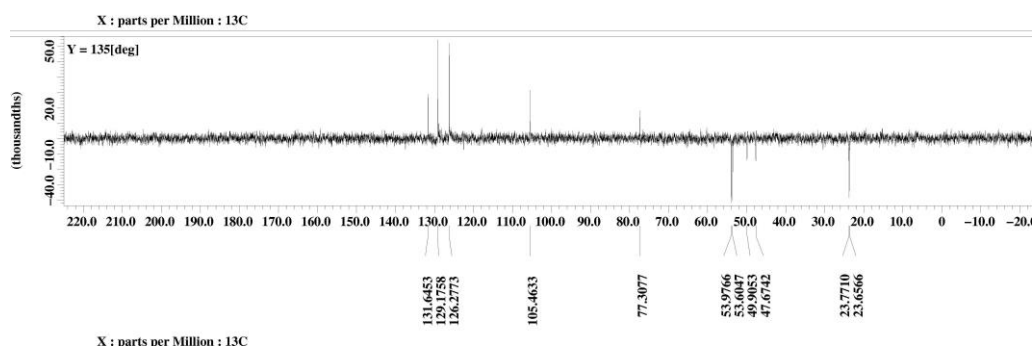
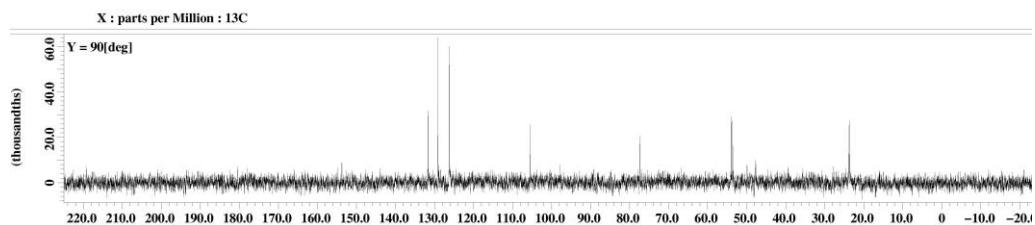
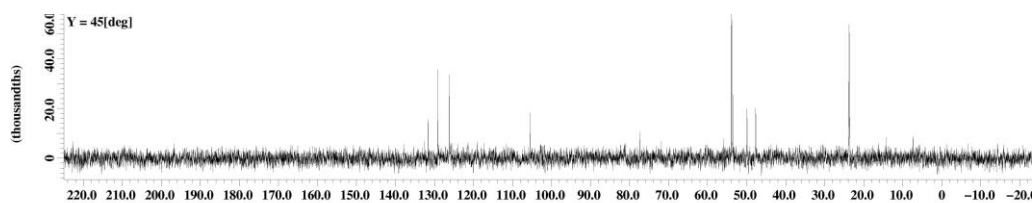
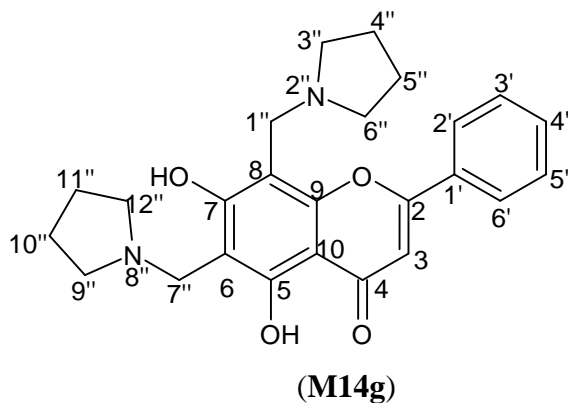


X : parts per Million : 13C

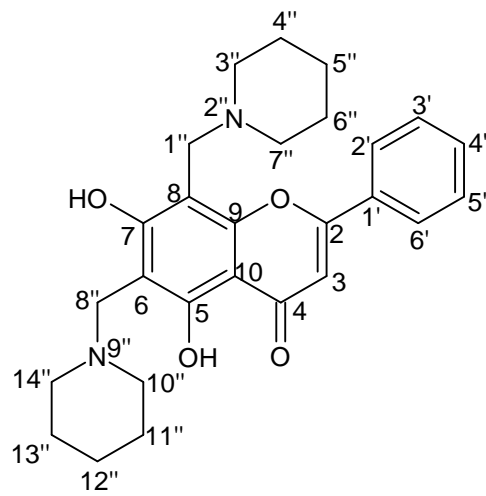
| | | |
|----------|----------|---------|
| 132.2555 | 114.3972 | 55.5879 |
| 130.9969 | 105.2822 | 50.1055 |
| 129.5667 | 100.6198 | 41.7437 |
| 126.6587 | | 39.9607 |
| | | 39.8273 |
| | | 39.7128 |

X : parts per Million : 13C

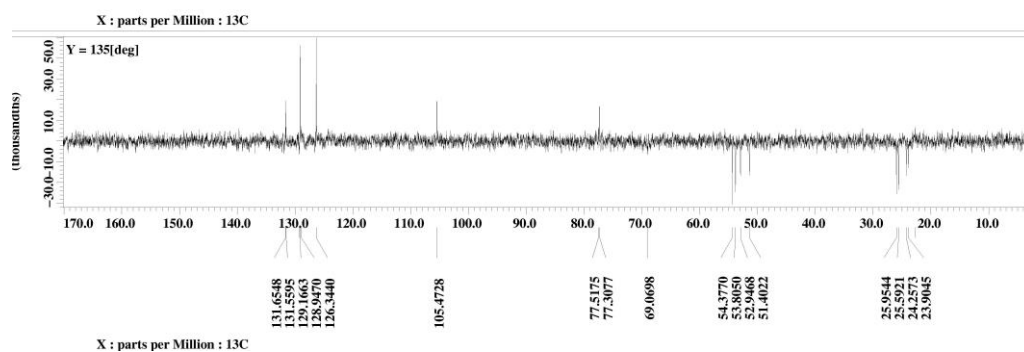
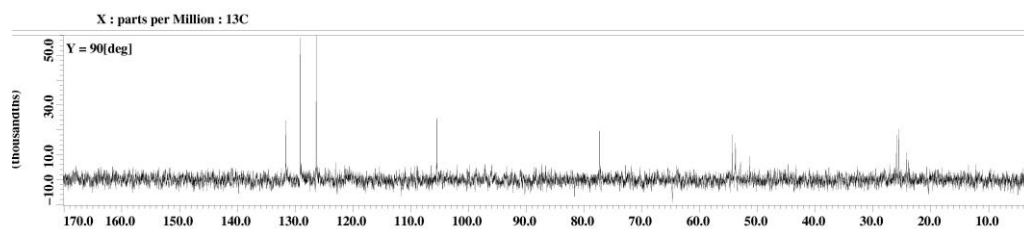
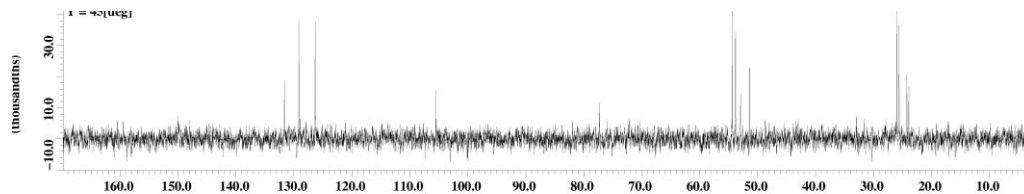
Appendix D69: DEPT Spectrum of 5,7-dihydroxy-8-(4-methoxybenzylamine)-2-phenyl-4H-chromen-4-one (M14f)



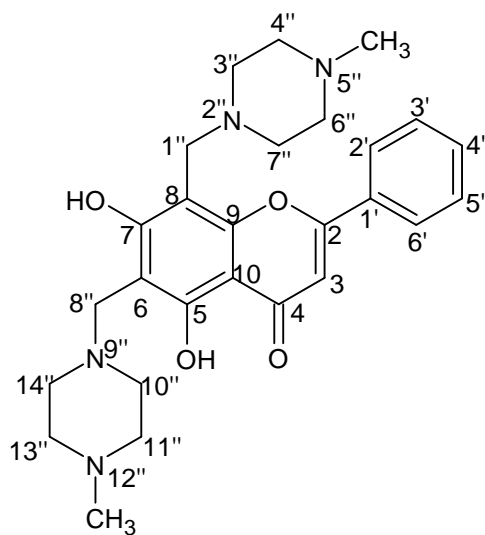
Appendix D70: DEPT Spectrum of 5,7-dihydroxy-6,8-bis(pyrrolidine-1-ylmethyl)-2-phenyl-4H-chromen-4-one (M14g)



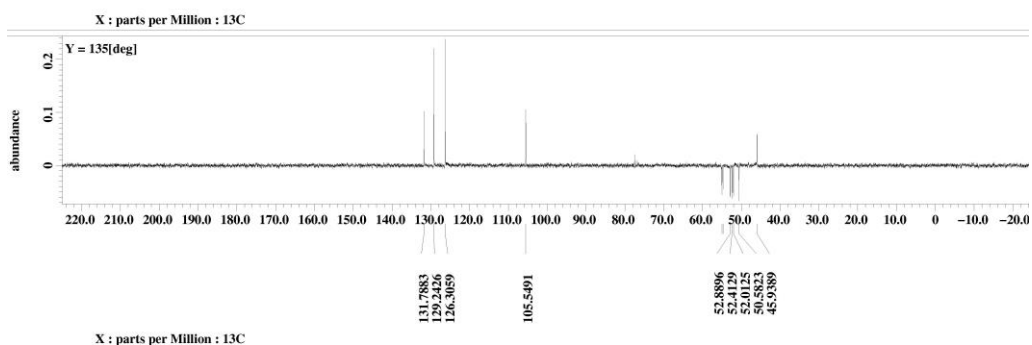
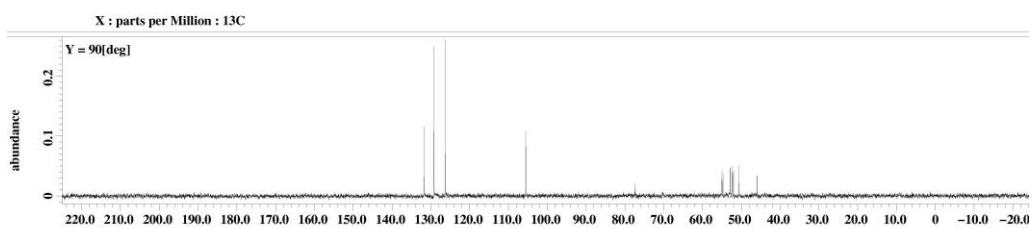
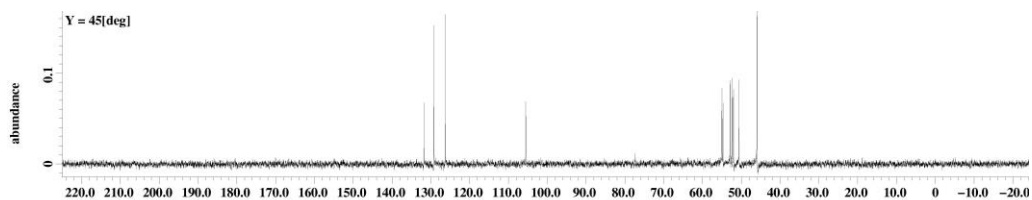
(M14h)



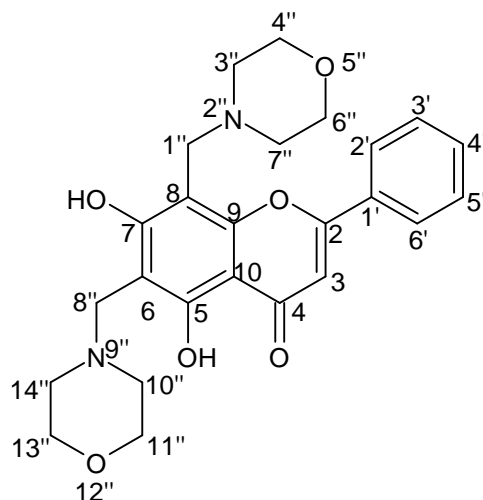
Appendix D71: DEPT Spectrum of 5,7-dihydroxy-6,8-bis(piperidin-1-ylmethyl)-2-phenyl-4H-chromen-4-one (M14h)



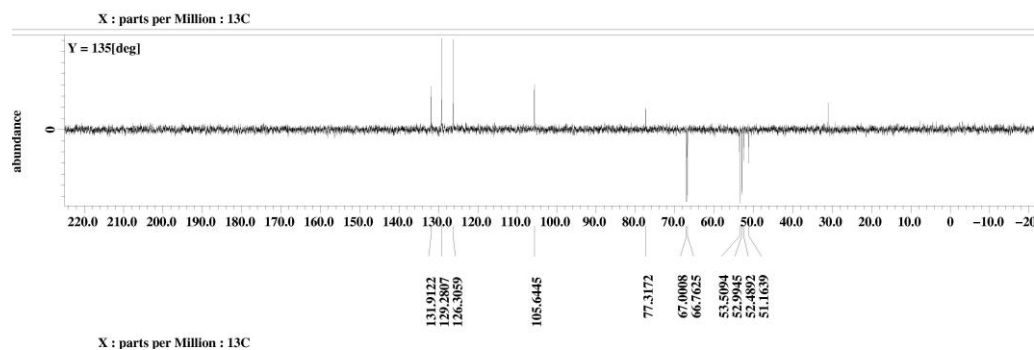
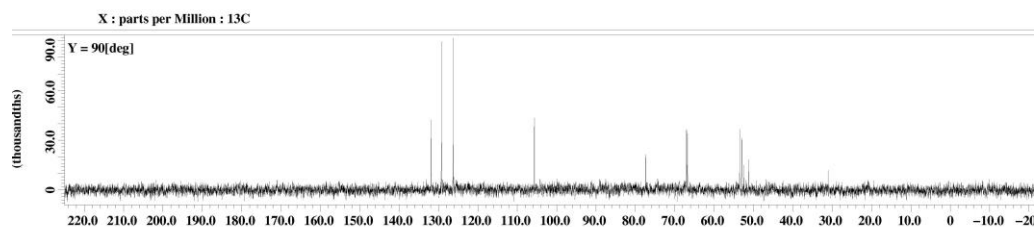
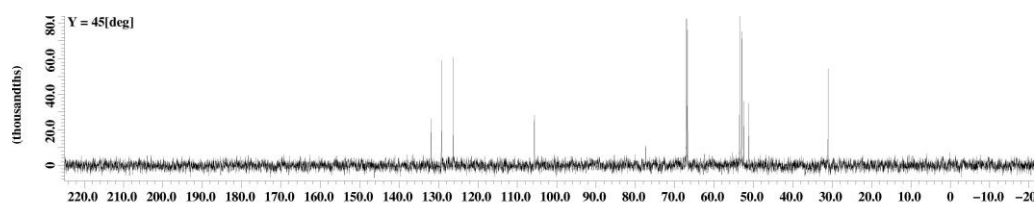
(M14i)



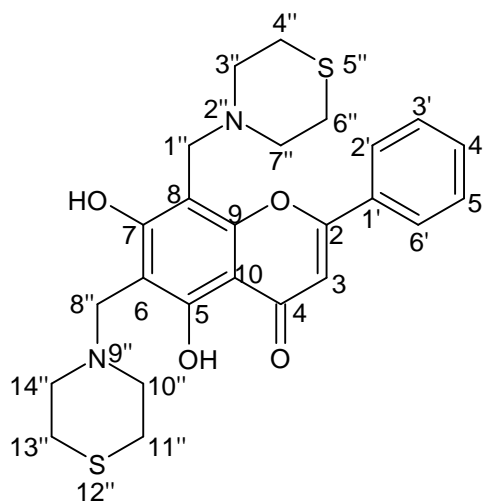
Appendix D72: DEPT Spectrum of 5,7-dihydroxy-6,8-bis(4-methylpiperazin-1-ylmethyl)-2-phenyl-4H-chromen-4-one (M14i)



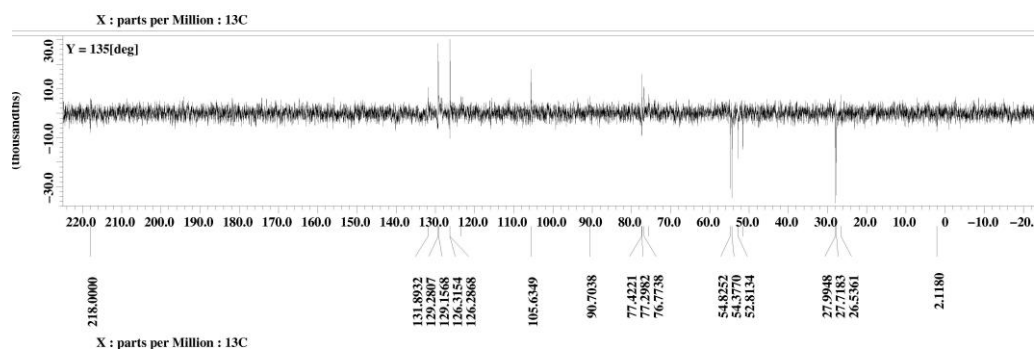
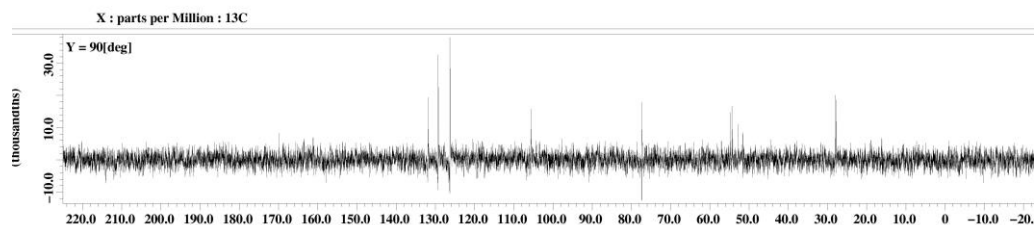
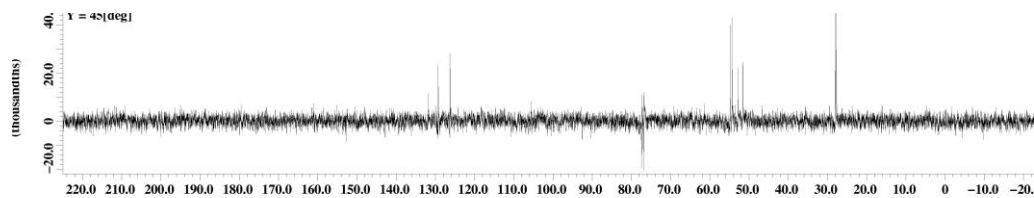
(M14j)



Appendix D73: DEPT Spectrum of 5,7-dihydroxy-6,8-bis(morpholinomethyl)-2-phenyl-4H-chromen-4-one (M14j)



(M14k)



Appendix D74: DEPT Spectrum of 5,7-dihydroxy-6,8-bis(thiomorphinomethyl)-2-phenyl-4H-chromen-4-one (M14k)